

Functionalization of Bicyclo[3.2.1] Sulfones

by

Chak Hong Andy Un  
B. Sc., University of British Columbia, 2016

A Thesis Submitted in Partial Fulfillment  
of the Requirements for the Degree of

MASTER OF SCIENCE

in the Department of Chemistry

© Chak Hong Andy Un, 2020  
University of Victoria

All rights reserved. This thesis may not be reproduced in whole or in part, by  
photocopy or other means, without the permission of the author.

## **Supervisory Committee**

Functionalization of Bicyclo[3.2.1] Sulfones

by

Chak Hong Andy Un  
B. Sc., University of British Columbia, 2016

### **Supervisory Committee**

Dr. Jeremy E. Wulff (Department of Chemistry)  
**Supervisor**

Dr. Fraser A. Hof (Department of Chemistry)  
**Departmental Member**

## Abstract

### Supervisory Committee

Dr. Jeremy E. Wulff (Department of Chemistry)  
**Supervisor**

Dr. Fraser A. Hof (Department of Chemistry)  
**Departmental Member**

Sulfones are useful bioisosteres in drug discovery, and have an unusual ability to engage in binding with both polar and nonpolar regions of target proteins. Despite this, they have seen limited use in drug-screening campaigns, compared with other functional groups. With the goal of generating a library of bicyclo[3.2.1]sulfone-containing molecules to probe biological function, a tandem 1,2-addition/anionic oxy-Cope/1,2-addition reaction proceeding from 3-sulfolene and discovered by previous members of our group was used to prepare highly substituted scaffolds for diversification. Functional group manipulations on this scaffold were partially successful, but ultimately provided limited scope for exploring three-dimensional space.

Moving to a less-substituted bicyclo[3.2.1]sulfone scaffold that could be accessed using methodology developed by the Chou group, it was found that a greater range of chemical diversification could be achieved. Using both substrate-directed methods and intrinsic functional group reactivity, about 70% of the skeletal framework was functionalized with high levels of regioselectivity and (in some cases) good levels of diastereoselectivity.

Cheminformatic analysis was performed on our collection of synthesized bicyclo[3.2.1]sulfone-containing molecules, and diverse molecular descriptors were obtained. Collaborations were established with industrial partners and non-profit institutions for the purpose of determining biological properties in medicinally relevant areas. Significantly, each of these partners joined the project with therapeutic expertise in a different field (oncology, neurodegenerative diseases, antimicrobial agents, and skin inflammation), thereby maximizing the chances of finding useful lead compounds for future development. Preliminary

biological screening data were obtained, which suggest future potential for sulfone-containing conformationally restricted small molecules to be impactful in therapeutic development.

## Table of Contents

Supervisory Committee .....	ii
Abstract .....	iii
Table of Contents .....	iv
List of Equations .....	v
List of Figures .....	vi
List of Schemes .....	x
List of Tables .....	xv
List of Abbreviation and Symbols .....	xvi
Acknowledgments .....	xxi
Chapter 1 - Introduction .....	1
1.1 Modern Evolution of Medicinal Chemistry .....	1
1.2 Predictors and Strategies in Drug Design .....	9
1.3 Academic-Industrial Collaboration in Drug Discovery .....	13
1.4 Sulfonamides and Sulfones in Medicinal Chemistry .....	16
Chapter 2 – Oxidative Cleavage of Previously Investigated Scaffold and Alternate Methods for Construction and Diversification .....	21
2.1 Tandem 1,2-addition/anionic oxy Cope reactions of Sulfolene Derivatives .....	21
2.2 Initial Construction of Bicyclo[3.2.1]Sulfone-Containing Library....	27
2.3 Alternative Approach to Generate Bicyclic Sulfones .....	38
Chapter 3 – Functionalization of Simpler Bicyclo[3.2.1]Sulfone-Containing Scaffold .....	43
3.1 Oxidation of Chou-type Bicyclic Sulfones .....	43
3.2 Expanding Chemical Space of Bicyclo[3.2.1] Sulfones.....	58
3.3 Bridgehead Alkylation of Bicyclic Sulfones .....	68
Chapter 4 – Biological Screening and Preliminary Data Analysis.....	79
4.1 Chemoinformatic Analysis of Bicyclo[3.2.1] Sulfones .....	79
4.2 Collaborations with Community for Open Antimicrobial Drug Discovery .....	89
4.3 Eli Lilly's Open Innovation Drug Discovery Platform .....	96
4.4 Eczema Assay Screening with LEO Pharma A/S .....	100
Chapter 5 – Future Directions.....	109
5.1 Further Functionalization of Bicyclo[3.2.1] Sulfones .....	109
5.2 Novel Methodology for Bicyclo[3.2.1]Sulfone Fragments .....	114
5.3 Alternative Evolution of Bicyclic Sulfones .....	117
Conclusion.....	119
Bibliography.....	120
Appendix A – Experimental Information .....	168
Experimental References .....	203
Appendix B – Spectral Data.....	204
Appendix A – Biological Data .....	250

## List of Equations

Equation 1. Simplified rate equation summarizing the cyclopropanation step and dimerized product <b>69</b> .....	63
--	----

## List of Figures

Figure 1. Simple overview of drug development timeline .....	1
Figure 2. Some of the most frequently used chemical reactions employed by medicinal chemists in recent years.....	2
Figure 3. Principle moments of inertia (PMI) plot constructed from a proportion of compounds in ChEMBL space. Obtained permission to reuse.....	3
Figure 4. An illustrative diagram to demonstrate how DOS results in skeletally comprehensive structures through functional group pairing. ....	7
Figure 5. List of benzofused lactams from DOS and their respective biological applications. ....	8
Figure 6. Comparison of molecular descriptors between three marketed-approval drugs. Criterias that violate Lipinski's rule of five are highlighted in red. ....	10
Figure 7. A list of representative sulfonamide-containing drugs that are currently approved or in development. ....	16
Figure 8. A list of all known sulfone-containing drugs that are currently approved or in development. ....	17
Figure 9. Functional group diversity of FDA-approved sulfur-containing drugs in US. ....	18
Figure 10. Close-up of co-crystal structure for small molecule <b>4</b> in BACE1 (left) and the chemical structure of small molecule <b>4</b> (right). PDB code: 4D8C. ....	19
Figure 11. Crystal structure comparison of compound <b>8a</b> (left, CCDC 766248) and enzyme-bound peramivir (right, PDB 1L7F).. ....	23
Figure 12. X-ray crystal structure of compounds <b>13</b> (top left), <b>14</b> (top middle) and <b>15</b> (top right) and their chemical structures (bottom). Included in each X-ray structure are the corresponding projection angle of the sulfone groups, with the exception of <b>14</b> (implied to be the inverse of 113.36° in a theoretically spherical model, which is 246.64°). ....	26
Figure 13. Overlapping <sup>1</sup> H NMR spectra of McMurry coupling using 5.0 equivalent (green), 3.5 equivalent (red), and 3.0 equivalent (blue) of TiCl <sub>4</sub> . Signals corresponding to diene <b>26</b> are highlighted as purple rectangles.	

Normalized based on peak height of singlet signal at $\delta$ 4.28 ppm (highlighted as yellow circles. ....	29
Figure 14. Rationalization of how decomposition originates from cleavage of C – SO <sub>2</sub> bond.....	35
Figure 15. Comparison of alkenes that demonstrate the highest reactivity as described by Mayr and coworkers. Highlighted in neon blue are the most reactive moieties in corresponding molecules <b>50</b> and <b>51</b> , while yellow highlighted regions indicate possible reactivity moieties with unknown preferences in compound <b>47</b> . ....	45
Figure 16. Grand scheme of site-selective functionalization of bicyclo[3.2.1]sulfone-containing frameworks. Coloured arrows indicate the direction of vectors that can be theoretically reached if the carbons with corresponding colours can be decorated. ....	46
Figure 17. Magnification of <sup>1</sup> H NMR reactivity monitoring spectrum of compound <b>46</b> and Pd(PPh <sub>3</sub> ) <sub>2</sub> Cl <sub>2</sub> . Highlighted in light green are diagnostic peaks corresponding to alkenyl protons of the 1,1-disubstituted <i>exo</i> -cyclic olefin. ....	55
Figure 18. Magnification of <sup>1</sup> H NMR reactivity monitoring spectrum of compound <b>46</b> and Pd(PPh <sub>3</sub> ) <sub>2</sub> Cl <sub>2</sub> . Highlighted in green are diagnostic peaks corresponding to C <sub>sp<sup>3</sup></sub> protons of the bridgehead position i.e. C–1 or C–5 positions of the bicyclo[3.2.1]sulfone-containing framework. ....	56
Figure 19. <sup>31</sup> P NMR reactivity monitoring spectrum of compound <b>47</b> and Pd(PPh <sub>3</sub> ) <sub>2</sub> Cl <sub>2</sub> . Highlighted in green are diagnostic peaks corresponding to Pd(PPh <sub>3</sub> ) <sub>2</sub> Cl <sub>2</sub> .....	57
Figure 20. <sup>1</sup> H NMR of compound <b>68a</b> and <b>68b</b> in CDCl <sub>3</sub> over prolonged period of time. Highlighted in purple circles are diagnostic peaks corresponding to sulfone <b>68a</b> , while highlighted in green diamonds are diagnostic peaks corresponding to sulfone <b>68b</b> . ....	62
Figure 21. <sup>1</sup> H NMR reactivity monitoring spectrum of compound <b>46</b> and GII. Highlighted in purple are diagnostic peaks corresponding to compound <b>46</b> ....	74

Figure 22. Downfield $^1\text{H}$ NMR reactivity monitoring spectrum of compound <b>47</b> and GII. Neon green circle indicates the vinyl proton of GII (Ru-CH $\underline{\text{H}}$ Ph). Orange circle indicates the formation of a new Ru-benzylidene species.....	75
Figure 23. $^{31}\text{P}$ NMR reactivity monitoring spectrum of compound <b>47</b> and GII. Green circle and light green square correspond to diagnostic signals of $\text{Cy}_3\text{P}=\text{O}$ and GII respectively.....	76
Figure 24. Zoomed in of $^1\text{H}$ NMR reactivity monitoring spectrum of compound <b>46</b> and GII. ....	77
Figure 25. First generation bicyclo[3.2.1]sulfone-containing small molecule library .....	79
Figure 26. Plane of best-fit distribution diagram of bicyclo[3.2.1]sulfone-containing molecules.....	86
Figure 27. Polar-dispersion distribution diagram of bicyclo[3.2.1]sulfone-containing molecules.....	86
Figure 28. Three-dimensionality distribution diagram of bicyclo[3.2.1]sulfone-containing molecules.....	87
Figure 29. Property space of bicyclo[3.2.1]sulfones, and corresponding spatial visualization of FDA-approved herbicides, insecticides, and drugs that target the central-nervous system, as highlighted in orange, green, and yellow respectively. ....	88
Figure 30. Principle moment of inertia plot of bicyclo[3.2.1]sulfone-containing molecules and selected examples that closely represents its corresponding axes.....	89
Figure 31. General mechanistic scheme illustrating natural ligands and function of NNMT. ....	99
Figure 32. Biological data of sulfone <b>41</b> in eczema-induced CCL2 release assay.....	104
Figure 33. Cyclopropanols and its transition-metal homoenolate counterparts .....	118
Figure 34. Greater three-dimensional control on a molecule level using sulfoximines. ....	120

## List of Schemes

Scheme 1. An overall reaction scheme of how sorafenib was discovered. ....	5
Scheme 2. An example of how DOS provides stereochemically different molecules. ....	8
Scheme 3. The evolution of maraviroc during hit-to-lead optimization until drug approval. ....	12
Scheme 4. An example of conformational restriction leading to improved biological properties. ....	13
Scheme 5. Development of cyclic sulfone <b>3</b> in the search of a novel BACE1 inhibitor.....	19
Scheme 6. Tandem 1,2-addition/anionic oxy-Cope cascade reaction.....	20
Scheme 7. Formation of cis-bicyclo[3.3.0]sulfone-containing molecules in a disastereoselective manner. ....	21
Scheme 8. Development of highly functionalized conformationally-restricted bicyclo[3.3.0]sulfone-containing neuraminidase inhibitor .....	24
Scheme 9. Diversity-orientated sulfone-containing scaffolds based on a common building block.....	25
Scheme 10. Synthesis of diarylidene ketones .....	27
Scheme 11. Synthesis of symmetrical diketone sulfides .....	27
Scheme 12. Synthesis of cyclic sulfones via deoxygenative annulation and sulfide oxidation.....	28
Scheme 13. Attempted improvement of sulfone synthesis via pinacol coupling. ....	29
Scheme 14. Attempted double arylation of cyclic alkenes via Heck reaction. ....	30
Scheme 15. Replication of tandem 1,2-addition/anionic oxy-Cope cascade reaction. ....	30
Scheme 16. Serendipitous discovery of iterative tandem 1,2-addition/ anionic oxy-Cope cascade. ....	32
Scheme 17. Attempted synthesis of sulfone-containing macrocycles. ....	32
Scheme 18. Synthesis of bicyclo[3.2.1]sulfone-containing compounds using different diarylidene ketones. ....	33

Scheme 19. Attempted oxidative cleavage of aryl alkenes under different redox workup conditions. ....	33
Scheme 20. Successful acylation of sterically hindered tertiary alcohol <b>31a</b> . .	34
Scheme 21. Attempted oxidative cleavage of aryl alkenes using either ozonolysis or Lemieux-Johnson oxidation. ....	34
Scheme 22. Postulated mechanism on how oxidative decomposition can arise during ozonolysis. ....	35
Scheme 23. Attempted allylic 1,3-oxygen transposition mediated by chromium reagents. ....	36
Scheme 24. Attempted transformation of one-pot Ireland-Claisen rearrangement to yield carboxylic acids. ....	36
Scheme 25. Acetylation of bicyclo[3.2.1]sulfone-containing compounds. ....	37
Scheme 26. Attempted demethylation of methyl aryl ethers under Lewis acidic conditions. ....	37
Scheme 27. Attempted synthesis of bicyclo[3.2.1]sulfone-containing compounds via nucleophilic substitution with organochlorides. ....	38
Scheme 28. Successful transformation of diaryl sulfones via double nucleophilic substitution with organohalides. ....	38
Scheme 29. Ozonolysis of terminal alkenes and subsequent reduction of ketones. ....	39
Scheme 30. Hydroboration of bicyclo[3.2.1]sulfone-containing alkenes. ....	40
Scheme 31. Attempted dipolar [3+2] cycloaddition of bicyclo[3.2.1]sulfone-containing compounds using <i>in situ</i> generated nitrile oxides. ....	40
Scheme 32. Regioselective dihydroxylation of bicyclo[3.2.1]sulfone-containing compounds. ....	41
Scheme 33. Attempted hydrogenation of tetra-substituted diaryl alkene region of bicyclo[3.2.1]sulfones. ....	41
Scheme 34. Formation of compound <b>47</b> using different dihalide species as the electrophile. ....	43
Scheme 35. Mechanism of how compound <b>47</b> is formed, as well as possible fragmentation pathway. ....	44

Scheme 36. Ozonolysis of compound <b>46</b> . Compound in brackets are not isolated but observed. ....	47
Scheme 37. Failed attempt to perform aldol-condensation between sulfone <b>51</b> and aldehyde <b>53</b> . ....	49
Scheme 38. Postulated $\beta$ -elimination pathway of compound <b>51</b> leading to the extrusion of sulfone moiety. ....	49
Scheme 39. Different regioselectivity in carbonyl reduction of compound <b>51</b> via different metal hydrides. ....	50
Scheme 40. Postulated mechanistic differences resulting in differing diastereoselectivity in reduction of ketone <b>52</b> using different metal-hydrides. ....	51
Scheme 41. Epoxidation of sulfone <b>47</b> (left) and the “butterfly” mechanistic transition state (right). ....	52
Scheme 42. Regioselective and diastereoselective hydroboration of sulfone <b>46</b> . ....	53
Scheme 43. Unexpected results from dihydroxylation of compound <b>47</b> using catalytic osmium tetroxide. ....	53
Scheme 44. Simplified catalytic cycle illustrating how compound <b>60</b> is formed. The rate-determining step of the mechanism is postulated to be the hydrolysis of <b>TS4b</b> . ....	54
Scheme 45. One-pot dihydroxylation/boronic ester formation from compound <b>46</b> . ....	55
Scheme 46. Weak bidentate chelation of sulfone <b>46</b> with Pd(II) species. ....	57
Scheme 47. Failed attempt at Baeyer-Villiger oxidation of compound <b>51</b> . ....	58
Scheme 48. Various O-substituted oximes formed via condensation with sulfone <b>52</b> . ....	59
Scheme 49. Rh-catalyzed cyclopropanation of sulfone <b>47</b> to yield conformationally restricted products. ....	60
Scheme 50. Simplified catalytic cycle that demonstrates the transformation of sulfones <b>68a</b> and <b>68b</b> . ....	65

Scheme 51. Reduction of the ester moieties of compound <b>68a</b> and <b>68b</b> . Isolated of compounds <b>71a</b> and <b>71b</b> were difficult due to negligible polarity differences as indicated in TLC. ....	66
Scheme 52. Mulzer's synthesis towards natural product branimycin. ....	67
Scheme 53. Failed attempts of allylic oxidation of sulfone <b>47</b> . ....	67
Scheme 54. Natural products that contains tropane skeleton as shown in blue. .....	68
Scheme 55. Deuteration via sulfone-assisted lithiation of compound <b>47</b> . ....	69
Scheme 56. Screening of base used in bridgehead lithiation to optimize isolated of sulfone ( <b>±</b> )- <b>76b</b> . ....	70
Scheme 57. Silylation of 2-bromoethanol under mild conditions. ....	71
Scheme 58. Successful attempts at bridgehead alkylation of compound <b>47</b> . .	72
Scheme 59. Failed attempts of bridgehead functionalization. Many different substrated were tested as shown and did not appear to be compatible with our current methodology. ....	73
Scheme 60. Unsuccessful attempts at furnishing sulfone ( <b>±</b> )- <b>76c</b> using cross- olefin metathesis. ....	74
Scheme 61. Failed attempts at Wacker-type oxidation of sulfone ( <b>±</b> )- <b>76c</b> . ....	78
Scheme 62. General schematic diagram of how methylation of nicotinamide proceeds (left) illustration of how 6-methoxynicotinamide interacts within the active site of NNMT. ....	101
Scheme 63. Postulated binding mode of amide <b>81</b> by covalent linkage within the active site of NNMT (left). Structural similarity between amide <b>81</b> and bicyclo[3.2.1]sulfone <b>31d</b> or <b>32d</b> as highlighted in red (right) . ....	102
Scheme 64. List of synthesized bicyclo[3.2.1]sulfone-containing molecules that participated in re-validation screening. ....	103
Scheme 65. Overall reaction schemes of synthesizing sulfones <b>82</b> and <b>83</b> , as well as postulated mechanism of how ketone <b>83</b> degrades under basic conditions. ....	105
Scheme 66. Structural similarity amongst all bioactive bicyclo[3.2.1]sulfones in eczema-induced CCL2 release assay, as highlighted in red. ....	108

Scheme 67. Structural similarity amongst all bioactive bicyclo[3.2.1]sulfones in IL-17 release from CD3/CD28/IL-23-induced assay, as highlighted in red. ..	109
Scheme 68. Functionalization of bicyclo[3.2.1]sulfone-containing ketone species using isocyanide-based multicomponent reactions. ....	111
Scheme 69. Rapid access of O-substituted hydroxylamines as substrates for oxime condensation. ....	112
Scheme 70. Radical-based ring-opening of epoxide <b>68</b> and subsequent trapping. ....	112
Scheme 71. Substrate-directed regioselective arylation of bicyclo[3.2.1]sulfone-containing molecules. ....	113
Scheme 72. Allylic functionalization methods that may accommodate our need for site-selective modification of bicyclo[3.2.1]sulfone-containing molecules. ....	113
Scheme 73. Rapid equilibrium of bicyclo[3.2.1]sulfone-containing benzoxaboronic esters. ....	114
Scheme 74. Quaternary allylic olefin metathesis as an alternative method for diversity-orientated synthesis of bicyclo[3.2.1]sulfone-containing molecules. ....	114
Scheme 75. Possible competition between C-H allylic functionalization and aziridination pathways. ....	115
Scheme 76. Cross-coupling between aryl diazonium salts and 3-sulfolene <b>4a</b> to generate diverse amounts of cyclic sulfones, which can act as substrates for our ongoing investigations. ....	116
Scheme 77. Formation of sulfone <b>82</b> using milder reactions conditions. ....	117
Scheme 78. Theorized oxidative cross-coupling between cyclic sulfones and cyclopropanols to generate bicyclo[3.2.1]sulfone-containing molecules. ....	118
Scheme 79. Formation of bicyclo[3.2.1]sulfone-containing molecules via tropinone derivatives. ....	119
Scheme 80. Possible two-step protocol to form bicyclo[3.2.1]sulfoximine-containing molecules from its sulfide counterparts. ....	120

## List of Tables

Table 1. Tabulation of varying catalyst loading of OsO <sub>4</sub> and their corresponding yields of sulfone <b>60</b> .....	54
Table 2. Rh-catalyzed cyclopropanation of sulfone <b>47</b> to yield conformationally restricted products. ....	61
Table 3. Chemoinformatic data of bicyclo[3.2.1]sulfone-containing molecules. MW, HBD, HBA, tPSA, cLogP, and RotB denotes molecular weight, number of hydrogen-bond donors, number of hydrogen-bond acceptors, topological polar surface area, calculated LogP, and number of rotatable bonds respectively. Checkmark in the column “Rule of 5?” indicates that such molecule fulfills the criteria proposed by Lipinski and coworkers. ....	84
Table 4. Summary of chemoinformatic data for FDA-approved herbicides, insecticides, and drugs, that target the central-nervous system. ....	87
Table 5. Summary of biological assay data of bicyclo[3.2.1]sulfone-containing molecules against yeast. Note that red, white and blue colour denotes performance at 19 <sup>th</sup> , 50 <sup>th</sup> , and 90 <sup>th</sup> percentile. . ....	93
Table 6. Summary of biological assay data of bicyclo[3.2.1]sulfone-containing molecules against bacteria. Note that red, white and blue colour denotes performance at 19 <sup>th</sup> , 50 <sup>th</sup> , and 90 <sup>th</sup> percentile.....	95
Table 7. Summary of biological assay data of bicyclo[3.2.1]sulfone-containing molecules against the enzyme NNMT. Note that red, white and blue colour denotes performance at 19 <sup>th</sup> , 50 <sup>th</sup> , and 90 <sup>th</sup> percentile. ....	100
Table 8. Summary of biological assay data from re-validation of bicyclo[3.2.1]sulfone-containing molecules. ....	107

## List of Abbreviation and Symbols

<i>A. baumannii</i>	<i>Acinetobacter baumannii</i>
Ac	acetyl
acac	acetylacetonate
AcOH	acetic acid
APP	amyloid precursor protein
aq	aqueous
Ar	aryl
Asp	aspartic acid
ATCC	American Type Culture Collection
BACE	beta-site APP-cleaving enzyme
BDE	bond dissociation energy
br	broad
Bu	butyl
Bn	benzyl
Bz	benzoyl
Boc	<i>tert</i> -butyloxycarbonyl
°C	degrees Celsius
<i>C. albicans</i>	<i>Candida albicans</i>
cat	catalytic
CatD	cathepsin D
CCDC	Cambridge Crystallographic Data Center
CCL2	C–C motif chemokine ligand 2
CD	cluster of differentiation
CH <sub>2</sub> Cl <sub>2</sub>	dichloromethane
CHO	Chinese hamster ovary
<i>CHO/APPwt</i> cells	CHO cells overexpressing human wild-type APP
clogP	calculated logarithm of the partition coefficient
cm <sup>-1</sup>	wavenumbers
<i>C. neoformans</i>	<i>Candida neoformans</i>
CNS	central nervous system
COSY	<sup>1</sup> H – <sup>1</sup> H correlation spectroscopy
Cu(OTf) <sub>2</sub>	cupric trifluoromethanesulfonate
Cy	cyclohexyl
Cys	cysteine
d	doublet
Da	dalton
dba	dibenzylideneacetone
DCM	dichloromethane
dd	doublet of doublets
ddd	doublet of doublet of doublets
DEPT	distortionless enhancement by polarization transfer

DFT	density functional theory
DIBAL-H	diisobutylaluminum hydride
DMAP	4-dimethylaminopyridine
DMF	N,N-dimethylformamide
DMS	dimethyl sulfide
DMSO	dimethyl sulfoxide
DOS	diversity-oriented synthesis
d.r.	diastereomeric ratio
dt	doublet of triplets
EC <sub>50</sub>	half maximal effective concentration
<i>E. coli</i>	<i>Escherichia coli</i>
EDG	electron donating group
e.g.	for example
eq	equivalents
ESI	electrospray ionization
Et	ethyl
EtOAc	ethyl acetate
etc	et cetera
EWG	electron withdrawing group
FDA	United States Food and Drug Administration
F <sub>sp<sup>3</sup></sub>	fraction of sp <sup>3</sup> hybridized centers in a molecule
g	grams
G-II	second-generation Grubbs catalyst
hr	hours
h	human
H <sup>+</sup>	acid
HBA	hydrogen-bond acceptor
HBD	hydrogen-bond donor
HEK	Human embryonic kidney
hERG	human <i>ether-à-go-go</i> -related gene
HG-II	second-generation Hoveyda–Grubbs catalyst
HMBC	heteronuclear multiple bond correlation
HMPA	hexamethylphosphoramide
HSQC	heteronuclear single quantum coherence
HTS	high throughput screening
<i>hν</i>	light
HRMS	high resolution mass spectrometry
Hz	Hertz, s <sup>-1</sup>
<i>i</i>	iso
IC <sub>50</sub>	half maximal inhibitory concentration
IFN	interferon
i.e.	that is
IL	interleukin
Imid	imidazole

iPr	isopropyl
IR	infrared
J	coupling constant
$k_{\text{cat}}$	catalytic rate constant
kDa	kiloDalton
$K_i$	inhibition rate constant
<i>K. pneumoniae</i>	<i>Klebsiella pneumoniae</i>
L	liter
LC	liquid chromatography
Leu	leucine
LDA	lithium diisopropylamide
LiHMDS	lithium hexamethyldisilazide
lit.	literature
LLAMA	Lead Likeness And Molecular Analysis
logP	logarithm of the partition coefficient
M	molar
m	multiplet
<i>m</i>	meta
m/z	mass to charge ratio
$M^+$	molecular ion
<i>m</i> CPBA	<i>meta</i> -chloroperbenzoic acid
MDCK	Madin-Darby Canine Kidney
MDR1	multi-drug resistance-1 gene
Me	methyl
MeCN	acetonitrile
MeOH	methanol
mg	milligrams
MHz	megaHertz
MIC <sub>90</sub>	minimum concentration required to inhibition growth of 90% of observed organisms
mp	melting point
min	minutes
mL	milliliters
mmol	millimoles
mol	moles
M	molar
mM	millimolar
MNA	<i>N</i> -methylnicotinamide
MRSA	methicillin-resistant <i>S. aureus</i>
MS	mass spectrometry
<i>M. tuberculosis</i>	<i>Mycobacterium tuberculosis</i>
MW	molecular Weight
<i>n</i>	straight chain
N/A	not applicable

NaBH <sub>4</sub>	sodium borohydride
NADH	nicotinamide adenine dinucleotide
NaHCO <sub>3</sub>	sodium bicarbonate
NaH	sodium hydride
NaOH	sodium hydroxide
NBS	N-bromosuccinimide
NCE	new chemical entity
n.d.	not determined
NEt <sub>3</sub>	triethylamine
NH <sub>4</sub> OH	ammonium hydroxide
nM	nanomolar
NMO	N-methylmorpholine oxide
NMR	nuclear magnetic resonance
NNMT	<i>nicotinamide N</i> -methyltransferase
No	number
nOe	nuclear Overhauser effect
NOESY	nuclear Overhauser enhanced spectroscopy
Nu	nucleophile
<i>o</i>	ortho
OAc	acetate
ox.	oxidation
[O]	an oxidative step
<i>p</i>	<i>para</i>
<i>P. aeruginosa</i>	<i>Pseudomonas aeruginosa</i>
P <sub>app</sub>	apparent permeability
pg.	page
PCC	pyridinium chlorochromate
PDB	Protein Data Bank
Pd(OAc) <sub>2</sub>	Palladium(II) acetate
PG	protecting group
Ph	phenyl
pH	potential hydrogen
PMI	principle moment of inertia
PPI	protein-protein interaction
ppm	parts per million
PPTS	pyridinium <i>p</i> -toluenesulfonate
pyr	pyridine
R	generalized substituent
R&D	research and development
Rh <sub>2</sub> (OAc) <sub>4</sub>	tetrakis(acetato)di-rhodium(II)
Rh <sub>2</sub> (oct) <sub>4</sub>	tetrakis(octanoato)di-rhodium(II)
RotB	rotatable bonds
RT	room temperature
rxn	reaction

s	singlet
<i>S. aureus</i>	<i>Staphylococcus aureus</i>
Ser	serine
SAH	S-adenosyl homocysteine
SAM	S-adenosyl methionine
SAR	structure activity relationship
S <sub>N</sub> Ar	nucleophilic aromatic substitution
S <sub>N</sub> 2	bimolecular nucleophilic substitution
SPS	solvent purification system
t	triplet
td	triplet of doublets
temp	temperature
<i>t</i> or <i>tert</i>	tertiary
TBAB	tetrabutylammonium bromide
TBAF	tetra-butylammonium fluoride
TBDPS	<i>tert</i> -butyldiphenylsilyl
TBS	<i>tert</i> -butyldimethylsilyl
<i>t</i> -BuOK	potassium <i>tert</i> -butoxide
Tf	trifluoromethanesulfonyl
THF	tetrahydrofuran
Thr	threonine
TLC	thin layer chromatography
TMS	trimethylsilyl
TNF	tumour necrotic factor
tol	<i>para</i> -methylphenyl
tPSA	topological polar surface area
TS	transition state
Tyr	tyrosine
UV	ultraviolet
Val	valine
vs	versus
<sup>1</sup> H	proton
<sup>13</sup> C	carbon-13
9-BBN	9-borabicyclo(3.3.1)nonane
α	alpha
β	beta
γ	gamma
δ	chemical shift
Δ	reflux
Å	angstroms
μL	microliters
μM	micromolar
~	approximately

## Acknowledgments

I would like to thank my supervisor Dr. Jeremy E. Wulff for never giving up on me throughout these two years. His dedication and drive towards progressing the field of synthetic organic chemistry serves as a role model for me. The one thing he influenced me the most is the paradigm of a good presentation augments the quality of science.

I would also extend my thanks of present and past members of the Wulff lab: Jun Chen, Ronan Hanley, Tong Li, Jon Sader, Derek Blevins, Cameron Zheng, Ivica Bratanovic, Lingxiao Lu, Asiyah Robinson, Katherine Krause, Hannah Shumka, Nathan Dao, James Saville, Jacob Davis, Kossivi Denanyoh, Michael Gignac, Rebecca Hof, Tyler Cuthbert, Chang Liu, Chakri Simhadri, Mathieu Lepage. Their presence makes this journey of mine more bearable, especially during difficult moments when one is engulfed by despair and hopelessness.

Appreciative thoughts are directed towards my thesis committee member Dr. Fraser A. Hof, who has provided me objective and constructive criticism. Many thanks towards the supportive staff members are warranted in my mind: Rosemary Pulez, Lori Aasebo, Penny Gordon, Sandra Carson, Sandra Baskett for their administrative support; Chris Barr, Dr. Ori Granot, Dr. Tyler Trefz, Andrew Macdonald, Mark Evans, Sean Adams for support in my research; Monica Reimer, Corrina Ewan, Dr. Peter Marrs, Kelli Fawkes for guiding me on how to become a better teacher.

The highly collaborative nature of this project would not have been able to proceed if not for the following: Lindsay Frehlick for ensuring that we stay out of legal troubles, Niclas Nilsson as liason between our lab and LEO Pharma.

Last but not least, I would like to thank my family and Meggy Li for their eternal emotional support. They are the reason why I am who I am and allows me to continuously improve and excel. They are always concerned about my wellbeing, although I may not fully express my reciprocated feelings and thoughts. I have nothing to repay but all my love.

## Chapter 1 - Introduction

### Chapter 1.1 Modern Evolution of Medicinal Chemistry.

Drug discovery is a complex and dynamic process where many strategies and ideas are developed in the pharmaceutical industry with the aim to improve human health. One of the most common strategies in medicinal chemistry<sup>1</sup> is oriented around prior understanding of the biological target of interest: its role in a given disease should be clearly validated in order to affirm its therapeutic value. Once an assay system has been developed, automated high-throughput screening of compound libraries can be performed in order to identify candidates with a good target affinity.<sup>2</sup> Once a favorable ligand is determined, rational optimization via chemical structure alteration will be performed to enhance target selectivity as well as to improve pharmacokinetic and pharmacodynamic properties.<sup>3</sup> Structure-activity relationships (SAR) can be derived as one performs data analysis to determine any correlation between changes of the chemical structure and variation in biological effects.<sup>4</sup> As a result, many chemical compounds are designed, built, and tested to derive a fundamental understanding of how the ligand works in the physiological environment, with the assistance of computer modelling and crystallographic data.

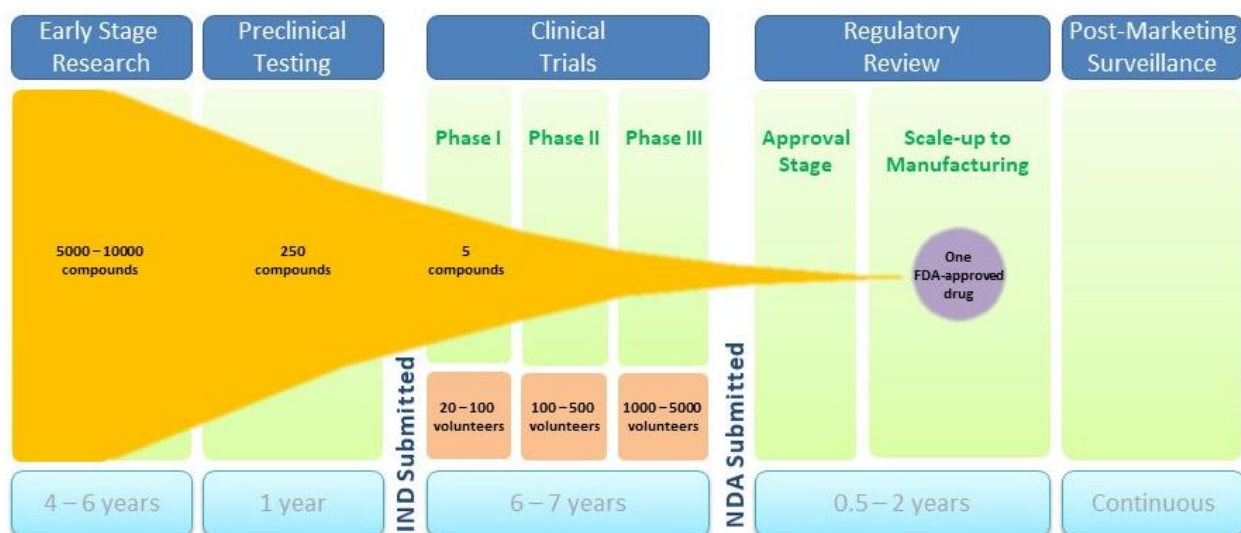


Figure 1. Simple Overview of Drug Development Timeline After Lead Identification.<sup>5</sup>

However, this approach requires huge investment in resources, manpower, and time<sup>6</sup> towards analogue chemical synthesis. Even then, depending on project difficulty, one may expect at least two to three years<sup>7</sup> of high-risk development in early-stage drug discovery. Figure 1 illustrates that on average, the time required for development of one market-approved drug requires between 12 to 16 years, with a minimum of 5000 to 10000 compounds required for early-stage screening after a suitable lead candidate has been identified. Realistically, there are many diseases for which we currently lack a full understanding of the underlying biology; as a result, one can expect an even higher barrier of entry to find a cure. To mitigate any obstacles that may arise from chemical synthesis, researchers tend to favor chemical reactions that are highly robust, provide good chemoselectivity and reactivity, offer high reproducibility, and are widely tolerant of functional groups.<sup>8</sup> These reactions include transition metal-catalyzed aryl-aryl cross-coupling reactions,<sup>9</sup> amide bond formations,<sup>10</sup> reductive aminations,<sup>11</sup> olefin metathesis,<sup>12</sup> and alkene hydrogenations.<sup>13</sup> As illustrated in Figure 2, most of the chemical reactions employed by medicinal chemists result in no change in hybridization, which leads to little or no change in overall molecular shape. Because the precursors in these coupling reactions tend to be  $sp^2$ -hybridized planar molecules, the resulting coupled products generally exhibit little deviation from planarity, barring the formation of atropisomers. An example would a typical Suzuki-Miyaura coupling reaction, in which a  $sp^2$ -hybridized organohalide reacts with a  $sp^2$ -hybridized boronic acid, resulting in formation of a  $C_{sp^2}-C_{sp^2}$  bond. These biases have a huge impact on the overall three-dimensional shape of drug candidates.<sup>14</sup>

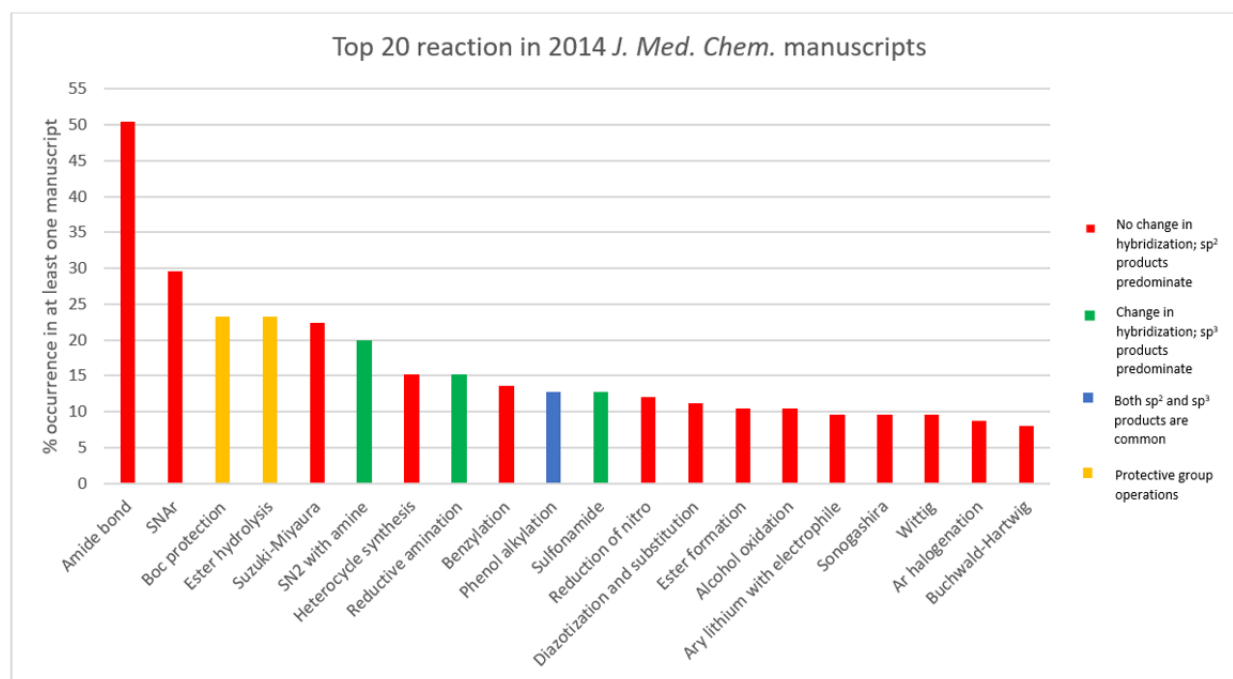


Figure 2. Some of the most frequently used chemical reactions employed by medicinal chemists in recent years.<sup>14c</sup> Chemical reactions highlighted in red do not change overall molecular shape.

For drug discovery campaigns where little to no information about the biological target(s) are provided, shape variation should be an important criterion to consider. If a given molecular shape does not interact favorably with any surface of biological target Y, then a library of molecules that have very similar 3D shapes will end up performing similarly, and generate little to no activity. Researchers may interpret these data incorrectly and term the biological target “undruggable”. In recent years, the community of medicinal chemists have gradually become more aware of how the three-dimensionality of synthesized molecules can be of importance in bestowing desired biological consequences.<sup>15</sup> Molecular shapes can be quantified using principal moments of inertia plots: this is done by normalizing Cartesian coordinate systems into a two-dimensional graph<sup>16</sup> containing an isosceles triangle, where each edge corresponds to various archetype shapes: linear (or sometimes referred to as rods), sphere, and disks.<sup>17</sup> Each molecule is represented as one coloured data point within the triangle. For molecules with a high proportion of sp<sup>2</sup>-hybridized carbons, one can envision distribution of data points near the edges indicating linear or disc shapes. Indeed,

Brown and coworkers have illustrated that as one surveys the ChEMBL database,<sup>18</sup> underpopulation of certain regions of medicinal chemical space can be identified, as shown in Figure 3.

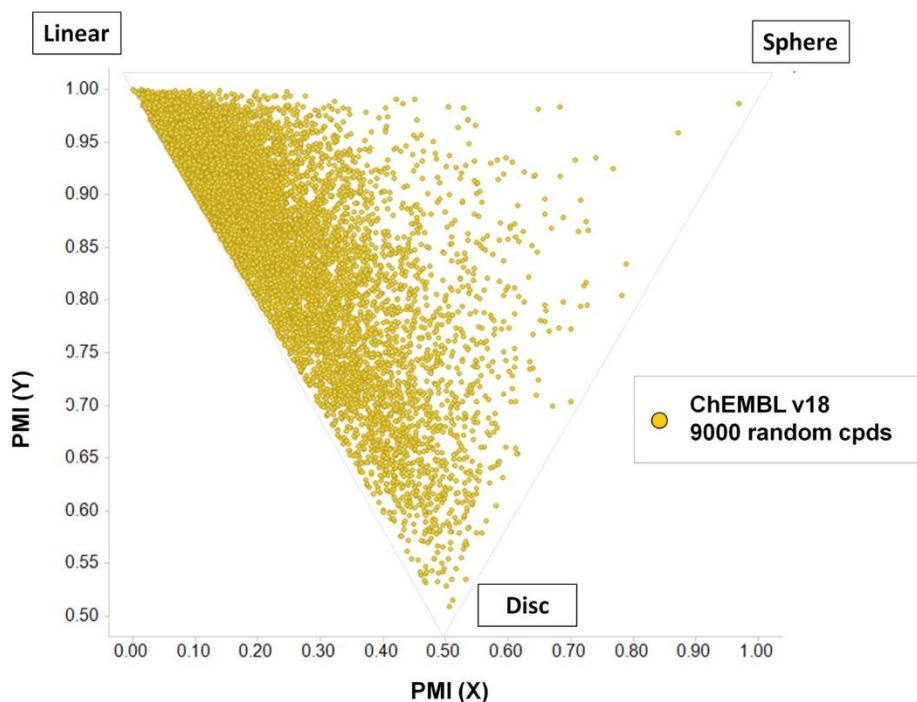


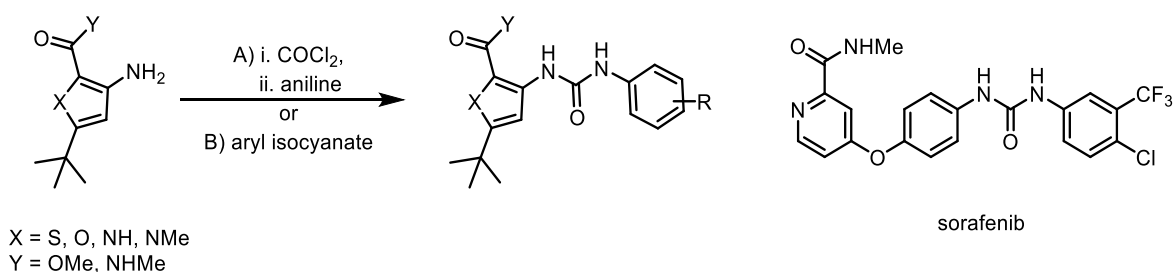
Figure 3. Principal moments of inertia (PMI) plot constructed from a proportion of compounds in ChEMBL space. Reproduced with permission.<sup>18</sup>

Biological interaction is reliant on chemical interaction on a three-dimensional scale; a molecule of more diverse and broader three-dimensional shape will occupy a greater amount of volume, thus leading to an increase in contact area overlap between two surfaces. This geometric change translates to higher chance of surface recognition between a small molecule and the biological enzyme of interest.<sup>19</sup> Highly planar drug candidates tend to have lower target selectivity,<sup>20</sup> leading to undesirable biological effects.<sup>21</sup> This mandates a new paradigm in drug discovery with an emphasis on crafting  $sp^3$ -rich compounds for medicinal chemistry applications.

Since the early 1960s, a new trend gradually emerged, in which commercially available chemical building blocks can be quickly assembled via simple chemical reactions.<sup>22</sup> The impact of this concept can lead to rapid expansion of chemical collections with various molecular sizes using a single chemical process. This new

ideology was coined combinatorial chemistry, and technologies emerged to support the rapid synthesis of compound libraries with minimal purification.<sup>23</sup> The grandeur of this idea was substantiated by many new discoveries, and it was once hailed by the pharmaceutical industry as the next revolution in drug research and discovery.<sup>24</sup>

One of the best examples of the power of combinatorial synthesis in medicinal chemistry is the discovery of the potent anticancer compound sorafenib.<sup>25</sup> During the early 2000s, Bayer was in collaboration with Onyx Pharmaceuticals to discover novel therapeutics aimed at the Ras/Raf/MEK/ERK kinases.<sup>26</sup> An initial biochemical screen of 200,000 compounds was performed to identify a project lead.<sup>27</sup> Afterwards, structure–activity evaluation was performed mainly via amino-isocyanate coupling (see scheme 1) using a robotic rapid parallel synthesizer. An additional 1,000 analogues were created for further testing in a cellular screening platform, which was used to evaluate Raf1 kinase inhibitory activity.<sup>28</sup> After several rounds of analogue synthesis by combinatorial chemistry to improve potency, a victor labelled BAY 43-9006 emerged. This drug candidate was later given the name sorafenib, and eventually went into widespread clinical use for the treatment of advanced renal cell carcinoma and hepatocellular carcinoma.<sup>29</sup>



*Scheme 1. An overall reaction scheme of how sorafenib was discovered.*

Since this time, however, the rate of successful discovery has rapidly dropped.<sup>30</sup> Data analysis revealed that this could be attributed to limited chemical space that can be encompassed by a single chemical reaction.<sup>31</sup> To make matters worse, Schmidt has suggested that combinatorial chemistry suffers from the same drawbacks, arguably more so, of traditional medicinal chemistry discovery: the low proportion of sp<sup>3</sup>-hybridized carbons and stereogenic centers.<sup>32</sup> Indeed, using limited templates to build a large collection of chemical compounds without providing for any changes in three-

dimensionality will result in little to no variation in structural topology, depending on the coupling building blocks. This is not to say, of course, that  $sp^2$ -rich compounds cannot be successful drugs. The majority of successful kinase inhibitors are comprised principally of  $sp^2$ -centres, and members of this family (e.g. imatinib, pazopanib, regorafenib, sorafenib, etc.) have proven to be phenomenally successful at treating a wide range of diseases. However, this is to some extent a “special case” (albeit an economically significant one!) since these molecules occupy a pocket that has evolved to bind the  $sp^2$ -rich adenine base within ATP. Biology in general exhibits substantially greater three-dimensionality than is found within the structure of ATP; it therefore stands to reason that molecules with less planar structures may be useful in targeting a broader selection of disease-specific targets.

Many critics have argued that the most successful examples of drug discovery arise from sufficient fundamental understanding of the biological target, including its structural information.<sup>33</sup> Rapid synthesis of a large collection of chemical structures without understanding how the template itself can interact with the biological target is meaningless: if the template does not orientate the substituents favorably for bioactivity, the whole collection will be rendered useless as no bioactive compounds can be discovered. Significant resources and time are committed for purification and characterization, which often exceeds initial expectation. Minimal SAR data will be generated despite the number of compounds made. All in all, the usage of solely combinatorial chemistry to develop drug candidates without proper guidance was doomed to fail. Despite the limited utility of combinatorial chemistry in early stage drug discovery,<sup>34</sup> one can argue that if a hit candidate is identified, small pools of chemical analogues can be assembled in a timely fashion using various chemical building blocks. Consequently, hit-to-lead optimization can proceed within a reasonable timeframe. Thus, the usage of combinatorial chemistry has remained as a powerful tool in advancing innovation within medicinal chemistry.<sup>35</sup>

In combinatorial chemistry, the diversity of molecular shapes is highly dependent on the type of building blocks and scaffolds, resulting in structurally similar chemical libraries. One can argue that with some exceptions, compounds with high structural similarity exhibit similar biological profiles, thus limiting the progress for searching novel

biological targets.<sup>36</sup> Instead, Schreiber and co-workers propose that if one were to design molecule libraries with an emphasis of broad structural diversity and molecular complexity, then larger chemical space can be occupied, thereby allowing rapid interrogation with a wide range of cellular targets, thus leading to higher probabilities of identifying novel lead compound.<sup>37</sup> Many biological applications have followed through using this concept, which is given the name diversity-orientated synthesis (DOS), spanning from usage in fragment-based drug discovery,<sup>38</sup> to the development of small molecular probes that helped elucidate novel biological pathways.<sup>39</sup> To help understand how to achieve the syntheses of small molecules with structurally unique architecture more efficiently, Nielson and Schreiber developed a rational guideline for systemically designing:<sup>40</sup>

- Build: Chemical building blocks with predefined stereochemistry are assembled using organic synthesis.
- Couple: Intermolecular coupling is carried out with different reagents and pre-synthesized building blocks in order to generate densely functionalized molecules.
- Pair: Based on analysis of all functional group present, pairing allows intramolecular coupling to occur. Different ring formation can arise from different combination of functional group pairing, thereby leading to diverse formation of skeletal frameworks.

An informative representation for these criteria is shown in Figure 4. During the building phase, chiral building blocks can be obtained either by enantio- and diastereoselective reactions or from natural origins (“chiral pool”).<sup>41</sup> The design of building blocks should allow for functional groups required during the coupling phase and pairing phase to be embedded, thus allowing for subsequent stereochemical diversity through mix-and-match.<sup>42</sup> Ideally, all stereoisomeric elements should be controlled during the coupling phase to allow the fully dense array of functional groups to remain intact during the subsequent pairing phase. Additionally, broader occupation of three-dimensional space can occur during the coupling phase, depending on building blocks of varying molecular weight and size. Consequently, an increase in molecular size translates to greater volume of occupation, which also leads to an increase in

interacting surface area between the synthesized molecule and any cellular proteins; thus one would expect greater perturbation of cellular function. Finally, identification of suitable functional group pairs can allow for highly diverse skeletal outcome. By capitalizing different functional group interaction amongst transition metals,<sup>43</sup> or pre-designed cyclization and pericyclic reactions,<sup>44</sup> compounds of uniquely different molecular frameworks and various ring sizes, which is an important attribute to the overall skeletal diversity within a screening collection, can be generated. Topological differences amongst chemical matters allow for different interaction, thereby leading to changes in binding selectivity amongst protein surfaces. Thus, divergent outcomes can arise from a common scaffold of systematic design, allowing for a diverse number of binding events to occur.

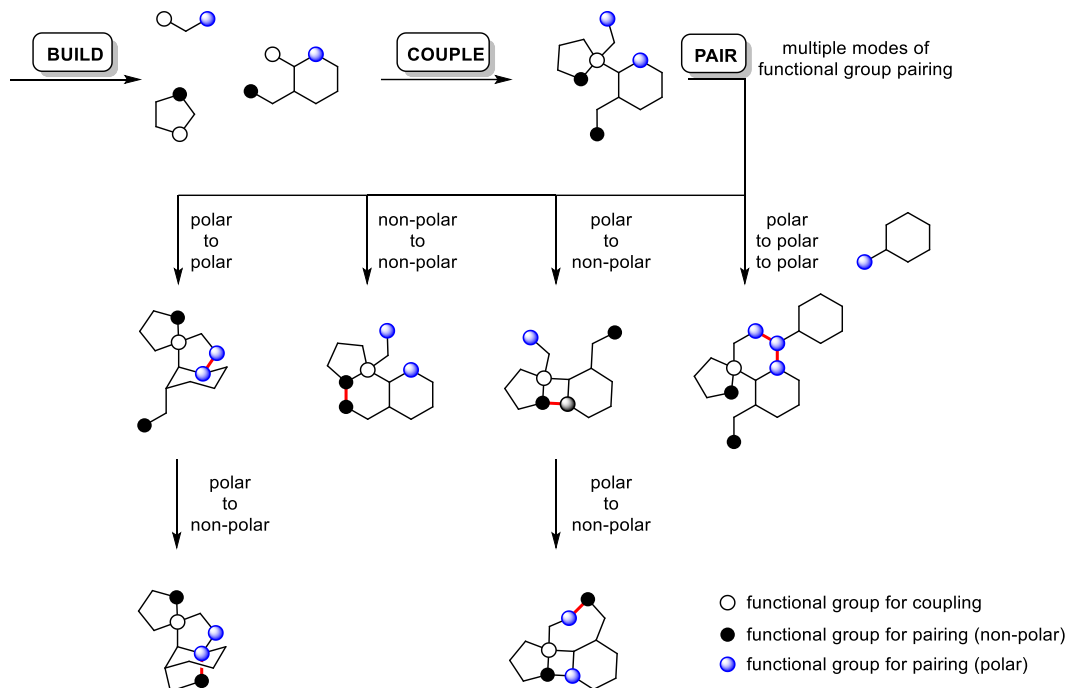
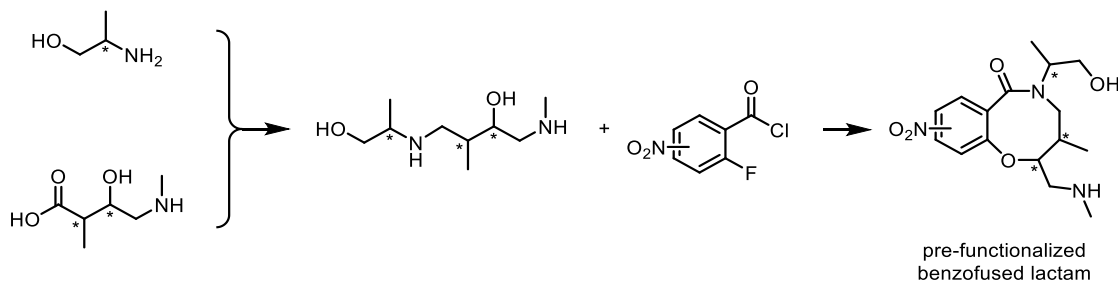


*Figure 4. An illustrative diagram to demonstrate how DOS results in skeletally comprehensive structures through functional group pairing.*

Over the past two decades, many research labs have adopted this strategy and have seen some success,<sup>45</sup> which have helped to identify new therapeutic targets and biological mechanisms of action,<sup>46</sup> as well as small molecule drug candidates capable of modulating the functions of these new targets.<sup>47</sup> For example, the central motif of 8-membered benzo-fused lactams can be generated via the build-couple-pair strategy

using readily synthesized amino alcohols, amino acids, and aryl acid halides, as shown in scheme 2.



*Scheme 2. An example of how DOS provides stereochemically different molecules.*

The convergent strategy to combine all linear building blocks allows rapid synthesis of the core macrocycle. Further investigation of all stereoisomers, as well as different appendage partners led to the identification of different bioactivity, with selected examples shown in Figure 5.<sup>48</sup>

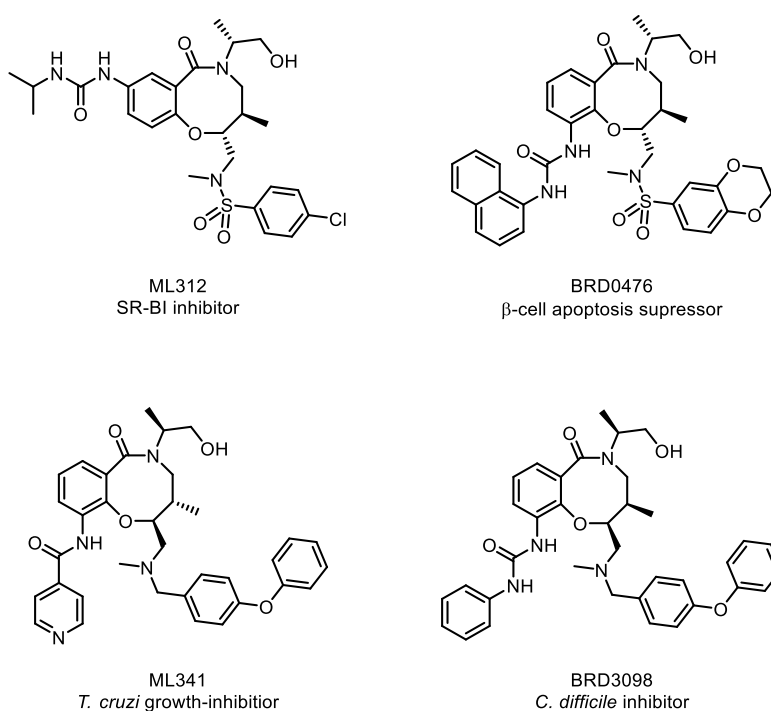


*Figure 5. List of benzofused lactams from DOS and their respective biological applications.*

## Chapter 1.2 Predictors and Strategies in Drug Design.

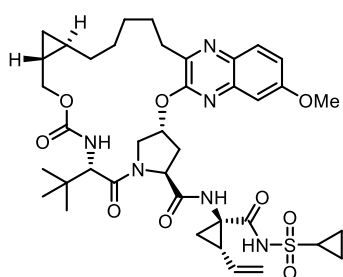
In the 1990s, Lipinski and coworkers published a landmark article that highlighted important parameters and changed the way people analyze drug candidates.<sup>49</sup> Using data from the World Drug Index, Lipinski and coworkers analyzed physicochemical

properties of all marketed drugs dating back to 1964 in order to determine parameters for identifying good cellular permeability. They discovered common trends which were later termed “the rule of five” – for any orally administered drug molecules that are not substrates for biological transporters:

- The molecular weight should not exceed 500 Da
- The number of hydrogen-bond donors should not exceed 5
- The number of hydrogen-bond acceptors should be less than 10
- The partition coefficient between octanol and water should not exceed 5.

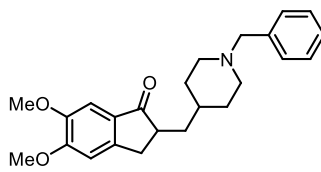
These criteria helped shape the mindset of the medicinal chemistry community, as many researchers viewed Lipinski’s rule of five as important guidelines for predicting if a molecule has the desired physicochemical properties for use as a drug.

Nonetheless, many exceptions to these rules are known,<sup>50</sup> and one should be careful to avoid an over-reliance on Lipinski’s guidelines. Figure 6 represents an informative comparison between three marketed drugs. Grazoprevir is an orally-administered drug approved for the treatment for hepatitis C.<sup>51</sup> However, its physicochemical properties clearly do not abide by all of Lipinski’s rule of five, as highlighted in red. On the other hand, donepezil and imatinib are orally-administered drugs that both abide by Lipinski’s rule of five. However, the former is ineffective for stopping progression of patients in Alzheimer’s disease,<sup>52</sup> whereas the latter is a blockbuster success in treating different types of cancer.<sup>53</sup>



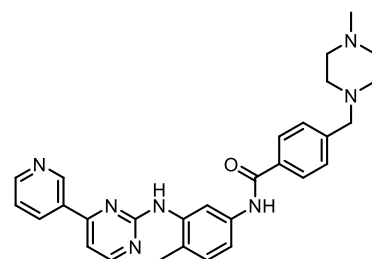
Grazoprevir

MW (g/mol)	766.903
PSA (Å)	205.69
log P	5.41
HBD	3
HBA	14



Donepezil

MW (g/mol)	379.492
PSA (Å)	38.77
log P	3.6
HBD	0
HBA	4



Imatinib

MW (g/mol)	493.6027
PSA (Å)	86.28
log P	3.0
HBD	2
HBA	8

*Figure 6. Comparison of molecular descriptors between three approved and marketed drugs. Criteria that violate Lipinski's rule of five are highlighted in red.* <sup>54</sup>

Many newly developed drug discovery programs have been heavily influenced by these criteria during the search for compounds that exhibit high “druglikeness”. An ideal druglike molecule would have the following properties:

- Soluble in both aqueous and organic phases.
  - The logarithm of partition coefficient in octanol and water, known as LogP, is a common measure of a molecule's solubility.
- High potency toward the desired biological target.
  - This is usually expressed as IC<sub>50</sub>, the maximum concentration at which half of the target population undergoes inhibition of function.
- Low molecular weight
  - Smaller molecular size leads to higher rate of cellular diffusion.

Variants based on Lipinski's rule of five later emerged to improve the prediction of molecular physicochemical properties of a drug candidate.<sup>55</sup> Veber and coworkers proposed that the molecular weight cutoff was highly arbitrary, and the following predictions are more suited to predict good oral bioavailability:<sup>56</sup>

- Number of rotatable bonds should be 10 or fewer
- Polar surface area should not exceed 140 Å<sup>2</sup>. The definition of polar surface area is the sum of all surface areas for all polar heteroatoms (usually oxygen or nitrogen) in a molecule.<sup>57</sup>

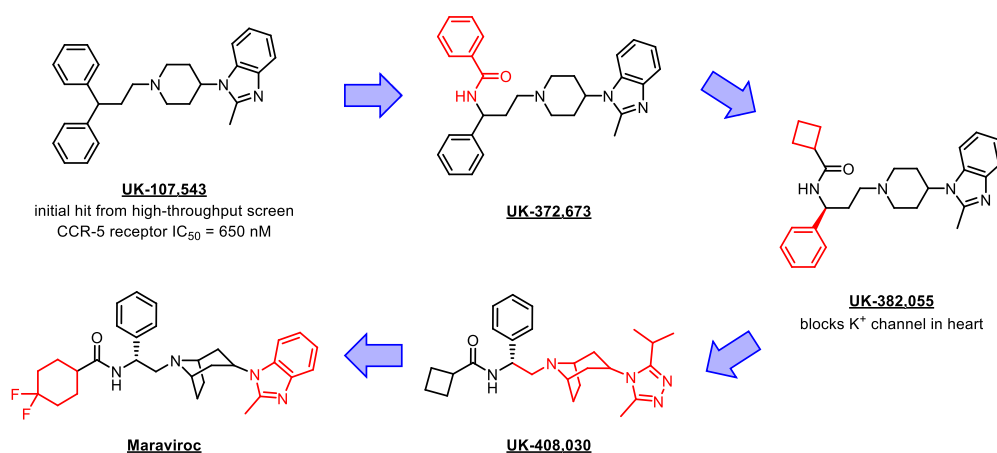
More recently, Lovering and coworkers have attempted to use identifiable molecular properties to address the importance of molecular complexity towards the community of medicinal chemists.<sup>58</sup> As discussed before, molecular architecture is important when considering any spatial interaction between ligand and biological target of interest. They proposed that the following parameters can be used to address this problem:

- F<sub>sp<sup>3</sup></sub>: fraction of sp<sup>3</sup>-hybridized carbons within a molecule of interest.
- Number of chiral centers in the molecule of interest.

Their analysis of the GVK BIO database identified that during transition from lead identification to drug candidate optimization, an increasing trend of saturated carbon counts can be observed. Combined with previous physicochemical filters, an active

approach to addressing pharmacological effects during drug design has been applied to the development of discovering new drug candidates.<sup>59</sup>

The development of maraviroc provides an illustrative case study.<sup>60</sup> Initial high-throughput screening (HTS) from Pfizer for an antagonist of the CCR5 receptor, which is expressed on the surface of leukocytes and is involved in HIV virion entry into human cells, yielded UK-107,543.<sup>61</sup> The molecule had weak affinity, but after some structural optimization, an increase in potency was observed for the structural analogue UK-382,005.<sup>62</sup> However, an inherent problem was that the inhibitor was also active towards CYP2D6, a metabolic enzyme expressed primarily in hepatocytes and the central nervous system.<sup>63</sup> This spelled trouble for the campaign, and during their venture towards minimizing CYP2D6 toxicity, they discovered that the solution was to replace the aminopiperidine moiety into a more structurally rigid tropane skeleton.<sup>64</sup> The resultant UK-408,300 had excellent binding affinity and antiviral activity yet exhibited no CYP2D6 activity. Further structural changes were necessary to mitigate inhibition of the hERG ion channel and to improve metabolic stability, ultimately leading to the emergence of maraviroc.<sup>65</sup> Due to its well-tolerated safety profile and remarkable potency to reduce at least 80% of viral load in a 48 week Phase II daily-dose trial over 48 weeks, maraviroc received approval from the FDA for marketing within 4 months of application review.<sup>66</sup>

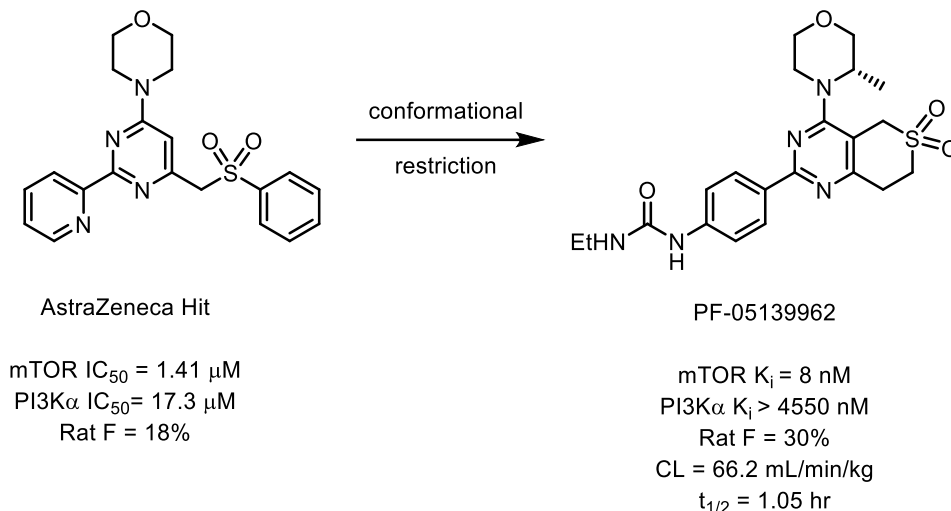


*Scheme 3. The evolution of maraviroc from hit-to-lead optimization until drug approval, with selected examples from the discovery campaign shown. Structural changes are highlighted in red.*

To achieve the desired physicochemical properties, appropriately positioned functional groups are necessary and can be accomplished by careful consideration of

synthetic planning. One such strategy is termed rigidification, or conformational restriction.<sup>67</sup> Complementary to the induced fit model proposed by Daniel Koshland,<sup>68</sup> ligands that are conformationally flexible may adopt different three-dimensional shapes, some of which will be energetically unfavorable during drug-protein interaction.<sup>69</sup> However, there exists some geometrical adjustments where the binding interactions between a ligand and its target are optimally maximized. Note that high degrees of conformational flexibility can induce ligand binding to other undesired biomolecules, leading to undesirable phenotypical responses. Therefore, if the ligand adopts a geometrically restricted conformation, and the three-dimensional shape of such matches with how it binds to the desired target, one can theoretically expect that only one binding event will occur between the ligand and the desired target, even amongst an environment swarmed with other proteins. Thus, by lowering the amount of rotatable bonds and restricting conformational variability, off target binding can be lowered,<sup>70</sup> thereby leading to an improved pharmacokinetic profile during lead optimization.

A model demonstrating the benefits of conformational restriction is shown below. AstraZeneca reported a hit candidate based on an inhibition assay for the enzyme mammalian target of rapamycin (mTOR).<sup>71</sup> Due to the enzyme being involved in regulating cell proliferation and survival,<sup>72</sup> many companies sought to target the enzyme as an alternative therapeutic for inhibiting tumour growth.<sup>73</sup> After much optimization and learning from their failure, researchers from Pfizer reported a strategy based on conformational restriction,<sup>74</sup> leading to drastic improvement in both bioavailability and selective inhibition of mTOR over PI3K $\alpha$ , a kinase that also participates in cellular signaling to equilibrate cellular growth.<sup>75</sup>



*Scheme 4. An example of conformational restriction leading to improved biological properties.*

### Chapter 1.3 Academic-Industrial Collaboration in Drug Discovery.

If one were to evaluate the number of new molecular entities (NMEs) approved by the Food and Drug Administration (FDA) throughout the past decades, one can observe a trend of stagnating output by evaluating the number of NMEs approved on an annual basis.<sup>76</sup> Considering the rapid growth of new biotechnological advances, one would expect the productivity to be higher instead due to more efficient tools to understand human biology and discover novel targets. Without a doubt, there is a significant productivity gap in research-and-development (R&D), between what was anticipated and what is currently delivered. Experts have concluded that many variables contribute to the lower rate of innovation in for-profit pharmaceuticals, including explosive growth of low-cost generics, escalating research and development (R&D) costs, as well as “low-hanging fruits” – biological targets with an in-depth fundamental understanding that are easily translatable to clinical success – being slowly reached and thus saturating the market.<sup>77</sup> To make matters worse, therapeutic targets are often chosen due to their marketability, instead of a full understanding of their biology, ultimately leading to late discovery of unattractive pharmacological properties. The cost of failure in drug discovery is enormous, as an FDA-approved drug comes with a hefty price of between 0.8 to 1.3 billion dollars.<sup>78</sup> On top of that, patent expiration of blockbuster drugs that was discovered by conglomerate pharmaceutical companies in the past two decades will face sharp decline in revenue sales primarily from generic

competition.<sup>79</sup> Coupled with rising costs in R&D investment within the pharmaceutical industry, the current economic model of drug discovery is unsustainable if the issue of low productivity in pipeline discovery is not dealt with.

Due to fiduciary responsibilities to shareholders and employees, many pharmaceutical companies are conservative and in favor of approaches that are low-risk yet yield moderate-to-high rewards. One most common decision is to develop “me-too” drugs – pharmaceutical products that are chemically related or structurally similar to other known drugs.<sup>80</sup> This strategy may allow one to recuperate heavy loss in R&D investment from other failed programs but diminishes any pioneering incentives for innovation in the grand scheme of things.<sup>81</sup> Other methods aimed at circumventing productivity issues include acquisitions of promising biotechnology start-ups, or liquidating assets that may result in higher R&D cost and time.<sup>82</sup> However, these business models only solve issues on a short-term basis and cannot be sustained forever. Coupled with the looming threat of antibiotic resistance,<sup>83</sup> therapy-resistant viral mutations,<sup>84</sup> and chemotherapy-resistant oncology cases,<sup>85</sup> the need for discovering novel, druggable biological targets has never been greater.<sup>86</sup> Many have expressed the desire for novel chemical agents to function as probes to perturb and understand unknown biological pathways,<sup>87</sup> since less than 3% of the numerous illness that afflicts humanity can be managed by currently known treatments, while less than 0.5% of the entire human genome can be targeted by all known FDA-approved drugs.<sup>88</sup>

Recognizing this global threat as well as the resources required to accomplish these lofty goals, many collaborative programs have been established through a combination of academic excellence and industrial resources.<sup>89</sup> Academics have an edge towards basic research with regards to target identification and validation, whilst their industrial counterpart is experienced in developing highly adaptable and applicable technological platforms, such as high-throughput biomarker studies or large-scale informatics processing and management.<sup>90</sup> This new business model, coined by Henry Chesbrough as “open innovation”,<sup>91</sup> where collaborative and free exchange of information and ideas occur, has gradually seen more adaptations in the modern era.<sup>92</sup> Statistics have shown that in the last four decades, about 60% of all new FDA-approved small molecules drugs were discovered through research programs that were publicly

funded.<sup>93</sup> Open accessible platforms will be of immense use in many fields of life science.

A successful and ongoing example is the European Lead Factory.<sup>93</sup> It is an open innovation platform with the objective of combining innovative ideas in chemistry and biology to accelerate research in drug discovery. Sponsored by the Innovative Medicine Initiative, the public-private partnership attracts more than 150 researchers all over Europe, from 7 pharmaceutical companies, 10 small-to-medium-sized enterprises, and 13 academic institutions.<sup>94</sup> The multidisciplinary center boasts an industry-standard HTS infrastructure, and state-of-the-art information technology to support any ongoing campaigns. Currently a total of 83 successful HTS evaluations has results in more than 4500 hit compounds with definitive biological profiles.<sup>95</sup> A combination of more than 460,000 novel compounds, based on more than 220 novel chemical architecture, have been generated by both academic scholars and pharmaceutical partners.<sup>96</sup> To date, at least one spin-out enterprise has been established based on publicly accessible information from the European Lead Factory, and other funding agencies such as the Wellcome Trust are invested in further developing their hit portfolios into new medical therapies.<sup>97</sup>

#### **Chapter 1.4 Sulfonamides and Sulfones in Medicinal Chemistry.**

Sulfonamide-containing molecules were among the first commercial antibiotics in the history of drug discovery. Under the leadership of Gerhard Domagk, a research team experimented with hundred of molecules under the hypothesis that dyes may be preferentially harmful to microbial organisms instead of humans.<sup>98</sup> After years of unfruitful search, Prontosil emerged in the facilities of Bayer AG in 1932 as a synthetic molecule capable of suppressing bacterial infection in mice.<sup>99</sup> This work also earned Gerhard Domagk the 1939 Nobel Prize in Medicine.<sup>100</sup> Since then, sulfonamides have emerged as one of the most common functional groups in pharmaceuticals.<sup>101</sup> Often, the group serves as a suitable bioisostere for carboxylic acid moieties.<sup>102</sup> Due to being reliable substitutes for optimizing molecular physicochemical properties, sulfonamides are applied in a wide variety of therapeutic areas, including anticancer,<sup>103</sup> antiviral,<sup>104</sup> anti-inflammatory,<sup>105</sup> anti-epileptic,<sup>106</sup> and many others (Figure 7).

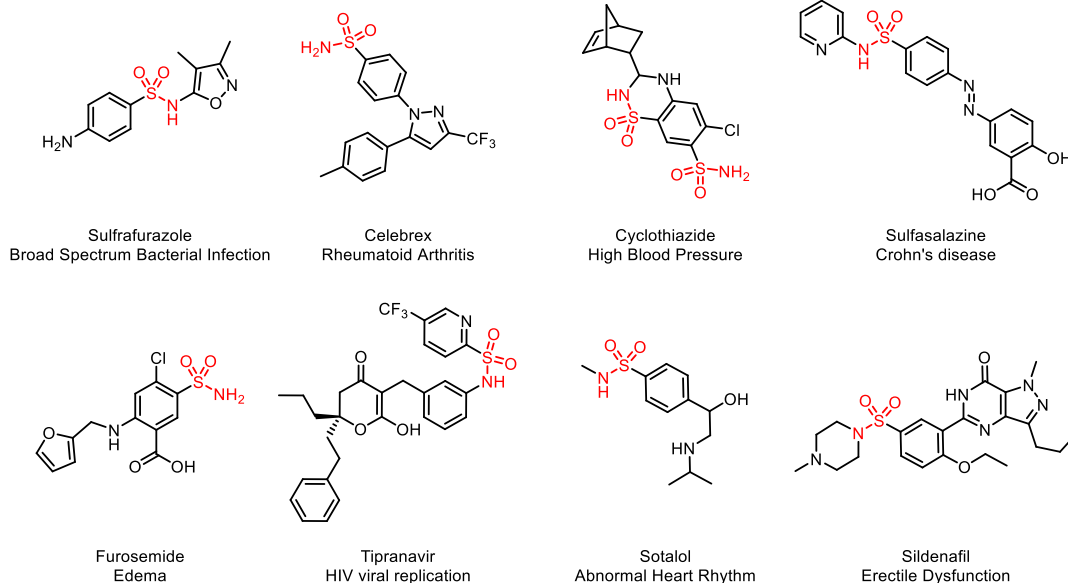
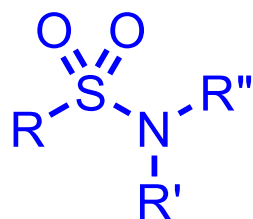
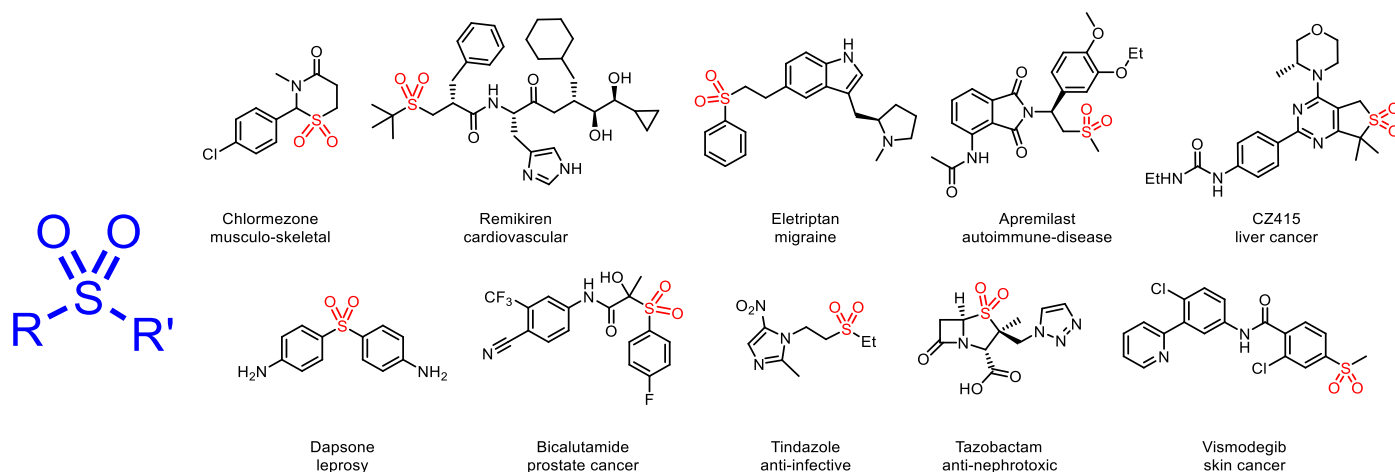


Figure 7. A list of representative sulfonamide-containing drugs that are currently approved or in development. Highlighted in blue is the general structure of a sulfonamide, where  $R$ ,  $R'$  and  $R''$  denotes any carbon-containing substituent.

Other sulfur-containing groups, such as thioethers, thiophenes, and sulfoxides, also appear in drugs or drug candidates. However, sulfones are unusual for their comparative absence among approved drug compounds or clinical candidates.

Sulfones are capable of both acting as hydrogen bond acceptors and interacting strongly with lipophilic regions.<sup>107</sup> This amphiphilic property is viewed favorably in the field of material sciences.<sup>108</sup> Beyond that, sulfone-containing molecules are also important in the commodity chemical industry: sulfolane is used as a privileged organic solvent, due to its thermal stability, and chemical robustness against highly corrosive acid-catalyzed reaction environments. The sulfone functional group in sulfolane allows for high solvating power towards cations, as well as introducing a high dipole moment and a high dielectric constant, compared to common polar aprotic solvents.<sup>109</sup>

The earliest example of a sulfone-containing drug that is FDA approved is chlormezanone, which is used for anxiety management and muscle relaxation.<sup>110</sup> Sulfones have also been used as ketone<sup>111</sup> and ether bioisosteres<sup>112</sup> in drug design.



*Figure 8. A list of all known sulfone-containing drugs that are currently approved or in development. Highlighted in blue is the general structure of a sulfone, where  $R$ , and  $R'$  denotes any carbon-containing substituent.*

However, if one were to evaluate all known sulfone-containing drugs (Figure 8), most of them contain at least one aryl substituent. Comparatively, the number of bis-alkyl sulfone-containing drugs appears to be underrepresented in the field of medicinal chemistry,<sup>113</sup> as only 1% of all FDA-approved-sulfur-containing drugs contain the bis-alkyl sulfone moiety, which is illustrated as the blue portion with the caption “Sulfones ( $sp^3-sp^3$ )” in Figure 9.<sup>114</sup> Such a low proportion amongst sulfur-containing drugs can be considered baffling, and yet we have not considered the fact that sulfur-absent drugs were omitted from this analysis! Furthermore, the inclusion of sulfones as part of the pharmacophore is relatively uncommon compared to other bioisosteres.<sup>115</sup> This phenomenon is puzzling as when considering the versatility of sulfones based on previous points, one would consider that incorporation of such an amazing functional group would be beneficial to early stage drug discovery and possibly during hit-to-lead optimization. And yet, reality has demonstrated that there is a sufficiently large gap in what should be expected and what is happening in real life. Nonetheless, this lack of practical usage represents a golden opportunity for one to explore any applications of sulfone-containing chemical matters in drug discovery.

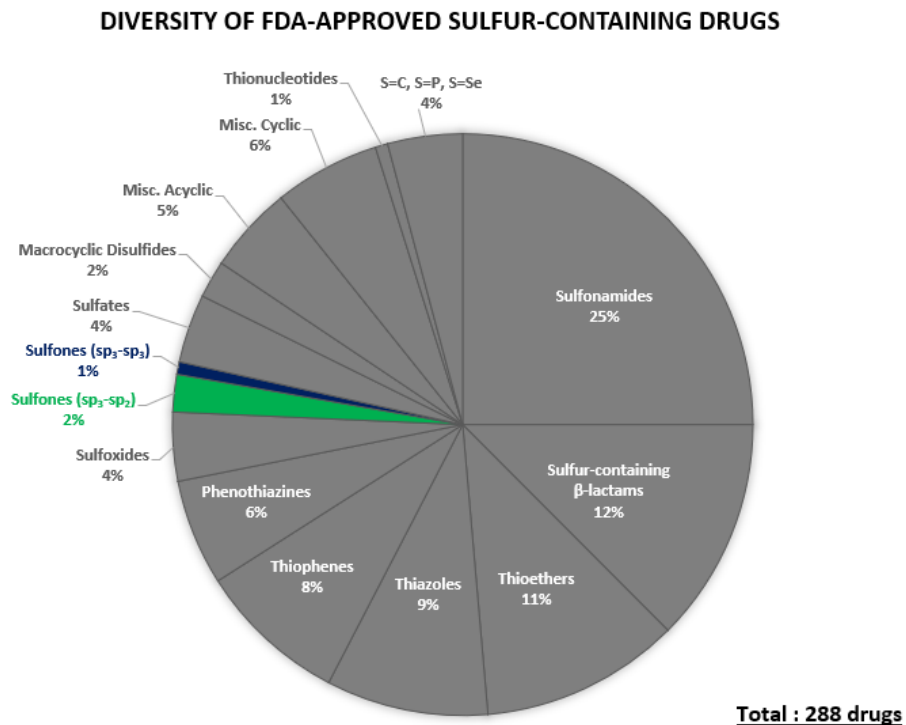
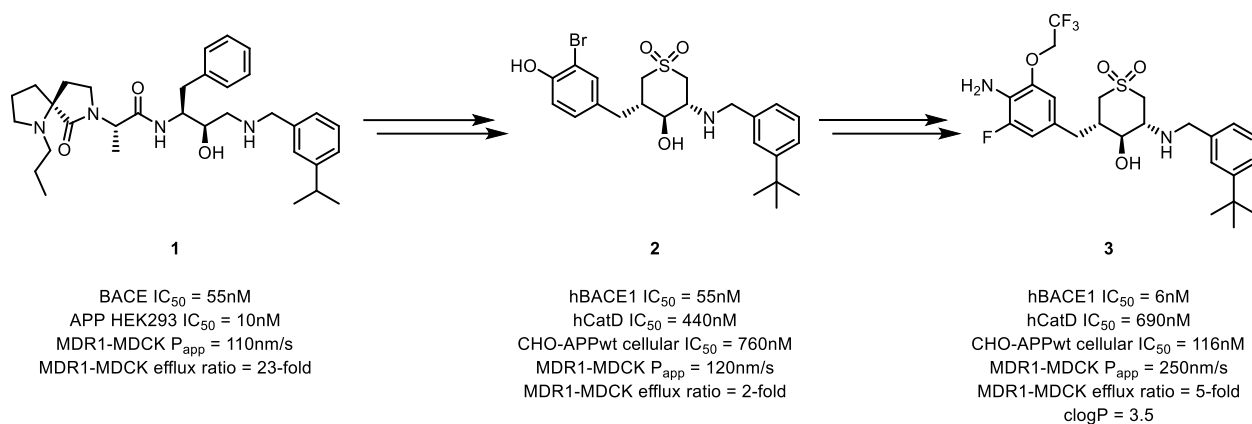


Figure 9. Functional Group Diversity of FDA-approved sulfur-containing drugs in US.

The sulfone moiety has proven to be a viable option as part of the pharmacophore during early stages of drug discovery. For example, cyclic sulfone **2** was developed as a cyclic transition-state mimetic of amide **1** in the hopes of developing a beta-secretase (BACE-1) inhibitor.<sup>116</sup> The decision to use sulfone **2** as a starting point originates from high ranking score in molecular docking, followed by preliminary experimental data demonstrating an improved pharmacokinetic profile compared to amide **1**, which exhibits poor oral bioavailability.<sup>117</sup> However, poor selectivity towards the cysteine protease cathepsin D (CatD) was observed, which left room for improvements: the inhibition of CatD is associated with build up of lipofuscin within human neuronal tissues.<sup>118</sup> Further site-modifications and biological data analysis led to the evolution of sulfone **3** with relatively superior potency and good pharmacokinetic and permeability profile,<sup>119</sup> as illustrated in scheme 5. Co-crystal structure of compound **4**, which evolved during the lead optimization campaign, and BACE reveals hydrogen-bonding interaction of the sulfonyl oxygen with the amide N–H of Gln73 and secondary alcohol O–H of Thr220, which was a key feature of how compound **2** was chosen as a good starting point due to optimal fit at the binding site

through computational docking. This case study serves to highlight the importance of cyclic bis-alkyl sulfones as a pharmacophore in drug discovery.



*Scheme 5. Development of cyclic sulfone 3 in the search of a novel BACE1 inhibitor.*

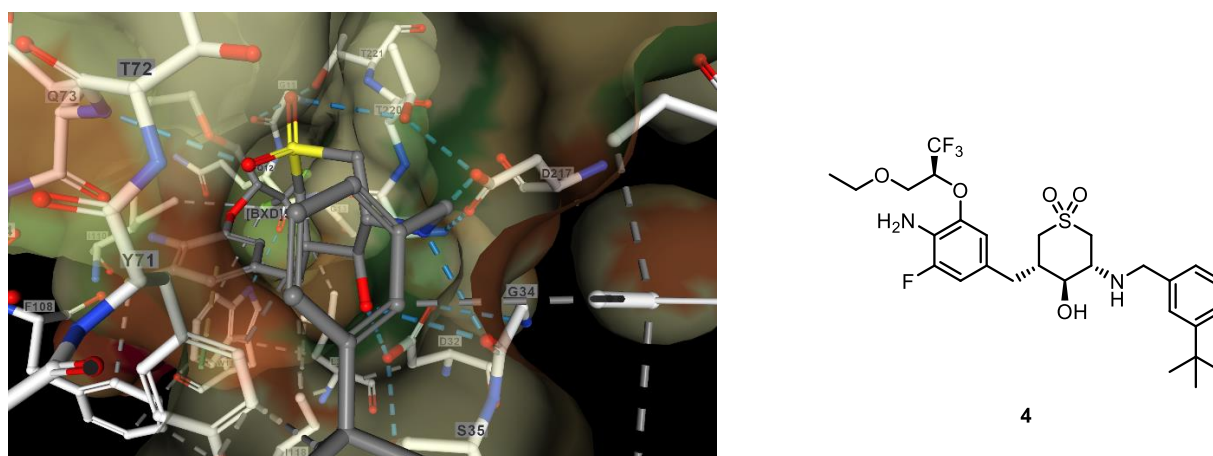


*Figure 10. Close-up of co-crystal structure for small molecule 4 in BACE1 (left) and the chemical structure of small molecule 4 (right). PDB code: 4D8C.*

As mentioned previously, incorporation of a cyclic bis-alkyl sulfone as part of the pharmacophore of a novel drug candidate can serve as an important strategy. Once again, the underrepresentation of said feature can be viewed as an opportunity for researchers to capitalize on. Upon further understanding of sulfone-containing chemical matters and how they can interact with biologically important proteins, one should expect a greater occurrence of practical application amongst both the academic sphere and the industrial community should follow through.

## Chapter 2 – Oxidative Cleavage of Previously Investigated Scaffold and Alternative Methods for Construction and Diversification

All compound syntheses, analysis and characterization of data was performed by C. H. Andy Un, except for characterization of compound **28**, which was performed by Dr. Jeremy E. Wulff. Dr. Tyler Trefz and Dr. Ori Granot collected the HRMS data.

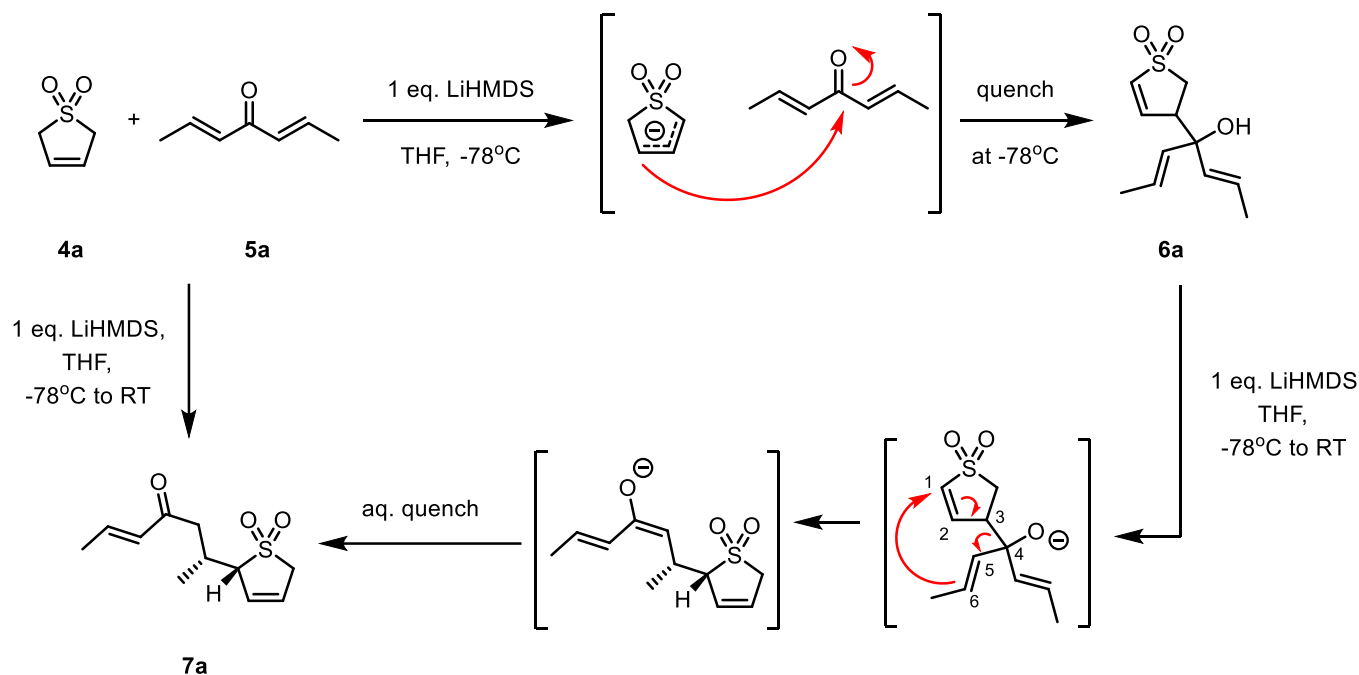
### Chapter 2.1 Synthetic access to bi- and tri-cyclic alkyl sulfones, and selection of the bicyclo[3.2.1]sulfone framework for diversification

As described in the previous Chapter, bis-alkyl sulfones have considerable promise as pharmacophores but have not yet been extensively explored. Conducting a thorough survey of biological properties for any set of molecules would require screening against a wide variety of microorganisms and enzymatic targets. This will necessarily result in large amounts of biological data being acquired. Making and testing molecules is resource-intensive, and analysis of the collected biological data will be time-consuming. It is therefore crucial to select at the outset the *right* bis-alkyl sulfone scaffold with which to undertake such a study.

This Chapter begins with a review of the Wulff group's existing methodology for the production of four different classes of bi- or tri-cyclic sulfones, and describes the decision process that led to the selection of a family of bicyclo[3.2.1]sulfones for further study. Among the four different structural archetypes that could be readily accessed, the bicyclo[3.2.1]sulfone framework was particularly attractive due to its conformational rigidity, its pronounced three-dimensionality, and the absence of any electrophilic alkenes that could trigger false-positive hits in biological screening. The remainder of the Chapter summarizes efforts to suitably derivatize this scaffold to generate compounds for biological testing.

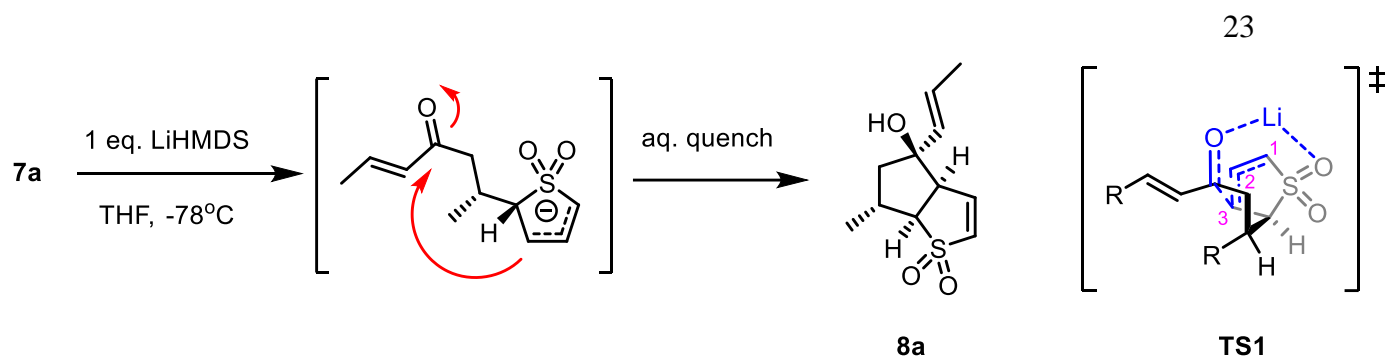
In earlier work, our group discovered a method of generating architecturally interesting molecules based on 3-sulfolene, illustrated as **4a** in scheme 6.<sup>120</sup> Lithiation of **4a**, followed by addition of bis-vinyl ketone **5a** produced  $\alpha$ -substituted sulfone **7a** as a single diastereomer. Mechanistic studies indicated that deprotonation of 3-sulfolene occurs prior to nucleophilic addition to ketone **5a** via 1,2-addition, followed by an anion

oxy-Cope rearrangement at low temperature. We have proved that the 1,2-addition product **6a** can be isolated, and at room temperature rearranged to the desired tandem product via a boat-shaped transition state, thus offering valuable evidence to support our mechanistic proposal.



*Scheme 6. Tandem 1,2-addition/anionic oxy-Cope cascade reaction.*

Prior work from our group showed that this methodology can tolerate multiple alkyl fragments on both the ketone and sulfone substrates, in each case provided the coupled product in moderate yield. Taking advantage of the presence of an  $\alpha,\beta$ -unsaturated ketone, **7a** can be subjected to a second deprotonation as part of an annulation strategy, resulting in the formation of a highly constrained sulfone-containing framework **8a**. The transformation is highly diastereoselective, and presumably occurs through nucleophilic addition at the 3-position of the sulfone-stabilized allylic anion, as highlighted in **TS1** within scheme 7.



*Scheme 7. Formation of cis-bicyclo[3.3.0]sulfone-containing molecules in a diastereoselective manner.*

Strategic recognition of all substituents and functional groups in the bicyclo[3.3.0]system revealed a geometrical match between **8a** and the enzyme-bound conformation of peramivir, a viral neuraminidase inhibitor, as shown in Figure 11. Computational data suggests that despite the high potency of peramivir, the conformational flexibility of peramivir in solution may not be ideal for high isoenzyme specificity. As such, our group envisioned that derivatization of the conformationally rigid bicyclo[3.3.0]sulfone-containing framework can lead to reduced entropy of binding and improved target selectivity, paving way to the development of the next generation influenza neuraminidase inhibitors.<sup>121</sup>

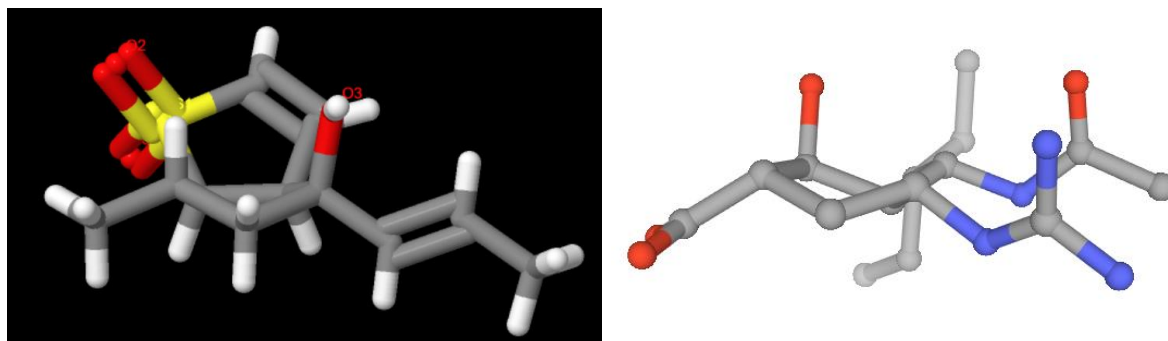
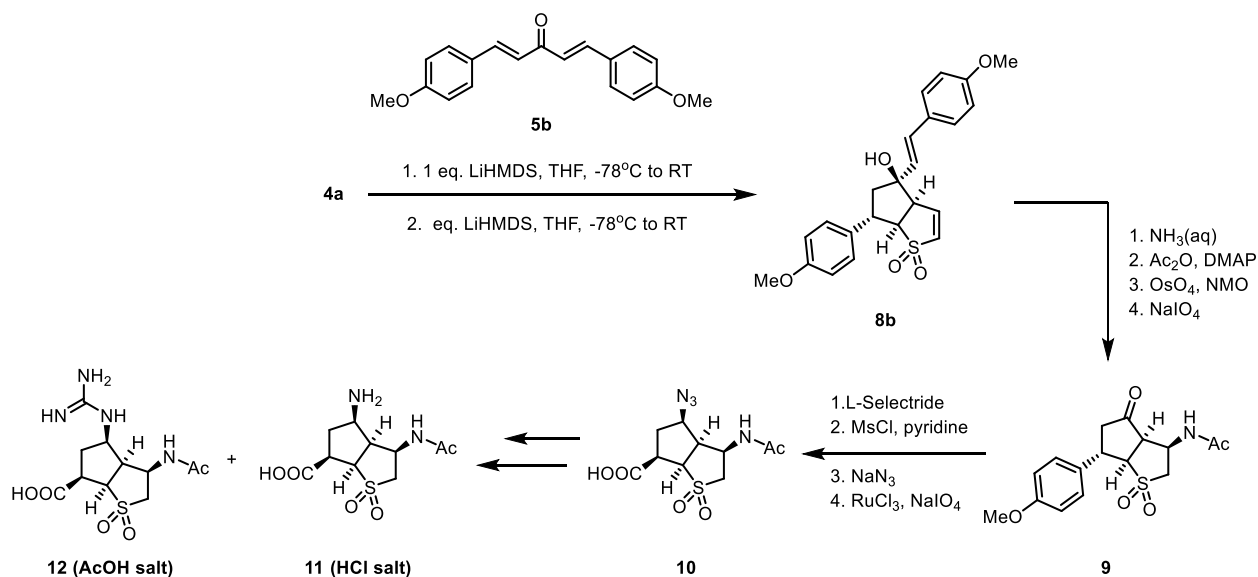


*Figure 11. Crystal structure comparison of compound **8a** (left, CCDC 766248) and enzyme-bound peramivir (right, PDB 1L7F). As discussed in reference 121, the core of sulfone **8a** is predisposed to position substituents in similar orientations to those found in the enzyme-bound structure—but not in the solid-state or solution-state structure—of peramivir.*

Mutation-induced resistance of influenza virus has become an ongoing healthcare issue that also has huge economical impact, especially after the 2009 pandemic.<sup>122</sup> Current available treatments have gradually become less effective in combatting this issue if the situation does not improve.<sup>123</sup> As it stands, novel neuraminidase inhibitors with new skeletal framework is required in order to inhibit

mutant influenza neuraminidase. Taking advantage of the peramivir-like conformation of our highly functionalized bicyclo[3.3.0]sulfone-containing framework, Dr. Mike G. Brant set out to test if derivatization of the scaffold into biologically-active neuraminidase inhibitors. Utilizing the aforementioned tandem cascade methodology, compound **8b** was synthesized as shown in scheme 8. Installation of an acetamide group was possible due to reaction with the vinyl sulfone moiety; subsequent oxidative cleavage allows for the formation of a versatile ketone group, thereby setting up a precursor **9** that can theoretically engage with all the sub-pockets of the neuraminidase active site. Dr. Brant envisioned that oxidative degradation of the aromatic fragment could offer a versatile functional group – a carboxylic acid for further derivatization. This transformation is not without literature precedent, as strong oxidants such RuO<sub>4</sub> can achieve said task.<sup>124</sup> Indeed, compound **10** was obtained successfully. Subsequent transformation lead to the emergence of amine **11** as an HCl salt, as well as its chemical analogue – guanidine **12** as an acetic acid salt.

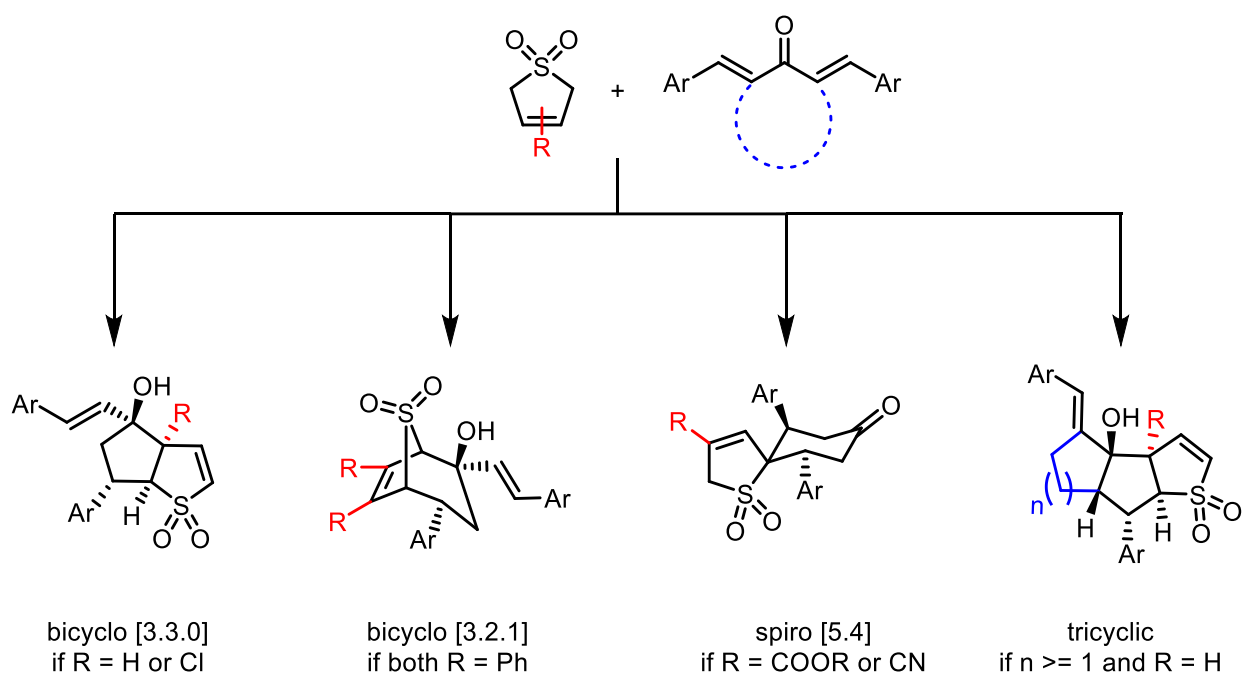


*Scheme 8. Development of highly functionalized conformationally-restricted bicyclo[3.3.0]sulfone-containing neuraminidase inhibitor.*

*In vitro* enzymatic assay against viral neuraminidase of amine **11** and guanidine **12** displayed promising activities, with K<sub>i</sub> values of 19 ± 1 μM and 4.5 ± 0.5 μM respectively. Both compounds were determined to be competitive inhibitors of neuraminidase, as well as showing higher bioactivity when compared to model

compounds based on zanamivir and peramivir. Thus, it was determined that bicyclic bis-alkyl sulfone-containing compounds were effective small molecules capable of modulating the activities of biological systems.

Dr. Brant and other previous Wulff group members (Jordan Friedmann and Connor Boulken) later discovered that a more extensive collection of interesting bicyclic frameworks can be synthetically achieved. By varying the steric and electronic environment using different 3-substituted 3-sulfolenes, the reaction with bis-vinyl ketones could be tuned to selectively provide three unique ring systems in a diastereoselective manner, as shown in Scheme 9.<sup>125</sup> This reactivity is analogous to dialkylative coupling between disubstituted alkyl halides and 3-sulfolene. Thus, one can gain access to a diverse set of sulfone-containing scaffolds with varying degrees of three-dimensionality.<sup>126</sup>



*Scheme 9. Diversity-orientated sulfone-containing scaffolds based on a common building block.*

Upon inspection of crystallographic data of all three frameworks, one can calculate the projection angle of the sulfone moiety, as shown in Figure 12. The projection angles can serve as useful references to guide researchers in constructing chemical matters that maximize the interaction between the sulfone functional group and any biological interface. The projection angle of the sulfone moiety relative to the 7-

membered carbon framework of the bicyclo[3.2.1]scaffold was determined to be approximately  $247^\circ$  using compound **14** as reference, as the angle shown in Figure 12 implied the spatial region of a spherical model that obstructs any theoretical biological interface that can interact with the sulfone. In contrast, the projection angles of the sulfone moiety relative to the scaffold framework of the bicyclo[3.3.0]framework and the spiro[5.4]framework were determined to be  $183^\circ$  and  $97^\circ$  respectively using compound **13** and **15** as references. Clearly, amongst all three conformationally-rigid sulfone-containing framework, the bicyclo[3.2.1]system appears to be fit for interacting with a greater range of three-dimensional volume due to being more spatially accessible.

Furthermore, we noted that electron-deficient alkenes (vinyl sulfones) were present in both the bicyclo[3.3.0]sulfone and the corresponding tricyclic structure, whereas the spiro[5.4]sulfone could *acquire* an electron-deficient alkene if the double bond were to migrate into proximity of the sulfone. Vinyl sulfone groups serve as potential electrophilic centres for conjugate addition reactions with various nucleophiles, (especially thiols) and are often found to be promiscuous (i.e. nonselective) binders in biological screening campaigns. While prior experience from our research group suggests that none of these three species are particularly electrophilic, we nonetheless felt it safer to deprioritize these three scaffolds. The bicyclo[3.2.1]sulfone contains a  $\beta$ -alkenyl sulfone like that present in the spirocyclic ring system, but while the double bond in the latter molecule can migrate toward the sulfone (creating a potentially risky vinyl sulfone motif, as described above) the alkene in the former molecule cannot, since doing so would violate Bredt's rule.

For all of the above reasons, the bicyclo[3.2.1]system served as a good starting point to probe novel biological interactions with sulfones serving as the pharmacophore. This presents a novel research frontier for our group to explore, in the hopes of discovering novel hit candidates or understanding unexplored physiological pathways. Thus, we aim to create highly functionalized analogues of bicyclo[3.2.1]sulfone-containing molecules as part of our campaign towards promoting conformationally-restricted sulfone-containing scaffolds in medicinal chemistry.

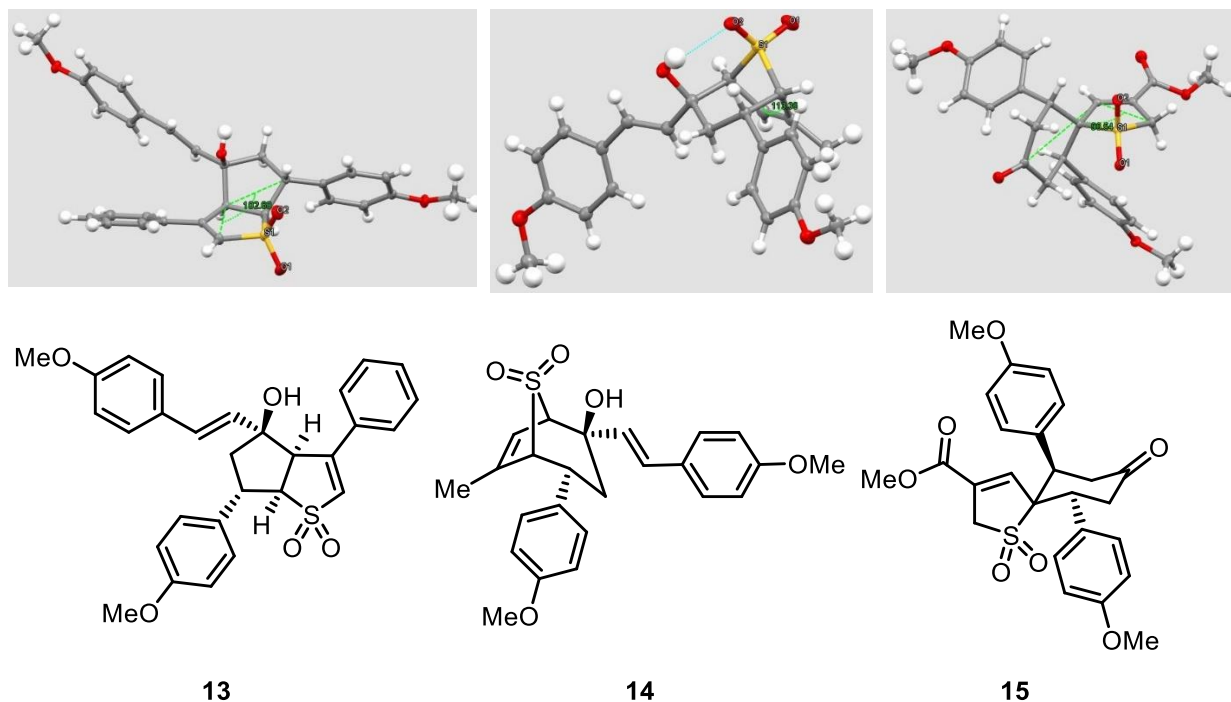
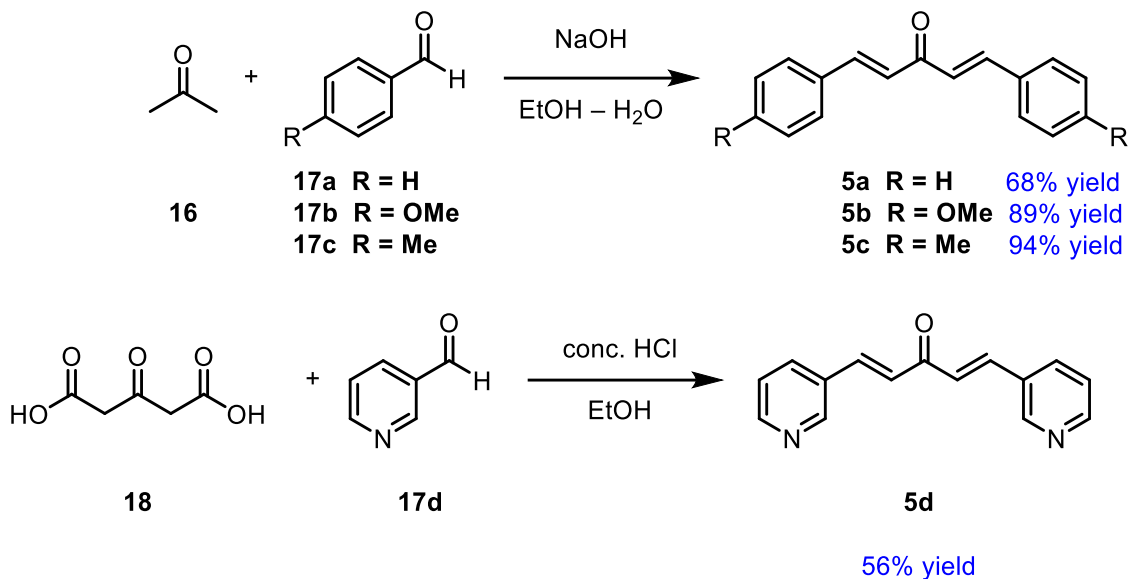


Figure 12. X-ray crystal structure of compounds **13** (top left), **14** (top middle) and **15** (top right) and their chemical structures (bottom). Included in each X-ray structure are the corresponding projection angle of the sulfone groups, with the exception of **14** (implied to be the inverse of  $113^\circ$  in a theoretically spherical model, which is approximately  $247^\circ$ ).

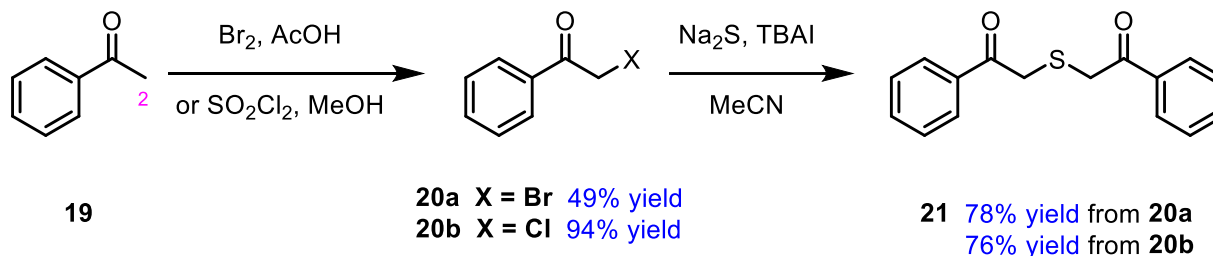
## Chapter 2.2 Initial Construction of Bicyclo[3.2.1]Sulfone-Containing Library.

Instead of constructing bicyclo[3.2.1]sulfone-containing molecules in a *de novo* manner, we devised a strategy based on our previously discovered tandem cascade methodology. As shown in Scheme 10, bis-aryl electrophiles were constructed via a simple double-aldol condensation method.<sup>127</sup> This strategy offered great variability due to usage of inexpensive aryl aldehyde and acetone **16** as feedstocks, and good yields were obtained for compounds **5a**, **5b**, and **5c**. However, for electron-poor aryl substituents such as 3-pyridyl, the protocol was not applicable. An alternative solution based on an acid-mediated aldol-decarboxylative condensation allowed us to obtain compound **5d**.<sup>128</sup>



*Scheme 10. Synthesis of diarylidene ketones.*

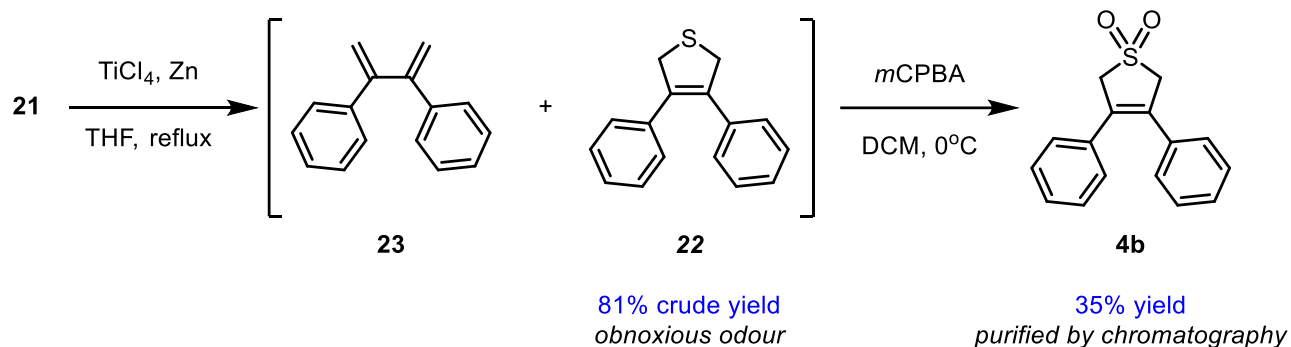
For construction of the bis-aryl sulfone, Nakyama and coworkers have described a viable synthetic route, which we relied upon.<sup>129</sup> Shown in Scheme 11, acetophenone **19** was brominated at the 2-position mediated by acetic acid,<sup>130</sup> which produced compound **20a** upon stirring at ambient temperature overnight. Alternatively, chlorination with sulfuryl chloride in methanol can yield the analogous compound **20b**.<sup>131</sup> Subsequent coupling with Na<sub>2</sub>S using either compound **20a** or **20b** provided the diketone **21** without the need for chromatography.<sup>132</sup>



*Scheme 11. Synthesis of symmetrical diketone sulfides*

Depicted in Scheme 12, initial McMurry coupling generated the annulated thioether species **22** in high conversion but low purity. Chromatographic purification was challenging because of the possibility of aromatization,<sup>133</sup> therefore we decided to telescope into the formation of sulfone **4b**. The transformation presumably occurs via reduction of TiCl<sub>4</sub> into Ti (III) species,<sup>134</sup> which can form a ketyl radical. Annulation occurs upon interaction of diketyl species, which under thermodynamic conditions can

undergo elimination to afford the tetra-substituted alkene **4b**. Our initial screening revealed a byproduct as indicated by  $^1\text{H}$  NMR signal of two doublets at  $\delta$  5.32 ppm and 5.55 ppm, with both signals displaying coupling constants of 1.6 Hz. The byproduct was assigned as diene **23** due to spectroscopic agreement with precedent literature.<sup>135</sup>



*Scheme 12. Synthesis of cyclic sulfones via deoxygenative annulation and sulfide oxidation.*

Careful optimization led to minimal formation of **23** via reduction of the stoichiometry of the terminal reductant zinc dust as well as the amount of titanium (III) precursor (from 5.0 equivalent to 3.0 equivalent), as shown in Figure 13. Presumably, the formation of the diene **23** is due to the harsh reductive condition leading to cleavage of the C-S bonds.<sup>136</sup> Attempts to use Fürstner's catalytic method yielded thiophenes instead.<sup>137</sup> Subsequent electrophilic oxidation with *m*CPBA offered higher yield compared to Oxone conditions.<sup>138</sup> Thus, after considerable optimization, we were able to obtain symmetrical sulfone **4b**.

Due to aforementioned obstacles, we also tried investigating whether other possible synthetic routes can yield **4b** in a more efficient manner. We decided to begin by performing pinacol coupling with acetophenone **19** in the presence of acetic anhydride to synthesize compound **24**, as shown in Scheme 13.<sup>139</sup> Good yields were obtained after moderate reaction time; subsequent elimination under thermodynamic conditions to afford the diene **23** was performed.<sup>140</sup> However, low yield was obtained due to competing pinacol rearrangement to give ketone **25** as the major product.<sup>137</sup> Despite our successful attempt at sulfur-dioxide transfer using compound **23** and sodium hydroxymethanesulfinate dihydrate, commonly referred to as Rongalite salt, to

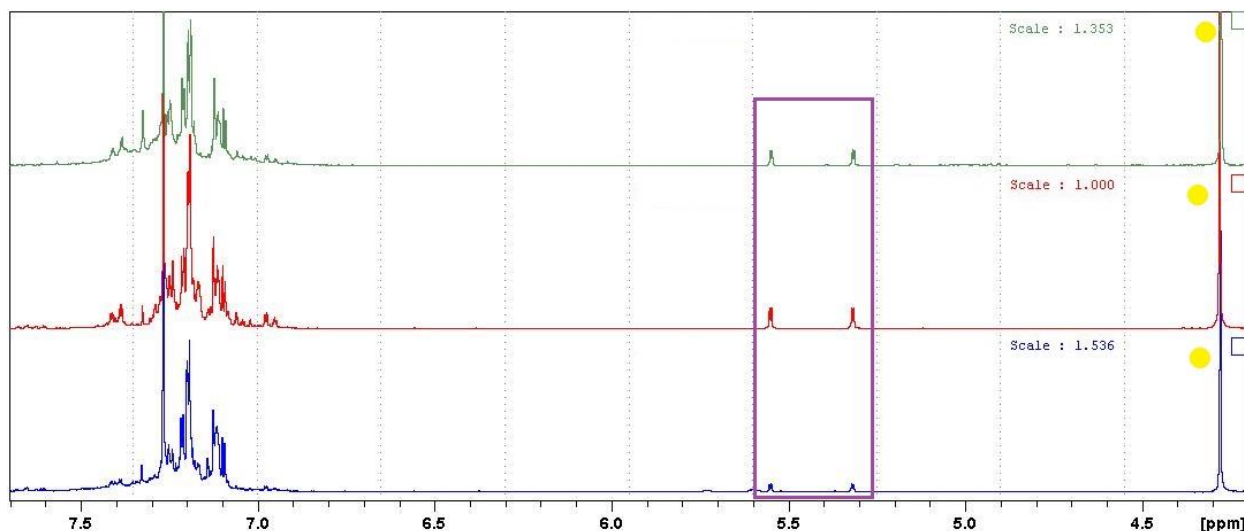
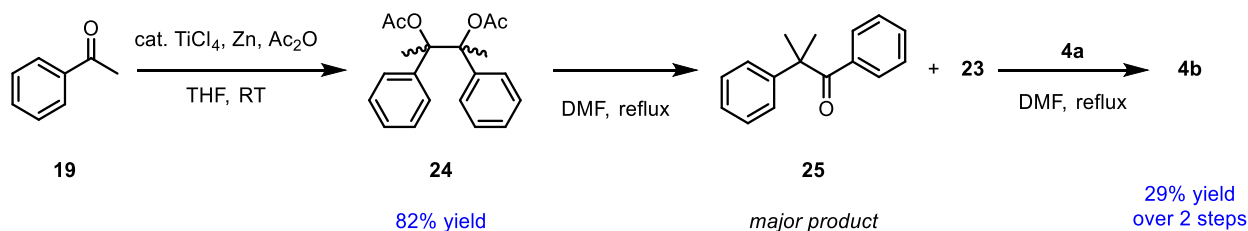


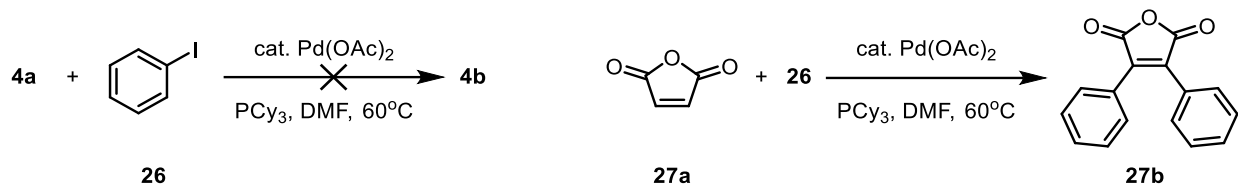
Figure 13. Overlapping  $^1\text{H}$  NMR spectra of McMurry coupling using 5.0 equivalent (green), 3.5 equivalent (red), and 3.0 equivalent (blue) of  $\text{TiCl}_4$ . Signals corresponding to diene **26** are highlighted as purple rectangle. Normalized based on peak height of singlet signal at  $\delta$  4.28 ppm (highlighted as yellow circles).

yield compound **4b**, the overall yield of this synthetic route was abysmally low and not deemed scalable due to the necessity of maintain an atmosphere of sulfur dioxide gas in the last step. Thus, we abandoned this synthetic route.



Scheme 13. Attempted improvement of sulfone synthesis via pinacol coupling.

Harrington and DiFiore have previously reported that iodobenzene **26** and 3-sulfolene **4a** served as suitable substrates for Pd-catalyzed cross-coupling reaction in order to yield 3-substituted sulfolenes.<sup>141</sup> As such, we sought to investigate whether their protocol could serve as a template for generating 3,4-disubstituted sulfolene derivatives. Despite their claim of obtaining mono-aryl sulfolenes, we were curious as to whether this protocol can lead to formation of the analogous sulfone **4b**. Instead of using triethylamine as a reductant to generate Pd(0) from Pd(II), we explored the possibilities of using tricyclohexylphosphine instead. However, we were unable to obtain either the mono-arylated or bis-arylated product, as iodobenzene and 3-sulfolene was recovered in all cases. These results are summarized in Scheme 14.

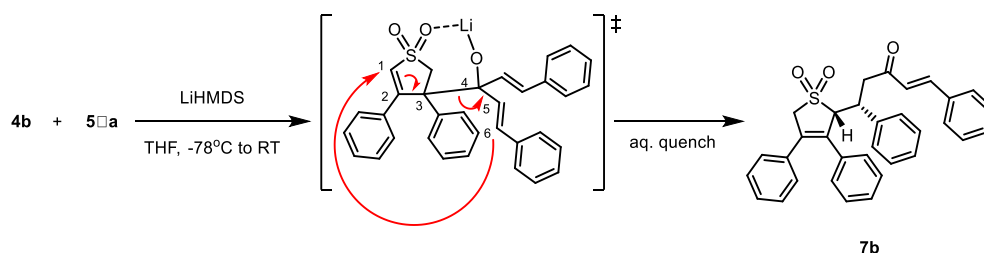


quantitative yield

*Scheme 14. Attempted double arylation of cyclic alkenes via Heck reaction.*

This is most likely due to the alkene being less-polarized and more electron-rich, thus requiring higher activation energy to overcome the rate-limiting reductive elimination step and less steric hinderance during oxidative addition. By contrast, the more electron-deficient maleic anhydride is capable of under going Pd-catalyzed double arylation at room temperature to yield **27b**.<sup>142</sup> It is known that the use of tetrabutylammonium bromide as an additive during palladium cross-coupling can generate Pd colloids,<sup>143</sup> which are catalytically active for aryl cross couplings.<sup>141</sup>

Nonetheless, the McMurry coupling route offered us the desired sulfone precursor in multigram quantity. Thus, we attempt to replicate the tandem 1,2-addition/anion-oxy Cope cascade reaction, as shown in Scheme 15. Initial attempts revealed that the reaction was successful, although only 50% conversion towards compound **7b** was achieved.

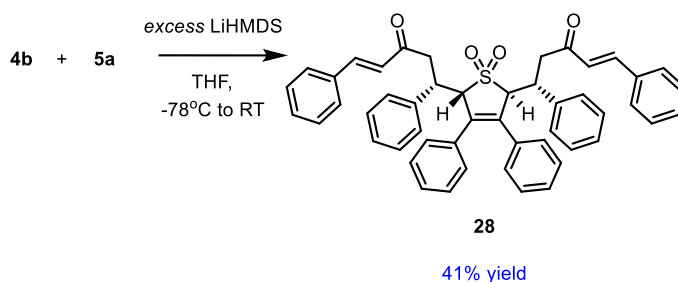


*Scheme 15. Replication of Tandem 1,2-addition/anionic oxy-Cope cascade reaction.*

We pondered whether the order of reagent addition was of importance, and after a series of investigations, no significant change in product conversion was observed. Introduction of tertiary amine additives are known to influence the aggregation state of the lithium hexamethyldisilazene (LiHMDS),<sup>144</sup> and we were curious whether introduction of DABCO could lead to any improvements. Unfortunately, our situation remained stagnant. It was not until we realized that the rate of addition of the base was of crucial importance: upon near-instantaneous addition of all LiHMDS in one portion

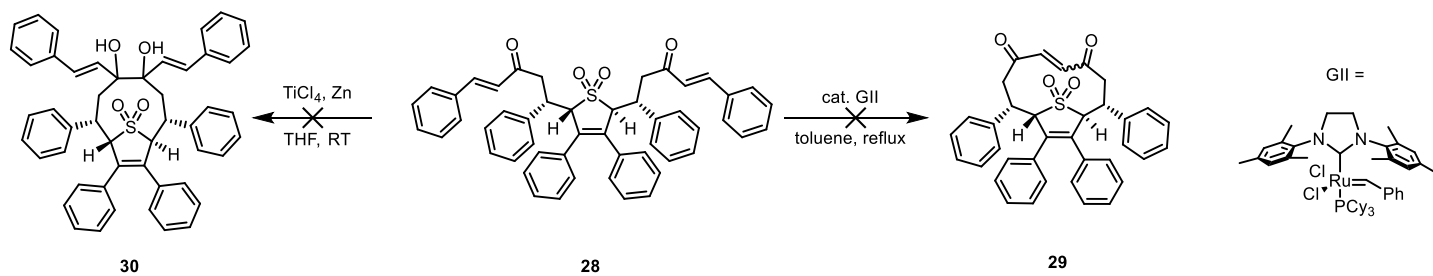
instead of gradual addition, we observed that the reaction mixture turned from clear, yellow to a persistent clear, brown colour. Note that previously when performing gradual addition, the reaction mixture gradually changed from clear, yellow to clear, light brown colour, which exhibit a lighter tone compared to the “instantaneous addition” method. Surprisingly, complete conversion into sulfone **7b** was observed using the “instantaneous addition” method upon workup and subsequent  $^1\text{H}$  NMR analysis. The crude product appeared as clear, brown oil, which turned into light brown foamy solid upon drying under reduced pressure. Thus, it is possible that the anionic oxy-Cope rearrangement requires a high concentration of lithium salt aggregates to perform at its full capacity.<sup>145</sup> The presence of sulfone moieties can also influence the aggregation state of lithium salts.<sup>146</sup> Initial purification was not successful in producing compound **7b** in high purity, as our early attempts to do so resulted in recovery of the substrates. Later replication attempts reveal that the product is highly unstable under acidic conditions, as presumably the acidic nature of silica leads to beta-elimination pathway and thus recovery of fragments **4b** and **5a**.<sup>147</sup> Suppression of said fragmentation can be done through addition of a small amount of triethylamine during elution of the product through chromatographic means.

Interestingly, we were able to generate compound **28** during our struggle to achieve complete conversion of compound **7b**, as shown in Scheme 16. We added an excessive amount of base in the attempts to generate compound **7b**, as we postulated that interference of residual water content in the reaction flask resulted in incomplete conversion towards compound **7b**. Presumably, the compound **28** arises from compound **7b** via another iteration of tandem 1,2-addition/anionic oxy-Cope reaction sequence.



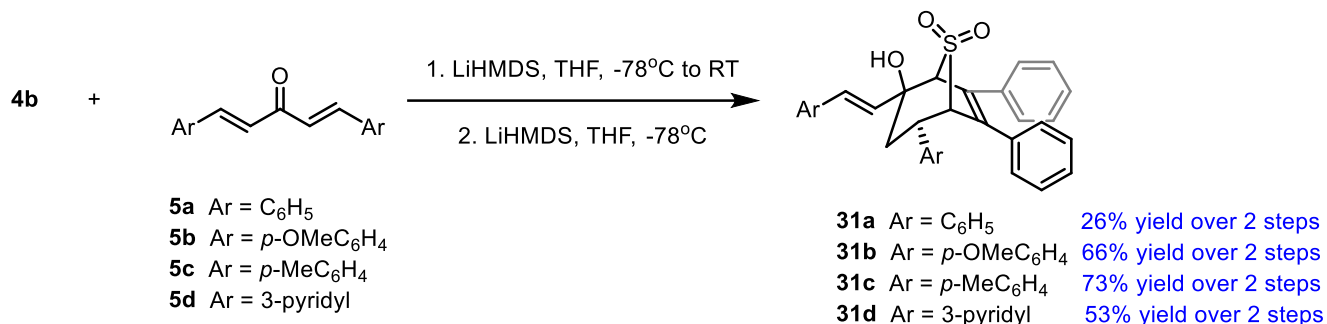
*Scheme 16. Serendipitous discovery of iterative tandem 1,2-addition/ anionic oxy-Cope cascade.*

We were curious whether ring-closing metathesis of compound **28** could occur at the activated alkenes and yield a 11-membered ring **29**.<sup>148</sup> Unfortunately, we only recovered starting material. Attempts to generate a 9-membered ring **30** via pinacol coupling was also met with failure, as shown in Scheme 17. Presumably, these transformations were unable to proceed as planned due to intrinsic nature of the two alkyl appendages being unable to geometrically be in close contact with each other.



*Scheme 17. Attempted synthesis of sulfone-containing macrocycles.*

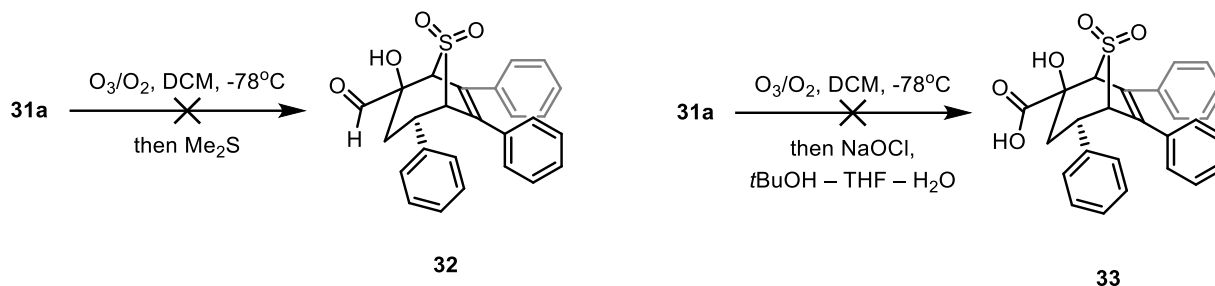
Once we resolved the issues surrounding the anionic oxy-Cope reaction, subsequent ring-closure proceeded smoothly,<sup>149</sup> although cautious purification via chromatographic means were warranted due to the bicyclic products also being acid-sensitive. The above sequence was tolerant of various aryl substituents, and we were able to synthesize various analogues **31a**, **31b**, **31c**, and **31d**, as shown in Scheme 18.



*Scheme 18. Synthesis of bicyclo[3.2.1]sulfone-containing compounds using different diarylidene ketones.*

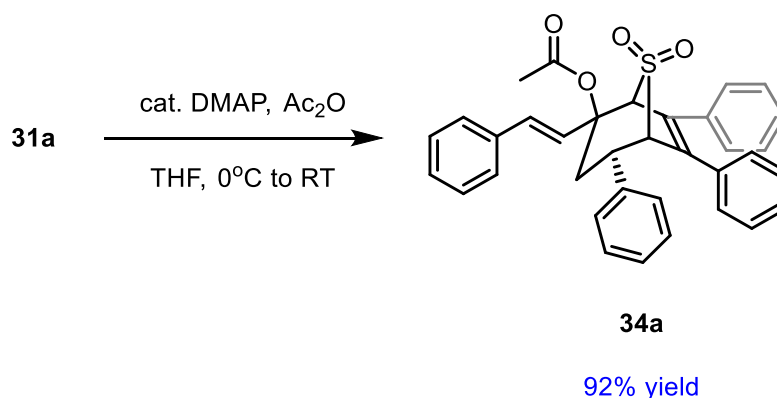
Our initial attempt at selective oxidative degradation to yield compound **32** was done under ozonolysis conditions. However, the crude product revealed no significant <sup>1</sup>H signals, let alone anything resembling compound **31a**. After various replications without success, we wondered whether the presumed aldehyde product was unstable, thus we decided to perform Pinnick oxidation directly after ozonolysis in the hopes of

isolating the carboxylic acid **33**. However, we were unable to isolate any material of significance, as shown in Scheme 19.



*Scheme 19. Attempted oxidative cleavage of aryl alkenes under different redox workup conditions.*

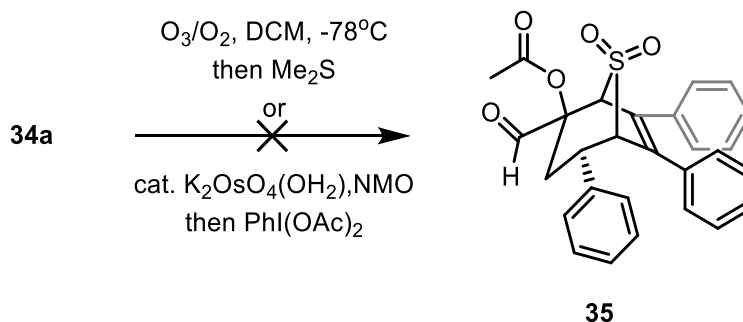
As such, we pondered whether the alcohol was of crucial importance leading to oxidative decomposition.<sup>150</sup> Thus, protection of the alcohol would be necessary, and we elected to install an acetyl group<sup>151</sup> as we envision the ester moiety would be capable of serving as a substrate to generate silylketene acetals *in situ* upon deprotonation with a strong base, which could then undergo [3,3]-sigmatropic rearrangement. Shown in Scheme 20, esterification using acetic anhydride and catalytic amounts of DMAP afforded compound **34a** albeit very slowly; 3 days of reaction time was required in order to reach complete conversion.<sup>152</sup>



*Scheme 20. Successful acylation of sterically hindered tertiary alcohol 31a.*

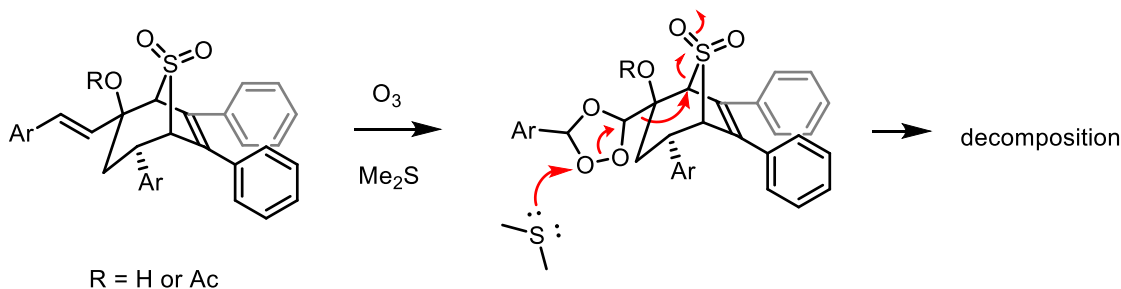
Despite protection of the alcohol, once again no identifiable products were observed under ozonolysis conditions. As such, we decided to employ a Lemieux-Johnson-type transformation as an alternative, as shown in Scheme 21.<sup>153,154</sup> However, we were met with no success again. Usage of other strong oxidants warrant our caution due to the possibility of oxidative degradation of any aryl fragments. As such, we

elected to abandon this route to more advanced bicyclo[3.2.1]sulfone-containing compounds.



*Scheme 21. Attempted oxidative cleavage of aryl alkenes using either ozonolysis or Lemieux-Johnson oxidation.*

Currently our hypothesis is that decomposition originates from elimination during reduction of our supposedly generated Criegee intermediate.<sup>155</sup> Upon inspection of the crystallographic data of the bicyclo[3.2.1]sulfone-containing framework using compound **14**, we discovered that the dihedral angle between C<sub>1</sub>-S<sub>1</sub> bond and C<sub>2</sub>-C<sub>3</sub> bond are nearly on the same plane, as illustrated in Figure 14. Thus, it may not be surprising to postulate that the C<sub>1</sub>-S<sub>1</sub> bond is cleaved via pathways similar to Grob-fragmentation,<sup>156, 157</sup> leading to ring-opening of the bicyclic framework as shown in Scheme 22, and further oxidative decomposition may arise.



*Scheme 22. Postulated mechanism on how oxidative decomposition can arise during ozonolysis.*

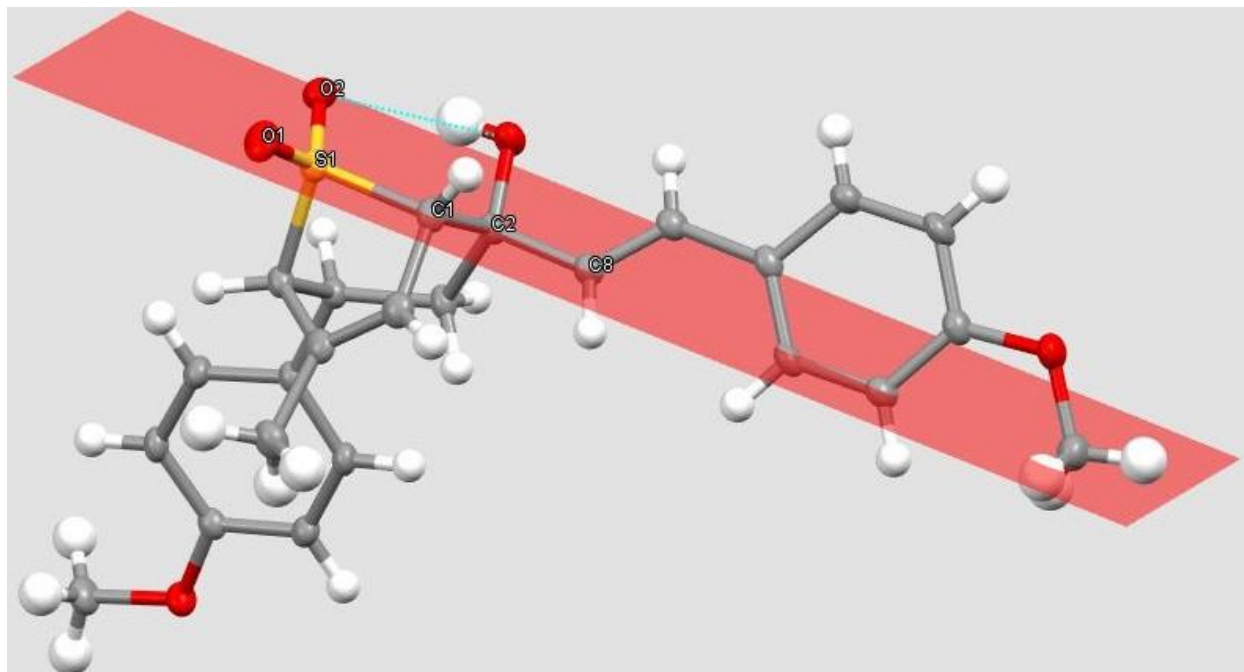
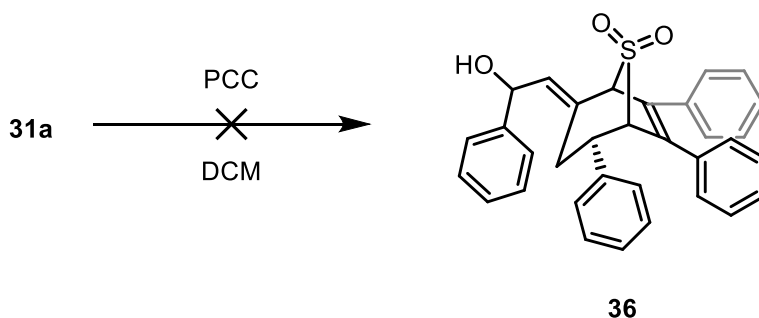


Figure 14. Rationalization of how decomposition originates from cleavage of C – SO<sub>2</sub> bond.

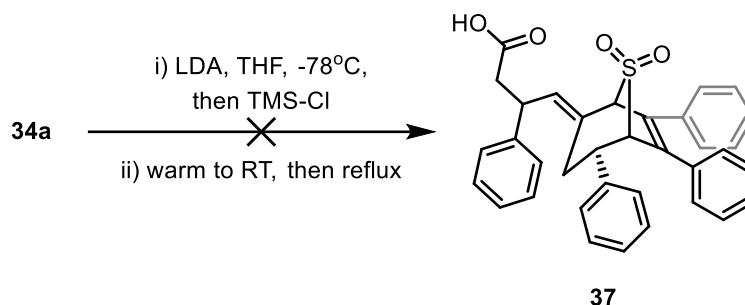
Despite the struggles, we were still optimistic about other ways to functionalize the bicyclo[3.2.1]framework. Due to the presence of the allylic alcohol, we envisioned obtaining compound **36** through allylic rearrangement of the alcohol moiety mediated by PCC, as shown in Scheme 23.<sup>158, 159</sup> However, no significant product was observed, nor did we recover any starting material.



Scheme 23. Attempted allylic 1,3-oxygen transposition mediated by chromium reagents.

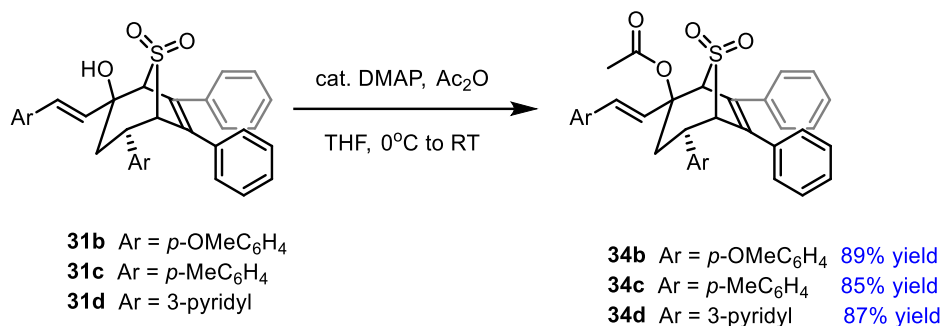
We speculated that cleavage of the C–O bond would lead to overall decomposition of the entire framework. Indeed, compound **34a** was investigated for its potential to undergo Ireland-Claisen rearrangement, as shown in Scheme 24,<sup>160, 161</sup> however, decomposition was also observed. Regardless of whether the pericyclic reactions undergo cationic or radical pathways,<sup>162</sup> it appears that deoxygenation in the

vicinal of the bicyclic sulfone moiety is key to decomposition, presumably the collapse of the C–SO<sub>2</sub> bond can alleviate ring strain imposed by the bicyclic framework.



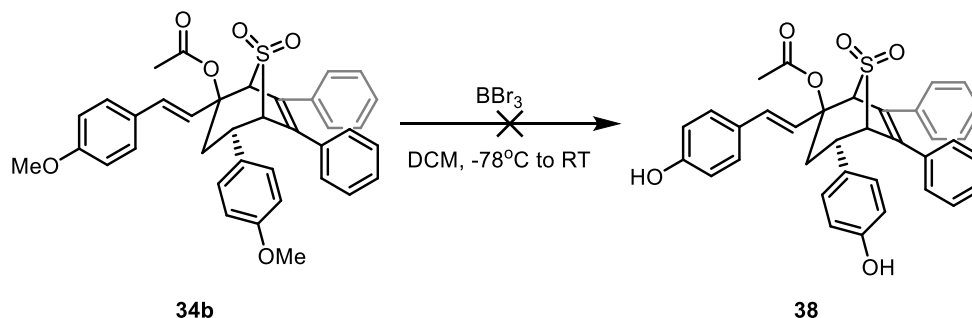
*Scheme 24. Attempted transformation of one-pot Ireland-Claisen rearrangement to yield carboxylic acids*

Our resilience against the face of continuous failures had started to wane, as we were only able to demonstrate acetylation of the tertiary alcohol moiety amongst all synthesized tetra-aryl sulfone-containing molecules, yet could not accomplish any further derivatization.



*Scheme 25. Acetylation of bicyclo[3.2.1]sulfone-containing compounds.*

Our final hope was to attempt to demethylate compound **34b** using BBr<sub>3</sub> in the hopes of obtaining compound **38**, as shown in Scheme 25. The reaction was performed under extremely low temperature,<sup>163</sup> but compound **34a** underwent rapid decomposition instead.



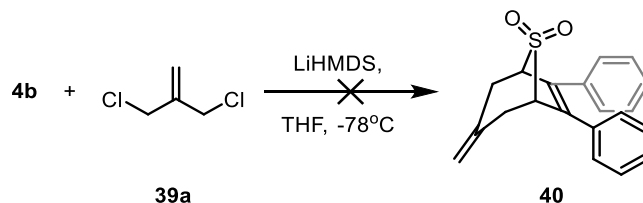
*Scheme 26. Attempted demethylation of methyl aryl ethers under Lewis acidic conditions.*

This can proceed via two decomposition pathway: (i) the oxygen of the sulfone coordinating to the Lewis acidic boron, thereby enhancing the electrophilicity of the sulfur, and cleavage of the C-S bond will alleviate the inherent ring strain from the bicyclic system, or (ii)  $\text{BBr}_3$  mediates the loss of an acetate group,<sup>164</sup> thus high degree of carbocation character on the tertiary carbon can result in bond migration and further uncontrolled rearrangement. All in all, we were not able to chemically transform the substrate as planned.

Nonetheless, we were able to construct a small collection of bicyclo[3.2.1]sulfone-containing small molecules. We anticipated acetylated products to be of different physicochemical properties compared to the free-alcohol products, thus evaluation of any future biological data would be useful, as we would be able to question the importance of the free alcohol. Variability amongst this small chemical collection is low, thus we seek other methods to generate the bicyclo[3.2.1]framework. Perhaps instead of starting from a densely functionalized template, a simpler skeleton framework can offer us better ways of installing substituents for future derivatization.

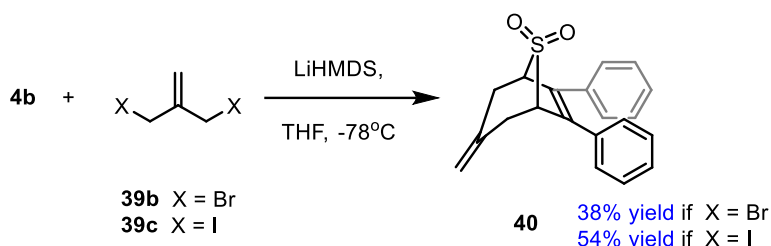
### Chapter 2.3 Alternative Approach to Generate Bicyclic Sulfones.

Chou and coworkers reported a simpler and more straightforward method of generating bicyclo[3.2.1]sulfone-containing molecules.<sup>165</sup> Taking inspiration from them, we were curious whether their protocol of double displacement using dihalide compound can generate the 7-membered ring framework. Commercially available dichloride **39a** was reacted with compound **4b**, but we only recovered both starting materials, as shown in Scheme 27. Note that due to safety concerns, we elected to not employ the usage of HMPA during our initial investigations.



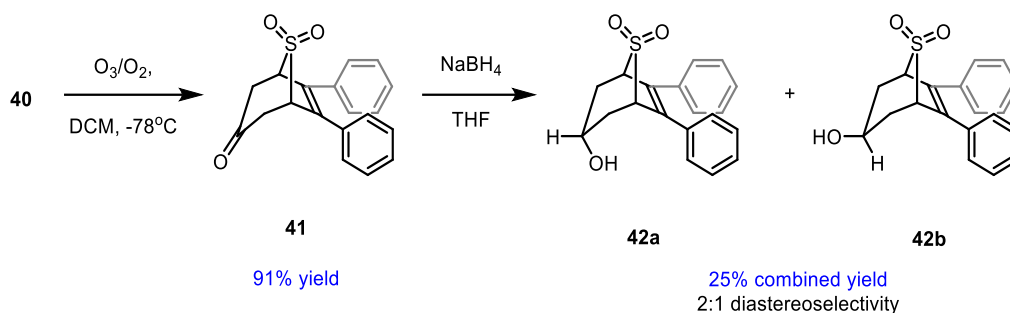
*Scheme 27. Attempted synthesis of bicyclo[3.2.1]sulfone-containing compounds via nucleophilic substitution with organochlorides.*

We rationalized that perhaps organochloride species **39a** were unreactive towards nucleophilic displacement, hence we needed to enhance the electrophilicity of the isobutene fragment. Under Finkelstein conditions,<sup>166</sup> compound **39a** was reacted with NaBr and NaI to afford compound **39b** and **39c** in quantitative yield respectively. Next, we subjected the compound **39b** under Chou's protocol, and we were able to isolate the novel diphenyl bicyclic compound, albeit in low yield. Compound **39c** proved to be more reactive, as shown in Scheme 28, and the usage of this led to a moderate yield after chromatographic purification.



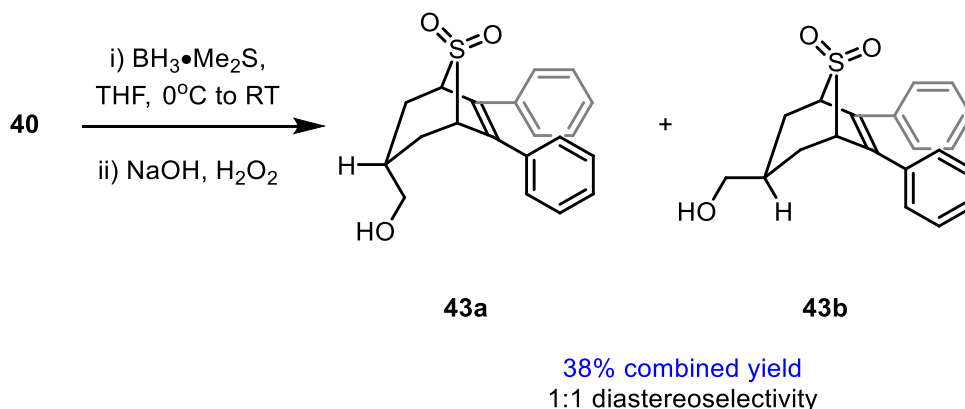
*Scheme 28. Successful transformation of diaryl sulfones via double nucleophilic substitution with organohalides.*

With the bicyclic framework in hand, we enthusiastically moved forward to perform oxidative cleavage on the terminal alkene. The transformation proceeded smoothly, and we were able to isolate ketone **41**. Reduction of the alcohol using NaBH<sub>4</sub> lead to a mixture of diastereomer alcohols **42a** and **42b**. Thorough spectroscopic analysis revealed the identity of both diastereomers, with **42a** being the major product in approximately 2:1 diastereoselectivity, as shown in Scheme 29. The identity of alcohols **42a** and **42b** were determined upon thorough spectroscopic analysis: the methine proton of the alcohol moiety in compound **42b** demonstrated a coupling constant of 11.2 Hz with the axial proton of the methylene carbon, which is within the range of values that one would expect of typical axial-axial <sup>3</sup>J<sub>HH</sub> coupling within a conformationally rigid cyclohexane skeleton when presented as chair form. From there, COSY and HSQC assisted in assigning the <sup>1</sup>H and <sup>13</sup>C signals. By process of elimination, we can also assign other <sup>1</sup>H and <sup>13</sup>C signals that correspond to alcohol **42a**.



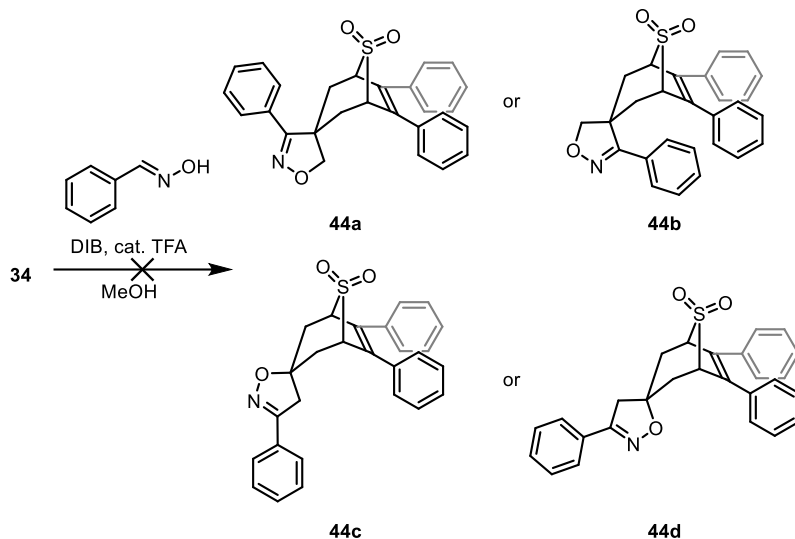
Scheme 29. Ozonolysis of terminal alkenes and subsequent reduction of ketones

Based on our results, we hypothesized that delivery of the hydride source via the concave face was unfavorable as the two phenyl groups introduced significant steric congestion. We also tried to perform hydroboration of the diaryl alkene<sup>167</sup> and obtained an equal mixture of diastereomers, compound **43a** and compound **43b**, as shown in Scheme 30. The possibility of other regioisomers were ruled out due to the lack of any observable signals that corresponded to the methyl resulting from anti-Markonikov hydride addition.



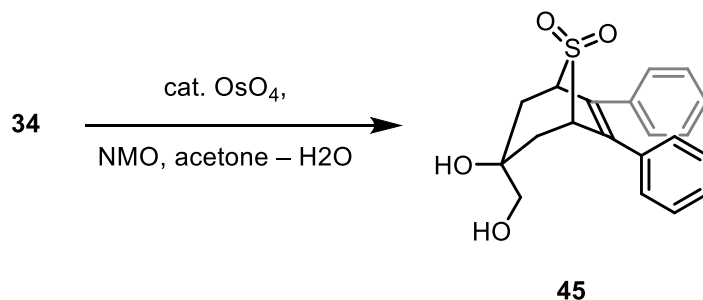
Scheme 30. Hydroboration of bicyclo[3.2.1]sulfone-containing alkenes

We were curious as to whether a 1,3-dipolar cycloaddition reaction with nitrile oxide species would be able to proceed to obtain either compound **44a** or **44b** as well as regioisomers **44c** and **44d**, as shown in Scheme 31. Sadly, under the prescribed conditions,<sup>168</sup> we were unable to collect anything but recovered **40**. Due to precedent report that indicates success of sterically hindered alkene substrates undergoing the desired [3+2] transformation, it may be that our current conditions are not optimized for said performance;<sup>169</sup> the strong acidic nature of trifluoroacetic acid (TFA) could result in degradation of compound **40** prior to undergoing the desired transformation.



*Scheme 31. Attempted dipolar [3+2] cycloaddition of bicyclo[3.2.1]sulfone-containing compounds using in situ generated nitrile oxides.*

Another method of regioselective functionalization of the terminal alkene was by dihydroxylation using catalytic amount of osmium tetroxide ( $\text{OsO}_4$ ): the tetra-substituted olefin of compound **34** did not react and instead we obtained compound **45** as a single diastereomer, as shown in Scheme 32.

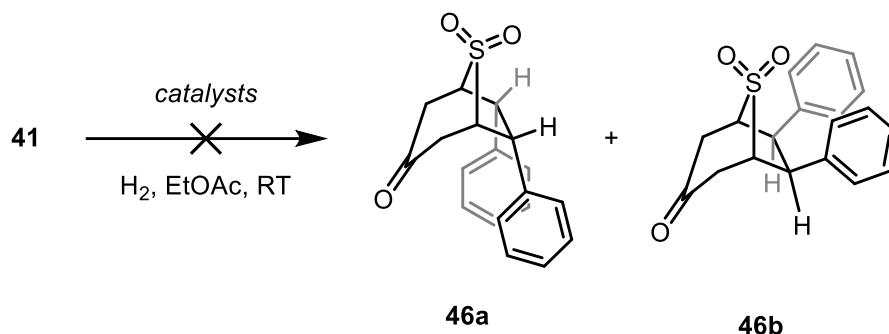


75% yield

*Scheme 32. Regioselective dihydroxylation of bicyclo[3.2.1]sulfone-containing compound.*

In theory, stereoselective hydrogenation could be performed on the tetra-substituted olefin using ketone **41** as the substrate.<sup>170</sup> Attempts to transform into compound **46a** or **46b** were futile using catalytic amount of Pd on carbon, as shown in Scheme 33. We recovered starting material even with up to 500 psi of hydrogen gas. Usage of different Pd sources such as Pearlman's catalyst did not improve the situation. Switching to different transition-metal such as Pt results in cleavage of the C-SO<sub>2</sub> bond. It is currently unknown whether the decomposition pathway proceeds via direct insertion

of Pt into the C-SO<sub>2</sub> bond, or perhaps via initial  $\pi$ -coordination of transition metals to the tetra-substituted olefin, followed by subsequent formation of  $\pi$ -allyl complex leading to sulfone cleavage. As such, we had to temporarily abandon the hydrogenation idea.



*Scheme 33. Attempted hydrogenation of tetra-substituted diaryl alkene region of bicyclo[3.2.1]sulfones.*

Arguably, many more robust chemical reactions can be used to functionalize the alkene region (and perhaps the allylic region), but we aimed to be more ambitious. Furthermore, we were concerned that since all synthesized compounds contained a stilbene moiety, it would be hard for us to assess well-defined structure–activity relationships. It would therefore be helpful to have access to a broader range of different substituents around the bicyclic core, and we therefore desired a simpler bicyclo[3.2.1]sulfone-containing scaffold in order to achieve this goal—for the simple reason that it's often easier to *add* functionality to a relatively simple scaffold than it is to take it away from a more complex one.

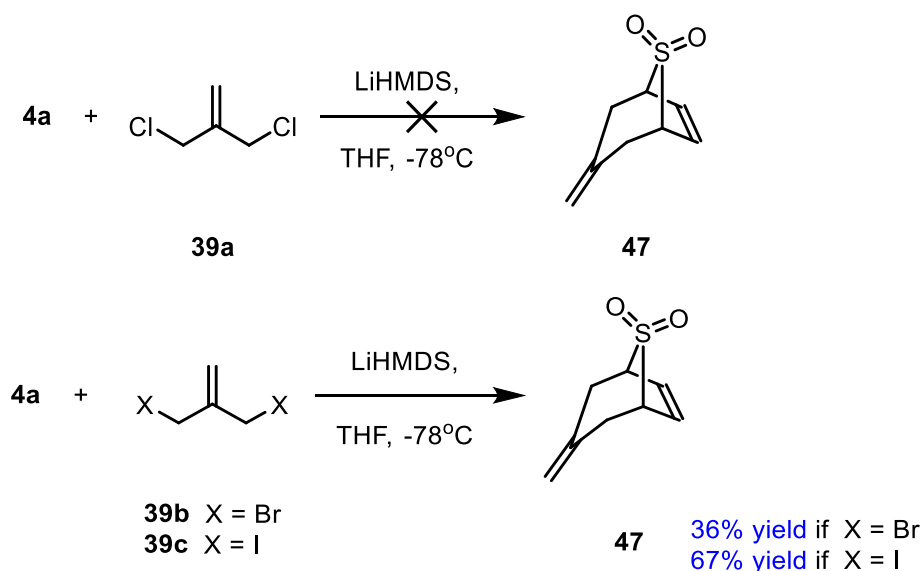
In conclusion, we realized that the approach outlined in this Chapter is very limited: the bicyclo[3.2.1]sulfone-containing molecules from tandem 1,2-addition/ anionic oxy-Cope cascade were difficult to functionalize, and already contained too many substituents. In the next Chapter, a route to alternative bicyclo[3.2.1]sulfone-containing molecules is presented. This was based upon a simpler double-nucleophilic substitution sequence, and allowed for much greater success in functionalization.

## Chapter 3 – Functionalization of Simpler Bicyclo[3.2.1]Sulfone-Containing Scaffold.

All compound syntheses, analysis and characterization of data was performed by C. H. Andy Un. Dr. Tyler Trefz and Dr. Ori Granot collected the HRMS data.

### Chapter 3.1 Oxidation of Chou-type Bicyclic Sulfones.

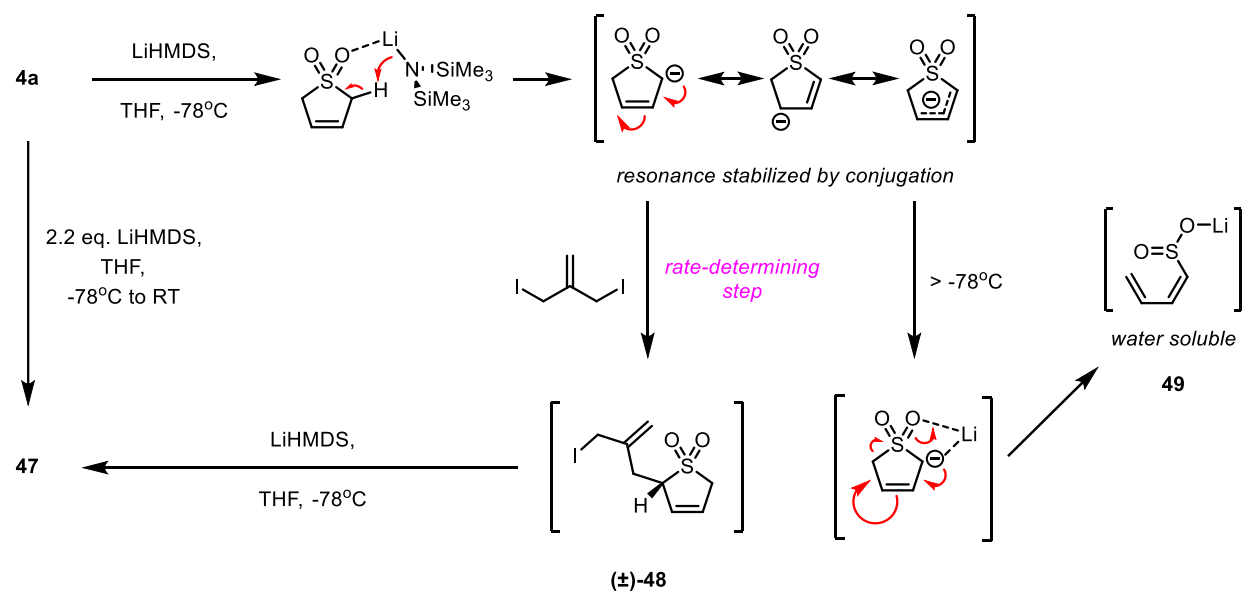
As mentioned previously, we sought simpler bicyclo[3.2.1]sulfone-containing building blocks, which would allow for a greater degree of functionalization. This strategy would not only permit the generation of more analogues in a rapid manner, but would also allow us to obtain greater vector control in probing three-dimensional space. To that end, we looked towards the original molecule **47** that Chou and coworkers described. Replication of their procedure yet without the use of carcinogenic HMPA afforded us crude sulfone **47** in relatively high purity. Similar to our screening of suitable electrophiles for the synthesis of sulfone **40**, we realized that only dibromide **39b** and diiodide **39c** were compatible to yield sulfone **47** in moderate to good yield, with isolated yields of 34% and 55% respectively, as shown in Scheme 34. This shows that electrophilicity of the dihalide is crucial for formation of Chou-type sulfone **47**. The diiodide **39c** was generally prepared freshly before being subjected to Chou's annulation method, as degradation was observed within one week despite storage in a  $-20^{\circ}\text{C}$  freezer and away from light.



Scheme 34. Formation of compound **47** using different dihalide species as the electrophile.

However, crude  $^1\text{H}$  NMR revealed the presence of the desired bicyclo[3.2.1]sulfone-containing product **47**, as well as unreacted diiodide **39c**. Although flash column chromatography is capable of purifying product **47** for later diversification, this issue is non-trivial for future scale-up purposes. Initially, we tried decreasing the amount of reaction solvent – THF – as our initial hypothesis was that the rate of nucleophilic displacement was too slow, and therefore increasing the concentrations of both reagents may assist in the initial bimolecular reaction step. However, the situation did not improve. Precipitate formation was noticeable as more LiHMDS was gradually added to the reaction flask during scale-up synthesis of sulfone **47**, which was presumably the formation of LiBr from double nucleophilic substitution of sulfone **4a**.

It is known that upon lithiation of the  $\alpha$ -position of **4a**, the lithiated intermediate is unstable above cryogenic temperature of  $-78^\circ\text{C}$  and undergoes fragmentation to generate sulfinate salt **49**, as shown in Scheme 35.<sup>171</sup> It may be possible that the sulfinate salt **49** is washed away during workup, hence why we could not observe the presence of unreacted butadiene sulfone.



Scheme 35. Mechanism of how compound **47** is formed, as well as possible fragmentation pathway.

To remedy this issue, we speculated that perhaps better heat dissipation during the presumably exothermic deprotonation step can be a solution; indeed, by adjusting to a slow addition of LiHMDS into the reaction mixture, we obtained an isolated yield of 65% on a multigram scale. Although Chou's original synthesis employs the addition of

4.0 equiv. of carcinogenic HMPA presumably to alter the aggregation state of organolithium species in solution, we did not see the value of introducing polar aprotic additives in the reaction mixture as the isolated yield of sulfone **47** drastically lowered to 8% yield upon changing the solvent composition from THF to a mixture of 1:1 THF:DMPU. These results may suggest that the aggregation states can be influential for optimal conformational alignment between the electrophilic carbon center and sulfone ( $\pm$ )-**48** during formation of the bicyclic sulfone **47**, although we are currently unsure if the aggregation state of delocalized lithiated **4a** anion is important for the initial nucleophilic substitution step and/or perhaps overall formation of bicyclic sulfone **47**. Nonetheless, we have established optimal conditions for obtaining sufficient quantities of the Chou-type sulfone **47** on a decagram scale that may be scalable in larger batches.

With the material in hand, we decided to chemically modify the alkene regions in a chemoselective manner: relative  $\pi$ -bond reactivity between a 1,1-disubstituted exocyclic olefin (such as compound **50**) and the 1,2-disubstituted internal olefin of a bicyclic system (such as compound **51**) can be distinguished, as Mayr and coworkers have described the reaction rates of these respective alkenes to differ by approximately 1000 times.<sup>172</sup> As we noted that the Mayr's parameter is evaluated towards electrophilic atomic centers,<sup>173</sup> we rationalized that reactions that employ alkenes as nucleophiles may serve as an initial point of investigation for chemoselective functionalization of the Chou-type bicycle [3.2.1]sulfone **47**, as indicated in Figure 15.

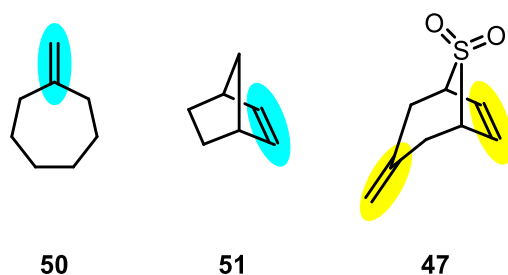


*Figure 15. Comparison of alkenes that demonstrate the highest reactivity as described by Mayr and coworkers. Highlighted in neon blue are the most reactive moieties in corresponding molecules **50** and **51**, while yellow highlighted regions indicate possible reactivity moieties with unknown preferences in compound **47**.*

Beyond this, we postulated that perhaps the relative position of the sulfone moiety can affect  $\pi$ -reactivity of either the 1,1-disubstituted exo-cyclic olefin or the 1,2-disubstituted internal olefin via inductive effects and/or electronic repulsion. Furthermore, allylic carbons are present in the framework, which offers activated C–H bonds that may prove to be versatile in selective functionalization.<sup>174</sup> Beyond that, although the bridgehead carbons appear to be sterically encumbered, it is highly likely that the electron-withdrawing properties of sulfone moieties can help stabilize any proximal carbanion formation,<sup>175</sup> which we can capitalize upon by employing different electrophiles of various three-dimensional shapes. Thus, it appears that the Chou-type bicyclo[3.2.1]sulfone-containing framework is poised for a fundamental investigation, where one should question whether chemoselective and regioselective functionalization of the carbon framework is possible, as indicated in Figure 16. If we can achieve this, then not only will the novel functionalized products that incorporate the bicyclo[3.2.1]sulfone-containing scaffold be generated, but also this can help assist in structure-activity relationship analysis during our lofty goal of eventually deploying  $sp^3$ -rich sulfone-containing small molecules for further understanding of biological mechanisms and development of impactful therapeutics.

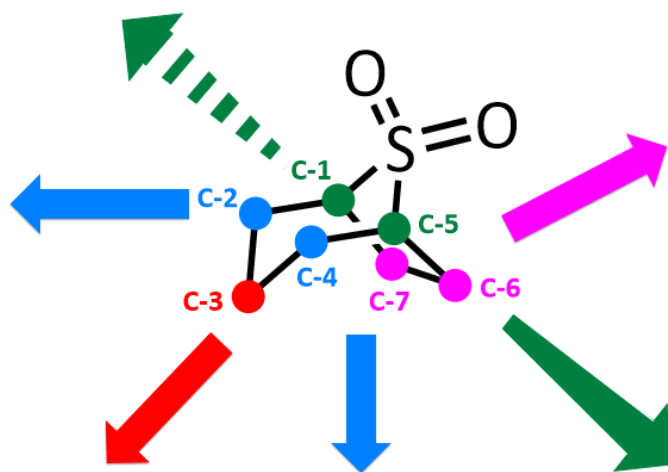
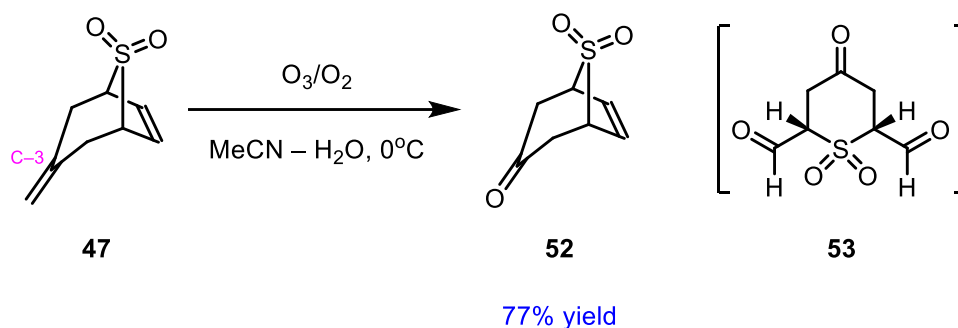


*Figure 16. Grand scheme of site-selective functionalization of bicyclo[3.2.1]sulfone-containing frameworks. Coloured arrows indicate the direction of vectors that can be theoretically reached if the carbons with corresponding colours can be decorated.*

As described by Criegee and coworkers,<sup>176</sup> the fundamental mechanism of ozonolysis requires the electrophilic ozone generated to approach with

an alkene in a bimolecular manner, leading to the formation of a 1,3-dipolar cycloadduct prior to fragmentation. Alkenes with increasing substitution may exhibit greater hyperconjugative stabilization of the polarized transition state,<sup>177</sup> which we further anticipated to be beneficial for our substrate: the 1,1-disubstituted exo-cyclic olefin was expected to react preferentially over the 1,2-disubstituted internal olefin. Indeed, *in situ* generated ozone reacted exactly as we predicted, yielding 66% of ketone **52** upon reductive workup using dimethyl sulfide, as shown in Scheme 36.

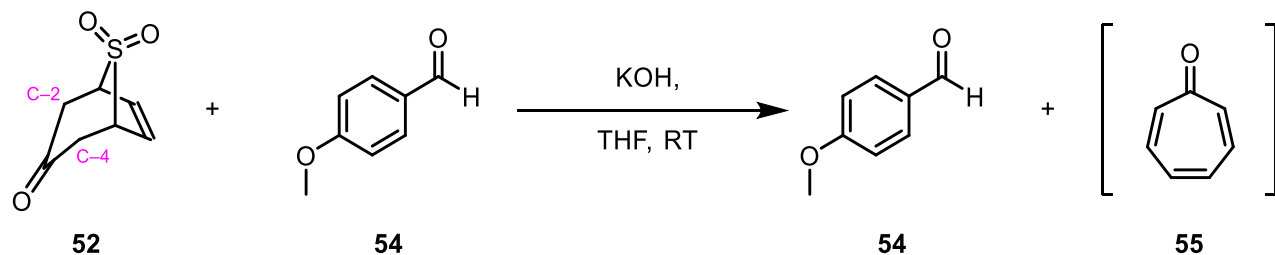


Scheme 36. Ozonolysis of compound **46**. Compound in brackets are not isolated but observed.

A binary solvent mixture of water and water-miscible organic solvents such as acetonitrile has been used as greener alternative to the conventional reaction environment of ozonolysis protocols,<sup>178</sup> where large amount of environmentally hazardous dichloromethane was needed; small amount of water content can also be used to quench the ozonides generated *in situ*, further making the process safer to working personnel. After testing the procedures described by Cochran, we observed comparable results.<sup>179</sup> Furthermore, we have also observed that depending on the feeding rate of ozone generated *in situ*, it is possible to perform oxidative ring-opening of the internal olefin. Therefore, close monitoring of the reaction progress was crucial to avoid overreaction leading to sulfone **53**; typically, at a feeding rate of 7L per minute of ozone, the reaction reaches complete conversion approximately after 90 min, with the assistance of TLC for reaction monitoring. Thus, we have successfully optimized the synthetic steps leading to ketone **52**.

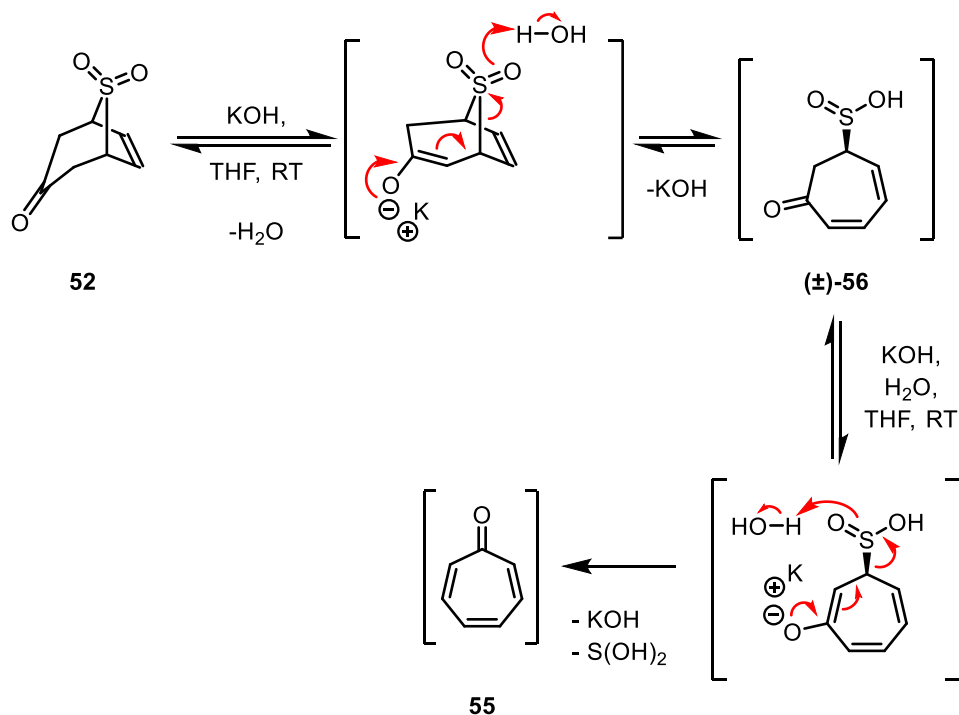
With ketone **52** in hand, we envisioned that the carbonyl moiety can serve as a versatile functional group handle, especially on forming new chemical bonds at either the C-2 or C-4 position. Aldol reactions were described by Majewski and coworkers on

analogues of ketone **52** (albeit the sulfone moiety was replaced with a thioether functional group instead),<sup>180</sup> therefore we had reason to believe that sulfones **41** or **52** would be capable of undergoing similar transformations. However, attempts of performing aldol condensation was not successful, and we only recovered the aldehyde component **54**, as shown in Scheme 37.



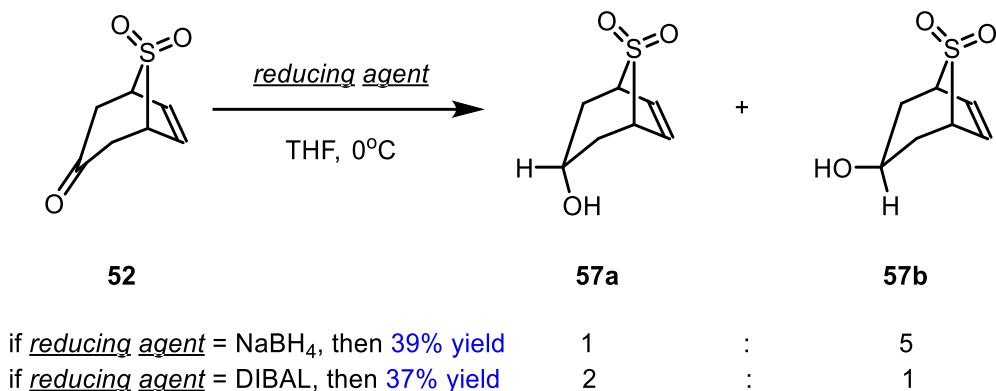
*Scheme 37. Failed attempt to perform aldol-condensation between sulfone **51** and aldehyde **53**.*

Interestingly, purification of ketone **52** via flash column chromatography using silica gel as the stationary phase failed, as we were also unable to recover any trace of ketone **52**. We speculate that the acidic nature of silica gel led to degradation of ketone **52**; however, even upon treating the silica gel with 5% v/v Et<sub>3</sub>N, recovery of ketone **52** was still not feasible. Thus, we have reason to believe that no matter the pH change, tautomerization of the carbonyl region will lead to  $\beta$ -elimination of the sulfone moiety to relieve ring strain, thus triggering a decomposition pathway that is undesirable, as shown in Scheme 38.<sup>181</sup> Literature precedent of sulfones acting as leaving groups exists,<sup>182</sup> although in our case, we believe that the identity of the nucleofuge is sulfoxylic acid (sulfur in +2 oxidation state). This is known to be an unstable species, and most likely oxidizes under aerobic conditions to gaseous sulfur dioxide (sulfur in +4 oxidation state).



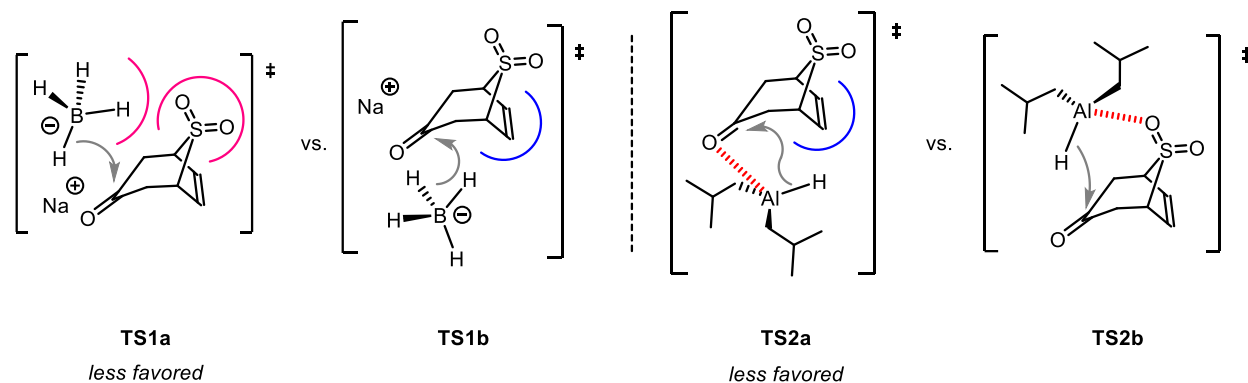
*Scheme 38. Postulated  $\beta$ -elimination pathway of compound **52** leading to the extrusion of sulfone moiety.*

Fortunately, reduction of the carbonyl afforded isolation of both diastereomers of alcohol **57** (i.e. alcohols **57a** and **57b**) in a 1:5 ratio, as shown in Scheme 39. Rapid bubbling was observed as soon as the reducing agent  $\text{NaBH}_4$  was transferred into the reaction flask, despite the use of freshly distilled anhydrous THF as the reaction solvent. Furthermore, a nauseous odour originated from the reaction vial as soon as the reduction proceeded. Thus, it may be possible that the exothermic process of generating a C-O bond from a C=O bond of ketone **52** triggered retro-cheletropic rearrangement of ketone **51**, thereby releasing foul sulfur dioxide gas that lingered within the workspace.<sup>183</sup> Note that the retro-cheletropic rearrangement under thermal conditions is a fundamentally different decomposition pathway to the  $\beta$ -elimination reaction described above, and occurs under different reaction conditions. Further dilution of the reaction via addition of more THF did not help dissipate the amount of heat transferred, nor did performing the reduction in an ice-water bath, as low yields of alcohols **57a** and **57b** were consistently obtained.



Scheme 39. Different regioselectivity in carbonyl reduction of compound **51** via different metal hydrides.

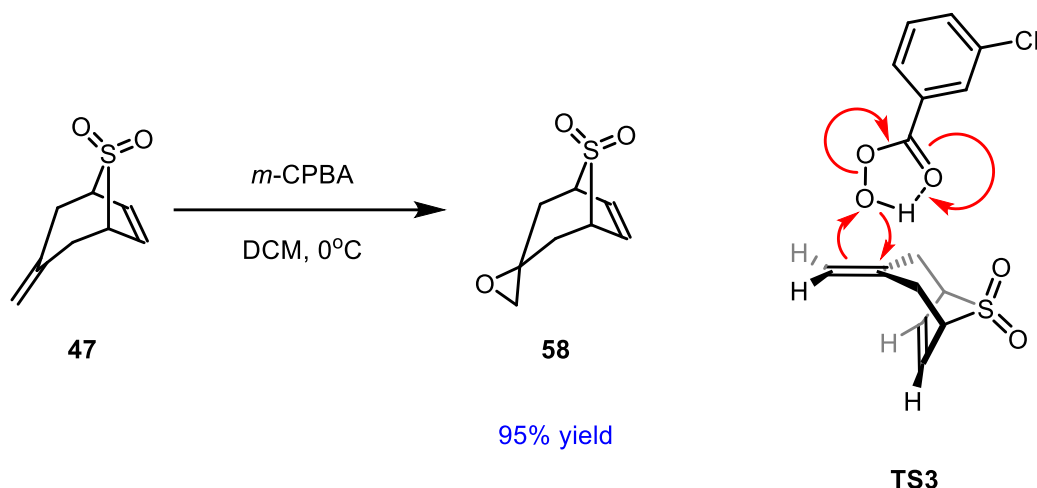
As NaBH<sub>4</sub> was our initial choice of reducing agent, we pondered whether screening alternative choices of both cations and anions would assist us in understanding what factors can influence the diastereoselectivity and perhaps isolated yields of alcohols **57a** and **57b**. Despite using LiBH<sub>4</sub> and Zn(BH<sub>4</sub>),<sup>184</sup> we did not see any major improvement in diastereoselectivity nor isolated yield. Thus, we concluded that the cations were not a primary factor.<sup>185</sup> Interestingly, changing the reducing agent to DIBAL-H lead to an observed reversal trend of diastereoselectivity: we isolated alcohols **57a** and **57b** in a 2:1 ratio. It is possible that the monomeric DIBAL-H coordinates with the oxygen atoms of the sulfone moiety, thereby directing the hydride transfer via the convex face of the scaffold i.e. **TS2b**. On the other hand, the tetrahedral borohydride anion is incapable of interacting with the sulfone moiety in such manner; instead, electronic repulsion between the two results in an energetically unfavorable process if the hydride transfer were to occur via the convex face i.e. **TS1a**, as shown in Scheme 40. This type of phenomenon was showcased by Schomaker and coworkers in their crusade to functionalize bicyclic substrates based on their methodology of Rh-catalyzed [4+3] cycloadditions of aziridines.<sup>186</sup>



*Scheme 40. Postulated mechanistic differences resulting in differing diastereoselectivity in reduction of ketone **52** using different metal-hydrides.*

We sought to confirm whether arguments of steric repulsion were affirmative, thus leading to our use of L-selectride; however, we did not obtain any material of interest, nor did we recover any starting material **52**. Furthermore, evaluation of the crude reaction mixture afforded none of the diagnostic protons of the internal alkene. As L-selectride can be considered as a “softer” hydride-transferring agent due to its prominent use in 1,4-reduction of  $\alpha,\beta$ -unsaturated carbonyl derivatives,<sup>187</sup> it may not be surprising to surmise that hydride deliver to the internal olefin may trigger elimination of the sulfone moiety through an  $S_N2'$  pathway.<sup>188</sup> Further investigations may be warranted.

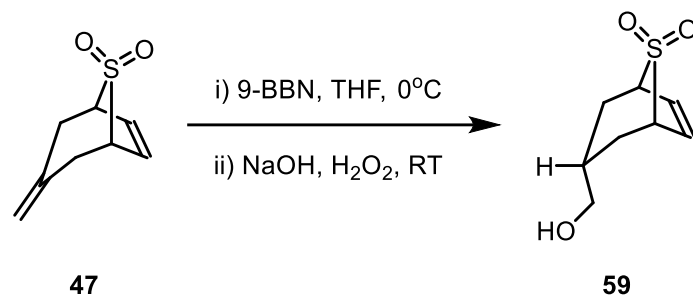
As we were able to showcase that the two alkenes can participate in chemical functionalization with differing reactivities, we wanted to test further reactions in order to derive different building blocks. Epoxidation using *m*CPBA was successful and epoxide **58** was generated in 96% isolated yield as a single diastereomer, as shown in Scheme 41. Increasing the concentration of both *m*CPBA and alkene **47** to 1.0 M lead to complete conversion into epoxide **58**.



Scheme 41. Epoxidation of sulfone **47** (left) and the “butterfly” mechanistic transition state (right).

It was noted that the “butterfly” transition state **TS3** is key towards the epoxidation,<sup>189</sup> since when we added saturated  $\text{NaHCO}_3$  during the reaction, only 12% of epoxide **58** was obtained. Presumably, *m*CPBA is deprotonated in situ and thus the loss of hydrogen-bonding interaction during the “butterfly” transition state leads to low conversion. It is currently unknown if hydrogen-bonding between *m*CPBA and the sulfone moiety is possible and whether it could assist in regiocontrol;<sup>190</sup> if so, the approach of *m*CPBA towards the concave face will not be determined based on the argument of steric congestion solely.

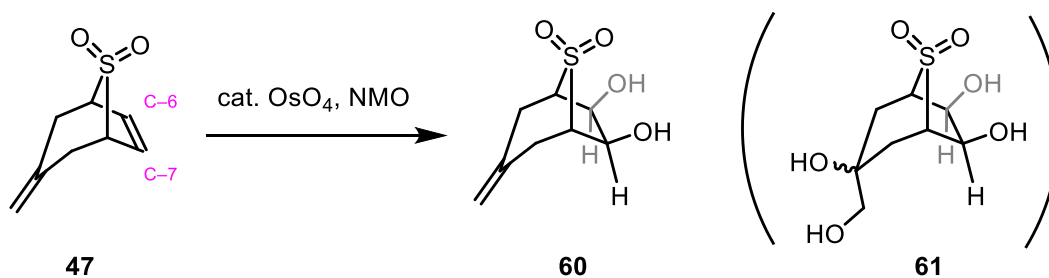
Hydroboration using sterically bulky 9-borabicyclo[3.3.1]nonane (9-BBN) afforded alcohol **59** in 30% isolated yield as a single region- and diastereomer, as shown in Scheme 42. Presumably, the sterically encumbered 9-BBN approaches the alkene from the convex face in order to avoid steric clash with the relatively congested concave face of the bicyclo[3.2.1]scaffold.<sup>191</sup> However, we noted that acid-catalyzed hydration was not successful, as we noticed decomposition of alkene **47**; in an effort to generate the Markonikov product, we pondered the possibility of performing Mukaiyama hydration,<sup>192</sup> but instead we were only able to recover alkene **47**. All in all, we have demonstrated that in the presence of electrophilic reagents, the 1,1-disubstituted alkene of alkene **47** would react preferentially, generating versatile building blocks where the C-3 position of the bicyclo[3.2.1]sulfone scaffold is functionalized.



57% yield

*Scheme 42. Regioselective and diastereoselective hydroboration of sulfone 46.*

Interestingly, as we turn our attention towards formation of diols via osmylation, unexpected results were obtained. Based on aforementioned difference in olefin reactivity from Mayr's nucleophilicity scale, we expected that the exo-olefin to participate in the reaction. Serendipitously, we were able to obtain diol **60** as a single regioisomer instead, as shown in Scheme 43.



50% yield

*not observed*

*Scheme 43. Unexpected results from dihydroxylation of compound 47 using catalytic osmium tetroxide.*

We found this finding to be extraordinary due to the following reasons:

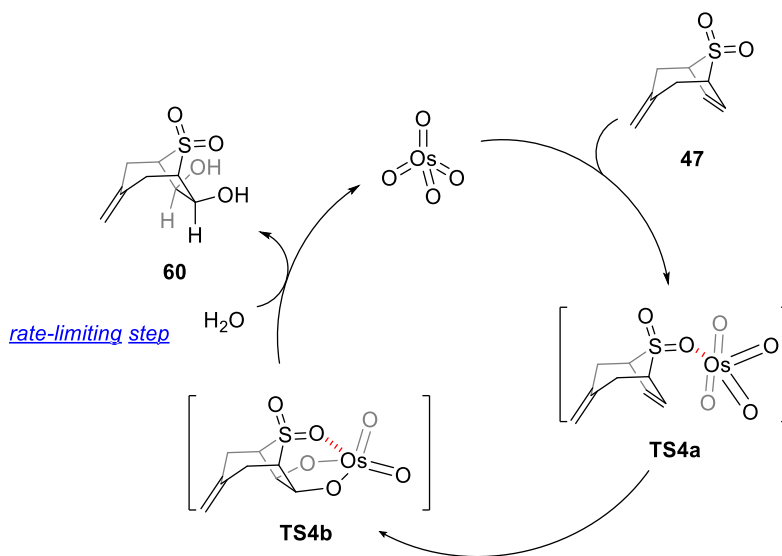
1. The reaction time required to achieve complete conversion was at least 48 hours, which was deemed to be significantly longer compared to literature precedent of substrates with similar framework undergoing similar transformations.
2. Minor improvements in isolated yield was obtained as we screened different catalyst loading, as shown in Table 1. Usage of either  $\text{K}_2[\text{OsO}_4(\text{H}_2\text{O})_2]$  or  $\text{OsO}_4$  in water as the osmium source did not yield any significant difference.

Table 1. Tabulation of varying catalyzing loading of OsO<sub>4</sub> and their corresponding yield of sulfone **60**.

Catalyst loading (mol %)	1	3	4	5	7
Yield (%)	22	28	30	28	23

3. Even as we increased the stoichiometry of terminal oxidant N-methylmorpholine N-oxide (NMO), overreaction was not observed i.e. we did not observe the appearance of tetra-ol **61**. Instead, we were only able to obtain diol **60**.

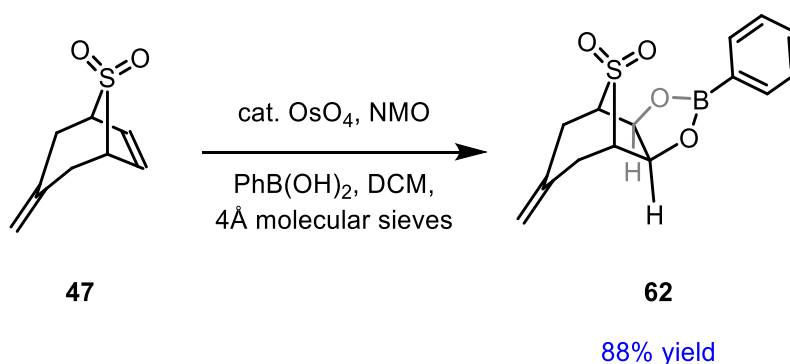
Based on these observations, we offer the following explanations: it is highly likely that the oxygen of the sulfone in our framework interacts with the osmium center in OsO<sub>4</sub> i.e. **TS4a**, thereby directing the transformation to occur in a regioselective manner. Literature precedent has demonstrated that late transition-metal centers can interact with analogous DMSO to form either S-adducts or O-adducts, with the former being more prevalent and equilibrium favored.<sup>193</sup> The aforementioned coordination between bicyclic sulfone **47** and OsO<sub>4</sub> is kinetically favorable, as we did not observe any signs of exo-olefin participating in osmylation regardless of the catalyst loading nor the stoichiometry of NMO used. Furthermore, the [3+2] adduct is stable enough to temporarily resist hydrolysis and subsequent liberation of diol **60**, which may explain the prolonged reaction time required as well as absence of tetraol **61** in the presence of excess NMO, as shown in Scheme 44.



Scheme 44. Simplified catalytic cycle illustrating how compound **60** is formed. The rate-determining step of the mechanism is postulated to be the hydrolysis of **TS4b**.

Narasaka and coworkers have reported a one-pot synthesis for transforming olefins into boronate esters.<sup>194</sup> The protocol essentially combines the essence of dihydroxylation and diol-boronate exchange within a single reaction vessel. Given that metathesis of diols between osmic esters and arylboronic acids occurs during the Narasaka reaction,<sup>195</sup> we anticipate that the faster reactivity of this protocol may be an alternative method to not only speed up reactivity of osmylation in our campaign to transform bicyclic sulfone **47**, but also to yield novel boronic ester **62** in a rapid manner.<sup>196</sup> Indeed, using reaction conditions described by Sharpless and coworkers,<sup>197</sup> we were able to obtain boronic ester **62** in excellent yield, as shown in Scheme 45. Furthermore, we observed that the reaction time required to achieve complete conversion is shortened to 24 hours instead, which serve to augment our hypothesis of facile transmetallation as a method to improve slow hydrolysis of osmic ester **TS4b**.

One interesting note is that presence of trace amounts of water during the transformation led to a mixture of diol **60** and boronic ester **62**. It is possible that the oxygen of the sulfone is geometrically incapable of coordinating the vacant  $\pi$ -orbital of the boron center, thereby instead of yielding a hydrolytically stable tetrahedral boronate salt, we obtained a neutral tri-coordinate boronic ester which is susceptible to hydrolysis. Addition of 4Å molecular sieves during the Narasaka reaction was able to circumvent this issue, and also assisted in product purification since residual osmium metal was coated on the surface of the molecular sieves.



*Scheme 45. One-pot dihydroxylation/boronic ester formation from compound **46**.*

This sulfone-chelation phenomenon was once again demonstrated when stoichiometric amounts of Pd(PPh<sub>3</sub>)<sub>2</sub>Cl<sub>2</sub> and bicyclic sulfone **47** were dissolved in C<sub>6</sub>D<sub>6</sub>. Interestingly, small upfield changes in chemical shifts in <sup>1</sup>H NMR were observed, which

are demonstrated in Figures 16, and 17. We rationalized that perhaps the upfield shifts of these signals are attributed from metal-ligand donation of the more electron dense Pd-center as two tris-aryl phosphine ligands are capable of forming two  $\sigma$ -bonds with the Pd-center.

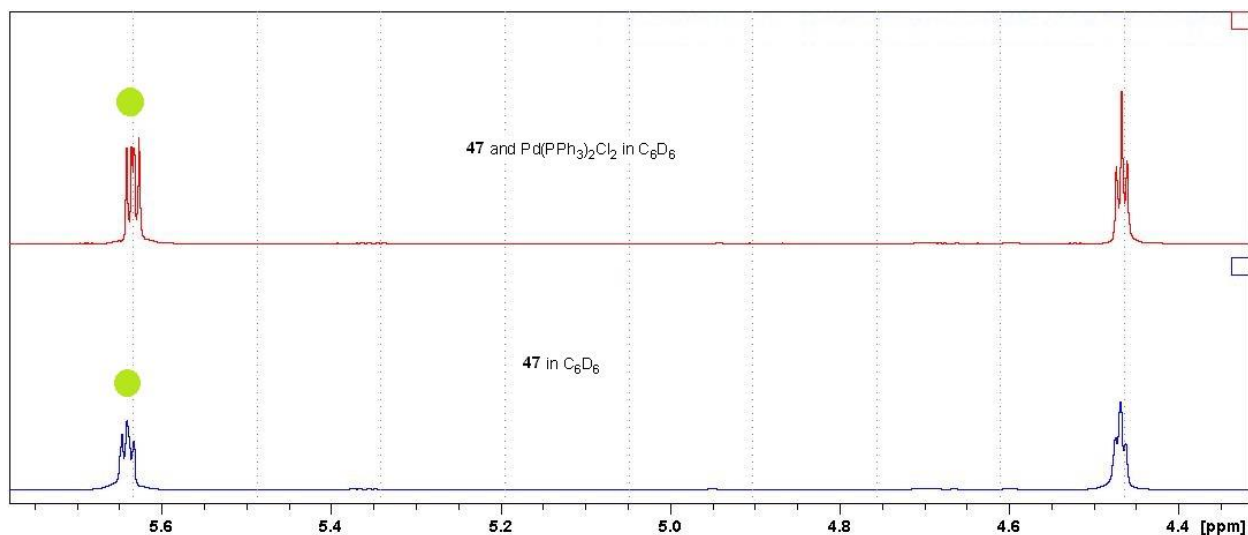


Figure 17. Magnification of  $^1\text{H}$  NMR reactivity monitoring spectrum of compound **46** and  $\text{Pd}(\text{PPh}_3)_2\text{Cl}_2$ . Highlighted in light green are diagnostic peaks corresponding to alkenyl protons of the 1,1-disubstituted *exo*-cyclic olefin.

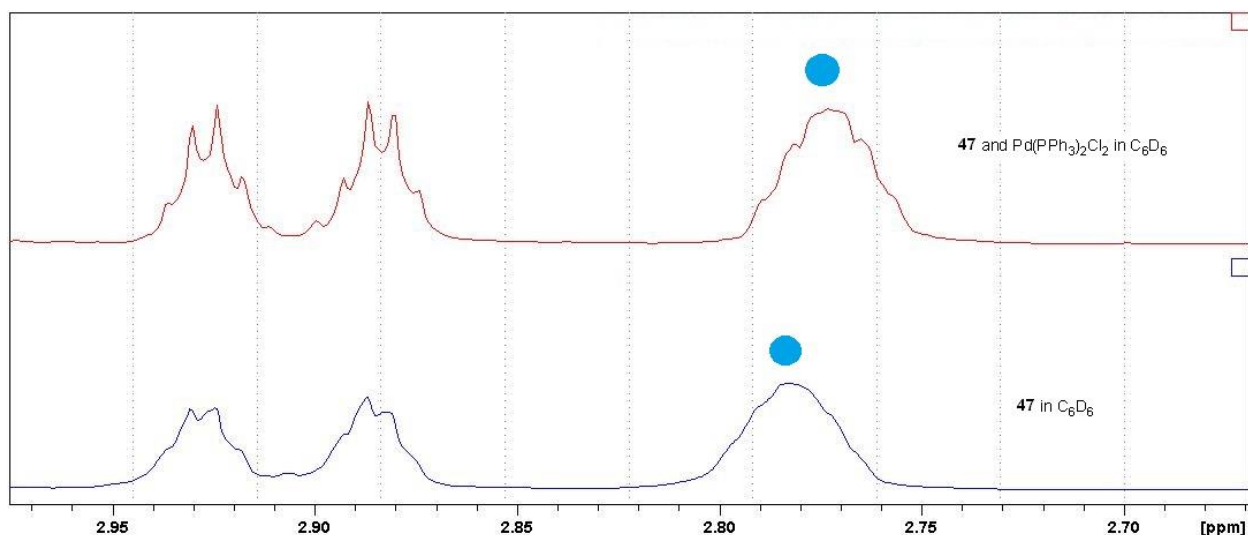
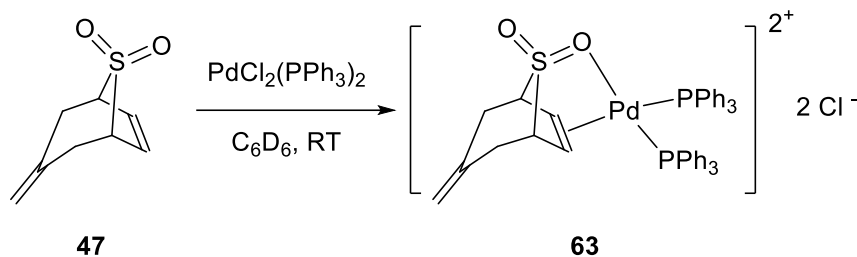


Figure 18. Magnification of  $^1\text{H}$  NMR reactivity monitoring spectrum of compound **46** and  $\text{Pd}(\text{PPh}_3)_2\text{Cl}_2$ . Highlighted in light green are diagnostic peaks corresponding to  $\text{C}_{\text{sp}^3}$  protons of bridgehead position i.e. C-1 or C-5 positions of the bicyclo[3.2.1]sulfone-containing framework.

Note that these signals correspond to the internal olefin of bicyclic sulfone **47**, yet the exocyclic olefin region demonstrated no change in either chemical shifts nor did it exhibit different coupling patterns. Thus, we can assume that a chelated adduct is formed from  $\text{Pd}(\text{PPh}_3)_2\text{Cl}_2$  to both the oxygen atom of the sulfone moiety and the internal olefin i.e. compound **63** as shown in Scheme 46.



*Scheme 46. Weak bidentate chelation of sulfone **46** with Pd(II) species.*

Salt formation was observed, which we attribute to the displacement of chloride anions resulting from the aforementioned chelation. New  $^{31}\text{P}$  signals occurred at  $\delta$  21.9 ppm and  $\delta$  13.6 ppm as soon as both substrates were dissolved into the solution, as shown in Figure 19; as the signals persisted over time, we attribute to the possibility of a new intermediate resulting from coordination geometry change from the square planar ( $\text{D}_{4h}$ )  $\text{Pd}(\text{PPh}_3)_2\text{Cl}_2$  to the unstable chelated adduct in solution.<sup>198</sup>

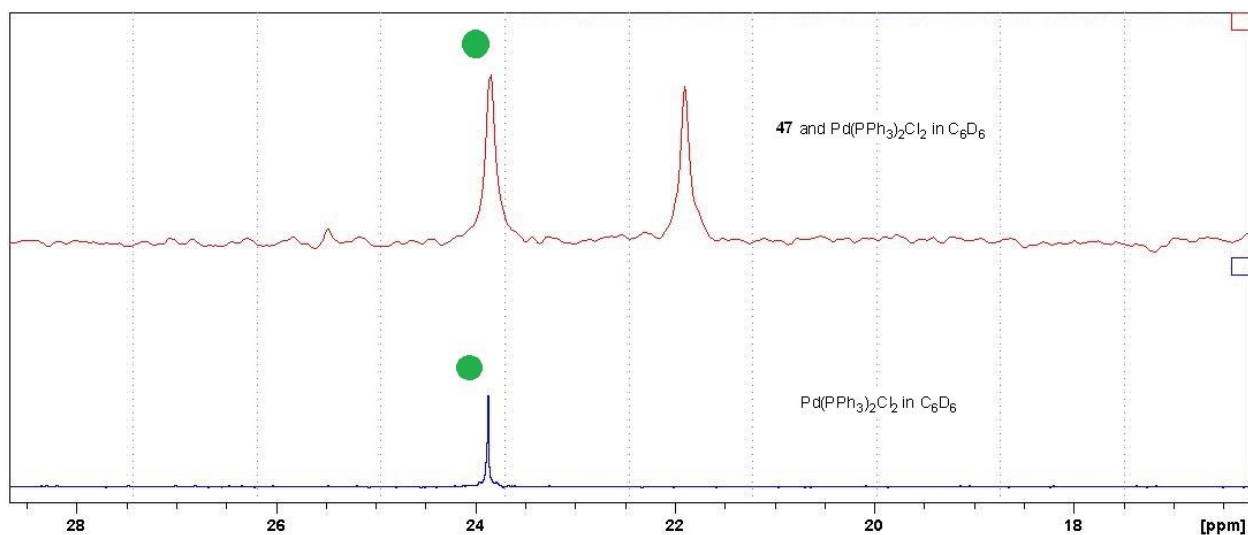


*Figure 19.  $^{31}\text{P}$  NMR reactivity monitoring spectrum of compound **47** and  $\text{Pd}(\text{PPh}_3)_2\text{Cl}_2$ . Highlighted in green are diagnostic peaks corresponding to  $\text{Pd}(\text{PPh}_3)_2\text{Cl}_2$ .*

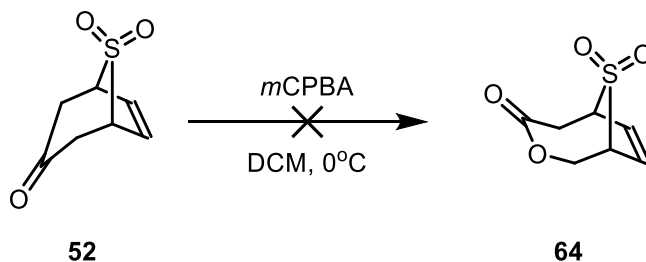
Despite not fully understanding the elementary steps relating to how the chelation phenomenon occurs, these results further augment our hypothesis of

regioselective chelation between bicyclic sulfone scaffolds and various transition-metals.

With that said, we were able to showcase the potential of functionalization of the bicyclic sulfone framework at selective positions using chemoselective methodologies that results in possibly regioselective outcomes.

### Chapter 3.2 Expanding Chemical Space of Bicyclo[3.2.1] Sulfones

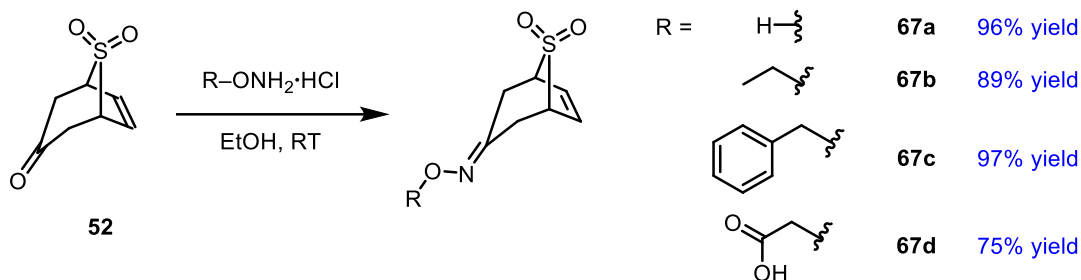
To further functionalize ketone **52**, we pondered whether a Baeyer-Villiger rearrangement could be performed; <sup>199</sup> particularly, we chose *m*CPBA as the nucleophilic oxidant <sup>200</sup> such that the electrophilic ketone can preferably react instead of the nucleophilic internal alkene. Unfortunately, we were only able to recover alkene **47**, and no signs of the desired product **64** was observed as shown in Scheme 47. We hypothesized that hydrogen-bonding between the oxygen of the sulfone bridge and the acidic *m*CPBA may hinder the desired transformation, since presumably hydrogen-bonding between the acidic *m*CPBA and the ketone moiety is necessary in order for the desired transformation to proceed.<sup>201</sup>



Scheme 47. Failed attempt at Baeyer-Villiger oxidation of compound **51**.

Fortunately, we were able to form oxime **67a** in 50% yield using hydroxylamine hydrochloride with ketone **52**, as shown in Scheme 48.<sup>202</sup> The fact that oxime formation was possible under ambient temperature and without the introduction of external sources of acid was encouraging to us, as we envisioned that substitution at the oxygen of hydroxylamine of oxime **67a** could lead to better coverage of three-dimensional space at a certain vector. To that end, we attempted to see if the alcohol can participate in phosphine-mediated etherification of methyl acrylate,<sup>203</sup> with the hopes that the theoretical ester can lead to further derivatization. However, we did not observe such transformation, and instead recovered oxime **67a**. We also attempted dehydration of the

alcohol moiety of oxime **67a** with cyanuric chloride in order to induce a Beckmann rearrangement, but to no avail.<sup>204</sup> We reasoned that the oxygen of hydroxylamine **67a** was insufficiently nucleophilic to participate in the desired transformation.<sup>205</sup>

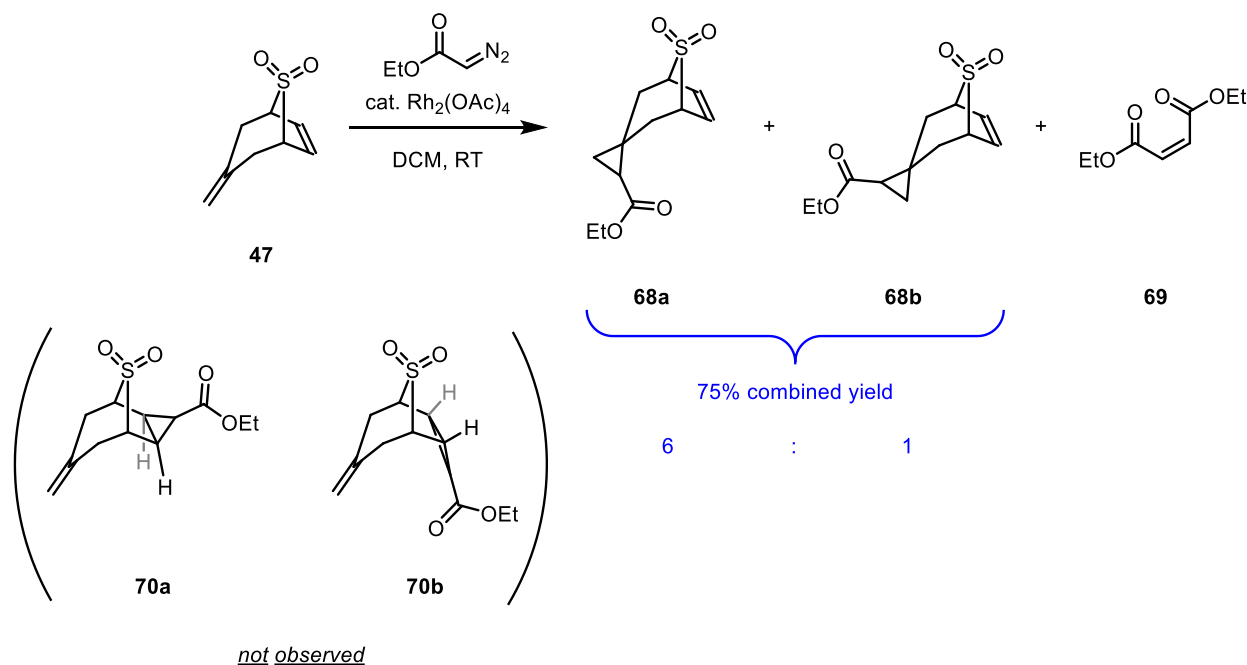


*Scheme 48. Various O-substituted oximes formed via condensation with sulfone **52**.*

Therefore, we sought to investigate whether O-substituted hydroxylamines were capable of undergoing condensation with ketone **52**. Indeed, using O-ethyl hydroxylamine hydrochloride and O-benzyl hydroxylamine hydrochloride under the same reaction conditions, we were able to obtain oxime **67b** and **67c** respectively. Both products were obtained in 89% yield and 97% yield respectively. Note that the reaction conditions required longer reaction time in order to achieve complete conversion, regardless of the stoichiometry of hydroxylamine hydrochloride salts, which we attribute to increasing steric hindrance. Oxime **67d** was also isolatable in 75% yield, which is encouraging to us since we were concerned about the stability of ketone **52** under acidic conditions. Based on the aforementioned results, perhaps the stability of the sulfone moiety in bicyclic substrates are highly dependent on pH, as we noted that recovery of sulfone **47** is possible despite submerging in glacial acetic acid over 48 hours.

We were interested to see if we could replicate an outcome similar to the aforementioned case of bicyclic sulfone **47** reacting with  $OsO_4$  in a regioselective manner via sulfone-guided directing. Currently many methodologies are known that convert alkenes of various kinds into functionalized cyclopropanes.<sup>206</sup> The presence of cyclopropanes in pharmaceutical drugs are considered to be beneficial due to improved metabolic stability and other pharmacokinetic properties;<sup>207</sup> as such, we anticipate that incorporation of cyclopropanes within our bicyclic sulfone scaffold will not only afford additional conformational restriction, but also direct functional groups along specific projection vectors that may be beneficial for interaction with protein surfaces. One of the

mildest methods of cyclopropanation involves transition-metal-catalyzed transformation between alkenes and activated diazo species.<sup>208</sup> We started our initial investigation by employing 5 mol% of  $\text{Rh}_2(\text{OAc})_4$  and 1.5 equivalent of commercially available ethyl diazoacetate, and we obtained the desired cyclopropanes **68a** and **68b** in 33% isolated yield, as shown in Scheme 49. Interestingly, beyond the occurrence of compound **69** which resulted from dimerization of ethyl diazoacetate, we did not observe diagnostic signals that corresponded to either compound **70a** or **70b** spectroscopically, as shown in Scheme 49.



*Scheme 49. Rh-catalyzed cyclopropanation of sulfone **47** to yield conformationally restricted products.*

Despite this exciting news, we faced many different obstacles, including optimization of the reaction conditions by varying catalyst loading, varying stoichiometry of ethyl diazoacetate, varying amount of solvent (DCM) in the reaction vessel, varying reaction temperature, and much more. After much extensive screening, the following was observed:

1. Optimal catalyst loading was determined to be at 5 mol% of  $\text{Rh}_2(\text{OAc})_4$ . Lower catalyst loading was achievable, but required significantly longer reaction time.
2. 8 equivalents of ethyl diazoacetate was required to achieve near-complete conversion (92.5%). Lower stoichiometry was not achievable, as

dimerization of ethyl diazoacetate in the presence of metal catalysts was far more rapid compared to cyclopropanation. However, stoichiometry of ethyl diazoacetate can be significantly reduced to 4 equivalents if slow addition of ethyl diazoacetate was performed i.e. addition rate of ethyl diazoacetate should be kept to 0.10mL/hr.

- The reaction can be performed at room temperature. Lower temperature (eg. 0 °C) did not appear to be beneficial in improving isolated yield or diastereomeric ratio. Higher temperature (eg. 40 °C) led to lower conversion of desired cyclopropanes **68a** and **68b**, and greater amount of dimerized product **69** to be formed.
- Lower amount of reaction solvent i.e. higher concentration of substrates appears to favor the formation of dimerized product **69**. Dilution appears to be beneficial for the formation of cyclopropanes **68a** and **68b**, and we deemed the ratio of 10mL of DCM for every mmol of bicyclic sulfone **47** to be the optimal concentration for our desired transformation to occur.
- Diastereomeric ratio maintained stagnant (3:1) despite any of the aforementioned changes.
- Usage of other transition-metals were explored, as shown in Table 2:<sup>209</sup> Pd(OAc)<sub>2</sub> did not afford any cyclopropanes **68a** and **68b** but instead we recovered bicyclic sulfone **47** and obtained dimerized product **69**. Cu(OTf)<sub>2</sub> appeared to afford higher diastereomeric ratio (~9:1), but at the cost of low conversion (9%).

*Table 2. Rh-catalyzed cyclopropanation of sulfone 47 to yield conformationally restricted products.*

<u>Catalyst</u>	<u>Combined conversion of 68a + 68b (%)</u>	<u>Diastereoselectivity (68a : 68b)</u>	<i>Note: all reactions were performed using a catalyst loading of 5 mol% and 4 equiv. of ethyl diazoacetate</i>
Rh <sub>2</sub> (OAc) <sub>4</sub>	60.00	2.99 : 1	
Pd(OAc) <sub>2</sub>	N/A		
Cu(OTf) <sub>2</sub>	8.97	8.76 : 1	

- Rh<sub>2</sub>(oct)<sub>4</sub> was deemed to be a more soluble catalyst compared to Rh<sub>2</sub>(OAc)<sub>4</sub>,<sup>210</sup> and we anticipated that usage of such transition-metal complex may assist in increasing surface area contact between substrates

and catalyst; however, no improvements in either substrate conversion, isolated yield, or diastereomeric ratio upon using the costlier  $\text{Rh}_2(\text{oct})_4$ .

Currently we have determined the optimal conditions for cyclopropanation of bicyclic sulfone **47** as the following: a reaction vessel was charged with 5 mol%  $\text{Rh}_2(\text{OAc})_4$ , bicyclic sulfone **47**, and DCM (10mL for every mmol of substrate **47**). Stirring of the reaction mixture was performed using a Teflon-coated magnetic stir bar; high revolution per minute (rpm) is encouraged; we usually try to aim for 750 – 900 rpm. Slow addition of a solution of ethyl diazoacetate in DCM (4 wt%) into the reaction vessel was accomplished using a syringe pump. After addition of ethyl diazoacetate is finished, the reaction vessel remains as is and continued stirring at ambient temperature for 30 minutes. Filtration of the reaction mixture through a short plug of Celite can assist in separation of insoluble  $\text{Rh}_2(\text{OAc})_4$  from the product mixture. Purification via column chromatography was performed in order to afford pure cyclopropanes **68a** and **68b**.

An interesting note is that compared to previous bicyclic sulfone derivatives, cyclopropane **68a** appears to demonstrate greater stability in the presence of aerobic  $\text{CDCl}_3$  i.e. acidic environment; however, it would appear that the minor diastereomer **68b** would eventually degrade upon standing in  $\text{CDCl}_3$  overnight, as indicated by Figure 20.

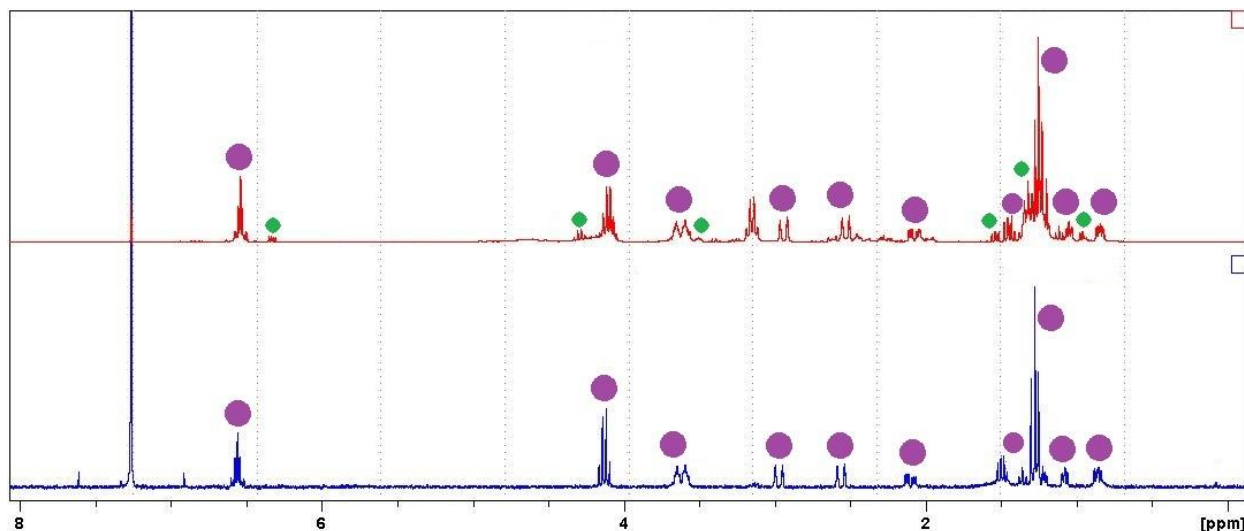


Figure 20.  $^1\text{H}$  NMR of cyclopropanes **68a** and **68b** in  $\text{CDCl}_3$  over prolonged period of time. Highlighted in purple circles are diagnostic peaks corresponding to sulfone **68a**, while highlighted in green diamonds are diagnostic peaks corresponding to sulfone **68b**.

Based on the optimization data, further understanding of the mechanistic cycle has been achieved, as demonstrated in Scheme 50. Oxidative addition of  $\text{Rh}_2(\text{OAc})_4$  with ethyl diazoacetate is moderately facile, as indicated by the presence of constant bubbling from molecular nitrogen and short lag in time between addition of ethyl diazoacetate and occurrence of bubbling in solution.

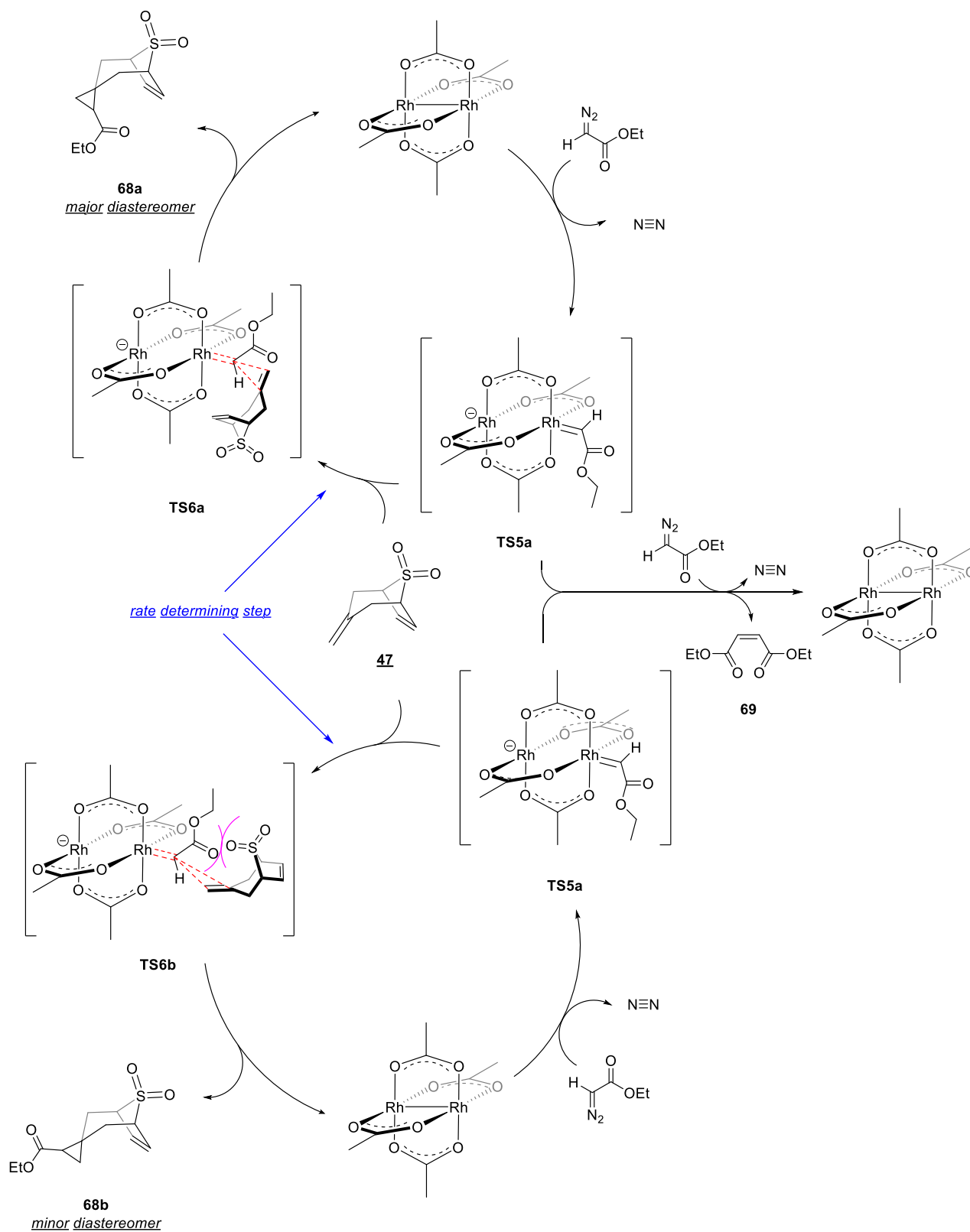
$$\frac{d[\mathbf{68a} + \mathbf{68b}]}{dt} = k_1[\text{ethyl diazoacetate}][\mathbf{47}] - k_2[\text{ethyl diazoacetate}]^2$$

*Equation 1. Simplified rate equation summarizing the cyclopropanation step and dimerized product **69**.*

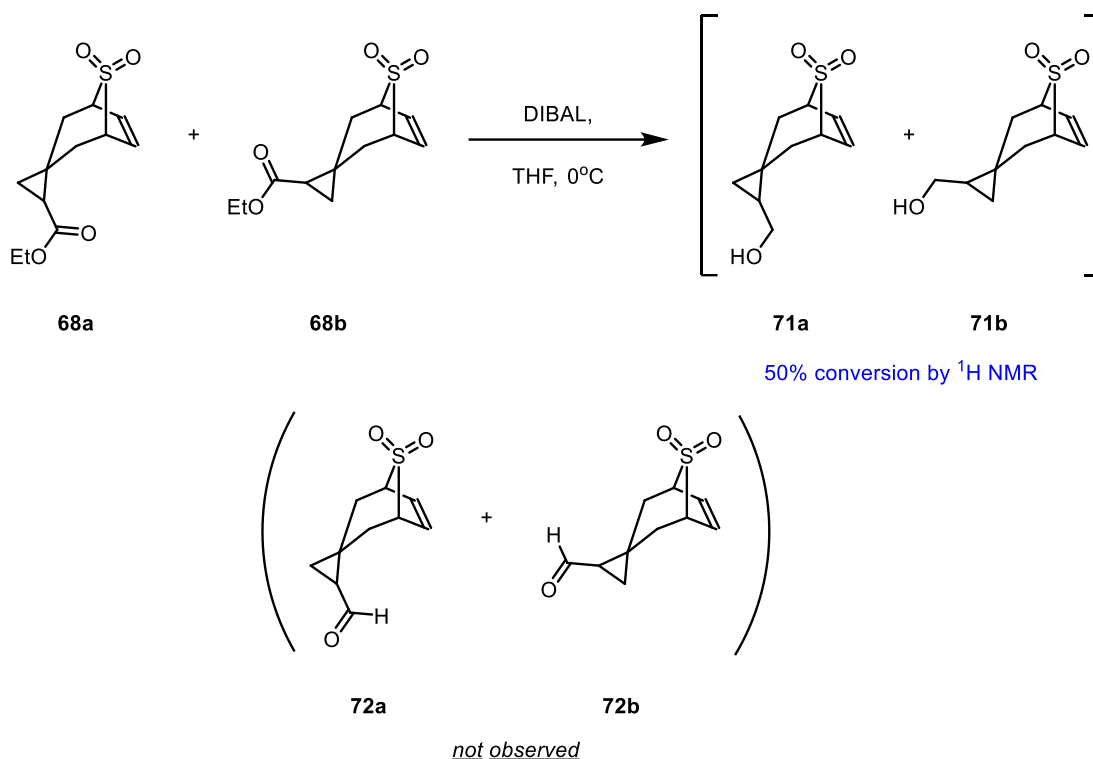
As we decrease the amount of DCM used i.e. higher concentration of both ethyl diazoacetate and sulfone **47**, greater amount of dimerized product **69** is formed. Significant amounts of both **68a** and **68b** can be isolated if we were to pursue the opposite direction and introduce more DCM as the reaction solvent i.e. lower concentration of both ethyl diazoacetate and sulfone **47**. The latter scenario indicates that upon dilution, the importance of the second component of equation 1 would be rendered relatively infinitesimal compared to the first component, even though the concentration of ethyl diazoacetate being significantly greater than the concentration of sulfone **47** in solution i.e. excess amount of ethyl diazoacetate. Due to the second component being the product of the square of the concentration of ethyl diazoacetate, if  $k_1$  and  $k_2$  are equivalent then the first component would be rendered less significant due to the lower concentration values of sulfone **47** in solution. However, this is in contrast to what we have observed experimentally; thus, the only explanation is that the inherent value of  $k_1$  is greater than  $k_2$ . As we assumed that **TS5a** is a common elementary step towards generation of both compound **69** and cyclopropane products **68a** and **68b**, this indicates that interaction of Rh-carbenoid complex **TS5a** with sulfone **47** is inherently more favorable compared to the interaction of a second equivalent of ethyl diazoacetate. This may be due to higher  $\pi$ -nucleophilicity of the exocyclic alkene moiety of sulfone **47** compared to the ylide form of ethyl diazoacetate.

As such, one way to minimize unproductive dimerization is to utilize physical means to control the amount of  $\text{Rh}_2(\text{OAc})_4$  being exposed to ethyl diazoacetate, which we have demonstrated via slow addition of ethyl diazoacetate using a syringe pump. Subsequently, upon interaction of exo-olefin with the Rh-carbenoid complex **TS5a** in a

putative butterfly-like transition state i.e. **TS6a** and **TS6b** should yield our desired cyclopropane **68a** and **68b**, as well as liberating the catalytic rhodium species to participate in the next catalytic cycle. We believe that based on these data, interaction of the sulfone moiety and the Rh-carbenoid species **TS5a** does not exist to a significant extent,<sup>211</sup> as we do not observe the formation of cyclopropanes **70a** and **70b**. Furthermore, we believe the “ $\pi$ -coordination” step from **TS5a** to **TS6a** or **TS6b** to be the rate-determining and diastereoselectivity-determining step in the mechanistic catalytic cycle. We also note that the nearly-constant diastereomeric ratio could be a result of conformational preference when the Rh-carbenoid species **TS5a** is interacting with either the concave or convex face of the exo-olefin. Currently we have assessed the identities of both the major and minor portion of the product mixture as cyclopropane diastereomers **68a** and **68b**: if cyclopropane **68b** was produced as the major portion, we would expect transfer of spin polarization through space between the alkenyl protons and the protons of the methylene carbon of the cyclopropane. As a side note, we have observed a nuclear Overhauser effect (NOE) between the protons of the internal and external olefin in sulfone **47**. However, upon irradiation of the alkenyl protons of the major cyclopropane diastereomer, we did not observe any cross relaxation that corresponded to any signals that we assigned to be the cyclopropane portion. Thus, we can confidently assign cyclopropane **68a** as the major diastereomer produced; however, further spectroscopic evidence may be beneficial in assessing our mechanistic hypothesis. We also anticipate that other Rh-containing dimer species with increasing steric bulkiness of ligand size may be helpful in achieving diastereoselective cyclopropanation of bicyclic sulfone **47**.<sup>212</sup>



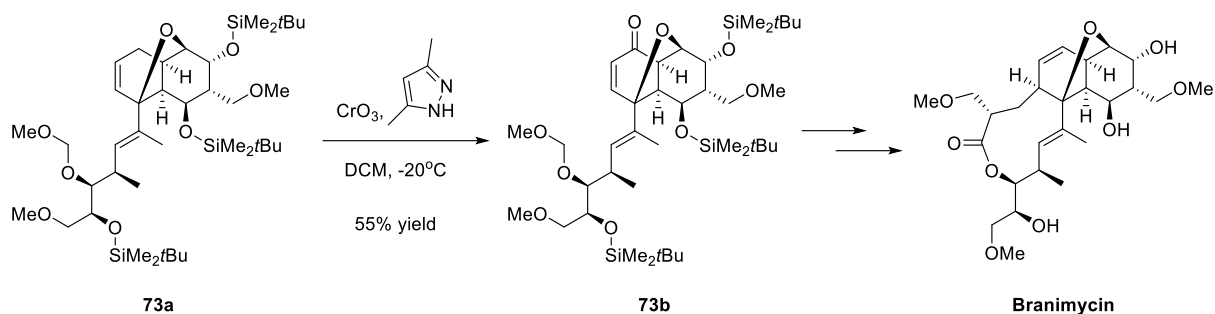
Attempts at transforming the cyclopropane ester moiety have been briefly investigated. Reduction of the ester functional group using DIBAL appears to yield the cyclopropanols **71a** and **71b** as 50% conversion and no signs of aldehydes **72a** and **72b**, as we do not observe any characteristic proton signals between  $\delta$  9 to 11 ppm that would correspond to any aldehydes, as shown in Scheme 51. However, separation of cyclopropanols **71a** and **71b**, as well as cyclopropanes **68a** and **68b**, is non-trivial. Therefore, future means of identifying methodologies that can selectively reduce the ester moiety without disrupting the bicyclic sulfone scaffold are desired.



*Scheme 51. Reduction of the ester moieties of compound **68a** and **68b**. Isolation of compounds **71a** and **71b** were difficult due to negligible polarity differences as indicated in TLC.*

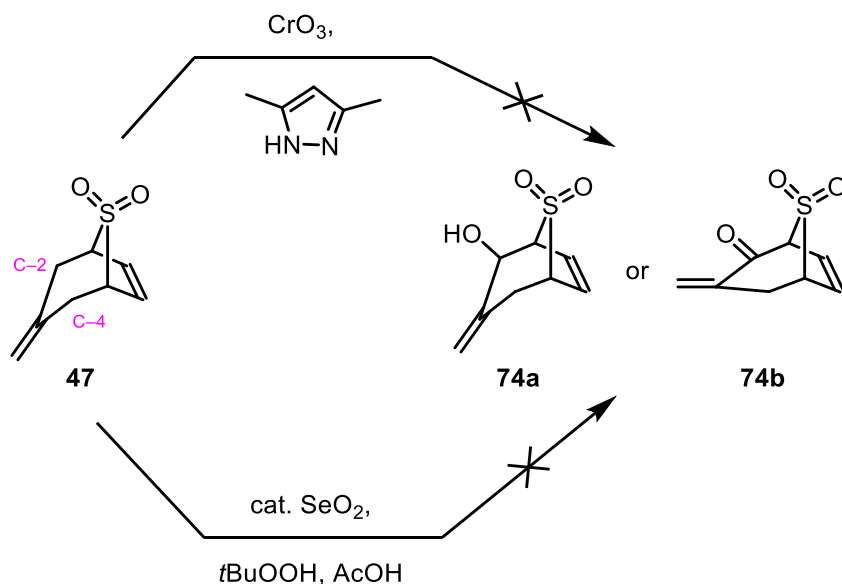
Next, we once again turn our attention towards functionalization of positions C-2 and C-4, after much effort in expanding chemical space at positions C-3, C-6 and C-7. Due to the positions of C-2 and C-4 being adjacent to the exo-olefins of sulfone **47**, we thought that functionalization at these allylic positions of sulfone **47** would be achieved. However, reality proved us differently. Many different allylic oxidation methods require the reaction to be performed at elevated temperature;<sup>213</sup> however, we were concerned about the thermal stability of bicyclic sulfone **47**, as we anticipated that retro-cheletropic

reaction would be facile.<sup>214</sup> Few examples were demonstrated in past literature where allylic functionalization was achievable under mild reaction conditions and without the need for elevated temperature, thus we decided to explore these conditions.



*Scheme 52. Mulzer's synthesis towards natural product branimycin.*

Mulzer and coworkers showcased that  $\alpha,\beta$ -unsaturated ketone **73b** can be synthesized from allylic oxidation using chromium trioxide and 3,5-dimethylpyrazole as additive in the reaction;<sup>215</sup> despite their success in achieving this transformation in the journey towards complex natural product branimycin shown in Scheme 52, instead our bicyclic sulfone **47** remain inert under such conditions and neither compound **74a** or **74b** was observed spectroscopically. Undeterred, we seek to use more conventional methods – selenium dioxide-mediated allylic oxidation.<sup>216</sup> Sharpless and coworkers have described the usage of catalytic amounts of selenium dioxide to afford allylic oxidation, with tert-butyl peroxide as the terminal oxidant and acetic acid to neutralize

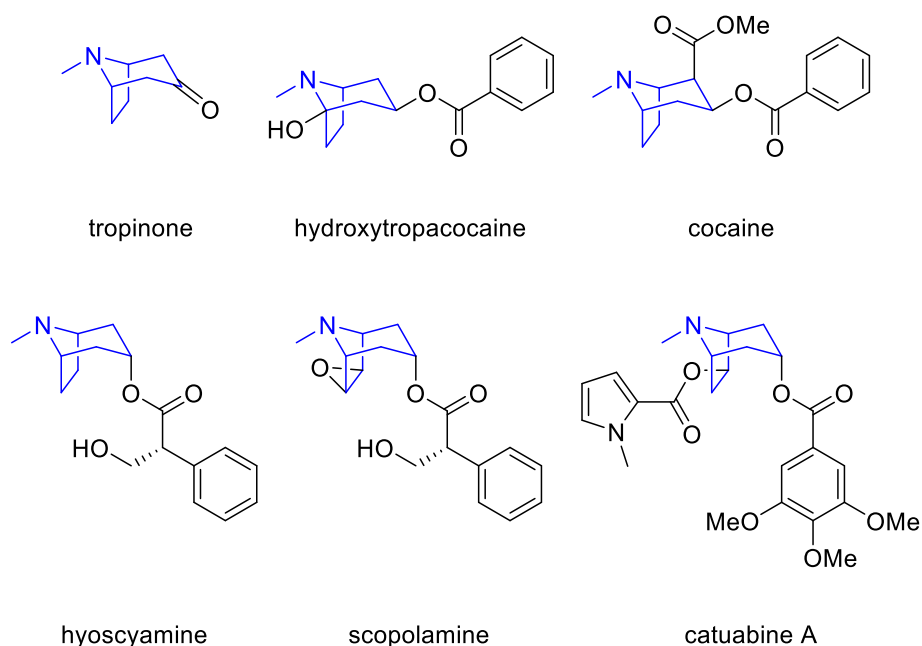


*Scheme 53. Failed attempts of allylic oxidation of sulfone 47.*

the pH level of the reaction environment.<sup>217</sup> Yet again, our bicyclic sulfone **47** shows robustness in resisting these oxidation techniques, as summarized in Scheme 53. Despite these setbacks, tetra-aryl sulfones **31a**, **31b**, **31c**, **31d**, **32a**, **32b**, **32c**, and **32d** featured functionalization at the desired carbons of the scaffold. Thus, we decided to rely on these molecules in order to gain us reliable and predictive insight on structure-activity relationship studies in future biological screening results.

### Chapter 3.3 Bridgehead Alkylation of Bicyclic Sulfones

Despite facing numerous obstacles, we remained strong at heart. The bridgehead positions at C-1 and C-5 of our bicyclic sulfone scaffold remains untouched, and we initially anticipated that functionalization at these positions would be the most difficult challenge to tackle. However, given the fact that these positions being adjacent to the sulfone moiety, we remained optimistic as the inductive effects of the sulfone functional group would be capable of stabilizing the resulting carbanion when presented with a strong base.<sup>218</sup> The anion could subsequently react with appropriate electrophiles in order to achieve our goal of selective functionalization at these positions of the bicyclic sulfone scaffold. Literature precedents for similar approaches have been described in several campaigns which pursued the chemical synthesis of polycyclic polyprenylated acylphloroglucinols (PPAPs).<sup>219</sup> Beyond that, our bicyclic sulfone

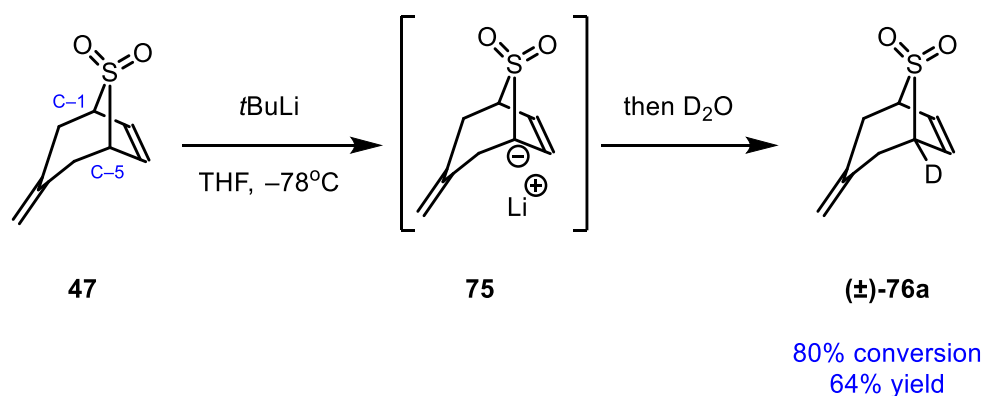


*Scheme 54. Natural products that contains tropine skeleton as shown in blue.*

scaffold highly resembles molecules derived from tropinone-type family of natural products, as shown in Scheme 54.<sup>220</sup>

Traditionally, synthesis of these tropinone derivatives employ multicomponent condensation such as Robinson's tandem Mannich reaction,<sup>221</sup> and functionalization at analogous positions require building blocks with substituents inherently featured.<sup>222</sup> Even so, these sterically demanding building blocks present a challenge in these conventional processes. As such, we have high hopes that our anticipated strategy of bridgehead functionalization of our bicyclo[3.2.1]sulfone-containing molecules can gain access to unnatural bioactive chemical structures that highly resemble natural products.

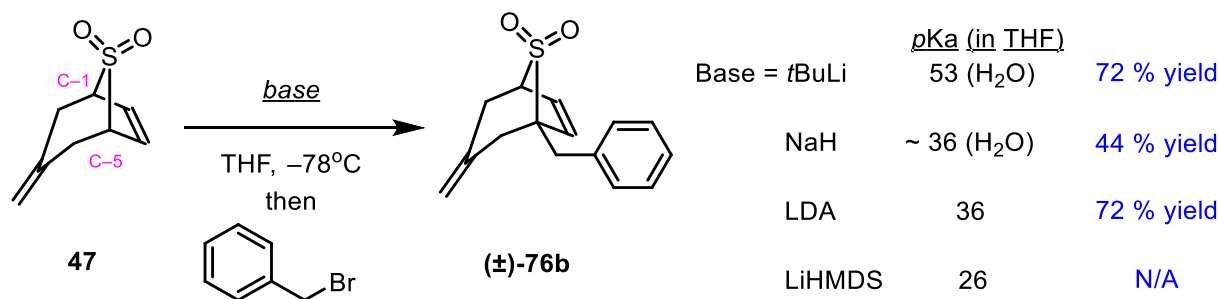
Indeed, during our initial investigation, deprotonation using 1.5 equivalent of tert-butyl lithium and subsequent quenching using 1.0 equivalent of D<sub>2</sub>O afforded mono-deuterated bicyclic sulfone (**±**)-**76a** in 80% isolated yield, as shown in Scheme 55. Spectroscopically, we determined that approximately 80% of bicyclic sulfone **47** was deuterated.



*Scheme 55. Deuteration via sulfone-assisted lithiation of compound 47.*

The results are not only encouraging as is, but also demonstrated that in the presence of excess amounts of strong base, no other C-H bonds are capable of being deprotonated, and ultimately the stoichiometry of the quenching agent determines the substrate conversion. Furthermore, we envisioned that by substituting the trapping agent with suitable electrophiles, the isolated products would be effectively desymmetrized.

Firstly, we decided to screen different organic bases with differing pKa in order to obtain a rough estimation of the acidity of the C–H bonds at position C-1 and C-5. Using benzyl bromide as the electrophile, we were able to demonstrate that tert-butyl lithium (pKa = 53 in H<sub>2</sub>O) was a suitable base for obtaining quaternary sulfone (**±**)-**76b** in 30% isolated yield. Significant amount of unreacted bicyclic sulfone **47** was recovered after chromatographic purification, thus we believe that instead of tert-butyl lithium acting as a base solely, it may also function as a nucleophile as well, which ended up interfering with our anticipated synthetic plans. Switching to NaH (pKa ~36 in H<sub>2</sub>O) was possible to yield quaternary sulfone (**±**)-**76b**, albeit with significantly more amounts of unreacted bicyclic sulfone **47** recovered. We theorize that although the deprotonated carbanion can be stabilized by the adjacent sulfone moiety, the species remain short-lived and may be potentially quenched by residual water content from the reaction environment despite rigorously ensuring anhydrous reaction conditions. Thus, we sought an alternative choice of base that is capable of deprotonating the desired C–H bond under kinetic control. LDA (pKa ~36 in THF) was able to perform its function as an organic base proficiently, as we were able to obtain quaternary sulfone (**±**)-**75b** in 66% isolated yield, as demonstrated in Scheme 56.

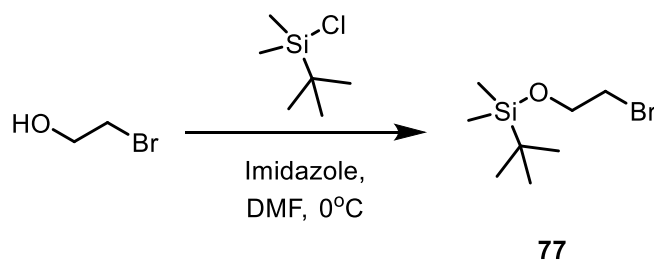


Scheme 56. Screening of base used in bridgehead lithiation to optimize isolation of sulfone (**±**)-**76b**.

An interesting note is that LiHMDS (pKa = 26 in THF) was incapable of deprotonating the C–H bonds at the bridgehead positions of our bicyclic sulfone scaffold. This matches with the expectation that  $\pi$ -conjugation in butadiene sulfone assisted in lowering the acidity of the  $\alpha$ -proton, and therefore complete deprotonation with a milder base such as LiHMDS is possible; thus, in the absence of such  $\pi$ -conjugation, deprotonation of sulfone **47** with LiHMDS is not kinetically and thermodynamically favorable. Indeed, Paquette and coworkers have briefly investigated the whether the

aforementioned phenomenon holds true in bicyclic sulfone-containing organic molecules, and they claim that in bicyclic bis-alkyl sulfone structures, the sulfone moiety serves to inductively stabilize the carbanion and if the adjacent alkene is incapable of sufficient orbital overlap, charge stabilization should not be expected.<sup>223</sup> Thus, our current optimal conditions for bridgehead alkylation is to employ 1.1 equivalent of LDA formed in situ, which acts to deprotonate bicyclic sulfone **47** at -78 °C. After 5 minutes of stirring to ensure complete deprotonation, 1.2 equivalent of appropriate electrophile is added in one bolus charge, and stirring at cryogenic temperature is maintained for several hours before quenching with aqueous NH<sub>4</sub>Cl.

Using the aforementioned method, we were able to synthesize quaternary sulfone (**±**)-**76c** using allyl bromide as the choice of electrophile, and we isolated the product in 50% yield. Other alkyl bromides were capable of participating in the bridgehead alkylation procedure: 2-bromoethanol was transformed into silyl ether **77** using TBS-Cl and imidazole as shown in Scheme 57,<sup>224</sup> and silyl ether **77** served as the electrophile during bridgehead alkylation in order to afford quaternary sulfone (**±**)-**76d** in 30% isolated yield, as shown in Scheme 58. A possibility that may result in the lower yield of quaternary sulfone (**±**)-**76d** is that either deprotonated sulfone **74** or LDA acts more as a base to perform hydrogen abstraction of bromide **77** i.e. the reaction rate of E2 is faster than S<sub>N</sub>2.

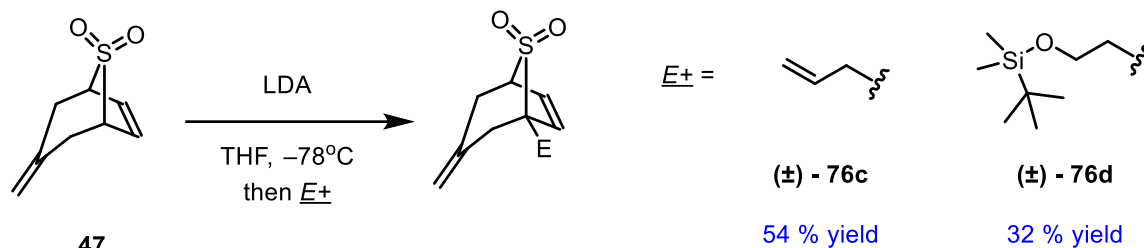


95 % yield

*Scheme 57. Silylation of 2-bromoethanol under mild conditions.*

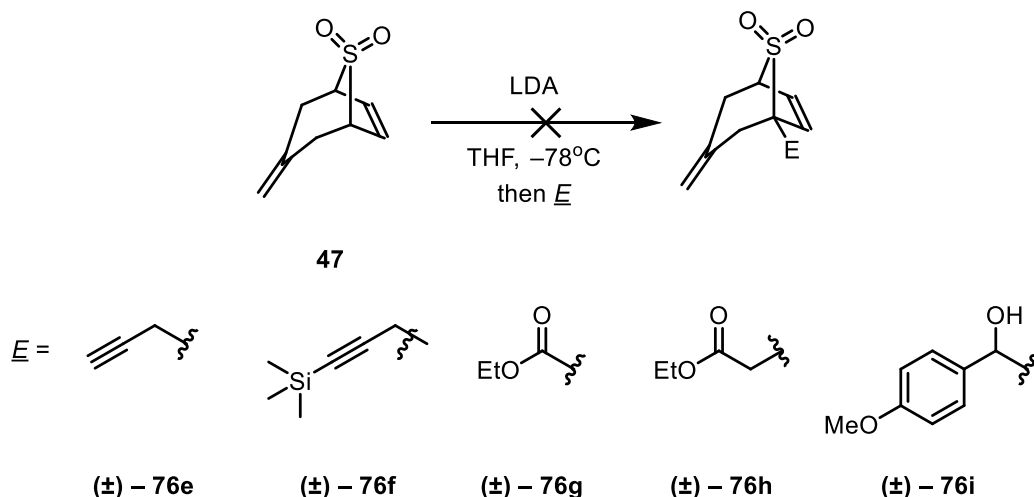
Despite this, not all alkyl bromides were compatible: in the presence of either propargylic bromide or TMS-propargylic bromide,<sup>225</sup> deprotonated bicyclic sulfone **74** did not undergo bridgehead alkylation, and we recovered bicyclic sulfone **47** instead. Note that in a previous allylation investigation with a slightly different substrate, we

isolated impurities that correspond to N-allyldiisopropylamine. A plausible explanation is that either LDA or DIPEA (from protonated LDA) exhibits nucleophilicity towards alkyl bromides, which results in direct competition against the more nucleophilic deprotonated bicyclic sulfone **75**.



*Scheme 58. Successful attempts at bridgehead alkylation of compound **47***

However, other activated electrophiles such as benzyl chloroformate were competent reactants, but yielded products that we were unable to successfully characterize; we observed signals that corresponded to protons of the aromatic region and the benzylic carbon, but we did not observe any signals that corresponded to either the alkenyl protons, diastereotopic protons of the methylene carbons, or the methane proton attached to the carbon adjacent to the sulfone moiety of compound **47** with comparable intensity to the benzylic portion. Thus, we attribute that perhaps degradation of the bicyclic core occurred in the presence of highly electrophilic species. Reactions using *p*-anisaldehyde as the source of electrophile did not yield any significant transformation; instead, we recovered both substrates upon work-up. Furthermore, when we were investigating the option of using ethyl 2-bromoacetate as the electrophile, we did not yield the desired bridgehead alkylated product. Instead, we

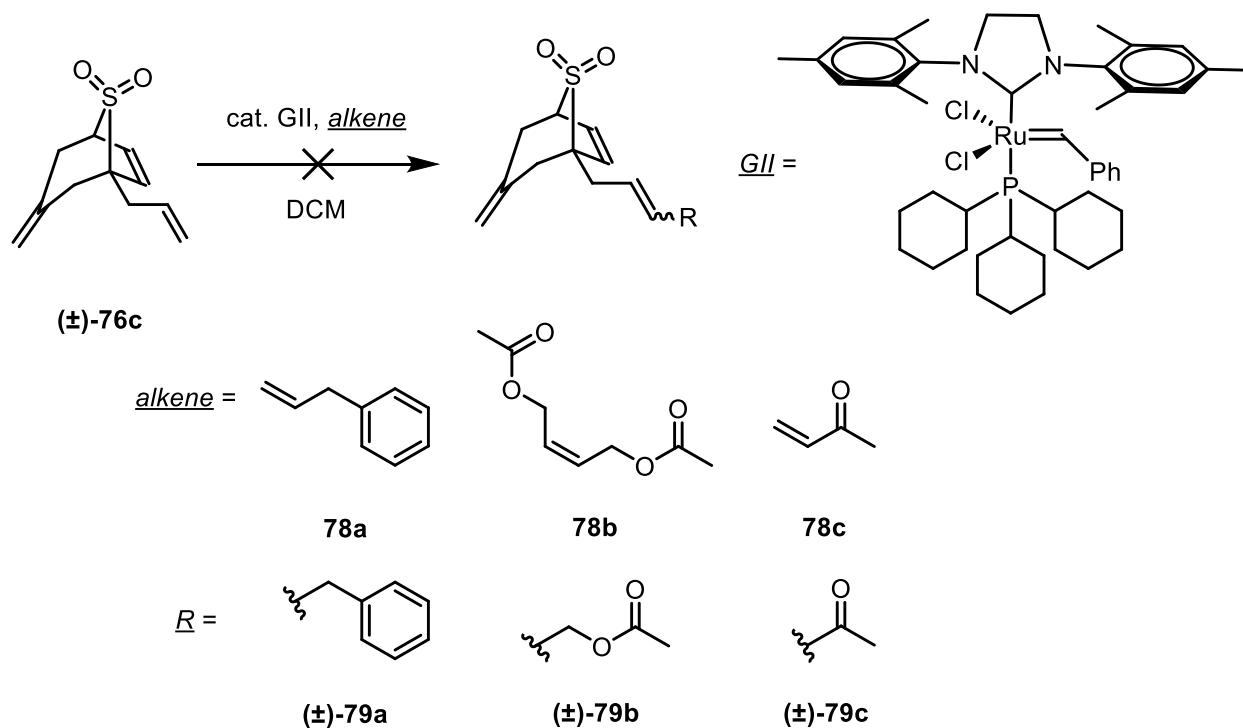


*Scheme 59. Failed attempts of bridgehead functionalization. Many different substituents were tested as shown and did not appear to be compatible with our current methodology.*

obtained unreacted bicyclic sulfone **47** and impurities that we identified as ethyl 2,4-dibromo-3-ethoxy-3-hydroxybutanoate. All failed attempts using various electrophile are summarized in Scheme 59.

Once again, we were able to understand the limitations of our methodology; however, in the process, we were able to achieve our goal of regioselective functionalization of certain positions of our bicyclic sulfone framework.

Despite some setbacks, we were interested in whether allylated bicyclic sulfone ( $\pm$ )-**76c** could undergo cross metathesis with other alkenes. If so, not only can we expand on accessible chemical space based on our bicyclic sulfone framework, but also showcase compatibility of transition-metals such as Ru-species towards bicyclic sulfone moieties. Our initial investigation employed 5 mol% of 2<sup>nd</sup>-generation Grubbs catalyst, with stoichiometric amount of allyl benzene **78a** as the coupling partner, as shown in Scheme 60. The reaction was performed at ambient temperature over the course of 24 hours, but we did not obtain cross-metathesis product ( $\pm$ )-**79a** nor self-metathesis products.



*Scheme 60. Unsuccessful attempts at furnishing sulfone ( $\pm$ )-**76c** using cross-olefin metathesis.*

Heating the reaction to 40 °C did not prove to be beneficial in improving the situation. We considered perhaps that the alkenes of both allylated bicyclic sulfone ( $\pm$ )-**76c** and allyl benzene **78a** exhibited mildly nucleophilic properties and resulted in a mismatch of chemo-compatibility. Thus we decided to test out methyl acrylate **78c**, which contains an activated alkene, as the coupling partner. Unfortunately, both substrates were recovered regardless of performing the reaction at ambient temperature or heating to 40 °C.

Allylated bicyclo[3.2.1]scaffolds were demonstrated by Miesch and coworkers as effective substrates that could undergo cross metathesis under analogous reaction conditions.<sup>226</sup> To that end, we decided to investigate whether bidentate chelation of the oxygen of the sulfone moiety and the internal olefin of compound ( $\pm$ )-**76c** and 2<sup>nd</sup>-generation Grubbs catalyst would interact prior to the formation of the ruthenacyclobutane structure.<sup>227</sup> Surprisingly, no significant changes in chemical shifts were observed in either <sup>1</sup>H and <sup>31</sup>P NMR after 24 hours of mixing, when a solution of stoichiometric equivalent of both bicyclic sulfone **47** and 2<sup>nd</sup>-generation Grubbs catalyst was prepared by dissolving in C<sub>6</sub>D<sub>6</sub>, as shown in Figures 20, 21 and 23.

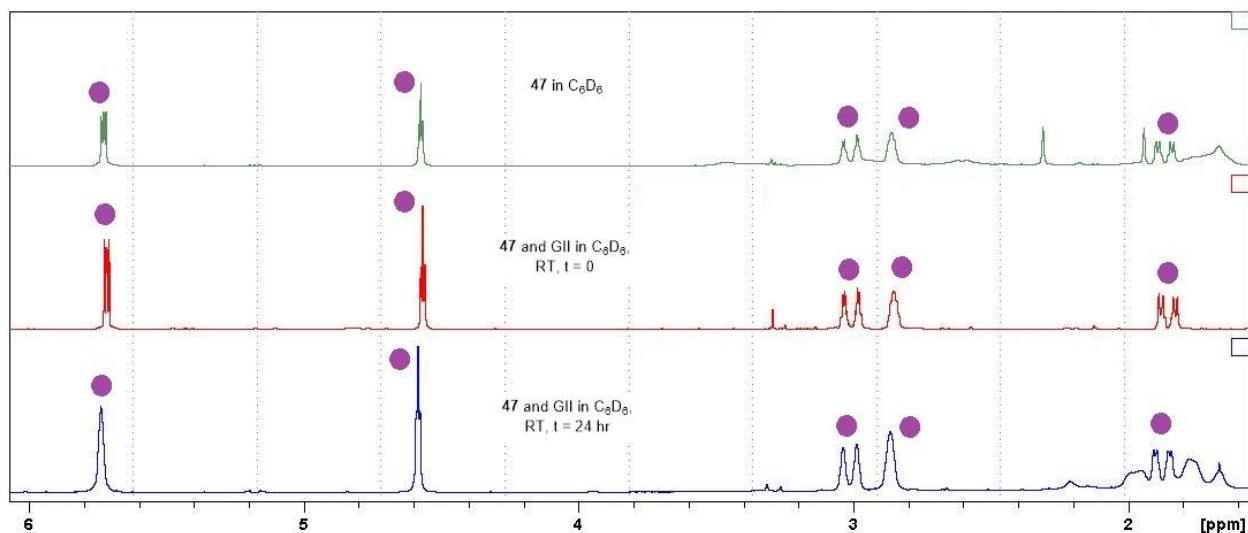


Figure 21. <sup>1</sup>H NMR reactivity monitoring spectrum of compound **46** and GII. Highlighted in purple are diagnostic peaks corresponding to compound **46**.

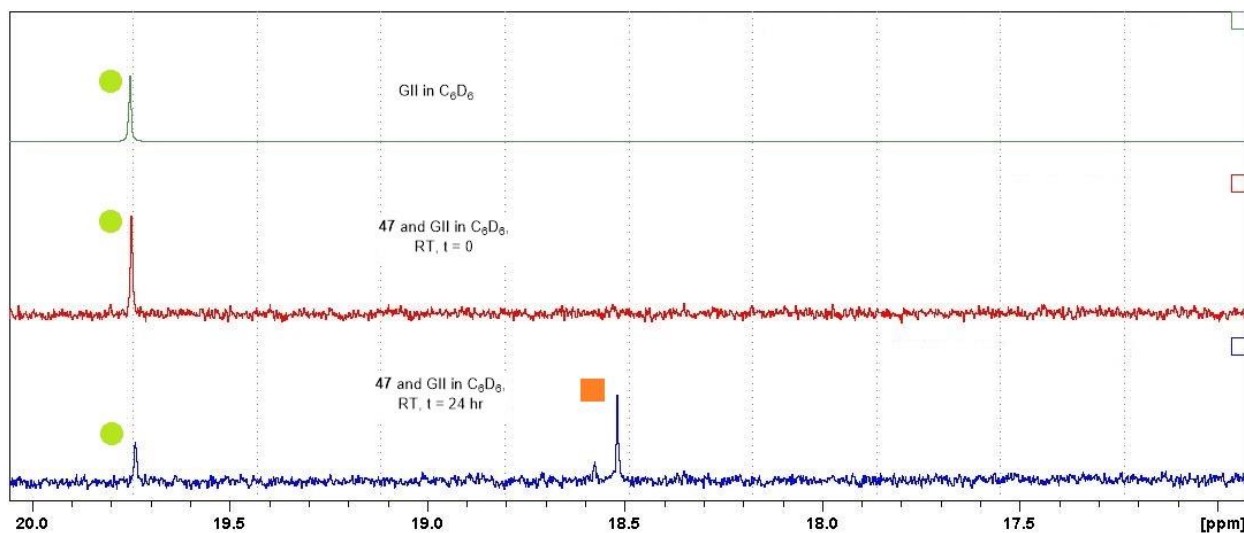


Figure 22. Downfield  $^1\text{H}$  NMR reactivity monitoring spectrum of compound **47** and *GII*. Neon green circle indicates the vinyl proton of *GII* ( $\text{Ru}=\text{CHPh}$ ). Orange circle indicates the formation of a new Ru-benzylidene species.

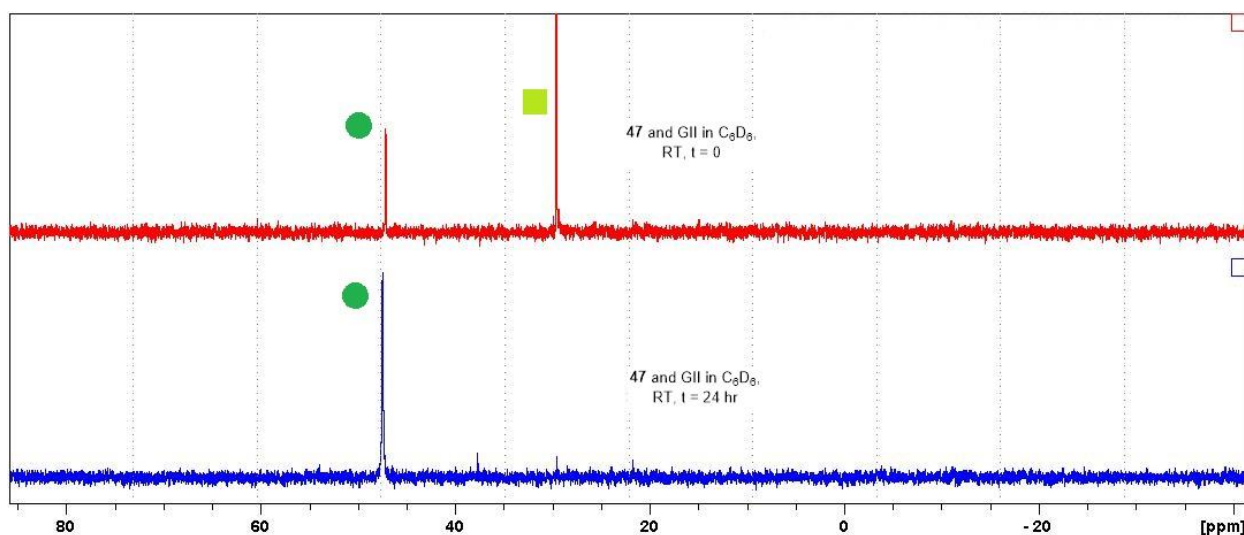


Figure 23.  $^{31}\text{P}$  NMR reactivity monitoring spectrum of compound **47** and *GII*. Green circle and light green square correspond to diagnostic signals of  $\text{Cy}_3\text{P}=\text{O}$  and *GII* respectively.

Interestingly, a new complex has formed based on the appearance of a singlet at  $\delta$  18.5 ppm, as highlighted in orange square in Figure 22. The chemical shift of this signal suggests that a Ru-benzylidene species to be present in solution. Figure 24 illustrated that upon standing for 24 hours, the signal corresponding to the bridgehead protons of sulfone **47** appears to be shifted towards downfield by 0.02. Based on all the above data, it is implicated that neither the exo-olefin and internal-olefin of the bicyclic sulfone framework has interacted with the Ru-center; instead, a plausible explanation is

that upon disassociation of PCy<sub>3</sub> in solution, the active NHC-containing Ru-benzylidene species is coordinated towards the oxygen of the sulfone moiety in compound **47**. Grela and colleagues have reported that amongst sulfone-chelating benzylidene species, the appearance of the sp<sup>2</sup> C–H of the Ru-benzylidene portion to be relatively downfield i.e. between  $\delta$  18.6 to 19 ppm.<sup>228</sup> They have also demonstrated that choices of NHC may have a non-trivial influence on the catalytic activity of the sulfone-chelated Ru-benzylidene species towards olefin metathesis.

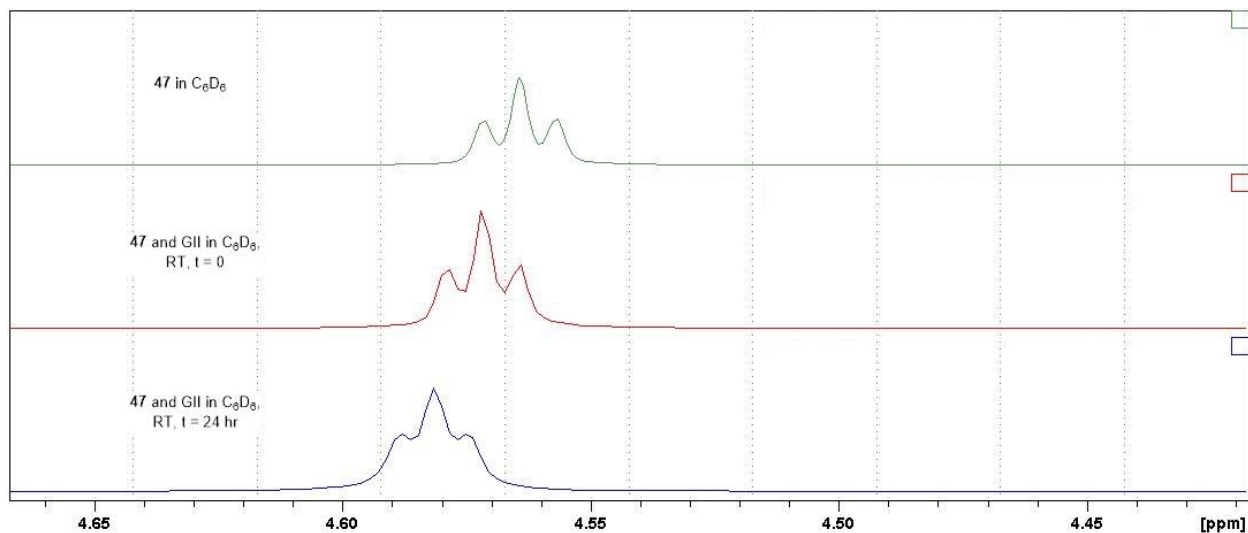
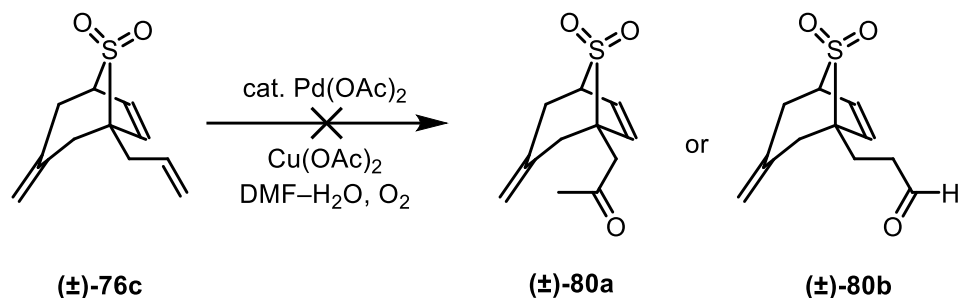


Figure 24. Zoomed in of <sup>1</sup>H NMR reactivity monitoring spectrum of compound **46** and GII.

In the early works by Paquette and colleagues, they postulated a potential pathway where chelation between the Ru-metal center and both the sulfone moiety and the alkene functional group of the substrate is necessary in order to direct the formation of sulfone-containing macrocycles via olefin metathesis.<sup>229</sup> In the absence of such effects, no activity of olefin metathesis have been observed. Therefore, we speculate that perhaps sulfone-coordination to Ru-metal center hampers the reactivity of the catalytically active species, and the olefin of the allyl portion of sulfone (**±**)-**76c** may not be geometrically flexible enough to coordinate to the Ru-metal center and subsequently displace the sulfone moiety.

We also sought other chemical processes to functionalize allylated bicyclic sulfone (**±**)-**76c**. One such approach that we pursued was to oxidize the allyl moiety via Wacker process.<sup>230</sup> Usage of Wacker oxidation is prominently featured in acyclic alkene substrates in natural product synthesis and development of novel methodologies.<sup>231</sup> We

anticipated that the allyl moiety in allylated bicyclic sulfone (**±**)-**76c** is less sterically congested compared to the exo-olefin and internal olefin region, which may be advantageous in yielding our desired transformation.



*Scheme 61. Failed attempts at Wacker-type oxidation of sulfone (**±**)-**76c**.*

Unfortunately, reality always has ways to enable one to embrace humility: after briefly screening various reaction conditions, we were unable to obtain the desired Wacker oxidation product, but instead recovered unreacted allylated bicyclic sulfone (**±**)-**76c** instead, as shown in Scheme 61. Based on previous experimental data with  $\text{Pd(PPh}_3)_2\text{Cl}_2$  and bicyclic sulfone **47**, we hypothesized that chelated adduct formation of allylated bicyclic sulfone (**±**)-**76c** and  $\text{Pd(OAc)}_2$  is not only possible, but thermodynamically stable enough such that the desired Wacker pathway cannot proceed as expected. Although the results appear to be tragic, one must always embrace failure and learn from it in order to reach the realms of success.

All in all, using the simpler bicyclo[3.2.1]sulfone-containing framework, we were able to achieve a much greater degree of functionalization than was the case with the more highly functionalized bicyclo[3.2.1]sulfones described in Chapter 2. Further understanding of the scaffold itself was realized, such as the inability to functionalize at the allylic positions. Moreover, between the two different sets of structures we were ultimately able to achieve our primary goal of manipulating functionality at every position around the bicycle—although in many cases we were not able to modify as extensively as we would have liked.

Although we have encountered much failure in our crusade to selectively functionalize our bicyclic sulfone scaffold, we have also achieved many treasurable successful moments by isolating novel functionalized bicyclic sulfone derivatives, as shown in Figure 25. We are curious to explore any meaningful functions that these

novel chemical matters can potentially harbor in early stages of drug discover and development, especially with regards to identification of novel biological pathways or undiscovered therapeutic targets.

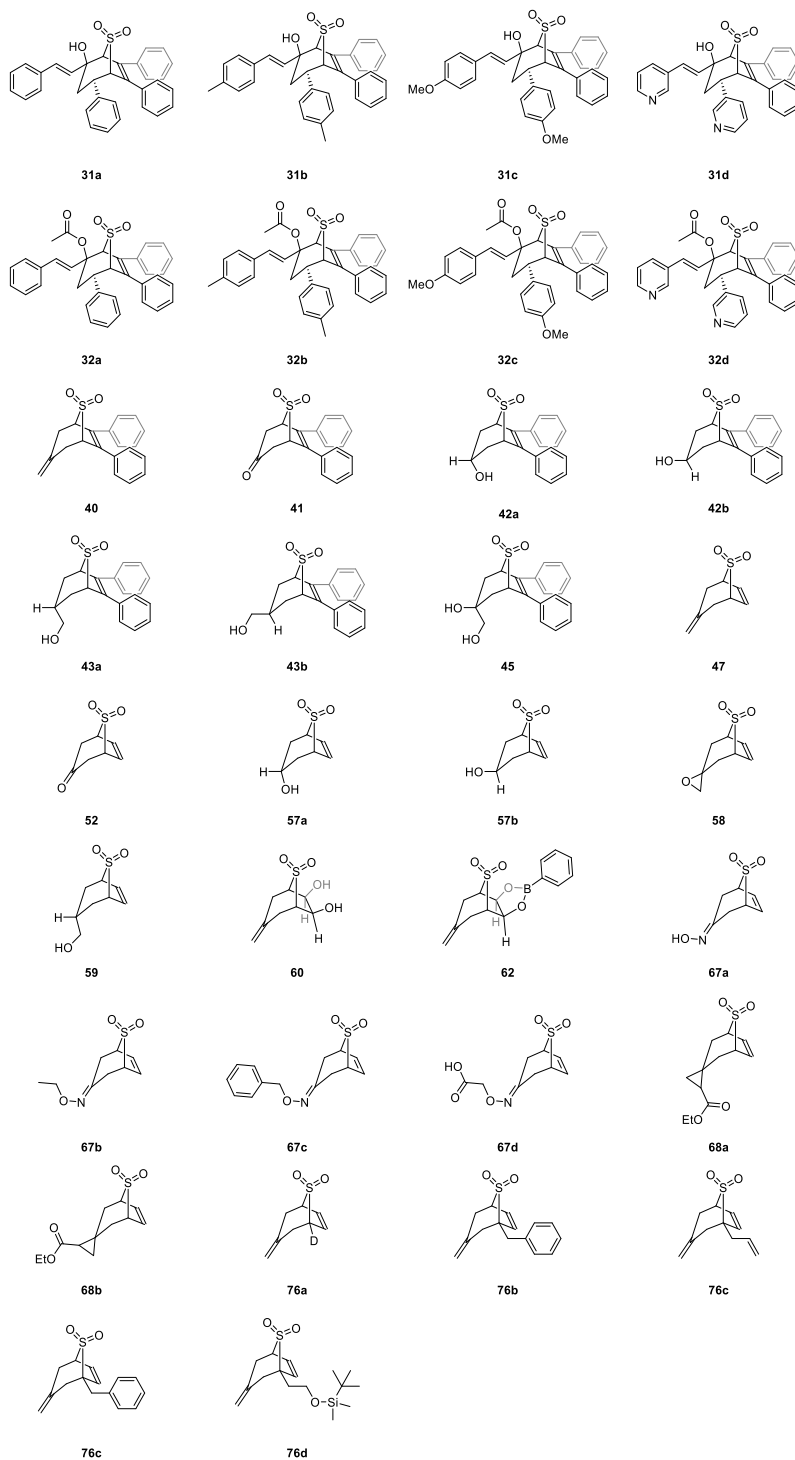


Figure 25. First generation bicyclo[3.2.1]sulfone-containing small molecule library.

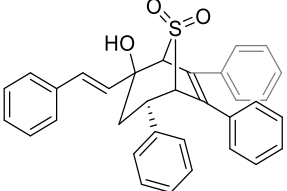
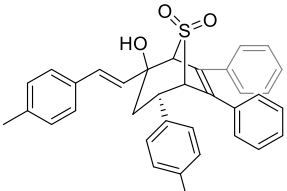
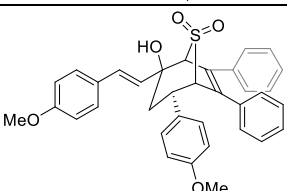
## Chapter 4 – Biological Screening and Preliminary Data Analysis

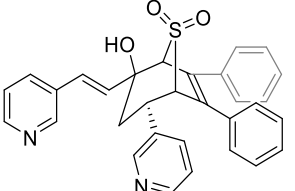
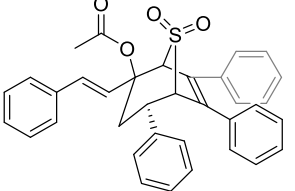
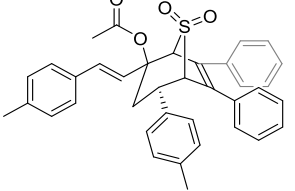
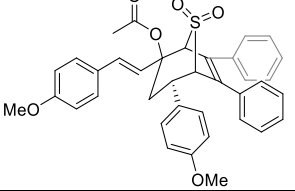
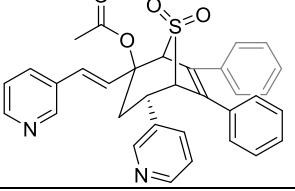
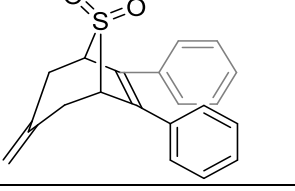
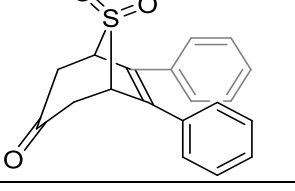
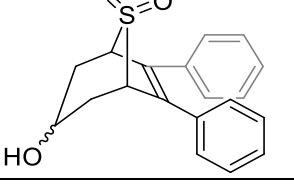
All chemoinformatic analysis was performed by C. H. Andy Un. All biological screening data were collected by respective collaborators at the Community for Open Antimicrobial Drug Discovery, Open Innovation Drug Discovery (OIDD) program at Eli Lilly & Company, and LEO Pharma A/S.

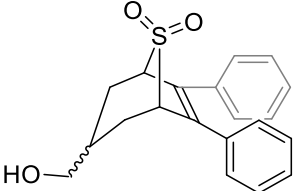
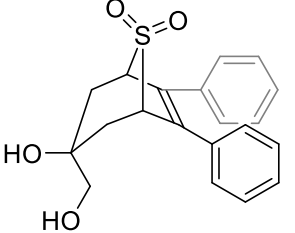
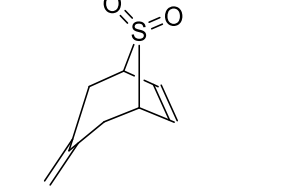
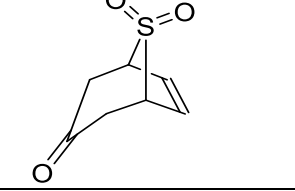
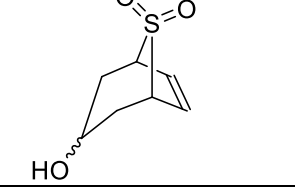
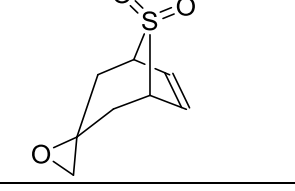
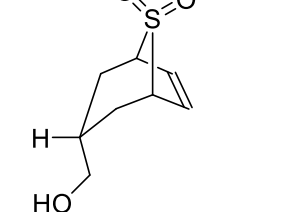
### Chapter 4.1 Chemoinformatic Analysis of Bicyclo[3.2.1] Sulfones

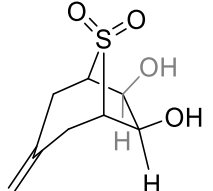
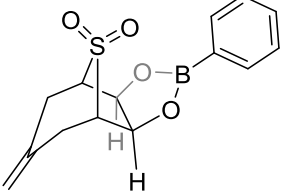
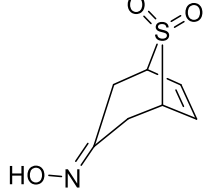
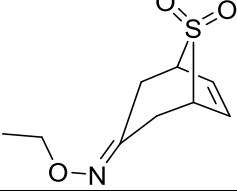
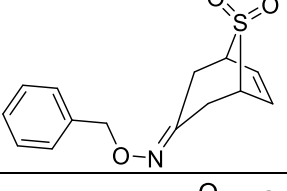
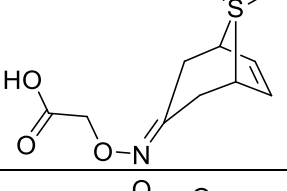
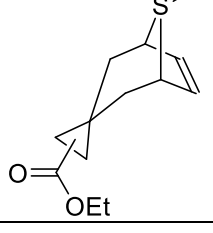
Once we finished assembling our library of bicyclo[3.2.1]sulfone-containing molecules, we sought to obtain chemoinformatic data to assess the degree of structural diversity within our collection of small molecules. Using the online engine ChemAxon,<sup>232</sup> we were able to obtain the following data, which is summarized in Table 3, after providing corresponding chemical structures (note that diastereomers and regioisomers are treated as equivalent structures):

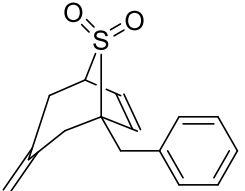
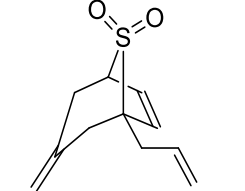
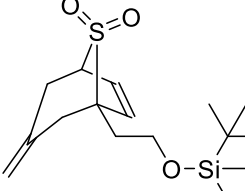
*Table 3. Chemoinformatic data of bicyclo[3.2.1]sulfone-containing molecules. MW, HBD, HBA, tPSA, cLogP, and RotB denotes molecular weight, number of hydrogen-bond donors, number of hydrogen-bond acceptors, topological polar surface area, calculated LogP, and number of rotatable bonds respectively. Checkmark in the column “Rule of 5?” indicates that such molecule fulfills the criteria proposed by Lipinski and coworkers.<sup>49</sup>*

No	Structure	MW (Da)	HBD	HBA	tPSA (Å <sup>2</sup> )	cLogP	RotB	F <sub>sp<sup>3</sup></sub>	Rule of 5?
31a		504.644	1	3	54.37	6.35	5	0.15	X
31b		532.698	1	3	54.37	7.37	5	0.20	X
31c		564.696	1	5	72.83	6.03	7	0.20	X

<b>31d</b>		505.620	1	5	80.15	3.91	5	0.16	X
<b>32a</b>		546.681	0	3	60.44	6.79	7	0.17	X
<b>32b</b>		574.735	0	3	60.44	7.82	7	0.22	X
<b>32c</b>		606.733	0	5	78.90	6.47	9	0.22	X
<b>32d</b>		545.657	0	5	86.22	4.35	7	0.18	X
<b>40</b>		322.422	0	2	34.14	3.60	2	0.20	✓
<b>41</b>		324.394	0	3	51.21	2.80	2	0.21	✓
<b>42</b>		326.410	1	3	54.37	2.13	2	0.26	✓

<b>43</b>		340.437	1	3	54.37	2.59	3	0.30	✓
<b>45</b>		356.436	2	4	74.60	1.37	3	0.30	✓
<b>47</b>		170.226	0	2	34.14	0.57	0	0.57	✓
<b>52</b>		172.198	0	3	51.21	-0.23	0	0.57	✓
<b>57</b>		174.214	1	3	54.37	-0.90	0	0.71	✓
<b>59</b>		186.225	0	3	46.67	-0.50	0	0.75	✓
<b>60</b>		188.241	1	3	54.37	-0.44	1	0.75	✓

<b>67a</b>		204.240	2	4	74.60	-1.22	0	0.75	✓
<b>67b</b>		290.140	0	4	52.60	2.77	1	0.43	✓
<b>67c</b>		185.241	1	4	66.73	-0.22	0	0.57	✓
<b>76b</b>		215.267	0	4	55.73	0.51	2	0.67	✓
<b>76c</b>		277.338	0	4	55.73	1.88	3	0.36	✓
<b>31a</b>		245.249	1	6	93.03	-0.63	3	0.56	✓
<b>31b</b>		256.316	0	3	60.44	0.48	3	0.75	✓

<b>31c</b>		260.351	0	2	34.14	2.66	2	0.33	✓
<b>31d</b>		210.291	0	2	34.14	1.67	2	0.45	✓
<b>32a</b>		328.542	0	3	43.37	2.45	5	0.75	✓

These data confirm that a wide range of physicochemical properties are contained within this library of bicyclo[3.2.1]sulfone-containing molecules. For example, the total-polar-surface-area of our bicyclo[3.2.1]sulfone-containing chemical library is very well spread-out, ranging from 34.14 Å<sup>2</sup> to 93.03 Å<sup>2</sup>; the same could be said about the  $F_{sp^3}$  values as they range from 0.15 to 0.75.

Furthermore, analysis of plane of best-fit (PBF) distribution<sup>233</sup> amongst all synthesized bicyclo[3.2.1]sulfone-containing molecules, which is summarized in Figure 26, are significantly above 0 Å<sup>2</sup>, which indicates that most molecules are not flat in overall shape. Note that similar to line-fitting in two-dimensions, three-dimensional “plane-fitting” of molecules will generate a plane where the distance of heavy atoms in the molecule away from the plane of best-fit is minimized. A quantitative description of three-dimensional molecular shape can be determined as one analyzes the average distance of all heavy atoms away from the PBF. A higher score will indicate that the analyzed molecule deviates farther away from two-dimensional shape. For reference, Blagg and colleagues have reported that the practical average PBF scores for drug-like small molecules and proteins are <2 and <10 respectively.<sup>233</sup>

Once the plane of best fit for a molecule has been determined, a PBF descriptor is calculated by dividing the sum of the distances of all heavy atoms away from the plane by the number of heavy atoms in the molecule. Using this methodology provided

by LLAMA, we can see that all of our bicyclo[3.2.1]sulfone-containing molecules have PBF scores above  $0.7 \text{ \AA}^2$ , with the mean and median PBF scores being  $1.09 \text{ \AA}^2$  and  $1.02 \text{ \AA}^2$  respectively. This testifies that none of our synthesized bicyclo[3.2.1]sulfone-containing molecule should be categorized as planar molecules, as our library contains diverse three-dimensionality. We attribute the rich three-dimensionality to the overall molecular shape of bicyclo[3.2.1]scaffolds.

However, upon visual analysis of Figures 27 and 28, it is clear that there is certain property space that we are lacking. For example, the  $F_{\text{sp}^3}$  values of some heavier bicyclo[3.2.1]sulfone-containing molecules (i.e. greater than 500Da) appears to be localized within 0.15 to 0.22, and leaves much to be desired. This is a consequence of adding non-polar substituents via acylation, as well as the molecules' innate ability to undergo oxidative cleavage to generate lighter bicyclo[3.2.1]sulfone-containing fragments for functionalization and redox manipulation. Noticeably, certain molecules contained properties that medicinal chemists would flag as not worthy for further investigation. For example, all tetra-aryl sulfones **31a-d** and **32a-d** exhibit high cLogP values, and do not abide by Lipinski's Rule of 5. Nonetheless, we argue that strict definition of physicochemical properties may lead to "tunnel vision" whereby only certain chemical space can be manipulated,<sup>234</sup> thereby leading to a small subset of biological matter being influenced. For example, currently development of proteolysis targeting chimera (PROTAC) has led to alternative ways that may potentially translate to improvement in human health via merely binding affinity as opposed to functionally-driven small molecule inhibitors,<sup>235</sup> and these PROTACS do not abide by Lipinski's Rule of 5.

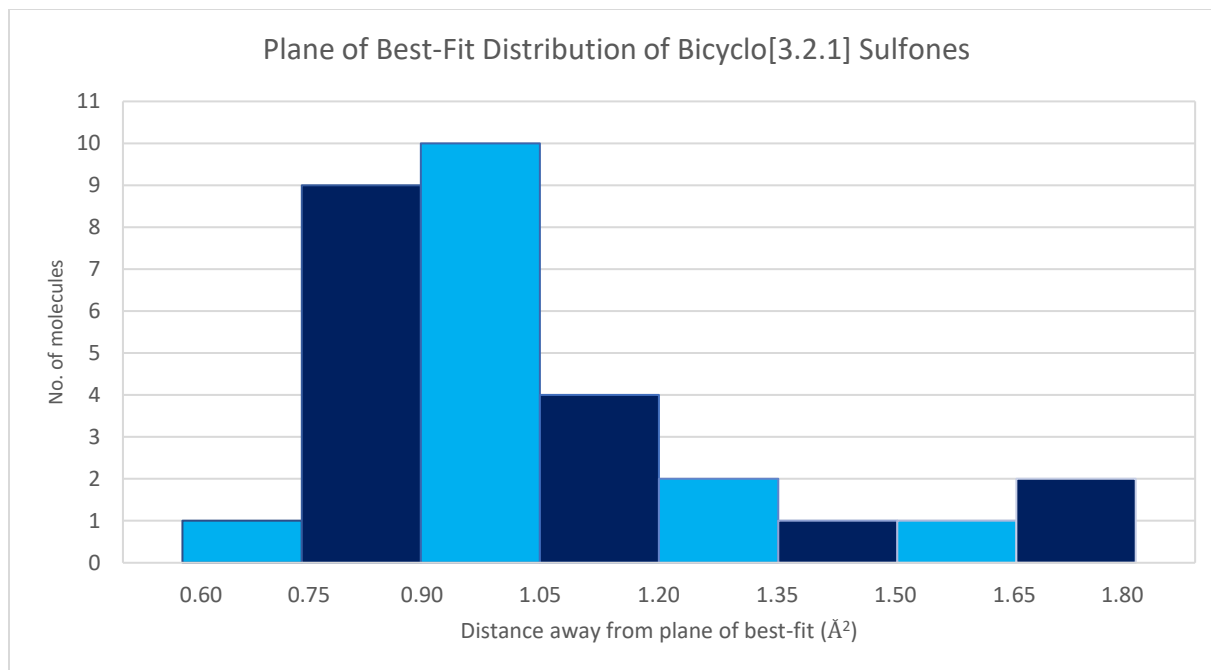


Figure 26. Plane of best-fit distribution diagram of bicyclo[3.2.1]sulfone-containing molecules from Table 3.

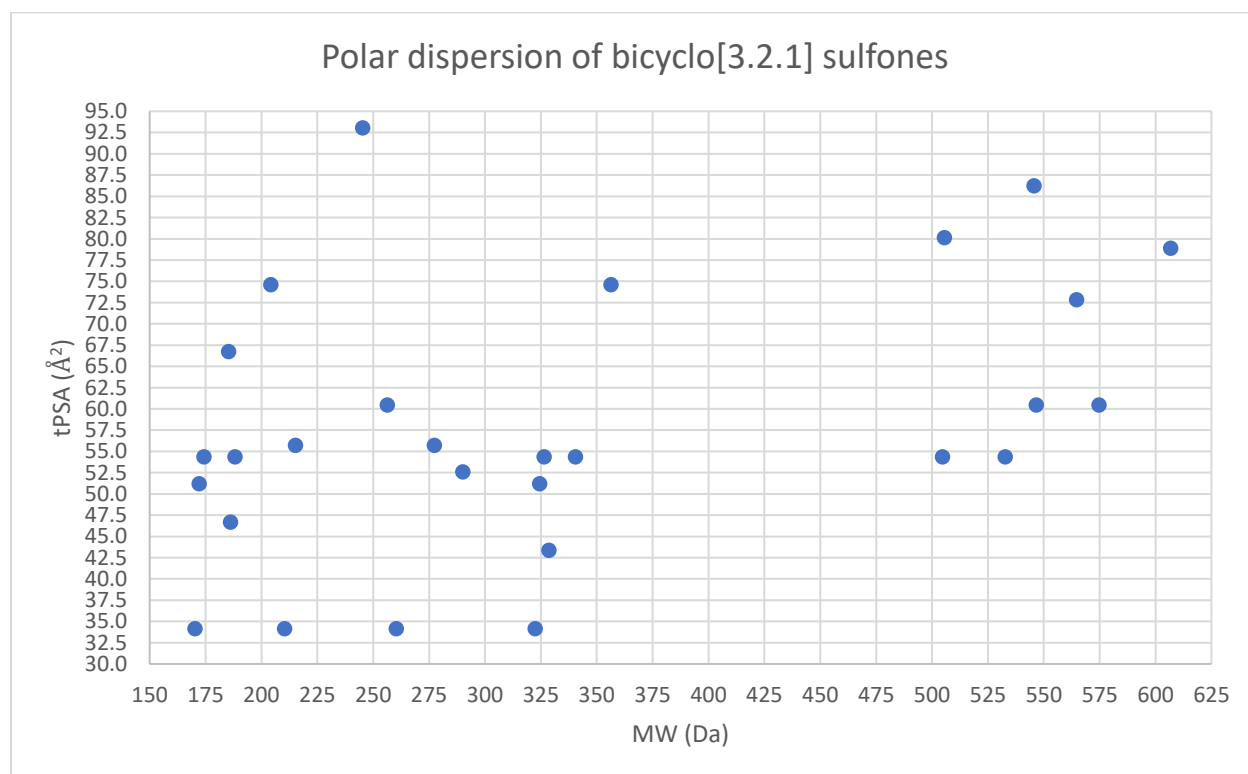


Figure 27. Distribution plot of polar surface area and molecular size of bicyclo[3.2.1]sulfone-containing molecules from Table 3.

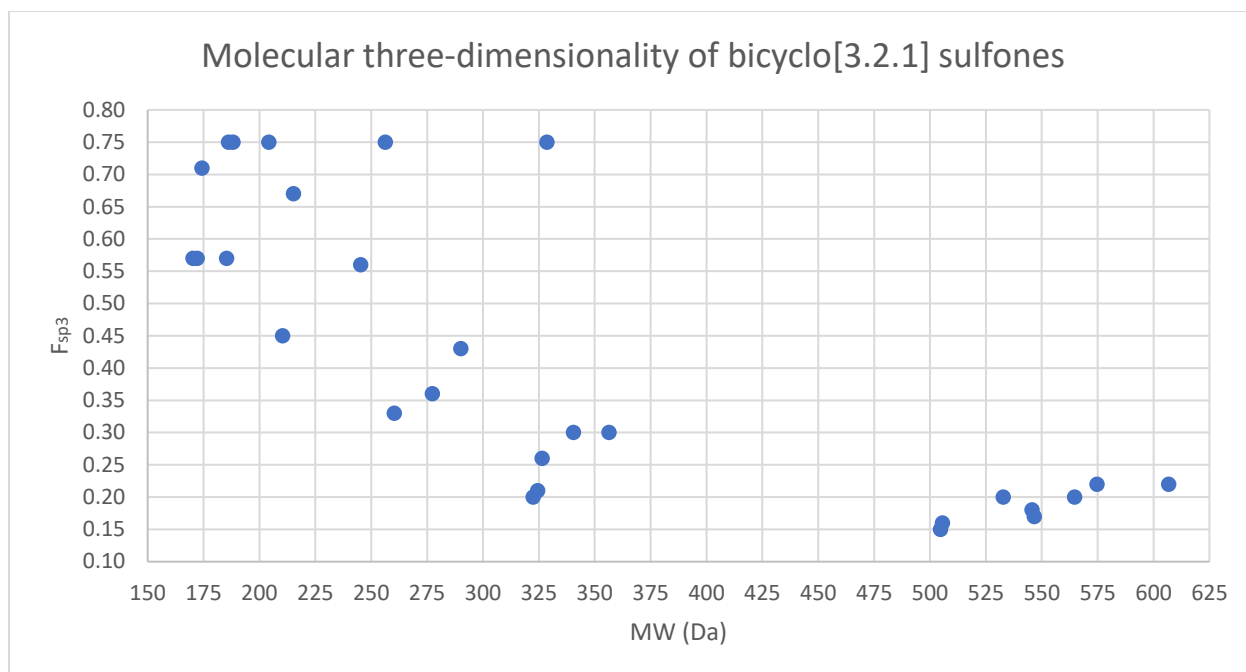


Figure 28. Three-dimensionality distribution diagram of bicyclo[3.2.1]sulfone-containing molecules from Table 3.

Chemoinformatic guidelines have been established for lead candidates serving as herbicides,<sup>236</sup> insecticides,<sup>237</sup> or acting against diseases targeted toward the central-nervous system (CNS),<sup>238</sup> as shown in Figure 29 and Table 4. By comparing the physicochemical parameters of our bicyclo[3.2.1]sulfone-containing molecular library to parameters summarized from Table 4, it is interesting that most of the synthesized molecules fit the aforementioned criteria.

Table 4. Summary of chemoinformatic data for FDA-approved herbicides, insecticides, and drugs that target the central-nervous system.

	<u>Herbicide</u>	<u>Insecticide</u>	<u>CNS</u>
<b>MW (Da)</b>	150 to 500		< = 360
<b>HBD</b>	< = 3	< = 2	< = 0.5
<b>HBA</b>	2 to 12	1 to 8	
<b>tPSA (Å<sup>2</sup>)</b>			40 to 90
<b>cLogP</b>	< = 5.0	0 to 6.5	< = 3.0
<b>RotB</b>	< = 12		

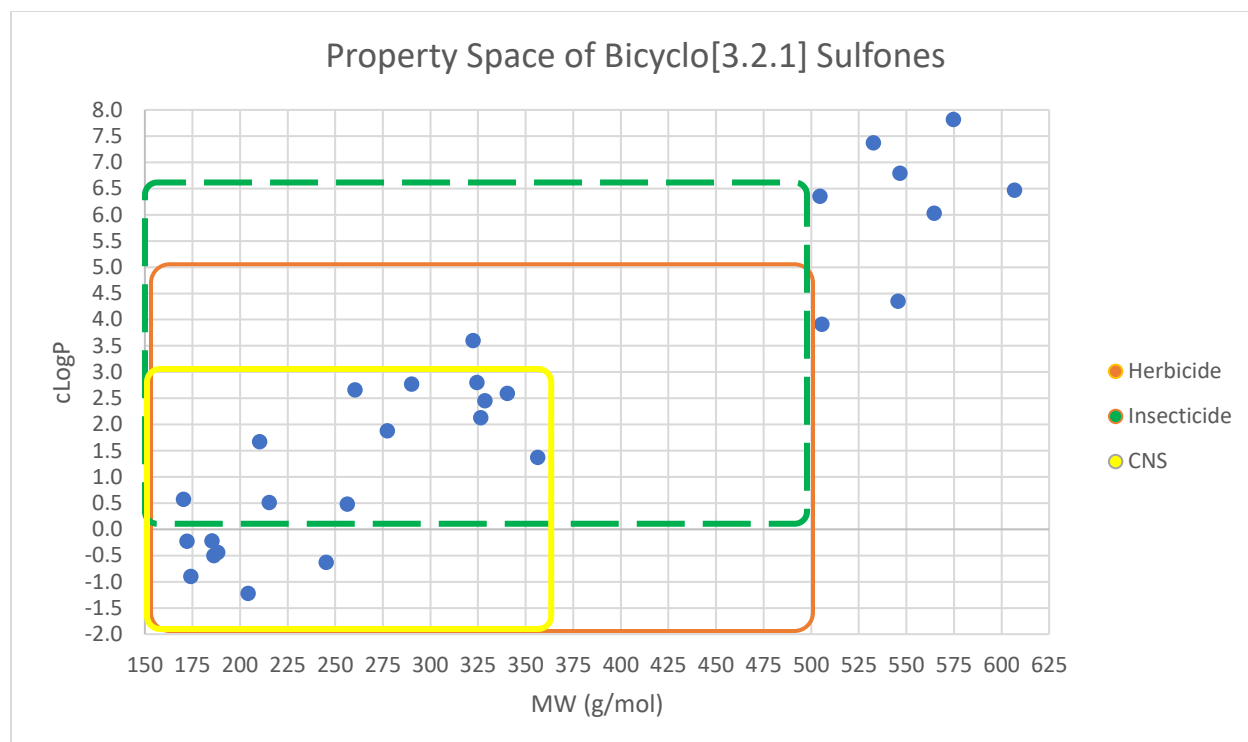


Figure 29. Property space of synthesized bicyclo[3.2.1]sulfones. Chemoinformatic properties of FDA-approved herbicides,<sup>236</sup> insecticides,<sup>237</sup> and central-nervous system-targeting drugs<sup>238</sup> are highlighted in orange, green, and yellow respectively.

We also constructed a principle moment of inertia (PMI) plot of our bicyclo[3.2.1]sulfone-containing library using the open software LLAMA,<sup>239</sup> as illustrated in Fig. 27. Generally speaking, the PMI of each molecule is calculated in three orthogonal vectors, which is usually represented as  $I_1$ ,  $I_2$ , and  $I_3$  in ascending magnitude. Normalization is done in order to minimize size-dependency by dividing the two lower variables by the highest one i.e. generating ratios  $\frac{I_1}{I_3}$  and  $\frac{I_2}{I_3}$ . A plot in the form of an isosceles triangle is generated, where its three corners are defined by the normalized ratios of various magnitudes ( $[1, 1]$ ,  $[0.5, 0.5]$ , and  $[0, 1]$ ). Note that these corners translate in three-dimensional space as spheres, discs, and rod-shapes respectively. Lastly, once all normalized ratios of each molecule are calculated, projection onto the isosceles triangle will afford the PMI plot.

Gratifyingly, the molecular shapes of our library are well-dispersed, which indicate diversity in three-dimensional space, as shown in Figure 30. Compared to Brown and coworker's PMI plot of known FDA-approved drugs (Figure 3),<sup>18</sup> our library

of bicyclo[3.2.1]sulfone-containing molecules demonstrate less bias towards either the rod or disk axes, as the mean PMI coordinate ( $I_1 = 0.434$ ,  $I_2 = 0.864$ ) is relatively close to the center of the PMI plot ( $I_1 = 0.5$ ,  $I_2 = 0.75$ ), which represents a balance of all three axes. Note that our current collection of molecules has not encompassed much chemical space near the spherical region; we anticipate that by discovering more methods to chemically functionalize bicyclo[3.2.1]sulfone-containing frameworks, greater vector control and strategies to increase hybridization (e.g. macrocyclization in the pairing phase of DOS) can help address this challenge. Although some molecules may not contain optimal physicochemical properties i.e. too many heavy atoms, high number of aromatic rings, or functional groups that may be labile or classified as pan-assay interfering,<sup>240</sup> we are nonetheless excited to showcase the possibility of bicyclo[3.2.1]sulfone-containing scaffolds in drug discovery once we have practical biological data.

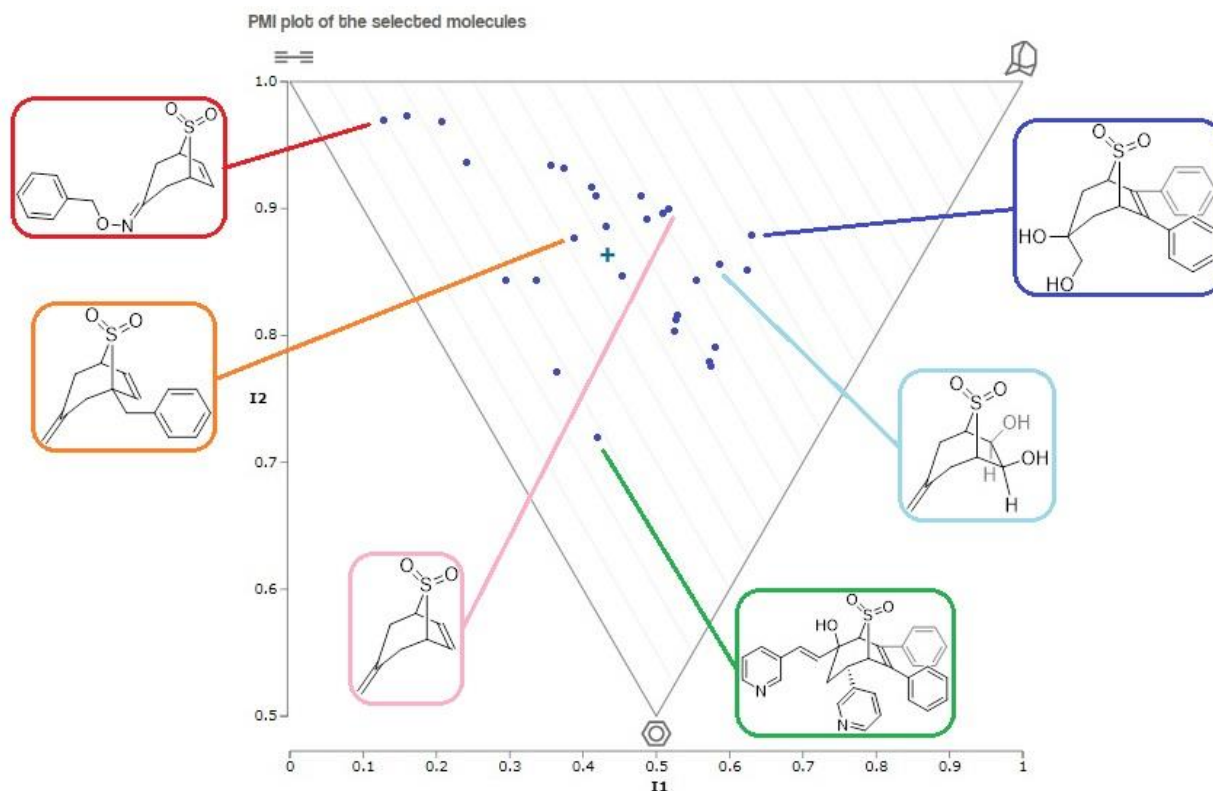


Figure 30. Principle moment of inertia plot of bicyclo[3.2.1]sulfone-containing molecules and selected examples that closely represents its corresponding axes. Mean PMI coordinates:  $I_1 = 0.434$ ,  $I_2 = 0.864$  (denoted by +).

## Chapter 4.2 Collaborations with Community for Open Antimicrobial Drug Discovery.

With our small library of bicyclo[3.2.1]sulfone-containing molecules in hand, we next sought to explore their biological importance. Without a specific biological target in mind, we decided to consult phenotypic assays provided by open-access biological screening platforms. Currently, many such initiatives have been established in order to increase overall productivity of drug discovery, and one such example is the Community for Open Antimicrobial Drug Discovery (CO-ADD) in Australia.<sup>241</sup> This initiative is established and co-managed by both academia and government agencies, and aims to resolve the healthcare crisis resulting from drug-resistant antibiotics.

Even in the early stages of understanding microbes, many renowned researchers including Sir Alexander Fleming have addressed the potential for prokaryotes to evolve across multiple generations of colonies, leading to hereditary transfer of genetic material that renders antibiotics powerless.<sup>242</sup> Currently this phenomenon has emerged to become more of an impactful matter to society: microbial infections are becoming resilient to most front-line medicines that mankind has developed,<sup>243</sup> and if this matter becomes worse, perhaps the healthcare standard may regress into the equivalent of early-1900s, where plagues and small wounds can become lethal.<sup>244</sup>

Thus, there have been many ongoing efforts towards improving this potentially apocalyptic crisis.<sup>245</sup> Despite this, many political and socioeconomical factors make the financial aspects of developing novel drug candidates for multidrug-resistant microorganisms not appealing to the private sector due to increasing overhead costs and low rate-of-return.<sup>246</sup> This creates an important role for academic labs to play in the drug discovery process.

Initial screening of select members of our compound library was performed by the CO-ADD, and results are presented in Table 5, below. Each compound shown in the table was tested against a panel of different microorganisms of various strains, including two pathogenic yeasts: *Cryptococcus neoformans* (ATCC 208821) and *Candida albicans* (ATCC 90028). Yeast infections represent one of the highly represented causes for high morbidity and mortality rates in immunocompromised patients.<sup>247</sup> Thus, the increasing prevalence of multidrug resistance in these

microorganisms is starting to become a serious healthcare concern. Many frontline antifungal agents are starting to experience decrease in efficiency,<sup>248</sup> and if humanity does not take this problem seriously, one cannot fathom the horrendous outcome associated with this issue.

Only one of our synthesized compounds is shown to be bioactive towards *C. neoformans*, as illustrated in Table 5. This particular strain is commonly known to serve as a reference strain for antimicrobial assays,<sup>249</sup> and has been well documented since its whole genome was sequenced.<sup>250</sup>

*C. albicans* is also used commonly as a reference strain, as this strain is known to be susceptible to many different antifungal agents and has been thoroughly studied within the community.<sup>251</sup> Only selected molecules from our screening library were shown to be bioactive, and no obvious relationship can be deduced based on structural information. However, compound **31c** and **76b** were shown to be the most potent out of all bioactive bicyclo[3.2.1]sulfone-containing molecules, as they exhibit approximately 50% and 40% inhibition at a concentration of 32 $\mu$ g/mL. Of course, these values are relatively unimpressive when we compare them to FDA-approved antifungal therapeutics (documented MIC<sub>90</sub> values for amphotericin B and itraconazole against *C. albicans* are 0.094  $\mu$ g/mL and 0.75  $\mu$ g/mL respectively).<sup>252(d)</sup> Nonetheless they are an intriguing glimpse into a previously undocumented type of activity for the class of molecules under study. We anticipate that further studies will help us to understand the pharmacophore, and elucidate the mechanism of action.

Table 5. Summary of biological assay data of bicyclo[3.2.1]sulfone-containing molecules against pathogenic yeast. Note that red, white, and blue colour coding denotes performance at 10<sup>th</sup>, 50<sup>th</sup>, and 90<sup>th</sup> percentile. Grey blocks indicate that negative inhibition was detected, or else a lack of statistical significance in the result.

Compound No.	Molecular Formula	MW (Da)	% inhibition at 32µg/mL	
			<i>C. albicans</i>	<i>C. neoformans</i>
<b>31a</b>	C <sub>33</sub> H <sub>28</sub> O <sub>3</sub> S	504.644	8.44	
<b>31b</b>	C <sub>35</sub> H <sub>32</sub> O <sub>3</sub> S	532.698	5.71	
<b>31c</b>	C <sub>35</sub> H <sub>32</sub> O <sub>5</sub> S	564.696	49.53	
<b>31d</b>	C <sub>31</sub> H <sub>26</sub> N <sub>2</sub> O <sub>3</sub> S	505.620	8.12	
<b>32a</b>	C <sub>35</sub> H <sub>30</sub> O <sub>4</sub> S	546.681		
<b>32b</b>	C <sub>37</sub> H <sub>34</sub> O <sub>4</sub> S	574.735	9.07	
<b>32c</b>	C <sub>37</sub> H <sub>34</sub> O <sub>6</sub> S	606.733	8.62	
<b>32d</b>	C <sub>33</sub> H <sub>28</sub> N <sub>2</sub> O <sub>4</sub> S	545.657	7.46	
<b>40</b>	C <sub>20</sub> H <sub>18</sub> O <sub>2</sub> S	322.422		
<b>41</b>	C <sub>19</sub> H <sub>16</sub> O <sub>3</sub> S	324.394	4.12	
<b>42</b>	C <sub>19</sub> H <sub>18</sub> O <sub>3</sub> S	326.410		
<b>43</b>	C <sub>20</sub> H <sub>20</sub> O <sub>3</sub> S	340.437	6.14	
<b>45</b>	C <sub>20</sub> H <sub>20</sub> O <sub>4</sub> S	356.436		
<b>47</b>	C <sub>8</sub> H <sub>10</sub> O <sub>2</sub> S	170.226		
<b>52</b>	C <sub>7</sub> H <sub>8</sub> O <sub>3</sub> S	172.198	5.67	6.10
<b>57</b>	C <sub>7</sub> H <sub>10</sub> O <sub>3</sub> S	174.214	5.11	
<b>59</b>	C <sub>8</sub> H <sub>12</sub> O <sub>3</sub> S	188.241		
<b>60</b>	C <sub>8</sub> H <sub>12</sub> O <sub>4</sub> S	204.240	4.68	
<b>67a</b>	C <sub>7</sub> H <sub>9</sub> NO <sub>3</sub> S	185.241	11.84	
<b>67b</b>	C <sub>9</sub> H <sub>13</sub> NO <sub>3</sub> S	215.267	6.39	
<b>67c</b>	C <sub>14</sub> H <sub>15</sub> NO <sub>3</sub> S	277.338		
<b>76b</b>	C <sub>15</sub> H <sub>16</sub> O <sub>2</sub> S	260.351		
<b>76c</b>	C <sub>11</sub> H <sub>14</sub> O <sub>2</sub> S	210.291	13.99	

10<sup>th</sup> percentile50<sup>th</sup> percentile90<sup>th</sup> percentile

In addition, five out of the six most commonly encountered drug-resistant microorganisms, which are known in the field as the acronym ESKAPE (*Enterococcus faecium*, *Staphylococcus aureus*, *Klebsiella pneumoniae*, *Acinetobacter baumannii*, *Pseudomonas aeruginosa*, and *Enterobacter species*)<sup>253</sup> were screened in order to access whether our library of bicyclo[3.2.1]sulfone-containing molecules are active against these organisms. Data are presented in Table 6.

For Gram-positive bacteria,<sup>254</sup> only strain ATCC 43300 of *S. aureus* was screened. Note that this strain of *S. aureus* has been documented to be resistant against methicillin, oxacillin, and other antibiotics via incorporation of the *mecA* gene.<sup>255</sup> This gene is responsible for encoding penicillin-binding protein A (PBP2a), in which its active site is unable to bind to  $\beta$ -lactam antibiotics and thus cell-wall synthesis can propagate in the presence of antibiotics.<sup>256</sup> Thus, strain ATCC 43300 of *S. aureus* is classified as one of the problematic methicillin-resistant *S. aureus* (MRSA), which is responsible for high mortality rates amongst patients diagnosed with bacterial infections. Only a few specific bicyclo[3.2.1]sulfone-containing molecules were shown to be active against this strain of *S. aureus*, as illustrated in Table 6. Without a reference strain or similar Gram-positive bacteria, it remains difficult for us to understand fully the underlying biological phenomenon. Further control experiments are required in order to accurately deduce the underlying effects.

*E. Coli* is one of the most well-understood Gram-negative bacteria in the scientific community, and certain strains are responsible for food poisoning and other gastrointestinal-related disorders.<sup>257</sup> In this case, strain ATCC 25922 was screened. This strain is known to be susceptible to all known antibiotics and commonly serves as a reference strain.<sup>258</sup> Having a positive control of this type in the screening campaign informs us of the inherent bioactivity of bicyclo[3.2.1]sulfone-containing molecules against microorganisms in general. As shown in Table 6, a wide range of inhibition percentage values were obtained using a fixed concentration of bicyclo[3.2.1]sulfone-containing molecules in DMSO. Even though maximum inhibition does not exceed approximately 21% inhibition across the entire panel, we can still extrapolate some useful trends from these screening results.

For example, with the exception of tetra-aryl sulfones **31a–d** and **32a–d**, almost all Chou-type bicyclo[3.2.1]sulfone-containing molecules performed moderately, with inhibition values generally varying between approximately 10% to 21%. This trend suggests that the bioactivity of bicyclo[3.2.1]sulfone-containing molecules is size-dependant; perhaps this phenomenon may be relevant to cell-permeability of the bicyclo[3.2.1]sulfone-containing molecules. O-substitution of oximes appear to follow the same trend, as inhibition values decrease when comparing oximes **67a**, **67b**, and

**67c**. Changes in overall polar-dispersity did not appear to be beneficial; however, it is noted that the hydroboration-oxidation product **59** appears to be slightly outperforming most of the Chou-type sulfones, yet alcohols **57a** and **59b** did not demonstrate such effect. However, compound **45** does not appear to fit the observing trend when compared to other di-aryl bicyclo[3.2.1]sulfone-containing molecules. Thus, based on emerging structure-activity-relationships as well as the inhibition values themselves, it appears that further development via library expansion is warranted. On the other hand, strain ATCC 19606 of *A. baumannii* is known to be a commonly used reference strains and is resistant against sulfonamides such as sulfamethoxazole,<sup>264</sup> as well as gentamycin<sup>265</sup> and carbapenem-based antibiotics.<sup>266</sup>

For example, with the exception of tetra-aryl sulfones **31a–d** and **32a–d**, almost all Chou-type bicyclo[3.2.1]sulfone-containing molecules performed moderately, with inhibitions values generally varying between approximately 10% to 21%. This trend suggests that the bioactivity of bicyclo[3.2.1]sulfone-containing molecules is size-dependant; perhaps this phenomenon may be relevant to cell-permeability of the bicyclo[3.2.1]sulfone-containing molecules. O-substitution of oximes appear to follow the same trend, as inhibition values decrease when comparing oximes **67a**, **67b**, and **67c**. Changes in overall polar-dispersity did not appear to be beneficial; however, it is noted that the hydroboration-oxidation product **59** appears to be slightly outperforming most of the Chou-type sulfones, yet alcohols **57a** and **59b** did not demonstrate such effect. However, compound **45** does not appear to fit the observing trend when compared to other di-aryl bicyclo[3.2.1]sulfone-containing molecules. Thus, based on emerging structure-activity-relationships as well as the inhibition values themselves, it appears that further development via library expansion is warranted. On the other hand, strain ATCC 19606 of *A. baumannii* is known to be a commonly used reference strains and is resistant against sulfonamides such as sulfamethoxazole,<sup>264</sup> as well as gentamycin<sup>265</sup> and carbapenem-based antibiotics.<sup>266</sup>

Table 6. Summary of biological assay data of bicyclo[3.2.1]sulfone-containing molecules against bacteria. Note that red, white, and blue colour coding denotes performance at 10<sup>th</sup>, 50<sup>th</sup>, and 90<sup>th</sup> percentile. Grey blocks indicate that negative inhibition was detected, or else a lack of statistical significance in the result.

Compound No.	Molecular Formula	MW (Da)	% inhibition at 32µg/mL					
			<i>S. aureus</i>	<i>E. Coli</i>	<i>K. pneumoniae</i>	<i>A. baumannii</i>	<i>P. aeruginosa</i>	<i>M. tuberculosis</i>
31a	C <sub>33</sub> H <sub>28</sub> O <sub>3</sub> S	504.644		13.85	11.95			2.34
31b	C <sub>35</sub> H <sub>32</sub> O <sub>3</sub> S	532.698						4.16
31c	C <sub>35</sub> H <sub>32</sub> O <sub>5</sub> S	564.696						
31d	C <sub>31</sub> H <sub>26</sub> N <sub>2</sub> O <sub>3</sub> S	505.620	8.47	7.75	8.39			12.42
32a	C <sub>35</sub> H <sub>30</sub> O <sub>4</sub> S	546.681						12.42
32b	C <sub>37</sub> H <sub>34</sub> O <sub>4</sub> S	574.735		8.34				
32c	C <sub>37</sub> H <sub>34</sub> O <sub>6</sub> S	606.733						1.21
32d	C <sub>33</sub> H <sub>28</sub> N <sub>2</sub> O <sub>4</sub> S	545.657		5.95	1.47			
40	C <sub>20</sub> H <sub>18</sub> O <sub>2</sub> S	322.422	6.48	15.83				5.32
41	C <sub>19</sub> H <sub>16</sub> O <sub>3</sub> S	324.394	12.66	17.94	11.70			
42	C <sub>19</sub> H <sub>18</sub> O <sub>3</sub> S	326.410		10.19				1.21
43	C <sub>20</sub> H <sub>20</sub> O <sub>3</sub> S	340.437		12.32	15.52	24.67		5.32
45	C <sub>20</sub> H <sub>20</sub> O <sub>4</sub> S	356.436		9.42				1.96
47	C <sub>8</sub> H <sub>10</sub> O <sub>2</sub> S	170.226		10.20	6.22			0.16
52	C <sub>7</sub> H <sub>8</sub> O <sub>3</sub> S	172.198	3.52	15.37				5.61
57	C <sub>7</sub> H <sub>10</sub> O <sub>3</sub> S	174.214		12.52	9.45			5.32
59	C <sub>8</sub> H <sub>12</sub> O <sub>3</sub> S	188.241	10.44	21.20	14.53			3.46
60	C <sub>8</sub> H <sub>12</sub> O <sub>4</sub> S	204.240						1.21
67a	C <sub>7</sub> H <sub>9</sub> NO <sub>3</sub> S	185.241	10.74	21.46				4.58
67b	C <sub>9</sub> H <sub>13</sub> NO <sub>3</sub> S	215.267		11.60	12.95			6.45
67c	C <sub>14</sub> H <sub>15</sub> NO <sub>3</sub> S	277.338		10.05				
76b	C <sub>15</sub> H <sub>16</sub> O <sub>2</sub> S	260.351		7.53	8.81			8.31
76c	C <sub>11</sub> H <sub>14</sub> O <sub>2</sub> S	210.291	17.98	15.22	16.82			0.84

10<sup>th</sup> percentile
50<sup>th</sup> percentile
90<sup>th</sup> percentile

Currently, we have insufficient data to understand why certain bicyclo[3.2.1]sulfone-containing molecules selectively act against the drug resistant microorganisms that we have screened. Elucidating which biochemical pathway bicyclo[3.2.1]sulfone-containing molecules interact with would require extensive effort, such as developing bicyclo[3.2.1]sulfone-containing photoaffinity probes to determine which biological target(s) they interact with, or testing mutant microorganisms with specific gene knockouts to determine which biological pathways are influenced by the presence of bicyclo[3.2.1]sulfone-containing molecules.

Nonetheless, we can derive interesting observations based on our results from the screening assays against drug resistant microorganisms. For example, one can argue that Gram-negative bacteria appear to be more susceptible than Gram-positive bacteria to be influenced by the presence of bicyclo[3.2.1]sulfone-containing molecules, if one were to qualitatively compare that number of bioactive hits amongst *S. aureus* strain ATCC 43300 and *K. pneumoniae* strain ATCC 700603. Given the fact that Gram-negative bacteria are more resistant against most known antibiotics due to their nearly-impenetrable cell wall,<sup>267</sup> this is a considerably interesting phenomenon, and we can foresee an opportunity may arise through future development that leads to emergence of bicyclic sulfone-containing antibiotics that are selective against Gram-negative bacteria. Alternatively, given the fact that at least four molecules of our bicyclo[3.2.1]sulfone-containing library exhibit similar bioactivity against both *S. aureus* and *K. pneumoniae*, exciting development can arise from further development of bicyclic sulfone-containing broad spectrum antibiotics.<sup>268</sup>

Drug resistant *M. tuberculosis* was also screened with the assistance of the team from Eli Lilly's Open Innovation Drug Discovery program.<sup>269</sup> In contrast to the microbes, *M. tuberculosis* cannot be definitively categorized using Gram test.<sup>270</sup> Nonetheless, this species represents one of the major challenges to be tackled as the wave of antibiotic resistance becomes more prevalent to our daily lives.<sup>271</sup> Screening against our library of bicyclic sulfone-containing small molecules reveal that low scores of inhibition values were obtained, with the maxima being approximately 12.5%. Comparison between chemical structures and their respective inhibition values reveal no obvious trends, which may be attributed to unfavorable cellular uptake of bicyclic sulfone-containing fragments by *M. tuberculosis*.<sup>272</sup> This phenomenon yet again demonstrates that different microorganisms exhibit different preference of bicyclic sulfone-containing small molecules, which at first glance may be challenging to tackle for long-term research focus of drug discovery development. However, surely every molecule synthesized has its own purpose in the realms of searching for bioactivity.

### Chapter 4.3 Eli Lilly's Open Innovation Drug Discovery Platform.

As mentioned previously, Eli Lilly provides a comprehensive open-access biological screening platform for academia and industrial partners for future collaboration.<sup>273</sup> In order to further validate the potential of our library of bicyclic sulfone-containing small molecules during our campaign, we determined that collaborative effort with Eli Lilly's Open Innovation Drug Discovery Platform would be a good fit. The pipelines of Eli Lilly orientate towards other therapeutic direction beyond antibiotics; instead, they aim to solidify their position as a global competitor in disciplines such as oncology, immunology, diabetes, and neurodegenerative diseases. To that end, we felt that their biological assays may yield further interesting results from our bicyclic sulfone-containing small molecule library.

Indeed, we received news that our library raised some attentions in a primary assay against an enzyme called nicotinamide N-methyl transferase (NNMT). This enzyme is capable of catalyzing the process of transferring a methyl group from S-adenosylmethionine (SAM) to the  $sp^2$ -hybridized nitrogen of the pyridine ring in nicotinamide, thereby generating N-methylated nicotinamide (MNAN) and S-adenosylhomocysteine (SAH) as products, as illustrated in Figure 31.<sup>274</sup>

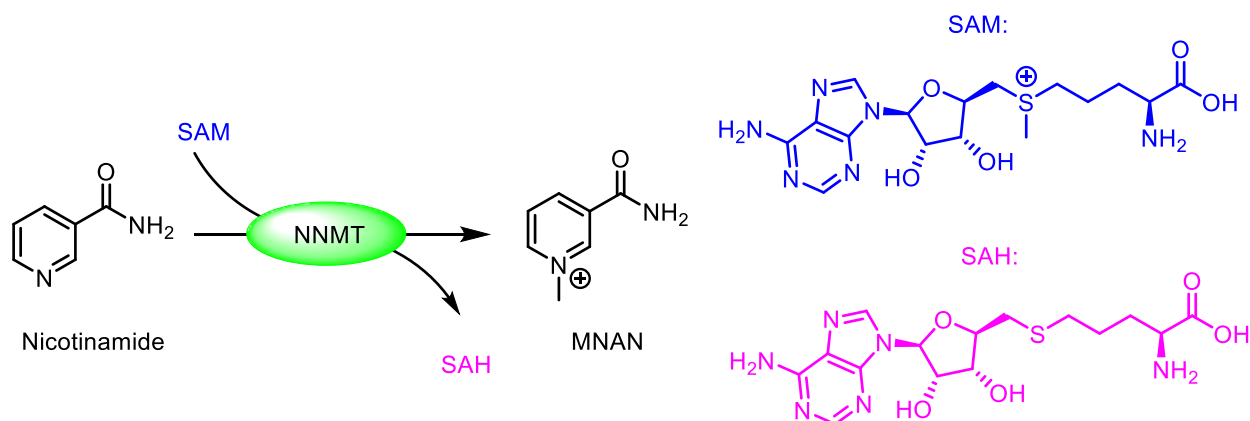


Figure 31. General mechanistic scheme illustrating natural ligands and function of NNMT.

Although this biochemical pathway sounds relatively straightforward, its biological implication can be tremendously significant: MNAN is involved in numerous cellular signaling pathways,<sup>275</sup> and consumption of SAM into SAH requires that methionine-dependant pathways perform methionine salvaging in order to be functional,<sup>276</sup> which is also associated with a wide variety of epigenetic cell expression. Furthermore,

nicotinamide is not the only competent substrate for NNMT, as there is evidence to support that vitamin B3 and other nitrogen-containing heterocycles can be methylated,<sup>277</sup> thereby implicating the enzyme into numerous biochemical pathways. Coupled with the fact that different expression level of NNMT has been observed in different tissues,<sup>278</sup> it is no surprise NNMT is a key player in many different types of cancer,<sup>279</sup> neurological disorders such as Parkinson's disease,<sup>280</sup> and various metabolic impairments.<sup>281</sup> Yet, the biological function of NNMT remains unclear.

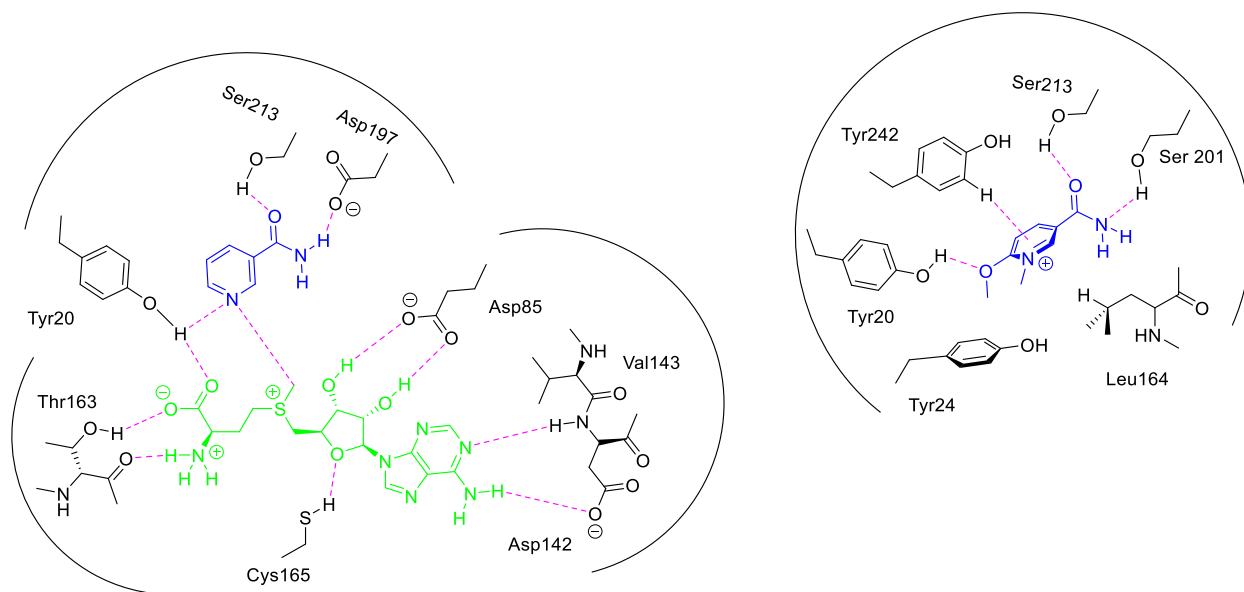
*Table 7. Summary of biological assay data of bicyclo[3.2.1]sulfone-containing molecules against the enzyme NNMT. Note that red, white, and blue colour coding denotes performance at 10<sup>th</sup>, 50<sup>th</sup>, and 90<sup>th</sup> percentile. Grey blocks indicate that negative inhibition was detected, or else a lack of statistical significance in the result.*

Compound No.	Molecular Formula	MW (Da)	% inhibition at 9.99 $\mu$ M	
			MNA	SAH
<b>31a</b>	C <sub>33</sub> H <sub>28</sub> O <sub>3</sub> S	504.64	8.393	
<b>31b</b>	C <sub>35</sub> H <sub>32</sub> O <sub>3</sub> S	532.7		
<b>31c</b>	C <sub>35</sub> H <sub>32</sub> O <sub>5</sub> S	564.7	15.17	
<b>31d</b>	C <sub>31</sub> H <sub>26</sub> N <sub>2</sub> O <sub>3</sub> S	505.62	35.15	38.14
<b>32a</b>	C <sub>35</sub> H <sub>30</sub> O <sub>4</sub> S	546.68	8.297	
<b>32b</b>	C <sub>37</sub> H <sub>34</sub> O <sub>4</sub> S	574.74		28.52
<b>32c</b>	C <sub>37</sub> H <sub>34</sub> O <sub>6</sub> S	606.73	17.49	
<b>32d</b>	C <sub>33</sub> H <sub>28</sub> N <sub>2</sub> O <sub>4</sub> S	545.66	17.31	28.65
<b>40</b>	C <sub>20</sub> H <sub>18</sub> O <sub>2</sub> S	322.42	10.67	
<b>41</b>	C <sub>19</sub> H <sub>16</sub> O <sub>3</sub> S	324.39	5.549	
<b>42</b>	C <sub>19</sub> H <sub>18</sub> O <sub>3</sub> S	326.41		
<b>43</b>	C <sub>20</sub> H <sub>20</sub> O <sub>3</sub> S	340.44	5.57	
<b>45</b>	C <sub>20</sub> H <sub>20</sub> O <sub>4</sub> S	356.44	1.471	
<b>47</b>	C <sub>8</sub> H <sub>10</sub> O <sub>2</sub> S	170.23	11.04	
<b>52</b>	C <sub>7</sub> H <sub>8</sub> O <sub>3</sub> S	172.2	11.4	
<b>57</b>	C <sub>7</sub> H <sub>10</sub> O <sub>3</sub> S	174.21	11.04	
<b>59</b>	C <sub>8</sub> H <sub>12</sub> O <sub>3</sub> S	188.24		
<b>60</b>	C <sub>8</sub> H <sub>12</sub> O <sub>4</sub> S	204.24	7.681	
<b>67a</b>	C <sub>7</sub> H <sub>9</sub> NO <sub>3</sub> S	185.24	19.42	
<b>67b</b>	C <sub>9</sub> H <sub>13</sub> NO <sub>3</sub> S	215.27		
<b>67c</b>	C <sub>14</sub> H <sub>15</sub> NO <sub>3</sub> S	277.34	2.327	
<b>76b</b>	C <sub>15</sub> H <sub>16</sub> O <sub>2</sub> S	260.35	12.13	
<b>76c</b>	C <sub>11</sub> H <sub>14</sub> O <sub>2</sub> S	210.29	1.837	

10<sup>th</sup> percentile50<sup>th</sup> percentile90<sup>th</sup> percentile

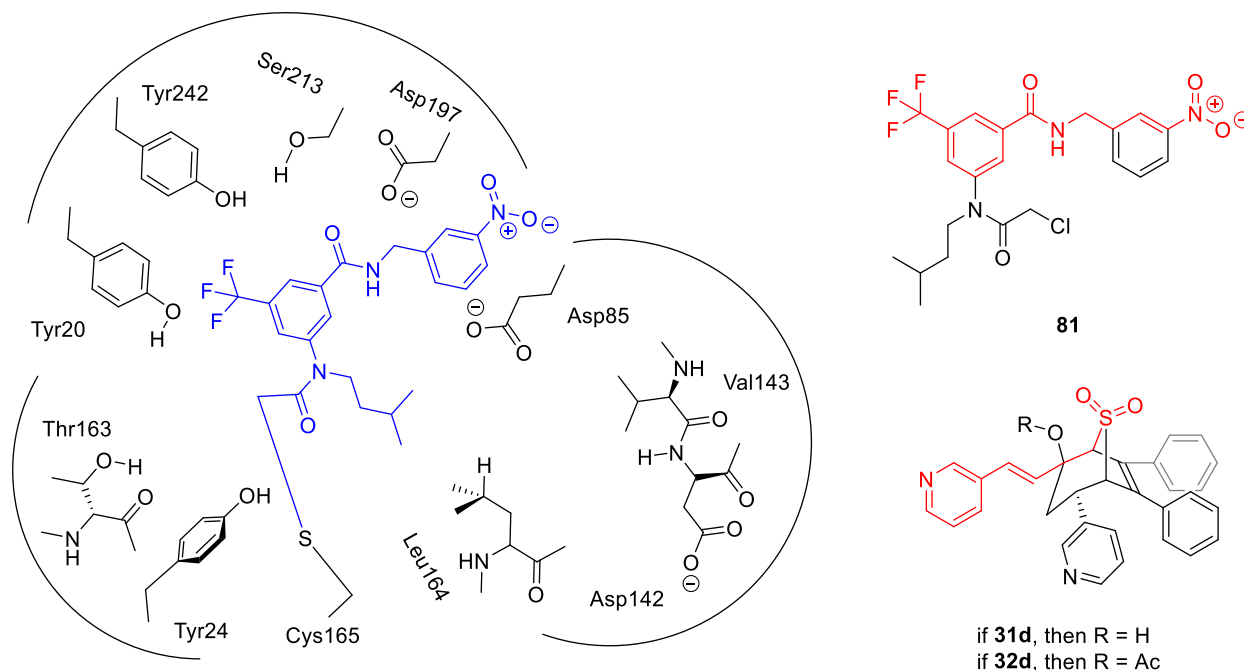
The primary assay used for determining inhibition of NNMT was prescribed by van Haren and colleagues,<sup>282</sup> although many different quantification assays have been developed since then.<sup>283</sup> In our case, monitoring of the MNA and SAH concentration values can offer further insight into the mechanism of how our bicyclic sulfone-containing small molecules interact with NNMT. Inhibition values derived from the concentration of MNA vary significantly, as shown in Table 7; however, their inhibition values are moderate at best.

Perhaps it is no surprise that sulfones **31d** and **32d** slightly outperformed the rest of the library, which we attribute to greater match between the pyridine moieties and the active site of NNMT.<sup>284</sup> Note that the *p*-anisole-containing sulfone **32c** also appears to be a competitive inhibitor, which exceeded our expectations. Given the fact that 6-methoxynicotinamide can function as a competitive inhibitor for NNMT,<sup>285</sup> which is summarized in Scheme 62, our hypothesis of pyridine-containing bicyclic sulfone-containing small molecules acting as competitive inhibitor for the active site of NNMT is further augmented. Martin and coworkers have demonstrated that favorable interaction between two regions of the active site of NNMT is necessary for optimal inhibitions,<sup>286</sup> and coupled with careful analysis of the co-crystal structure of human NNMT and natural ligands nicotinamide and SAM,<sup>287</sup> our hypothesis where the bicyclic sulfone scaffold may be interacting with a pocket in close proximity to the active site of NNMT is further strengthened.



*Scheme 62. General schematic diagram of how methylation of nicotinamide proceeds (left) illustration of how 6-methoxynicotinamide interacts within the active site of NNMT.*

Cravatt and coworkers have showcased an  $\alpha$ -chloroacetamide-based chemical probe with extraordinary selectivity for NNMT *in vitro*;<sup>288</sup> if one were to assume that the trifluoromethyl moiety acts as a hydrogen-bond accepting bioisostere to interact with Tyr-20 and/or its vicinity, then one may be able to see parallelism between their rightmost portion of the chemical probe and our compounds **31d** and **32d**: the aryl amide and nitro moiety functions similar to our trans-alkene and bicyclic sulfone moieties, as illustrated in Scheme 63. The high proportion of  $sp^2$ -hybridized atoms in both the aryl amide and trans-alkene moiety could be a geometrical match, while both the nitro and bicyclic sulfone functional group could act as hydrogen-bond acceptors presumably in a pocket nearby the nicotinamide-binding region. It is possible that the low reactivity could be due to a combination of steric hindrance between the bulky tetra-aryl **31d** or **32d** with the active site of NNMT, as well as insufficient binding affinity due to suboptimal geometry between interacting regions. Excitingly, we should anticipate that further optimization and truncating certain regions of our pyridine-containing bicyclo[3.2.1]sulfone-containing molecules can lead to improved potency; fragment extension in order to reach the cysteine-amino-acid-binding region should also lead improved binding affinity and increased selectivity amongst other SAM-dependant methyltransferases.<sup>289</sup>



*Scheme 63. Postulated binding mode of amide **81** by covalent linkage within the active site of NNMT (left). Structural similarity between amide **81** and bicyclo[3.2.1]sulfone **31d** or **32d** as highlighted in red (right).*

Arguably, the present analysis has no computational or crystallographic evidence to directly support our hypothesis. Nonetheless, we believe ongoing development of fragment coupling as well as further structure-activity relationship development may be helpful in developing structures that not only contain bicyclic alkyl sulfone moieties, but also achieve desirable physiological outcome by interacting favorably with NNMT, whether competitively or not.

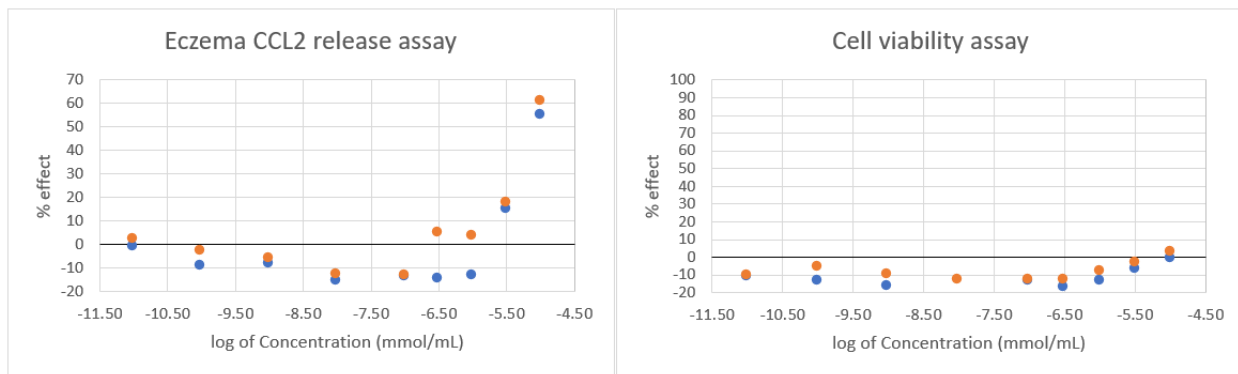
#### Chapter 4.4 Eczema Assay Screening with LEO Pharma A/S.

To further explore any potential biological applications for our bicyclic sulfone-containing small molecule library, we decided to collaborate with another industrial partner, this time with a focus towards a different therapeutic area. LEO Pharma A/S is a Denmark-based pharmaceutical that specializes in developing novel therapeutic treatments with regards to skin-related disorders and diseases related to cellular signaling.<sup>290</sup> In particular, they have had long-lasting collaborations with academic partners on a global scale.<sup>291</sup>

The open innovation platform offered by LEO Pharma focuses on four biological assays:<sup>292</sup>

1. Eczematous inflammation in human keratinocytes: human keratinocytes are incubated with a cytokine cocktail containing IL-4, IL-13, IL-22 and IFN-gamma to induce an eczema-relevant response, which is characterized by an increase in CCL2 expression.
2. T-cell inflammation assay: an inflammatory response is induced in human CD4+ T-cells via exposure to beads coated in CD2, CD3 and CD28. The response is measured by the secretion level of IL-2 and IL-4.
3. Psoriatic inflammation in human keratinocytes: Increase in IL-8 expression is used to indicate the presence of a psoriasis-relevant inflammatory response when human keratinocytes are stimulated with a cytokine cocktail of TNF- $\alpha$  and IL-7.
4. Peripheral blood mononuclear cells (PBMC) inflammation assay: Human PMBC are to be used to induce an inflammatory response as indicated by the expression level of IL-17. This is done by exposure of PMBC with beads coated in CD3 and CD28, followed by incubation in a medium rich in IL-23.

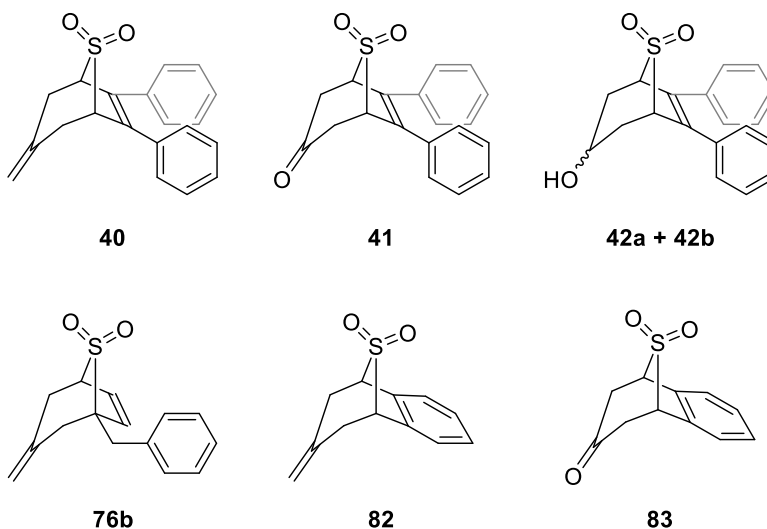
Our bicyclic sulfone-containing fragment library was tested against the aforementioned assays, with additional testing of cellular viability in order to ensure minimization of cytotoxicity during exposure to our library of small molecules. Many of our synthesized molecules did not perform well nor yield any interesting results, with one exception being ketone **41**, which demonstrated an EC<sub>50</sub> value of approximately 8.12 $\mu$ M during observation of inhibition of CCL2 expression, as shown in Figure 32. Beyond that, additional data suggested that cell viability was well-maintained, which indicated that cellular damage was kept to a minimum. These results are very encouraging for primary screening, as we obtained a hit candidate within a relatively small library. However, other bicyclic sulfone-containing analogues did not perform as well, such as alcohol **42a**, **42b** or alkene **40**, which suggests improved activity may not come easily.



Data: Abs EC<sub>50</sub> = 8120 nM , Max Effect = 61.2 %      Abs EC<sub>50</sub> > 10000 nM , Max Effect = 3.15 %

Figure 32. Biological data of sulfone **41** in eczema induced CCL2 release assay. Data points highlighted in orange and blue represent two separate trials.

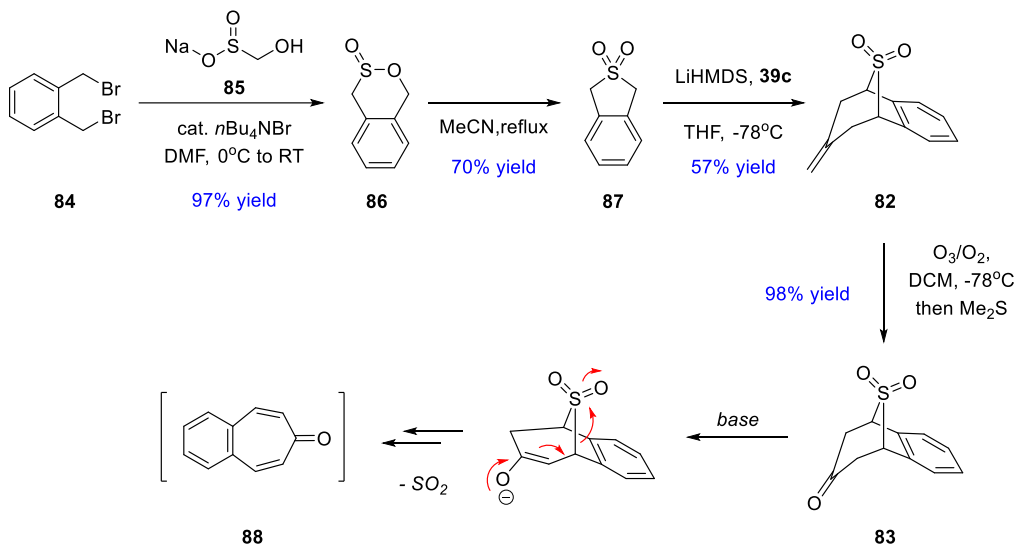
In order to revalidate the data obtained from the primary phenotypic assays, we decided to re-test several bicyclic sulfones with the goal of obtaining a full inhibition curve if appropriate. These molecules were chosen due to high structural similarity, as well as our desire for further understanding the pharmacophore required for phenotypic activity, and full toxicity curve induced by the corresponding molecule. As such, compounds **40**, **41**, **42a**, **42b**, **76b**, **82**, and **83** were screened, as shown in Scheme 64.



Scheme 64. List of synthesized bicyclo[3.2.1]sulfone-containing molecules that were used in re-validation screening.

Compounds **82** and **83** were synthesized as a part of our ongoing efforts to continue exploring novel bicyclo[3.2.1]sulfone-containing molecules and investigate novel bioactivity. Sulfone **82** was synthesized using Chou's double alkylation protocol from sulfone **87**,<sup>293</sup> while ketone **83** was generated from **82** via ozonolysis, as illustrated

in Scheme 65. It is interestingly that we observed ketone **83** being degraded within a week when dissolved in a solution of hexane with 5% v/v NEt<sub>3</sub>, thus augmenting our previous hypothesis that enolization leads to  $\beta$ -elimination of the sulfone moiety in bicyclo[3.2.1]sulfone-containing molecules.



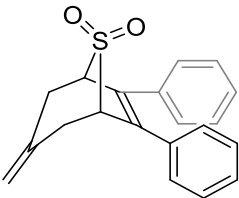
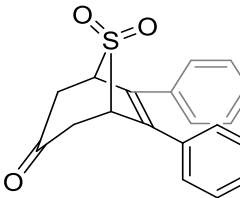
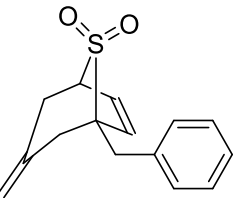
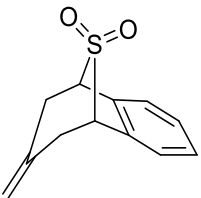
*Scheme 65. Overall reaction schemes of synthesizing sulfones **82** and **83**, as well as postulated mechanism of how ketone **83** degrades under basic conditions.*

The biological data from re-validation is summarized in Table 8. Note that in our analysis, assays results are deemed insignificant when the potency values are approximately equal to (or less than) cell viability values. Interestingly, sulfone **41** performed arguably similar in the IL-8 assay as well as the CCL2-assay, due to similarity between their potency values (7.35  $\mu$ M and 5.47 $\mu$ M). However, we also observed that sulfones **76b** and **40** showing bioactivity in the assay, as their inhibition values were determined to be 20.3 $\mu$ M and 9.12 $\mu$ M respectively; unfortunately, sulfone **82** did not show any significant cellular events.

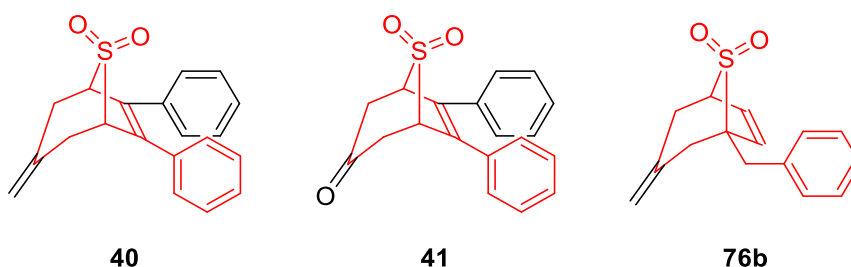
We also obtained other interesting results: sulfone **41** performed relatively well in the psoriasis IL-8 assay and is the only bioactive bicyclo[3.2.1]sulfone-containing molecule to demonstrate significant results in the assay during our secondary screen. Furthermore, sulfone **41** showed moderate inhibition in the IL-17 assay which was not seen previously. This fluctuation in cellular outcome could be due to biological inconsistency in whole-cell screenings. Note that sulfone **40** also performed in a decent manner in IL-17 assay as it demonstrated a potency of 21.4 $\mu$ M.

Simply evaluating by potency values alone without considering toxicity would be misleading. Although much remains to be elucidated i.e. mechanism of action, more refined structure-activity relationship studies, pharmacophore determination, pharmacodynamics and pharmacokinetic profile, we believe that adapting therapeutic index (TI), which is a quantitative measurement of the relative safety of a drug, could be beneficial in our analysis, as we seek to minimize any potential side-effects. In our case, we can derive the therapeutic index using the ratio of half maximal assay output concentration and the half maximal cell viability concentration. For example, the “therapeutic index” of sulfone **40** in CCL2 assay is  $\frac{9.12\mu\text{M}}{35.0\mu\text{M}} = 0.261$ .

Table 8. Summary of biological assay data from re-validation of bicyclo[3.2.1]sulfone-containing molecules.

	No.	<b>40</b>	<b>41</b>	<b>76b</b>	<b>82</b>
Assay types	Structure				
Psoriasis-induced IL-8 assay	Potency	Insignificant	7.35 $\mu\text{M}$	Insignificant	Insignificant
	Cell Viability		9.63 $\mu\text{M}$		
	TI values		0.763		
Eczema-induced CCL2 release assay	Potency	9.12 $\mu\text{M}$	5.47 $\mu\text{M}$	20.3 $\mu\text{M}$	
	Cell Viability	35.0 $\mu\text{M}$	11.8 $\mu\text{M}$	56.6 $\mu\text{M}$	
	TI values	0.261	0.464	0.359	
Inhibition of IL-17 release from CD3/CD28/IL-23-induced assay	Potency	21.4 $\mu\text{M}$	27.1 $\mu\text{M}$	Insignificant	
	Cell Viability	40.4 $\mu\text{M}$	64.2 $\mu\text{M}$		
	TI values	0.530	0.422		
Inhibition of IL-2 and IL-4 release from CD2/CD3/CD28-induced assay	Potency	Insignificant	Insignificant	Insignificant	
	Cell Viability				
	TI values				

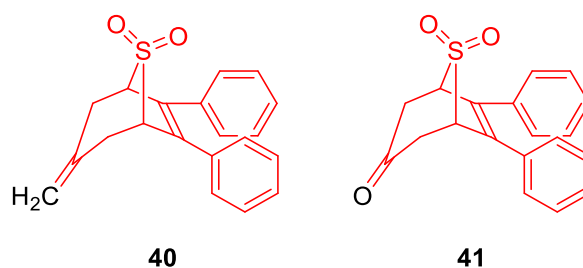
Using such standards, sulfones **41**, **76b**, and **40** offered TI values of 0.464, 0.359, and 0.261 respectively when comparing results from CCL2 assays. Despite the fact that sulfone **40** outperforming ketone **41** in terms of potency values, the fact that sulfone **40** offered higher TI values may indicate that the ketone moiety may be responsible for higher cellular toxicity events. Currently we are unsure if the changes in polarity alone (tPSA of ketone **41** = 51.21 Å<sup>2</sup> while sulfone **40** = 34.14 Å<sup>2</sup>) can explain the observation that ketone **41** is twice as effective than sulfone **40**. Serendipitously, although sulfone **76b** has a TI value that is inbetween that of ketone **41** and sulfone **40**, the values of cell viability of sulfones **76b** and **40** are significantly higher than ketone **41**, which further supports our hypothesis that the ketone moiety is leading to unproductive cellular outcomes. Thus, we believe that the higher potency values of sulfone **76b** compared to sulfone **40** are due to geometric mismatch of the phenyl moiety between target pocket. The fact that the inflexible benzene ring is featured in sulfone **82**, and coupled with its insignificant results, has lead us to infer that a flexible phenyl ring at an appropriate geometric distance away from the protruding sulfone moiety of the bicyclo[3.2.1]scaffold is most likely the pharmacophore, as shown in Scheme 66. However, further screening of new bicyclo[3.2.1]sulfone-containing molecules are needed in order to validate our hypothesis, as well as more accurately determine the biological target.



*Scheme 66. Structural similarity amongst all bioactive bicyclo[3.2.1]sulfones in eczema-induced CCL2 release assay, as highlighted in red.*

During analysis of IL-17 assay data, the TI values of sulfone **40** is slightly higher than ketone **41**, which is directly in contrast to what was observed in the first round of assays. When comparing the IL-17 assay data between ketone **41** and sulfone **40**, almost all data appears to be comparable, despite slight differences of cell viability. This

implies that either change in overall polarity does not induce significant phenotypic responses in the CCL2 assay, or that substitution at the C-3 position is irrelevant to inducing any changes in cellular outcome. Interestingly, alcohols **43a**, **43b** and diol **45** did not demonstrate any significant bioactivity in the IL-17 assay; these molecules feature  $sp^3$ -hybridization at the C-3 position and changes in overall polarity. Coupled with the fact that neither sulfone **47** nor ketone **52** performed outstandingly well during primary screens, it is possible that an exo-cyclic  $sp^2$ -hybridized moiety, as well as di-aryl stilbene moiety incorporated a bicyclo[3.2.1]sulfone scaffold is necessary in order to achieve comparable phenotypic outcome, as shown in Scheme 67.



*Scheme 67. Structural similarity amongst all bioactive bicyclo[3.2.1]sulfones in inhibition of IL-17 release from CD3/CD28/IL-23-induced assay, as highlighted in red.*

Despite the intriguing results mentioned previously, we are currently unsure if the mechanism of action induced by bicyclo[3.2.1]sulfones are as straightforward as one might imagine. Currently, we require more experimental data not only for structure-activity relationship studies, but also to elucidate the biological target responsible for the observed cellular outcome. For example, JAK-STAT pathways are thoroughly studied and is known to be highly involved in immunodeficiency disorders<sup>294</sup> and different types of cancer cases.<sup>295</sup> The enzyme JAK3 is responsible for regulating activation of various receptors such as IL-2, IL-4, IL-15, and IL-21, amongst other cytokine receptors.<sup>296</sup> Faulty JAK-STAT signaling pathways have been observed to be associated with high prevalence of skin disorders.<sup>297</sup> Overexpression of STAT3 has been associated with psoriasis,<sup>298</sup> as STAT3 is known to regulate production of IL-23 receptors and thus indirectly controlling the development of Th17 cells, which can induce psoriasis.<sup>299</sup> Also, STAT6 has been demonstrated as a crucial component for mediating IL-4-induced signaling,<sup>300</sup> which produces various physiological responses.<sup>301</sup> Beyond IFN- $\gamma$  or TNF- $\alpha$ ,<sup>302</sup> it has been demonstrated that IL-4, IL-13, and IL-23 can lead to signal induction of

JAK-STAT pathways.<sup>303</sup> In addition, IL17 expression has been known to be influenced by cooperativity between STAT3 and the receptor ROR $\gamma$ t.<sup>304</sup> Beyond that, JAK2 has been examined to play an important role in regulating IL-8 transcription.<sup>305</sup> However, currently there are many variables that may refute our hypotheses, thus, continuation of this program would require re-validation and reassessment on top of additional experimental data to support our claims.

Despite this, the reduction of CCL2 expression is a good starting point for therapeutic development. The cytokine is responsible for attracting various types of monocytes, memory T-cells, and dendritic cells to sites of inflammation when tissue injuries or infections occurs.<sup>306</sup> Thus, CCL2 is implicated in pathogenesis of not only psoriasis, but also of rheumatoid arthritis and atherosclerosis.<sup>307</sup> Furthermore, the polypeptide is involved in neuroinflammatory processes which are characterized by neuronal degeneration, such as epilepsy,<sup>308</sup> brain ischemia,<sup>309</sup> Alzheimer's disease,<sup>310</sup> experimental autoimmune encephalomyelitis,<sup>311</sup> and traumatic brain injury.<sup>312</sup> Beyond that, high levels of CCL2 can lead to hypomethylation of CpG sites and upregulation of amylin expression through ERK1/ERK2/JNK-AP1 and NF- $\kappa$ B related signaling pathways, which are responsible for vascular complications and insulin resistance.<sup>313</sup> Thus, we anticipate that further optimization of bicyclo[3.2.1]sulfone-containing molecules can lead to improved reduction of CCL2 levels without significantly damaging cell proliferability, and ultimately lead to improvement in human health.

Similarly, the ability to alter expression levels of cytokines IL-8 and IL-17 can be beneficial in advancing human healthcare. IL-8 not only serves a prominent role in the development of gingivitis and psoriasis,<sup>314</sup> but also been implied in various other disorders, such as obesity,<sup>315</sup> colorectal carcinomas,<sup>316</sup> cystic fibrosis,<sup>317</sup> as well as schizophrenia.<sup>318</sup> The severity of asthma is highly correlated with the expression level of IL-17.<sup>319</sup> Thus, we can foresee that biological testing with more bicyclo[3.2.1]sulfone-containing molecules will help chart through unknown territory and expand human knowledge.

In summary, small molecule candidates with promising biological applications have been achieved. This work showcases that bicyclic alkyl sulfones have the potential

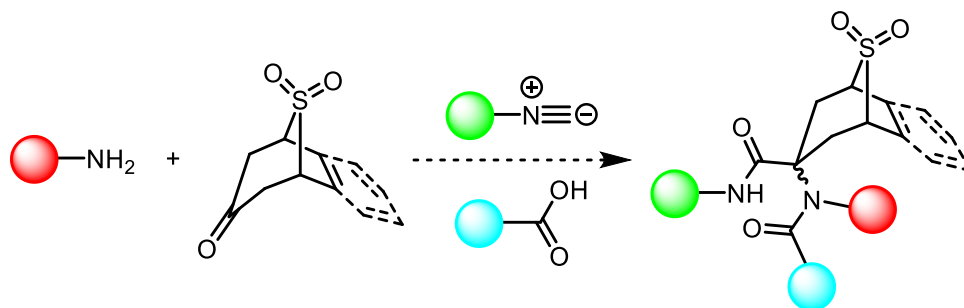
to become an important cornerstone that no medicinal chemists should dismiss in the pursuit of drug discovery.

## Chapter 5 – Future Directions on Functionalization

### Chapter 5.1 Further Functionalization of Bicyclo[3.2.1]Sulfones

As mentioned in previous chapters, we have made significant progress in site-selective functionalization of bicyclo[3.2.1]alkyl sulfone-containing skeletons. Our strategy so far has allowed us to realize many biological activities. However, our lofty goal of complete vector control via site-selective functionalization has not yet been fully realized. Greater dedication in reaction screening is required in order to further expand chemical space and exert molecular control.

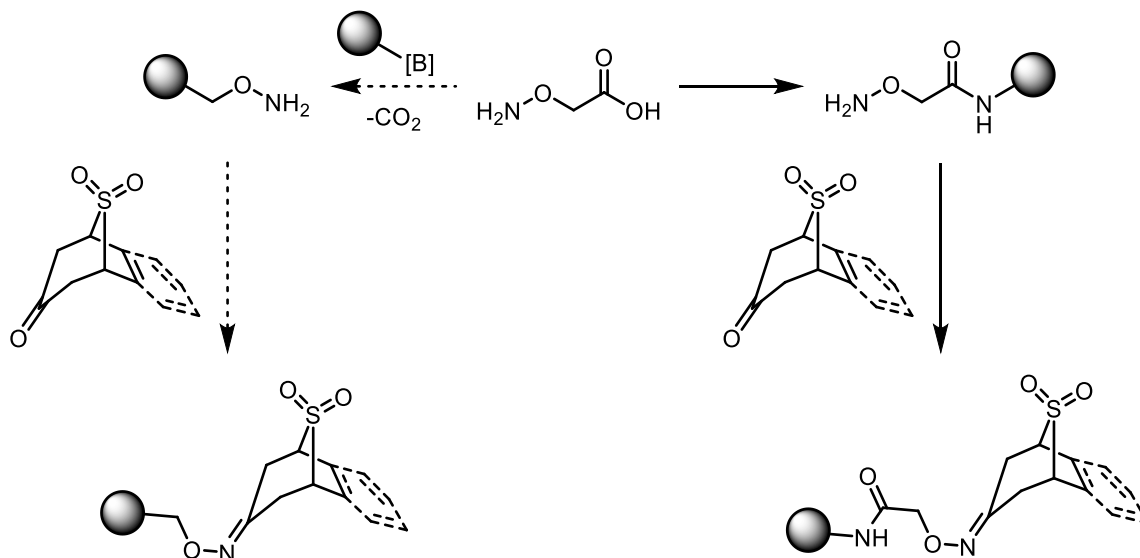
For example, despite ketone **52** being sensitive to changes in pH, the fact remains that oxime formation via condensation presents the ketone moiety as an opportunity for us to capitalize upon. One can envision other nucleophilic reagents to perform 1,2-addition selectively with the carbonyl moiety, such as isocyanides.<sup>320</sup> As such, we can envision that ketone **52** can be further decorated using multicomponent reactions, such as Ugi-type 4 component coupling reactions, as shown in Scheme 68.<sup>321</sup>



*Scheme 68. Functionalization of bicyclo[3.2.1]sulfone-containing ketone species using isocyanide-based multicomponent reactions*

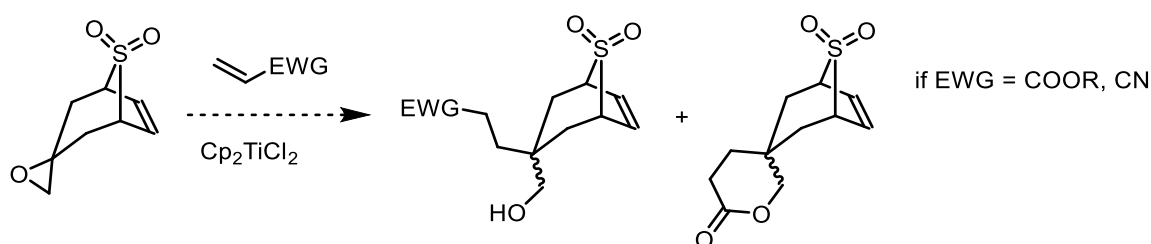
Our success in forming oxime **67d** using aminoxyacetic acid is also an interesting direction to focus upon. One can imagine multiple derivatizations using the carboxylic acid functional group, which may include amide bond formation using different amine-containing building blocks.<sup>322</sup> Other carboxylic derivatives such as ketones, aldehydes, esters can also be derived. Alternatively, one may perform decarboxylative cross couplings with other simple, inexpensive metal-containing building blocks.<sup>323</sup> The decarboxylatively-trapped products can once more lead to

diverse hydroxylamine building blocks, which can be very helpful in controlling three-dimensional chemical space with possible vectorial control, as shown in Scheme 69.



*Scheme 69. Rapid access to O-substituted hydroxylamines as substrates for oxime condensation.*

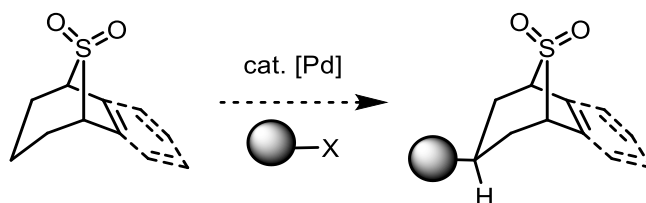
Although we were presented with considerable difficulties in performing ring-opening of epoxide **68** under mild conditions, we can exhibit other strategies for functionalization. For example, Giese-type addition of electron-deficient alkenes<sup>324</sup> can be performed by radical ring-opening of epoxides mediated by transition-metal complexes.<sup>325</sup> A possibility that may arise from this research direction is lactone installation, as shown in Scheme 70.<sup>326</sup> The hypothetical 6-membered lactone can lead to numerous opportunities, either via  $\alpha$ -functionalization or  $\beta$ -functionalization. Beyond that, epoxides have been shown to be capable substrates for transition-metal-catalyzed cross-coupling reactions.<sup>327</sup>



*Scheme 70. Radical-based ring-opening of epoxide **68** and subsequent trapping.*

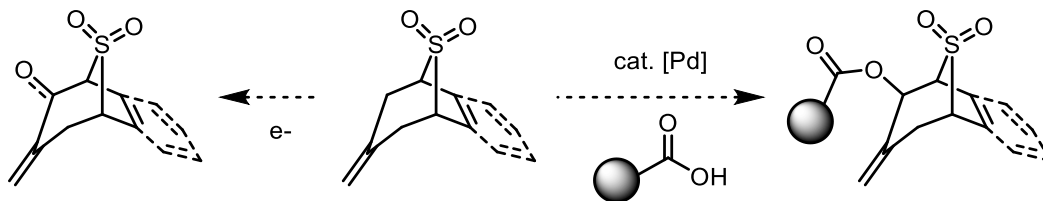
Despite our extensive efforts that showcase the capability of installing substituents at the C-3 position, it would appear that we are becoming increasingly

reliant on the ketone moiety. Recently, Sanford and coworkers have demonstrated C-H functionalization of tropane frameworks using directing groups to install aryl building blocks both regioselectively and diastereoselectively.<sup>328</sup> It would perhaps be an interesting approach to investigate whether the oxygen of the sulfone moiety is capable of performing the same trick, as perhaps coordination to the Pd followed by subsequent elementary steps can allow us to accomplish the same feat on our bicyclo[3.2.1]sulfone-containing scaffold, as shown in Scheme 71.



*Scheme 71. Substrate-directed regioselective arylation of bicyclo[3.2.1]sulfone-containing molecules.*

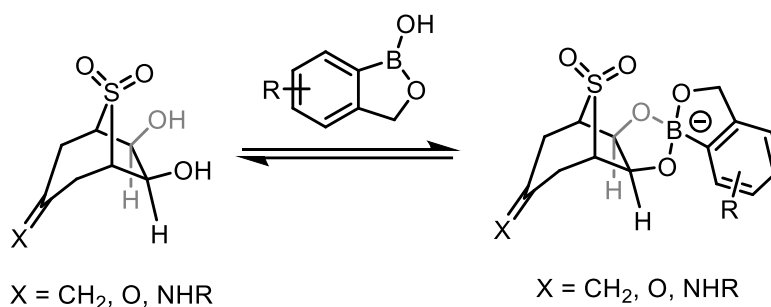
We faced significant challenges in order to functionalize the allylic carbon of the bicyclo[3.2.1]sulfone-containing framework, and it is possible that perhaps we have not fully explored all allylic oxygenation protocols. Transition-metal-catalyzed C-H functionalization would represent one of the most ideal situations for scaffold functionalization, and perhaps we may be tempted to investigate installation of carboxylic acids of various types onto C-2 or C-4 positions of bicyclo[3.2.1]sulfone-containing molecules.<sup>329</sup> Electrochemical organic synthesis<sup>330</sup> may offer us an alternative solution, with the promise of greater reproducibility, as shown in Scheme 72. A point of concern will be whether the sulfone moiety is capable of undergoing reductive cleavage under electrochemical reaction conditions.<sup>331</sup>



*Scheme 72. Allylic functionalization methods that may accommodate our need for site-selective modification of bicyclo[3.2.1]sulfone-containing molecules.*

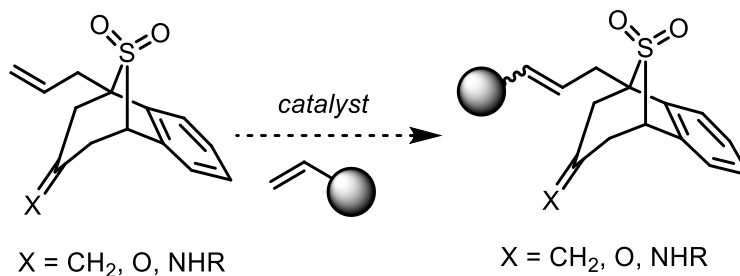
Although we have not yet extensively used boronic ester **62**, one can envision formation of boronate salts using benzoxaboroles, as shown in Scheme 73. Reaction equilibrium can be determined using either NMR titration,<sup>332</sup> or UV-Visible

spectroscopic analysis.<sup>333</sup> Due to precedent literature on using benzoboraxole as antimicrobial agent,<sup>334</sup> we can envision biological applications of a pro-drug delivery system: further functionalization of the bicyclo[3.2.1]sulfone skeleton can lead to selective cellular intake or binding with a particular enzyme of interest, whereupon the benzoboraxole can be released under physiological conditions in order to inhibit the activity of the cellular target, leading to a desired physiological outcome.<sup>335</sup> One may also capitalize on the increase in buried volume due to the formation of boronic esters to develop bicyclo[3.2.1]sulfone-containing boronic esters as novel ligands for asymmetric catalysis.<sup>338</sup>



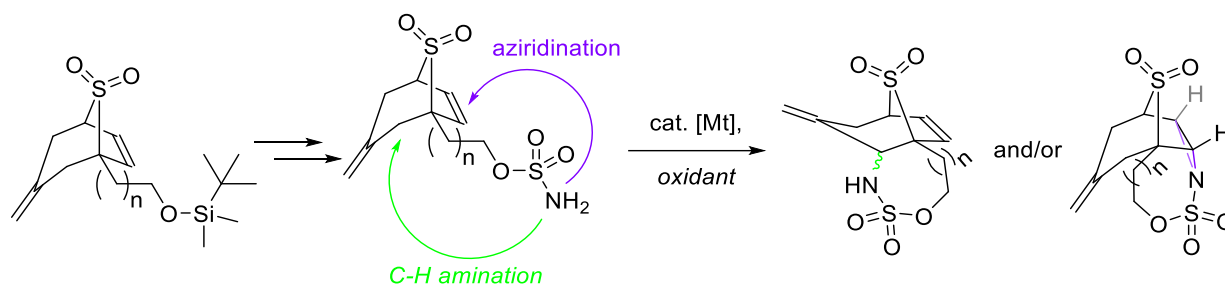
*Scheme 73. Rapid equilibrium of bicyclo[3.2.1]sulfone-containing benzoxaboronic esters.*

Despite the unsuccessful outcome of olefin cross metathesis in our preliminary test results against allylated sulfone **76c**, more extensive reaction screening may be required in order to obtain our desired product under mild reaction conditions. With the plethora of commercially available molybdenum<sup>337</sup> and ruthenium-based<sup>338</sup> catalysts for testing, it is doubtful that optimization will be a major obstacle. The promise of a modular synthetic strategy to yield a diverse set of bicyclo[3.2.1]alkyl sulfone-containing molecules remains an attractive option for continue pursuing this research direction, as shown in Scheme 74.



*Scheme 74. Quaternary allylic olefin metathesis as an alternative method for diversity-orientated synthesis of bicyclo[3.2.1]sulfone-containing molecules.*

One may ponder what results would come out of the silyl-protected primary alcohol moiety of sulfone **76d**, and we foresaw beyond simple coupling chemistry with electrophilic building blocks. We pondered that perhaps if we were to construct a sulfamate moiety from the primary alcohol, then it is possible upon exposure to catalytic amounts of a suitable transition-metal catalyst in an oxidative environment, intramolecular C-H functionalization at the allylic position would end up creating a C-N bond, as shown in Scheme 75.<sup>339</sup> We envision that regioselectivity would depend on many variables, including the identity of the catalyst as well as conformational preference.



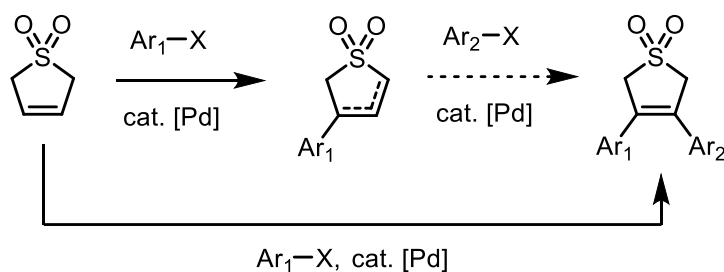
*Scheme 75. Possible competition between C-H allylic functionalization and aziridination pathways.*

Desulfonation selectively at the sulfamate would be desirable, as newly converted secondary amine and primary alcohols would be labile for selective coupling with electrophilic building blocks. Not only would that allow us to control the overall solubility of the bicyclo[3.2.1]sulfone-containing scaffold, but also control of three-dimensional chemical space in designated vectors. Also, one may change the tethering length by employing different silyl-protected alcohol-containing alkyl bromides, and perhaps we may even see competing aziridination if conformationally-allowed.<sup>340</sup>

The reactions listed above are but a tip of the iceberg if one desired to further functionalize the carbon skeleton of the 7-membered ring. As one incorporates more building blocks and increases the diversity of functional groups, one can envision different combination of functional group pairing that may give rise to novel molecular architecture.

## Chapter 5.2 Novel Methodology for Bicyclo[3.2.1] Sulfone Fragments

Despite obtaining some interesting biological data from open screening collaboration with industrial partners and not-for-profit research organizations, our current progress of rapid generation of bicyclo[3.2.1]sulfone-containing molecules has been hindered due to lengthy synthesis and lack of modularity. In particular, unsymmetrical cyclic sulfones cannot be obtained using our current protocol, thus new synthetic possibilities should be entertained. Current methodologies in constructing cyclic alkyl sulfones are insufficient in meeting our needs,<sup>341</sup> as many require tedious efforts for substrate manufacturing, or perhaps lack of chemical versatility. Despite our lack of success in performing Heck-type arylation of sulfolene **4a**, we can envision analogous concepts using aryldiazonium salts. Sigman and coworkers<sup>342</sup> have communicated such ideas to form functionalized carbocycles with high reactivity, and our preliminary tests have revealed that **4a** can be functionalized via Heck-Matsuda reactions<sup>343</sup> that can afford either mono-arylated products or di-arylated products. We envisioned that a two-step protocol from the mono-arylated product to afford unsymmetrical cyclic sulfones, as shown in Scheme 76. Alternatively, symmetrical cyclic sulfones can also be assembled presumably in a one-pot manner using aforementioned methods.

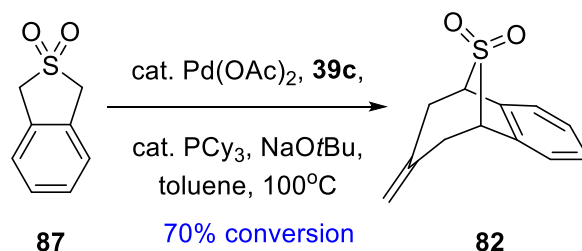


*Scheme 76. Cross-coupling between aryl diazonium salts and 3-sulfolene **4a** to generate diverse amounts of cyclic sulfolenes, which can act as substrates for our ongoing investigations.*

In order to verify our hypothesis of pyridine-containing bicyclic sulfones serving as competitive inhibitors of NMMT, we need to synthesize more analogues with selective modifications on certain structural regions. For example, analogues with the tertiary allylic alcohol moiety but without the stilbene fragment can perhaps offer useful biological data for future development. However, currently our synthetic route requires

the use of sulfone **4b** as substrate, which provides limited utility for future structural-activity relationship deconvolution. Thus, there is a need for obtaining bicyclo[3.2.1]sulfone-containing scaffolds that are structurally similar but do not proceed through the tandem vinylogous 1,2-addition/ anionic oxy-Cope cascade reaction.

One interesting aspect would be to modulate the nucleophilicity of the lithiated sulfone intermediate via addition of late transition-metals such as Cu or Zn, which should direct the carbanion to proceed via Michael-reaction instead of aldol-reactions. Diastereoselective or enantioselective  $\alpha$ -functionalization of alkyl sulfones via conjugate addition with activated alkenes are known; however, current paradigm requires the presence of electron-withdrawing groups at the  $\alpha$ -position in order to stabilize the resulting carbanion.<sup>344</sup> Removal of these substituents is non-trivial,<sup>345</sup> and we foresee tremendous efforts required to apply such concept onto our campaign in constructing diverse bicyclo[3.2.1]sulfone-containing compounds. Interestingly,  $\alpha$ -functionalization of alkyl sulfones relies on conventional lithiation protocols at cryogenic temperature; arguably,  $\alpha$ -arylation would be expected when applying transition-metal-catalyzed cross-coupling methods,<sup>348</sup> followed by decarboxylative allylation.<sup>349</sup> More so, cyclic alkyl sulfones are rarely featured as substrates in aforementioned areas of research development. Note that these lack of thorough development amongst the academic sphere represents an opportunity for us to capitalize on: we have been able to furnish sulfone **82** from sulfone **87** in good conversion using catalytic amounts of Pd(OAc)<sub>2</sub> and PCy<sub>3</sub> as the ligand, and NaOtBu as the base, as shown in Scheme 77.



*Scheme 77. Formation of sulfone **82** using milder reaction conditions.*

By applying the concepts of transition-metal-catalyzed cross-coupling, it is not impractical for us to achieve modular synthetic methods that can furnish novel bicyclo[3.2.1]sulfone-containing molecular frameworks as well as post-annulation functionalization.

Another theoretically interesting methodology would require the involvement of cyclopropanols, which can act as 3-carbon synthons in the form of homoenolates, as illustrated in Figure 33.<sup>348</sup>

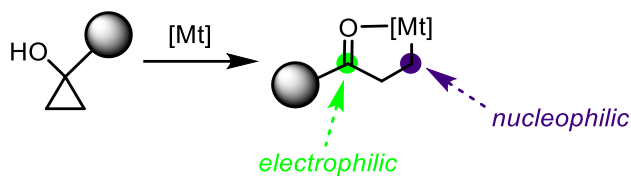
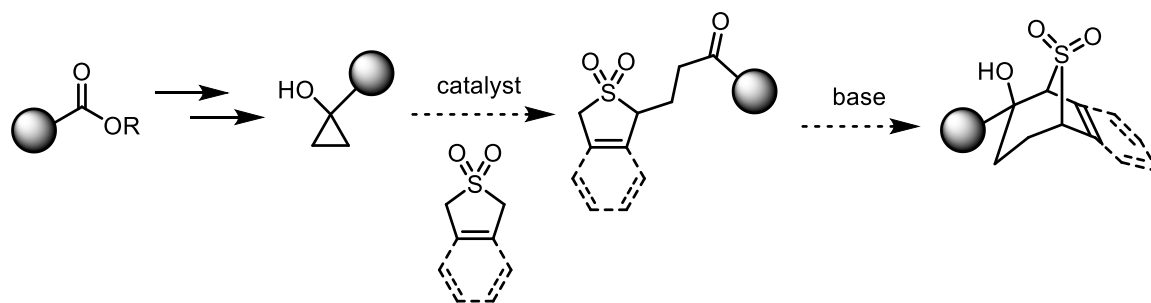


Figure 33. Cyclopropanols and their transition-metal homoenolate counterparts.

Literature precedents for homoenolates participating in Pd-catalyzed cross-coupling reactions are known;<sup>349</sup> in order to afford formation of the desired C-C bond, we have to envision reaction environments that can bring together the nucleophilic carbon of homoenolates and the nucleophilic carbon of sulfones.<sup>350</sup> Thus, C-C bond formation would require oxidative cross-coupling of sulfones and cyclopropanols, which can be readily accessed from Kulinkovich reactions.<sup>351</sup> If proven successful, a one-pot protocol can evolve as additional amounts of strong base can not only deprotonate sulfones during the cross-coupling phase, but also serve an important role during aldol-ring-closure to afford our desired bicyclo[3.2.1]sulfone-containing scaffolds, as shown in Scheme 78.



Scheme 78. Theorized oxidative cross-coupling between cyclic sulfones and cyclopropanols to generate bicyclo[3.2.1]sulfone-containing molecules.

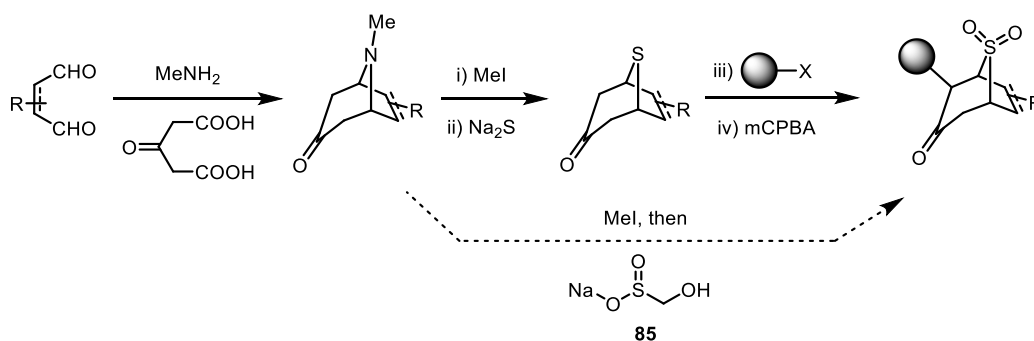
Thus, we can predict an academically-productive feedback loop, where development of novel synthetic methodologies leads to rapid construction of bicyclo[3.2.1]sulfone-containing molecules with densely populated chemical handles for late-stage functional group interconversion, as well as investigation of biological activity of novel chemical matter incorporating bicyclo[3.2.1]sulfone-containing frameworks to

reveal interesting screening results and thus promoting demand for more precise molecular control for proper structure-activity relationship studies.

### Chapter 5.3 Alternative Evolution of Bicyclic Sulfones.

As mentioned in chapter 3.1, Majewski and coworkers have described the generation of bicyclo[3.2.1]sulfide-containing compounds. In particular, their substrates were capable of undergoing aldol reactions with various aldehydes. These discoveries are particularly of value to us, as sulfides can readily be oxidized into sulfoxides or sulfones, and Majewski's aldol products are structurally functionalized at the framework where our efforts at allylic functionalization have failed. Thus, it would be an interesting idea to functionalize using bicyclo[3.2.1]sulfide-containing molecules, which can then be subjected to late-stage oxidation to yield bicyclo[3.2.1]sulfone-containing congener.

Moreover, these bicyclo[3.2.1]sulfide-containing compounds are readily accessible via the analogue tropinones: <sup>352</sup> generation of quaternary ammonium salts using methyl iodide can weaken the C-N bonds, where introduction of sodium sulfide can perform double substitution in order to create new C-S bonds. Substituted tropinones can be generated quite readily using various di-aldehyde species using conditions reported by Robinson, and can be amenable for scale-up safely. Furthermore, we can also investigate whether ronalite, which in solution can act as a doubly nucleophilic synthon, <sup>353</sup> can undergo substitution with quaternary ammonium tropinone salts, as shown in Scheme 79. These efforts will be complementary to our crusade in gaining topological control of bicyclo[3.2.1]sulfone-containing molecules on a molecular scale.



Scheme 79. Formation of bicyclo[3.2.1]sulfone-containing molecules via tropinone derivatives.

There has been an increasing amount of literature describing the use of sulfoximines,<sup>354</sup> as the functional group features a chiral sulfur center as well as the possibility of controlling further three-dimensional space through various substituents at the sulfoximine nitrogen, as illustrated in Figure 34.

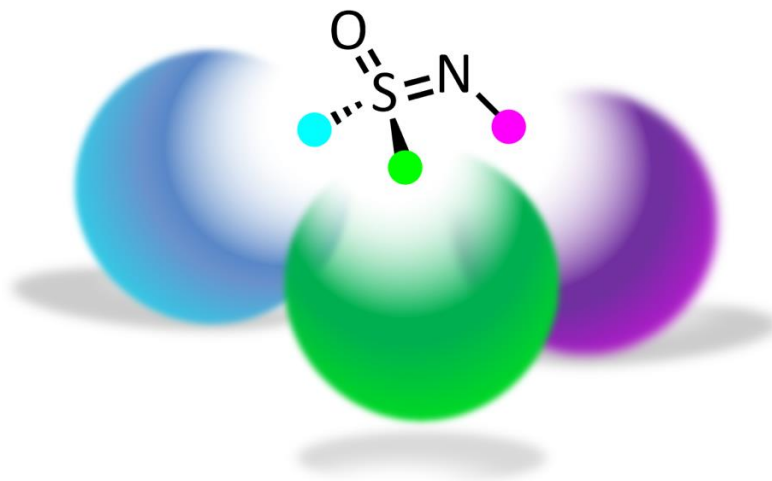
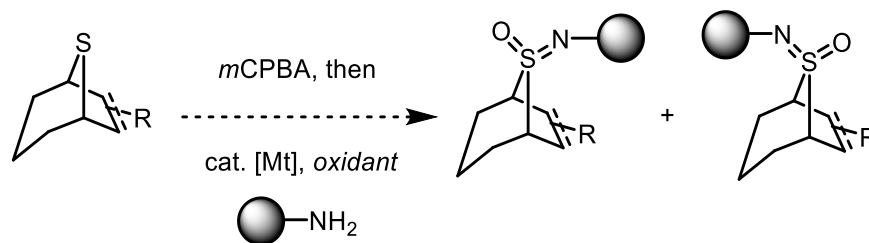


Figure 34. Greater three-dimensional control on a molecular level using sulfoximines.

Evolution from bicyclo[3.2.1]sulfone-containing molecules into the analogous bicyclo[3.2.1]sulfoximine-containing molecules will allow for greater sampling of chemical space, which will attract more attention for medicinal chemists to incorporate during early stages of drug discovery campaigns. Diastereoselective bicyclo[3.2.1]sulfoximines may possibly be generated from bicyclo[3.2.1]sulfoxides using electrophilic nitrogen sources in oxidative environments, as shown in Scheme 80.<sup>355</sup> We can also expect the “imine fragment” of bicyclo[3.2.1]sulfoximine-containing scaffolds and the internal olefin to coordinate to transition-metal centers via a bidentate coordination,<sup>356</sup> thus opening up new possibilities of sulfoxomines as novel ligands in catalytic applications.<sup>357</sup> Overall, much potential remains untapped and explored.



Scheme 80. Possible two-step protocol to form bicyclo[3.2.1]sulfoximine-containing molecules from its sulfide counterparts.

## Conclusion

In summary, we have successfully demonstrated the potential of using sulfones to serve as part of the pharmacophore. With the foresight of combining the concepts of conformational rigidification and site-selective functionalization, we were able to obtain a collection of molecules that together encompass a wide degree of physicochemical properties, such as three-dimensionality. Interesting biological screening data was observed across many therapeutic areas, which proves that our strategy is viable, and our dreams of developing bicyclic sulfone-containing drugs may one day come to fruition. Granted, much is left for us to explore, such as how to overcome the intrinsic limits of bicyclo[3.2.1]sulfone-containing scaffolds in order to achieve complete site-selective functionalization, and elucidating which biochemical pathway our molecules interact favorably with.

We are highly encouraged that our fundamental ideas can possibly be translated into such diverse amounts of novel research directions. One must never forget that basic research is the foundation that leads to technological improvements which leads to an overall improvement in societal standards. If one does not truly understand sufficiently about their own research, or be allowed to have the appropriate resources to support their intellectual creativity, then the cornerstone of what scientific research stands for is lost.

## Bibliography

1. a) Swinney, D. C.; Anthony, J. *Nat. Rev. Drug Discov.*, **2011**, *10*, 507 – 519. b) Eder, J.; Sedrani, R.; Wiesmann, C. *Nat. Rev. Drug Discov.*, **2014**, *13*, 577 – 587.
2. Macarron, R.; Bankds, M. N.; Bojanic, D.; Burns, D. J.; Cirovic, D. A.; Garyantes, T.; Green, D. V.; Hertzberg, R. P.; Janzen, W. P.; Paslay, J. W.; Schopfer, U.; Sittampalam, G. S. *Nat. Rev. Drug Discov.*, **2011**, *10*, 188 – 195.
3. a) Bleicher, K. H.; Bohm, H, J.; Muller, K.; Alanine, A. I. *Nat. Rev. Drug Discov.*, **2003**, *2*, 369 – 378. b) Kesery, G. M.; Makara, G. M. *Drug Discov. Today*, **2006**, *11*, 741 – 748.
4. Brown, A. C.; Fraser, T. R. *Trans. R. Soc. Edinb.*, **1865**, *25*, 1968 – 1969.
5. *The Pharmaceutical Industry and Global Health, Facts and Figures 2012*. International Federation of Pharmaceutical Manufacturers and Associations [https://www.ifpma.org/wp-content/uploads/2016/01/IFPMA\\_-\\_Facts\\_And\\_Figures\\_2012\\_LowResSinglePage.pdf](https://www.ifpma.org/wp-content/uploads/2016/01/IFPMA_-_Facts_And_Figures_2012_LowResSinglePage.pdf) (Accessed Oct 7th, 2018)
6. a) Dimasi, J. A.; Hansen, R. W.; Grabowski, H. G. *J. Health Econ.*, **2003**, *22*, 151 – 185. b) Kraljevic, S.; Stambrook, P. J.; Pavelic, K. *EMBO Rep.*, **2004**, *5*, 837 – 842. c) Paul, S. M.; Mytelka, D. S.; Dunwiddie, C. T.; Persinger, C. C.; Munos, B. H.; Lindborg, S. R.; Schacht, A. L. *Nat. Rev. Drug Discov.*, **2010**, *9*, 203 – 214.
7. Brown, D. *Drug Discov. Today*, **2007**, *12*, 1007 – 1012.
8. Roughley, S. D.; Jordan, A. M. *J. Med. Chem.*, **2011**, *54*, 3451 – 3479.
9. Magano, J.; Dunetz, J. R. *Chem. Rev.*, **2011**, *111*, 2177 – 2250.
10. Dunetz, J. R.; Magano, J.; Weisenburger, G. A. *Org. Process Res. Dev.*, **2016**, *20*, 140 – 177.
11. Abdel-Magid, A. F.; Mehrman, S. J. *Org. Process Res. Dev.*, **2005**, *10*, 971 – 1031.
12. a) Binder, J. B.; Raines, R. T. *Curr. Opin. Chem. Biol.*, **2008**, *12*, 767 – 773. b) Higman, C. S.; Lummiss, J. A. M.; Fogg, D. E. *Angew. Chem. Int. Ed.*, **2016**, *55*, 3552 – 3565. c) Hughes, D.; Wheeler, P.; Ene, D. *Org. Process Res. Dev.*, **2017**, *21*, 1938 – 1962.

13. a) Cerveny, L., Ed. *Catalytic Hydrogenation*; Elsevier: Amsterdam, **1986**. b) de Vries, J. G.; Elsevier, C. J. *The Handbook of Homogeneous Hydrogenation*; Wiley-VCH: Weinheim, **2007**. c) Andersson, P. G.; Munslow, I. J. *Modern Reduction Methods*; Wiley-VCH Verlag GmbH & Co. KGaA: Weinheim, **2008**.
14. a) Aldeghi, M.; Malhotra, S.; Selwood, D. L.; Chan, A. W. *Chem. Biol. Drug Des.*, **2014**, *83*, 450 – 461 b) Brown, D.; Gagnon, M. M.; Boström, J. *J. Med. Chem.*, **2015**, *58*, 2390 – 2405. c) Brown, D.; Boström, J. *J. Med. Chem.*, **2016**, *59*, 4443 – 4458. d) Meyers, J.; Carter, M.; Mok, N. Y.; Brown, N. *Future Med. Chem.*, **2016**, *8*, 1753 – 1767.
15. a) Clemons, P. A.; Bodycombe, N. E.; Carrinski, H. A.; Wilson, J. A.; Shamji, A. F.; Wagner, B. K.; Koehler, A. N.; Schreiber, S. L. *Proc. Natl. Acad. Sci. USA*, **2010**, *107*, 18787 – 18792. b) Ritchie, T. J.; Macdonald, S. J. F.; Young, R. J.; Pickett, S. D. *Drug Discov. Today*, **2011**, *16*, 164 – 171. c) Meanwell, N. A. *Chem. Res. Toxicol.*, **2016**, *29*, 564 – 616.
16. Sauer, W. H. B.; Schwarz, M. K. *Chim. Int. J. Chem.*, **2003**, *43*, 987 – 1003.
17. Aldeghi, M.; Malhotra, S.; Selwood, D. L.; Chan, A. W. E. *Chem. Biol. Drug Des.*, **2013**, *83*, 450 – 461.
18. Gaulton, A.; Bellis, L. J.; Bento, A. P.; Chambers, J.; Davies, M.; Hersey, A.; Light, Y.; McGlinchey, S.; Michalovich, D.; Al – Lazikani, B.; Overington, J. P. *Nucleic Acids Res.*, **2012**, *40*, 1100 – 1107.
19. a) Haigh, J. A.; Pickup, B. T.; Grant, J. A.; Nicholls, A. *J. Chem. Inform. Model.*, **2005**, *45*, 673 – 684. b) Hajduk, P. J.; Galloway, W. R. J. D.; Spring, D. R. *Nature*, **2011**, *470*, 42 – 43.
20. a) Hann, M. M.; Leach, A. R.; Harper, G. *J. Chem., Inf. Comput. Sci.*, **2001**, *41*, 856 – 864. b) Monteleone, S.; Fuchs, J. E.; Liedl, K. R. *Front. Pharmacol.*, **2017**, *8*, 552.
21. Lovering, F. *Med. Chem. Commun.*, **2013**, *4*, 515 – 519.
22. a) Merrifield, R. B. *J. Am. Chem. Soc.*, **1963**, *85*, 2149 – 2154. b) Geysen, H. M.; Meloan, R. H.; Barteling, S. J. *Proc. Natl. Acad. Sci. USA*, **1984**, *81*, 3998 – 4002. c) Merrifield, R. B. *Science*, **1986**, *232*, 341 – 347.

23. a) Lam, K. S.; Salmon, S. E.; Hersh, E. M.; Hruby, V. J.; Kazmierski, W. M.; Knapp, R. J. *Nature*, **1991**, *354*, 82 – 84. b) Fodor, S. P.; Read, J. L.; Pirrung, M. C.; Stryer, L.; Lu, A. T.; Solas, D. *Science*, **1991**, *251*, 767 – 773. c) Booth, R. J.; Hodges, J. C. *Acc. Chem. Res.*, **1999**, *32*, 18 – 26. d) Guillier, F.; Orain, D.; Bradley, M. *Chem. Rev.*, **2000**, *100*, 2091 – 2157.
24. a) Bunin, B. A.; Plunkett, M. J.; Ellman, J. A. *Proc. Natl. Acad. Sci. USA*, **1994**, *91*, 4708 – 4712. b) Villhauer, E. B.; Brinkman, J. A.; Naderi, G. B.; Burkey, B. F.; Dunning, B. E.; Prasad, K.; Mangold, B. L.; Russell, M. E.; Hughes, T. E. *J. Med. Chem.*, **2003**, *46*, 2774 – 2789. c) Bang-Andersen, B.; Ruhland, T.; Jørgensen, M.; Smith, G.; Frederiksen, K.; Jensen, K. G.; Zhong, H.; Neilsen, S. M.; Hogg, S.; Mørk, A.; Stensbøl, T. B. *J. Med. Chem.*, **2011**, *54*, 3206 – 3221.
25. White, P. T.; Cohen, M. S. *Expert Opin. Drug Discov.*, **2015**, *10*, 427 – 439.
26. Wilhelm, S.; Carter, C.; Lynch, M.; Lowinger, T.; Dumas, J.; Smith, R. A.; Schwartz, B.; Simantov, R.; Kelley, S. *Nat. Rev. Drug Discov.*, **2006**, *5*, 835 – 844.
27. Lyons, J. F.; Wilhelm, S.; Hibner, B.; Bollag, G. *Endocr. Relat. Cancer*, **2001**, *8*, 219 – 225.
28. Smith, R. A.; Barbosa, J.; Blum, C. L.; Bobko, M. A.; Caringal, Y. V.; Dally, R.; Johnson, J. S.; Katz, M. E.; Kennure, N.; Kingery-Wood, J.; Lee, W.; Lowinger, T. B.; Lyons, J.; Marsh, V.; Rogers, D. H.; Swartz, S.; Walling, T.; Wild, H. *Bioorg. Med. Chem. Lett.*, **2001**, *11*, 2775 – 2778.
29. Wan, P. T.; Garnett, M. J.; Roe, S. M.; Lee, S.; Niculescu-Duvaz, D.; Good, V. M.; Jones, C. M.; Marshall, C. J.; Springer, C. J.; Barford, D.; Marais, R. *Cell*, **2004**, *116*, 855 – 867.
30. Kennedy, J. P.; Williams, L.; Bridges, T. M.; Daniels, R. N.; Weaver, D.; Lindsley, C. W. *J. Comb. Chem.*, **2008**, *10*, 346 – 354.
31. Sauer, W. H. B.; Schwarz, M. K. *Chim. Int. J. Chem.*, **2003**, *57*, 276 – 283.
32. Feher, M.; Schmidt, J. M. *J. Chem. Inf. Comput. Sci.*, **2003**, *43*, 218 – 227.
33. Carroll, J. *Biotechnol. Healthc.*, **2005**, *2*, 26 – 27.
34. Borman, S. *C&EN*, **2003**, *81*, 45 – 56.
35. Borman, S. *C&EN*, **2004**, *82*, 32 – 40.

36. Spring, D. R. *Org. Biomol. Chem.* **2003**, *1*, 3867.
37. Schreiber, S. L. *Science*, **2000**, *287*, 1964 – 1969.
38. a) Hung, A. W.; Ramek, A.; Wang, Y.; Kaya, T.; Wilson, A.; Clemons, P. A.; Young, D. W. *Proc. Natl. Acad. Sci. USA*, **2011**, *108*, 6799 – 6804. b) Haftchenary, S.; Nelson, Jr., S. D.; Furst, L.; Dandapani, S.; Ferrara, S. J.; Bošković, Z. V.; Lazú, S. F.; Guerrero, A. M.; Serrano, J. C.; Crews, D. K.; Brackeen, C.; Mowat, J.; Brumby, T.; Bauser, M.; Schreiber, S. L.; Phillips, A. J. *ACS Comb. Sci.*, **2016**, *18*, 5569 – 574. c) Kidd, S. L.; Osberger, T. J.; Mateu, N.; Sore, H. F.; Spring, D. R. *Front. Chem.*, **2018**, *16*, 460.
39. a) Kim, J.; Jung, J.; Cho, W.; Lee, W. S.; Kim, C.; Park, W.; Park, S. B. *Nat. Commun.*, **2016**, *7*, 13196. b) Gerry, C. J.; Schreiber, S. L. *Nat. Rev. Drug Discov.*, **2018**, *17*, 333 – 352.
40. Neilsen, T. E.; Schreiber, S. L. *Angew. Chem. Int. Ed.*, **2008**, *47*, 48 – 56.
41. a) Hanessian, S. *Total Synthesis of Natural Products: The Chiron Approach*. Pergamon Press: Oxford, UK, 1983. b) Blaser, H.-U. *Chem. Rev.*, **1992**, *92*, 935 – 952.
42. a) Spiegel, D. A.; Schroeder, F. C.; Duvall, J. R.; Schreiber, S. L. *J. Am. Chem. Soc.*, **2006**, *128*, 14766 – 14767. b) Comer, E.; Rohan, E.; Deng, L.; Porco, J. A. *Org. Lett.*, **2007**, *9*, 2123 – 2126.
43. a) Kumagai, N.; Muncipinto, G.; Schreiber, S. L. *Angew. Chem. Int. Ed.*, **2006**, *45*, 3635 – 3638. b) Chattopadhyay, S. K.; Karmakar, S.; Biswas, T.; Majumdar, K. C.; Rahaman, H.; Roy, B. *Tetrahedron*, **2007**, *63*, 3919 – 3952.
44. a) Tan, D. S.; Foley, M. A.; Shair, M. D.; Schreiber, S. L. *J. Am. Chem. Soc.*, **1998**, *120*, 8565 – 8566. b) Lee, D.; Sello, J. K.; Schreiber, S. L. *J. Am. Chem. Soc.*, **1999**, *121*, 10648 – 10649
45. a) Ostresh, J. M.; Husaw, G. R.; Blondelle, S. E.; Dörner, B.; Weber, P. A.; Houghten, R. A. *Proc. Natl. Acad. Sci. USA*, **1994**, *91*, 11138 – 11142. b) Tempest, P. A.; Armstrong, R. W. *J. Am. Chem. Soc.*, **1997**, *119*, 7607 – 7608. c) Haggarty, S. J.; Koeller, K. M.; Wong, J. C.; Grozinger, C. M.; Schreiber, S. L. *Proc. Nat. Acad. Sci. USA*, **2003**, *100*, 4389 – 4394. d) Ng, P. Y.; Tang, Y.; Knosp, W. M.; Stadler, H. S.; Shaw, J. T. *Angew. Chem. Int. Ed.*, **2007**, *46*, 5352

- 5355. e) Galloway, W. R. J. D.; Bender, A.; Welch, M.; Spring, D. R.; Chem. Commun., **2009**, 0, 2446 – 2462. f) Kim, J.; Kim, H.; Park, S. B. *J. Am. Chem. Soc.*, **2014**, 136, 14629 – 14638. g) Colomer, I.; Adeniji, O.; Burslem, G. M.; Craven, P.; Rasmussen, M. O.; Willaume, A.; Kalliokoski, T.; Foster, R.; Marsden, S. P.; Nelson, A. *Bioorg. Med. Chem. Lett.*, **2015**, 23, 2736 – 2740. h) Lenci, E.; Menchi, G.; Trabocchi, A. *Org. Biomol. Chem.*, **2016**, 14, 808 – 825.
46. a) Mayer, T. U.; Kapoor, T. M.; Haggarty, S. J.; King, R. W.; Schreiber, S. L.; Mitchison, T. J. *Science*, **1999**, 286, 971 – 974. b) Kuruvilla, F. G.; Shamji, A. F.; Sternson, S. M.; Hergenrother, P. J.; Schreiber, S. L. *Nature*, **2002**, 416, 653 – 657. dc Stanton, B. Z.; Peng, L. F.; Maloof, N.; Nakai, K.; Wang, X.; Herlihy, K. M.; Duffner, J. L.; Taveras, K. M.; Hyman, J. M.; Lee, S. W.; Koehler, A. N.; Chen, J. K.; Fox, J. L.; Mandinova, A.; Schreiber, S. L. *Nat. Chem. Biol.*, **2009**, 5, 154 – 156. d) Collins, I.; Jones, A. M. *Molecules*, **2014**, 19, 17221 – 17255.
47. a) Heidebrecht, Jr., R. W.; Mulrooney, C.; Austin, C. P.; Barker, Jr., R. H.; Beaudoin, J. A.; Cheng, K. C.-C.; Comer, E.; Dandapani, S.; Dick, J.; Duvall, J. R.; Ekland, E. H.; Fidoc, D. A.; Fitzgerald, M. E.; Foley, M.; Guha, R.; Hinkson, P.; Kramer, M.; Lukens, A. K.; Masi, D.; Marcaurelle, L. A.; Su, X.-Z.; Thomas, C. J.; Weïwer, M.; Wiegand, R. C.; Wirth, D.; Xia, M.; Yuan, J.; Zhao, J.; Palmer, M.; Munoz, B.; Schreiber, S. L. *ACS Med. Chem. Lett.*, **2012**, 3, 112 – 117. b) Comer, E.; Beaudoin, J. A.; Kato, N.; Fitzgerald, M. E.; Heidebrecht, R.; duPont Lee, IV, M.; Masi, D.; Mercier, M.; Mulrooney, C.; Muncipinto, G.; Rowley, A.; Crespo-Llado, K.; Serrano, A. E.; Lukens, A. K.; Wiegand, R. C.; Wirth, D. F.; Palmer, M. A.; Foley, M. A.; Munoz, B.; Scherer, C. A.; Duvall, J. R.; Schreiber, S. L. *J. Med. Chem.*, **2014**, 57, 8469 – 8502. c) Dandapani, S.; Germain, A. R.; Jewett, I.; le Quement, S.; Marie, J.-C.; Muncipinto, G.; Duvall, J. R.; Carmody, L. C.; Perez, J. R.; Engel, J. C.; Gut, J.; Kellar, D.; Siqueira-Neto, J. L.; McKerrow, J. H.; Kaiser, M.; Rodriguez, A.; Palmer, M. A.; Foley, M.; Schreiber, S. L.; Munoz, B. *ACS Med. Chem. Lett.*, **2014**, 5, 149 – 153.
48. a) Chou, D. H.-C.; Duvall, J. R.; Gerald, B.; Liu, H.; Pandya, B. A.; Suh, B.-C.; Forbeck, E. M.; Wagner, B. K.; Marcaurelle, L. A. *ACS Med. Chem. Lett.*, **2011**, 2, 698 – 702. b) Dandapani, S.; Germain, A. R.; Jewett, I.; le Quement, S.; Marie,

- J.-C.; Muncipinto, G.; Duvall, J. R.; Carmody, L. C.; Perez, J. R.; Engel, J. C.; Gut, J.; Kellar, D.; Siqueira-Neto, J. L.; McKerrow, J. H.; Kaiser, M.; Rodriguez, A.; Palmer, M. A.; Foley, M.; Schreiber, S. L.; Munoz, B. *ACS Med. Chem. Lett.*, **2014**, 5, 149 – 153. c) Dockendorff, C.; Faloon, P. W.; Pu, J.; Yu, M.; Johnston, S.; Bennion, M.; Penman, M.; Neiland, T. J. F.; Dandapani, S.; Perez, J. R.; Munoz, B.; Palmer, M. A.; Schreiber, S. L.; Krieger, M. *Bioorg. Med. Chem. Lett.*, **2015**, 25, 2100 – 2105. d) Duvall, J. R.; Bedard, L.; Naylor-Olsen, A. M.; Manson, A. L.; Bittker, J. A.; Sun, W.; Fitzgerald, M. E.; He, Z.; Lee, IV, M. D.; Marie, J.-C.; Muncipinto, G.; Rush, D.; Xu, D.; Xu, H.; Zhang, M.; Earl, A. M.; Palmer, M. A.; Foley, M. A.; Vacca, J. P.; Scherer, C. A. *ACS Infect. Dis.*, **2017**, 3, 349 – 359.
49. a) Lipinski, C. A.; Lombardo, F.; Dominy, B. W.; Feeney, P. J. *Adv. Drug Deliv. Rev.*, **1997**, 23, 3 – 25. b) Lipinski, C. A.; Lombardo, F.; Dominy, B. W.; Feeney, P. J. *Adv. Drug Deliv. Rev.*, **2001**, 46, 3 – 26.
50. a) Alex, A.; Millan, D. S.; Perez, M.; Wakenhut, F.; Whitlock, G. A. *Med. Chem. Commun.*, **2011**, 2, 669 – 674. b) Paolini, G. V.; Shapland, R. B.; van Hoorn, W. P.; Mason, J. S.; Hopkins, A. L. *Nat. Biotechnol.*, **2006**, 24, 805 – 815. c) Vieth, M.; Sutherland, J. J. *J. Med. Chem.*, **2006**, 49, 3451 – 3453. d) Leeson, P. D.; Springthorpe, B. *Nat. Rev. Drug Discov.*, **2007**, 6, 881 – 890.
51. a) Harper, S.; McCauley, J. A.; Rudd, M. T.; Ferrara, M.; DiFilippo, M.; Crescenzi, B.; Koch, U.; Petrocchi, A.; Holloway, M. K.; Butcher, J. W.; Romano, J. J.; Bush, K. J.; Gilbert, K. F.; McIntyre, C. J.; Nguyen, K. T.; Nizi, E.; Carroll, S. S.; Ludmerer, S. W.; Burlein, C.; DiMuzio, J. M.; Graham, D. J.; McHale, C. M.; Stahlhut, M. W.; Olsen, D. B.; Monteagudo, E.; Cianetti, S.; Giuliano, C.; Pucci, V.; Trainor, N.; Fandozzi, C. M.; Rowley, M.; Coleman, P. J.; Vacca, J. P.; Summa, V.; Liverton, N. J. *ACS Med. Chem. Lett.*, **2012**, 3, 332 – 336. b) Gentile, I.; Buonomo, A. R.; Borgia, F.; Zappulo, E.; Castaldo, G.; Borgia, G. *Expert. Opin. Investig. Drugs.*, **2014**, 23, 719 – 728.
52. a) Sugimoto, H.; Ogura, H.; Arai, Y.; Limura, Y.; Yamanishi, Y. *Jpn. J. Pharmacol.*, **2002**, 89, 7 – 20. b) Shaw, K. E.; Bondi, C. O.; Light, S. H.; Massimino, L. A.; McAloon, R. L.; Monaco, C. M.; Kline, A. E. *J. Neurotrauma*,

- 2013**, *30*, 557 – 564. c) Lee, J. H.; Jeong, S. K.; Kim, B. C.; Park, K. W.; Dash, A. *Acta. Neurol. Scand.*, **2015**, *131*, 259 – 267.
53. a) Capdeville, R.; Silberman, S. *Semin. Hematol.*, **2003**, *40*, 15 – 20. b) Deininger, M.; Buchdunger, E.; Druker, B. J. *Blood*, **2005**, *105*, 2640 – 2653. c) Bruker, B. J. *Nat. Med.*, **2009**, *15*, 1149 – 1152.
54. Steele, L. S.; Glazier, R. H. *Can. Fam Physician*, **1999**, *45*, 917 – 919.
55. a) Ghose, A. K.; Viswanadhan, V. N.; Wendoloski, J. J. *J. Comb. Chem.*, **1999**, *1*, 55 – 68. b) Congreve, M.; Carr, R.; Murray, C.; Jhoti, H. *Drug, Discov. Today*, **2003**, *8*, 876 – 877.
56. Veber, D. F.; Johnson, S. R.; Cheng, H.-Y.; Smith, B. R.; Ward, K. W.; Kopple, K. D. *J. Med. Chem.*, **2002**, *45*, 2615 – 2623.
57. a) Palm, K.; Stenberg, P.; Luthman, K.; Artursson, P. *Pharm. Res.*, **1997**, *14*, 568 – 571. b) Ertl, P.; Rohde, B.; Selzer, P. *J. Med. Chem.*, **2000**, *43*, 3714 – 3717.
58. Lovering, F.; Bikker, J.; Humblet, C. *J. Med. Chem.*, **2009**, *52*, 6752 – 6756.
59. a) Meanwell, N. A. *Chem. Res. Toxicol.*, **2011**, *24*, 1420 – 1456. b) Cumming, J. G.; Davis, A. M.; Muresan, S.; Haeberlein, M.; Chen, H. *Nat. Rev. Drug Discov.*, **2013**, *12*, 948 – 962.
60. a) Ochoa-Callejero, L.; Pérez-Martínez, L.; Rubio-Mediavilla, S.; Oteo, J. A.; Martínez, A.; Blanco, J. R. *PLoS ONE*, **2013**, *8*, e53992. b) Pérez-Martínez, L.; Pérez-Matute, P.; Aguilera-Lizarraga, J.; Rubio-Mediavilla, S.; Narro, J.; Receio, E.; Ochoa-Callejero, L.; Oteo, J. A.; Blanco, J. R. *J. Antimicrob. Chemother.*, **2014**, *69*, 1903 – 1910. c) Vann der Ryst, E.; Heera, J.; Demarest, J.; Knirsch, C. *Ann. N. Y. Acad. Sci.*, **2015**, *1346*, 7 – 17.
61. Dorr, P.; Westby, M.; Dobbs, S.; Griffin, P.; Irvine, B.; Macartney, M.; Mori, J.; Rickett, G.; Smith-Burchnell, C.; Napier, C.; Webster, R.; Armour, D.; Price, D.; Stammen, B.; Wood, A.; Perros, M. *Antimicrob., Agents Chemother.*, **2005**, *49*, 4721 – 4732.
62. a) Veljkovic, N.; Vucicevic, J.; Tassini, S.; Glisic, S.; Veljkovic, V.; Radi, M. *Expert. Opin. Drug Discov.*, **2015**, *10*, 671 – 684. b) Woollard, S. M.; Kanmogne, G. D. *Drug Des. Devel. Ther.*, **2015**, *9*, 5447 – 5468.

63. a) Ingelman-Sundberg, M. *Pharmacogenomics J.*, **2005**, 5, 6 – 13. b) Wang, B.; Yang, L. P.; Zhang, X. Z.; Huang, S. Q.; Bartlam, M.; Zhou, S. F. *Drug Metab. Rev.*, **2009**, 41, 573 – 643. c) Wang, X.; Li, J.; Dong, G.; Yue, J. *Eur. J. Pharmacol.*, **2014**, 724, 211 – 218. d) Gopisankar, M. G. *Egypt. J. Med. Hum. Genet.*, **2017**, 18, 309 – 313.
64. a) Armour, D. R.; de Groot, M. J.; Price, D. A.; Stammen, B. L. C.; Wood, A.; Perros, M.; Burt, C. *Chem. Biol. Drug Des.*, **2006**, 67, 305 – 308. b) Price, D. A.; Armour, D.; de Groot, M.; Leishman, D.; Napier, C.; Perros, M.; Stammen, B. L.; Wood, A. *Bioorg. Med. Chem. Lett.*, **2006**, 16, 4633 – 4637.
65. a) Kramer, V. G.; Schader, S. M.; Oliveira, M.; Colby-Germinario, S. P.; Donahue, D. A.; Singhroy, D. N.; Tressler, R.; Sloan, R. D.; Wainberg, M. A. *Antimicrob., Agents Chemother.*, **2012**, 56, 4154 – 4160. b) Reshef, R.; Luger, S. M.; hexner, E. O.; Loren, A. W.; Frey, N. V.; Nasta, S. D.; Goldstein, S. C.; Stadtmauer, E. A.; Smith, J.; Bailey, S.; Mick, R.; Heitjan, D. F.; Emerson, S. G.; Hoxie, J. A.; Vonderheide, R. H.; Porter, D. L. *N. Engl. J. Med.*, **2012**, 367, 135 – 145. c) Puertas, M. C.; Massanella, M.; Llibre, J. M.; Ballester, M.; Buzon, M. J.; Ouchi, D.; Esteve, A.; Boix, J.; Manzardo, C.; Miró, J. M.; Gatell, J. M.; Clotet, B.; Blanco, J.; Martinez-Picado, J. *AIDS*, **2014**, 28, 325 – 334.
66. a) Stephenson, J. *JAMA*, **2007**, 297, 1535 – 1536. b) Vandekerckhove, L.; Verhofstede, C.; Vogelaers, D. *J. Antimicrob. Chemother.* **2009**, 63, 1087–1096. c) Ford, N.; Calmy, A. *Expert Opin. Pharmacother.*, **2012**, 13, 1083 – 1085.
67. a) Walters, W. P. *Expert Opin. Drug Discov.*, **2012**, 7, 99 – 107. b) Yang, T.; Engkivst, O.; Llinàs, A.; Chen, H. *J. Med. Chem.*, **2012**, 55, 3667 – 3677. c) Fang, Z.; Song, Y.; Zhan, P.; Zhang, Q.; Liu, X. *Future Med. Chem.*, **2014**, 6, 885 – 901. d) Zheng, Y.; Tice, C. M.; Singh, S. B. *Bioorg. Med. Chem. Lett.*, **2017**, 27, 2825 – 2837. e) Friederich, N.-O.; Simir, M.; Kirchmair, J. *Front. Chem.*, **2018**, 6, 68.
68. Koshland, Jr., D. E. *Proc. Natl. Acad. Sci. USA*, **1958**, 44, 98 – 104.
69. Harrold, M. W. *Am. J. Pharm. Educ.*, **1996**, 60, 192 – 197.
70. a) He, M. W.; Lee, P. S.; Sweeney, Z. K. *ChemMedChem.*, **2015**, 10, 238 – 244. b) Doak, B. C.; Kihlberg, J. *Expert Opin. Drug Discov.*, **2017**, 12, 115 – 119. c)

- Bakali, J. E.; Muccioli, G. G.; Body-Malapel, M.; Djouina, M.; Klupsch, F.; Ghinert, A.; Baryczyk, A.; Renault, N.; Chavatte, P.; Desreumaux, P.; Lambert, D. M.; Millet, R. *ACS Med. Chem. Lett.*, **2015**, 6, 198 – 203. d) Focken, T.; Chowdhury, S.; Zenova, A.; Grimwood, M. E.; Chabot, C.; Sheng, T.; Hemeon, I.; Decker, S. M.; Wilson, M.; Bichler, P.; Jia, Q.; Sun, S.; Young, C.; Lin, S.; Goodchild, S. J.; Stuart, N. G.; Chang, E.; Xie, Z.; Li, B.; Khakh, K.; Bankar, G.; Waldbrook, M.; Kwan, R.; Nelkenbrecher, K.; Tari, P. K.; Chahal, N.; Sojo, L.; Robinette, C. L.; White, A. D.; Chen, C.-A.; Zhang, Y.; Pang, J.; Chang, J. H.; Hackos, D. H.; Johnson, Jr., J. P.; Cohen, C. J.; Ortwine, D. F.; Sutherland, D. P.; Dehnhardt, C. M.; Safina, B. S. *J. Med. Chem.*, **2018**, 61, 4810 – 4831.
71. a) Morris, J. J.; Pike, K. G. WO 2009007748, Jan. 15, 2009. b) Finlay, M. R. V.; Buttar, D.; Critchlow, S. E.; Dishington, A. P.; Fillery, S. M.; Fisher, E.; Glossop, S. C.; Graham, M. A.; Johnson, T.; Lamont, G. M.; Mutton, S.; Perkins, P.; Pike, K. G.; Slater, A. M. *Bioorg. Med. Chem. Lett.*, **2012**, 22, 4163 – 4168.
72. a) Sarbassov, D. D.; Ali, S. M.; Sabatini, D. M. *Curr. Opin. Cell Biol.*, **2005**, 17, 596 – 603. b) Engelman, J. A.; Luo, J.; Cantley, L. C. *Nat. Rev. Genet.*, **2006**, 7, 606 – 619. c) Guertin, D. A.; Sabatini, D. M. *Sci. Signaling*, **2009**, 2, pe24.
73. a) Richard, D. J.; Verheijen, J. C.; Zask, A. *Curr. Opin. Drug Discov.*, **2010**, 13, 428 – 435. b) Roychowdhury, A.; Sharma, R.; Kumar, S. *Future Med. Chem.*, **2010**, 2, 1577 – 1589. c) García-Echeverría, C. *Bioorg. Med. Chem. Lett.*, **2010**, 20, 4308 – 4312. d) Zask, A.; Verheijen, J. C.; Richard, D. J. *Expert Opin. Ther. Patents*, **2011**, 7, 1109 – 1127. e) Fasolo, A.; Sessa, C. *Expert Opin. Investig. Drugs*, **2011**, 20, 381 – 384.
74. Liu, K. K.-C.; Bailey, S.; Dinh, D. M.; Lam, H.; Li, C.; Wells, P. A.; Yin, M.-J.; Zou, A. *Bioorg. Med. Chem. Lett.*, **2015**, 22, 5114 – 5117.
75. a) Sun, S.-Y.; Rosenberg, L. M.; Wang, X.; Zhou, Z.; Yue, P.; Fu, H.; Khuri, F. R. *Cancer Res.*, **2005**, 65, 7052 – 7058. b) Liu, P.; Cheng, H.; Roberts, T. M.; Zhao, J. J. *Nat. Rev. Drug Discov.*, **2009**, 8, 627 – 644. c) Utermark, T.; Rao, T.; Cheng, H.; Wang, Q.; Lee, S. H.; Wang, Z. C.; Iglehart, J. D.; Roberts, T. M.; Muller, W. J.; Zhao, J. J. *Genes Dev.*, **2012**, 26, 1573 – 1586.

76. a) Ruffolo, R. R. *Expert Opin. Drug Discov.*, **2006**, *1*, 99 – 102. b) Schuhmacher, A.; Gassmann, O.; Hinder, M. *J. Transl. Med.*, **2016**, *14*, 105. c) Jarvis, L. M. *C&EN*, **2017**, *95*, 28 – 32.
77. a) Wellman-Labadie, O.; Zhou, Y. *Health Policy (New York)*, **2009**, *24*, 24. b) Williams, M. J. *Pharmacol. Exp. Ther.*, **2011**, *336*, 3 – 8. c) Lessl, M.; Schoepe, S.; Sommer, A.; Schneider, M.; Asadullah, K. *Drug Discov. Today*, **2011**, *16*, 288 – 292.
78. a) Vernon, J. A.; Golec, J. H.; Dimasi, J. A. *Health Econ.*, **2010**, *19*, 1002 – 1005. b) Roy, A.; Chaguturu. R. *Collaborative Innovation in Drug Discovery: Strategies for Public and Private Partnerships*, 1<sup>st</sup> ed. John Wiley & Sons, Inc.: Hoboken, USA, **2014**.
79. *Pharma 2020: Virtual R&D*. PriceWaterhouseCoopers, June 2008 [https://www.pwc.com/gx/en/pharma-life-sciences/pdf/pharma2020\\_virtualrd\\_final2.pdf](https://www.pwc.com/gx/en/pharma-life-sciences/pdf/pharma2020_virtualrd_final2.pdf) (Accessed Sept 18th, 2019)
80. a) Garattini, S. *J. Nephrol.*, **1997**, *10*, 283 – 294. b) Lichtenberg, F. R.; Philipson, T. *J. Law Econ.*, **2002**, *45*, 643 – 672. c) Gastala, N. M.; Wingrove, P.; Gaglioti, A.; Petterson, S.; Bazemore, A. *Health Aff. (Millwood)*, **2016**, *35*, 1237 – 1240. d) Hernandez, I.; Zhang, Y. *J. Pharm. Innov.*, **2017**, *12*, 105 – 109. e) Gyawali, B.; Prasad, V. *Nat. Rev. Clin. Oncol.*, **2017**, *14*, 653 – 654.
81. a) Graul, A. I.; Proud, J. R. *Drug News Perspect.*, **2007**, *20*, 57 – 68. b) Barden, C. J.; Weaver, D. F. *Drug Discov. Today*, **2010**, *15*, 84 – 87. c) Medina-Franco, J. L.; Giulianotti, M. A.; Welmaker, G. S.; Houghten, R. A. *Drug Discov. Today*, **2013**, *18*, 495 – 501.
82. a) Ellinger, B.; Gribbon, P. *Expert Opin. Drug Discov.*, **2016**, *11*, 333 – 336. b) Dierks, R. M. L.; Bruyère, O.; Reginster, J. Y. *Expert Rev. Pharmacoecon. Outcomes Res.*, **2018**, *18*, 147 – 160. c) Roy, A. *High-Throughput*, **2018**, *7*, 4.
83. a) Davies, J.; Davies, D. *Microbiol. Mol. Biol. Rev.*, **2010**, *74*, 417 – 433. b) Llor, C.; Bjerrum, L. *Ther. Adv. Drug Saf.*, **2014**, *6*, 25 – 64. c) Fair, R. J.; Tor, Y. *Perspect. Medicin. Chem.*, **2014**, *6*, 25 – 64. d) Zaman, S. B.; Hussain, M. A.; Nye, R.; Mehta, V.; Mamun, K. T.; Hossain, N. *Cureus*, **2017**, *9*, e1403. e)

- Kapoor, G.; Saigal, S.; Elongavan, A. *J. Anaesthesiol. Clin. Pharmacol.*, **2017**, 33, 300 – 305. f) Li, B.; Webster, T. J. *J. Orthop. Res.*, **2018**, 36, 22 – 32.
84. a) Marmor, M.; Hertzmark, K.; Thomas, S. M.; Halkitis, P. N.; Vogler, M. *J. Urban Health*, **2006**, 83, 5 – 17. b) Poland, G. A.; Jacobson, R. M.; Ovsyannikova, I. G. *Clin. Infect. Dis.*, **2009**, 48, 1254 – 1256. c) Taubenberger, J. K.; Kash, J. C. *Cell Host Microbe*, **2011**, 25, 440 – 451. d) Pizzorno, A.; Abed, Y.; Boivin, G. *Semin. Respir. Crit. Care Med.*, **2011**, 32, 409 – 422. e) van der Vries, E.; Schutten, M.; Fraaij, P.; Boucher, C.; Osterhaus, A. *Adv. Pharmacol.*, **2013**, 67, 217 – 246. f) Li, T. C. M.; Chan, M. C. W.; Lee, N. *Viruses*, **2015**, 7, 4929 – 4944. g) Hussain, M.; Galvin, H. D.; Haw, T. Y.; Nutsford, A. N.; Husain, M. *Infect. Drug Resist.*, **2017**, 10, 121 – 134.
85. a) Lungmani, Y. A. *Med. Princ. Pract.*, **2005**, 14, 35 – 48. b) Raguz, S.; Yagüe, E. *Br. J. Cancer*, **2008**, 99, 387 – 391. c) Housman, G.; Byler, S.; Heerboth, S.; Lapinska, K.; Longacre, M.; Snyder, N.; Sarkar, S. *Cancers*, **2014**, 6, 1769 – 1792. d) Alfarouk, K. O.; Sotck, C.-M.; Taylor, S.; Walsh, M.; Muddathir, A. K.; Verduzco, D.; Bashir, A. H. H.; Mohammed, O. Y.; Elhassan, G. O.; Harguindey, S.; Reshkin, S. J.; Ibrahim, M. E.; Rauch, C. *Cancer Cell Int.*, **2015**, 15, 71.
86. a) Austin, C. P. *Annu. Rev. Med.*, **2004**, 55, 1 – 13. b) Glimcher, L. H.; Lindvall, O.; Aguirre, V.; Topalian, S. L.; Musunuru, K. Fauci, A. S. *Cell*, **2012**, 148, 1077 – 1078. c) Earm, K.; Earm, Y. E. *Integr. Med. Res.*, **2014**, 3, 211 – 216.
87. a) Austin, C. P.; Brady, L. S.; Insel, T. R.; Collins, F. S. *Science*, **2004**, 306, 1138 – 1139. b) Oprea, T. I.; Bologa, C. G.; Boyer, S.; Curpan, R. F.; Glen, R. C.; Hopkins, A. L.; Lipinski, C. A.; Marshall, G. R.; Martin, Y. C.; Ostopovici-Halip, L.; Rishton, G.; Ursu, O.; Vaz, R. J.; Waller, C.; Waldmann, H.; Sklar, L. A. *Nat. Chem. Biol.*, **2009**, 5, 441 – 447. c) Roy, A.; McDonald, P. R.; Sittampalam, S.; Chaguturu, R. *Curr. Pharm. Biotechnol.*, **2010**, 11, 764 – 778.
88. a) Hopkins, A. L.; Groom, C. R. *Nat. Rev. Drug Discov.*, **2002**, 1, 727 – 730. b) Lindsay, M. A. *Nat. Rev. Drug Discov.*, **2003**, 2, 831 – 838. c) Overington, J. P.; Al-Lazikani, B.; Hopkins, A. L. *Nat. Rev. Drug Discov.*, **2006**, 5, 993 – 996.
89. a) Clark, R. L.; Johnston, B. F.; Mackay, S. P.; Breslin, C. J.; Robertson, M. N.I Harvey, A. L. *Drug Discov. Today*, **2010**, 15, 679 – 683. c) McCarthy, A. *Chem.*

- Biol.*, **2010**, *17*, 549 – 550. d) Wang, Y.; Cheng, T.; Bryant, S. H. *SLAS Discov.*, **2017**, *22*, 655 – 666. e) Tresadern, G.; Rombouts, F. J. R.; Oehlrich, D.; Macdonald, G.; Trabanco, A. A. *Drug Discov. Today*, **2017**, *22*, 1478 – 1488.
90. a) Frye, S. V. *Hematology Am. Soc. Hematol. Educ. Program*, **2013**, *2013*, 300 – 305. b) Laterza, O. F.; Plump, A.; Ming, J. E.; Richards, S.; Burczynski, M. E.; Wagner, J. A.; Patterson, S. D. *Clin. Chem.*, **2015**, *61*, 579 – 583. c) Lee, W. H. *PLoS Biol.*, **2015**, *13*, e1002164. d) Nilsson, N.; Felding, J. *Future Med. Chem.*, **2015**, *7*, 1853 – 1859. e) Bergauer, T.; Ruppert, T.; Essioux, L.; Spleiss, O. *Ther. Innov. Regul. Sci.*, **2016**, *50*, 769 – 776. f) Williams, S. P.; McDermott, U. *Cell Chem. Biol.*, **2017**, *24*, 1066 – 1074.
91. Chesbrough, H. *Open Innovation: The New Imperative for Creating and Profiting from Technology*. Harvard Business School Press: Cambridge, USA, **2003**.
92. a) Chin-Dusting, J.; Mizrahi, J.; Jennings, G.; Fitzgerald, D. *Nat. Rev. Drug Discov.*, **2005**, *4*, 891 – 897. b) Tralau-Stewart, C. J.; Wyatt, C. A.; Kleyn, D. E.; Ayad, A. *Drug Discov. Today*, **2009**, *14*, 95 – 101. c) Paul, S. M.; Mytelka, D. S.; Dunwiddie, C. T.; Persinger, C. C.; Munos, B. H.; Lindborg, S. R.; Schacht, A. L. *Nat. Rev. Drug Discov.*, **2010**, *9*, 203 – 214.
93. a) Roy, A.; McDonald, P. R.; Sittampalam, S.; Chaguturu, R. *Curr. Pharm. Biotechnol.*, **2010**, *11*, 764 – 778. b) Robertson, G. M.; Mayr, L. M. *Future Med. Chem.*, **2011**, *3*, 1995 – 2020. c) Moos, W. H.; Kodukula, K. *Curr. Med. Chem.*, **2011**, *18*, 3437 – 3440. d) Stevens, A. J.; Jensen, J. J.; Wyller, K.; Kilgore, P. C.; Chatterjee, S.; Rohrbaugh, M. L. *N. Engl. J. Med.*, **2011**, *364*, 535 – 541. e) Alvim-Gaston, M.; Grese, T.; Mahoui, A.; Palkowitz, A. D.; Pineiro-Nunez, M.; Watson, I. *Curr. Top. Med. Chem.*, **2014**, *14*, 294 – 303.
94. a) Nelson, A.; Roche, D. *Bioorg. Med. Chem.*, **2015**, *23*, 2613. b) Besnard, J.; Jones, P. S.; Hopkins, A. L.; Pannifer, A. D. *Drug Discov. Today*, **2015**, *20*, 181 – 186. c) Gottwald, M.; Becker, A.; Bahr, I.; Mueller-Fahrnow, A. *Archiv. Der Pharmazie*, **2016**, *349*, 692 – 697. d) Paillard, G.; Cochrane, P.; Jones, P. S.; van Hoorn, W. P.; Caracoti, A.; van Vlijmen, H.; Pannifer, A. D. *Drug Discov. Today*, **2016**, *21*, 97 – 102.

95. Karawajczyk, A.; Giordanetto, F.; Benningshof, J.; Hamza, D.; Kalliokoski, T.; Pouwer, K.; Morgentin, R.; Nelson, A.; Piechot, A.; Tzalis, D. *Drug Discov. Today*, **2015**, *20*, 1310 – 1316.
96. Mullard, A. *Nat. Rev. Drug Discov.*, **2013**, *12*, 173 – 175.
97. a) Karawajczyk, A.; Orrling, K. M.; de Vlieger, J. S. B.; Rijnders, T.; Tzalis, D. *Front. Med.*, **2017**, *3*, 75. b) Morgentin, R.; Dow, M.; Aimon, A.; Karageorgis, G.; Kalliokoski, T.; Roche, D.; Marsden, S.; Nelson, A. *Drug Discov. Today*, **2018**, *23*, 1578 – 1583.
98. Otten, H. *J. Antimicrob. Chemother.*, **1986**, *17*, 689 – 696.
99. Hager, T. *The Demon Under the Microscope: From Battlefield Hospitals to Nazi Labs, One Doctor's Heroic Search for the World's First Miracle Drug*. Harmony Books: New York City, N.Y., 2006.
100. a) Kyle, R. A.; Shampo, M. A. *JAMA*, **1982**, *247*, 2581. b) Raju, T. N. *Lancet*, **1999**, *353*, 681.
101. a) Carta, F.; Scozzafava, A.; Supuran, C. T. *Expert Opin. Ther. Pat.*, **2012**, *22*, 747 – 758. b) Ajeet; Mishra, A. K.; Kumar, A. *Am. J. Pharmacol. Sci.*, **2015**, *3*, 18 – 24. c) Gokcen, T.; Gulcin, I.; Ozturk, T.; Goren, A. C. *J. Enzyme Inhib. Med. Chem.*, **2016**, *31*, 180 – 188. d) Lavanya, R. *Int. J. Pharm. Sci. Invent.*, **2017**, *6*, 1 – 3.
102. Ballatore, C.; Hury, D. M.; Smith, III, A. B. *ChemMedChem*, **2013**, *8*, 385 – 395.
103. a) Han, T.; Goralski, M.; Gaskill, N.; Capota, E.; Kim, J.; Ting, T. C.; Xie, Y.; Williams, N. S.; Nijhawan, D. *Science*, **2017**, *356*, eaal3755. b) Gul, H. I.; Yamali, C.; Sakagami, H.; Angeli, A.; Leitans, J.; Kazaks, A.; Tars, K.; Ozgun, D. O.; Supuran, C. T. *Bioorg. Chem.*, **2018**, *77*, 411 – 419.
104. Scozzafava, A.; Owa, T.; Mastrolorenzo, A.; Supuran, C. T. *Curr. Med. Chem.*, **2003**, *10*, 925 – 953.
105. Ottonello, L.; Dapino, P.; Scirocco, M. C.; Balbi, A.; Bevilacqua, M.; Dallergrì, F. *Clin. Sci. (Lond.)*, **1995**, *88*, 331 – 336.
106. a) Masereel, B.; Rolin, S.; Abbate, F.; Scozzafava, A.; Supuran, C. T. *J. Med. Chem.*, **2002**, *45*, 312 – 320. b) Thiry, A.; Dogné, J. M.; Supuran, C. T.;

- Masereel, B. *Curr. Pharm. Des.*, **2008**, *14*, 661 – 671. c) Siddiqui, N.; Arshad, M. F.; Khan, S. A.; Ahsan, W. *J. Enzyme Inhib. Med. Chem.*, **2010**, *25*, 485 – 491.
107. Bissantz, C.; Kuhn, B.; Stahl, M. *J. Med. Chem.*, **2010**, *53*, 5061 – 5084.
108. Fujii, S.; McCarthy, T. J. *Langmuir*, **2016**, *32*, 765 – 771.
109. a) Tilstam, U. *Org. Process Res. Dev.*, **2012**, *16*, 1273 – 1278. b) Butawan, M.; Benjamin, R. L.; Bloomer, R. J. *Nutrients*, **2017**, *9*, 290.
110. a) Ghosh, A. K. *J. Med. Chem.*, **2008**, *52*, 2163 – 2176. b) Ghosh, A. K.; Chapsal, B. D.; Weber, I. T.; Mitsuya, H. *Acc. Chem. Res.*, **2008**, *41*, 78 – 86.
111. Feng, M.; Tang, B.; Liang, S. H.; Jiang, X. *Curr. Top. Med. Chem.*, **2016**, *16*, 1200 – 1216.
112. Vandyck, K.; Cummings, M. C.; Nyanguile, O.; Boutton, C. W.; Vendeville, S.; McGowan, D.; Devogelaere, B.; Amssoms, K.; Last, S.; Rombauts, K.; Tahri, A.; Lory, P.; Hu, L.; Beauchamp, D. A.; Simmen, K.; Raboisson, P. *J. Med. Chem.*, **2009**, *52*, 4099 – 4102.
113. a) Rickels, K.; Pereira-Ogan, J. A.; Case, W. G.; Csanalosi, I.; Mirman, M. J.; Nathanson, J. E.; Parish, L. C. *Am. J. Psychiatry*, **1974**, *131*, 592 – 595. b) Gautier, V.; Vinçon, G.; Demotes-Mainard, F.; Albin, H. *Therapie*, **1990**, *45*, 315 – 319. c) Pattrick, M.; Swannell, A.; Doherty, M. *Br. J. Rheumatol.*, **1993**, *32*, 55 – 58. d) Seeling, A.; Oelschläger, H.; Rothley, D. *Pharmazie*, **2000**, *55*, 293 – 296. e) Wollina, U.; Hipler, U. C.; Seeling, A.; Oelschläger, H. *Skin Pharmacol. Physiol.*, **2005**, *18*, 132 – 138.
114. a) Ilardi, E. A.; Vitaku, E.; Njardarson, J. T. *J. Med. Chem.*, **2014**, *57*, 2832 – 2842. b) Scott, K. A.; Njardarson, J. T. *Top. Curr. Chem.*, **2018**, *376*, 5.
115. a) Fang, S.-H.; Padmavathi, V.; Rao, Y. K.; Subbaiah, D. R. C. V.; Thriveni, P.; Geethangili, M.; Padmaja, A.; Tzeng, Y.-M. *Int. Immunopharmacol.*, **2006**, *6*, 1699 – 1705. b) Chen, X.; Hussain, S.; Parveen, S.; Zhang, S.; Yang, Y.; Zhu, C. *Curr. Med. Chem.*, **2012**, *19*, 3578 – 3604. c) Athar, M.; Lone, M. Y.; Khedkar, V. M.; jha, P. C. *J. Biomol. Struct. Dyn.*, **2016**, *34*, 1282 – 1297. d) Bollong, M. J.; Lee, G.; Coukos, J. S.; Yun, H.; Zambaldo, C.; Chang, J. W.; Chin, E. N.; Ahmad, I.; Chatterjee, A. K.; Lairson, L. L.; Schultz, P. G.; Moellering, R. E. *Nature*, **2018**, *562*, 600 – 604.

116. Auberson, Y.; Glatthar, R.; Salter, R.; Simic, O.; Tintelnot-Blomley, M. WO2005035535, April 21, 2005.
117. a) Seelig, A.; Landwojtowicz, E. *Eur. J. Pharm. Sci.*, **2000**, *12*, 31–40. (b) Seelig, A. *Eur. J. Biochem.*, **1998**, *251*, 252–261. (c) Cianchetta, G.; Singleton, R. W.; Zhang, M.; Wildgoose, M.; Giesing, D.; Fravolini, A.; Cruciani, G.; Vaz, R. *J. J. Med. Chem.*, **2005**, *48*, 2927–2935. (d) Didziapetris, R.; Japertas, P.; Avdeef, A.; Petrauskas, A. *J. Drug Target*, **2003**, *11*, 391–406.
118. a) Shacka, J. J.; Roth, K. A. *Autophagy* **2007**, *3*, 474–476. b) Pearce, D. A.; Ramirez-Montealegre, D.; Rothberg, P. G. *Brain*, **2006**, *129*, 1353–1356.
119. Rueeger, H.; Lueoend, R.; Rogel, O.; Rondeau, J.-M.; Möbitz, H.; Machauer, R.; Jacobson, L.; Staufenbiel, M.; Desrayaud, S.; Neumann, U. *J. Med. Chem.* **2012**, *55*, 3364–3386.
120. Brant, M. G.; Bromba, C. M.; Wulff, J. E. *J. Org. Chem.*, **2010**, *75*, 6312 – 6315.
121. a) Richards, M. R.; Brant, M. G.; Boulanger, M. J.; Cairo, C. W.; Wulff, J. E. *Med. Chem. Commun.*, **2014**, *5*, 1483 – 1488. b) Brant, M. G.; Wulff, J. E. *Org. Lett.*, **2012**, *14*, 5876 – 5879.
122. a) Dharan, N. J.; Gubareva, L. V.; Meyer, J. J.; Okomo-Adhiambo, M.; McClinton, R. C.; Marshall, S. A.; St. George, K.; Epperson, S.; Brammer, L.; Klimov, A. I.; Bresee, J. S.; Fry, A. M. *JAMA*, **2009**, *301*, 1034 – 1041. b) Dixit, R.; Khandaker, G.; Ilgoutz, S.; Rashid, H.; Booy, R. *Infect. Disord. Drug Targets*, **2013**, *13*, 34 – 45.
123. Shao, W.; Li, X.; Goraya, M. U.; Wang, S.; Chen, J. L. *Int. J. Mol. Sci.*, **2017**, *18*, 1650. d) Samson, M.; Pizzorno, A.; Abed, Y.; Boivin, G. *Antiviral Res.*, **2013**, *98*, 174 – 185. e) Hurt, A. C. *Curr. Opin. Virol.*, **2014**, *8*, 22 – 29.
124. Caputo, J. A.; Fuchs, R. *Tetrahedron Lett.*, **1967**, *8*, 4729 – 4731. b) Piatak, D. M.; Herbst, G.; Wicha, J.; Caspi, E. *J. Org. Chem.*, **1969**, *34*, 116 – 120. c) Clayden, J.; Menet, C. J.; Tchabanenko, K. *Tetrahedron*, **2002**, *58*, 4727 – 4733. d) Tabatabaeian, K.; Mamaghani, M.; Mahmoodi, N. O.; Khorshidi, A. *Catal. Commun.*, **2008**, *9*, 416 – 420.

125. Brant, M. G.; Friedmann, J. N.; Bohlken, C. G.; Oliver, A. G.; Wulff, J. E. *Org. Biomol. Chem.*, **2015**, *13*, 4581 – 4588.
126. Y. T. Tao, C. L. Liu, S. J. Lee and S. S. P. Chou. *J. Org. Chem.*, **1986**, *51*, 4718 – 4721.
127. Conrad, C. R.; Dolliver, M. A. *Org. Synth.*, **1932**, *12*, 22.
128. Jagt, D. V.; Deck, L.; Abcouwer, S.; Bobrovnikova – Marjon, E.; Weber, W. U.S. Patent 20060276536 A1, December 7, 2004.
129. Nakayama, J.; Machida, H.; Saito, R.; Akimoto, K.; Hoshino, M. *Chem. Lett.*, **1985**, *14*, 1173–1176.
130. Klingenberg, J. J. *Org. Synth.*, **1955**, *35*, 11.
131. Siegel, W.; Dobler, W.; John, M. U.S. Patent 5710341A, January 20, 1998.
132. Eller, C.; Kehr, G.; Daniliuc, C. G.; Stephan, D. W.; Erker, G. *Chem. Commun.*, **2015**, *51*, 7226 – 7229.
133. Nakayama, J.; Machida, H.; Hoshino, M. *Tetrahedron Lett.*, **1985**, *26*, 1981 – 1982.
134. a) Mukaiyama, T.; Sato, T.; Hanna, J. *Chem. Lett.*, **1973**, *2*, 1041 – 1044. b) McMurry, J. E.; Felming, M. P. *J. Am. Chem. Soc.*, **1974**, *96*, 4708 – 4709. c) McMurry, J. E. *Chem. Rev.*, **1989**, *89*, 1513 – 1524. d) Fürstner, A.; Bogdanović, B. *Angew. Chem. Int. Ed.*, **1996**, *98*, 2442 – 2469. f) Ephritikhine, M. *Chem. Commun.*, **1998**, *0*, 2549 – 2554.
135. a) Engman, L.; Bystrom, S. E. *J. Org. Chem.*, **1985**, *50*, 3170 – 3173. b) Takahashi, T.; Xi, Z.; Fischer, R.; Huo, S.; Xi, C.; Nakajima, K. *J. Am. Chem. Soc.*, **1997**, *119*, 4561 – 4562. c) Xi, Z.; Liu, X.; Lu, J.; Bao, F.; Fan, H.; Li, Z.; Takahashi, T. *J. Org. Chem.* **2004**, *69*, 8547 – 8549. d) Lee, P. H.; Seomoon, D.; Lee, K. *Org. Lett.* **2005**, *7*, 343 – 345.
136. Takeda, T.; Horikawa, Y.; Nomura, T.; Watanabe, M.; Miura, I.; Fujiwara, T. *Phosphorus Sulfur Silicon Relat. Elem.*, **1997**, *120*, 391 – 392.
137. Fürstner, A.; Hupperts, A. *J. Am. Chem. Soc.*, **1995**, *117*, 4468 – 4475.
138. Webb, K. S. Patent WO1994021603 A1, July 31, 1996.

139. Hirao, T.; Takeuchi, H.; Ogawa, A.; Sakurai, H. *Synlett*, **2000**, 11, 1658 – 1660.
140. Juteau, H.; Gareau, Y. *Synth. Commun.*, **1998**, 28, 3795 – 3805.
141. Harrington, P. J.; DiFiore, K. A. *Tetrahedron Lett.*, **1987**, 28, 495 – 498.
142. a) Canto, K.; da Silva Ribeiro, R.; Biajoli, A. F. P.; Correia, C. R. D. *Eur. J. Org. Chem.*, **2013**, 0, 8004 – 8013. b) Lim, L. H.; Zhou, J. *Chem. Front.*, **2015**, 2, 775 – 777.
143. a) Jeffery, T. *J. Chem. Soc., Chem. Commun.*, **1984**, 0, 1287 – 1289. b) Jeffery, T. *Tetrahedron Lett.* **1985**, 26, 2667 – 2670. c) Jeffery, T. *Tetrahedron*, **1996**, 52, 10113 – 10130. d) Reetz, T. M.; Breinbauer, R.; Wanninger, K. *Tetrahedron Lett.*, **1996**, 37, 4499 – 4502.
144. a) Kiwi, J.; Grätzel, M. *J. Am. Chem. Soc.*, **1979**, 101, 7214 – 7217. b) Reetz, M. T.; Helbig, W.; S. A. Quaiser, S. A.; Stimming, U.; Breuer, N.; Vogel, R. *Science*, **1995**, 267, 367 – 369. c) M. T. Reetz, M. T.; Winter, M.; Breinbauer, R.; T. Thurn-Albrecht, T.; Vogel, W. *Chem. Eur. J.*, **2001**, 7, 1084–1094.
145. a) Lucht, B. L.; Collum, D. B. *J. Am. Chem. Soc.*, **1994**, 116, 6009 – 6010. b) Lucht, B. L.; Collum, D. B. *J. Am. Chem. Soc.*, **1995**, 117, 9863 – 9874. c) Lucht, B. L.; Collum, D. B. *J. Am. Chem. Soc.*, **1996**, 118, 2217 – 2225. d) Lucht, B. L.; Collum, D. B. *Acc. Chem. Res.*, **1999**, 32, 1035 – 1042.
146. a) Evans, D. A.; Golob, A. M. *J. Am. Chem. Soc.*, **1975**, 117, 4765 – 4766. b) Gajewski, J. J.; Gee, K. R. *J. Am. Chem. Soc.*, **1991**, 113, 967 – 971. c) Msayib, K. J.; Watt, C. I. F. *Chem. Soc. Rev.*, **1992**, 21, 237 – 243.
147. Reich, H. *J. Chem. Rev.*, **2013**, 113, 7130 – 7178.
148. a) Li, L.; Liu, Y.; Peng, Y.; Yu, L.; Wu, X.; Yan, H. *Angew. Chem. Int. Ed.*, **2016**, 55, 331 – 335. b) Liu, X.; Guo, X.; Wang, F.; Lei, G.; Luo, D. *Nucleosides Nucleotides Nucleic Acids*, **2007**, 26, 45 – 49.
149. Fürstner, A.; Müller, C. *Chem. Commun.*, **2005**, 0, 5583 – 5585.
150. a) DeNinno, M. P. *J. Am. Chem. Soc.*, **1995**, 117, 9927 – 9928. b) Vlad, P. F.; Aryku, A. N.; Chokyrlan, A. G. *Russ. Chem. Bull.* **2004**, 53, 443 – 446. c) García Martínez, A.; Teso Vilar, E.; García Fraile, A.; de la Moya Cerero, S.; Lora Maroto, B. *Tetrahedron Lett.* **2005**, 46, 5157 – 5159.

151. a) Höfle, G.; Steglich, W.; Vorbrüggen, H. *Angew. Chem. Int. Ed.*, **1978**, *17*, 569 – 583. b) Scriven, E. F. V. *Chem. Soc. Rev.*, **1983**, *12*, 129 – 161. c) Xu, S.; Held, I.; Kempf, B.; Mayr, H.; Steglich, W.; Zipse, H. *Chem. Eur. J.*, **2005**, *11*, 4751 – 4757.
152. Hasegawa, M.; Iwata, S.; Sone, Y.; Endo, J.; Matsuzawa, H.; Mazaki, Y. *Molecules*, **2014**, *19*, 2829 – 2841.
153. Nicolaou, K. C.; Adsool, V. A.; Hale, C. R. H. *Org. Lett.*, **2010**, *12*, 1552 – 1555.
154. a) Pappo, R.; Allen, Jr., D. S.; Lemieux, R. U.; Johnson, W. S. *J. Org. Chem.*, **1956**, *21*, 478 – 479. b) Yu, W.; Mei, Y.; Kang, Y.; Hua, Z.; Jin, Z. *Org. Lett.*, **2004**, *6*, 3217 – 3219.
155. a) Criegee, R. *Angew. Chem. Int. Ed.*, **1975**, *14*, 745 – 752. b) Geletneky, C.; Berger, S. *Eur. J. Org. Chem.*, **1998**, *8*, 1625 – 1627. c) Welz, O.; Savee, J. D.; Osborn, D. L.; Vasu, S. S.; Percival, C. J.; Shallcross, D. E.; Taatjes, C. *Science*, **2012**, *335*, 204 – 207. d) Su, Y.-T.; Huang, Y.-H.; Witek, H. A.; Lee, Y.-P. *Science*, **2013**, *340*, 174 – 176.
156. Schreiber, S. L.; Liew, W. F. *J. Am. Chem. Soc.*, **1985**, *107*, 2980 – 2982.
157. a) Eschemoser, A.; Frey, A. *Helv. Chim. Acta.*, **1952**, *35*, 1660 – 1666. b) Grob, C. A.; Baumann, W. *Helv. Chim. Acta.*, **1955**, *38*, 594 – 610. c) Prantz, K.; Mulzer, J. *Chem. Rev.*, **2010**, *110*, 3741 – 3766. d) Grob, C. A.; Krasnobajew, V. *Helv. Chim. Acta.*, **1964**, *47*, 2145 – 2155. e) Grob, C. A. *Helv. Chim. Acta.*, **1969**, *8*, 535 – 546.
158. Luzzio, F. A.; Moore, W. J. *J. Org. Chem.*, **1993**, *58*, 2966 – 2971.
159. a) Babler, J. H.; Coghlan, J. J. *Synth. Commun.*, **1976**, *6*, 469 – 474. b) Dauben, W. G.; Michno, D. M. *J. Org. Chem.*, **1977**, *42*, 682 – 685. c) Wietzerbin, K.; Bernadou, J.; Meunier, B. *Eur. J. Inorg. Chem.*, **2000**, *0*, 1391 – 1406. d) Nagata, H.; Miyazawa, N.; Ogasawara, K. *Chem. Commun.*, **2001**, *0*, 1094 – 1095.
160. He, F.; Bo, Y.; Altom, J. D.; Corey, E. J. *J. Am. Chem. Soc.*, **1999**, *121*, 6771 – 6772.

161. a) Ireland, R. E.; Mueller, R. H. *J. Am. Chem. Soc.*, **1972**, *94*, 5897 – 5898. b) Ireland, R. E.; Willard, A. K. *Tetrahedron Lett.*, **1975**, *16*, 3975 – 3978. c) Ireland, R. E.; Mueller, R. H.; Willard, A. K. *J. Am. Chem. Soc.*, **1976**, *98*, 2868 – 2877. d) Ireland, R. E.; Wipf, P.; Armstrong, J. D. *J. Org. Chem.*, **1991**, *56*, 650 – 657. e) Ireland, R. E.; Wipf, P.; Xiang, J. N. *J. Org. Chem.*, **1991**, *56*, 3572 – 3582. f) Chai, Y.; Hong, S.; Lindsay, H. A.; McFarland, C.; McIntosh, M. C. *Tetrahedron*, **2002**, *58*, 2905 – 2928.
162. a) Bauld, N. L.; Bellville, D. J.; Pabon, R.; Chelsky, R.; Green, G. *J. Am. Chem. Soc.*, **1983**, *105*, 2378 – 2382. b) Gajewski, J. J.; Emrani, J. *J. Am. Chem. Soc.*, **1984**, *106*, 5733 – 5734. c) Burns, J. D. Ph.D. Dissertation, University of Queensland, Brisbane, Australia, 2015.
163. Ida, Y.; Matsubara, A.; Nemoto, T.; Saito, M.; Hirayama, S.; Fujii, H.; Nagase, H. *Bioorg. Med. Chem.*, **2012**, *20*, 5810 – 5831.
164. Olah, G. A.; Karpeles, R.; Narang, S. C. *Synthesis*, **1982**, *11*, 963 – 965.
165. Chou, T. S.; Lee, S. J.; Tso, H. H.; Yu, C. F. *J. Org. Chem.*, **1987**, *52*, 5082 – 5085.
166. a) John, J. P.; Jost, J.; Novikov, A. V. *J. Org. Chem.*, **2009**, *74*, 6083 – 6091. b) Biftu, T.; Sinha – Roy, R.; Chen, P.; Qian, X.; Feng, D.; Kuethe, J. T.; Scapin, G.; Gao, Y. D.; Yan, Y.; Krueger, D.; Bak, A.; Eiermann, G.; He, J.; Cox, J.; Hicks, J.; Lyons, K.; He, H.; Salituro, G.; Tong, S.; Patel, S.; Doss, G.; Petrov, A.; Wu, J.; Xu, S. S.; Sewall, C.; Zhang, X.; Zhang, B.; Thornberry, N. A.; Weber, A. E. *J. Med. Chem.*, **2014**, *57*, 3205 – 3212.
167. Andrez, J. – C.; Chowdhury, S.; Decker, S.; Dehnhardt, C. M.; Focken, T.; Grimwood, M. E.; Hemeon, I. W.; Jia, Q.; Li, J.; Ortwine, D.; Safina, B.; Sheng, T.; Sun, S.; Sutherlin, D. P.; Wilson, M. S.; Zenova, A. Y. *PCT Int. Appl.* 2013177224, May 21, 2013. b) Jain, N.; Ciufolini, M. A. *Synlett.*, **2015**, *26*, 631 – 634. c) Jain, N.; Xu, S.; Ciufolini, M. A. *Chem. Eur. J.*, **2017**, *23*, 4542 – 4546.
168. Mendelsohn, B.; Lee, S.; Kim, S.; Teyssier, F.; Aulakh, V. S.; Ciufolini, M. A. *Org. Lett.*, **2009**, *11*, 1539 – 1542.
169. a) Pin, F.; Vercouille, J.; Ouach, A.; Mavel, S.; Gulhan, Z.; Chicheri, G.; Jarry, C.; Massip, S.; Deloye, J. – B.; Guilloteau, D.; Suzenet, F.; Chalon, S.;

- Routier, S. *Eur. J. Med. Chem.*, **2014**, *82*, 214 – 224. b) Dallanoce, C.; Canovi, M.; Matera, C.; Mennini, T.; De Amici, M.; Gobbi, M.; De Micheli, C. *Bioorg. Med. Chem.*, **2012**, *20*, 6344 – 6355. c) Borsini, E.; Broggin, G.; Colombo, F.; Khansaa, M.; Fasana, A.; Galli, S.; Passarella, D.; Riva, E.; Riva, S. *Tetrahedron: Asymmetry*, **2011**, *22*, 264 – 269.
170. Chou, T.-S.; Tso, H.-H.; Chang, L. J. *J. Chem. Soc., Perkin Trans. 1*, **1985**, *0*, 515 – 519.
171. a) Mayr, H.; Kempf, B.; Ofial, A. R. *Acc. Chem. Res.*, **2003**, *36*, 66 – 77. b) Ammer, J.; Nolte, C.; Mayr, H. *J. Am. Chem. Soc.*, **2012**, *134*, 13902 – 13911.
172. a) Mayr, H.; Bug, T.; Gotta, M. F.; Hering, N.; Irrgang, B.; Janker, B.; Kempf, B.; Loos, R.; Ofial, A. R.; Remennikov, G.; Schimmel, H. *J. Am. Chem. Soc.*, **2001**, *123*, 9500 – 9512. b) Mayr, H.; Ofial, A. R. *J. Phys. Org. Chem.*, **2003**, *21*, 584 – 595.
173. a) Khursan, S. L.; Mikhailov, D. A.; Yanborisov, V. M.; Borisov, D. I. *React. Kinet. Catal. Lett.*, **1997**, *61*, 91 – 95. b) Nakamura, A.; Nakada, M. *Synthesis*, **2013**, *45*, 1421 – 1451. c) Deshlahra, P.; Iglesia, E. *J. Phys. Chem. C*, **2015**, *120*, 16741 – 16760.
174. a) Zimmerman, H. E.; Thyagarajan, B. S. *J. Am. Chem. Soc.*, **1960**, *82*, 2505 – 2511. b) Boche G.; Marsch, M.; Harms, K.; Sheldrick, G. M. *Angew. Chem. Int. Ed.*, **1985**, *24*, 573 – 575. c) Boche, G. *Angew. Chem. Int. Ed.*, **1989**, *28*, 277 – 297.
175. a) Story, P. R.; Alford, J. A.; Burgess, J. R.; Ray, W. C. *J. Am. Chem. Soc.*, **1971**, *93*, 3042 – 3044. b) Criegee, R. *Angew. Chem. Int. Ed.*, **1975**, *14*, 745 – 752. c) Geletneky, C.; Berger, S. *Eur. J. Org. Chem.*, **1998**, *1998*, 1625 – 1627.
176. a) Fliszár, S.; Renard, J. *Can. J. Chem.*, **1970**, *48*, 3002 – 3018. b) Fisher, T. J.; Dussault, P. H. *Tetrahedron*, **2017**, *73*, 4233 – 4258.
177. a) Schiaffo, C. E.; Dussault, P. H. *J. Org. Chem.*, **2008**, *73*, 4688 – 4690. b) Cochran, B. M.; Corbett, M. T.; Correll, T. L.; Fang, Y.-Q.; Flick, T. G.; Jones, S. C.; Smith, A. G.; Tucker, J. L.; Vounatsos, F.; Wells, G.; Yeung, D.; Walker, S. D.; Bio, M. W.; Caille, S. *J. Org. Chem.*, **2019**, *84*, 4763 – 4779.

178. Cochran, B. M. *Synlett*, **2016**, 27, 245 – 248.
179. a) Coggins, P.; Gaur, S.; Simpkins, N. S. *Tetrahedron Lett.*, **1995**, 36, 1545 – 1548. b) Majewski, M.; DeCaire, M.; Nowak, P.; Wang, F. *Can. J. Chem.*, **2001**, 79, 1792 – 1798. c) Sikorska, L. M.Sc. Dissertation, University of Saskatchewan, 2008.
180. Chen, Z.; Gonzalez, M. D.; Blundell, P.; Meltzer, P. C. *Tetrahedron Lett.*, **1997**, 38, 6823 – 6824.
181. a) Baker-Glenn, C. A. G.; Barrett, A. G. M.; Gray, A. A.; Procopiou, P. A.; Ruston, M. *Tetrahedron Lett.*, **2005**, 46, 7427 – 7430. b) Zhao, F.; Luo, J.; Tan, Q.; Liao, Y.; Peng, S.; Deng, G.-J. *Adv. Syn. Catal.*, **2012**, 354, 1914 – 1918. c) Gauthier, Jr, D. R.; Yoshikawa, N. *Org. Lett.*, **2016**, 18, 5994 – 5997.
182. a) Issacs, N. S.; Laila, A. A. R. *Tetrahedron Lett.*, **1976**, 17, 715 – 716. b) Suárez, D.; Sordo, T. L.; Sordo, J. A. *J. Org. Chem.*, **1995**, 60, 2848 – 2852. c) Desimoni, G.; Faita, G.; Garau, S.; Righetti, P. P. *Tetrahedron*, **1996**, 52, 6241 – 6248. d) Suárez, D.; Iglesias, E.; Sordo, T. L.; Sordo, J. A. *J. Phys. Org. Chem.*, **1996**, 9, 17 – 20. e) Fernandez, T.; Sordo, J. A.; Monnat, F.; Deguin, B.; Vogel, P. *J. Am. Chem. Soc.*, **1998**, 120, 13276 – 13277. f) Monnat, F.; Vogel, P.; Sordo, J. A. *Helv. Chim. Acta.*, **2002**, 85, 713 – 732.
183. Ranu, B. C. *Synlett*, **1993**, 1993, 885 – 892.
184. a) Scouten, C. G.; Brown, H. C. *J. Org. Chem.*, **1973**, 38, 4092 – 4094. b) Gung, B. W. *Chem. Rev.*, **1999**, 99, 1377 – 1386. c) Neufeldt, S. R.; Jiménez-Osés, G.; Comins, D. L.; Houk, K. N. *J. Org. Chem.*, **2014**, 79, 11609 – 11618.
185. a) Gerstner, N. C.; Adams, C. S.; Tretbar, M.; Schomaker, J. M. *Angew. Chem. Int. Ed.*, **2016**, 128, 13434 – 13437.
186. a) Fortunato, J. M.; Ganem, B. *J. Org. Chem.*, **1976**, 41, 2194 – 2200. b) Crisp, G. T.; Scott, W. J.; Stille, J. K. *J. Am. Chem. Soc.*, **1984**, 106, 7500 – 7506. c) Knight, S. D.; Overman, L. E.; Paireau, G. *J. Am. Chem. Soc.*, **1993**, 115, 9293 – 9294.
187. a) Gupton, J. T.; Layman, W. J. *J. Org. Chem.*, **1987**, 52, 3683 – 3686. b) Gamero-Melo, P.; Villanueva-García, M.; Robles, J.; Contreras, R.; Paz-Sandoval, M. A. *J. Organomet. Chem.*, **2005**, 690, 1379 – 1395.

188. a) Bartlett, P. D. *Rec. Chem. Prog.*, **1950**, *11*, 47 – 51. b) Singleton, D.; Merrigan, S. R.; Liu, J.; Houk, K. N. *J. Am. Chem. Soc.*, **1997**, *119*, 3385 – 3386.
189. a) Takaishi, N.; Takahashi, H.; Yamashita, O.; Inamoto, Y. *J. Org. Chem.*, **1986**, *51*, 4862 – 4865. b) Neelamkavil, S. F.; Neustadt, B. R.; Stamford, A.; Xia, Y.; Harris, J. M.; Boyle, C. D.; Chackalamannil, S.; Biswas, D.; Liu, H.; Hao, J.; Lankin, C. M.; Shah, U. G. WO2010114958, October 4<sup>th</sup>, 2010.
190. a) Alvarez-Idaboy, J. R.; Reyes, L. *J. Org. Chem.*, **2007**, *72*, 6580 – 6583. b) Hoveyda, A. H.; Evans, D. A.; Fu, G. C. b) Alvarez-Idaboy, J. R.; Reyes, L. *Chem. Rev.*, **1993**, *93*, 1307 – 1370.
191. a) Brown, H. C.; Knights, E. V.; Scouten, C. G. *J. Am. Chem. Soc.*, **1974**, *96*, 7765 – 7770. b) Brown, H. C.; Liotta, R.; Scouten, C. G. *J. Am. Chem. Soc.*, **1976**, *98*, 5297 – 5301. c) Brown, H. C.; Liotta, R.; Brener, L. *J. Am. Chem. Soc.*, **1977**, *99*, 3427 – 3432. d) Liotta, R.; Brown, H. C. *J. Org. Chem.*, **1977**, *42*, 2836 – 2839.
192. a) Mockus, N. V.; Petersen, J. L.; Rack, J. J. *Inorg. Chem.*, **2006**, *45*, 8 – 10. b) Rack, J. J. *Coord. Chem. Rev.*, **2009**, *253*, 78 – 85.
193. a) Teruaki, M.; Isayama, S.; Inoki, S.; Kato, K.; Yamada, T.; Takai, T. *Chem. Lett.*, **1989**, *18*, 449 – 452. b) Inoki, S.; Kato, K.; Takai, T.; Isayama, S.; Yamada, T.; Mukaiyama, T. *Chem. Lett.*, **1989**, *18*, 515 – 518. c) Isayama, S.; Mukaiyama, T. *Chem. Lett.*, **1989**, *18*, 1071 – 1074. d) Kato, K.; Yamada, T.; Takai, T.; Inoki, S.; Isayama, S. *Chem. Lett.*, **1990**, *63*, 179 – 186. e) Crossley, S. W. M.; Obradors, C.; Martinez, R. M.; Shenvi, R. A. *Chem. Rev.*, **2016**, *116*, 8912 – 9000.
194. a) Iwasawa, N.; Kato, T.; Narasaka, K. *Chem. Lett.*, **1988**, *17*, 1721 – 1724. b) Sakurai, H.; Iwasawa, N.; Narasaka, K. *Bull. Chem. Soc. Jpn.*, **1996**, *69*, 2585 – 2594.
195. Hövelmann, C. H.; Muñiz, K. *Chem. Eur. J.*, **2005**, *11*, 3951 – 3958.
196. Gypser, A.; Michel, D.; Nirschl, D. S.; Sharpless, K. B. *J. Org. Chem.*, **1998**, *63*, 7322 – 7327.
197. Chapman, C. J.; Frost, C. G.; Mahon, M. F. *Dalton Trans.*, **2006**, *2006*, 2251 – 2262.

198. a) Renz, M.; Meunier, B. *Eur. J. Org. Chem.*, **1999**, 1999, 737 – 750. b) ten Brink, G.-J.; Arends, I. W. C. E.; Sheldon, R. A. *Chem. Rev.*, **2004**, *104*, 4105 – 4124.
199. Baeyer, A.; Villiger, V. *Ber. Dtsch. Chem. Ges.*, **1899**, *32*, 3625 – 3633.
200. a) Yamabe, S.; Yamazaki, S. *J. Org. Chem.*, **2007**, *72*, 3031 – 3041. b) Xu, S.; Wang, Z.; Li, Y.; Zhang, X.; Wang, H.; Ding, K. *Chem. Eur. J.*, **2010**, *16*, 3021 – 3035. c) Kotlewska, A. J.; van Rantwijk, F.; Sheldon, R. A.; Arends, I. W. C. E. *Green Chem.*, **2011**, *13*, 2154 – 2160.
201. Hartung, J.; Schwarz, M. *Org. Synth.*, **2002**, *79*, 228.
202. a) Bhuniya, D.; Mohan, S.; Narayanan, S. *Synthesis*, **2003**, *0*, 1018 – 1024. b) Bertelsen, S.; Dinér, P.; Johansen, R. L.; Jørgensen, K. A. *J. Am. Chem. Soc.*, **2007**, *129*, 1536 – 1537. c) Zhang, F.-G.; Yang, Q.-Q.; Xuan, J.; Lu, H.-H.; Duan, S.-W.; Chen, J.-R.; Xiao, W.-J. *Org. Lett.*, **2010**, *12*, 5636 – 5639.
203. a) Blatt, A. H. *Chem. Rev.*, **1933**, *12*, 215 – 260. b) De Luca, L.; Giacomelli, G.; Porcheddu, A. *J. Org. Chem.*, **2002**, *67*, 6272 – 6274. c) Furuya, Y.; Ishihara, K.; Yamamoto, H. *J. Am. Chem. Soc.*, **2005**, *127*, 11240 – 11241. d) Taber, D. F.; Straney, P. J. *J. Chem. Educ.*, **2010**, *87*, 1392 – 1392.
204. Bolotin, D. S.; Burianova, V. K.; Novikov, A. S.; Demakova, M. Y.; Pretorius, C.; Mokolokolo, P. P.; Roodt, A.; Bokach, N. A.; Suslonov, V. V.; Zhdanov, A. P.; Zhizhin, K. Y.; Kuznetsov, N. T.; Kukushkin, V. Y. *Organometallics*, **2016**, *35*, 3612 – 3623.
205. a) Gololobov, Y. G.; Nesmeyanov, A. N.; Iysenko, V. P.; Boldeskul, I. E. *Tetrahedron*, **1987**, *43*, 2609 – 2651. b) Lebel, H.; Marcoux, J.-F.; Molinaro, C.; Charette, A. B. *Chem. Rev.*, **2003**, *103*, 977 – 1050. c) Fedoryński, M. *Chem. Rev.*, **2003**, *103*, 1099 – 1132.
206. Talele, T. T. *J. Med. Chem.*, **2016**, *59*, 8712 – 8756.
207. a) Doyle, M. P. *Chem. Rev.*, **1986**, *86*, 919 – 939. b) Davies, H. M. L.; Denton, J. R. *Chem. Soc. Rev.*, **2009**, *38*, 3061 – 3071.
208. a) Anciaux, A. J.; Demonceau, A.; Noels, A. F.; Warin, R.; Hubert, A. J.; Teyssié, P. *Tetrahedron*, **1983**, *39*, 2169 – 2173. b) Doyle, M. P.; Wang, L. C.; Loh, K.-L. *Tetrahedron Lett.*, **1984**, *25*, 4087 – 4090.

209. Doyle, M. P.; Davies, H.; Manning, J. R. *Encyclopedia of Reagents in Organic Synthesis*, **2006**,  
<https://onlinelibrary.wiley.com/doi/full/10.1002/047084289X.rd462.pub2>.
210. Nobushige, K.; Hirano, K.; Satoh, T.; Miura, M. *Tetrahedron*, **2015**, *71*, 6506 – 6512.
211. a) Nowlan, D. T.; Gregg, T. M.; Davies, H. M. L.; Singleton, D. A. *J. Am. Chem. Soc.*, **2003**, *125*, 15902 – 15911. b) Thornton, A.; Martin, V. I.; Blakey, S. B. *J. Am. Chem. Soc.*, **2009**, *131*, 2434 – 2435. c) Caballero, A.; Prieto, A.; Díaz-Requejo, M. M.; Pérez, P. J. *Eur. J. Inorg. Chem.*, **2009**, *73*, 1137 – 1144. d) Wang, H.; Guptill, D. M.; Varela-Alvarez, A.; Musaev, D. G.; Davies, H. M. L. *Chem. Sci.*, **2013**, *4*, 2844 – 2850.
212. a) Djerassi, C. *Chem. Rev.*, **1948**, *43*, 271 – 317. b) Kharasch, M. S.; Sosnovsky, G. *J. Am. Chem. Soc.*, **1958**, *80*, 756 – 756. c) Andrus, M. B.; Lashley, J. C. *Tetrahedron*, **2002**, *58*, 845 – 866. d) Bayeh, L.; Tambar, U. K. *ACS Catal.*, **2017**, *7*, 8533 – 8543. e) Corey, E. J.; Fleet, G. W. J. *J. Am. Chem. Soc.*, **1973**, *45*, 4499 – 4501. f) Salmond, W. G.; Barta, M. A.; Havens, J. L. *J. Org. Chem.*, **1978**, *43*, 2057 – 2059.
213. a) Durst, T.; Lancaster, M.; Smith, D. J. H. *J. Chem. Soc., Perkin Trans. 1*, **2008**, *0*, 1846 – 1848. b) Chou, T.-S.; Chang, C.-Y. *J. Org. Chem.*, **1991**, *56*, 4560– 4563. c) Nakayama, J.; Iguchi, K.; Fujihara, T. . *Phosphorus, Sulfur, and Silicon*, **2010**, *185*, 1131 – 1141.
214. Enev, V. S.; Felzmann, W.; Gromov, A.; Marchart, S.; Mulzer, J. *Chem. Eur. J.*, **2012**, *18*, 9651 – 9668.
215. a) Riley, H. L.; Morley, J. F.; Friend, N. A. C. *J. Chem. Soc.*, **1932**, *1932*, 1875 – 1883. b) Rapoport, H.; Bhalerao, U. T. *J. Am. Chem. Soc.*, **1971**, *93*, 4835 – 4840. c) Trachtenberg, E. N.; Nelson, C. H.; Carver, J. R. *J. Org. Chem.*, **1970**, *35*, 1653 – 1658. d) Warpehoski, M. A.; Chabaud, B.; Sharpless, K. B. *J. Org. Chem.*, **1982**, *47*, 2897 – 2900. e) Shafer, C. M.; Morse, D. I.; Molinski, T. F. *Tetrahedron*, **1996**, *52*, 14475 – 14486. f) Singleton, D. A.; Hang, C. *J. Org. Chem.*, **2000**, *65*, 7554 – 7560.

216. Umbreit, M. A.; Sharpless, K. B. *J. Am. Chem. Soc.*, **1977**, *99*, 5526 – 5528.
217. Pine, S. H.; Shen, G.; Bautista, J.; Sutton, Jr., C.; Yamada, W.; Apodaca, L. *J. Org. Chem.*, **1990**, *55*, 2234 – 2237. b) Streitwieser, A.; Wang, G. P.; Bors, D. A. *Tetrahedron*, **1997**, *53*, 10103 – 10112. c) Gais, H.-J.; van Gumpel, M.; Schleusner, M.; Raabe, G.; Runsink, J.; Vermeeren, C. *Eur. J. Org. Chem.*, **2001**, *2001*, 4275 – 4303. d) Scholz, R.; Hellmann, G.; Rohs, S.; Raabe, G.; Runsink, J.; Özdemir, D.; Luche, O.; Heß, T.; Giesen, A. W.; Atodiresei, J.; Lindner, H. J.; Gais, H.-J. *Eur. J. Org. Chem.*, **2010**, *2010*, 4559 – 4587.
218. a) Siegel, D. R.; Danishefsky, S. J. *J. Am. Chem. Soc.*, **2006**, *128*, 1048 – 1049. b) Rodeschini, V.; Simpkins, N. S.; Wilson, C. *J. Org. Chem.*, **2007**, *72*, 4265 – 4267. c) Mehta, G.; Dhanbal, T.; Bera, M. K. *Tetrahedron Lett.*, **2010**, *51*, 5302 – 5305. d) Richard, J.-A.; Pouwer, R. H.; Chen, D. Y.-K. *Angew. Chem. Int. Ed.*, **2012**, *51*, 4536 – 4561. e) Simpkins, N. S. *Chem. Commun.*, **2013**, *49*, 1042 – 1051.
219. a) Gryniewicz, G.; Gadzikowska, M. *Pharmacol. Rep.*, **2008**, *60*, 439 – 463. b) O'Hagan, D. *Nat. Prod. Rep.*, **2000**, *17*, 435 – 446.
220. a) Birch, A. J. *Notes Rec. R. Soc. Lond.*, **1993**, *47*. b) Medley, J. W.; Movassaghi, M. *Chem. Commun.*, **2013**, *49*, 10775 – 10777.
221. a) Keana, J. F. K.; Heo, G. S.; Gaughan, G. T. *J. Org. Chem.*, **1985**, *50*, 2346 – 2351. b) Baylis, A. M.; Davies, M. P. H.; Thomas, E. J. *Org. Biomol. Chem.*, **2007**, *5*, 3139 – 3155. c) Huang, S.-Y.; Chang, Z.; Tuo, S.-C.; Gao, L.-H.; Wang, A.-E.; Huang, P.-Q. *Chem. Commun.*, **2013**, *49*, 7088 – 7090. d) Shanahan, C. S.; Fang, C.; Paull, D. H.; Martin, S. F. *Tetrahedron*, **2013**, *69*, 7592 – 7607. e) Li, Y.; Jackson, K. E.; Charlton, A.; Neve-Foster, B. L.; Khurshid, A.; Rudy, H.-K. A.; Thompson, A. L.; Paton, R. S.; Hodgson, D. M. *J. Org. Chem.*, **2017**, *82*, 10479 – 10488.
222. Paquette, L. A.; Meisinger, R. H.; Gleiter, R. *J. Am. Chem. Soc.*, **1973**, *95*, 5414 – 5416.
223. Borbas, K. E.; Mroz, P.; Hamblin, M. R.; Lindsey, J. S. *Bioconjugate Chem.*, **2006**, *17*, 638 – 653.

224. Schaefer, M.; Hanik, N.; Kilbinger, A. F. M. *Macromolecules*, **2012**, *17*, 6807 – 6818.
225. Peter, C.; Geoffroy, P.; Miesch, M. *Org. Biomol. Chem.*, **2018**, *16*, 1381 – 1389.
226. a) Hérisson, J.-L.; Chauvin, Y. *Die Makromolekulare Chemie*, **1971**, *141*, 161 – 176. b) Schrock, R. R.; Meakin, P. *J. Am. Chem. Soc.*, **1974**, *96*, 5288 – 5290. c) Grubbs, R. H.; Burk, P. L.; Carr, D. D. *J. Am. Chem. Soc.*, **1975**, *97*, 3265 – 3267. d) Trnka, T. M.; Grubbs, R. H. *Acc. Chem. Res.*, **2001**, *34*, 18 – 29. e) La, D. S.; Sattely, E. S.; Ford, J. G.; Schrock, R. R.; Hoveyda, A. H. *J. Am. Chem. Soc.*, **2001**, *123*, 7767 – 7778. f) Chauvin, Y. *Angew. Chem. Int. Ed.*, **2006**, *45*, 3740 – 3747.
227. Szadkowska, A.; Żukowska, K.; Pazio, A. E.; Woźniak, K.; Kadyrov, R.; Grela, K. *Organometallics*, **2011**, *30*, 1130 – 1138.
228. a) Paquette, L. A.; Fabris, F.; Tae, J.; Gallucci, J. C.; Hofferberth, J. E. *J. Am. Chem. Soc.*, **2000**, *122*, 3391 – 3398. b) Szadkowska, A.; Zukowska, K.; Pazio, A. E.; Woźniak, K.; Kadyrov, R.; Grela, K. *Organometallics*, **2011**, *30*, 1130 – 1138.
229. a) Smidt, J.; Hafner, W.; Jira, R.; Sedlmeier, J.; Sieber, R.; Rüttinger, R.; Kojer, H. *Angew. Chem. Int. Ed.*, **1959**, *71*, 176 – 182. b) Smidt, J.; Hafner, W.; Jira, R.; Sieber, R.; Sedlmeier, J.; Sabel, A. *Angew. Chem. Int. Ed.*, **1962**, *1*, 80 – 88. c) Tsuji, J.; Shimizu, I.; Yamamoto, K. *Tetrahedron Lett.*, **1976**, *17*, 2975 – 2976. d) Tsuji, J. *Synthesis*, **1984**, *1984*, 369 – 384. e) Jira, R. *Angew. Chem. Int. Ed.*, **2009**, *48*, 9034 – 9037.
230. a) Larock, R. C.; Lee, N. H. *J. Am. Chem. Soc.*, **1991**, *113*, 7815 – 7816. b) Barth, R.; Mulzer, J. *Tetrahedron*, **2008**, *64*, 4718 – 4735. c) Smith, T. E.; Kuo, W.-H.; Bock, V. D.; Roizen, J. L.; Balskus, E. P.; Theberge, A. B. *Org. Lett.*, **2007**, *9*, 1153 – 1155. d) Lorenz, M.; Kabir, M. S.; Cook, J. M. *Tetrahedron Lett.*, **2010**, *51*, 1095 – 1098. a) Baiju, T. V.; Gravel, E.; Doris, E.; Namboothiri, I. N. N. *Tetrahedron Lett.*, **2016**, *57*, 3993 – 4000.
231. a) Swain, M. *J. Chem. Inf. Comput. Sci.*, **2012**, *52*, 613 – 615. b) Southan, C.; Stracz, A. *J. Cheminform.*, **2013**, *5*, 1 – 10.

232. a) Firth, N. C.; Brown, N.; Blagg, J. *J. Chem. Inf. Model.*, **2012**, *52*, 2516 – 2525. b) Meyers, J.; Carter, M.; Mok, N. Y.; Brown, N. *Future Med. Chem.*, **2016**, *8*, 1753 – 1767.
233. Sauer, W. H. B.; Schwarz, M. K. *J. Chem. Inf. Comput. Sci.*, **2003**, *43*, 987 – 1003.
234. a) Sakamoto, K. M.; Kim, K. B.; Kumagai, A.; Mercurio, F.; Crews, C. M.; Deshaies, R. J. *Proc. Natl. Acad. Sci.*, **2001**, *98*, 8554 – 8559. b) Cermakova, K.; Hodges, H. C. *Mol. Ther.*, **2018**, *23*, 1958. c) Gu, S.; Cui, D.; Chen, X.; Xiong, X.; Zhao, Y. *BioEssays*, **2018**, *40*, 1700247. d) An, S.; Fu, L. *EBioMedicine*, **2018**, *36*, 553 – 562. e) Zou, Y.; Ma, D.; Wang, Y. *Cell Biochem. Funct.*, **2019**, *37*, 21 – 30.
235. a) Tice, C. M. *Pest Manag. Sci.*, **2001**, *16*, 3 – 16. b) Tice, C. M. *Pest Manag. Sci.*, **2002**, *233*, 219 – 233. c) Gandy, M. N.; Corral, M. G.; Mylne, J. S.; Stubbs, K. A. *Org. Biomol. Chem.*, **2015**, *13*, 5586 – 5590.
236. a) Lindell, S. D.; Pattenden, L. C.; Shannon, J. *Bioorg. Med. Chem.*, **2009**, *17*, 4035 – 4046. b) Rao, H.; Huangfu, C.; Wang, Y.; Wang, X.; Tang, T.; Zeng, X. *Mol. Inf.*, **2015**, *34*, 331 – 338.
237. a) Wager, T. T.; Hou, X.; Verhoest, P. R.; Villalobos, A. *ACS Chem. Neurosci.*, **2010**, *1*, 435 – 449. b) Foley, D. J.; Nelson, A.; Marsden, S. P. *Angew. Chem. Int. Ed.*, **2016**, *55*, 13650 – 13657.
238. a) Colomer, I.; Empson, C. J.; Craven, P.; Owen, Z.; Doveston, R. G.; Churcher, I.; Marsden, P.; Nelson, A. *Chem. Commun.*, **2016**, *52*, 7175 – 7316. b) Lenci, E.; Trabocchi, A. *ChemBioChem*, **2019**, *20*, 1115 – 1123.
239. a) Baell, J. B.; Holloway, G. A. *J. Med. Chem.*, **2010**, *53*, 2719 – 2740. b) Dahlin, J. L.; Walters, M. A. *Future Med. Chem.*, **2014**, *6*, 1265 – 1290. c) Dahlin, J. L.; Nissink, J. W. M.; Strasser, J. M.; Francis, S.; Higgins, L.; Zhou, H.; Zhang, Z.; Walters, M. A. *J. Med. Chem.*, **2015**, *58*, 2091 – 2113. d) Baell, J. B. *J. Nat. Prod.*, **2016**, *79*, 616 – 628. e) Jasial, S.; Hu, Y.; Bajorath, J. *J. Med. Chem.*, **2017**, *60*, 3879 – 3886. f) Baell, J. B.; Nissink, J. W. M. *ACS Chem. Biol.*, **2018**, *13*, 36 – 44.

240. a) Blaskovich, M. A. T.; Zuegg, J.; Elliott, A. G.; Cooper, M. A. *ACS Infect. Dis.*, **2015**, *1*, 285 – 287. b) Cooper, M. A. *Nat. Publ. Gr.*, **2015**, *14* (9), 587 – 588. c) Desselle, M. R.; Hansford, K. A.; Zuegg, J.; Alysha, G.; Blaskovich, M. A. *T. Futur. Sci. OA*, **2017**, *3*, FSO171.
241. a) Rosenblatt-Farrell, N. *Environ. Health Perspect.*, **2009**, *117*, A244 – A250. b) Fleming, A. *Clin. Infect. Dis.*, **1980**, *2*, 129 – 139. c) Tan, S. Y.; Tatsumura, Y. *Singapore Med. J.*, **2015**, *56*, 366 – 367.
242. a) Davies, J.; Davies, D. *Microbiol. Mol. Biol. Rev.*, **2010**, *74*, 417 – 433. b) Macgowan, A.; Albur, M. *Clin. Med.*, **2013**, *13*, 263 – 268. c) Auer, J.; Rahman, K. M. *J. Drug Des. Res.*, **2015**, *2*, 1018. d) Zaman, S. Bin; Hussain, M. A.; Nye, R.; Mehta, V.; Taib, K. *Cureus*, **2017**, *9* (6), e1403. e) Naylor, N. R.; Atun, R.; Zhu, N.; Kulasabanathan, K.; Silva, S.; Chatterjee, A.; Knight, G. M.; Robotham, J. V. *Antimicrob. Resist. Infect. Control*, **2018**, *7*, 1 – 17. f) Hofer, U. *Nat. Rev. Microbiol.*, **2019**, *17*, 3.
243. a) Acar, J. F. *Clin. Infect. Dis.*, **1997**, *24*, S17 – S18. b) Michael, C. A.; Dominey-howes, D.; Labbate, M.; Maria, C.; Elisabeth, J. *Front. Public Heal.*, **2014**, *2*, 1 – 8. c) Friedman, N. D.; Temkin, E.; Carmeli, Y. *Clin. Microbiol. Infect.*, **2016**, *22* (5), 416 – 422.
244. a) Power, E. *Clin. Microbiol. Infect.*, **2006**, *12*, 25 – 34. b) Simpkin, V. L.; Renwick, M. J.; Kelly, R.; Mossialos, E. *J. Antibiot.(Tokyo)*, **2017**, *70*, 1087 – 1096. c) Renwick, M.; Mossialos, E.; Renwick, M.; Mossialos, E. *Expert Opin. Drug Discov.*, **2018**, *13* (10), 889 – 892. d) Moreno, S. G.; Epstein, D. *J. Mark. Access Heal. Policy*, **2019**, *7* (1).
245. a) Gulshan, K.; Moye-rowley, W. S. *Eukaryot. Cell*, **2007**, *6*, 1933 – 1942. b) Costa, C.; Dias, P. J.; Sá-correia, I.; Teixeira, M. C. *Front. Physiol.*, **2014**, *5*, 197. c) Xie, J. L.; Polvi, E. J.; Shekhar-guturja, T.; Cowen, L. E. *Future Microbiol.*, **2014**, *9*, 523 – 542. d) Arikan-akdagli, S.; Ghannoum, M.; Meis, J. F. *J. Fungi*, **2018**, *4*, 129.
246. a) Ghannoum, M. A.; Rice, L. B. *Clin. Microbiol. Rev.*, **1999**, *12*, 501 – 517. b) Cowen, L. E.; Sanglard, D.; Howard, S. J.; Rogers, P. D.; Perlin, D. S. *Cold Spring Harb. Perspect. Med.*, **2015**, *5*, a019752. c) Wiederhold, N. P. *Infect.*

- Drug Resist.*, **2017**, *10*, 249 – 259. e) Fisher, M. C.; Hawkins, N. J.; Sanglard, D.; Gurr, S. J. *Science*, **2018**, *360*, 739 – 742. d) Kanafani, Z. A.; Perfect, J. R. *Antimicrob. Resist.*, **2008**, *46*, 120 – 128.
247. Arras, S. D. M.; Ormerod, K. L.; Erpf, P. E.; Espinosa, M. I.; Carpenter, A. C.; Blundell, R. D.; Stowasser, S. R.; Schulz, B. L.; Tanurdzic, M.; Fraser, J. A. *Sci. Rep.*, **2017**, *7*, 17918.
248. a) Morrow, C. A.; Lee, I. R.; Chow, E. W. L.; Ormerod, K. L.; Goldinger, A.; Iii, J. B.; Nielsen, K. *MBio*, **2012**, *3*, e00310 – 11. b) Janbon, G.; Ormerod, K. L.; Paulet, D.; Iii, E. J. B.; Yadav, V.; Gaillardin, C.; Gerik, K. J.; Goldberg, J.; Gonzalez-Hilarion, S.; Gujja, S.; Hamlin, J. L.; Hsueh, Y.-P.; Ianiri, G.; Jones, S.; Kodira, C. D.; Kozubowski, L.; Lam, W.; Marra, M.; Mesner, L. D.; Mieczkowski, P. A.; Moyrand, F.; Nielsen, K.; Proux, C.; Rossignol, T.; Schein, J. E.; Sun, S.; Wollschlaeger, C.; Wood, I. A.; Zeng, Q.; Neuvéglise, C.; Newlon, C. S.; Perfect, J. R.; Lodge, J. K.; Idnurm, A.; Stajich, J. E.; Kronstad, J. W.; Sanyal, K.; Heitman, J.; Fraser, J. A.; Cuomo, C. A.; Dietrich, F. S. *PLoS Genet.*, **2014**, *10*, e1004261.
249. a) Pancholi, P.; Park, S.; Perlin, D.; Kubin, C.; Della-Latta, P. *J. Clin. Microbiol.*, **2004**, *42*, 5938 – 5939. b) Carvalhinho, S.; Margarida, A.; Sampaio, A. *Mycopathologia*, **2012**, *174*, 69 – 76. c) Sanitá, P. V.; Oliveira, G. De. *Oral Surg. Oral Med. Oral Pathol Oral Radiol.*, **2013**, *116* (5), 562 – 569. d) Song, Y. B.; Suh, M. K.; Ha, G. Y.; Kim, H. *Ann. Dermatol.*, **2015**, *27*, 715 – 720.
250. a) Sheehan, D. J.; Hitchcock, C. A.; Sibley, C. M. *Clin. Microbiol. Rev.*, **1999**, *12*, 40 – 79. b) Vermes, A.; Guchelaar, H.; Dankert, J. *Antimicrob. Chemother.*, **2000**, *46*, 171 – 179. c) Cappelletty, D.; Pharm, D.; Eiselstein-Mckitrick, K.; Pharm, D. *Pharmacotherapy*, **2007**, *27*, 369 – 388. d) Baginski, M.; Czub, J. *Curr. Drug Metabol.*, **2009**, *10*, 459 – 469. e) Ameen, M. *Clin. Dermatol.*, **2010**, *28*, 197 – 201. f) Scorzoni, L.; Paula, A. C. A. De; Marcos, C. M.; Assato, P. A.; Melo, W. C. M. A. De; Oliveira, H. C. De; Costa-orlandi, C. B.; Mendes-Giannini, M. J. S.; Fusco-Almeida, A. M. *Front. Microbiol.*, **2017**, *8*, 36.
251. a) Sirijan, S.; Nitaya, I. *Biomed Res. Int.*, **2006**, *2016*, 1 – 8. b) Boucher, H. W.; Talbot, G. H.; Bradley, J. S.; Edwards, J. E.; Gilbert, D.; Rice, L. B.; Scheld,

- M.; Spellberg, B.; Bartlett, J. *IDSA Rep. Dev. Pipeline*, **2009**, *48*, 1 – 12. c) Pendleton, J. N.; Gorman, S. P.; Gilmore, B. F.; Pendleton, J. N.; Gilmore, B. F. *Expert Rev. Anti. Infect. Ther.*, **2014**, *11*, 297 – 308. d) Xu, S.; Wang, Q.; Zhang, Q.; Zhang, L.; Zuo, L.; Jiang, J. D.; Hu, H. Y. *Chem. Commun.*, **2017**, *53*, 11177 – 11180. e) Smith, P. A.; Koehler, M. F. T.; Girgis, H. S.; Yan, D.; Chen, Y.; Chen, Y.; Crawford, J. J.; Durk, M. R.; Higuchi, R. I.; Kang, J.; Murray, J.; Paraselli, P.; Park, S.; Phung, W.; Quinn, J. G.; Roberts, T. C.; Rougé, L.; Schwarz, J. B.; Skippington, E.; Wai, J.; Xu, M.; Yu, Z.; Zhang, H.; Tan, M.-W.; Heise, C. E. *Nature*, **2018**, *561*, 189 – 194.
252. a) Austrian, R. *Bacteriol. Rev.*, **1960**, *24*, 261 – 265. b) Menichetti, F. *Clin. Microbiol. Infect.*, **2005**, *11*, 22 – 28. c) Galperin, M. Y. *Microbiol. Spectr.*, **2013**, *1*, TBS-0015-2012. d) Amran, F.; Aziz, M. N.; Ibrahim, H. M.; Atiqah, N. H.; Parameswari, S.; Hafiza, M. R.; Ifwat, M. *J. Med. Microbiol.*, **2011**, *60*, 1312 – 1316.
253. a) Felten, A.; Grandry, B.; Lagrange, P. H.; Casin, I. *J. Clin. Microbiol.*, **2002**, *40*, 2766 – 2771. b) Lowy, F. D.; Lowy, F. D. *J. Clin. Invest.*, **2003**, *111*, 1265 – 1273. c) Ah, U. Von; Wirz, D.; Daniels, A. U. *J. Clin. Microbiol.*, **2008**, *46*, 2083 – 2087. d) Stenholm, T.; Hakanen, A. J.; Vaarno, J.; Pihlasalo, S.; Terho, P.; Vuopio-varkila, J.; Huovinen, P.; Kotilainen, P. *Antimicrob. Agents Chemother.*, **2009**, *53*, 5088 – 5094. e) Pyzik, E.; Marek, A.; Hauschild, T. *Bull. Vet. Inst. Pulawy.*, **2014**, *58*, 57 – 63.
254. Ubukata, K.; Nonoguchi, R.; Matsushashi, M.; Konno, M. *J. Bacteriol.*, **1989**, *171*, 2882 – 2885.
255. a) Chambers, H. F. *J. Infect. Dis.*, **1999**, *179*, 353 – 359. b) Wielders, C. L. C.; Fluit, A. C.; Brisse, S.; Verhoef, J.; Schmitz, F. J. *J. Clin. Microbiol.*, **2002**, *40*, 3970 – 3975. c) Chen, F.; Wang, C.; Chen, C.; Hsu, Y.; Wang, K. *Antimicrob. Agents Chemother.*, **2014**, *58*, 1047 – 1054.
256. a) Hardy, K. J.; Hawkey, P. M.; Gao, F.; Oppenheim, B. A. *Br. J. Anaesth.*, **2004**, *92*, 121 – 130. b) Wyllie, D. H.; Crook, D. W.; Peto, T. E. A. *BMJ*, **2006**, *333*, 281. c) Blot, S. I.; Vandewoude, K. H.; Hoste, E. A.; Colardyn, F. A. *Arch. Intern. Med.*, **2019**, *162*, 2229 – 2235.

257. a) Lee, S. Y. *Trends Biotechnol.*, **1996**, *14*, 98 – 105. b) Russo, E. *Nature*, **2003**, *421*, 456 – 457. c) Tenailleon, O.; Skurnik, D.; Picard, B.; Denamur, E. *Nat. Rev. Microbiol.*, **2010**, *8*, 207 – 217. d) Youn, J.; Yoon, J. W.; Hovde, C. J. *J. Microbiol. Biotechnol.*, **2010**, *20*, 1 – 10. e) Croxen, M. A.; Law, R. J.; Scholz, R.; Keeney, K. M.; Wlodarska, M.; Finlay, B. B. *Clin. Microbiol. Rev.*, **2013**, *26*, 822 – 880.
258. a) Lobry, J. R.; Carret, G.; Flandrois, J. P. *J. Antimicrob. Chemother.*, **1992**, *29*, 121 – 127. b) Qi, J.; Du, Y.; Bai, H.; Zhu, X.; Hu, M.; Luo, Y.; Liu, Y. *Microb. Drug Resist.*, **2013**, *19*, 6 – 14. c) Minogue, T. D.; Daligault, H. A.; Davenport, K. W.; Bishop-Lilly, K. A.; Broomall, S. M.; Bruce, D. C.; Chain, P. S.; Chertkov, O.; Coyne, S. R.; Freitas, T.; Frey, K. G.; Gibbons, H. S.; Jaissle, J.; Redden, C. L.; Rosenzweig, C. N.; Xu, Y.; Johnson, S. L. *Genome Announc.*, **2014**, *2*, e00969 – 14.
259. Elliott, A. G.; Ganesamoorthy, D.; Coin, L.; Cooper, M. A. *Genome Announc.*, **2016**, *4*, 3 – 4.
260. Rasheed, J. K.; Anderson, G. J.; Yigit, H.; Queenan, A. M.; Swenson, J. M.; Biddle, J. W.; Ferraro, M. J.; Jacoby, G. A.; Tenover, F. C. *Antimicrob. Agents Chemother.*, **2000**, *44*, 2382 – 2388.
261. a) (1) Marti, L.; Alberti, N. *J. Bacteriol.*, **1999**, *181*, 2726–2732. b) Dome, A.; Conejo, C.; Pascual, A.; Toma, J. M. *Antimicrob. Agents Chemother.*, **2003**, *47*, 3332 – 3335.
262. Formosa, C.; Herold, M.; Vidailac, C.; Duval, R. E.; Dague, E. *J. Antimicrob. Chemother.*, **2015**, *70*, 2261 – 2270.
263. Paterson, D. L.; Bonomo, R. A. *Clin. Microbiol. Rev.*, **2005**, *18*, 657 – 686.
264. a) Fernando, D.; Zhanel, G.; Kumar, A. *Can. J. Infect. Dis. Med. Microbiol.*, **2013**, *24*, 17 – 22. b) Hamidian, M.; Hall, R. M. *Antimicrob. Agents Chemother.*, **2017**, *61*, e01991 – 16. c) Moon, K. H.; Weber, B. S.; Feldman, F. *Antimicrob. Agents Chemother.*, **2017**, *61*, e00778 – 17.
265. a) Valentine, S. C.; Contreras, D.; Tan, S.; Real, L. J.; Chu, S.; Xu, H. H.; Al, V. E. T. *J. Clin. Microbiol.*, **2008**, *46*, 2499 – 2507. b) Chusri, S.; Villanueva, I.; Voravuthikunchai, S. P.; Davies, J. *J. Antimicrob. Chemother.*, **2009**, *64*, 1203 –

1211. c) Nie, L.; Lv, Y.; Yuan, M.; Hu, X.; Nie, T. *Acta Pharm. Sin. B*, **2014**, *4*, 295 – 300.
266. a) Kuo, H.; Chang, K.; Kuo, J.; Yueh, H.; Liou, M. *Int. J. Antimicrob. Agents*, **2012**, *39*, 33 – 38. b) Swe-han, K. S.; Pillay, M.; Schnugh, D.; Koleka, P.; Baba, K.; Pillay, M. *South. African J. Infect. Dis.*, **2017**, *32*, 119 – 126. c) Lenhard, J. R.; Bulitta, B.; Connell, T. D.; King-lyons, N.; Landersdorfer, C. B.; Cheah, S.; Thamlikitkul, V.; Shin, B. S.; Rao, G.; Holden, P. N.; Walsh, T. J.; Forrest, A.; Nation, R. L.; Li, J.; Tsuji, B. T. *J. Antimicrob. Chemother.*, **2017**, *72*, 153 – 165.
267. a) Richter, M. F.; Hergenrother, P. J. *Chem*, **2017**, *3*, 10 – 13. b) Richter, M. F.; Drown, B. S.; Riley, A. P.; Garcia, A.; Shirai, T.; Svec, R. L.; Hergenrother, P. J. *Nature*, **2017**, *545*, 299. c) Drown, B. S.; Hergenrother, P. J. *Proc. Natl. Acad. Sci.*, **2018**, *115*, 6530 – 6532. d) Richter, M. F.; Hergenrother, P. J. *Ann. N. Y. Acad. Sci.*, **2019**, *1435*, 18 – 38.
268. Carroll, G. P.; Srivastava, S.; Volini, A. S.; Piñeiro-Núñez, M. M.; Vetman, T. *Drug Discov. Today*, **2017**, *22*, 776 – 785.
269. a) Fu, L. M.; Fu-Liu, C. S. *Tuberculosis*, **2002**, *82*, 85 – 90. b) de Souza Luna, L. K.; Panning, M.; Grywna, K.; Pfefferle, S.; Drosten, C. *J. Infect. Dis.*, **2007**, *195*, 675 – 679. c) Cudahy, P.; Shenovi, S. V. *Postgrad. Med. J.*, **2016**, *92*, 187 – 193.
270. a) Gillespie, S. H. *Antimicrob. Agent Chemother.*, **2002**, *46*, 267 – 274. b) Keshavjee, S.; Farmer, P. E. *New. Engl. J. Med.*, **2012**, *367*, 931 – 936. c) Fonesca, J. D.; Knight, G. M.; McHugh, T. D. *Int. J. Infect. Dis.*, **2015**, *32*, 94 – 100. d) Nguyen, L. *Arch. Toxicol.*, **2016**, *90*, 1585 – 1604. e) Gygli, S. M.; Borrell, S.; Trauner, A.; Gagneux, S. *FEMS Microb. Rev.*, **2017**, *41*, 354 – 373.
271. a) Louw, G. E.; Warren, R. M.; Gey van Pittius, N. C.; McEvoy, C. R. E.; Van Helden, P. D.; Victor, T. C. *Antimicrob. Agent Chemother.*, **2009**, *53*, 3181 – 3189. b) Baptista, R.; Bhowmick, S.; Nash, R. J.; Baillie, L.; Mur, A. J. L. *Future Med. Chem.*, **2018**, *10*, 811 – 822.
272. Alvim-gaston, M.; Grese, T.; Mahoui, A.; Palkowitz, A. D.; Pineiro-nunez, M.; Watson, I. *Curr. Top. Med. Chem.*, **2014**, *14*, 294 – 303.

273. a) Ramsden, D. B.; Waring, R. H.; Barlow, D. J.; Parsons, R. B. *Int. J. Tryptophan Res.*, **2017**, *10*, 1 – 19. b) Lu, X. M.; Long, H. *Neoplasma*, **2018**, *65*, 656 – 663.
274. Blazejczyk, A.; Switalska, M.; Chlopicki, S.; Marcinek, A.; Gebicki, J.; Nowak, M.; Nasulewicz-Goldeman, A.; Wietrzyk, J. *J. Exp. Clin. Cancer Res.*, **2016**, *35*, 110.
275. a) Sauter, M.; Moffatt, B.; Saechao, M. C.; Wirtz, M. *Biochem. J.*, **2013**, *154*, 145 – 154. b) Miller, D. V.; Rauch, B. J.; Harich, K.; Xu, H.; Perona, J. J.; White, R. H. *Microbiology*, **2019**, *164*, 969 – 981.
276. Pissios, P. *Trends Endocrinol. Metab.*, **2017**, *28* (5), 340 – 353.
277. a) Aksoy, S.; Szumlanski, C. L.; Weinshilbourns, R. M. *J. Biol. Chem.*, **1994**, *269*, 14835 – 14840. b) Aksoy, S.; Brandriff, B. F.; Ward, A.; Little, P. F. R.; Weinshilbourn, R. M. *Genomics*, **1995**, *561*, 555 – 561.
278. a) Kassem, Heba, S.; Sangar, V.; Cowan, R.; Clarke, N.; Margison, G. P. *Int. J. Cancer*, **2002**, *460*, 454 – 460. b) Roe, M.; Rollinger, W.; Palme, S.; Hagmann, M.; Berndt, P.; Engel, A. M.; Schneidinger, B.; Pfeffer, M.; Andres, H.; Karl, J.; Bodenmüller, H.; Rüschoff, J.; Henkel, T.; Rohr, G.; Rossol, S.; Rösch, W.; Langen, H.; Zolg, W.; Tacke, M. *Clin. Cancer Res.*, **2005**, *11*, 6550 – 6558. c) Xu, J.; Capezzone, M.; Xu, X.; Hershman, J. M. *Mol. Endocrinol.*, **2005**, *19*, 527 – 539. d) Li, Z. S.; Kannt, A.; Pfenninger, A.; Tönjes, A.; Blüher, M. *Diabetologia*, **2015**, *58*, 2193 – 2194.
279. a) Mateuszuk, Ł.; Khomich, T. I.; Słomińska, E.; Gajda, M.; Wójcik, L.; Łomnicka, M.; Gwóźdź, P.; Chłopicki, S. *Pharmacol. Reports*, **2009**, *61*, 76 – 85. b) Neelakantan, H.; Brightwell, C. R.; Graber, T. G.; Maroto, R.; Wang, H.-Y. L.; Mchardy, S. F.; Papaconstantinou, J.; Fry, C. S.; Watowich, S. J. *Biochem. Pharmacol.*, **2019**, *163*, 481 – 492.
280. Williams, A. C.; Cartwright, L. S.; Ramsden, D. B. *Q. J. Med.*, **2005**, *98*, 215 – 226.
281. Van Haren, M. J.; Sastre, J.; Sartini, D.; Emanuelli, M.; Parsons, R. B.; Martin, N. I. *Biochemistry*, **2016**, *55*, 5307 – 5315.

282. a) Neelakantan, H.; Vance, V.; Wang, H. L.; Mchardy, S. F.; Watowich, S. *J. Biochemistry*, **2017**, *56*, 824 – 832. b) Akhtar, M. K.; Vijay, D.; Umbreen, S.; Mclean, C. J.; Cai, Y. *Front. Bioeng. Biotechnol.*, **2018**, *6*, 146. c) Chen, C.; Bönisch, D.; Penzis, R.; Winckler, T.; Scriba, G. K. E. *Chromatographia*, **2018**, *81*, 1439 – 1444. d) Sen, S.; Mondal, S.; Zheng, L.; Salinger, A. J.; Fast, W. *ACS Chem. Biol.*, **2019**, *14*, 613 – 618.
283. Neelakantan, H.; Wang, H. Y.; Vance, V.; Hommel, J. D.; McHardy, S. F.; Watowich, S. J. *J. Med. Chem.*, **2017**, *60*, 5015 – 5028.
284. Kannt, A.; Rajagopal, S.; Kadnur, S. V.; Suresh, J.; Kanth Bhamidipati, R.; Swaminathan, S.; Siddappa Hallur, M.; Kristam, R.; Elvert, R.; Czech, J.; Pfenninger, A.; Rudolph, C.; Schreuder, H.; Chandrasekar, D. V.; Mane, V. S.; Birudukota, S.; Shaik, S.; Zope, B. R.; BUrri, R. R.; Anad, N. N.; Thakur, M. K.; Singh, M.; Parveen, R.; Kandan, S.; Mullangi, R.; Yura, T.; Gosu, R.; Ruf, S.; Dhakshinamoorthy, S. *Sci. Rep.*, **2018**, *8*, 3660.
285. Van Haren, M. J.; Taig, R.; Kuppens, J.; Toraño, J. S.; Moret, E. E.; Parsons, R. B.; Sartini, D.; Emanuelli, M.; Martin, N. I. *Org. Biomol. Chem.*, **2017**, *15*, 6656 – 6667.
286. Peng, Y.; Sartini, D.; Pozzi, V.; Wilk, D.; Emanuelli, M.; Yee, V. C. *Biochemistry*, **2011**, *50*, 7800 – 7808.
287. a) Horning, B. D.; Suciu, R. M.; Ghadiri, D. A.; Ulanovskaya, O. A.; Matthews, M. L.; Lum, K. M.; Backus, K. M.; Brown, S. J.; Rosen, H.; Cravatt, B. F. *J. Am. Chem. Soc.*, **2016**, *138*, 13335 – 13343. b) Lee, H.-Y.; Suciu, R. M.; Horning, B. D.; Vinogradova, E. V.; Ulanovskaya, O. A.; Cravatt, B. F. *Bioorg. Med. Chem. Lett.*, **2018**, *28*, 2682 – 2687.
288. Policarpo, R. L.; Decultot, L.; May, E.; Kuzmi, P.; Carlson, S.; Huang, D.; Wright, B.; Dhakshinamoorthy, S.; Kannt, A.; Rani, S.; Dittakavi, S.; Panarese, J.; Gaudet, R.; Shair, M. D. *ChemRxiv*, **2019**, Preprint.
289. Nilsson, N.; Felding, J. *Future Med. Chem.*, **2015**, *7*, 1853 – 1859.
290. a) Bornholdt, J.; Felding, J.; Kristensen, J. L. *J. Org. Chem.*, 2010, *75*, 7454 – 7457. b) Michaudel, Q.; Ishihara, Y.; Baran, P. S. *Acc. Chem. Res.*, **2015**, *48*, 712 – 721. c) Jin, Y.; Yeh, C.-H.; Kuttruff, C. A.; Jørgensen, L.; Dünstl, G.;

- Felding, J.; Natarajan, S. R.; Baran, P. S. *Angew. Chem. Int. Ed.*, **2015**, *54*, 14044 – 14048. d) Kawamura, S.; Chu, H.; Felding, J.; Baran, P. S. *Nature*, **2016**, *532*, 90 – 93. e) Egbewande, F. A.; Nilsson, N.; White, J. M.; Coster, M. J.; Davis, R. A. *Bioorg. Med. Chem. Lett.*, **2017**, *27*, 3185 – 3189. f) Parker, C. G.; Kuttruff, C. A.; Galmozzi, A.; Jørgensen, L.; Yeh, C.-H.; Hermanson, D. J.; Wang, Y.; Artola, M.; McKerrall, S. J.; Josyln, C. M.; Nørremark, B.; Dünstl, G.; Felding, J.; Saez, E.; Baran, P. S.; Cravatt, B. F. *ACS Cent. Sci.*, **2017**, *3*, 1276 – 1285. g) Chu, H.; Smith, J. M.; Felding, J.; Baran, P. S. *ACS Cent. Sci.*, **2017**, *3*, 47 – 51. h) Merchant, R. R.; Oberg, K. M.; Lin, Y.; Novak, A. J. E.; Felding, J.; Baran, P. S. *J. Am. Chem. Soc.*, **2018**, *140*, 7462 – 7465.
291. LEO Pharma: Open Innovation – Assays you can access. LEO Pharma Open Innovation. <http://openinnovation.leo-pharma.com/Science-and-diseases/Assays-you-can-access.aspx> (Accessed August 15<sup>th</sup>, 2019)
292. a) Hoey, M. D.; Dittmer, D. C. *J. Org. Chem.*, **1991**, *56*, 1947 – 1948. b) Malwal, S. R.; Chakrapani, H. *Org. Biomol. Chem.*, **2015**, *13*, 2399 – 2406.
293. a) Villarino, A. V.; Kanno, Y.; Ferdinand, J. R.; O’Shea, J. J. *J. Immunol.*, **2015**, *194*, 21 – 27. b) Au-Yeung, N.; Mandhana, R.; Horvath, C. M. *JAK-STAT*, **2014**, *2*, e23931.
294. Thomas, S. J.; Snowden, J. A.; Zeidler, M. P.; Danson, S. J. *Br. J. Cancer*, **2015**, *113*, 365 – 371. b) Messina, J. L.; Yu, H.; Riker, A. I.; Munster, P. N.; Jove, R. L.; Daud, A. I. *Cancer Control*, **2008**, *15*, 196 – 201. c) Groner, B.; von Manstein, V. *Mol. Cell. Endocrinol.*, **2017**, *451*, 1 – 14.
295. Pesu, M.; Candotti, F.; Husa, M.; Hofmann, S. R.; Notarangelo, L. D.; O’Shea, J. J. *Immunol. Rev.*, **2005**, *203*, 127 – 142.
296. Aaronson, D. S.; Horvath, C. M. *Science*, **2002**, *296*, 1653 – 1655.
297. Welsch, K.; Holstein, J.; Laurence, A.; Ghoreschi, K. *Eur. J. Immunol.*, **2017**, *47*, 1096 – 1107.
298. Ghoreschi, K.; Laurence, A.; Yang, X.-P.; Hirahara, K.; O’Shea, J. J. *Trends Immunol.*, **2011**, *32*, 395 – 401.
299. a) Takeda, K.; Tanaka, T.; Shi, W.; Matsumoto, M.; Minami, M.; Kashiwamura, S.; Nakanishi, K.; Yoshida, N.; Nishimoto, T.; Akira, S. *Nature*,

- 1996**, 380, 627 – 630. b) Kaplan, M. H.; Schindler, U.; Smiley, S. T.; Grusby, M. J. *Immunity*, **1996**, 4, 313 – 319.
300. a) Chen, Z.; Lund, R.; Aittokallio, T.; Kosonen, M.; Nevalainen, O.; Lahesmaa, R. *J. Immunol.*, **2003**, 171, 3627 – 3635. b) Khaled, W. T.; Read, E. K. C.; Nicholson, S. E.; Baxter, F. O.; Brennan, A. J.; Came, P. J.; Sprigg, N.; McKenzie, A. N. J.; Watson, C. J. *Development*, **2007**, 134, 2739 – 2750. c) Ricardo-Gonzalez, R. R.; Eagle, A. R.; Odegaard, J. I.; Jouihan, H.; Morel, C. R.; Heredia, J. E.; Mukundan, L.; Wu, D.; Locksley, R. M.; Chawla, A. *Proc. Nat. Acad. Sci.*, **2010**, 107, 22617 – 22622.
301. a) Guo, D.; Dunbar, J. D.; Yang, C. H.; Pfeffer, L. M.; Donner, D. B. J. *Immunology*, **1998**, 160, 2742 – 2750. b) Miscia, S.; Marchisio, M.; Grilli, A.; Di Valerio, V.; Centurione, L.; Sabatino, G.; Garaci, F.; Zauli, G.; Bonvini, E.; Di Baldassarre, A. *Cell Growth Differ.*, **2002**, 13, 13 – 18. c) Horvath, C. M. *Sci STKE*, **2004**, 260, tr8. d) Gough, D. J.; Levy, D. E.; Johnstone, R. W.; Clarke, C. J. *Cytokine Growth Factor Rev.*, **2008**, 19, 383 – 394. e) O'Connell, D.; Bouazza, B.; Kokalari, B.; Amrani, Y.; Khatib, A.; Ganther, J. D.; Tliba, O. *Am. J. Physiol. Lung Cell Mol. Physiol.*, **2015**, 309, L348 – L359.
302. a) Quelle, F. W.; Shimoda, K.; Thierfelder, W.; Fischer, C.; Kim, A.; Ruben, S. M.; Cleveland, J. L.; Pierce, J. H.; Keegan, A. D.; Nelms, K. *Mol. Cell. Biol.*, **1995**, 15, 3336 – 3343. b) Murata, T.; Noguchi, P. D.; Puri, R. K. J. *Immunology*, **1996**, 156, 2972 – 2978. c) Rolling, C.; Treton, D.; Pellegrini, S.; Galanaud, P.; Richard, Y. *FEBS Lett.*, **1996**, 393, 53 – 56. d) Lischke, A.; Moriggl, R.; Brändlein, S.; Berchtold, S.; Kammer, W.; Sebald, W.; Groner, B.; Liu, X.; Hennighausen, L.; Friedrich, K. *J. Biol. Chem.*, **1998**, 273, 31222 – 31229. e) Chang, T. L.; Peng, X.; Fu, X. Y. *J. Biol. Chem.*, **2000**, 275, 10212 – 10217. f) Parham, C.; Chirica, M.; Timans, J.; Vaisberg, E.; Travis, M.; Cheung, J.; Pflanz, S.; Zhang, R.; Singh, K. P.; Vega, F.; To, W.; Wagner, J.; O'Farrell, A. M.; McClanahan, T.; Zurawski, S.; Hannum, C.; Gorman, D.; Rennick, D. M.; Kastelein, R. A.; de Waal Malefyt, R.; Moore, K. W. J. *Immunology*, **2002**, 168, 5699 – 5708. g) Wang, I. M.; Lin, H.; Goldman, S. J.; Kobayasi, M. *Mol.*

- Immunol.*, **2004**, *41*, 873 – 884. h) Lin, L.; Benson, Jr, D. M.; DeAngelis, S.; Bakan, C. E.; Li, P. K.; Li, C.; Lin, J. *Int. J. Cancer*, **2012**, *130*, 1459 – 1469.
303. Bell, E. *Nat. Rev. Immunol.*, **2007**, *7*, 581.
304. a) Gharavi, N. M.; Alva, J. M.; Mouillesseaux, K. P.; Lai, C.; Yeh, M.; Yeung, W.; Johnson, J. Szeto, W. L.; Hong, L.; Fishbein, M.; Wei, L.; Pfeffer, L. M.; Berliner, J. A. *J. Biol. Chem.*, **2007**, *282*, 31460 – 31468. b) Britschgi, A.; Andraos, R.; Brinkhaus, H.; Klebba, I.; Romanet, V.; Muller, U.; Murakami, M.; Radimerski, T.; Bentires-Alj, M. *Cancer Cell.*, **2012**, *22*, 796 – 811. c) Singh, J. K.; Simões, B. M.; Howell, S. J.; Farnie, G.; Clarke, R. B. *Breast Cancer Res.*, **2013**, *15*, 210.
305. a) Carr, M. W.; Roth, S. J.; Luther, E.; Rose, S. S.; Springer, T. A. *Proc. Nat. Acad. Sci.*, **1994**, *91*, 3652 – 3656. b) Xu, L. L.; Warren, M. K.; Rose, W. L.; Gong, W.; Wang, J. M. *J. Leukoc. Biol.*, **1996**, *60*, 365 – 371.
306. Xia, M.; Sui, Z. *Expert Opin. Ther. Pat.*, **2009**, *19*, 295 – 303.
307. a) Foresti, M. L.; Arisi, G. M.; Katki, K.; Montañez, A.; Sanchez, R. M.; Shapiro, L. A. *J. Neuroinflammation*, **2009**, *6*, 40. b) Fabene, P. F.; Bramanti, P.; Constanin, G. *J. Neuroimmunol.*, **2010**, *224*, 22 – 27.
308. Kim, J. S.; Gautam, S. C.; Chopp, M.; Zagola, C.; Jones, M. L.; Ward, P. A.; Welch, K. M. *J. Neuroimmunol.*, **1995**, *56*, 127 – 134.
309. a) Gerald, C.; Rollins, B. J. *Nat. Immunol.*, **2001**, *2*, 108 – 115. b) Hickman, S. E.; El Khoury, J. *CNS Neurol. Disord. Drug Target*, **2010**, *9*, 168 – 173.
310. Ransohoff, R. M.; Hamilton, T. A.; Tani, M.; Stoler, M. H.; Shick, H. E.; Major, J. A.; Estes, M. L.; Thomas, D. M.; Tuohy, V. K. *FASEB J.*, **1993**, *7*, 592 – 600.
311. Semple, B. D.; Bye, N.; Rancan, M.; Ziebell, J. M.; Morganti-Kossmann, M. C. *J. Cereb. Blood Flow Metab.*, **2010**, *30*, 769 – 782.
312. a) Liu, Z. H.; Chen, L. L.; Deng, X. L.; Song, H. J.; Liao, Y. F.; Zeng, T. S.; Zheng, J.; Li, H. Q. *J. Endocrinol. Invest.*, **2012**, *35*, 585 – 589. b) Cai, K.; Qi, D.; Hou, X.; Wang, O.; Chen, J.; Deng, B.; Qian, L.; Liu, X.; Le, Y. *PLoS ONE*, **2011**, *6*, e19559.

313. a) Lagdive, S. S.; Marawar, P. P.; Byakod, G.; Lagdive, S. B. *Indian J. Dent. Res.*, **2013**, *24*, 188 – 192. b) Finoti, L. S.; Nepomuceno, R.; Pigossi, S. C.; Corbi, S. C.; Secolin, R.; Scarel-Carminaga, R. M. *Medicine (Baltimore)*, **2017**, *96*, e6932.
314. Sharabiani, M. T.; Vermeulen, R.; Scocciati, C.; Hosnijeh, F. S.; Minelli, L.; Sacerdote, C.; Palli, D.; Krogh, V.; Tumino, R.; Chiodini, P.; Panico, S.; Vineis, P. *Biomarkers*, **2011**, *16*, 243 – 251.
315. a) Brew, R.; Erikson, J. S.; West, D. C.; Kinsella, A. R.; Slavin, J.; Christmas, S. E. *Cytokine*, **2000**, *12*, 78 – 85. b) Itoh, Y.; Joh, T.; Tanida, S.; Sasaki, M.; Kataoka, H.; Itoh, K.; Oshima, T.; Ogasawara, N.; Togawa, S.; Wada, T.; Kubota, H.; Mori, Y.; Ohara, H.; Nomura, T.; Higashiyama, S.; Itoh, M. *Cytokine*, **2005**, *29*, 275 – 282.
316. Reeves, E. P.; Williamson, M.; O'Neill, S. J.; Grealley, P.; McElvaney, N. G. *Am. J. Respir. Crit. Care Med.*, **2011**, *183*, 1571 – 1523.
317. a) Brown, A. S.; Hooton, J.; Schaefer, C. A.; Zhang, H.; Petkova, E.; Babulas, V.; Perrin, M.; Gorman, J. M.; Susser, E. S. *Am. J. Psychiatry*, **2004**, *161*, 889 – 895. b) Zhang, X. Y.; Zhou, D. F.; Cao, L. Y.; Zhang, P. Y.; Wu, G. Y.; Shen, Y. C. *J. Clin. Psychiatry*, **2004**, *65*, 940 – 947.
318. Kawaguchi, M.; Kokubu, F.; Fujita, J.; Huang, S. K.; Hizawa, N. *Inflamm. Allergy Drug Targets*, **2009**, *8*, 383 – 389.
319. a) Ugi, I.; Werner, B.; Dömling, A. *Molecules*, **2003**, *8*, 53 – 66. b) Dömling, A. *Chem. Rev.*, **2006**, *106*, 17 – 89. c) Akrtopoulou-Zanze, I. *Curr. Opin. Chem. Biol.*, **2008**, *12*, 324 – 331. d) Koopmanschap, G.; Ruijter, E.; Orru, R. V. A. *Beilstein J. Org. Chem.*, **2014**, *10*, 544 – 598. e) Sadjadi, S.; Heravi, M. M.; Nazari, N. *RSC Adv.*, **2016**, *6*, 53203 – 53272.
320. a) Hardy, G. W.; Doyle, P. M.; Smith, T. W. *Eur. J. Med. Chem.*, **1987**, *22*, 331 – 335. b) Kazmaier, U.; Ackermann, S. *Org. Biomol. Chem.*, **2005**, *3*, 3184 – 3187. c) Kysil, V.; Tkachenko, S.; Khvat, A.; Williams, C.; Tsirolnikov, S.; Churakova, M.; Ivachtchenko, A. *Tetrahedron Lett.*, **2007**, *48*, 6239 – 6244. d) Simila, S. T. M.; Martin, S. F. *Tetrahedron Lett.*, **2008**, *49*, 4501 – 4504. e)

- Malaquin, S.; Jida, M.; Gesquiere, J. C.; Deprez-Poulain, R.; Deprez, B.; Laconde, G. *Tetrahedron Lett.*, **2010**, *51*, 2983 – 2985.
321. a) Yang, D.; Ng, F. F.; Li, Z. J.; Wu, Y. D.; Chan, K. W. K.; Wang, D. P. *J. Am. Chem. Soc.*, **1996**, *118*, 9794 – 9795. b) Kinzel, O.; Fattori, D.; Ingallinella, P.; Bianchi, E.; Pessi, A. *J. Pept. Sci.*, **2003**, *9*, 375 – 385. c) Vanderesse, R.; Thevenet, L.; Marraud, M.; Boggetto, N.; Reboud, M.; Corbier, C. *J. Pept. Sci.* **2003**, *9*, 282 – 299. d) Kurono, M.; Shimomura, A.; Isobe, M. *Tetrahedron*, **2004**, *60*, 1773 – 1780. e) Bertin, D.; Gigmes, D.; Marque, S. R. A.; Tordo, P. *Tetrahedron*, **2005**, *61*, 8752 – 8761. f) Paulick, M. G.; Hart, K. M.; Brinner, K. M.; Tjandra, M.; Charych, D. H.; Zuckermann, R. N. *J. Comb. Chem.*, **2006**, *8*, 417 – 426. g) Shimaoka, H.; Kuramoto, H.; Furukawa, J. I.; Miura, Y.; Kurogochi, M.; Kita, Y.; Hinou, H.; Shinohara, Y.; Nishimura, S. I. *Chem. Eur. J.*, **2007**, *13*, 1664 – 1673. h) Katritzky, A. R.; Avan, I.; Tala, S. R. *J. Org. Chem.*, **2009**, *74*, 8690 – 8694. m) Evelyn, C. R.; Bell, J. L.; Ryu, J. G.; Wade, S. M.; Kocab, A.; Harzdorf, N. L.; Hollis Showalter, H. D.; Neubig, R. R.; Larsen, S. D. *Bioorganic Med. Chem. Lett.*, **2010**, *20*, 665 – 672. i) Crisalli, P.; Hernández, A. R.; Kool, E. T. *Bioconjug. Chem.*, **2012**, *23*, 1969 – 1980. j) Ichikawa, K.; Kojima, N.; Hirano, Y.; Takebayashi, T.; Kowata, K.; Komatsu, Y. *Chem. Commun.*, **2012**, *48*, 2143 – 2145. k) Novoa-Carballal, R.; Pfaff, A.; Müller, A. H. E. *Polym. Chem.*, **2013**, *4*, 2278 – 2285. l) Netirojjanakul, C.; Witus, L. S.; Behrens, C. R.; Weng, C. H.; Iavarone, A. T.; Francis, M. B. *Chem. Sci.*, **2013**, *4*, 266 – 272. m) Obermeyer, A. C.; Jarman, J. B.; Netirojjanakul, C.; El Muslemany, K.; Francis, M. B. *Angew. Chemie. Int. Ed.*, **2014**, *53*, 1057 – 1061. n) Kutty, S. K.; Barraud, N.; Ho, K. K. K.; Iskander, G. M.; Griffith, R.; Rice, S. A.; Bhadbhade, M.; Willcox, M. D. P.; Black, D. S.; Kumar, N. *Org. Biomol. Chem.*, **2015**, *13*, 9850 – 9861. o) Lamping, M.; Grell, Y.; Geyer, A. *J. Pept. Sci.*, **2016**, *22*, 228 – 235. p) Rahimoff, R.; Kosmatchev, O.; Kirchner, A.; Pfaffeneder, T.; Spada, F.; Brantl, V.; Müller, M.; Carell, T. *J. Am. Chem. Soc.*, **2017**, *139*, 10359 – 10364.
322. a) Bi, H. P.; Zhao, L.; Liang, Y. M.; Li, C. J. *Angew. Chemie. Int. Ed.*, **2009**, *48*, 792 – 795. b) Toriyama, F.; Cornella, J.; Wimmer, L.; Chen, T.; Dixon, D. D.; Creech, G.; Baran, P. S. *J. Am. Chem. Soc.*, **2016**, *11*, 22 – 25. c) Wang,

- J.; Qin, T.; Chen, T.; Wimmer, L.; Edwards, J. T.; Cornella, J.; Vokits, B.; Shaw, S. A.; Baran, P. S. *Angew. Chemie. Int. Ed.*, **2016**, *55*, 9676 – 9679. d) Li, C.; Wang, J.; Barton, L. M.; Yu, S.; Tian, M.; Peters, D. S.; Kumar, M.; Yu, A. W.; Johnson, K. A.; Chatterjee, A. K.; Yan, M.; Baran, P. S. *Science*, **2017**, *356*, eaam7355. e) Qin, T.; Malins, L. R.; Edwards, J. T.; Merchant, R. R.; Novak, A. J. E.; Zhong, J. Z.; Mills, R. B.; Yan, M.; Yuan, C.; Eastgate, M. D.; Baran, P. S. *Angew. Chemie. Int. Ed.*, **2017**, *56*, 260 – 265. f) Wang, J.; Shang, M.; Lundberg, H.; Feu, K. S.; Hecker, S. J.; Qin, T.; Blackmond, D. G.; Baran, P. S. *ACS Catal.*, **2018**, *8*, 9537 – 9542. h) Jin, Y.; Yang, H.; Fu, H. *Chem. Commun.*, **2016**, *52*, 12909 – 12912. i) Degruyter, J. N.; Malins, L. R.; Wimmer, L.; Clay, K. J.; Lopez-Ogalla, J.; Qin, T.; Cornella, J.; Liu, Z.; Che, G.; Bao, D.; Stevens, J. M.; Qiao, J. X.; Allen, M. P.; Poss, M. A.; Baran, P. A. *Org. Lett.*, **2017**, *19*, 6196 – 6199.
323. a) Giese, B.; Gonzalez-Gomez, J. A.; Witzel, T. *Angew. Chem. Int. Ed.*, **1984**, *23*, 69 – 70. b) Giese, B. *Angew. Chem. Int. Ed.*, **1983**, *22*, 753 – 764. c) Zhang, W. *Tetrahedron*, **2001**, *57*, 7237 – 7262. d) Srikanth, G. S. C.; Castle, S. L. *Tetrahedron*, **2005**, *61*, 10377 – 10441.
324. a) Nugent, W. A.; RajanBabu, T. V. *J. Am. Chem. Soc.*, **1988**, *110*, 8561 – 8562. b) RajanBabu, T. V.; Nugent, W. A. *J. Am. Chem. Soc.*, **1989**, *111*, 4525 – 4527. c) Morcillo, S. P.; Miguel, D.; Campaña, A. G.; de Cienfuegos, L. Á.; Justicia, J.; Cuerva, J. M. *Org. Chem. Front.*, **2014**, *1*, 15 – 32. d) Rosales, A.; Rodríguez-García, I.; Muñoz-Bascón, J.; Roldan-Molina, E.; Padial, N. M.; Morales, L. P.; García-Ocaña, M.; Oltra, J. E. *Eur. J. Org. Chem.*, **2015**, *2015*, 4567 – 4591.
325. a) RajanBabu, T. V.; Nugent, W. A. *J. Am. Chem. Soc.*, **1994**, *116*, 986 – 997. b) Gansäuer, A.; Bluhm, H.; Rinker, B.; Narayan, S.; Schick, M.; Lauterbach, T.; Pierobon, M. *Chem. Eur. J.*, **2003**, *9*, 531 – 542.
326. a) Molinaro, C.; Jamison, T. F. *J. Am. Chem. Soc.*, **2003**, *125*, 8076 – 8077. b) Molinaro, C.; Jamison, T. F. *Angew. Chemie. Int. Ed.*, **2004**, *44*, 129 – 132. c) Nielsen, D. K.; Doyle, A. G. *Angew. Chemie. Int. Ed.*, **2011**, *50*, 6056 – 6059. d) Zhao, Y.; Weix, D. J. *J. Am. Chem. Soc.*, **2015**, *137*, 3237 – 3240.

327. a) Aguilera, E. Y.; Sanford, M. S. *Organometallics*, **2018**, *38*, 138 – 142. b) Cabrera, P. J.; Lee, M.; Sanford, M. S. *J. Am. Chem. Soc.*, **2018**, *140*, 5599 – 5606. c) Lee, M.; Adams, A.; Cox, P.; Sanford, M. *Synlett*, **2019**, *2*, 1 – 6.
328. a) Chen, M. S.; White, M. C. *J. Am. Chem. Soc.*, **2004**, *126*, 1346 – 1347. b) Fraunhoffer, K. J.; Bachovchin, D. A.; White, M. C. *Org. Lett.*, **2005**, *7*, 223 – 226. c) Vermeulen, N. A.; Delcamp, J. H.; White, M. C. *J. Am. Chem. Soc.*, **2010**, *132*, 11323 – 11328. d) Gormisky, P. E.; White, M. C. *J. Am. Chem. Soc.*, **2011**, *133*, 12584 – 12589. e) Howell, J. M.; Liu, W.; Young, A. J.; White, M. C. *J. Am. Chem. Soc.*, **2014**, *136*, 5750 – 5754. f) Ma, R.; White, M. C. *J. Am. Chem. Soc.*, **2018**, *140*, 3202 – 3205.
329. a) Pearson, A. J.; Chen, Y. S.; Hsu, S. Y.; Ray, T. *Tetrahedron Lett.*, **1984**, *25*, 1235 – 1238. b) Masui, M.; Hosomi, K.; Tsuchida, K.; Ozaki, S. *Chem. Pharm. Bull.*, **1985**, *33*, 4798 – 4802. c) Shing, T. K. M.; Yeung, Y. Y.; Su, P. L. *Org. Lett.*, **2006**, *8*, 3149 – 3151. d) Horn, E. J.; Rosen, B. R.; Chen, Y.; Tang, J.; Chen, K.; Eastgate, M. D.; Baran, P. S. *Nature*, **2016**, *533*, 77 – 81.
330. a) Horner, L.; Neumann, H. *Chem. Ber.*, **1965**, *98*, 1715 – 1721. b) Cox, J. A.; Ozment, C. L. *J. Electroanal. Chem.*, **1974**, *51*, 75 – 83. c) Delaunay, J.; Mabon, G.; El Badre, M. C.; Orliac, A.; Simonet, J. *Tetrahedron Lett.*, **1992**, *33*, 2149 – 2150. d) Pilard, J.-F.; Fourets, O.; Simonet, J.; Klein, L. J.; Peters, D. G. *J. Electrochem. Soc.*, **2001**, *148*, E171 – E175. e) Schoenenbeck, F.; Murphy, J. A.; Zhou, S.-Z.; Uenoyama, Y.; Miclo, Y.; Tuttle, T. *J. Am. Chem. Soc.*, **2007**, *129*, 13368 – 13369.
331. a) Lascano, S.; Zhang, K. Da; Wehlauch, R.; Gademann, K.; Sakai, N.; Matile, S. *Chem. Sci.*, **2016**, *7*, 4720 – 4724. b) Wuttke, A.; Geyer, A. *J. Pept. Sci.*, **2017**, *23*, 549 – 555. c) Kusano, S.; Konishi, S.; Yamada, Y.; Hayashida, O. *Org. Biomol. Chem.*, **2018**, *16*, 4619 – 4622.
332. a) Bérubé, M.; Dowlut, M.; Hall, D. G. *J. Org. Chem.*, **2008**, *73*, 6471 – 6479. b) Tomsho, J. W.; Benkovic, S. J. *J. Org. Chem.*, **2012**, *77*, 11200 – 11209.
333. Seiradake, E.; Mao, W.; Hernandez, V.; Baker, S. J.; Plattner, J. J.; Alley, M. R. K.; Cusack, S. *J. Mol. Biol.*, **2009**, *390*, 196 – 207.

334. a) Hu, Q.-H.; Liu, R.-J.; Fang, Z.-P.; Zhang, J.; Ding, Y.-Y.; Tan, M.; Wang, M.; Pan, W.; Zhou, H.-C.; Wang, E.-D. *Sci. Rep.*, **2013**, *3*, 2475. b) Nocentini, A.; Supuran, C. T.; Winum, J. Y. *Expert Opin. Ther. Pat.*, **2018**, *28*, 493 – 504. c) Gamrat, J. M.; Mancini, G.; Burke, S. J.; Colandrea, R. C.; Sadowski, N. R.; Figula, B. C.; Tomsho, J. W. *J. Org. Chem.*, **2018**, *83*, 6193 – 6201. d) Zhang, J.; Zhang, J.; Hao, G.; Xin, W.; Yang, F.; Zhu, M.; Zhou, H. *J. Med. Chem.*, **2019**, *62*, 6765 – 6784. e) Lunde, C. S.; Stebbins, E. E.; Jumani, R. S.; Hasan, M. M.; Miller, P.; Barlow, J.; Freund, Y. R.; Berry, P.; Stefanakis, R.; Gut, J.; Rosenthal, P. J.; Love, M. S.; McNamara, C. W.; Easom, E.; Plattner, J. J.; Jacobs, R. T.; Huston, C. D. *Nat. Commun.*, **2019**, *10*, 2816. f) Romero-Aguilar, K. S.; Arciniega-Martínez, I. M.; Farfán-García, E. D.; Campos-Rodríguez, R.; Reséndiz-Albor, A. A.; Soriano-Ursúa, M. A. *Expert Opin. Ther. Pat.*, **2019**, *29*, 339 – 351. g) Swain, B.; Angeli, A.; Angapelly, S.; Thacker, P. S.; Singh, P.; Supuran, C. T.; Arifuddin, M. *J. Enzyme Inhib. Med. Chem.*, **2019**, *34*, 1199 – 1209. h) Arrington, K.; Barcan, G. A.; Calandra, N. A.; Erickson, G. A.; Li, L.; Liu, L.; Nilson, M. G.; Strambeanu, I. I.; VanGelder, K. F.; Woodward, J. L.; Xie, S.; Allen, C. L.; Kowalski, J. A.; Leitch, D. C. *J. Org. Chem.*, **2019**, *84*, 4680 – 4694. i) Fernandes, G. F. S.; Denny, W. A.; Dos Santos, J. L. *Eur. J. Med. Chem.*, **2019**, *179*, 791 – 804.
335. Hashimoto, T.; Gálvez, A. O.; Maruoka, K. *J. Am. Chem. Soc.*, **2013**, *135*, 17667 – 17670.
336. a) Schrock, R. R. *Acc. Chem. Res.*, **1986**, *19*, 342 – 348. b) Schrock, R. R.; Jamieson, J. Y.; Dolman, S. J.; Miller, S. A.; Bonitatebus, P. J.; Hoveyda, A. H. *Organometallics*, **2002**, *21*, 409 – 417. c) Schrock, R. R.; Hoveyda, A. H. *Angew. Chem. Int. Ed.*, **2003**, *42*, 4592 – 4633. d) Schrock, R. R.; Czekelius, C. *Adv. Syn. Catal.*, **2007**, *349*, 55 – 77. e) Yu, M.; Wang, C.; Kyle, A. F.; Jakubec, P.; Dixon, D. J.; Schrock, R. R.; Hoveyda, A. H. *Nature*, **2011**, *479*, 88 – 93. f) Meek, S. J.; O'Brien, R. V.; Llaveria, J.; Schrock, R. R.; Hoveyda, A. H. *Nature*, **2011**, *471*, 461 – 466.
337. a) Bieniek, M.; Bujok, R.; Cabaj, M.; Lugan, N.; Lavigne, G.; Arlt, D.; Grela, K. *J. Am. Chem. Soc.*, **2006**, *128*, 13652 – 13653. b) Hoveyda, A. H.;

- Lombardi, P. J.; O'Brien, R. V.; Zhugralin, A. R. *J. Am. Chem. Soc.*, **2009**, *131*, 8378 – 8379. c) Montgomery, T. P.; Johns, A. M.; Grubbs, R. H. *Catalysts*, **2017**, *7*, 87.
338. a) Parker, K. A.; Chang, W. *Org. Lett.*, **2003**, *5*, 1997 – 1999. b) Parker, K. A.; Chang, W. *Org. Lett.*, **2005**, *6*, 7 – 10. c) Lorpitthaya, R.; Suryawanshi, S. B.; Wang, S.; Pasunooti, K. K.; Cai, S.; Ma, J.; Liu, X.-W. *Angew. Chemie. Int. Ed.*, **2011**, *50*, 12054 – 12057. d) Malik, G.; Est, A.; Retailleau, P.; Dauban, P. *J. Org. Chem.*, **2011**, *76*, 7438 – 7448. e) Takahashi, K.; Yamaguchi, D.; Ishihara, J.; Hatakeyama, S. *Org. Lett.*, **2012**, *14*, 4158 – 4160.
339. a) Evans, D. A.; Faul, M. M.; Bilodeau, M. T. *J. Am. Chem. Soc.*, **1994**, *116*, 2742 – 2753. b) Au, S.-M.; Huang, J.-S.; Yu, W.-Y.; Fung, W.-H.; Che, C.-M. *J. Am. Chem. Soc.*, **1999**, *121*, 9120 – 9132. c) Guthikonda, K.; Du Bois, J. *J. Am. Chem. Soc.*, **2002**, *124*, 13672 – 13673. d) Padwa, A.; Flick, A. C.; Leverett, C. A.; Stengel, T. *J. Org. Chem.*, **2004**, *69*, 6377 – 6386. e) Catino, A. J.; Nichols, J. M.; Forslund, R. E.; Doyle, M. P. *Org. Lett.*, **2005**, *7*, 2787 – 2790. f) Hayes, C. J.; Beavis, P. W.; Humphries, L. A. *Chem. Commun.*, **2006**, *0*, 4501 – 4502. g) Guthikonda, K.; Wehn, P. M.; Caliendo, B. J.; Du Bois, J. *Tetrahedron*, **2006**, *62*, 11331 – 11342. h) Driver, T. G. *Org. Biomol. Chem.*, **2010**, *8*, 3831 – 3846. i) Jung, N.; Bräse, D. *Angew. Chem. Int. Ed.*, **2012**, *51*, 5538 – 5540. j) Unsworth, W. P.; Clark, N.; Ronson, T. O.; Stevens, K.; Thompson, A. L.; Lamont, S. G.; Robertson, J. *Chem. Commun.*, **2014**, *50*, 11393 – 11396. k) Tao, J.; Jin, L.-M.; Zhang, X. P. *Beilstein J. Org. Chem.*, **2014**, *10*, 1282 – 1289. l) Jat, J. L.; Paudyal, M. P.; Gao, H.; Xu, Q.-L.; Yousufuddin, M.; Devarajan, D.; Ess, D. H.; Kürti, L.; Falck, J. R. *Science*, **2014**, *343*, 61 – 65. m) Chanda, B. M.; Vyas, R.; Bedekar, A. V. *J. Org. Chem.*, **2001**, *66*, 30 – 34. n) Crandell, D. W.; Muñoz, III, S. B.; Smith, J. M.; Baik, M.-H. *Chem. Sci.*, **2018**, *9*, 9692 – 9695.
340. a) Yao, Q. *Org. Lett.*, **2002**, *4*, 427 – 430. b) Ferguson, A. C.; Adlington, R. M.; Martyres, D. H.; Rutledge, P. J.; Cowley, A.; Baldwin, J. E. *Tetrahedron*, **2003**, *59*, 8233 – 8243. c) Kotha, S.; Khedkar, P.; Ghosh, A. K. *Eur. J. Org. Chem.*, **2005**, *2005*, 3581 – 3585. d) Morita, N.; Krause, N. *Angew. Chem. Int. Ed.*, **2006**, *45*, 1897 – 1899. e) Brichacek, M.; Njardarson, J. T. *Org. Biomol.*

- Chem.*, **2009**, *7*, 1761 – 1770. f) Alam, M. A.; Shimada, K.; Jahan, A.; Khan, M. W.; Bhuiyan, M. H.; Alam, M. S.; Matin, M. M. *Nat. Prof. Chem. Res.*, **2018**, *6*, 350.
341. a) Werner, E. W.; Sigman, M. S. *J. Am. Chem. Soc.*, **2011**, *133*, 9692 – 9695. b) Avila, C. M.; Patel, J. S.; Reddi, Y.; Saito, M.; Nelson, H. M.; Shunatona, H. P.; Sigman, M. S.; Sunoj, R. B.; Toste, F. D. *Angew. Chemie. Int. Ed.*, **2017**, *56*, 5806 – 5811.
342. a) Sengupta, S.; Bhattacharyya, S. *Synth. Commun.*, **1996**, *26*, 231 – 236. b) Ko, C. - W.; Chou, T. *Tetrahedron Lett.*, **1997**, *38*, 5315 – 5318. c) Correia, C. R. D.; Oliveira, C. C.; Salles, A. G.; Santos, E. A. F. *Tetrahedron Lett.*, **2012**, *53*, 3325 – 3328. d) Angnes, R. A.; Oliveira, J. M.; Oliveira, C. C.; Martins, N. C.; Correia, C. R. D. *Chem. Eur. J.*, **2014**, *20*, 13117 – 13121. e) De Oliveira Silva, J.; Angnes, R. A.; Menezes Da Silva, V. H.; Servilha, B. M.; Adeel, M.; Braga, A. A. C.; Aponick, A.; Correia, C. R. D. *J. Org. Chem.* **2016**, *81*, 2010 – 2018. f) Brant, M. G.; Wulff, J. E. *Synthesis*, **2016**, *48*, 1 – 17. g) Khan, I. U.; Kattela, S.; Hassan, A.; Correia, C. R. D. *Org. Biomol. Chem.*, **2016**, *14*, 9476 – 9480. h) Kattela, S.; Heerdt, G.; Correia, C. R. D. *Adv. Synth. Catal.*, **2017**, *359*, 260 – 267. i) Frota, C.; Polo, E. C.; Esteves, H.; Correia, C. R. D. *J. Org. Chem.*, **2018**, *83*, 2198 – 2209.
343. a) Britten-Kelly, M.; Willis, B. J. *Synthesis*, **1980**, *1980*, 27 – 29. b) Ueno, Y.; Ohta, M.; Okawara, M. *J. Organomet. Chem.*, **1980**, *197*, C1 – C4. d) Barton, D. H. R.; Swift, K. A. D.; Tachdjian, C. *Tetrahedron*, **1995**, *51*, 1887 – 1892. e) Pulkkinen, J.; Aburel, P. S.; Halland, N.; Jørgensen K. A. *Adv. Synth. Catal.*, **2004**, *346*, 1077 – 1080. f) Taylor, M. S.; Zatan, D. N.; Lerchner, A. M.; Jacobsen, E. N. *J. Am. Chem. Soc.*, **2005**, *127*, 1313 – 1317. g) Moon, H. W.; Cho, M. J.; Kim, D. Y. *Tetrahedron Lett.*, **2009**, *50*, 4896 – 4898. h) Kiren, S.; Padwa, A. *J. Org. Chem.*, **2009**, *74*, 7781 – 7789. i) Kamlar, M.; Bravo, N.; Alba, A.-N. R.; Hybelbauerová, S.; Císařová, I.; Veselý, J.; Moyano, A.; Rios, R. *Eur. J. Org. Chem.*, **2010**, *2010*, 5464 – 5470. j) Bera, K.; Namboothiri, I. N. N. *Chem. Commun.*, **2013**, *49*, 10632 – 10634. k) Bera, K.; Namboothiri, I. N. N. *Org. Biomol. Chem.*, **2014**, *12*, 6425 – 6431.

344. a) Ogura, K.; Yahata, N.; Minoguchi, M.; Ohtsuki, K.; Takahashi, K.; Iida, H. *J. Org. Chem.*, **1986**, *51*, 508 – 512. b) Opekar, S.; Pohl, R.; Eigner, V.; Beier, P. *J. Org. Chem.*, **2013**, *78*, 4573 – 4579. c) Chan, C.-K.; Chen, Y.-H.; Hsu, R.-T.; Chang, M.-Y. *Tetrahedron*, **2017**, *73*, 46 – 54.
345. a) Niwa, T.; Yorimitsu, H.; Oshima, K. *Tetrahedron*, **2009**, *65*, 1971 – 1976. b) Zhou, G.; Ting, P.; Aslanian, R. G. *Tetrahedron Lett.*, **2010**, *51*, 939 – 941. c) Zheng, B.; Jia, T.; Walsh, P. J. *Org. Lett.*, **2013**, *15*, 1690 – 1693. d) Nambo, M.; Crudden, C. M. *Angew. Chem. Int. Ed.*, **2013**, *53*, 742 – 746. e) Solé, D.; Pérez-Janer, F.; Mancuso, R. *Chem. Eur. J.*, **2015**, *21*, 4580 – 4584. f) Knauber, T.; Tucker, J. *J. Org. Chem.*, **2016**, *81*, 5636 – 5648. g) Solé, D.; Pérez-Janer, F.; Zulaica, E.; Guastavino, J. F.; Fernandez, I. *ACS Catal.*, **2016**, *6*, 1691 – 1700. h) Gao, G.; Zheng, B.; Fu, Y.; Li, M.; Chen, X.-Z.; Zhang, Y.-Y.; Liu, J.-J.; Hou, S.-C.; Walsh, P. J. *Asian J. Org. Chem.*, **2017**, *6*, 654 – 657. i) Nambo, M.; Keske, E. C.; Rygus, J. P. G.; Yim, J. C.-H.; Crudden, C. M. *ACS Catal.*, **2017**, *7*, 1108 – 1112.
346. a) Weaver, J. D.; Tunge, J. A. *Org. Lett.*, **2008**, *10*, 4657 – 4660. b) Weaver, J. D.; Ka, B. J.; Morris, D. K.; Thompson, W.; Tunge, J. A. *J. Am. Chem. Soc.*, **2010**, *132*, 12179 – 12181. c) Shibata, N.; Fukushi, K.; Furukawa, T.; Suzuki, S.; Tokunaga, E.; Cahard, D. *Org. Lett.*, **2012**, *14*, 5366 – 5369. d) Kong, H. I.; Gill, M. A.; Hrdina, A. H.; Crichton, J. E.; Manthorpe, J. M. *J. Fluorine Chem.*, **2013**, *153*, 151 – 161.
347. a) Nickon, A.; Lambert, J. L. S. *J. Am. Chem. Soc.*, **1962**, *84*, 4604 – 4605. b) Kuwajima, I.; Kato, M. *J. Chem. Soc., Chem. Commun.*, **1979**, *0*, 708 – 709. c) Werstiuk, N. H. *Tetrahedron*, **1983**, *39*, 205 – 268. d) Nakamura, E.; Kuwajima, I. *J. Am. Chem. Soc.*, **1983**, *105*, 651 – 652. e) Nakamura, E.; Shimada, J.; Kuwajima, I. *Organometallics*, **1985**, *4*, 641 – 646. Nakamura, E.; Oshino, H.; Kuwajima, I. *J. Am. Chem. Soc.*, **1986**, *108*, 3745 – 3755. f) Nakamura, E.; Aoki, S.; Sekiya, K.; Oshino, H.; Kuwajima, I. *J. Am. Chem. Soc.*, **1987**, *109*, 8056 – 8066. g) Mills, L. R.; Rousseaux, S. *Eur. J. Org. Chem.*, **2018**, *2019*, 8 – 26.

348. a) Tamaru, Y.; Ochiai, H.; Nakamura, T.; Yoshida, Z. *Tetrahedron Lett.*, **1986**, 27, 955 – 958. b) Aoki, S.; Fujimura, T.; Nakamura, E.; Kuwajima, I. *J. Am. Chem. Soc.*, **1988**, 110, 3296 – 3298. c) Aoki, S.; Nakamura, E.; Kuwajima, I. *Tetrahedron Lett.*, **1988**, 29, 1541 – 1542. d) Rosa, D.; Orellana, A. *Org. Lett.*, **2011**, 13, 110 – 113. e) Nithiy, N.; Rosa, D.; Orellana, A. *Synthesis*, **2013**, 45, 3199 – 3210. f) Rosa, D.; Orellana, A. *Chem. Commun.*, **2013**, 49, 5420 – 5422. g) Nikolaev, A.; Nithiy, N.; Orellana, A. *Synlett*, **2014**, 25, 2301 – 2305. h) Nithiy, N.; Orellana, A. *Org. Lett.*, **2014**, 16, 5854 – 5857. i) Ye, Z.; Gettys, K. E.; Shen, X.; Dai, M. *Org. Lett.*, **2015**, 17, 6074 – 6077. j) Shen, M. - H.; Lu, X. - L.; Xu, H. - D. *RSC Adv.*, **2015**, 5, 98757 – 98761. k) Nikolaev, A.; Orellana, A. *Synthesis*, **2016**, 48, 1741 – 1768. j)
349. a) Rathke, M. W.; Lindert, A. *J. Am. Chem. Soc.*, **1971**, 93, 4605 – 4606. b) Ito, Y.; Konoike, T.; Harada, T.; Saegusa, T. *J. Am. Chem. Soc.*, **1977**, 99, 1487 – 1493. c) Frazier, R. H.; Harlow, R. L. *J. Org. Chem.*, **1980**, 45, 5408 – 5411. d) Julia, M.; Thuillier, G. L.; Rolando, C.; Saussine, L. *Tetrahedron. Lett.*, **1982**, 23, 2453 – 2456. e) Chiba, S.; Cao, Z.; El Bialy, S. A. A.; Narasaka, K. *Chem. Lett.*, **2006**, 35, 18 – 19. f) Baran, P. S.; DeMartino, M. P. *Angew. Chem. Int. Ed.*, **2006**, 45, 7083 – 7086. g) DeMartino, M. P.; Chen, K.; Baran, P. S. *J. Am. Chem. Soc.*, **2008**, 130, 11546 – 11560. h) Martin, C. L.; Overman, L. E.; Rohde, J. M. *J. Am. Chem. Soc.*, **2008**, 130, 7568 – 7569. i) Guo, F.; Clift, M. D.; Thomson, R. J. *Eur. J. Org. Chem.*, **2012**, 2012, 4881 – 4896. j) Amaya, T.; Maegawa, Y.; Masuda, T.; Osafune, Y.; Hirao, T. *J. Am. Chem. Soc.*, **2015**, 137, 10072 – 10075. k) Parida, K. N.; Pathe, G. K.; Maksymenko, S.; Szpilman, A. M. *Beilstein J. Org. Chem.*, **2018**, 14, 992 – 997. l) Tanaka, T.; Tanaka, T.; Tsuji, T.; Yazaki, R.; Ohshima, T. *Org. Lett.*, **2018**, 20, 3541 – 3544.
350. a) Kulinkovich, O. G.; Savchenko, A. I.; Sviridov, S. V.; Vasilevski, D. A. *Mendeleev Commun.*, **1993**, 3, 230 – 231. b) Corey, E. J.; Rao, S. A.; Noe, M. C. *J. Am. Chem. Soc.*, **1994**, 116, 9345 – 9346. d) Kasatkin, A.; Sato, F. *Tetrahedron Lett.*, **1995**, 36, 6079 – 6082. e) Lee, J.; Kim, H.; Cha, J. K. *J. Am. Chem. Soc.*, **1996**, 118, 4198 – 4199. f) Esposito, A.; Taddei, M. *J. Org. Chem.*, **2000**, 65, 9245 – 9248. g) Kulinkovich, O. G.; De Meijere, A. *Chem. Rev.*, **2000**,

- 100, 2789 – 2834. h) Kim, S. - H.; Sung, M. J.; Cha, J. K. *Org. Synth.*, **2003**, *80*, 111. i) Wolan, A.; Six, Y. *Tetrahedron*, **2010**, *66*, 15 – 61. j) Wolan, A.; Six, Y. *Tetrahedron*, **2010**, *66*, 3097 – 3133. k) Haym, I.; Brimble, M. A. *Org. Biomol. Chem.* **2012**, *10*, 7649 – 7665.
351. a) Coggins, P.; Gaur, S.; Simpkins, N. S. *Tetrahedron Lett.*, **1995**, *36*, 1545 – 1548. b) Majewski, M.; Decaire, M.; Nowak, P.; Wang, F. *Tetrahedron*, **2000**, *9*, 1321 – 1323. d) Majewski, M.; DeCaire, M.; Nowak, P.; Wang, F. *Can. J. Chem.*, **2001**, *79*, 1792 – 1798. e) Majewski, M.; Wang, F. *Tetrahedron*, **2002**, *58*, 4567 – 4571. f) Högermeier, J.; Reissig, H. U.; Brüdgam, I.; Hartl, H. *Adv. Synth. Catal.*, **2004**, *346*, 1868 – 1879.
352. Kotha, S.; Khedkar, P. *Chem. Rev.*, **2012**, *112*, 1650 – 1680.
353. a) Bolm, C.; Hildebrand, J. P. *J. Org. Chem.*, **2000**, *65*, 169 – 175. b) Hackenberger, C. P. R.; Raabe, G.; Bolm, C. *Chem. Eur. J.*, **2004**, *10*, 2942 – 2952. c) Okamura, H.; Bolm, C. *Org. Lett.*, **2004**, *6*, 1305 – 1307. d) Gae, Y. C.; Rémy, P.; Jansson, J.; Moessner, C.; Bolm, C. *Org. Lett.*, **2004**, *6*, 3293 – 3296. e) Cheng, Y.; Dong, W.; Wang, L.; Parthasarathy, K.; Bolm, C. *Org. Lett.*, **2014**, *16*, 2000 – 2002. f) Goldberg, F. W.; Kettle, J. G.; Xiong, J.; Lin, D. *Tetrahedron*, **2014**, *70*, 6613 – 6622. g) Wang, L.; Priebbenow, D. L.; Dong, W.; Bolm, C. *Org. Lett.*, **2014**, *16*, 2661 – 2663. h) Chen, X. Y.; Wang, L.; Frings, M.; Bolm, C. *Org. Lett.*, **2014**, *16*, 3796 – 3799. i) Aithagani, S. K.; Dara, S.; Munagala, G.; Aruri, H.; Yadav, M.; Sharma, S.; Vishwakarma, R. A.; Singh, P. P. *Org. Lett.*, **2015**, *17*, 5547 – 5549. j) Bohnen, C.; Bolm, C. *Org. Lett.*, **2015**, *17*, 3011 – 3013. k) Zou, Y.; Xiao, J.; Peng, Z.; Dong, W.; An, D. *Chem. Commun.*, **2015**, *51*, 14889 – 14892. l) Teng, F.; Cheng, J.; Bolm, C. *Org. Lett.*, **2015**, *17*, 3166 – 3169. m) Wang, H.; Cheng, Y.; Becker, P.; Raabe, G.; Bolm, C. *Angew. Chemie. Int. Ed.*, **2016**, *55*, 12655 – 12658.
354. a) Lacote, E.; Amatore, M.; Fensterbank, L.; Malacria, M. *Synlett*, **2002**, *1*, 116 – 118. b) Leca, D.; Song, K.; Amatore, M.; Fensterbank, L.; Lacôte, E.; Malacria, M. *Chem. Eur. J.*, **2004**, *10*, 906 – 916. c) Miao, J.; Richards, N. G. J.; Ge, H. *Chem. Commun.*, **2014**, *50*, 9687 – 9689. d) Buglioni, L.; Bizet, V.; Bolm, C. *Adv. Synth. Catal.*, **2014**, *356*, 2209 – 2213. e) Dannenberg, C. A.; Bizet, V.;

- Bolm, C. *Synthesis*, **2015**, *47*, 1951 – 1959. f) Gutmann, B.; Elsner, P.; O’Kearney-Mcmullan, A.; Goundry, W.; Roberge, D. M.; Kappe, C. O. *Org. Process Res. Dev.*, **2015**, *19*, 1062 – 1067. g) Zenzola, M.; Doran, R.; Luisi, R.; Bull, J. A. *J. Org. Chem.*, **2015**, *80*, 6391 – 6399. h) Lebel, H.; Piras, H.; Borduy, M. *ACS Catal.*, **2016**, *6*, 1109 – 1112. i) Tota, A.; Zenzola, M.; Chawner, S. J.; John-Campbell, S. S.; Carlucci, C.; Romanazzi, G.; Degennaro, L.; Bull, J. A.; Luisi, R. *Chem. Commun.*, **2017**, *53*, 348 – 351. j) Bull, J. A.; Degennaro, L.; Luisi, R. *Synlett*, **2017**, *28*, 2525 – 2538.
355. a) Quin, L. D.; Littlefield, L. B. *J. Org. Chem.*, **1978**, *43*, 3508 – 3512. b) Dierkes, P.; Leeuwen, P. W. N. M. Van. *J. Chem. Soc. Dalt. Trans.* **1999**, 1519 – 1529. c) Shintani, R.; Duan, W. L.; Nagano, T.; Okada, A.; Hayashi, T. *Angew. Chemie. Int. Ed.*, **2005**, *44*, 4611 – 4614. d) Duan, W. L.; Iwamura, H.; Shintani, R.; Hayashi, T. *J. Am. Chem. Soc.*, **2007**, *129*, 2130 – 2138. e) Shintani, R.; Narui, R.; Tsutsumi, Y.; Hayashi, S.; Hayashi, T. *Chem. Commun.*, **2011**, *47*, 6123 – 6125. f) Mansell, S. M. *Dalton Trans.* **2017**, *46*, 15157 – 15174.
356. a) Bolm, C.; Verrucci, M.; Simic, O.; Cozzi, P. G.; Raabe, G.; Okamura, H. *Chem. Commun.*, **2003**, *0*, 2826 – 2827. b) Langner, M.; Bolm, C. *Angew. Chem. Int. Ed.*, **2004**, *43*, 5984 – 5987. c) Rémy, P.; Langner, M.; Bolm, C. *Org. Lett.*, **2006**, *8*, 1209 – 1211. d) Bolm, C.; Martin, M.; Gescheidt, G.; Palivan, C.; Stanoeva, T.; Bertagnolli, H.; Feth, M.; Schweiger, A.; Mitrikas, G.; Harmer, J. *Chem. Eur. J.*, **2007**, *13*, 1842 – 1850. e) Lu, S.-M.; Bolm, C. *Adv. Syn. Catal.*, **2008**, *350*, 1101 – 1105. f) Frings, M.; Bolm, C. *Eur. J. Org. Chem.*, **2009**, *2009*, 4085 – 4090. g) Benetskiy, E. B.; Bolm, C. *Tetrahedron: Asymmetry*, **2011**, *22*, 373 – 378.

## Appendix A – Experimental Information

### General Experimental Details:

All reactions were performed in single-neck, oven-dried, round-bottom flasks fitted with rubber septa under a positive pressure of argon, unless otherwise noted.

Liquid reagents and solvents were either transferred via plastic syringes with stainless steel needles of suitable gauge sizes, or transferred via cannula needle. Organic solutions were concentrated at appropriate temperatures using a water bath by rotary evaporation under vacuum.

Analytical thin-layer chromatography (TLC) was performed using aluminum plates pre-coated with silica gel (0.20 mm, 60 Å pore-size, 230-400 mesh, Macherey-Nagel) impregnated with a fluorescent indicator (254 nm). TLC plates were visualized by exposure to ultraviolet light, or developed using chemical stains of  $\text{KMnO}_4$  solution or phosphomolybdic acid (PMA) solution.

Flash column chromatography was performed over untreated silica gel (60 Å, 63-200  $\mu\text{M}$ , Caledon) from Silicycle<sup>®</sup> unless otherwise noted.

Unless otherwise noted, all compounds isolated by chromatography were sufficiently pure (>80 % by NMR) for use in subsequent preparative reactions.

### General Materials:

Commercial solvents and reagents were used as received with the following exceptions: THF was dried by distillation over  $\text{Na}^0$  and benzophenone. DCM and THF (when > 100 mL of solvent was used in the reaction) were dried by passage through alumina in a commercial solvent purification system (SPS).

### Instrumentation:

Proton nuclear magnetic resonance spectra ( $^1\text{H}$  NMR) were recorded at 300 MHz or 500 MHz using Bruker AVANCE III<sup>™</sup> 300MHz, AVANCE I<sup>™</sup> 500MHz, or AVANCE NEO<sup>™</sup> 500MHz respectively at 23 °C. Proton chemical shifts are expressed in parts per million (ppm,  $\delta$  scale) downfield from tetramethylsilane, and are referenced to residual protium in the NMR solvent ( $\text{CD}_3\text{C}(\text{O})\text{CD}_3$  or  $d_6$ -ace,  $\delta$  2.05;  $\text{CDCl}_3$ ,  $\delta$  7.26;  $\text{CD}_3\text{S}(\text{O})\text{CD}_3$  or  $d_6$ -DMSO,  $\delta$  2.50). Data are represented as follows: chemical shift, multiplicity (s = singlet, d = doublet, t = triplet, q = quartet, sext = sextet, m = multiplet and/or multiple resonances, br = broad), coupling constant (three significant figures) in Hertz, and relative integration.

Carbon nuclear magnetic resonance spectra ( $^{13}\text{C}$  NMR) were recorded at 75 MHz using Bruker AVANCE III<sup>™</sup> 300MHz at 23 °C. Carbon chemical shifts are reported in parts per million downfield from tetramethylsilane and are referenced to the carbon resonance of

the solvent ( $\text{CD}_3\text{C}(\text{O})\text{CD}_3$  or  $d_6$ -ace,  $\delta$  29.85;  $\text{CDCl}_3$ ,  $\delta$  77.22;  $\text{CD}_3\text{S}(\text{O})\text{CD}_3$  or  $d_6$ -DMSO,  $\delta$  39.52). Carbon assignments (e.g.  $\text{CH}_2$ ) were inferred using DEPT-135 spectra.

Infrared (IR) spectra were obtained using a Perkin Elmer 1000 FT-IR spectrometer referenced to a polystyrene standard with an air background. Diagnostic peaks are represented as follows: frequency of absorption ( $\text{cm}^{-1}$ ).

High-resolution mass spectra were obtained at the UVic Chemistry Mass Spectrometry Facility (CMSF) using a Thermo Fisher Scientific Exactive™ Orbitrap-LCMS instrument.

### General Procedure A:

A round-bottom flask was charged with an appropriate stir bar, sulfone (1.0 equiv.) and bis-aryl ketone (1.0 equiv.) prior to dissolving in THF (10 mL/mmol), and the solution was cooled to  $-78^\circ\text{C}$  using a cooling bath composed of dry ice and acetone. Commercially available LiHMDS (1.1 equiv., 1.0 M in THF) was added as one portion at  $-78^\circ\text{C}$ . The reaction mixture was stirred for 1 hr at  $-78^\circ\text{C}$ , then removed from the cooling bath and stirred for 30 min. at ambient temperature. Subsequently, the reaction mixture was quenched with saturated aqueous  $\text{NH}_4\text{Cl}$  (1.0 mL/mmol), prior to concentration under reduced pressure to remove THF. EtOAc (3 x 10 mL/mmol) was used for extraction, and the combined organic extracts were washed with  $\text{H}_2\text{O}$  (3 x 10 mL/mmol) and brine (2 x 10 mL/mmol). The organic layer was dried with anhydrous  $\text{Na}_2\text{SO}_4$  before concentration under reduced pressure to provide a coloured oil. The crude product instantaneously turned into coloured foam upon subjecting to high vacuum. The crude coloured foam was carried to the next step with no further purification.

Hexamethyldisilazane (1.1 equiv.) was dissolved to THF (1.0 mL/mmol) prior to cooling to  $0^\circ\text{C}$  using a cooling bath of ice and water. Commercially available  $n\text{BuLi}$  (1.1 equiv., 2.5M in hexane) was added to the solution in a dropwise manner at  $0^\circ\text{C}$ . The clear, yellow LiHMDS solution was allowed to stir for 10 min. Another round-bottom flask was charged with an appropriate stir bar and the aforementioned crude foam (1.0 equiv.) prior to dissolving in THF (20 mL/mmol). The solution was cooled to  $-78^\circ\text{C}$  using a cooling bath composed of dry ice and acetone. LiHMDS solution was then added into the reaction mixture in a dropwise manner at  $-78^\circ\text{C}$ . The reaction mixture was stirred for 1 hr at  $-78^\circ\text{C}$ , before being quenched with saturated aqueous  $\text{NH}_4\text{Cl}$  (1.0 mL/mmol). The quenched reaction mixture was then concentrated under reduced pressure to remove THF. EtOAc (3 x 10 mL/mmol) was used for extraction, and the combined organic extracts were washed with  $\text{H}_2\text{O}$  (3 x 10 mL/mmol) and brine (2 x 10 mL/mmol). The organic layer was dried with anhydrous  $\text{Na}_2\text{SO}_4$  before concentration under reduced pressure to provide a coloured oil. The crude product instantaneously turned into coloured foam upon subjecting to high vacuum. The crude coloured foam was then purified by flash column chromatography using DCM (spiked with 5% v/v  $\text{NEt}_3$ ) in order to afford  $\geq 90\%$  pure product as a lightly coloured foam.

**General Procedure B:**

A round-bottom flask was charged with an appropriate stir bar, sulfone (1.0 equiv.) prior to dissolving in THF (2.0 mL/mmol). Ac<sub>2</sub>O (5.0 equiv.) and DMAP (10 mol%) was added into the reaction mixture at 0 °C using a cooling bath composed of ice and water. The reaction mixture was then stirred for 3 days while warming gradually to ambient temperature. H<sub>2</sub>O (1.0 mL/mmol) was used to quench the reaction, prior to concentration under reduced pressure to remove THF. EtOAc (3 x 10 mL/mmol) was used for extraction, and the combined organic extracts were washed with H<sub>2</sub>O (3 x 10 mL/mmol) and brine (2 x 10 mL/mmol). The organic layer was dried with anhydrous Na<sub>2</sub>SO<sub>4</sub> before concentration under reduced pressure to provide ≥ 90% pure product as coloured oils.

**General Procedure C:**

Hexamethyldisilazane (2.2 equiv.) was dissolved to THF (1.0 mL/mmol) prior to cooling to 0 °C using a cooling bath of ice and water. Commercially available *n*BuLi (2.2 equiv., 2.5M in hexane) was added to the solution in a dropwise manner at 0°C. The clear, yellow LiHMDS solution was allowed to stir for 10 min. Another round-bottom flask was charged with an appropriate stir bar, sulfone (1.0 equiv.) and di-iodide **39c** (1.0 equiv.) prior to dissolving in THF (5.0 mL/mmol). The solution was cooled to –78 °C using a cooling bath composed of dry ice and acetone. LiHMDS solution was then added into the reaction mixture in a dropwise manner at –78°C. The addition rate should be properly controlled such that the cooling bath should not exceed –78°C for prolonged periods. The reaction mixture was then stirred for 2 hr at –78°C, before being quenched with saturated aqueous NH<sub>4</sub>Cl (1.0 mL/mmol). The quenched reaction mixture was then concentrated under reduced pressure to remove THF. Et<sub>2</sub>O (3 x 10 mL/mmol) was used for extraction, and the combined organic extracts were washed with H<sub>2</sub>O (3 x 10 mL/mmol) and brine (2 x 10 mL/mmol). The organic layer was dried with anhydrous Na<sub>2</sub>SO<sub>4</sub> before concentration under reduce pressure to provide yellow-coloured solids. The crude product was then purified by flash column chromatography using a column volume of hexane (spiked with 5% v/v NEt<sub>3</sub>) and subsequently gradient elution in order to afford ≥90% pure product as lightly-coloured solids.

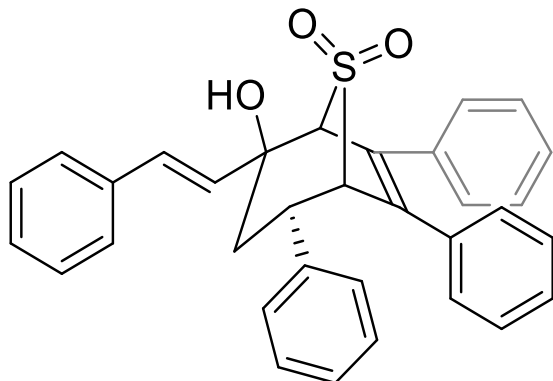
**General Procedure D:**

Under open atmosphere, a round-bottom flask was charged with an appropriate stir bar, ketone **52** (1.0 equiv.) prior to dissolving in EtOH (1.5 mL/mmol). Hydroxylamine hydrochloride salts (1.3 equiv.) were added in one portion at ambient temperature. The reaction mixture was stirred at ambient temperature in an open atmosphere until TLC indicated complete consumption of ketone **52**. The reaction mixture was then concentrated under reduced pressure to remove EtOH. EtOAc (3 x 10 mL/mmol) was used for extraction, and the combined organic extracts were dried with anhydrous Na<sub>2</sub>SO<sub>4</sub>. Subsequent concentration under reduced pressure provided ≥ 90% pure product as coloured solids.

**General Procedure E:**

Diisopropylamine (1.2 equiv.) was dissolved to THF (1.0 mL/mmol) prior to cooling to 0 °C using a cooling bath of ice and water. Commercially available *n*BuLi (1.2 equiv., 2.5M in hexane) was added to the solution in a dropwise manner at 0°C. The clear, yellow LDA solution was allowed to stir for 10 min. Another round-bottom flask was charged with an appropriate stir bar and sulfone **47** (1.0 equiv.) prior to dissolving in THF (2.0 mL/mmol). The solution was cooled to -78 °C using a cooling bath composed of dry ice and acetone. LDA solution was then added into the reaction mixture in a dropwise manner at -78°C. After stirring at -78 °C for 10 min., alkyl bromides (1.1 equiv.) were then added into the reaction mixture in one portion at -78 °C. The reaction mixture was then stirred for 4 hr at -78°C, before being quenched with saturated aqueous NH<sub>4</sub>Cl (1.0 mL/mmol). The quenched reaction mixture was then concentrated under reduced pressure to remove THF. Et<sub>2</sub>O (3 x 10 mL/mmol) was used for extraction, and the combined organic extracts were washed with H<sub>2</sub>O (3 x 10 mL/mmol) and brine (2 x 10 mL/mmol). The organic layer was dried with anhydrous Na<sub>2</sub>SO<sub>4</sub> before concentration under reduce pressure to provide brown oils. The crude product was then purified by flash column chromatography using gradient elution of 4:1 Hexane: Et<sub>2</sub>O (spiked with 5% v/v NEt<sub>3</sub>) to 1:1 Hexane: Et<sub>2</sub>O (spiked with 5% v/v NEt<sub>3</sub>) in order to afford ≥ 90% pure product.

**Synthesis of (1S,2S,4S,5S)-2-hydroxy-4,6,7-triphenyl-2-[(1E)-2-phenylethenyl]-8λ<sup>6</sup>-thiabicyclo[3.2.1]oct-6-ene-8,8-dione **31a****



Using **general procedure A**, alcohol **31a** was obtained as 0.5853g (63% yield) of yellow solid from sulfone **4b** and ketone **5a** on a 1.85 mmol scale.

**Melting Point:** 111 – 112°C

**TLC solvent:** ( $R_f = 0.24$ ) 3:1 hexane : EtOAc

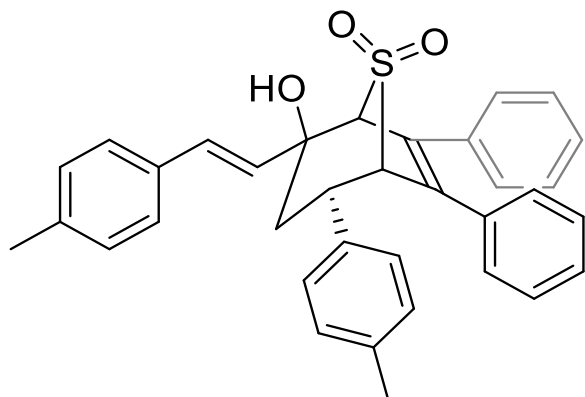
**<sup>1</sup>H NMR:** 7.33 – 7.39 (m, 5H), 7.16 – 7.21 (m, 5H), 7.06 – 7.13 (m, 3H), 6.99 (dm,  $J = 8.0$  Hz, 2H), 6.90 – 6.96 (m, 3H), 6.86 (d,  $J = 15.7$  Hz, 1H), 6.59 (dm,  $J = 7.4$  Hz, 2H), 5.89 (dd,  $J = 15.6$  Hz, 1.8 Hz, 1H), 5.56 (d,  $J = 1.8$  Hz, 1H), 4.32 (dd,  $J = 12.9$  Hz, 4.4 Hz, 1H), 4.20 – 4.24 (m, 1H), 4.10 (dm,  $J = 2.5$  Hz, 3H), 2.66 (dd,  $J = 15.0$  Hz, 13.0 Hz, 1H), 2.13 (dd,  $J = 14.8$  Hz, 4.5 Hz, 1H)

**<sup>13</sup>C NMR:** 139.99, 138.25, 136.42, 136.15, 135.43, 132.77, 129.72, 129.34, 129.31, 129.29, 128.73, 128.64, 128.56, 128.42, 128.38, 128.05, 127.92, 127.88, 126.65, 73.68, 73.22, 72.27, 39.73, 37.26

**IR (cm<sup>-1</sup>):** 3582, 3055, 2957, 1600, 1495, 1302, 1205, 1124, 1071, 971, 754, 695, 576

**HRMS:** calcd. for C<sub>33</sub>H<sub>28</sub>O<sub>3</sub>SNa [M+Na<sup>+</sup>]: 527.16569, found 527.16521

**Synthesis of (1S,2S,4S,5S)-2-hydroxy-4-(4-methylphenyl)-2-[(1E)-2-(4-methylphenyl)ethenyl]-6,7-diphenyl-8λ<sup>6</sup>-thiabicyclo[3.2.1]oct-6-ene-8,8-dione **31b****



Using **general procedure A**, alcohol **31b** was obtained as 0.3642g (66% yield) of yellow solid from sulfone **4b** and ketone **5b** on a 0.96 mmol scale.

**Melting Point:** 105 – 108°C

**TLC solvent:** ( $R_f = 0.25$ ) 3:1 hexane : EtOAc

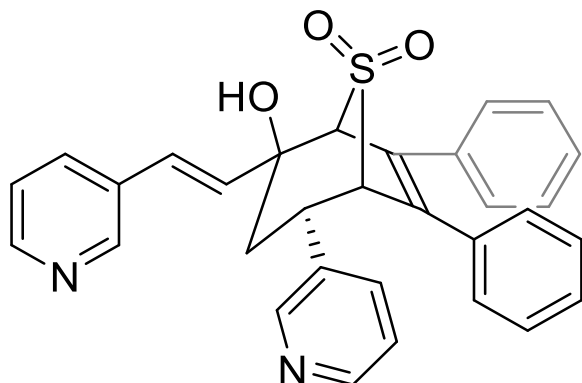
**<sup>1</sup>H NMR:** 7.30 – 7.34 (m, 5H), 7.18 – 7.22 (m, 5H), 7.00 (dm,  $J = 8.2$  Hz, 4H), 6.83 (d,  $J = 8.2$  Hz, 2H), 6.81 (d,  $J = 15.7$  Hz, 1H), 6.63 (dm,  $J = 6.8$  Hz, 2H), 5.84 (dd,  $J = 15.5$  Hz, 1.8 Hz, 1H), 5.53 (d,  $J = 1.83$  Hz, 1H), 4.27 (dd,  $J = 12.9$  Hz, 4.3 Hz, 1H), 4.18 – 4.22 (m, 1H), 4.08 (d,  $J = 2.5$  Hz, 1H), 2.62 (dd,  $J = 14.4$  Hz, 13.4 Hz, 1H), 2.38 (s, 3H), 2.29 (s, 3H), 2.10 (dd,  $J = 14.8$  Hz, 4.3 Hz, 1H)

**<sup>13</sup>C NMR:** 138.22, 137.72, 136.97, 136.20, 135.48, 135.28, 133.61, 131.82, 129.86, 129.79, 129.49, 129.37, 129.25, 129.04, 128.65, 128.57, 128.48, 128.34, 127.78, 126.54, 73.73, 73.23, 72.26, 39.42, 37.50, 21.28, 21.19

**IR (cm<sup>-1</sup>):** 3585, 3053, 2920, 1601, 1514, 1443, 1300, 1204, 1109, 1032, 973, 799, 763, 696, 579, 526

**HRMS:** calcd. for C<sub>35</sub>H<sub>30</sub>O<sub>4</sub>SNa [ $M+Na^+$ ]: 555.19699, found 555.19628

**Synthesis of (1S,2S,4S,5S)-2-hydroxy-6,7-diphenyl-4-(pyridin-3-yl)-2-[(1E)-2-(pyridin-3-yl)ethenyl]-8 $\lambda^6$ -thiabicyclo[3.2.1]oct-6-ene-8,8-dione **31d****



Using **general procedure A**, alcohol **31d** was obtained in 0.5073g (54% yield) of light yellow solid from sulfone **4b** and ketone **5d** on a 1.85 mmol scale.

**Melting Point:** 126 – 127°C

**TLC solvent:** ( $R_f$  = 0.32) 2:1 hexane : EtOAc

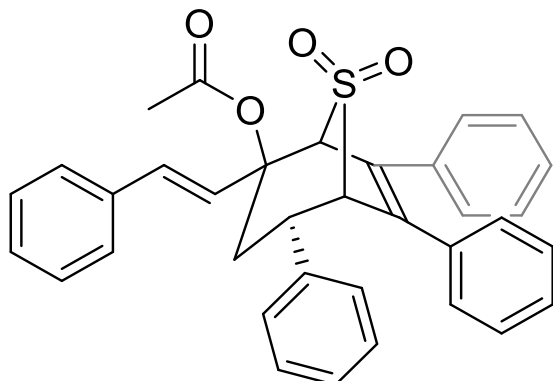
**$^1\text{H NMR}$ :** 8.53 – 8.57 (m, 3H), 8.47 (dd,  $J$  = 4.8 Hz, 1.6 Hz, 2H), 8.19 (d,  $J$  = 2.1 Hz, 1H), 7.88 (dt,  $J$  = 8.0 Hz, 2.0 Hz, 1H), 7.76 (qt,  $J$  = 8.1 Hz, 1.9 Hz, 1H), 7.21 – 7.26 (m, 5H), 7.14 – 7.21 (m, 3H), 7.04 – 7.09 (m, 1H), 6.83 (tt,  $J$  = 8.2 Hz, 2.0 Hz, 2H), 5.89 (dd,  $J$  = 15.6 Hz, 1.7 Hz, 1H), 5.55 (d,  $J$  = 1.8 Hz, 1H), 4.68 (dd,  $J$  = 13.3 Hz, 4.3 Hz, 1H), 4.33 – 4.36 (m, 1H), 4.22 – 4.25 (m, 1H), 2.99 (dd,  $J$  = 17.2 Hz, 15.5 Hz, 1H), 2.73 (dd,  $J$  = 17.1 Hz, 4.7 Hz, 1H)

**$^{13}\text{C NMR}$ :** 148.65, 148.09, 147.68, 146.29, 137.22, 136.16, 135.44, 133.19, 132.09, 129.01, 128.53, 128.26, 127.10, 126.84, 126.42, 126.28, 122.11, 121.60, 73.59, 73.33, 72.30, 39.75, 37.45

**IR ( $\text{cm}^{-1}$ ):** 3380, 3059, 2958, 1699, 1578, 1480, 1305, 1290, 1216, 1113, 962, 768, 707, 701, 557

**HRMS:** calcd. for  $\text{C}_{31}\text{H}_{26}\text{N}_2\text{O}_3\text{SNa}$  [ $\text{M}+\text{Na}^+$ ]: 529.15618, found 529.15648

**Synthesis of (1S,2S,4S,5S)-8,8-dioxo-4,6,7-triphenyl-2-[(1E)-2-phenylethenyl]-8λ<sup>6</sup>-thiabicyclo[3.2.1]oct-6-en-2-yl acetate **32a****



Using **general procedure B**, ester **32a** was obtained as 0.2632g (93% yield) of bright yellow solid from alcohol **31a** on a 0.52mmol scale.

**Melting Point:** 86 – 87°C

**TLC solvent:** ( $R_f = 0.60$ ) 2:1 hexane : EtOAc

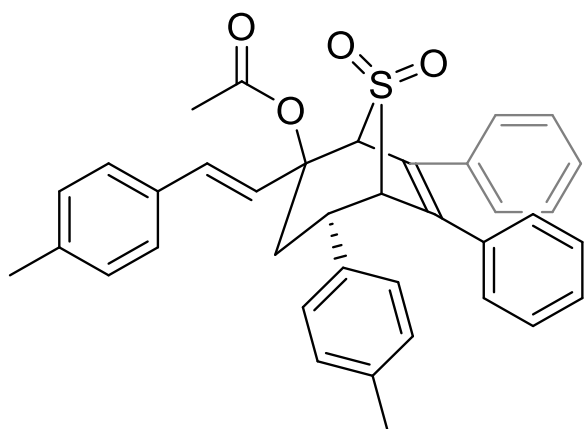
**<sup>1</sup>H NMR:** 7.30 – 7.33 (m, 5H), 7.15 – 7.23 (m, 5H), 7.01 – 7.10 (m, 3H), 6.89 – 6.99 (m, 5H), 6.59 (dm,  $J = 7.3$  Hz, 2H), 6.49 (d,  $J = 16.7$  Hz, 1H), 6.21 (d,  $J = 16.3$  Hz, 1H), 5.51 (d,  $J = 2.2$  Hz, 1H), 4.43 (dd,  $J = 12.2$  Hz, 4.0 Hz, 1H), 4.16 – 4.20 (m, 1H), 2.62 (dd,  $J = 14.4$  Hz, 12.5 Hz, 1H), 2.41 (dd,  $J = 14.2$  Hz, 4.2 Hz, 1H), 2.20 (s, 3H)

**<sup>13</sup>C NMR:** 168.59, 139.95, 138.20, 136.44, 136.12, 135.43, 135.18, 132.75, 129.76, 129.35, 129.33, 129.25, 128.72, 128.69, 128.53, 128.40, 128.38, 128.01, 128.00, 127.82, 126.63, 76.25, 73.22, 72.26, 39.72, 37.23, 22.15

**IR (cm<sup>-1</sup>):** 3053, 2923, 1732, 1594, 1484, 1311, 1259, 1123, 965, 763, 697, 591

**HRMS:** calcd. for C<sub>35</sub>H<sub>30</sub>O<sub>4</sub>SNa [M+Na<sup>+</sup>]: 569.17625, found 569.17579

**Synthesis of (1S,2S,4S,5S)-4-(4-methylphenyl)-2-[(1E)-2-(4-methylphenyl)ethenyl]-8,8-dioxo-6,7-diphenyl-8λ<sup>6</sup>-thiabicyclo[3.2.1]oct-6-en-2-yl acetate **32b****



Using **general procedure B**, ester **32b** was obtained in 0.1001g (89% yield) of light yellow oily solid from alcohol **31b** on a 0.19 mmol scale.

**Melting Point:** 78 – 82°C

**TLC solvent:** ( $R_f = 0.50$ ) 2:1 hexane : EtOAc

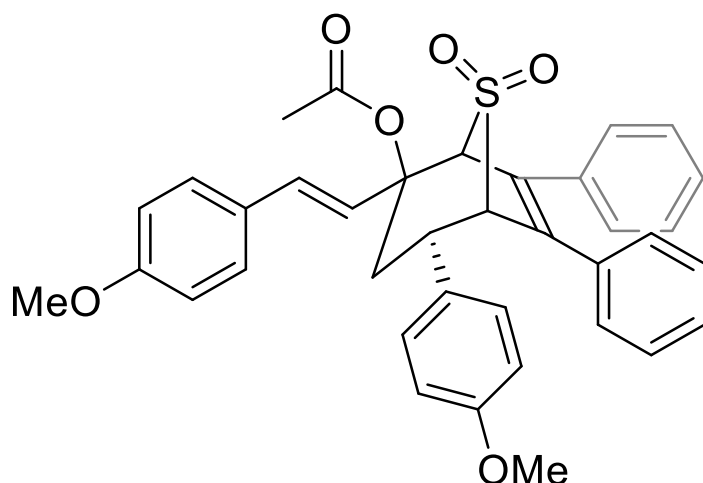
**<sup>1</sup>H NMR:** 7.28 – 7.32 (m, 5H), 7.18 – 7.22 (m, 2H), 7.15 – 7.18 (m, 2H), 6.96 – 7.02 (m, 5H), 6.85 (dm,  $J = 7.8$  Hz, 2H), 6.64 (dd,  $J = 7.4$  Hz, 1.3 Hz, 2H), 6.46 (d,  $J = 16.5$  Hz, 1H), 6.17 (d,  $J = 16.3$  Hz, 1H), 5.48 (d,  $J = 2.3$  Hz, 1H), 4.62 (dd,  $J = 13.1$  Hz, 4.7 Hz, 1H), 4.15 (dm,  $J = 1.1$  Hz, 1H), 2.97 (dd,  $J = 13.5$  Hz, 8.2 Hz, 1H), 2.68 (dd,  $J = 8.4$  Hz, 4.9 Hz, 1H), 2.38 (s, 3H), 2.29 (s, 3H), 2.19 (s, 3H)

**<sup>13</sup>C NMR:** 165.56, 138.20, 137.71, 136.92, 136.16, 135.40, 135.29, 133.69, 131.88, 129.86, 129.79, 129.49, 129.37, 129.35, 128.97, 128.62, 128.08, 127.77, 127.47, 127.39, 126.52, 75.73, 73.22, 72.21, 39.49, 37.43, 23.85, 21.29, 21.18

**IR (cm<sup>-1</sup>):** 3057, 2921, 1740, 1602, 1513, 1444, 1305, 1209, 1034, 974, 811, 760, 697, 578

**HRMS:** calcd. for C<sub>37</sub>H<sub>34</sub>O<sub>4</sub>SNa [M+Na<sup>+</sup>]: 597.20755, found 597.20686

**Synthesis of (1S,2S,4S,5S)-4-(4-methoxyphenyl)-2-[(1E)-2-(4-methoxyphenyl)ethenyl]-8,8-dioxo-6,7-diphenyl-8 $\lambda^6$ -thiabicyclo[3.2.1]oct-6-en-2-yl acetate **32c****



Using **general procedure B**, ester **32c** was obtained in 0.8956g (85% yield) of bright yellow oily solid from alcohol **31c** on a 1.20 mmol scale.

**Melting Point:** 85 – 89°C

**TLC solvent:** ( $R_f = 0.25$ ) 2:1 hexane : EtOAc

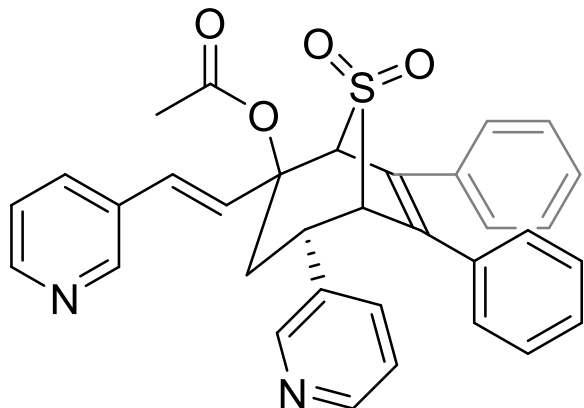
**$^1\text{H NMR}$ :** 7.43 – 7.45 (m, 2H), 7.29 – 7.30 (m, 2H), 6.94 – 7.00 (m, 4H), 6.88 – 6.92 (m, 5H), 6.73 (dd,  $J = 8.8$  Hz, 1.8 Hz, 3H), 6.64 (dd,  $J = 7.2$  Hz, 1.4 Hz, 2H), 6.43 (d,  $J = 16.3$  Hz, 1H), 6.08 (d,  $J = 16.2$  Hz, 1H), 5.48 (d,  $J = 2.3$  Hz, 1H), 4.35 (dd,  $J = 12.8$  Hz, 4.1 Hz, 1H), 4.13 – 4.15 (m, 1H), 3.84 (s, 3H), 3.78 (s, 3H), 2.56 (dd,  $J = 13.8$  Hz, 12.8 Hz, 1H), 2.36 (dd,  $J = 14.0$  Hz, 4.0 Hz, 1H), 2.21 (s, 3H)

**$^{13}\text{C NMR}$ :** 169.46, 138.24, 136.25, 135.42, 135.29, 132.01, 130.75, 129.38, 129.25, 129.14, 129.10, 128.99, 128.68, 128.41, 127.85, 124.55, 123.97, 75.81, 73.23, 72.25, 55.54, 55.38, 39.12, 37.77, 22.08

**IR ( $\text{cm}^{-1}$ ):** 3055, 2934, 1730, 1600, 1511, 1443, 1303, 1247, 1029, 979, 827, 766, 698

**HRMS:** calcd. for  $\text{C}_{37}\text{H}_{34}\text{O}_6\text{SNa}$  [ $\text{M}+\text{Na}^+$ ]: 629.19738, found 629.19684

**Synthesis of (1S,2S,4S,5S)-8,8-dioxo-6,7-diphenyl-4-(pyridin-3-yl)-2-[(1E)-2-(pyridin-3-yl)ethenyl]-8 $\lambda^6$ -thiabicyclo[3.2.1]oct-6-en-2-yl acetate **32d****



Using **general procedure B**, ester **32d** was obtained in 0.0891g (87% yield) of white solid from alcohol **31d** on a 0.18 mmol scale.

**Melting Point:** 98 – 100°C

**TLC solvent:** ( $R_f = 0.53$ ) 2:1 hexane : EtOAc

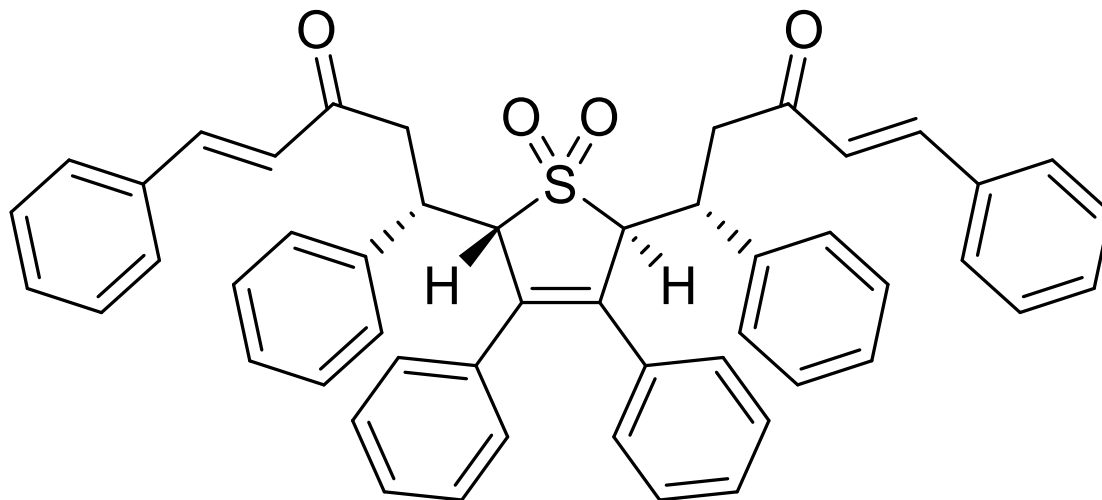
**$^1\text{H NMR}$ :** 8.73 – 8.75 (dm,  $J = 2.3$  Hz, 1H), 8.60 (dd,  $J = 4.8$  Hz, 1.6 Hz, 1H), 8.15 (dd,  $J = 4.4$  Hz, 2.1 Hz, 1H), 7.89 (ddd,  $J = 7.9$  Hz, 2.1 Hz, 1.6 Hz, 2H), 7.68 (dd,  $J = 2.1$  Hz, 1.0 Hz, 2H), 7.32 – 7.39 (m, 5H), 7.02 – 7.10 (m, 3H), 6.83 – 6.85 (m, 3H), 6.46 (d,  $J = 16.6$  Hz, 1H), 6.17 (d,  $J = 16.2$  Hz, 1H), 5.48 (d,  $J = 2.4$  Hz, 1H), 4.68 (dd,  $J = 19.2$  Hz, 5.3 Hz, 1H), 4.08 – 4.12 (m, 1H), 2.71 (dd,  $J = 19.3$  Hz, 17.6 Hz, 1H), 2.55 (dd,  $J = 16.7$  Hz, 5.6 Hz, 1H), 2.30 (s, 3H)

**$^{13}\text{C NMR}$ :** 165.35, 148.65, 148.09, 147.68, 146.29, 137.22, 136.16, 135.45, 133.18, 132.09, 129.01, 128.53, 128.26, 127.09, 126.85, 126.43, 126.28, 122.12, 121.60, 76.59, 73.32, 72.29, 39.76, 37.45, 22.61

**IR ( $\text{cm}^{-1}$ ):** 3059, 2957, 1759, 1713, 1699, 1494, 1446, 1306, 1205, 1124, 963, 760, 695, 579

**HRMS:** calcd. for  $\text{C}_{33}\text{H}_{28}\text{N}_2\text{O}_4\text{SNa}$  [ $\text{M}+\text{Na}^+$ ]: 571.16675, found 571.16699

**Synthesis of (S,E)-1-((2S,5S)-1,1-dioxido-5-((S,E)-3-oxo-1,5-diphenylpent-4-en-1-yl)-3,4-diphenyl-2,5-dihydrothiophen-2-yl)-1,6-diphenylhex-5-en-3-one **28****



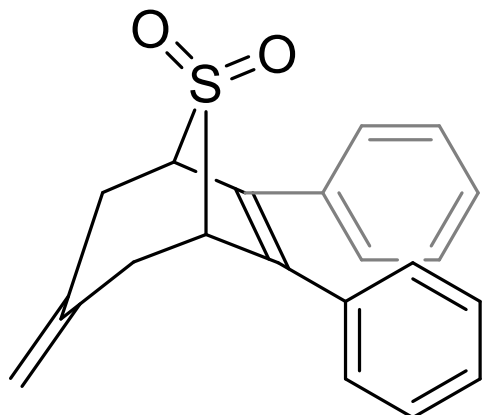
Using **general procedure A** albeit with two equivalent of LiHMDS, sulfone **28** was obtained as 0.315g (41% yield) of yellow solid from sulfone **4b** on a 1.04 mmol scale.

**TLC solvent:** ( $R_f = 0.35$ ) 7:2 hexane: EtOAc

**$^1\text{H NMR}$ :** 7.45 – 7.39 (m, 4H), 7.42 (dd,  $J = 15.84$  Hz, 2H), 7.32 – 7.29 (m, 7H), 7.12 – 7.07 (m, 8H), 7.07 – 7.03 (dm,  $J = 7.33$  Hz, 4H), 7.03 – 6.98 (m, 5H), 6.66 (dm,  $J = 7.84$  Hz, 2H), 6.63 (dd,  $J = 16.26$  Hz, 2H), 4.24 (d,  $J = 4.36$  Hz, 2H), 3.82 – 3.76 (m, 2H), 3.55 (dd,  $J = 17.7$  Hz, 6.9 Hz, 2H), 3.06 (dd,  $J = 16.5$  Hz, 7.4 Hz, 2H)

**$^{13}\text{C NMR}$ :** 197.72, 143.06, 138.51, 135.99, 134.51, 134.44, 130.66, 129.47, 129.05, 128.48, 128.35, 128.07, 127.90, 127.26, 126.10, 70.66, 47.78, 38.74

Synthesis of 3-methylidene-6,7-diphenyl-8 $\lambda^6$ -thiabicyclo[3.2.1]oct-6-ene-8,8-dione  
**40**



Using **general procedure C**, sulfone **40** was obtained as 1.02g (61% yield) of crystalline white solid from sulfone **4b** on a 5.18 mmol scale.

**Melting Point:** 142 – 144°C

**TLC solvent:** ( $R_f = 0.33$ ) 5:1 hexane: EtOAc

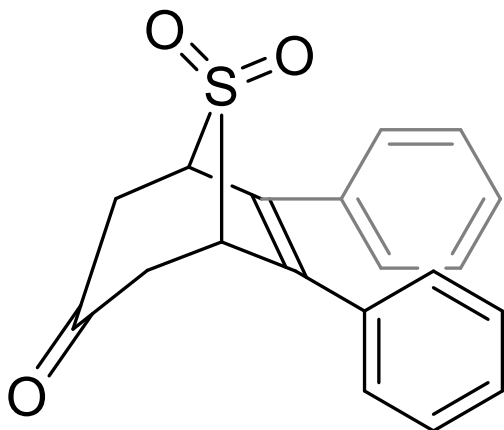
**$^1\text{H NMR}$ :** 7.22 – 7.27 (m, 6H), 7.13 – 7.18 (m, 4H), 4.99 (t,  $J = 2.0$  Hz, 2H), 3.96 (dm,  $J = 2.7$  Hz, 2H), 3.34 (dd,  $J = 15.8$  Hz, 2.3 Hz, 2H), 2.82 (dd,  $J = 16.0$  Hz, 4.8 Hz, 2H)

**$^{13}\text{C NMR}$ :** 137.17, 136.38, 135.21, 128.77, 128.40, 128.22, 118.15, 65.00, 36.67

**IR ( $\text{cm}^{-1}$ ):** 3057, 2911, 1651, 1497, 1444, 1294, 1253, 1175, 1109, 911, 762, 700, 582, 561

**HRMS:** calcd. for  $\text{C}_{20}\text{H}_{18}\text{O}_2\text{S}$  [ $\text{M}+\text{H}^+$ ]: 323.11058, found 323.11009

### Synthesis of 6,7-diphenyl-8λ<sup>6</sup>-thiabicyclo[3.2.1]oct-6-ene-3,8,8-trione **41**



Under open atmosphere, a round-bottom flask was charged with an appropriate stir bar, sulfone **40** (0.2611g, 0.81mmol, 1.0 equiv.) prior to dissolving in DCM (50 mL, 60 mL/mmol). The reaction flask was allowed to stir at  $-78^{\circ}\text{C}$  using a cooling bath of dry ice and acetone, before  $\text{O}_3$  being introduced into the reaction mixture via bubbling at a flow rate of 7L/min. The introduction of  $\text{O}_3$  was continued for 15 min., followed by the addition of  $\text{Me}_2\text{S}$  to quench the reaction mixture. The solution was allowed to continue stirring overnight and gradually warm to ambient temperature. The yellow reaction mixture was then concentrated under reduced pressure to remove DCM. 3 x 20mL EtOAc was used for extraction, and then washed with 3 x 20mL  $\text{H}_2\text{O}$  and 2 x 20mL brine sequentially. The combined organic extracts were dried with anhydrous  $\text{Na}_2\text{SO}_4$ , and subsequent concentration under reduced pressure provided crude product **41** as a reddish-brown solid. Purification was done via flash column chromatography using a gradient elution of 5:1 hexane: EtOAc (spiked with 5% v/v  $\text{NEt}_3$ ) to 2:1 hexane: EtOAc (spiked with 5% v/v  $\text{NEt}_3$ ) to afford a total of 0.2425g (92% yield)  $\geq 90\%$  pure product as crystalline white solids.

**Melting Point:** 138 – 140 $^{\circ}\text{C}$

**TLC solvent:** ( $R_f = 0.26$ ) 3:1 hexane: EtOAc

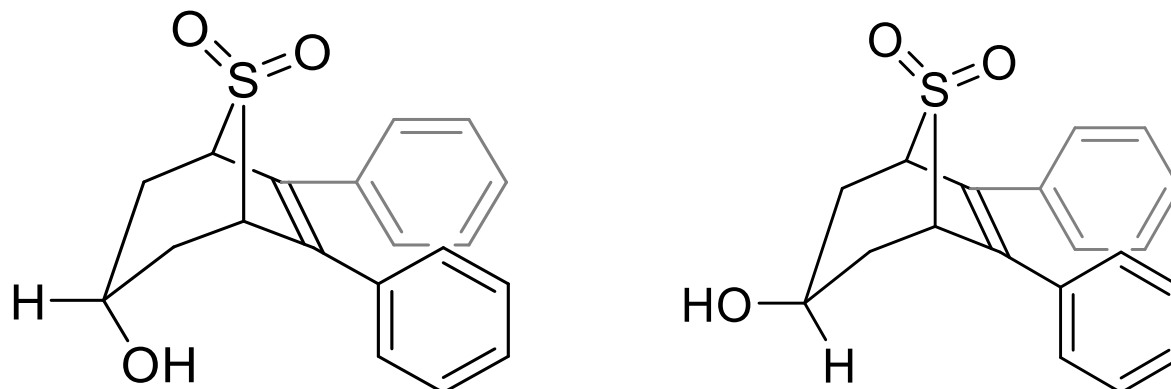
**$^1\text{H NMR}$ :** 7.29 (dd,  $J = 5.0$  Hz, 2.1 Hz, 6H), 7.13 – 7.18 (m, 4H), 4.16 – 4.21 (m, 2H), 3.52 (dm,  $J = 17.0$  Hz, 2H), 3.04 (dm,  $J = 17.0$  Hz, 2H)

**$^{13}\text{C NMR}$  (in acetone- $d_6$ ):** 201.49, 139.52, 135.48, 129.61, 129.51, 129.06, 63.85, 45.37

**IR ( $\text{cm}^{-1}$ ):** 3055, 2965, 1714, 1575, 1489, 1305, 1259, 1183, 1115, 761, 693, 561, 444

**HRMS:** calcd. for  $\text{C}_{19}\text{H}_{16}\text{O}_3\text{SNa}$  [ $\text{M}+\text{Na}^+$ ]: 347.07178, found 347.07100

### Synthesis of 3-hydroxy-6,7-diphenyl-8λ<sup>6</sup>-thiabicyclo[3.2.1]oct-6-ene-8,8-dione **42a** and **42b**



A round-bottom flask was charged with an appropriate size stir bar and ketone **41** (0.100g, 100mg, 0.31 mmol), and then dissolved in THF (1.5mL, 5 mL/mmol). The solution was then placed under a cooling bath of 0°C using ice and H<sub>2</sub>O. Subsequently, NaBH<sub>4</sub> (0.0620g, 1.64mmol, 5 equiv.) was added into the reaction mixture in one portion. The reaction was stirred for 24 hours and gradually warm to ambient temperature, or until TLC indicated complete consumption of ketone **41**. Subsequently, the reaction mixture was quenched with a mixture of 1:1 MeOH: H<sub>2</sub>O, and allowed to stir at ambient temperature for 15 min. Concentration under reduced pressure was performed to remove THF, before extraction with EtOAc (4 x 10mL). The combined organic extracts were then washed with 4 x 10mL H<sub>2</sub>O and 2 x 10mL brine sequentially, and dried over anhydrous Na<sub>2</sub>SO<sub>4</sub>. The crude product was obtained after concentration under reduced pressure as light yellow solids. Purification was performed via flash column chromatography using a gradient elution of 3:1 hexane: EtOAc (spiked with 5% v/v NEt<sub>3</sub>) to 1:2 hexane:EtOAc (spiked with 5% v/v NEt<sub>3</sub>) to yield a total of 0.0607g (61% yield) of both alcohol **42a** and **42b** as white solids. Both regioisomers were inseparable by column chromatography.

**Melting Point:** 136 – 137°C

**TLC solvent:** (R<sub>f</sub> = 0.08) 2:1 hexane: EtOAc

**<sup>1</sup>H NMR (major diastereomer):** 7.24 – 7.30 (m, 6H), 7.16 – 7.20 (m, 4H), 4.22 – 4.30 (dd, J = 11.2 Hz, 5.3 Hz, 1H), 3.93 (d, J = 4.6 Hz, 2H), 2.92 (dd, J = 15.3 Hz, 4.9 Hz, 2H), 2.47 (dm, J = 15.6 Hz, 2H), 1.74 (d, J = 6.0 Hz, 1H)

**<sup>1</sup>H NMR (minor diastereomer):** 7.24 – 7.30 (m, 6H), 7.16 – 7.20 (m, 4H), 4.03 – 4.12 (m, 1H), 4.00 (d, J = 4.9 Hz, 2H), 2.57 – 2.69 (m, 2H), 2.51 (d, J = 10 Hz, 2H), 1.48 (d, J = 8.0 Hz, 1H)

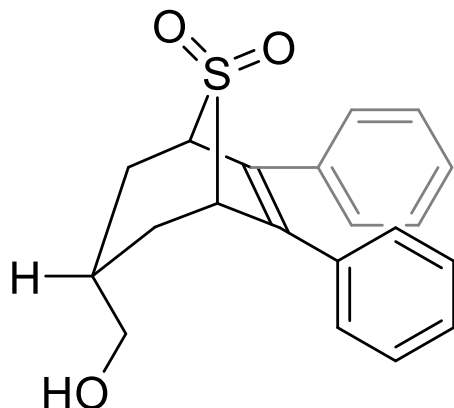
**<sup>13</sup>C NMR (major diastereomer, in acetone-d<sub>6</sub>):** 137.92, 136.38, 129.58, 129.14, 129.07, 65.36, 63.92, 35.96

**<sup>13</sup>C NMR (minor diastereomer, in acetone-d<sub>6</sub>):** 137.37, 135.97, 129.26, 129.11, 128.53, 64.72, 62.73, 34.63

**IR (cm<sup>-1</sup>):** 3508, 3058, 2959, 1599, 1489, 1292, 1111, 1061, 761, 694, 558

**HRMS:** calcd. for C<sub>19</sub>H<sub>19</sub>O<sub>3</sub>S [M+H<sup>+</sup>]: 327.10549, found 327.10490

### Synthesis of 3-(hydroxymethyl)-6,7-diphenyl-8λ<sup>6</sup>-thiabicyclo[3.2.1]oct-6-ene-8,8-dione **43**



A round-bottom flask was charged with an appropriate stir bar, sulfone **40** (0.500g, 1.55mmol, 1.0 equiv.) prior to dissolving in THF (8.0 mL, 5 mL/mmol). The reaction flask was allowed to stir at 0 °C using a cooling bath of ice and water, before the addition of 9-BBN (0.2843g, 4.66 mL, 2.23mmol, 1.5 equiv., 0.5M in THF) in dropwise manner. The reaction mixture was allowed to continue stirring at 0 °C and gradually warm to ambient temperature for 3 hr or until TLC indicated complete consumption of sulfone **40**. Subsequently, the reaction mixture was then transferred into an Erlenmyer flask containing 1M NaOH(aq.) (15.5mL, 15.5mmol, 5 equiv.) and placed at 0 °C prior to the addition of H<sub>2</sub>O<sub>2</sub> (0.527g, 1.51mL, 15.5mmol, 5 equiv., 35% w/v) in a dropwise manner. The reaction mixture was allowed to continue stirring for 1 hr, and then concentrated under reduce pressure to remove THF. Extraction was performed using 3 x 20mL EtOAc, and the combined organic layer was then washed with 3 x 20mL H<sub>2</sub>O and 3 x 20mL brine sequentially. The organic layer was then dried over anhydrous Na<sub>2</sub>SO<sub>4</sub>, and then concentrated under reduce pressure to provide a total of 0.2277g (43% yield) of ≥ 90% pure product as white oily solid.

**Melting Point:** 98 – 100°C

**TLC solvent:** (R<sub>f</sub> = 0.36) 2:1 hexane: EtOAc

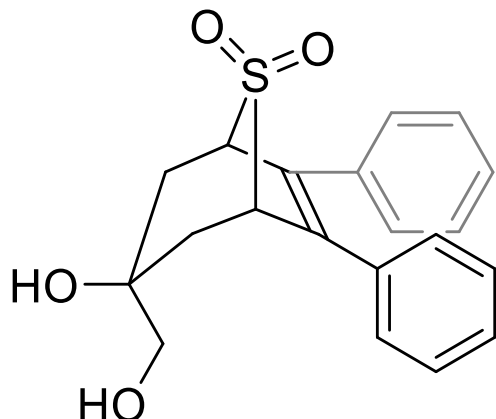
**<sup>1</sup>H NMR:** 7.23 – 7.30 (m, 6H), 7.07 – 7.15 (m, 4H), 3.95 (dd, J = 6.3 Hz, 2.7 Hz, 2H), 3.64 (dd, J = 7.4 Hz, 2.7 Hz, 2H), 2.77 (dq, J = 14.6 Hz, 3.2 Hz, 1H), 2.58 (dq, J = 14.6 Hz, 2.3 Hz, 1H), 2.43 (br s, 1H), 2.29 (ddd, J = 12.0 Hz, 3.0 Hz, 1.3 Hz, 1H), 2.18 (ddd, J = 12.8 Hz, 3.0 Hz, 1H), 2.08 – 2.15 (m, 1H)

**<sup>13</sup>C NMR (in acetone-d<sub>6</sub>):** 136.53, 132.34, 129.59, 129.40, 129.03, 71.58, 67.25, 61.49, 35.35, 32.82, 27.29

**IR (cm<sup>-1</sup>):** 3445, 2922, 1683, 1599, 1491, 1410, 1297, 1250, 1109, 1132, 1066, 759, 694, 563, 469

**HRMS:** calcd. for C<sub>20</sub>H<sub>21</sub>O<sub>3</sub>S [M+H<sup>+</sup>]: 341.12114, found 341.12135

**Synthesis of 3-hydroxy-3-(hydroxymethyl)-6,7-diphenyl-8λ<sup>6</sup>-thiabicyclo[3.2.1]oct-6-ene-8,8-dione 45<sup>1</sup>**



A round-bottom flask was charged with an appropriate size stir bar and sulfone **40** (0.400g, 1.24 mmol), and then dissolved in a mixture of 4:1 acetone: H<sub>2</sub>O (6.5mL, 5 mL/mmol). Subsequently, OsO<sub>4</sub> (0.0017g, 0.43mL, 1 mol%, 0.0065 mmol, 4 wt% in H<sub>2</sub>O) and NMO (0.2905g, 2.0 equiv., 2.48 mmol) was added into the reaction mixture sequentially. The reaction was stirred at ambient temperature for 24 hours, and then quenched with Na<sub>2</sub>S<sub>2</sub>O<sub>4</sub>. H<sub>2</sub>O was added into the reaction mixture for dilution, and allowed to stir at ambient temperature for 15 min. before extraction with EtOAc (4 x 10mL). The combined organic extracts were then washed with 4 x 10mL H<sub>2</sub>O and 2 x 10mL brine sequentially, and dried over anhydrous Na<sub>2</sub>SO<sub>4</sub>. The product was obtained after concentration under reduced pressure to yield a total of 0.1501g (75% yield) of white solid.

**Melting Point:** 124 – 122°C

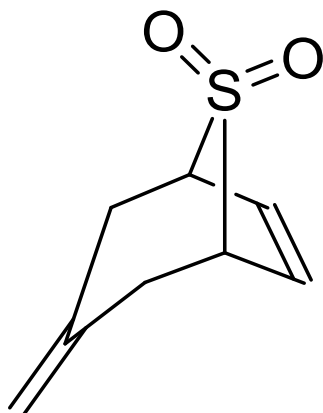
**TLC solvent:** (R<sub>f</sub> = 0.38) 3:1 hexane: EtOAc

**<sup>1</sup>H NMR:** 7.12 – 7.20 (m, 6H), 7.04 – 7.12 (m, 4H), 3.88 – 3.83 (m, 2H), 3.42 (s, 2H), 2.86 – 3.05 (br s, 2H), 2.57 (dd, J = 15.2 Hz, 3.8 Hz, 2H), 2.47 (dd, J = 15.2 Hz, 1.8 Hz, 2H)

**<sup>13</sup>C NMR:** 128.96, 127.92, 127.46, 127.19, 127.09, 70.48, 69.54, 63.96, 35.58

**IR (cm<sup>-1</sup>):** 3516, 3391, 3046, 2924, 1654, 1599, 1490, 1444, 1292, 1251, 1116, 1093, 1068, 1051, 760, 694, 562, 455

**HRMS:** calcd. for C<sub>20</sub>H<sub>20</sub>O<sub>4</sub>SNa [M+Na<sup>+</sup>]: 379.09800, found 379.09750

**Synthesis of 3-methylidene-8 $\lambda^6$ -thiabicyclo[3.2.1]oct-6-ene-8,8-dione **47****

Using **general procedure C**, followed by purification via flash column chromatography with a column volume of hexane (spiked with 5% v/v NEt<sub>3</sub>), and a gradient elution of 3:1 hexane: EtOAc (spiked with 5% v/v NEt<sub>3</sub>) to 2:1 hexane: EtOAc (spiked with 5% v/v NEt<sub>3</sub>), sulfone **47** was obtained as 7.98g (67% yield) of crystalline colourless solid from sulfone **4a** on a 71.45 mmol scale.

**Melting Point:** 64 – 68°C

**TLC solvent:** (R<sub>f</sub> = 0.41) 3:1 hexane: EtOAc

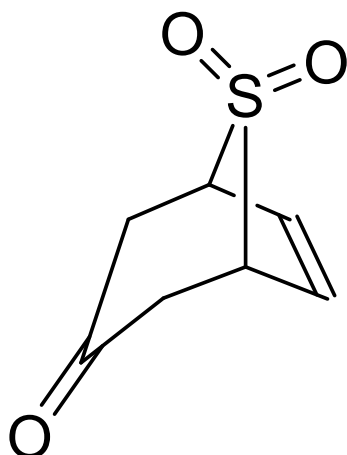
**<sup>1</sup>H NMR:** 6.44 (d, J = 2.9 Hz, 2H), 4.85 (t, J = 2.1 Hz, 2H), 3.57 – 3.62 (m, 2H), 3.16 (dd, J = 15.8 Hz, 2.0 Hz, 2H), 2.54 (dd, J = 15.8 Hz, 4.5 Hz, 2H)

**<sup>13</sup>C NMR:** 136.94, 130.82, 118.03, 58.75, 36.41

**IR (cm<sup>-1</sup>):** 3048, 2960, 2920, 1646, 1420, 1343, 1289, 1182, 1122, 897, 751, 702, 613

**HRMS:** calcd. for C<sub>8</sub>H<sub>10</sub>O<sub>2</sub>SNa [M+Na<sup>+</sup>]: 193.02992, found 193.02952

### Synthesis of 8 $\lambda^6$ -thiabicyclo[3.2.1]oct-6-ene-3,8,8-trione **52**



Under open atmosphere, a round-bottom flask was charged with an appropriate stir bar, sulfone **47** (2.50g, 17.62mmol, 1.0 equiv.) prior to dissolving in a mixture of 9:1 MeCN: H<sub>2</sub>O (88 mL, 5 mL/mmol). The reaction flask was allowed to stir at 0°C using a cooling bath of ice and water, before O<sub>3</sub> being introduced into the reaction mixture via bubbling at a flow rate of 7L/min until TLC indicated complete consumption of ketone **52**. The yellow reaction mixture was then concentrated under reduced pressure to remove MeCN. 3 x 50mL EtOAc was used for extraction, and then washed with 3 x 50mL H<sub>2</sub>O and 2 x 50mL brine sequentially. The combined organic extracts were dried with anhydrous Na<sub>2</sub>SO<sub>4</sub>, and subsequent concentration under reduce pressure provided a total of 1.900g (77% yield) of ≥ 90% pure product as light yellow solids.

**Melting Point:** 58 – 62°C

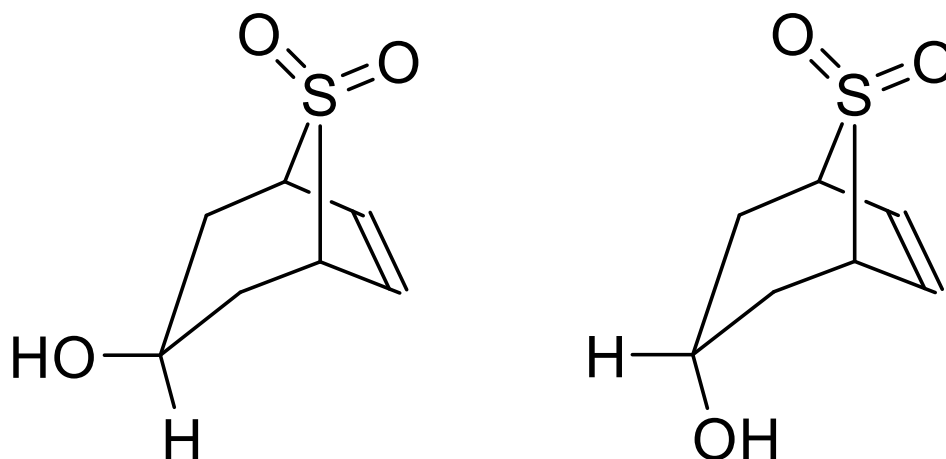
**TLC solvent:** (R<sub>f</sub> = 0.21) 3:1 hexane: EtOAc

**<sup>1</sup>H NMR:** 6.68 (d, J = 2.9 Hz, 2H), 3.80 – 3.91 (m, 2H), 3.34 (dd, J = 18.6 Hz, 2.4 Hz, 2H), 2.76 (dd, J = 19.1 Hz, 2.4 Hz, 2H)

**<sup>13</sup>C NMR:** 200.99, 133.34, 56.80, 45.17

**HRMS:** calcd. for C<sub>7</sub>H<sub>8</sub>O<sub>3</sub>SNa [M+Na<sup>+</sup>]: 195.00861, found 195.00870

**Synthesis of 3-hydroxy-8λ<sup>6</sup>-thiabicyclo[3.2.1]oct-6-ene-8,8-dione **57a** and **57b****



A round-bottom flask was charged with an appropriate stir bar, ketone **52** (0.400g, 400mg, 2.35 mmol, 1.0 equiv.) prior to dissolving in THF (10 mL, 5 mL/mmol). The reaction flask was then placed at 0 °C using a cooling bath of ice and water, before the addition of NaBH<sub>4</sub> (0.1334g, 133.4mg, 3.53mmol, 1.5 equiv.) in one portion at 0 °C. The reaction mixture was allowed to stir overnight or until TLC indicated complete consumption of ketone **52**. The reaction mixture was then quenched by the addition of MeOH at 0 °C in a dropwise manner, and then diluted with H<sub>2</sub>O. Concentration under reduced pressure was done to remove THF and MeOH, and then 4 x 10mL EtOAc was used for extraction. The combined organic extracts were then washed with 3 x 10mL H<sub>2</sub>O and 2 x 10mL brine sequentially before drying under anhydrous Na<sub>2</sub>SO<sub>4</sub>. Subsequent concentration under reduce pressure provided a total of 0.0674g (67.4mg, 39% yield) of ≥ 90% pure product as white solids. Both diastereomers **57a** and **57b** were inseparable by flash column chromatography.

**Melting Point:** 118 – 120°C

**TLC solvent:** (R<sub>f</sub> = 0.25) EtOAc

**<sup>1</sup>H NMR (major diastereomer):** 6.47 (d, J = 2.1 Hz, 2H), 3.70 – 3.80 (m, 1H), 3.63 – 3.69 (m, 2H), 2.33 – 2.41 (m, 2H), 2.24 – 2.33 (m, 2H)

**<sup>1</sup>H NMR (minor diastereomer):** 6.67 (d, J = 2.1 Hz, 2H), 3.70 – 3.80 (m, 1H), 3.56 – 3.65 (m, 2H), 3.47 (dd, J = 16.3 Hz, 7.4 Hz, 2H), 2.15 – 2.21 (m, 2H)

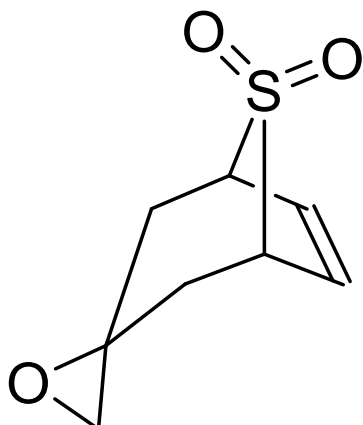
**<sup>13</sup>C NMR (major diastereomer):** 129.81, 63.84, 58.20, 33.42

**<sup>13</sup>C NMR (minor diastereomer):** 134.18, 63.80, 58.20, 33.20

**IR (cm<sup>-1</sup>):** 3535, 3059, 2933, 1652, 1449, 1338, 1281, 1186, 747, 701, 605

**HRMS:** calcd. for C<sub>7</sub>H<sub>10</sub>O<sub>3</sub>SNa [M+Na<sup>+</sup>]: 197.02431, found 197.02429

### Synthesis of 8 $\lambda^6$ -thiaspiro[bicyclo[3.2.1]octane-3,2'-oxiran]-6-ene-8,8-dione 58<sup>2</sup>



Under open atmosphere, a round-bottom flask was charged with an appropriate stir bar, sulfone **47** (1.00g, 5.87mmol, 1.0 equiv.) prior to dissolving in DCM (6.0 mL, 1 mL/mmol). The reaction flask was allowed to stir at 0 °C using a cooling bath of ice and water, before the addition of *m*CPBA (1.9745g, 8.81mmol, 1.5 equiv., max 77% purity) in one portion. The reaction mixture was allowed to continue stirring at 0 °C and gradually warm to ambient temperature overnight or until TLC indicated complete consumption of sulfone **47**. Filtration was performed in order to remove *m*CBA, and then diluted with DCM. The combined organic layer was then washed with 4 x 30mL NaHCO<sub>3</sub>(aq), and 3 x 30mL brine sequentially before drying over anhydrous Na<sub>2</sub>SO<sub>4</sub>. Concentration under reduced pressure provided a total of 1.05g (95% yield) of  $\geq 90\%$  pure product as crystalline white solids.

**Melting Point:** 130 – 131°C

**TLC solvent:** ( $R_f = 0.07$ ) 2:1 hexane: EtOAc

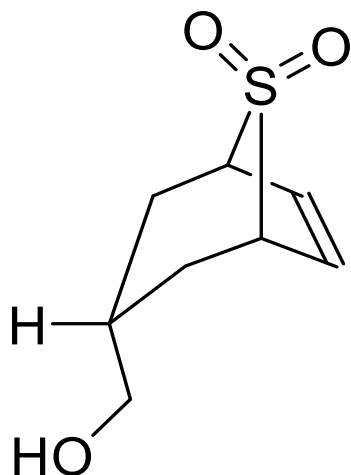
**<sup>1</sup>H NMR (in acetone-d<sub>6</sub>):** 6.65 (d,  $J = 2.9$  Hz, 2H), 3.70 – 3.73 (m, 2H), 3.00 (dd,  $J = 15.5$  Hz, 1.5 Hz, 2H), 2.40 (s, 2H), 1.67 (ddm,  $J = 15.4$  Hz, 1.2 Hz, 2H)

**<sup>13</sup>C NMR (in acetone-d<sub>6</sub>):** 133.70, 58.96, 52.48, 46.61, 38.44

**IR (cm<sup>-1</sup>):** 3054, 2990, 1599, 1347, 1247, 1228, 1120, 842, 766, 729, 597

**HRMS:** calcd. for C<sub>8</sub>H<sub>10</sub>O<sub>3</sub>SNa [ $M+Na^+$ ]: 209.02483 found 209.02426

### Synthesis of 3-(hydroxymethyl)-8λ<sup>6</sup>-thiabicyclo[3.2.1]oct-6-ene-8,8-dione **59**



A round-bottom flask was charged with an appropriate stir bar, sulfone **47** (0.500g, 2.94mmol, 1.0 equiv.) prior to dissolving in THF (15 mL, 5 mL/mmol). The reaction flask was allowed to stir at 0 °C using a cooling bath of ice and water, before the addition of 9-BBN (0.5381g, 8.82 mL, 4.41mmol, 1.5 equiv., 0.5M in THF) in dropwise manner. The reaction mixture was allowed to continue stirring at 0 °C and gradually warm to ambient temperature for 3 hr or until TLC indicated complete consumption of sulfone **47**.

Subsequently, the reaction mixture was then transferred into an Erlenmeyer flask containing 1M NaOH(aq.) (14.7mL, 14.7mmol, 5 equiv.) and placed at 0 °C prior to the addition of H<sub>2</sub>O<sub>2</sub> (0.500g, 1.43mL, 14.7mmol, 5 equiv., 35% w/v) in a dropwise manner. The reaction mixture was allowed to continue stirring for 1 hr, and then concentrated under reduce pressure to remove THF. Extraction was performed using 3 x 15mL EtOAc, and the combined organic layer was then washed with 3 x 15mL H<sub>2</sub>O and 3 x 15mL brine sequentially. The organic layer was then dried over anhydrous Na<sub>2</sub>SO<sub>4</sub>, and then concentrated under reduce pressure to provide crude product **59**. Purification via flash column chromatography using a gradient elution of 3:1 hexane: EtOAc (spiked with 5% v/v NEt<sub>3</sub>) to 1:2 hexane:EtOAc (spiked with 5% v/v NEt<sub>3</sub>) afforded a total of 0.3165g (57% yield) of ≥ 90% pure product as light yellow oil.

**TLC solvent:** (R<sub>f</sub> = 0.20) 2:1 hexane: EtOAc

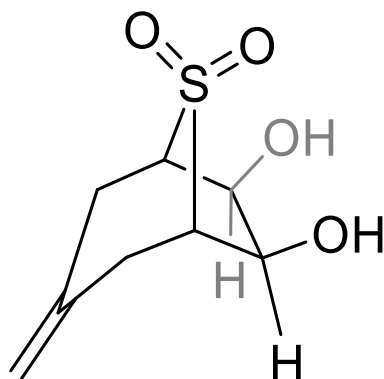
**<sup>1</sup>H NMR:** <sup>1</sup>H NMR: 6.42 – 6.48 (dm, J = 8.4 Hz, 2H), 3.77 – 3.85 (dm, J = 9.5 Hz, 2H), 3.52 – 3.59 (m, 2H), 2.38 (dm, J = 15.1 Hz, 1H), 2.19 – 2.28 (dm, J = 12.0 Hz, 1H), 2.14 – 2.23 (dd, J = 15.1 Hz, 4.0 Hz, 1H), 1.98 – 2.04 (dm, J = 12.7 Hz, 1H), 1.87 (t, J = 9.4 Hz, 1H)

**<sup>13</sup>C NMR:** 129.78, 129.57, 71.79, 59.26, 58.63, 39.73, 32.56, 18.82

**IR (cm<sup>-1</sup>):** 3054, 2990, 1599, 1347, 1247, 1228, 1120, 842, 766, 729, 597

**HRMS:** calcd. for C<sub>8</sub>H<sub>10</sub>O<sub>3</sub>SNa [M+Na<sup>+</sup>]: 209.02483 found 209.02426

**Synthesis of (1R,5S,6R,7S)-6,7-dihydroxy-3-methylidene-8 $\lambda$ <sup>6</sup>-thiabicyclo[3.2.1]octane-8,8-dione **60**<sup>3</sup>**



A round-bottom flask was charged with an appropriate size stir bar and sulfone **47** (0.100g, 100mg, 0.59 mmol), and then dissolved in a mixture of 4:1 acetone: H<sub>2</sub>O (3.0mL, 5 mL/mmol). Subsequently, NMO (0.1043g, 1.5 equiv., 0.89 mmol) and OsO<sub>4</sub> (0.010g, 0.25mL, 7 mol%, 0.004 mmol, 4 wt% in H<sub>2</sub>O) was added into the reaction mixture sequentially. The reaction was stirred at ambient temperature for 48 hours, and then quenched by adding Na<sub>2</sub>S<sub>2</sub>O<sub>4</sub> and allowed to stir at ambient temperature for 15 min. Concentration under reduced pressure was performed in order to remove acetone. Extraction was done using EtOAc (4 x 15mL), and the combined organic extracts were then washed with 3 x 15mL H<sub>2</sub>O and 2 x 15mL brine sequentially. The organic layer was dried over anhydrous Na<sub>2</sub>SO<sub>4</sub>, and concentrated under reduced pressure to yield a total of 0.050g (500mg, 50% yield) of diol **60** as white solid.

**Melting Point:** 76 – 78°C

**TLC solvent:** (R<sub>f</sub> = 0.24) 3:1 hexane: EtOAc

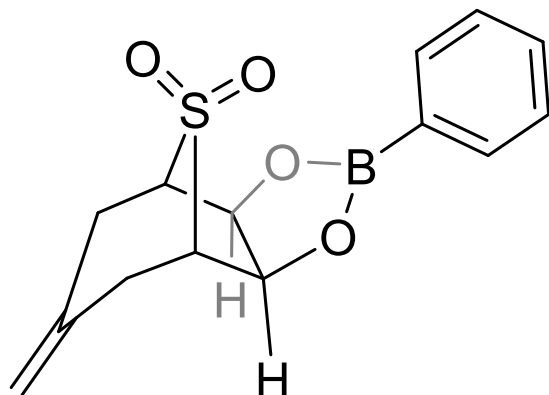
**<sup>1</sup>H NMR:** 5.02 (t, J = 2.1 Hz, 2H), 4.28 – 4.34 (m, 2H), 3.18 (dd, J = 5.9 Hz, 2.5 Hz, 2H), 3.13 (dm, J = 15.4 Hz, 2H), 2.63 (dm, J = 15.4 Hz, 4.87 Hz, 2H)

**<sup>13</sup>C NMR:** 137.00, 117.60, 69.78, 61.79, 36.75

**IR (cm<sup>-1</sup>):** 3449, 3375, 3046, 2986, 1647, 1434, 1413, 1307, 1290, 1173, 1161, 1112, 873, 582, 565

**HRMS:** calcd. for C<sub>8</sub>H<sub>12</sub>O<sub>4</sub>SNa [M+Na<sup>+</sup>]: 227.03540, found 227.03475

**Synthesis of (1R,2S,6R,7S)-9-methylidene-4-phenyl-3,5-dioxo-11 $\lambda^6$ -thia-4-boratricyclo[5.3.1.0<sup>2,6</sup>]undecane-11,11-dione **62****



A round-bottom flask was charged with an appropriate size stir bar, sulfone **47** (0.200g, 200mg, 1.17 mmol, 1.0 equiv.), PhB(OH)<sub>2</sub> (0.5706g, 4.68mmol, 4.0 equiv.), and 4Å molecular sieves (1.17g, 1.0 g/mmol) prior to dissolving in DCM (12.0mL, 10 mL/mmol). Subsequently, NMO (0.5483g, 4.68 mmol, 4.0 equiv.) and OsO<sub>4</sub> (0.0153g, 0.38mL, 5 mol%, 0.06 mmol, 4 wt% in H<sub>2</sub>O) was added into the reaction mixture sequentially at ambient temperature. The reaction was stirred at ambient temperature overnight or until TLC indicated complete consumption of sulfone **47**. The reaction mixture was then quenched by adding Na<sub>2</sub>S<sub>2</sub>O<sub>4</sub> and allowed to stir at ambient temperature for 15 min. Decantation was performed and the reaction vessel was washed with 2 x 10mL DCM. The combined organic extracts were then washed with 2 x 15mL brine sequentially and dried over anhydrous Na<sub>2</sub>SO<sub>4</sub>. Concentration under reduced pressure was done to yield a total of 1.199g (88% yield) of boronic ester **62** as flaky amber solid.

**Melting Point:** 114 – 118°C

**TLC solvent:** (R<sub>f</sub> = 0.34) 1:1 hexane : EtOAc

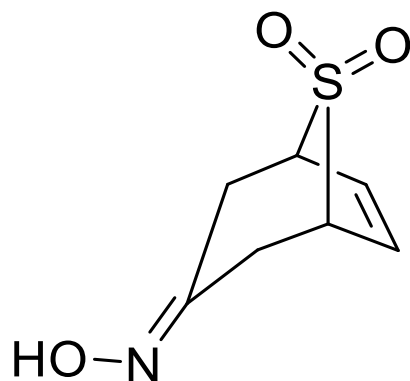
**<sup>1</sup>H NMR:** 7.68 – 7.76 (m, 2H), 7.36 – 7.49 (m, 1H), 7.27 – 7.36 (m, 2H), 4.98 (m, 2H), 3.33 – 3.38 (m, 2H), 3.29 – 3.33 (m, 2H), 3.16 (dd, J = 15.3 Hz, 2.1 Hz, 2H), 2.56 (dd, J = 15.7 Hz, 4.7 Hz, 2H)

**<sup>13</sup>C NMR:** 136.71, 134.97, 131.91, 128.71, 128.00, 118.10, 59.93, 59.17, 36.83

**IR (cm<sup>-1</sup>):** 3057, 2923, 1368, 1329, 1207, 1165, 1124, 1089, 698, 648, 586, 498, 412

**HRMS:** calcd. for C<sub>14</sub>H<sub>15</sub>O<sub>4</sub>SBNa [M+Na<sup>+</sup>]: 313.06761, found 313.06726

**Synthesis of 3-(hydroxyimino)-8λ<sup>6</sup>-thiabicyclo[3.2.1]oct-6-ene-8,8-dione **67a****



Using **general procedure D**, oxime **67a** was obtained as 0.1056g (96% yield) of bright yellow-orange solid from ketone **52** on a 0.59 mmol scale.

**Melting Point:** 98 – 100°C

**TLC solvent:** ( $R_f = 0.10$ ) 2:1 hexane:EtOAc

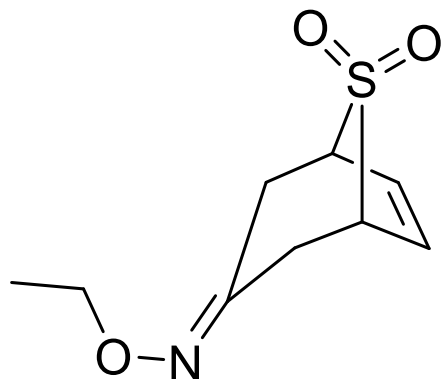
**<sup>1</sup>H NMR (acetone-d<sub>6</sub>):** 6.56 (d,  $J = 3.0$  Hz, 2H), 3.78 – 3.86 (m, 2H), 3.60 (dm,  $J = 17$  Hz, 2H), 3.06 (d,  $J = 16.6$  Hz, 2H), 2.79 (dm,  $J = 16.0$  Hz, 2H), 2.67 (dm,  $J = 17.2$  Hz, 2H)

**<sup>13</sup>C NMR (acetone-d<sub>6</sub>):** 149.67, 133.50, 132.88, 58.46, 57.36, 35.32, 29.40

**IR (cm<sup>-1</sup>):** 3387, 3050, 2954, 1716, 1647, 1346, 1268, 1184, 960, 715, 585

**HRMS:** calcd. for C<sub>8</sub>H<sub>11</sub>NO<sub>2</sub>SNa [M+Na<sup>+</sup>]: 210.01952, found 210.01989

**Synthesis of 3-(ethoxyimino)-8 $\lambda^6$ -thiabicyclo[3.2.1]oct-6-ene-8,8-dione **67b****



Using **general procedure D**, oxime **67b** was obtained as 0.1251g (89% yield) of light orange solid from ketone **52** on a 0.59 mmol scale.

**Melting Point:** 94 – 97°C

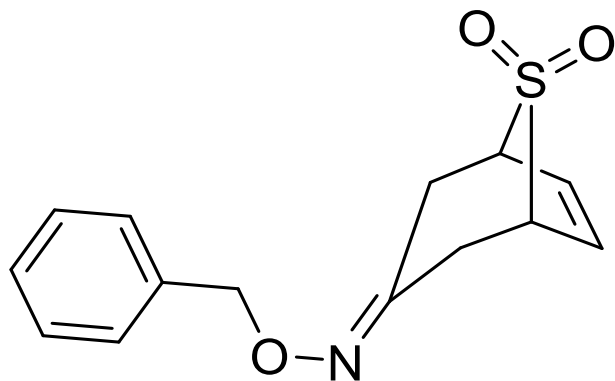
**TLC solvent:** ( $R_f = 0.26$ ) 2:1 hexane : EtOAc

**$^1\text{H NMR}$ :** 6.54 (d,  $J = 3.0$  Hz, 2.4 Hz, 2H), 4.06 (qd,  $J = 7.1$  Hz, 2.5 Hz, 2H), 3.71 – 3.76 (m, 1H), 3.67 – 3.71 (m, 1H), 3.56 (dm,  $J = 17.0$  Hz, 1H), 3.25 (dm,  $J = 16.1$  Hz, 1H), 2.83 (dm,  $J = 16.1$  Hz, 1H), 1.27 (t,  $J = 14.4$  Hz, 3H)

**$^{13}\text{C NMR}$ :** 148.63, 132.48, 131.86, 69.65, 57.78, 56.71, 34.77, 29.54, 14.57

**IR ( $\text{cm}^{-1}$ ):** 3056, 2979, 1703, 1655, 1301, 1262, 1122, 1043, 961, 690, 581

**HRMS:** calcd. for  $\text{C}_9\text{H}_{13}\text{O}_3\text{SNa}$  [ $\text{M}+\text{Na}^+$ ]: 238.05082, found 238.05105

**Synthesis of 3-[(benzyloxy)imino]-8 $\lambda^6$ -thiabicyclo[3.2.1]oct-6-ene-8,8-dione **67c****

Using **general procedure D**, oxime **67c** was obtained as 0.1594g (97% yield) of flaky beige-white solid from ketone **52** on a 0.59 mmol scale.

**Melting Point:** 126 – 127°C

**TLC solvent:** ( $R_f = 0.07$ ) 2:1 hexane:EtOAc

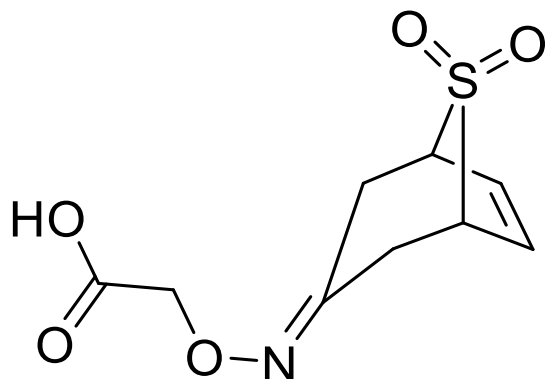
**$^1\text{H NMR}$ :** 7.30 – 7.40 (m, 5H), 6.51 (m, 2H), 3.70 (dm,  $J = 14.8$  Hz, 2H), 3.25 (dm,  $J = 16.4$  Hz, 2H), 2.79 – 2.88 (m, 2H)

**$^{13}\text{C NMR}$ :** 132.44, 131.89, 128.53, 128.11, 76.10, 57.78, 56.71, 45.23, 34.81, 29.74

**IR ( $\text{cm}^{-1}$ ):** 3064, 3031, 2954, 1737, 1651, 1586, 1496, 1320, 1144, 1126, 1082, 1058, 943, 753, 733, 693, 607, 459

**HRMS:** calcd. for  $\text{C}_{14}\text{H}_{15}\text{O}_3\text{SNa}$  [ $\text{M}+\text{Na}^+$ ]: 300.06703, found 300.06654

**Synthesis of [(8,8-dioxo-8 $\lambda^6$ -thiabicyclo[3.2.1]oct-6-en-3-ylidene)amino]oxy]acetic acid **67d****



Using **general procedure D**, oxime **67d** was obtained as 0.1154g (75% yield) of orange-yellow oil from ketone **52** on a 0.59 mmol scale.

**TLC solvent:** ( $R_f = 0.90$ ) 9:1 DCM: MeOH

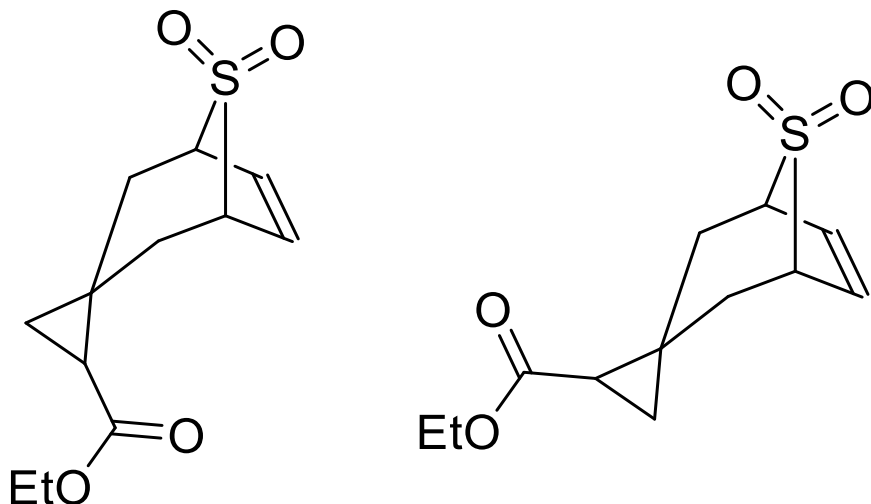
**$^1\text{H NMR}$ :** 6.51 – 6.60 (m, 2H), 4.20 – 4.28 (m, 2H), 3.70 – 3.78 (m, 2H), 3.66 (dm,  $J = 16.9$  Hz, 1H), 3.24 (dm,  $J = 16.2$  Hz, 1H), 2.90 (dm,  $J = 16.3$  Hz, 1H), 2.81 (dm,  $J = 16.2$  Hz, 1H)

**$^{13}\text{C NMR}$ :** 173.99, 169.88, 132.57, 131.73, 61.15, 57.63, 56.67, 34.62, 29.76

**IR ( $\text{cm}^{-1}$ ):** 3425, 3066, 2957, 1732, 1399, 1335, 1300, 1122, 1080, 961, 699, 587

**HRMS:** calcd. for  $\text{C}_9\text{H}_{11}\text{NO}_5\text{SNa}$  [ $\text{M}+\text{Na}^+$ ]: 268.02556, found 268.02574

**Synthesis of ethyl 8,8-dioxo-8 $\lambda^6$ -thiaspiro[bicyclo[3.2.1]octane-3,1'-cyclopropan]-6-ene-2'-carboxylate **68a** and **68b** <sup>4</sup>**



A round-bottom flask was charged with an appropriate size stir bar, sulfone **47** (0.300g, 1.76 mmol, 1.0 equiv.), and Rh<sub>2</sub>(OAc)<sub>4</sub> (0.0701g, 70.1mg, 0.09mmol, 5 mol%) prior to dissolving in DCM (18mL, 10 mL/mmol). Subsequently, ethyl diazoacetate (1.0098g, 0.93mL, 8.85 mmol, 5.0 equiv., 7.4% w/w in DCM) was added into the reaction mixture using a syringe pump at an addition rate of 0.01mL/min at ambient temperature. Upon completion of the addition of ethyl diazoacetate, the reaction mixture was allowed to stir at ambient temperature for 30 min, followed by filtration via Celite plug in order to separate Rh<sub>2</sub>(OAc)<sub>4</sub>. After washing with additional DCM, the combined organic layer was concentrated under reduced pressure to yield crude product mixture containing cyclopropane esters **68a** and **68b**. Purification via flash column chromatography was performed using a gradient elution of 2:1 hexane: Et<sub>2</sub>O (spiked with 5% v/v NEt<sub>3</sub>) to 1:4 hexane: Et<sub>2</sub>O (spiked with 5% v/v NEt<sub>3</sub>) to afford a total of 0.3383g (75% yield) of cyclopropane ester **68a** as amber-orange oil.

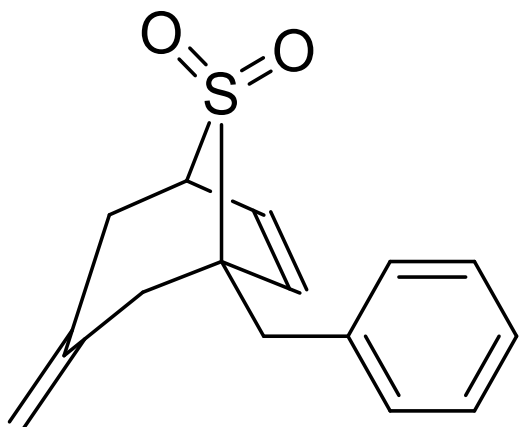
**TLC solvent:** (R<sub>f</sub> = 0.16) 1:2 hexane: Et<sub>2</sub>O

**<sup>1</sup>H NMR:** 6.56 (m, 2H), 4.13 (q, J = 7.1 Hz, 2H), 3.68 (m, 1H), 3.61 (m, 1H), 2.98 (dt, J = 14.3 Hz, 1.7 Hz, 1H), 2.56 (dt, J = 14.7 Hz, 1.7 Hz, 1H), 2.10 (ddd, J = 14.7 Hz, 5.3 Hz, 2.7 Hz, 1H), 1.48 (dd, J = 8.5 Hz, 5.9 Hz, 1H), 1.28 (t, J = 7.2 Hz, 3H), 1.24 (ddd, J = 14.3 Hz, 5.1 Hz, 2.5 Hz, 1H), 1.08 (td, J = 10.7 Hz, 1.8 Hz, 1H), 0.87 (ddd, J = 8.1 Hz, 4.9 Hz, 1.6 Hz, 1H)

**<sup>13</sup>C NMR (in acetone-d<sub>6</sub>):** 172.22, 132.15, 132.00, 61.00, 60.00, 59.87, 38.69, 27.26, 21.94, 21.53, 19.72, 14.61

**HRMS:** calcd. for C<sub>12</sub>H<sub>16</sub>O<sub>4</sub>SN<sub>a</sub> [M+Na<sup>+</sup>]: 279.06670, found 279.06610

**Synthesis of 1-benzyl-3-methylidene-8λ<sup>6</sup>-thiabicyclo[3.2.1]oct-6-ene-8,8-dione **76b****



Using **general procedure E**, sulfone **76b** was obtained as 1.10g (72% yield) of light yellow-orange solid from sulfone **47** on a 5.87 mmol scale.

**Melting Point:** 121 – 125°C

**TLC solvent:** ( $R_f = 0.26$ ) 2:1 hexane:EtOAc

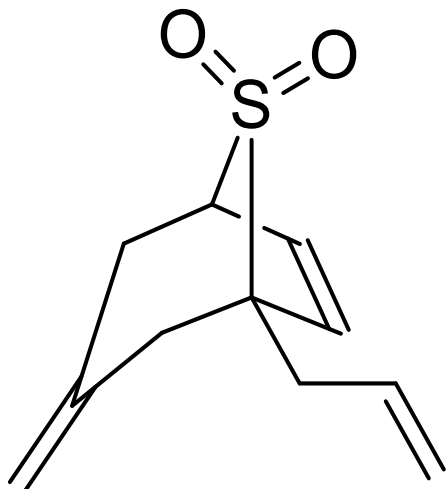
**<sup>1</sup>H NMR:** 7.30 – 7.40 (m, 3H), 7.24 – 7.30 (m, 2H), 6.37 (dd,  $J = 8.2$  Hz, 4.6 Hz, 1H), 6.26 (d,  $J = 8.1$  Hz, 1H), 4.77 (dd,  $J = 12.0$  Hz, 1.8 Hz, 2H), 3.71 (td,  $J = 4.6$  Hz, 2.2 Hz, 1H), 3.19 – 3.12 (m, 1H), 3.15 (dd,  $J = 24.6$  Hz, 14.2 Hz, 1H), 2.96 (dd,  $J = 15.0$  Hz, 2.0 Hz, 2H), 2.50 (ddd,  $J = 15.0$  Hz, 4.3 Hz, 2.0 Hz, 1H), 2.41 (dd,  $J = 15.0$  Hz, 2.0 Hz, 1H)

**<sup>13</sup>C NMR:** 138.12, 134.47, 134.15, 130.65, 128.74, 128.67, 127.40, 117.70, 66.29, 59.79, 40.64, 35.96, 33.12

**IR (cm<sup>-1</sup>):** 3056, 2961, 1651, 1605, 1495, 1283, 1255, 1138, 1110, 1093, 906, 761, 705, 698, 557, 433

**HRMS:** calcd. for C<sub>15</sub>H<sub>16</sub>O<sub>2</sub>SNa [M+Na<sup>+</sup>]: 283.07687, found 283.07629

Synthesis of 3-methylidene-1-(prop-2-en-1-yl)-8λ<sup>6</sup>-thiabicyclo[3.2.1]oct-6-ene-8,8-dione **76c**



Using **general procedure E**, sulfone **76c** was obtained as 1.344g (54% yield) of brown oil from sulfone **47** on a 11.75 mmol scale.

**TLC solvent:** ( $R_f = 0.22$ ) 3:1 hexane : EtOAc

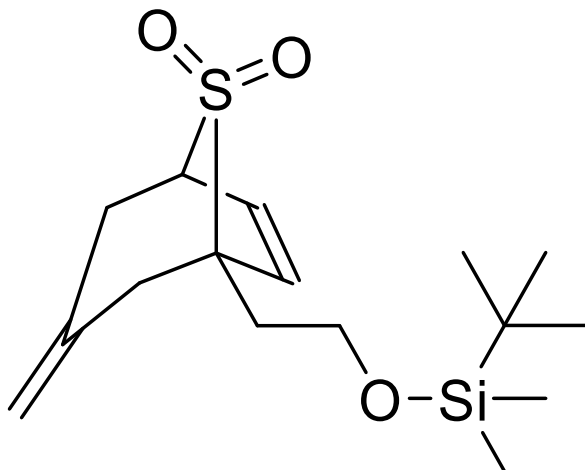
**<sup>1</sup>H NMR:** 6.38 (dd,  $J = 8.6$  Hz, 4.9 Hz, 1H), 6.24 (d,  $J = 8.3$  Hz, 1H), 5.84 – 5.95 (m, 1H), 5.25 (dm,  $J = 11.8$  Hz, 2H), 4.82 – 4.86 (m, 2H), 3.65 – 3.71 (m, 1H), 3.16 (dm,  $J = 15.9$  Hz, 1H), 3.04 (dm,  $J = 15.3$  Hz, 1H), 2.58 (dd,  $J = 14.3$  Hz, 7.4Hz, 1H), 2.52 (ddd,  $J = 15.1$  Hz, 4.7 Hz, 2.2 Hz, 1H), 2.43 (dd,  $J = 15.0$  Hz, 1.6 Hz, 1H)

**<sup>13</sup>C NMR:** 136.93, 132.98, 129.71, 127.64, 119.15, 116.27, 64.41, 58.57, 39.66, 34.72, 30.94

**IR (cm<sup>-1</sup>):** 3089, 2983, 2943, 1812, 1646, 1420, 1343, 1290, 1262, 1122, 986, 898, 703, 614, 593

**HRMS:** calcd. for C<sub>11</sub>H<sub>14</sub>O<sub>2</sub>SNa [M+Na<sup>+</sup>]: 233.06122, 233.06099

**Synthesis of 1-{2-[(tert-butyl)dimethylsilyl]oxy}ethyl}-3-methylidene-8 $\lambda$ <sup>6</sup>-thiabicyclo[3.2.1]oct-6-ene-8,8-dione **76d****



Using **general procedure E**, sulfone **76d** was obtained as 0.7527g (33% yield) of beige-white solid from sulfone **47** on a 7.0 mmol scale.

**Melting Point:** 146 – 148°C

**TLC solvent:** ( $R_f = 0.38$ ) 3:1 hexane: EtOAc

**<sup>1</sup>H NMR:** 6.35 – 6.38 (m, 1H), 6.31 – 6.34 (m, 1H), 4.85 (dd,  $J = 10.0$  Hz, 2.1 Hz, 2H), 3.86 – 3.90 (m, 2H), 3.60 – 3.62 (m, 1H), 3.16 (dd,  $J = 16.0$  Hz, 2.4 Hz, 1H), 3.03 (dd,  $J = 15.0$  Hz, 1.6 Hz, 1H), 2.58 (dd,  $J = 14.9$  Hz, 1.8 Hz, 1H), 2.49 (dd,  $J = 14.8$  Hz, 2.1 Hz, 1H), 2.10 – 2.20 (m, 2H), 0.90 (s, 9H), 0.08 (s, 6H)

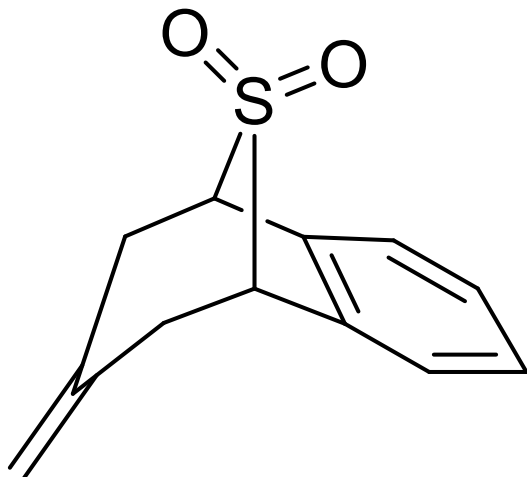
**<sup>13</sup>C NMR:** 134.23, 128.90, 120.41, 117.52, 63.66, 59.83, 58.08, 35.98, 34.56, 32.20, 25.80, 17.83, 5.29

136.93, 132.98, 129.71, 127.64, 119.15, 116.27, 64.41, 58.57, 39.66, 34.72, 30.94

**IR (cm<sup>-1</sup>):** 3055, 2969, 1654, 1294, 1123, 1090, 909, 702, 588, 579

**HRMS:** calcd. for C<sub>16</sub>H<sub>29</sub>O<sub>3</sub>SSi [M+H<sup>+</sup>]: 329.16067, found 329.16097

**Synthesis of 7-methylene-6,7,8,9-tetrahydro-5*H*-5,9-epithiobenzo[7]annulene 10,10-dioxide 82**



Using **general procedure C**, sulfone **76b** was obtained in 1.8848 g (93% yield) from sulfone **47** on a 9.2 mmol scale.

**Melting Point:** 124 – 126°C

**TLC solvent:** ( $R_f = 0.52$ ) 3:1 hexane: EtOAc

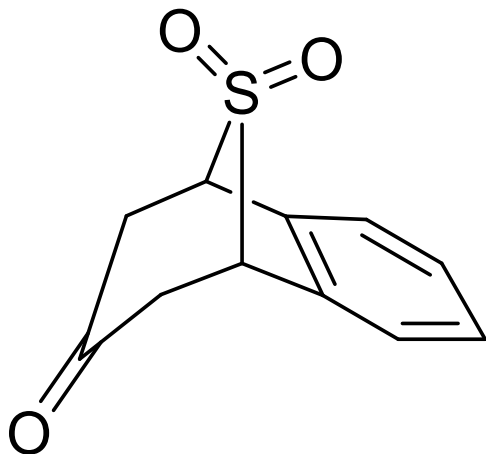
**$^1\text{H NMR}$ :** 7.33 – 7.40 (m, 4H), 4.65 (t,  $J = 1.2$  Hz, 2H), 4.15 – 4.18 (dm,  $J = 1.4$  Hz, 2H), 3.39 (dd,  $J = 9.2$  Hz, 1.2 Hz, 2H), 2.69 (dd,  $J = 9.3$  Hz, 2.8 Hz, 2H)

**$^{13}\text{C NMR}$ :** 136.17, 135.94, 128.96, 125.03, 118.33, 61.91, 39.22

**IR ( $\text{cm}^{-1}$ ):** 3086, 2984, 1645, 1472, 1454, 1295, 1244, 1217, 1114, 1102, 1082, 1025, 990, 912, 761, 743, 550, 486

**HRMS:** calcd. for  $\text{C}_{12}\text{H}_{14}\text{O}_2\text{S}$  [ $\text{M}+\text{H}^+$ ]: 222.06363, found 222.06381

**Synthesis of 5,6,8,9-tetrahydro-7H-5,9-epithiobenzo[7]annulen-7-one 10,10-dioxide **83****



Under open atmosphere, a round-bottom flask was charged with an appropriate stir bar, sulfone **82** (1.00 g, 4.54mmol, 1.0 equiv.) prior to dissolving in DCM (140 mL, 30 mL/mmol). The reaction flask was allowed to stir at  $-78^{\circ}\text{C}$  using a cooling bath of dry ice and acetone, before  $\text{O}_3$  being introduced into the reaction mixture via bubbling at a flow rate of 7L/min. The introduction of  $\text{O}_3$  was continued for 15 min., followed by the addition of  $\text{Me}_2\text{S}$  to quench the reaction mixture. The solution was allowed to continue stirring overnight and gradually warm to ambient temperature. The yellow reaction mixture was then concentrated under reduced pressure to remove DCM. 3 x 30mL EtOAc was used for extraction, and then washed with 3 x 30mL  $\text{H}_2\text{O}$  and 2 x 30mL brine sequentially. The combined organic extracts were dried with anhydrous  $\text{Na}_2\text{SO}_4$ , and subsequent concentration under reduce pressure provided a total of 0.5752 g (57% yield) of ketone **83** as beige-white needles.

**Melting Point:** 98 – 102 $^{\circ}\text{C}$

**TLC solvent:** ( $R_f = 0.33$ ) 3:1 hexane: EtOAc

**$^1\text{H NMR}$ :** 7.44 – 7.47 (m, 5H), 4.39 (tm,  $J = 3.5$  Hz, 2H), 3.56 (dm,  $J = 16.0$  Hz, 2H), 2.91 (dm,  $J = 15.6$  Hz, 2H)

**$^{13}\text{C NMR}$ :** 200.98, 136.15, 129.99, 125.80, 59.93, 47.46

**IR ( $\text{cm}^{-1}$ ):** 3019, 2962, 1709, 1473, 1306, 1187, 1108, 1016, 982, 761, 699

**HRMS:** calcd. for  $\text{C}_{11}\text{H}_{10}\text{O}_3\text{SNa}$  [ $\text{M}+\text{Na}^+$ ]: 245.02483, found 245.02497

**Experimental References**

1. Rice, K.; Markley, D. WO2016068106 A2, May 24<sup>th</sup> 2012.
2. Qi, X.; Khaybullin, R.; Okuneiff, P.; Zhang, M. WO2016077581, May 19<sup>th</sup> 2016.
3. Chen, J.; Kilpatrick, B.; Oliver, A. G.; Wulff, J. E. *J. Org. Chem.*, **2015**, *80*, 8979 – 8989.
4. Leung, S.-K.; Chiu, P. *Tetrahedron Lett.*, **2005**, *46*, 2709 – 2712.

## Appendix B – Spectral Data

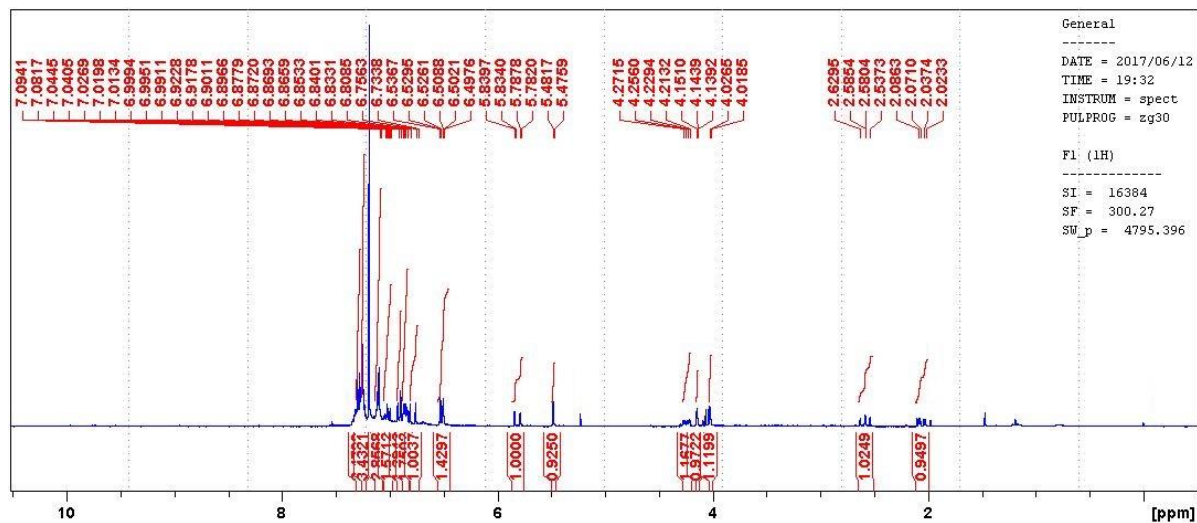


Figure E1. <sup>1</sup>H NMR Spectra of compound **31a** in CDCl<sub>3</sub>.

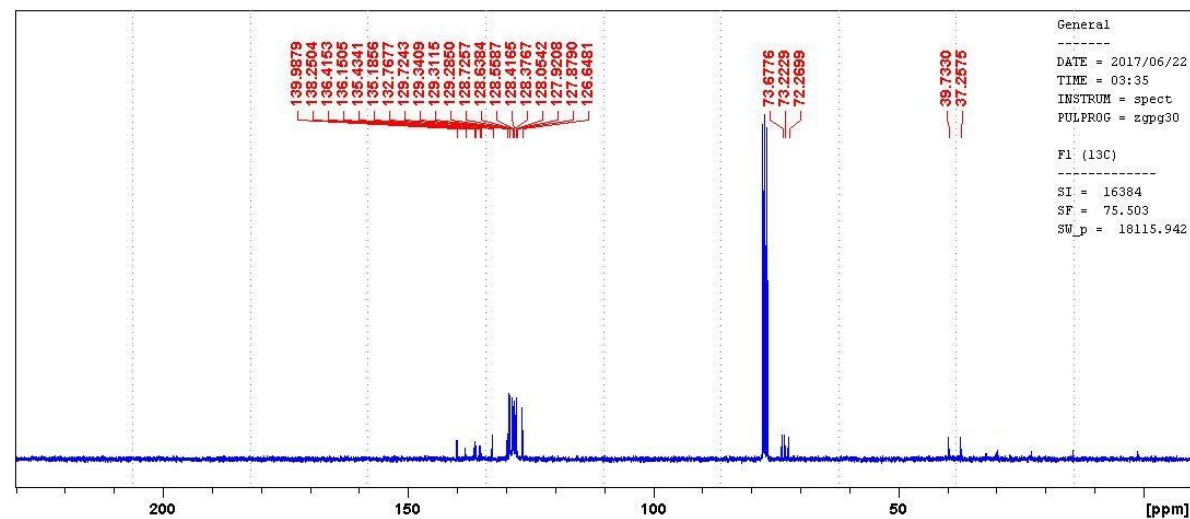


Figure E2. <sup>13</sup>C NMR Spectra of compound **31a** in CDCl<sub>3</sub>.

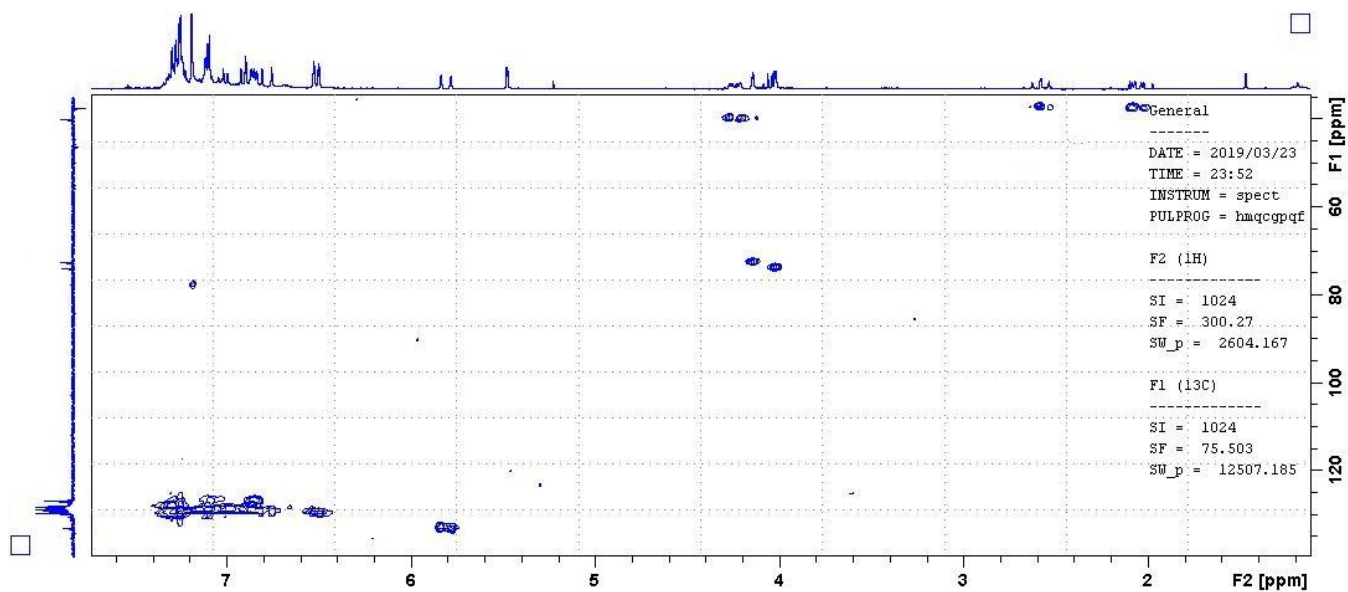


Figure E3. HSQC NMR Spectra of compound **31a** in  $\text{CDCl}_3$ .

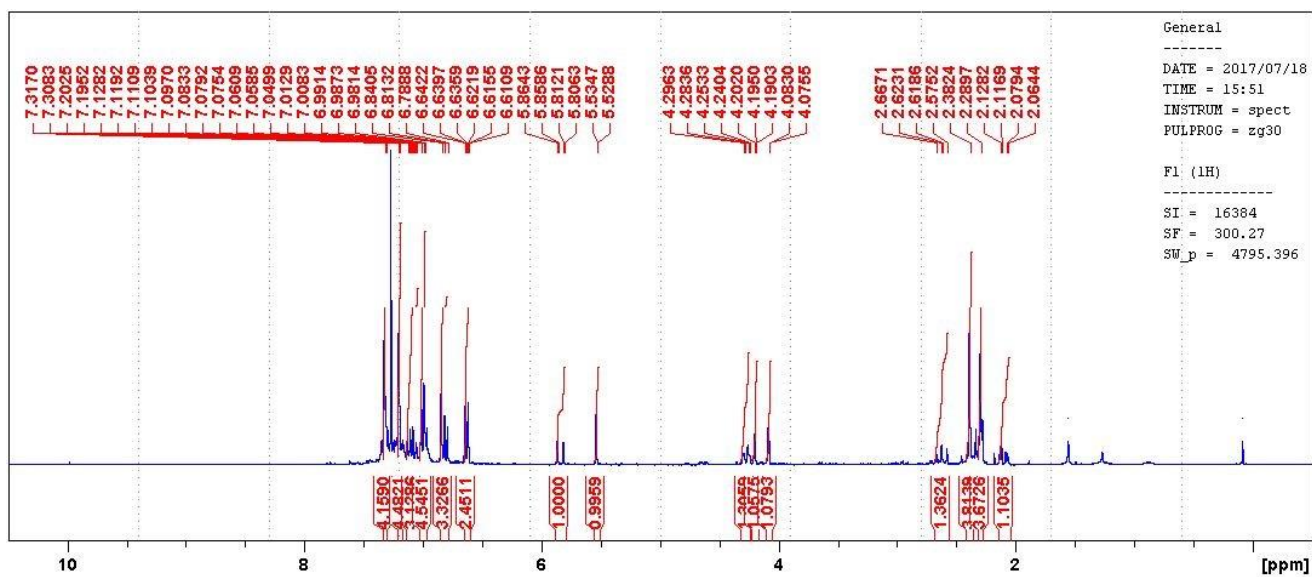


Figure E4.  $^1\text{H}$  NMR Spectra of compound **31b** in  $\text{CDCl}_3$ .

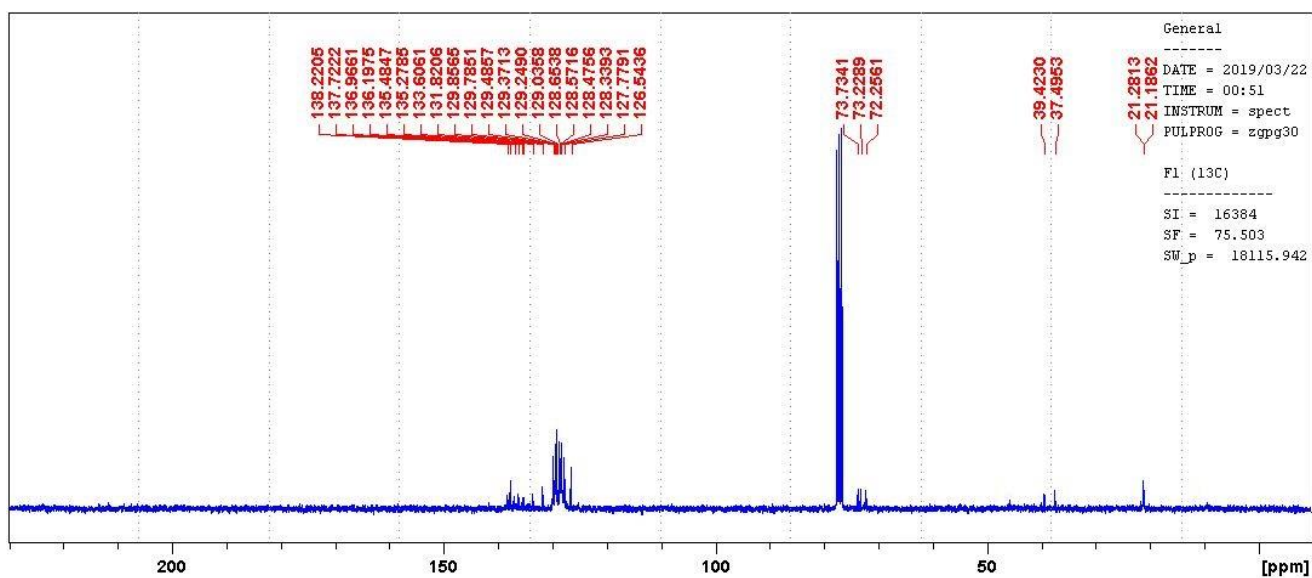


Figure E5.  $^{13}\text{C}$  NMR Spectra of compound **31b** in  $\text{CDCl}_3$ .

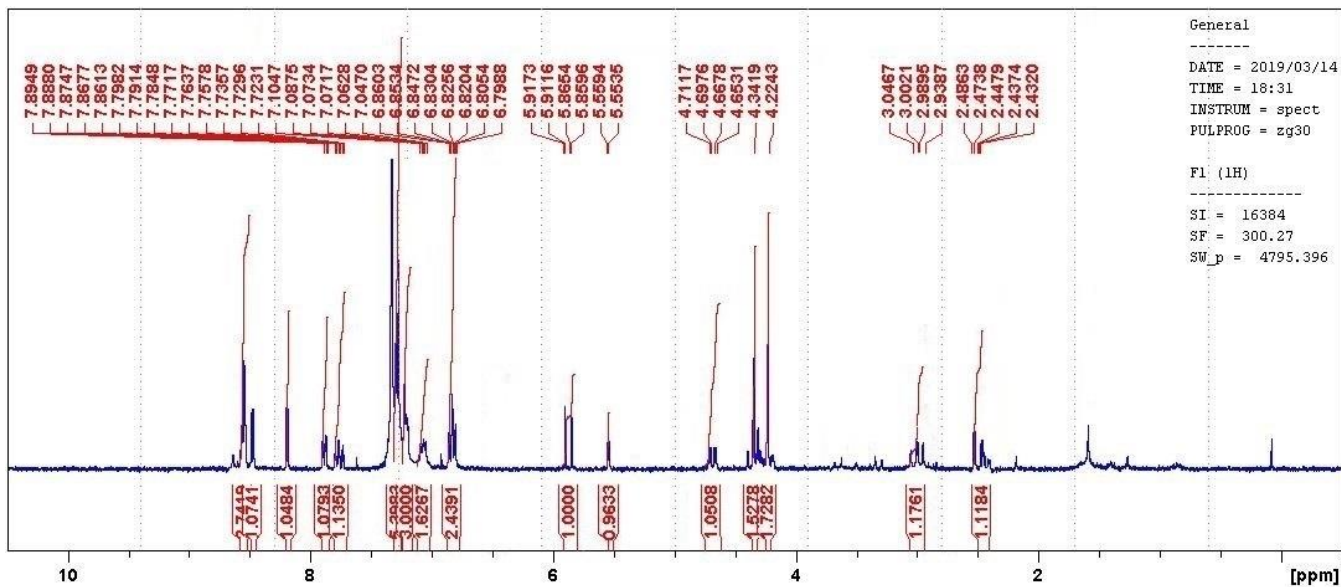


Figure E6.  $^1\text{H}$  NMR Spectra of compound **31d** in  $\text{CDCl}_3$ .

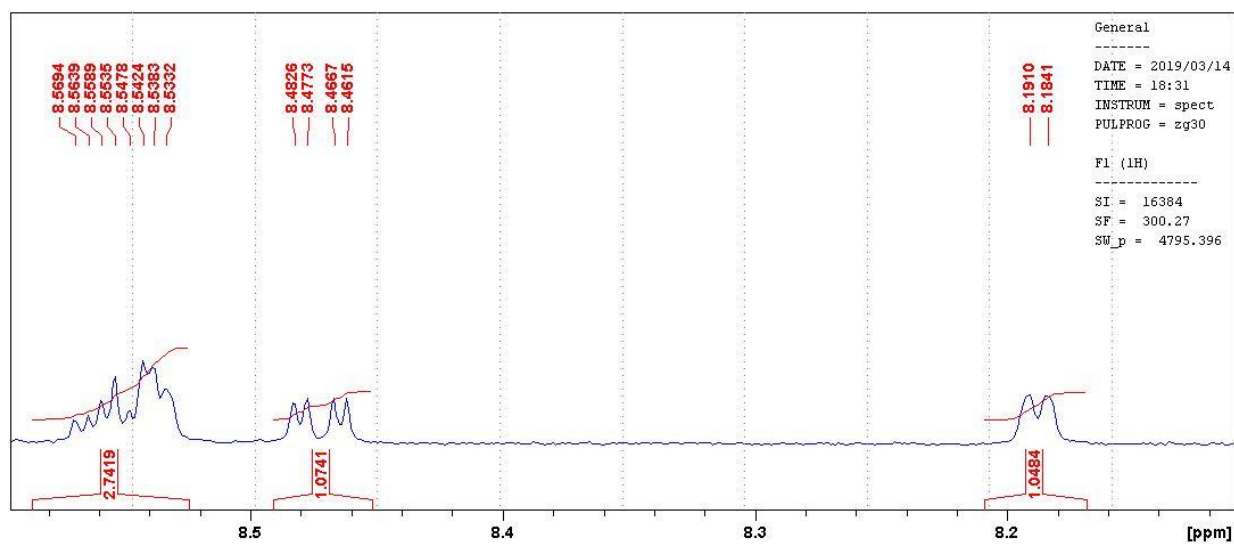


Figure E7. Extended aromatic regions of  $^1\text{H}$  NMR Spectra of compound **31d** in  $\text{CDCl}_3$ .

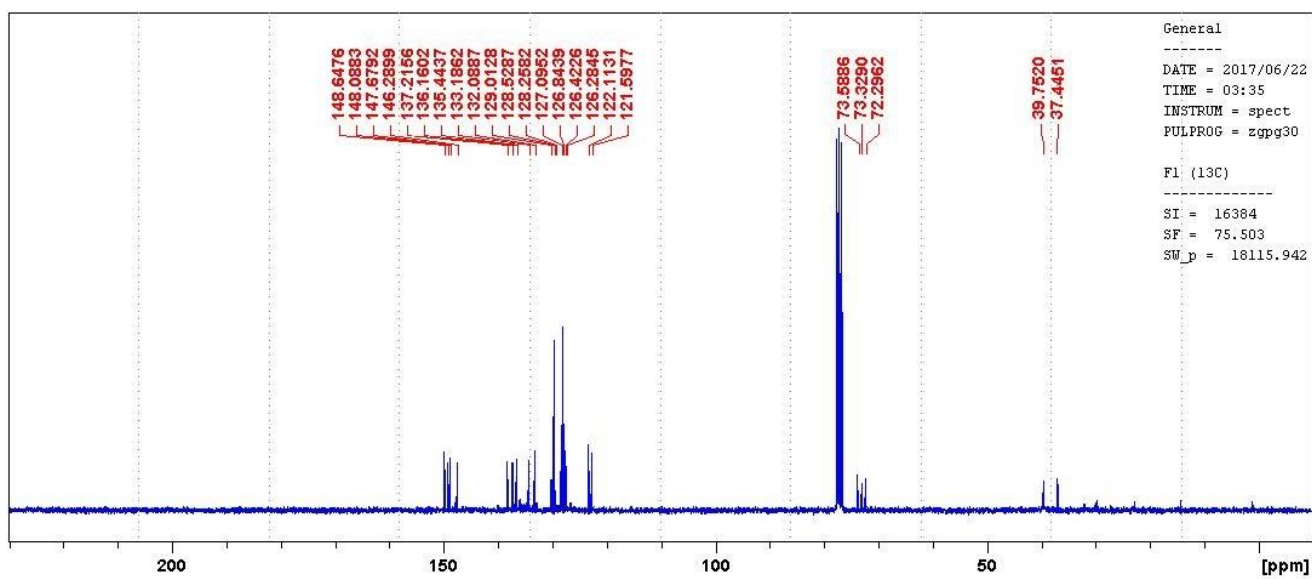


Figure E8.  $^{13}\text{C}$  NMR Spectra of compound **31d** in  $\text{CDCl}_3$ .

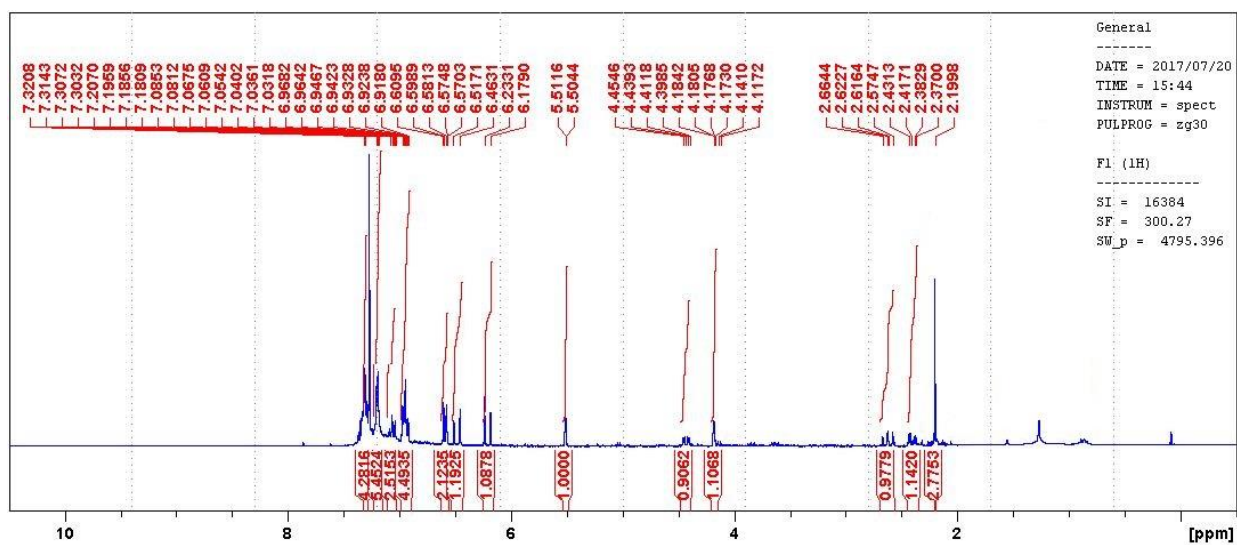


Figure E9.  $^1\text{H}$  NMR Spectra of compound **32a** in  $\text{CDCl}_3$ .

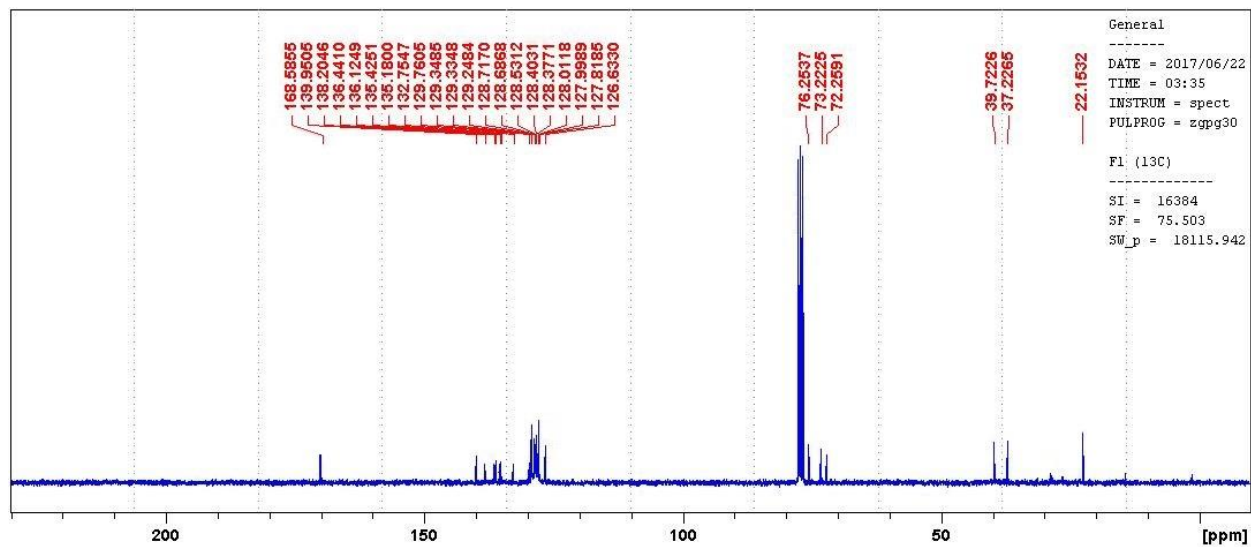


Figure E10.  $^{13}\text{C}$  NMR Spectra of compound **32a** in  $\text{CDCl}_3$ .

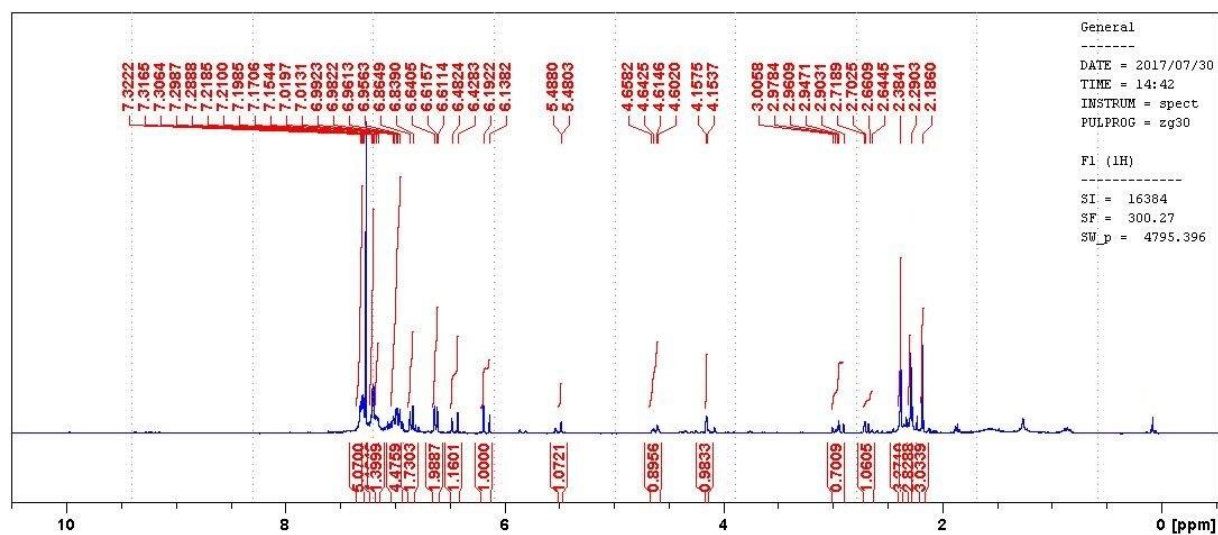


Figure E11.  $^1\text{H}$  NMR Spectra of compound **32b** in  $\text{CDCl}_3$ .

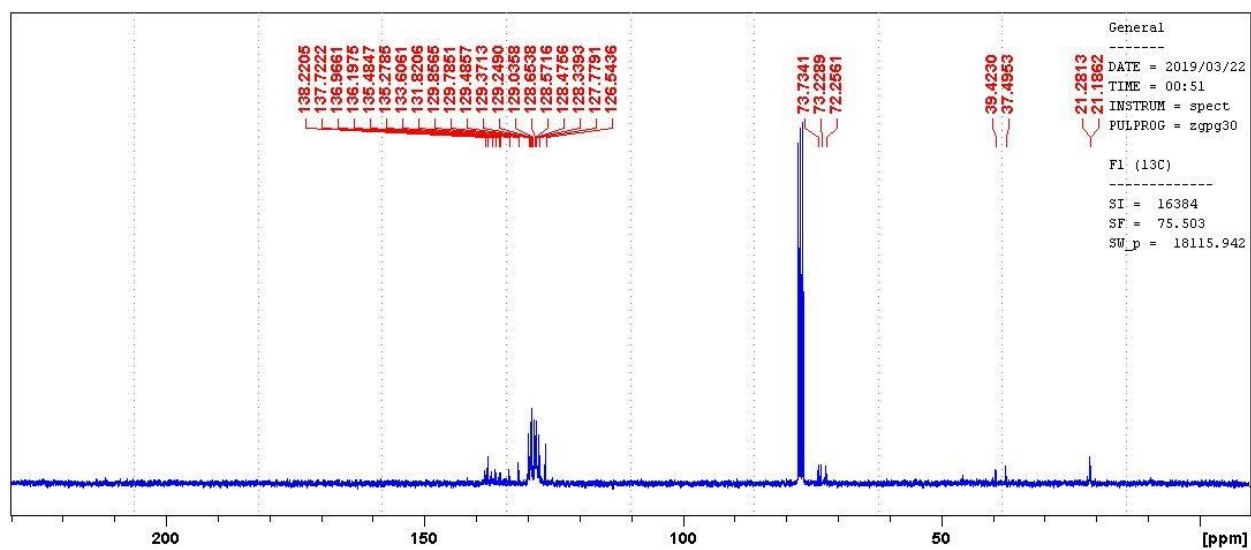


Figure E12.  $^{13}\text{C}$  NMR Spectra of compound **32b** in  $\text{CDCl}_3$ .

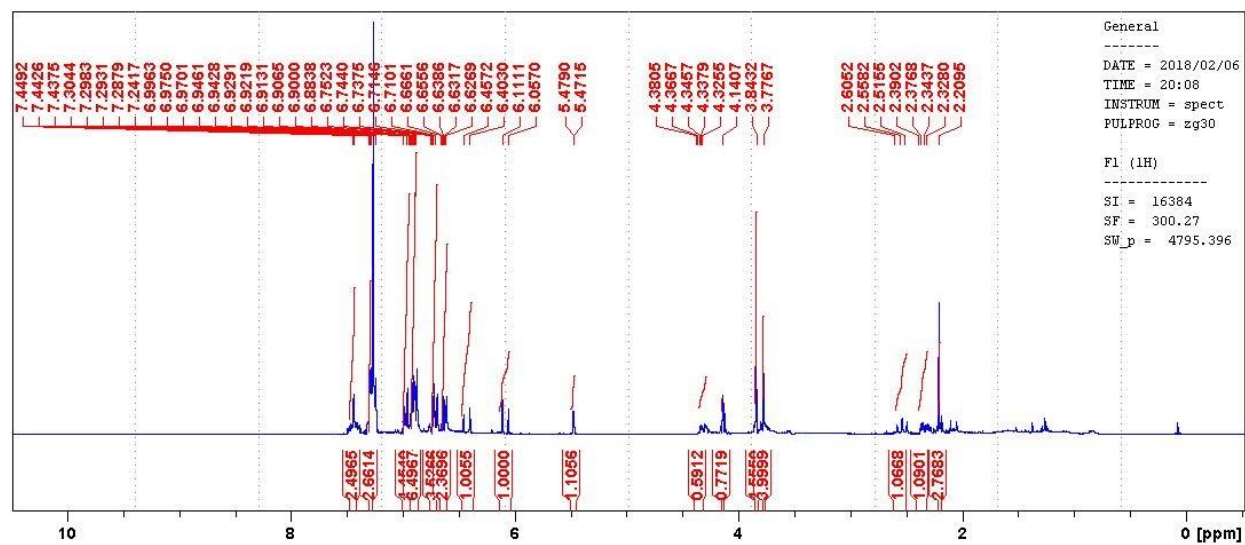


Figure E13.  $^1\text{H}$  NMR Spectra of compound **32c** in  $\text{CDCl}_3$ .

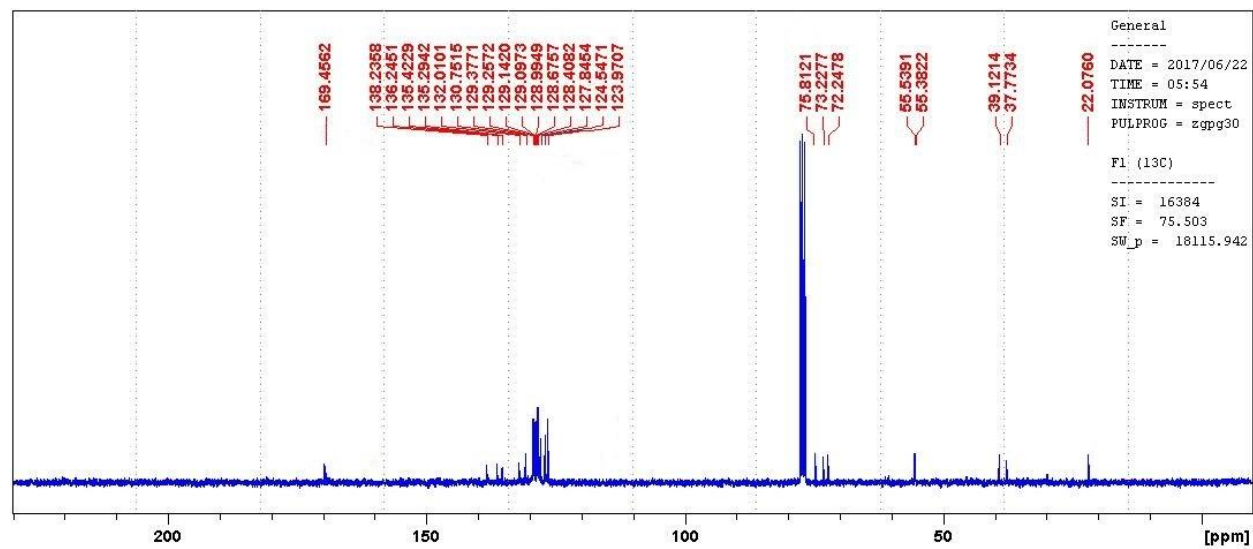


Figure E14.  $^{13}\text{C}$  NMR Spectra of compound **32c** in  $\text{CDCl}_3$ .

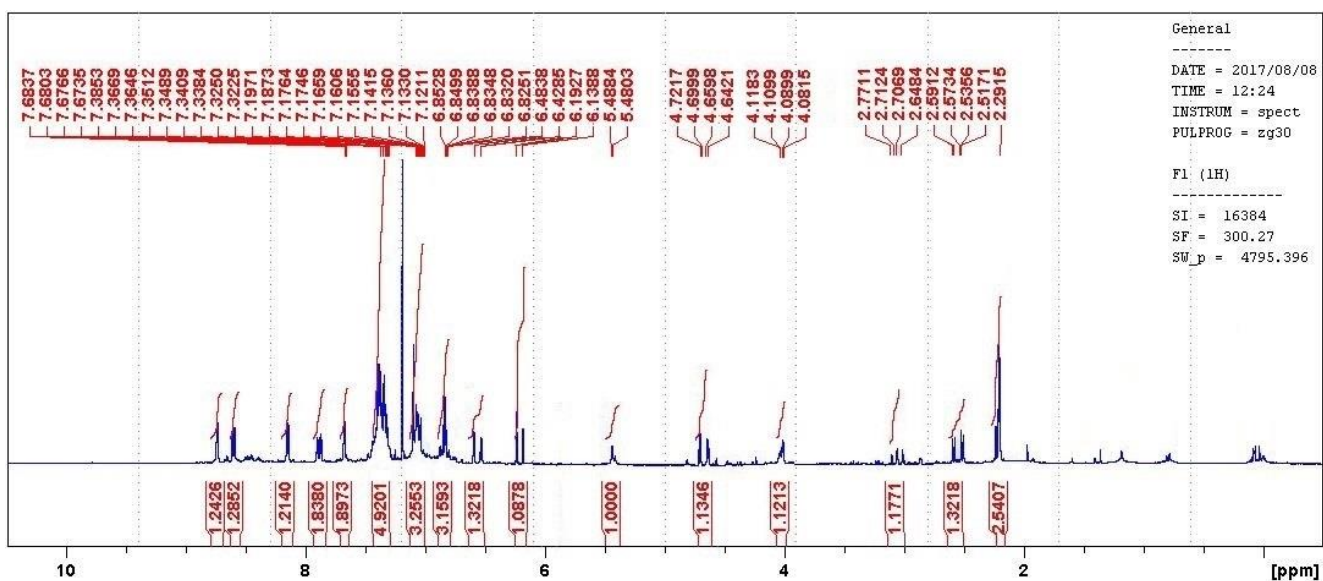


Figure E15.  $^1\text{H}$  NMR Spectra of compound **32d** in  $\text{CDCl}_3$ .

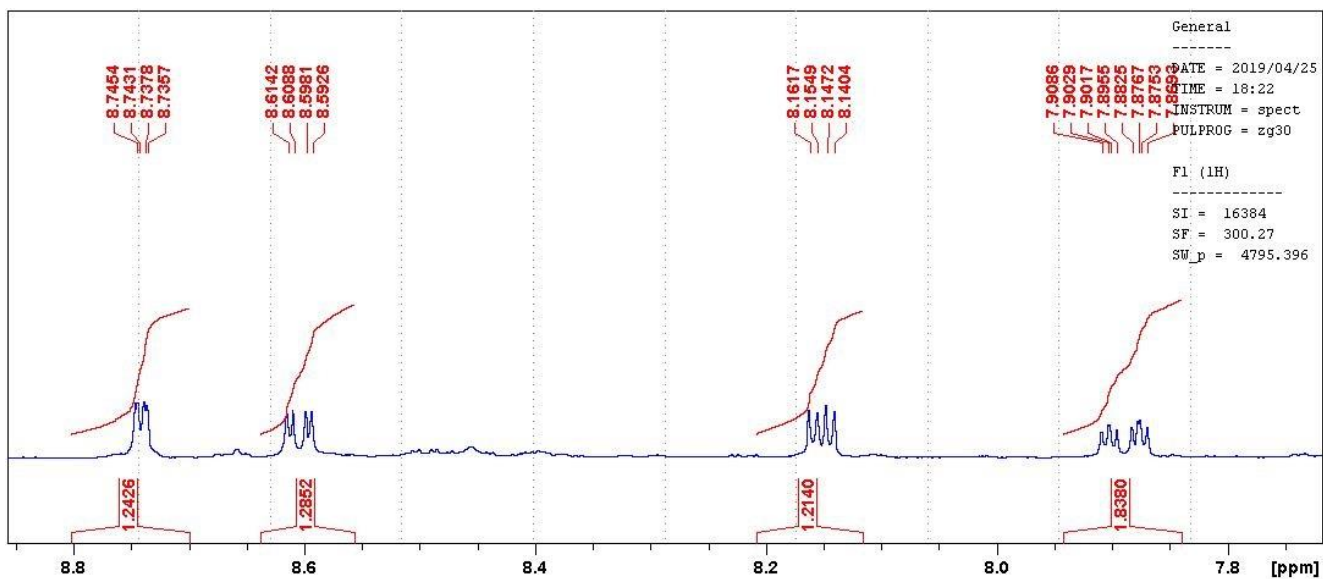


Figure E16. Extended aromatic regions of  $^1\text{H}$  NMR Spectra of compound **32d** in  $\text{CDCl}_3$ .

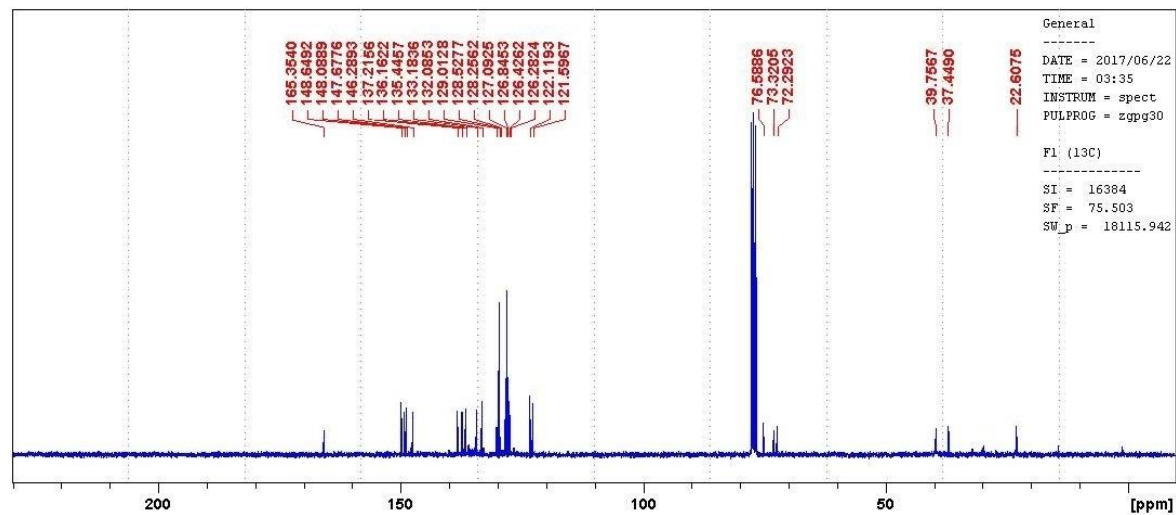


Figure E17.  $^{13}\text{C}$  NMR Spectra of compound **32d** in  $\text{CDCl}_3$ .

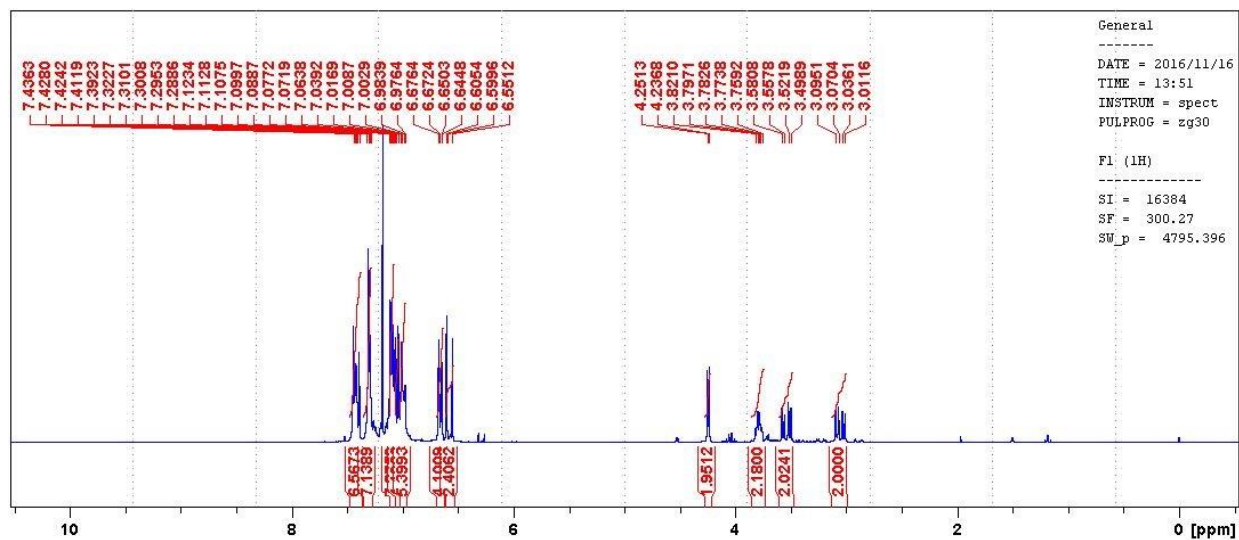


Figure E18.  $^1\text{H}$  NMR Spectra of compound **28** in  $\text{CDCl}_3$ .

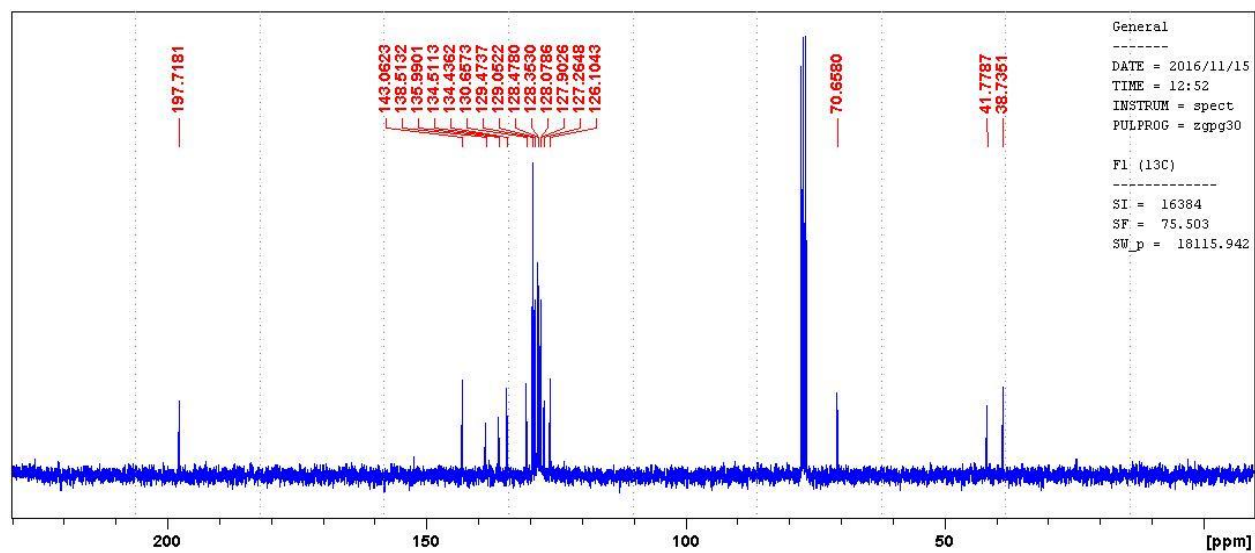


Figure E19.  $^{13}\text{C}$  NMR Spectra of compound **28** in  $\text{CDCl}_3$ .

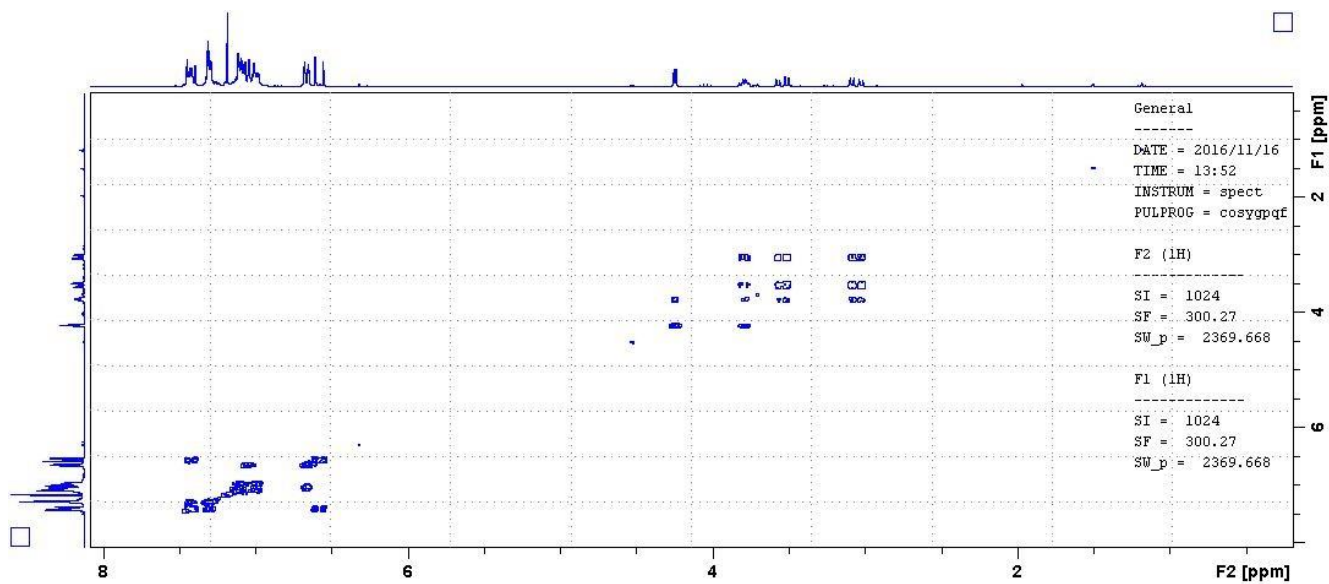


Figure E20. COSY NMR Spectra of compound **28** in  $\text{CDCl}_3$ .

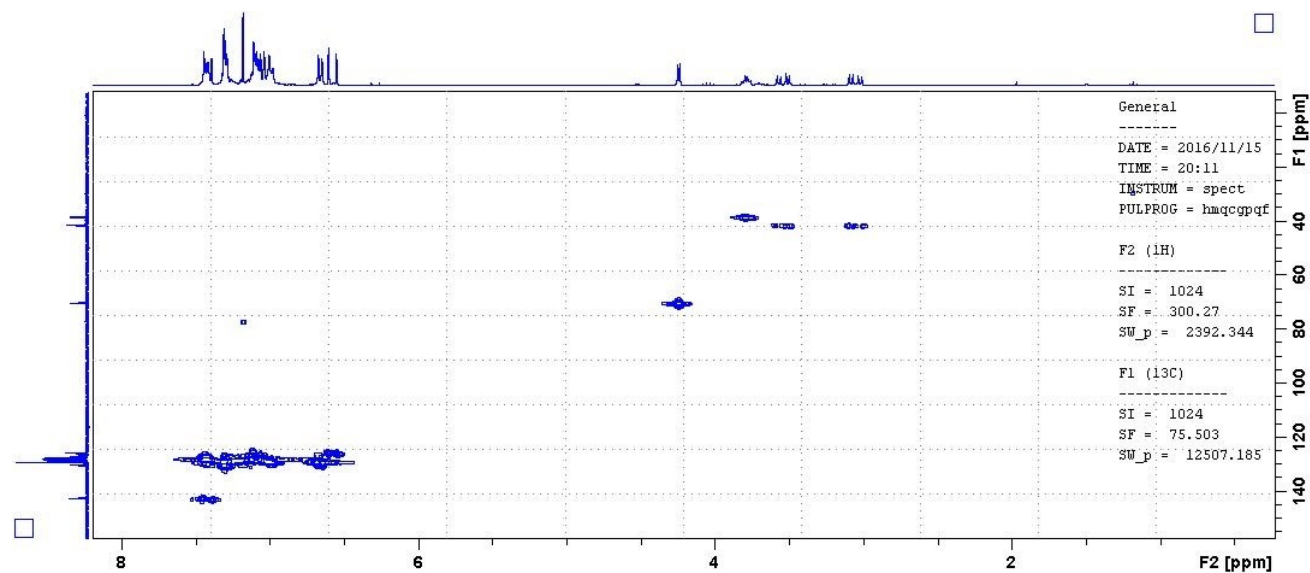


Figure E21. HSQC NMR Spectra of compound **28** in  $\text{CDCl}_3$ .

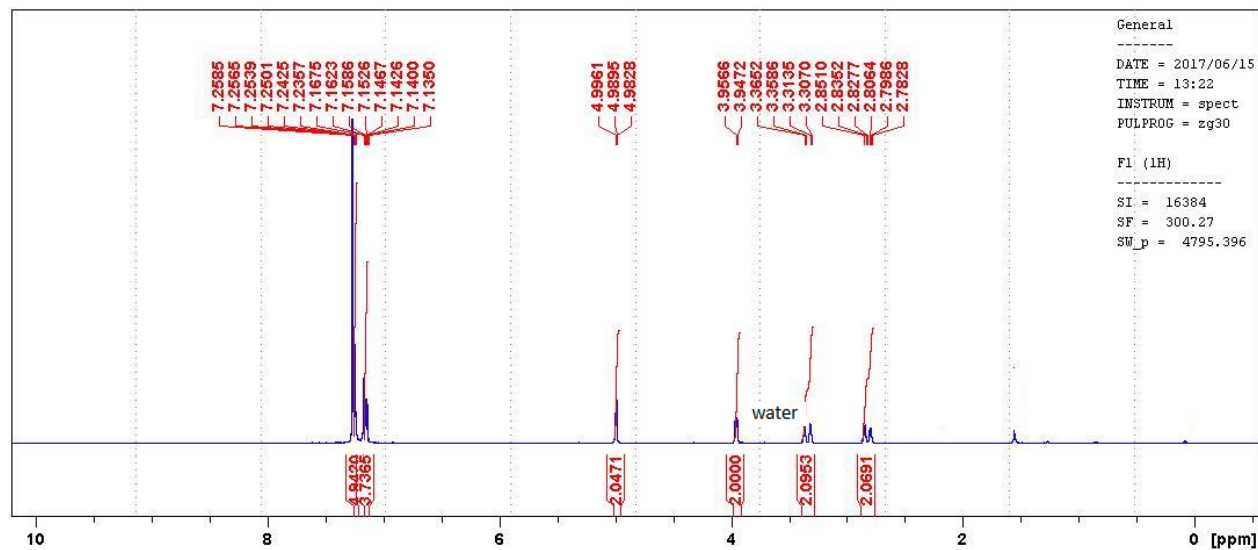


Figure E22.  $^1\text{H}$  NMR Spectra of compound **40** in  $\text{CDCl}_3$ .

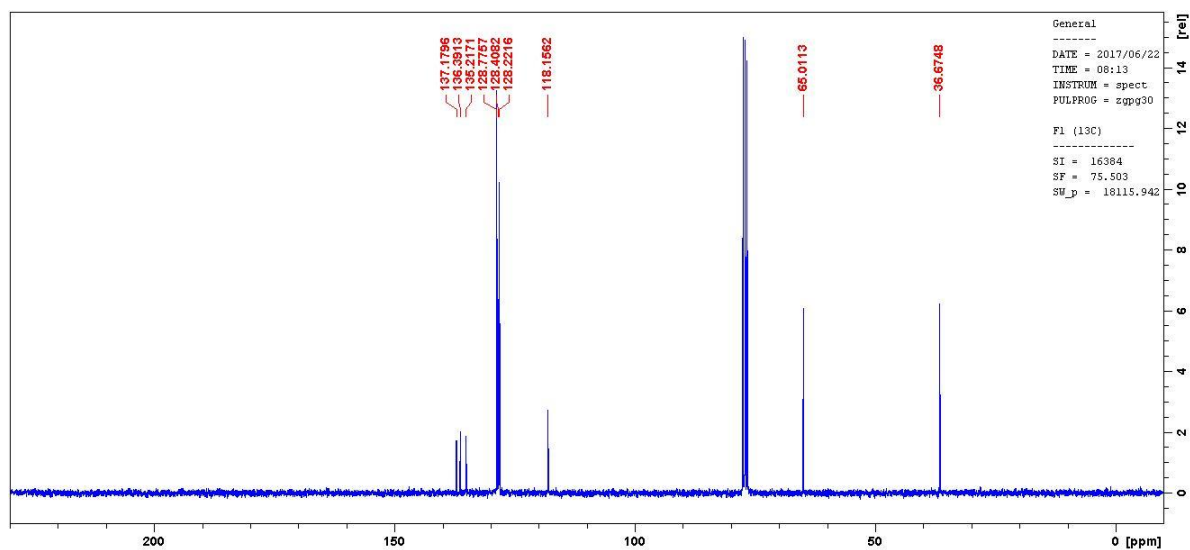


Figure E23.  $^{13}\text{C}$  NMR Spectra of compound **40** in  $\text{CDCl}_3$ .

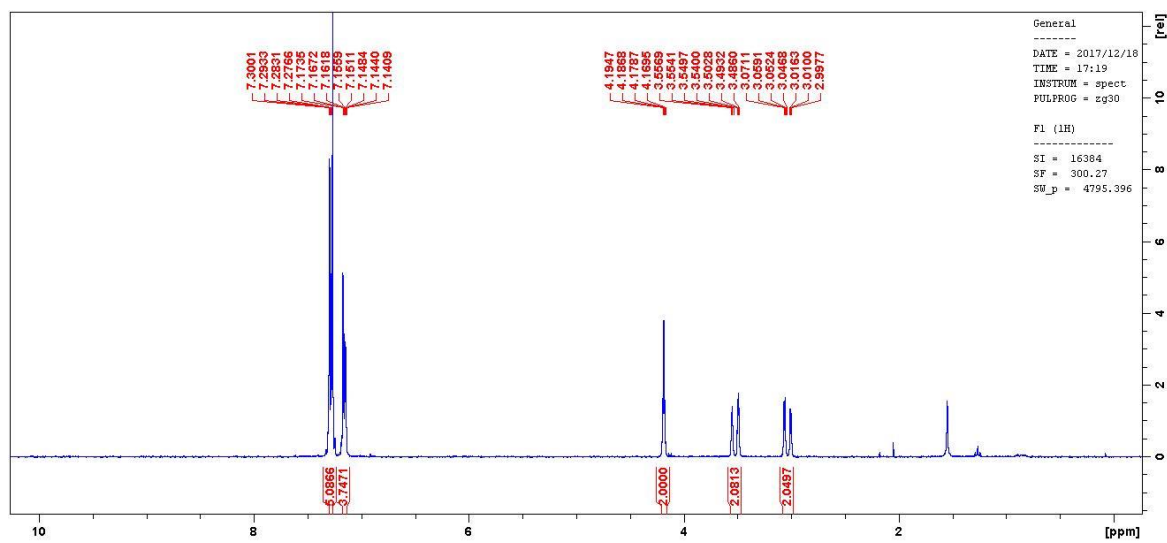


Figure E24.  $^1\text{H}$  NMR Spectra of compound **41** in  $\text{CDCl}_3$ .

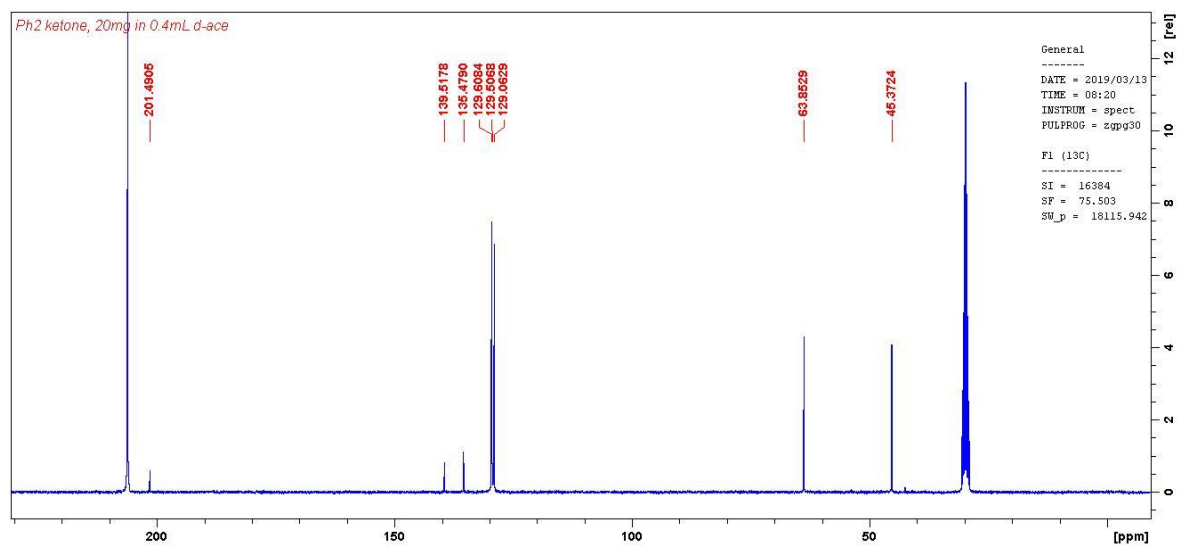


Figure E25.  $^{13}\text{C}$  NMR Spectra of compound **41** in acetone- $d_6$ .

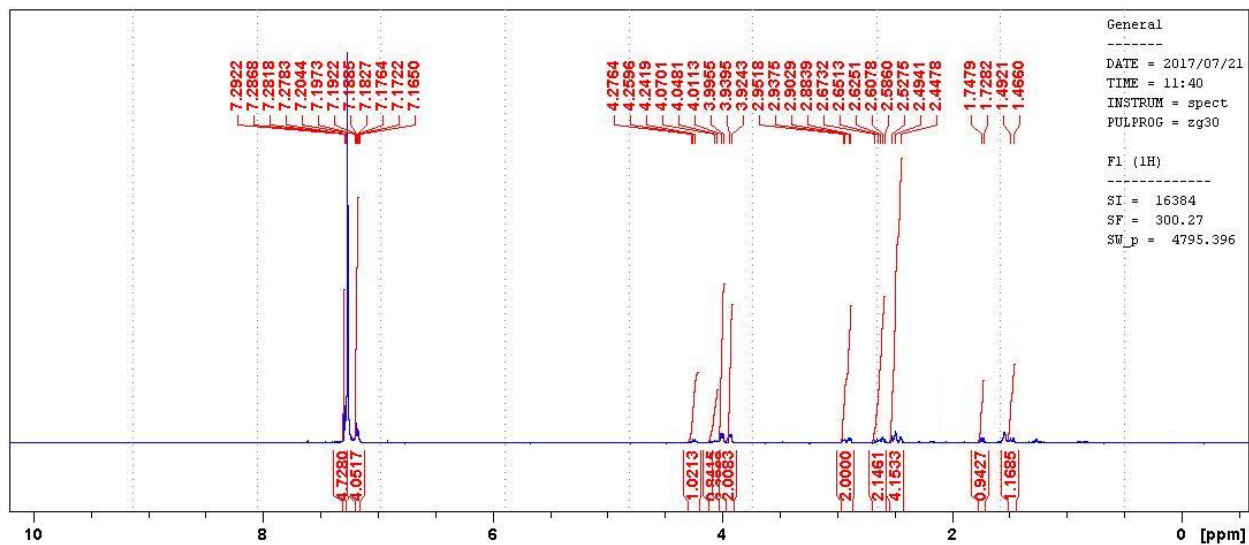


Figure E26.  $^1\text{H}$  NMR Spectra of compounds **42a** and **42b** in  $\text{CDCl}_3$ .

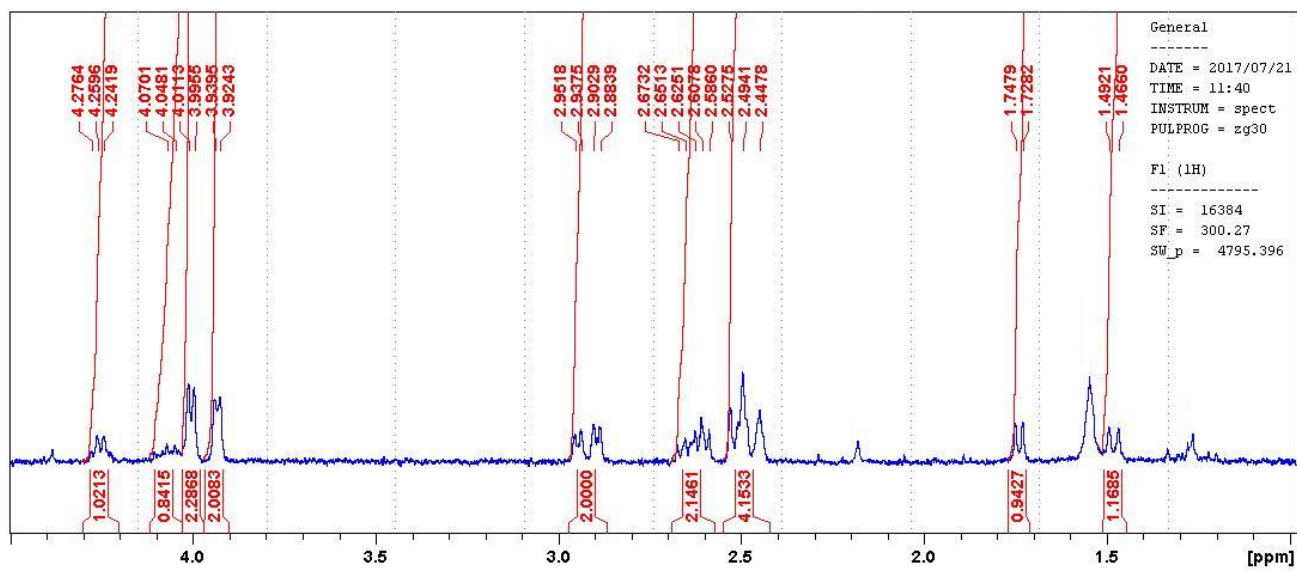


Figure E27. Magnified regions of  $^1\text{H}$  NMR Spectra of compounds **42a** and **42b** in  $\text{CDCl}_3$ .

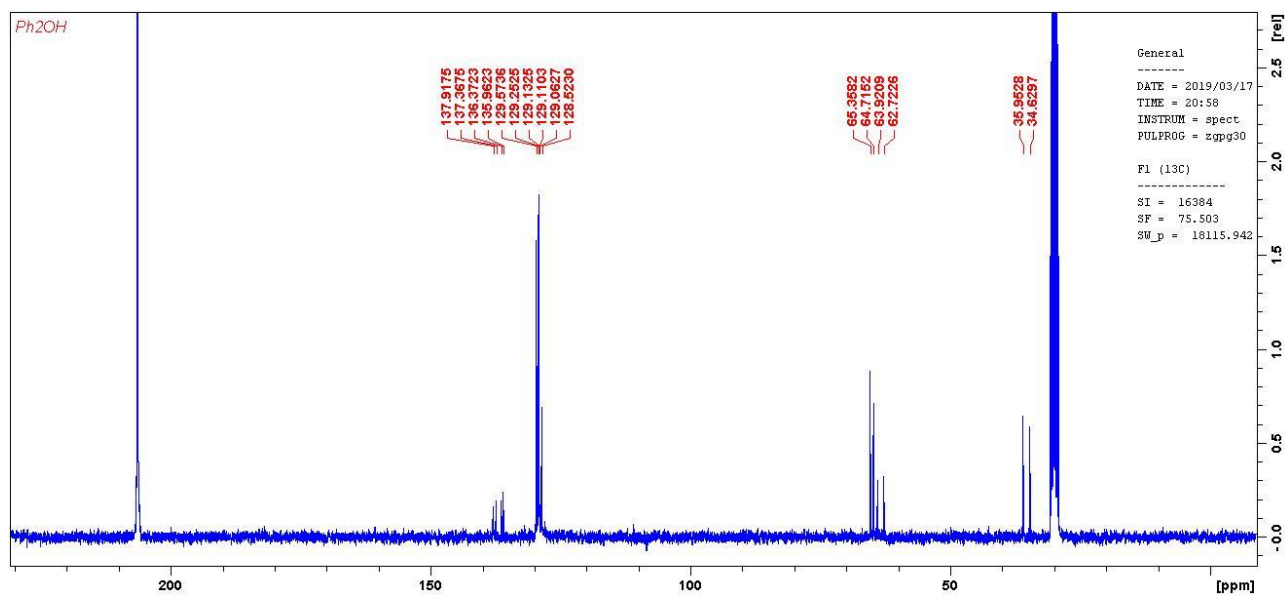


Figure E28.  $^{13}\text{C}$  NMR Spectra of compounds **42a** and **42b** in acetone- $d_6$ .

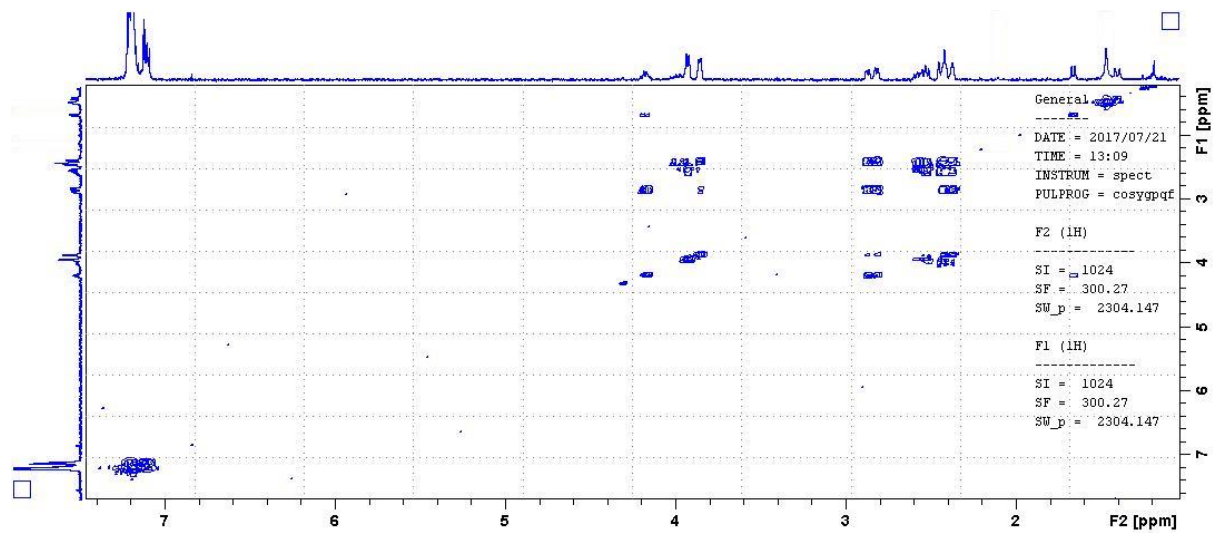


Figure E29. COSY NMR Spectra of compounds **42a** and **42b** in  $\text{CDCl}_3$ .

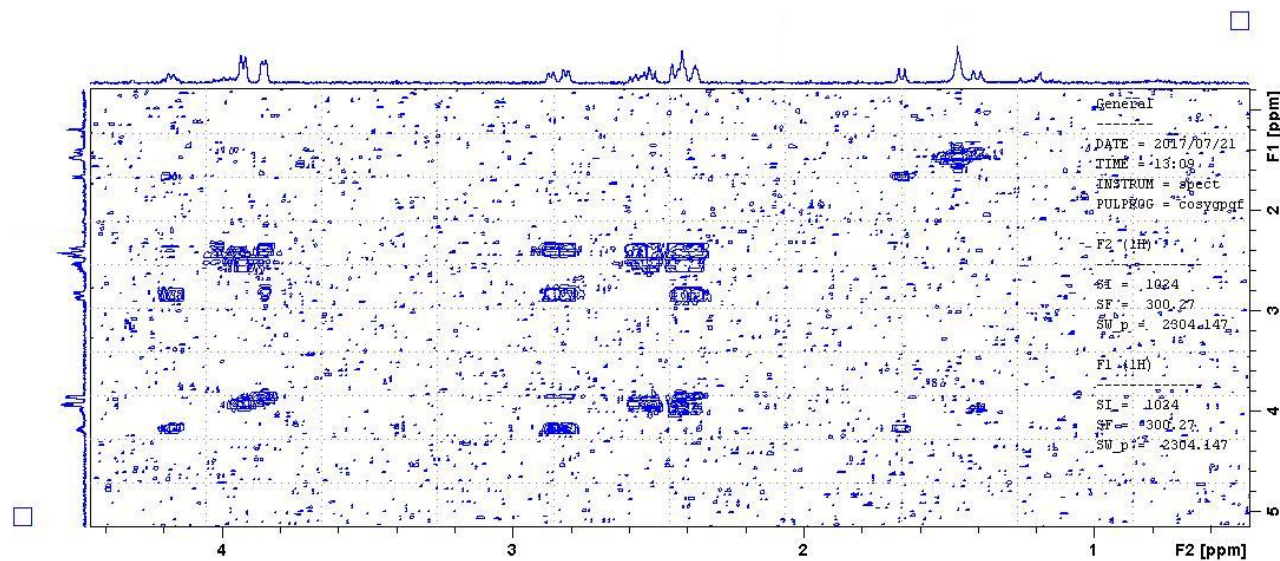


Figure E30. Magnified regions of COSY NMR Spectra of compounds **42a** and **42b** in  $\text{CDCl}_3$ .

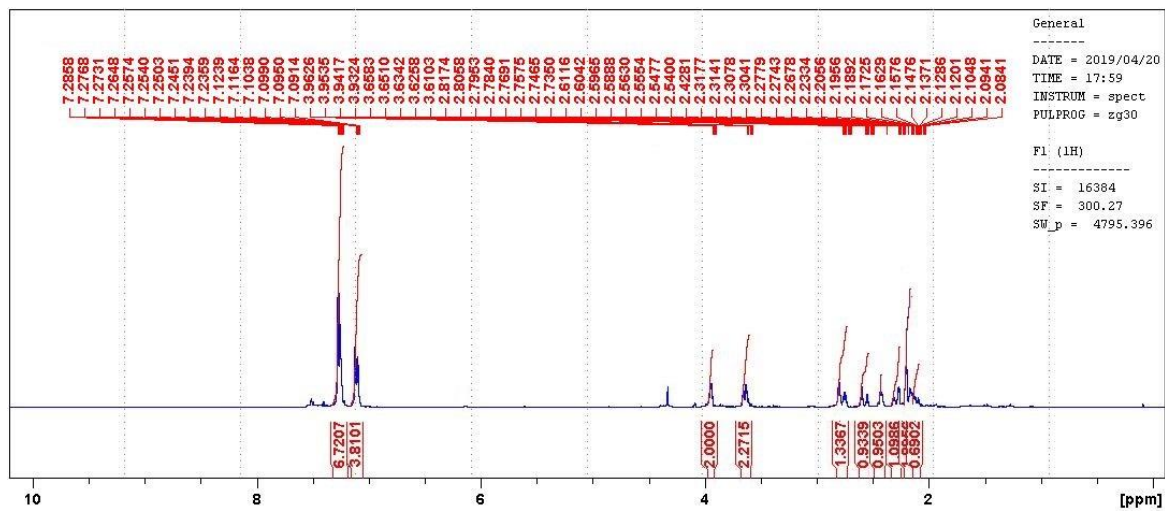


Figure E31.  $^1\text{H}$  NMR Spectra of compound **43** in  $\text{CDCl}_3$ .

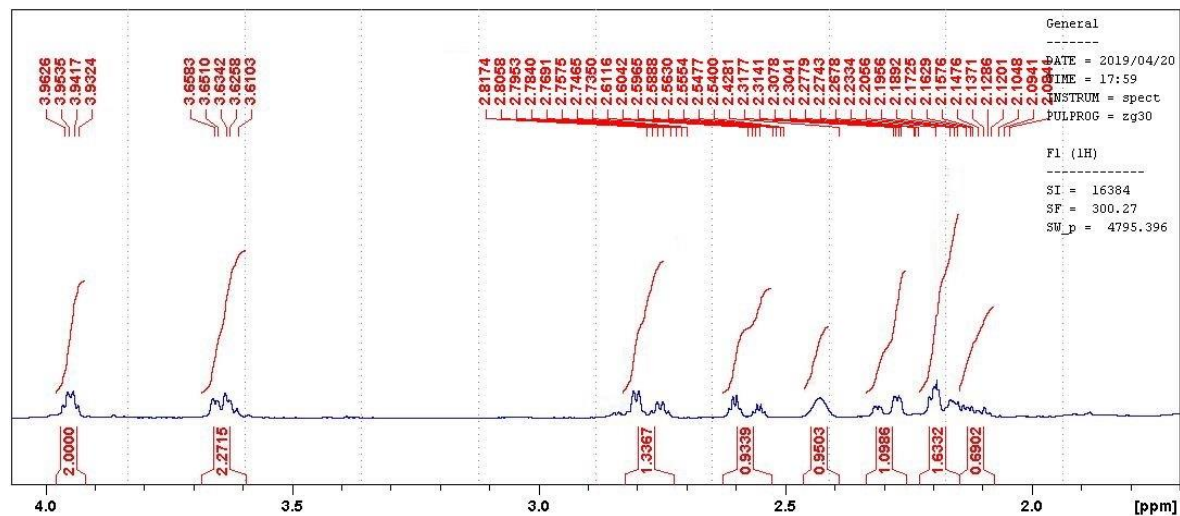


Figure E32. Magnified regions of  $^1\text{H}$  NMR Spectra of compound **43** in  $\text{CDCl}_3$ .

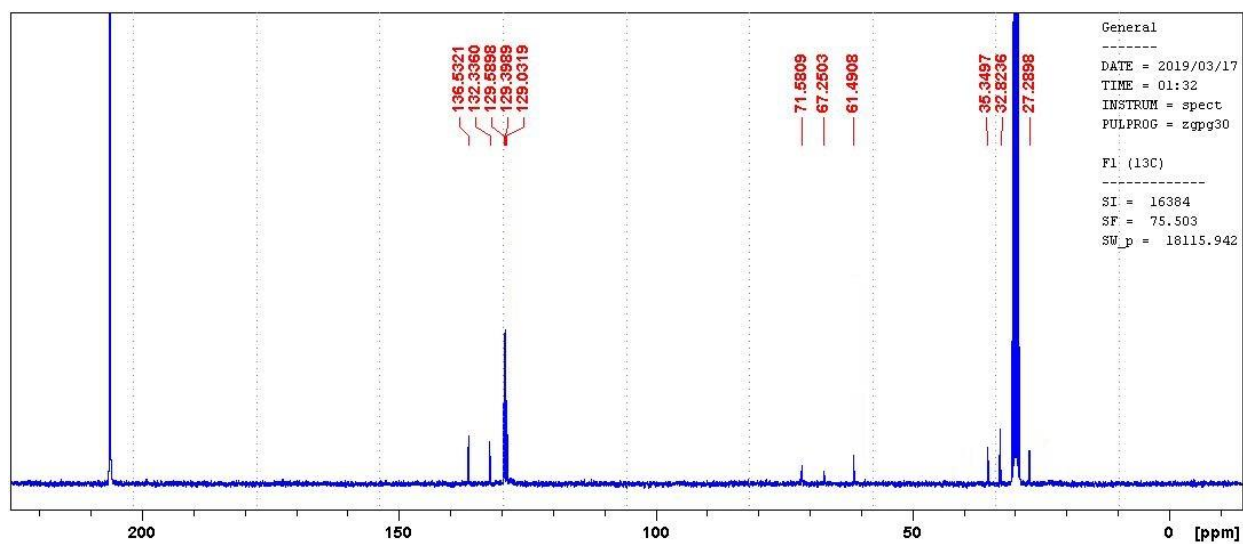


Figure E33.  $^{13}\text{C}$  NMR Spectra of compound **43** in acetone- $d_6$ .

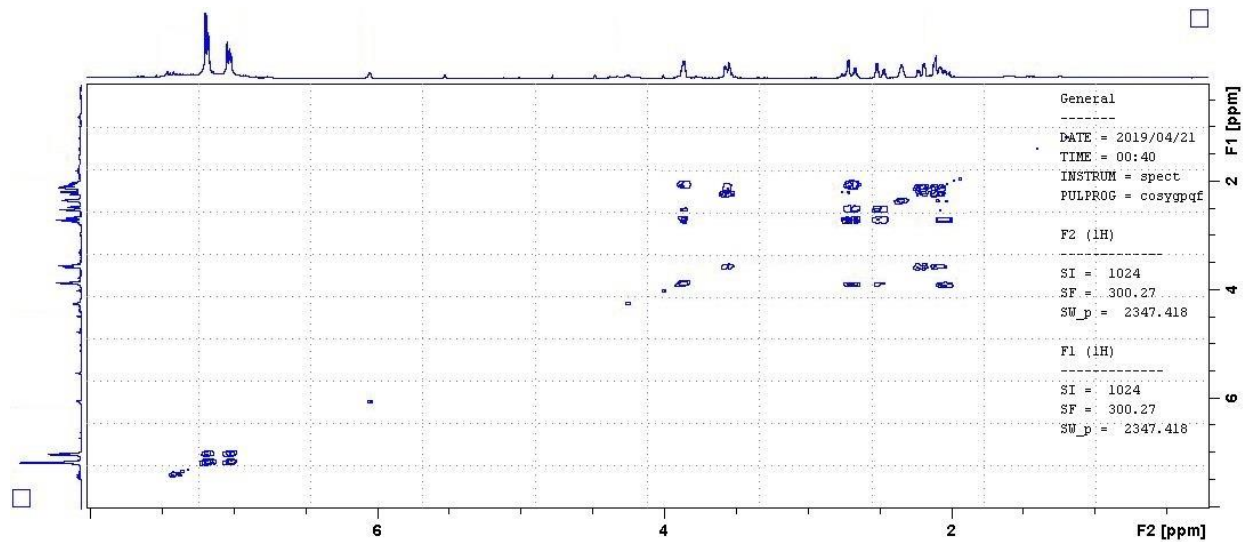


Figure E34. COSY NMR Spectra of compound **43** in  $\text{CDCl}_3$ .

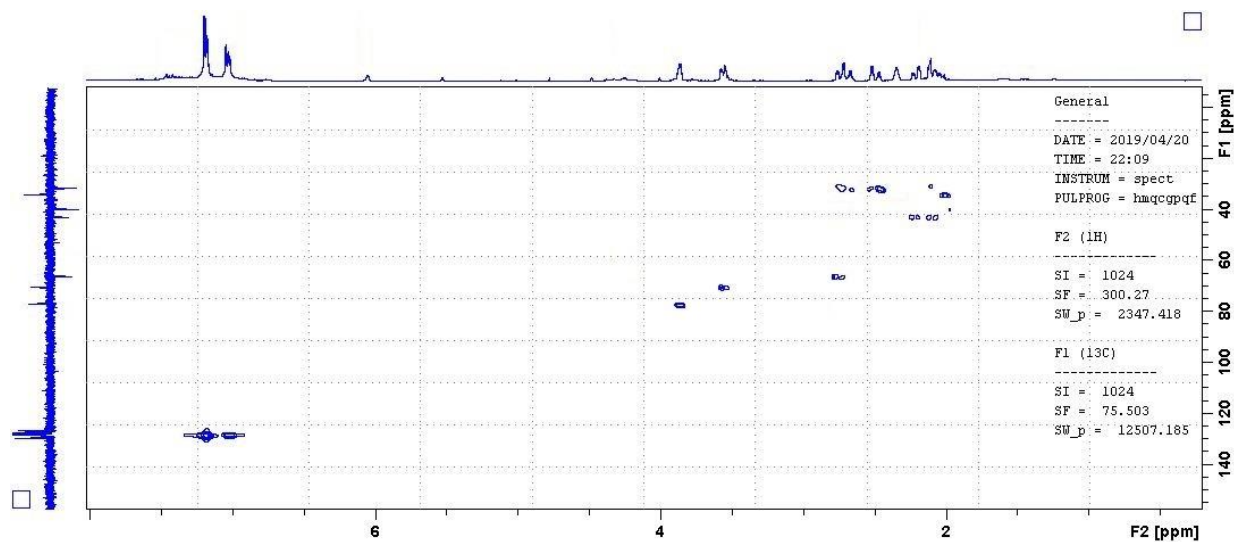


Figure E35. HSQC NMR Spectra of compound **43** in  $\text{CDCl}_3$ .

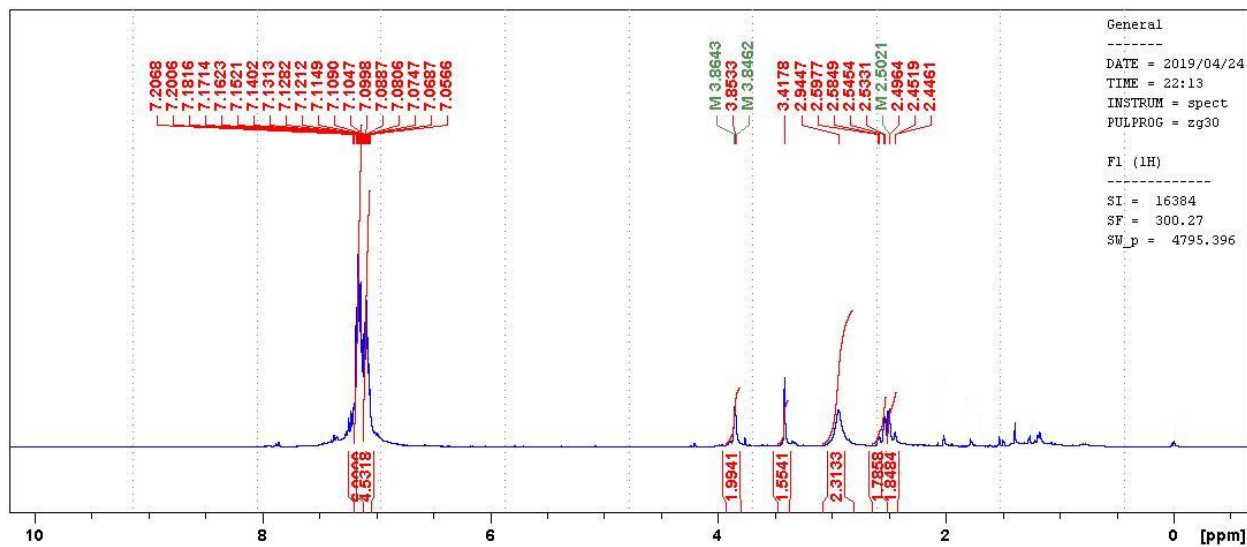


Figure E36.  $^1\text{H}$  NMR Spectra of compound **45** in  $\text{CDCl}_3$ .

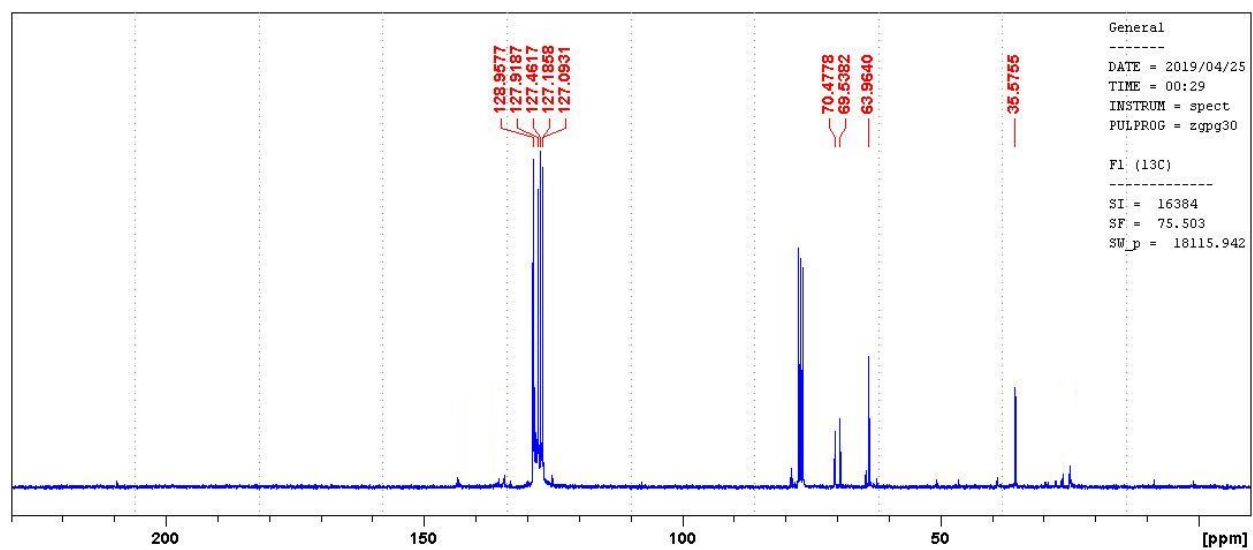


Figure E37.  $^{13}\text{C}$  NMR Spectra of compound **45** in  $\text{CDCl}_3$ .

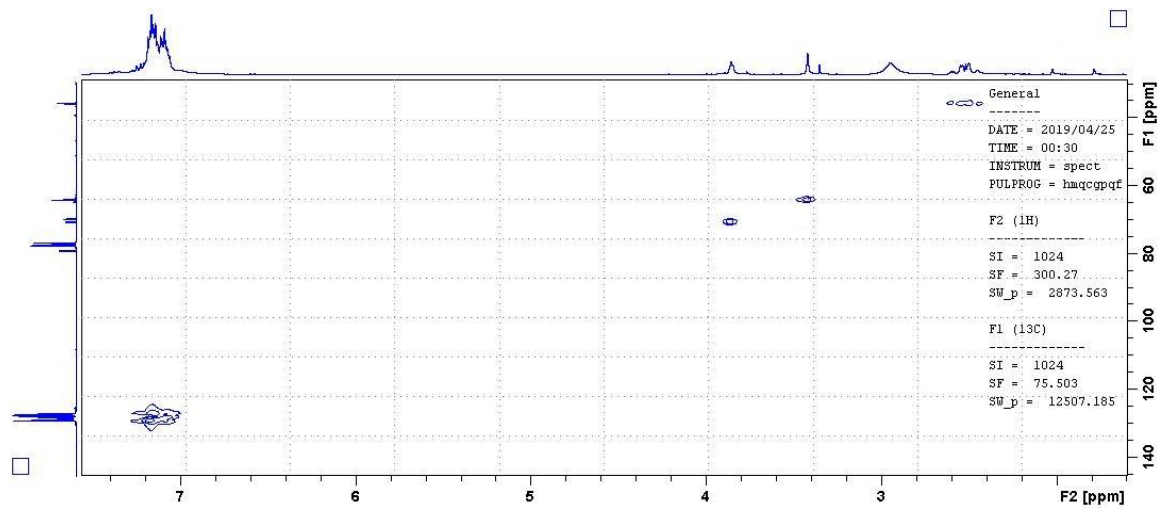
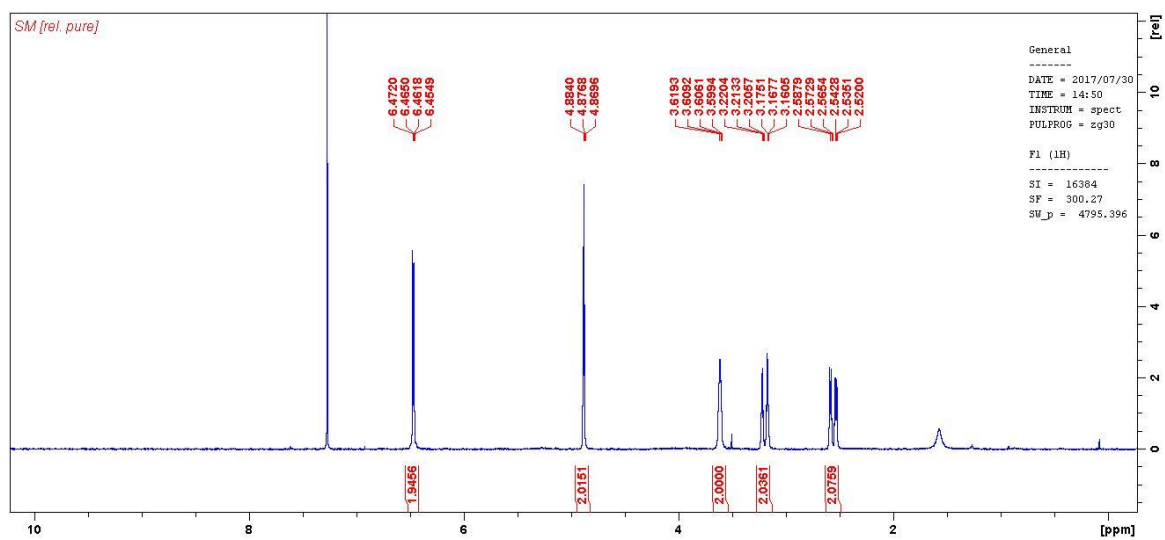
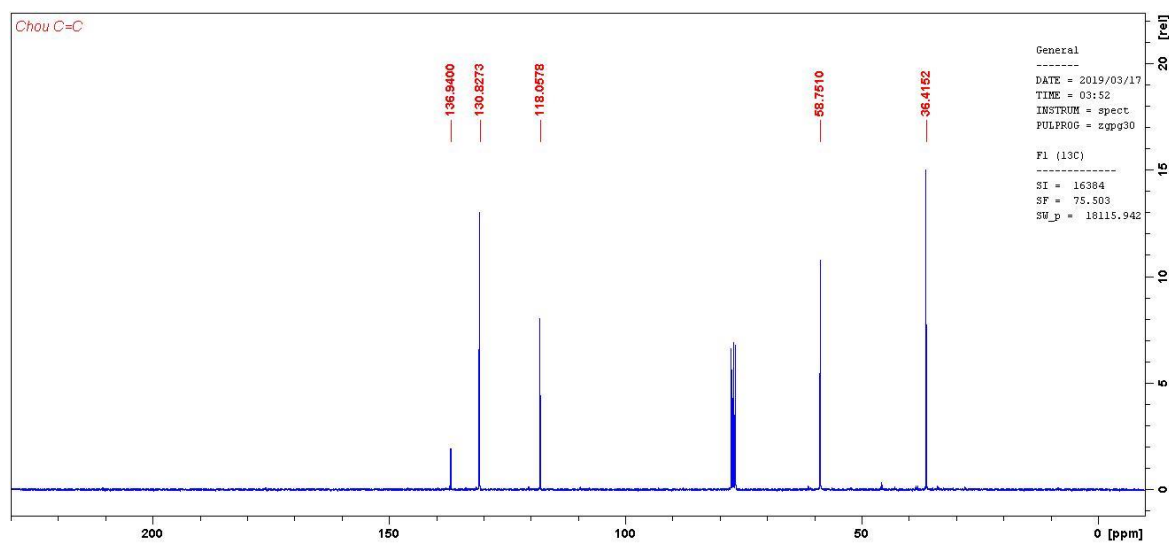


Figure E38. HSQC NMR Spectra of compound **45** in  $\text{CDCl}_3$ .

Figure E39.  $^1\text{H}$  NMR Spectra of compound **47** in  $\text{CDCl}_3$ .Figure E40.  $^{13}\text{C}$  NMR Spectra of compound **47** in  $\text{CDCl}_3$ .

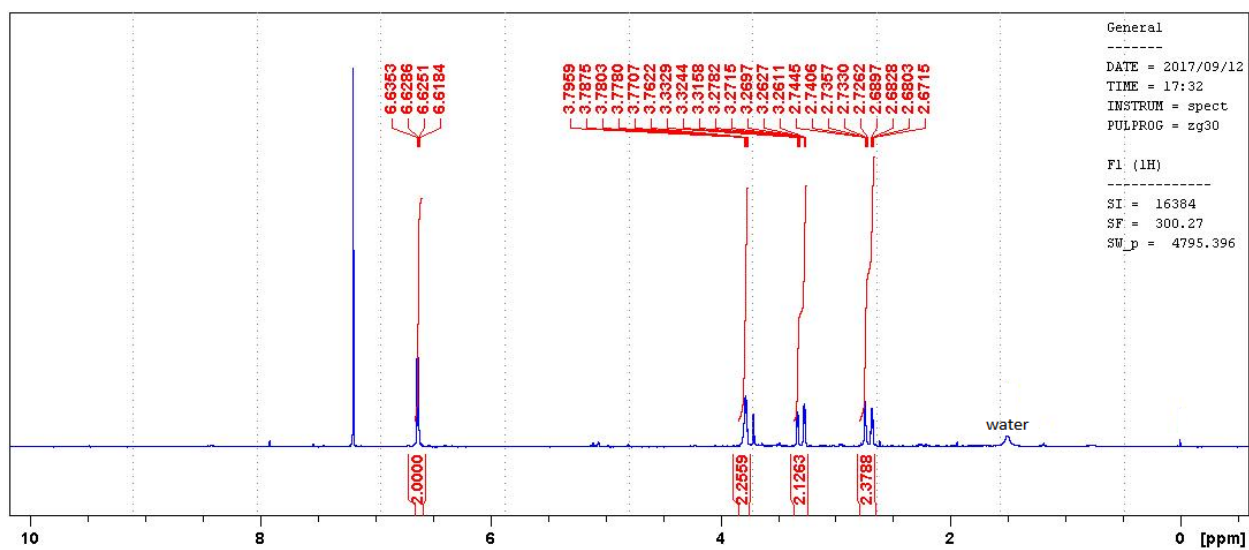


Figure E41.  $^1\text{H}$  NMR Spectra of compound **52** in  $\text{CDCl}_3$ .

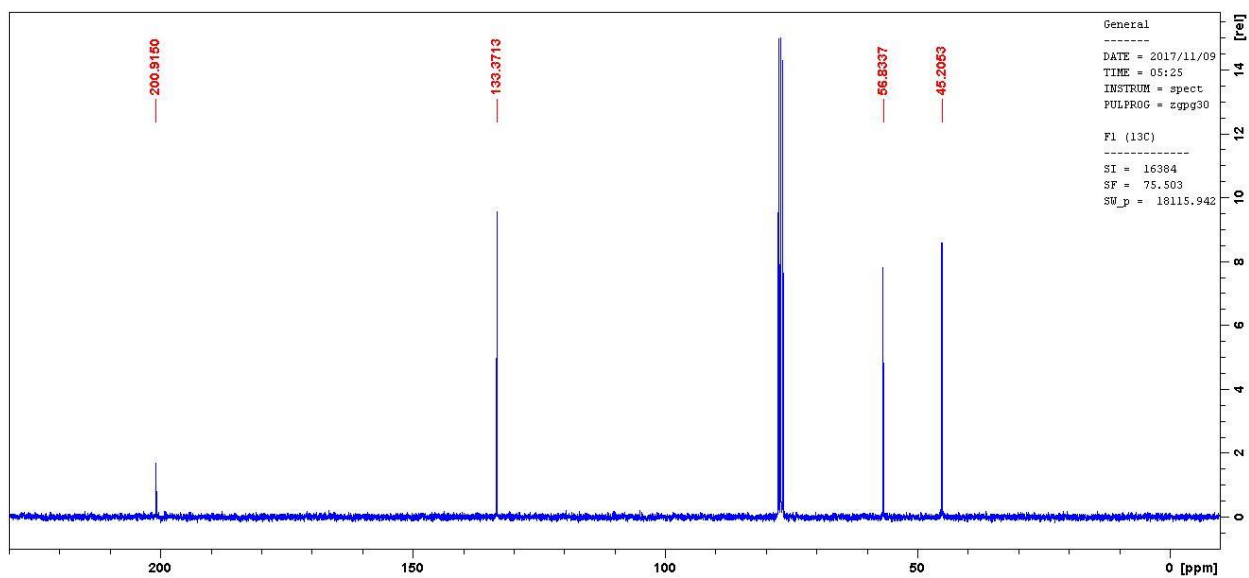


Figure E42.  $^{13}\text{C}$  NMR Spectra of compound **52** in  $\text{CDCl}_3$ .

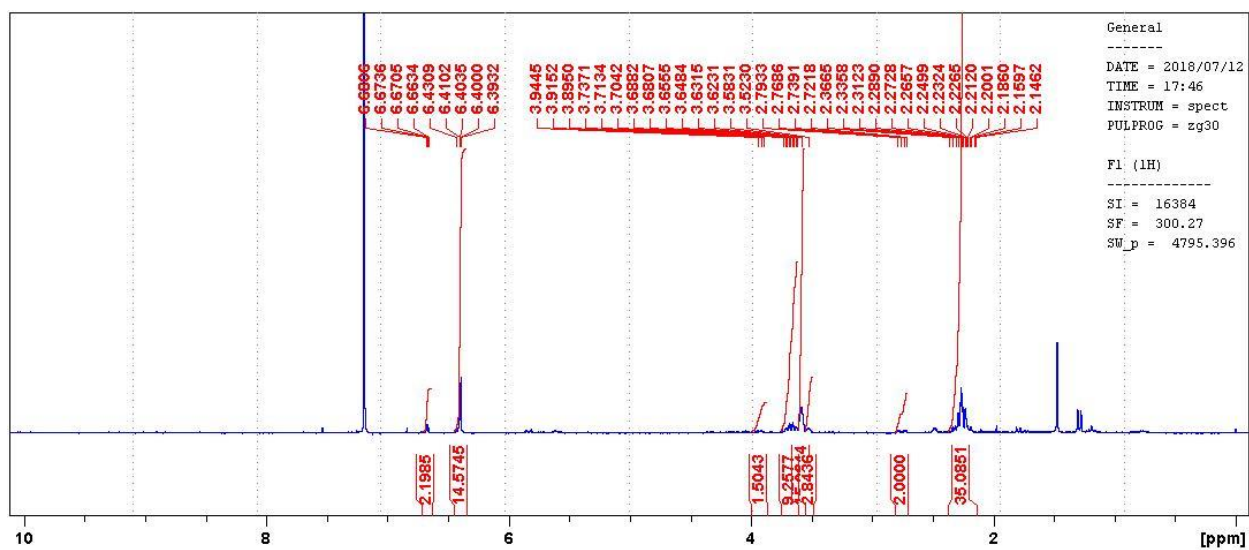


Figure E43.  $^1\text{H}$  NMR Spectra of compounds **57a** and **57b** in  $\text{CDCl}_3$ .

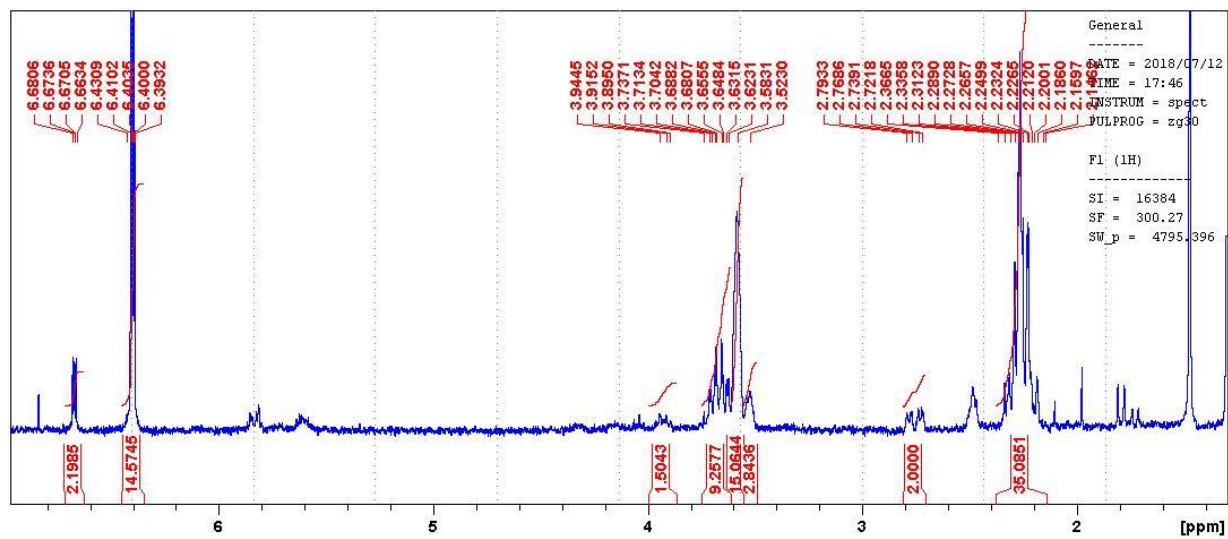


Figure E44. Magnified regions of  $^1\text{H}$  NMR Spectra of compounds **57a** and **57b** in  $\text{CDCl}_3$ .

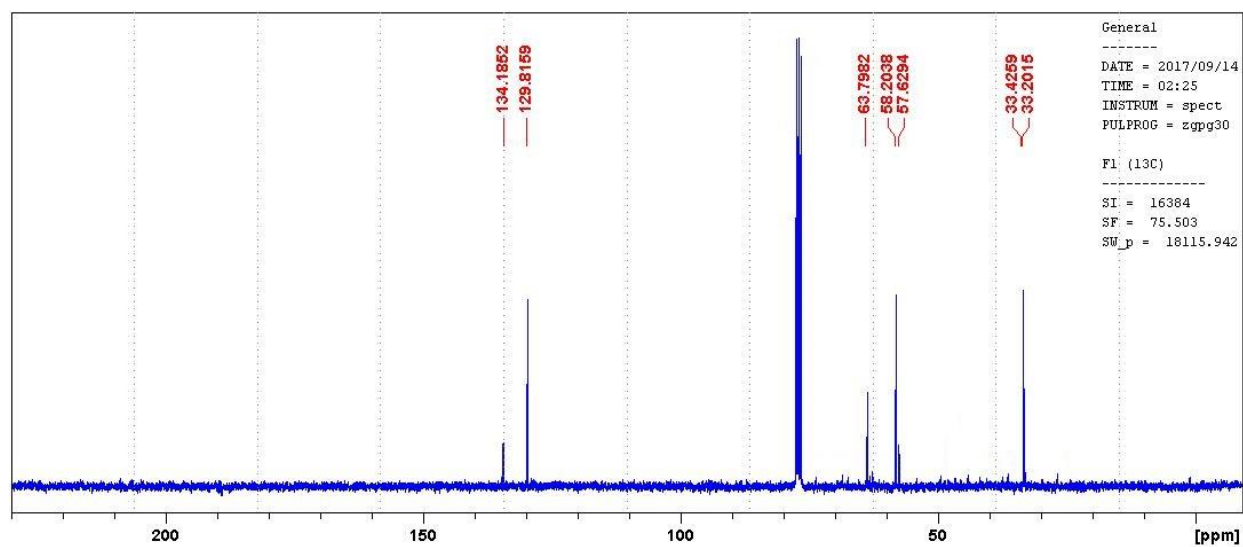


Figure E45.  $^{13}\text{C}$  NMR Spectra of compounds **57a** and **57b** in  $\text{CDCl}_3$ .

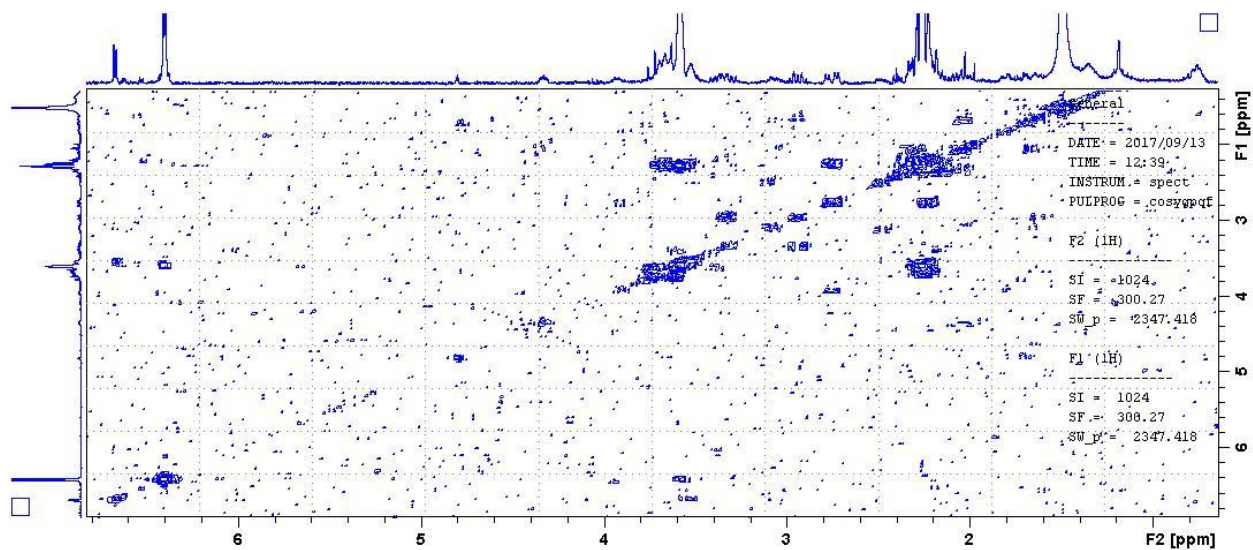


Figure E46. COSY NMR Spectra of compounds **57a** and **57b** in  $\text{CDCl}_3$ .

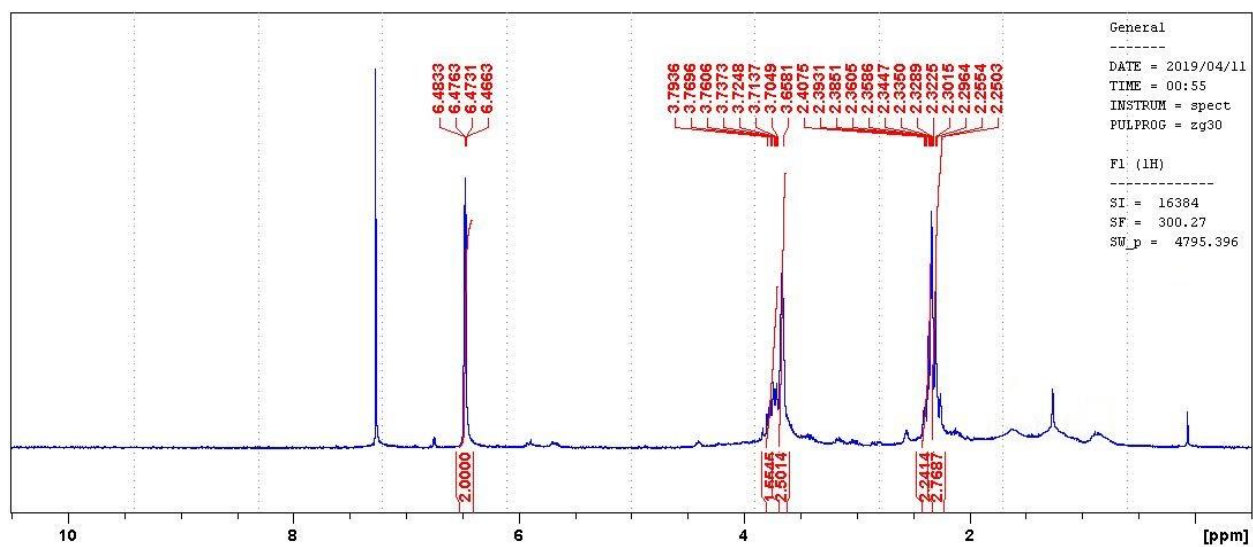


Figure E47.  $^1\text{H}$  NMR Spectra of compound **57a** in  $\text{CDCl}_3$ .

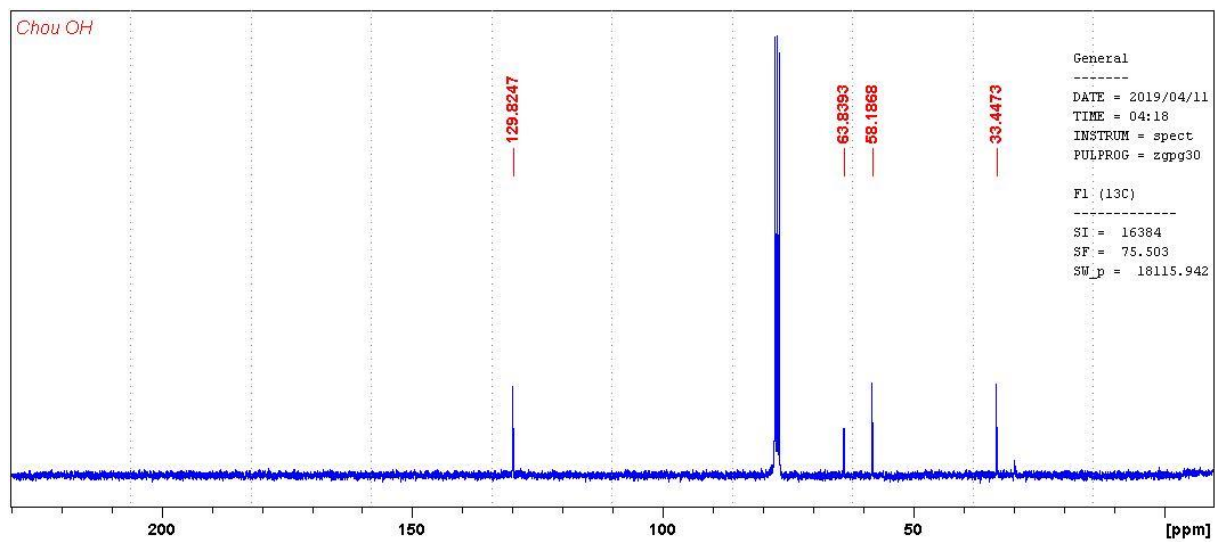


Figure E48.  $^{13}\text{C}$  NMR Spectra of compound **57a** in  $\text{CDCl}_3$ .

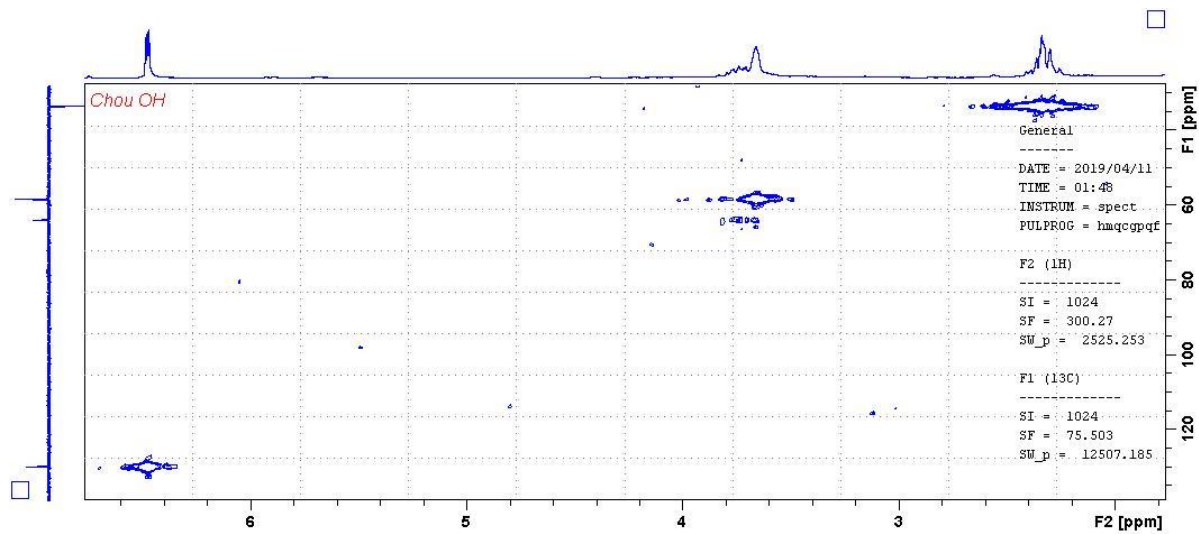


Figure E49. HSQC NMR Spectra of compound **57a** in  $\text{CDCl}_3$ .

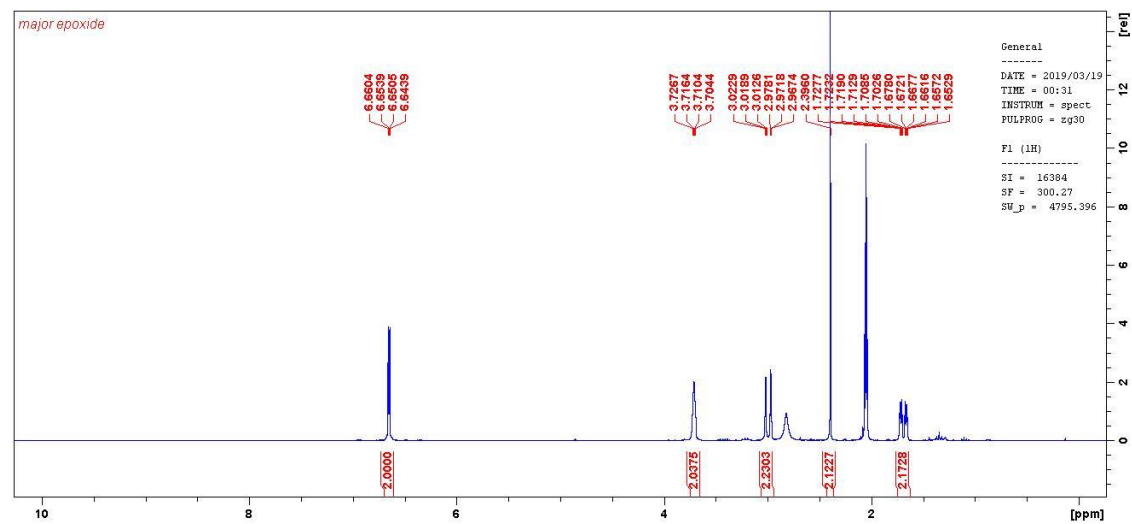


Figure E50.  $^1\text{H}$  NMR Spectra of compound **58** in  $\text{acetone-d}_6$ .

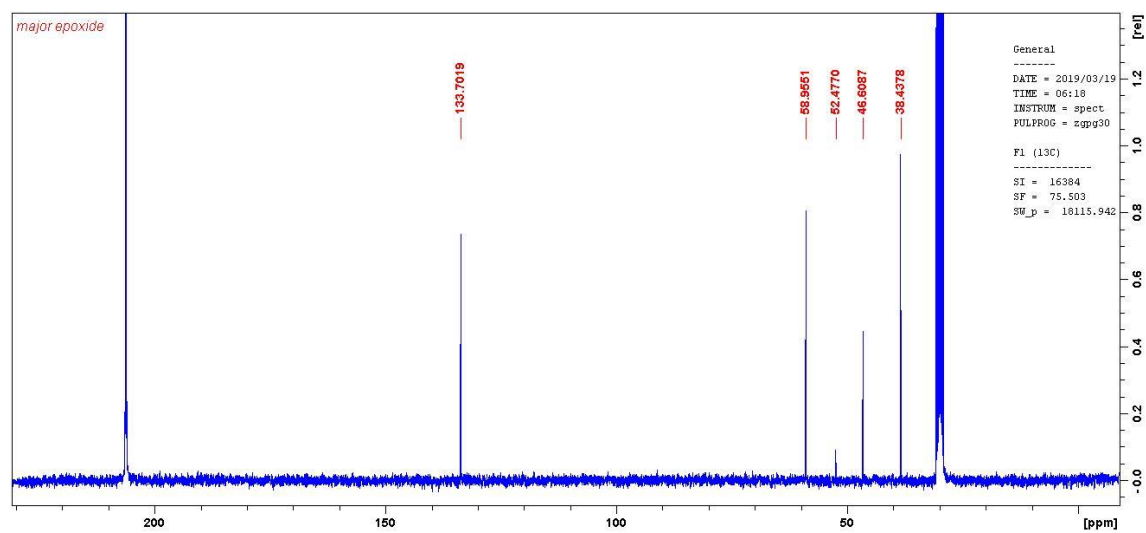


Figure E51.  $^{13}\text{C}$  NMR Spectra of compound **58** in acetone- $d_6$ .

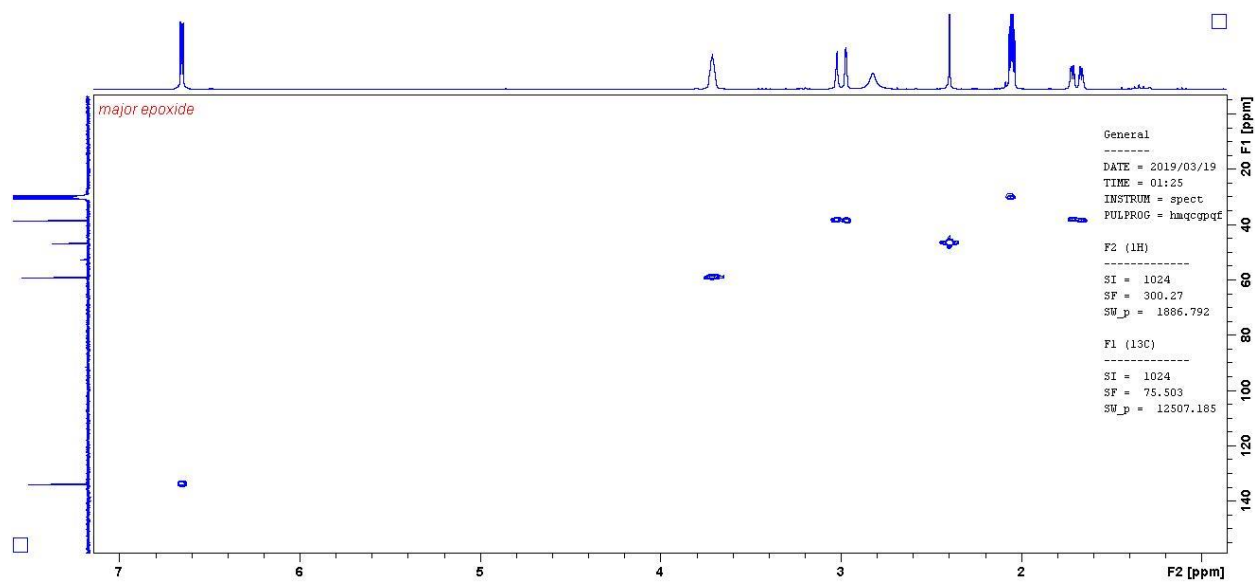


Figure E52. COSY NMR Spectra of compound **58** in acetone- $d_6$ .

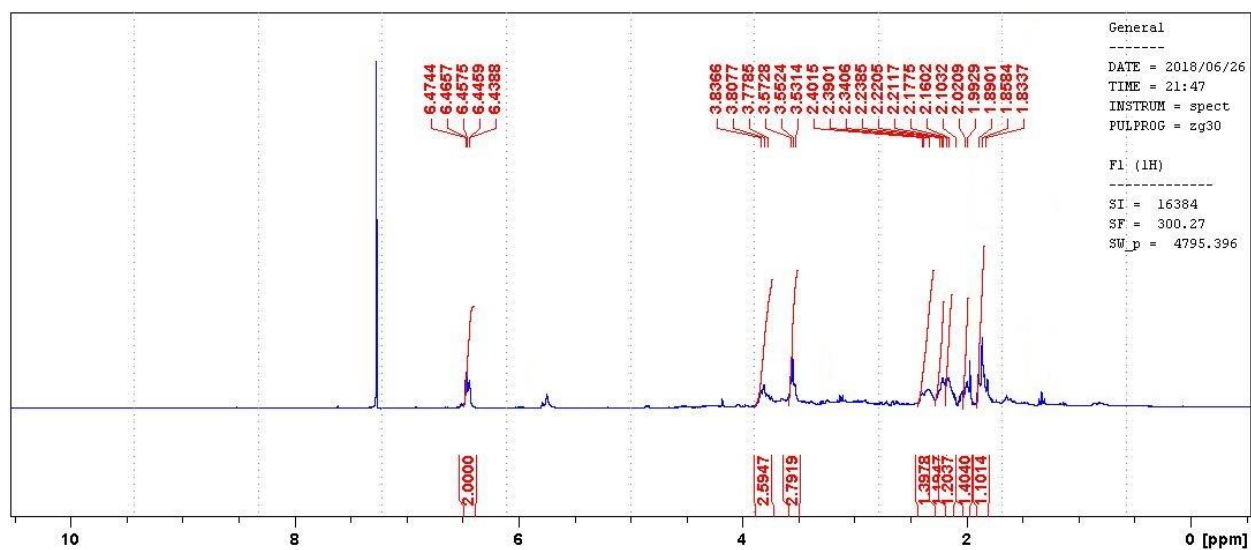


Figure E53.  $^1\text{H}$  NMR Spectra of compound **59** in  $\text{CDCl}_3$ .

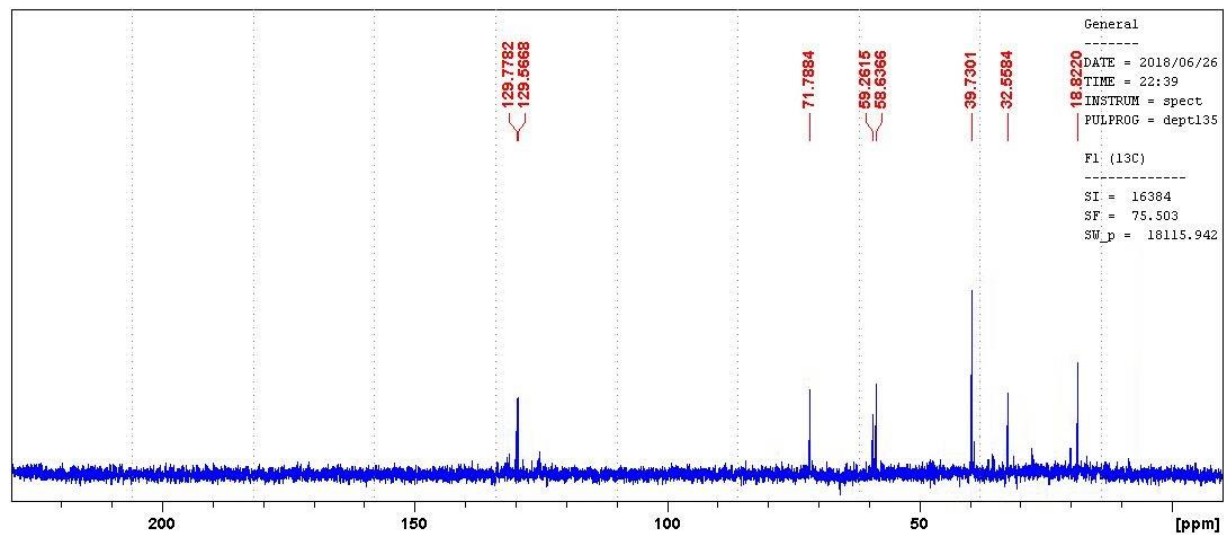


Figure E54.  $^{13}\text{C}$  NMR Spectra of compound **59** in  $\text{CDCl}_3$ .

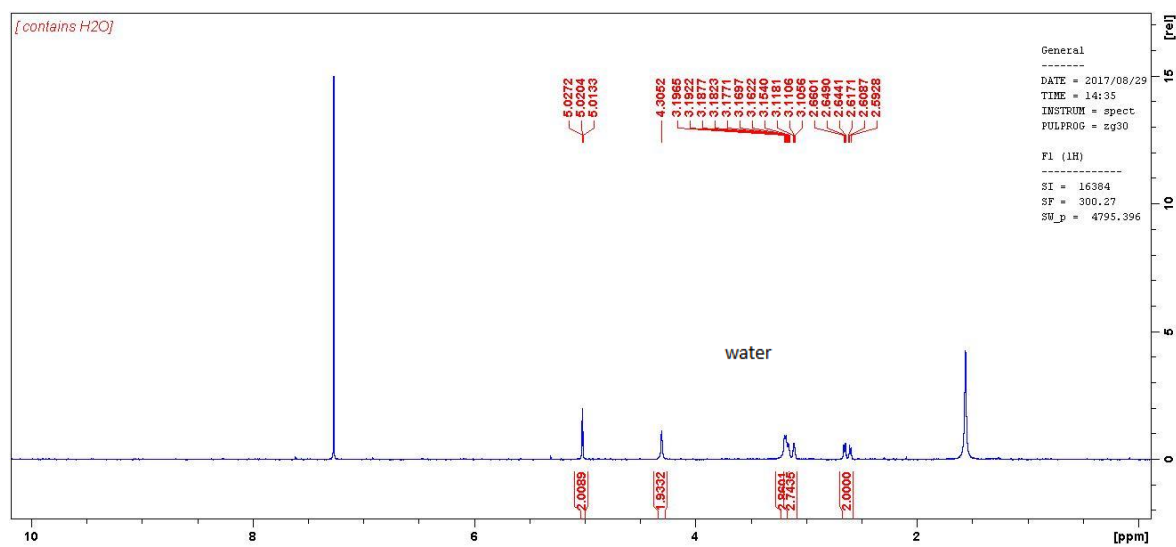


Figure E55. <sup>1</sup>H NMR Spectra of compound **60** in CDCl<sub>3</sub>.

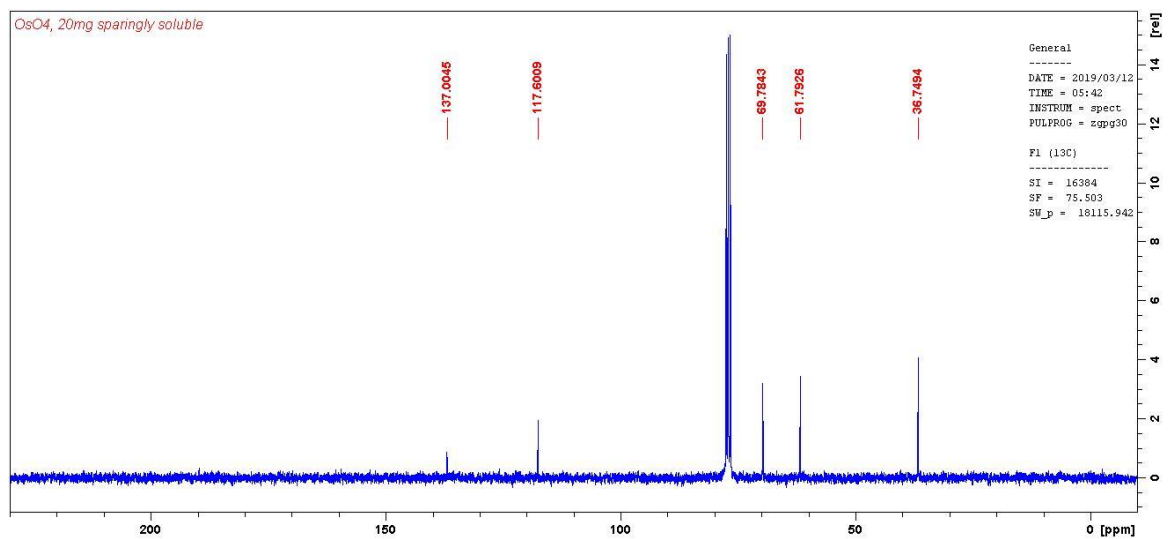


Figure E56. <sup>13</sup>C NMR Spectra of compound **60** in CDCl<sub>3</sub>.

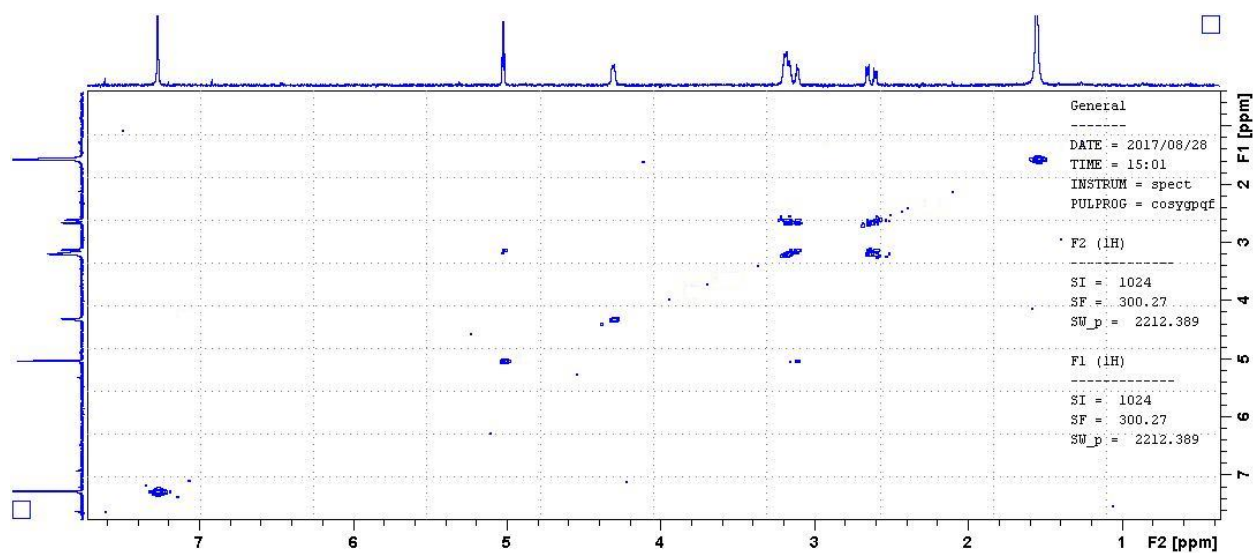


Figure E57. COSY NMR Spectra of compound **60** in  $\text{CDCl}_3$ .

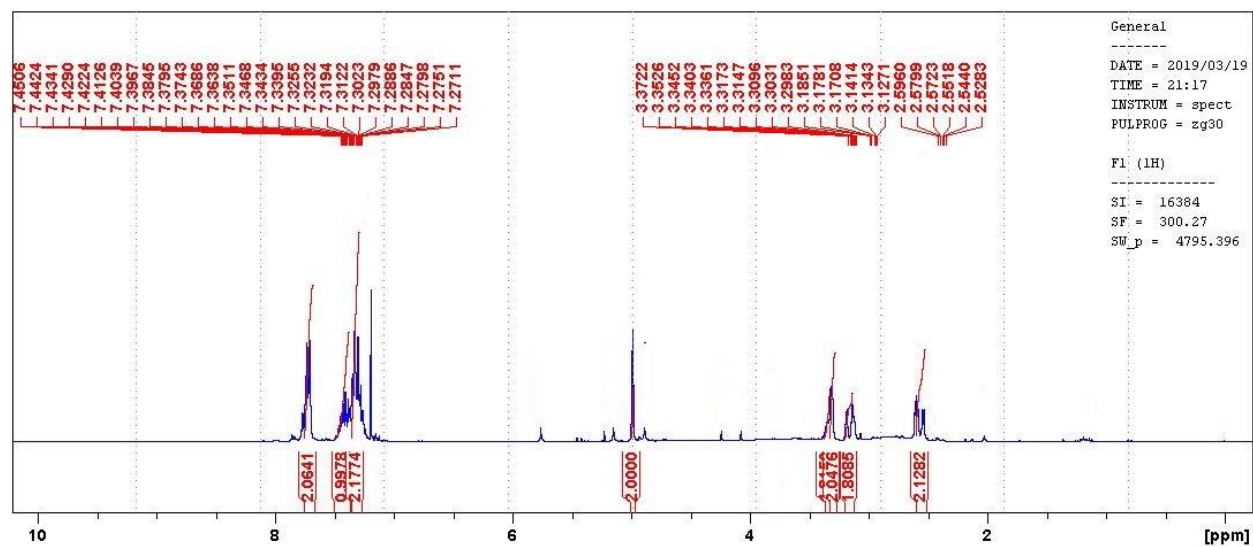


Figure E58.  $^1\text{H}$  NMR Spectra of compound **62** in  $\text{CDCl}_3$ .

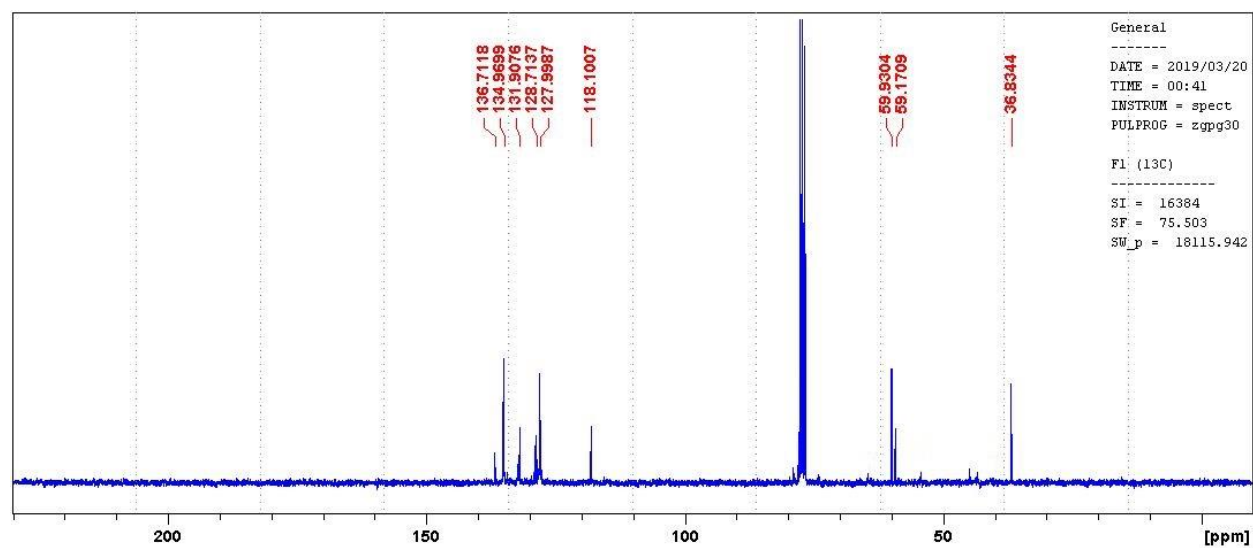


Figure E59.  $^{13}\text{C}$  NMR Spectra of compound **62** in  $\text{CDCl}_3$ .

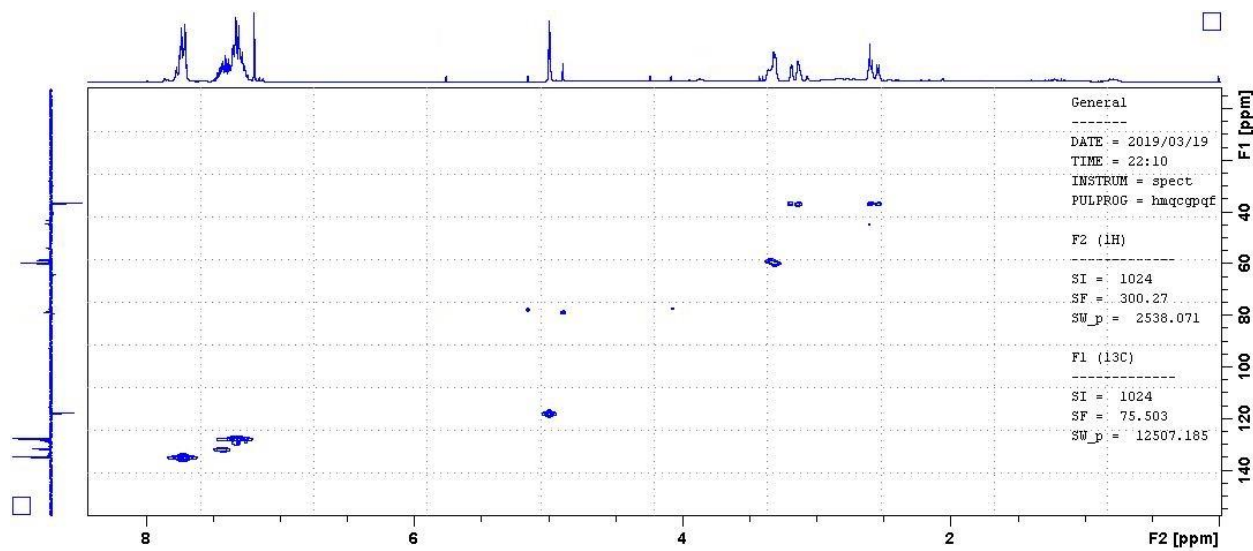


Figure E60. HSQC NMR Spectra of compound **62** in  $\text{CDCl}_3$ .

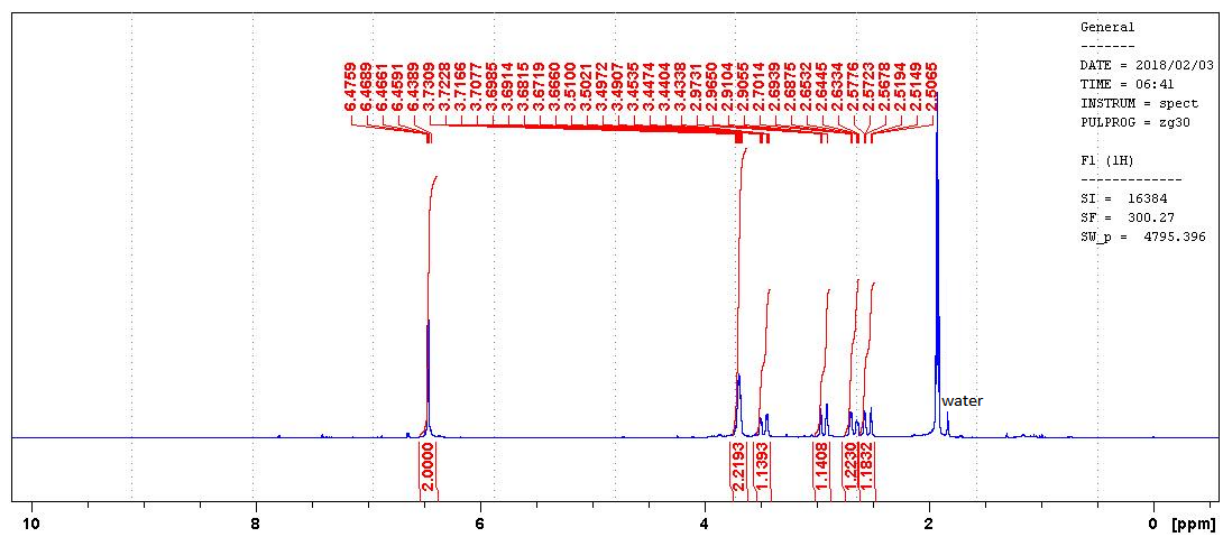


Figure E61.  $^1\text{H}$  NMR Spectra of compound **67a** in acetone- $d_6$ .

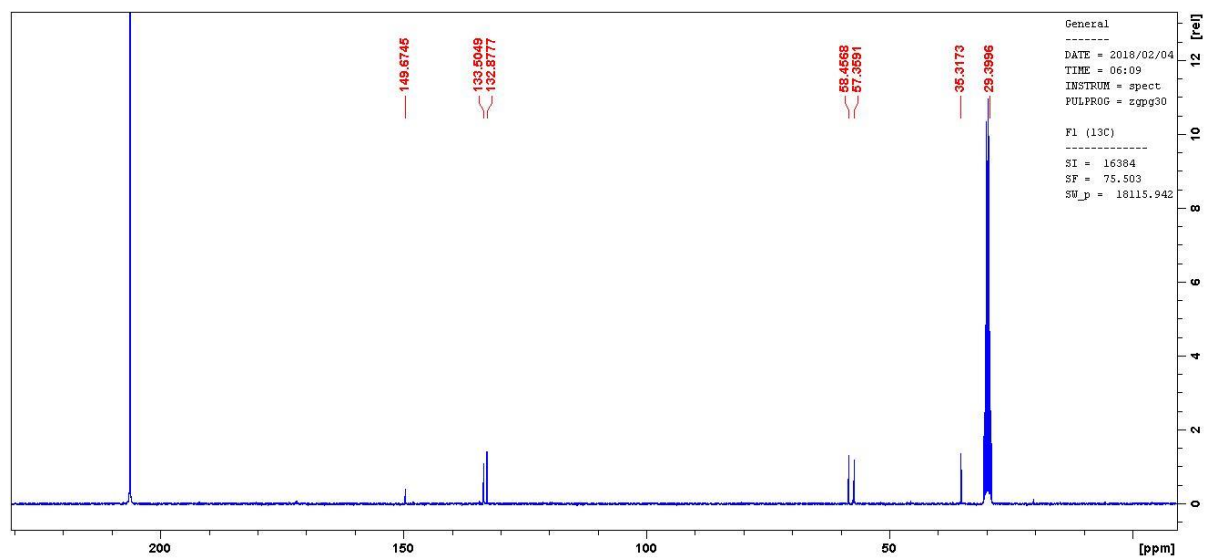


Figure E62.  $^{13}\text{C}$  NMR Spectra of compound **67a** in acetone- $d_6$ .

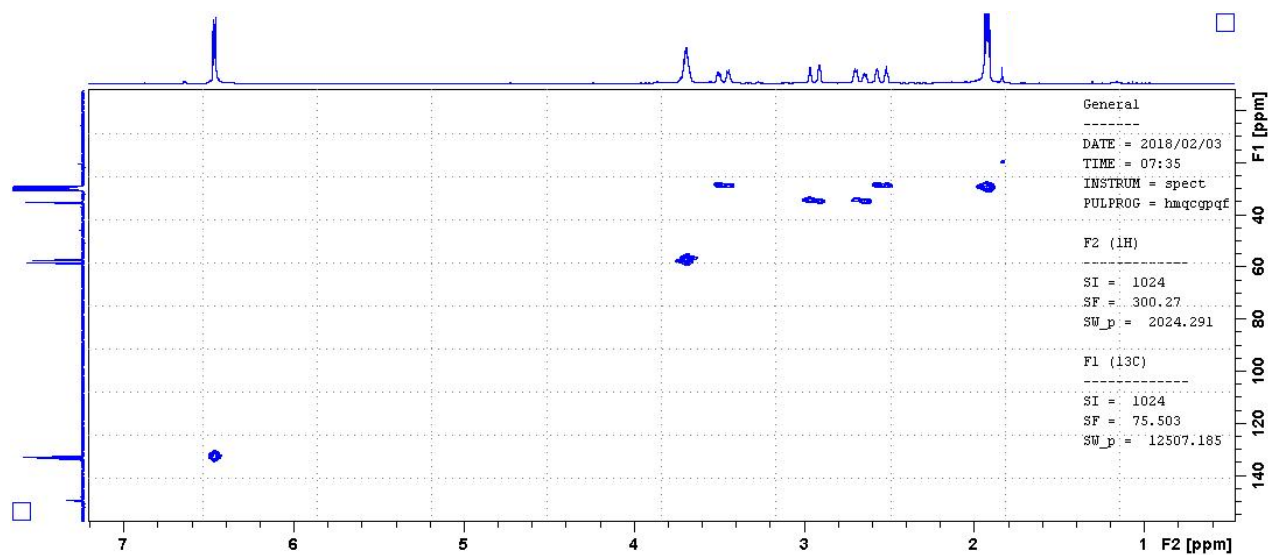


Figure E63. HSQC NMR Spectra of compound **67a** in acetone- $d_6$ .

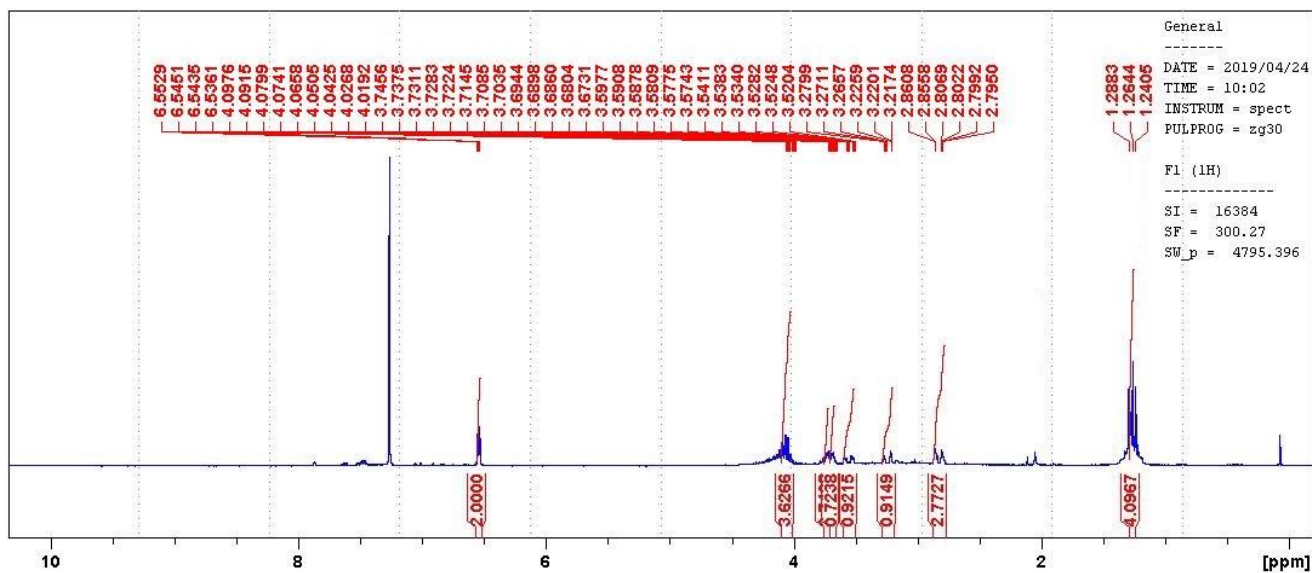


Figure E64.  $^1\text{H}$  NMR Spectra of compound **67b** in  $\text{CDCl}_3$ .

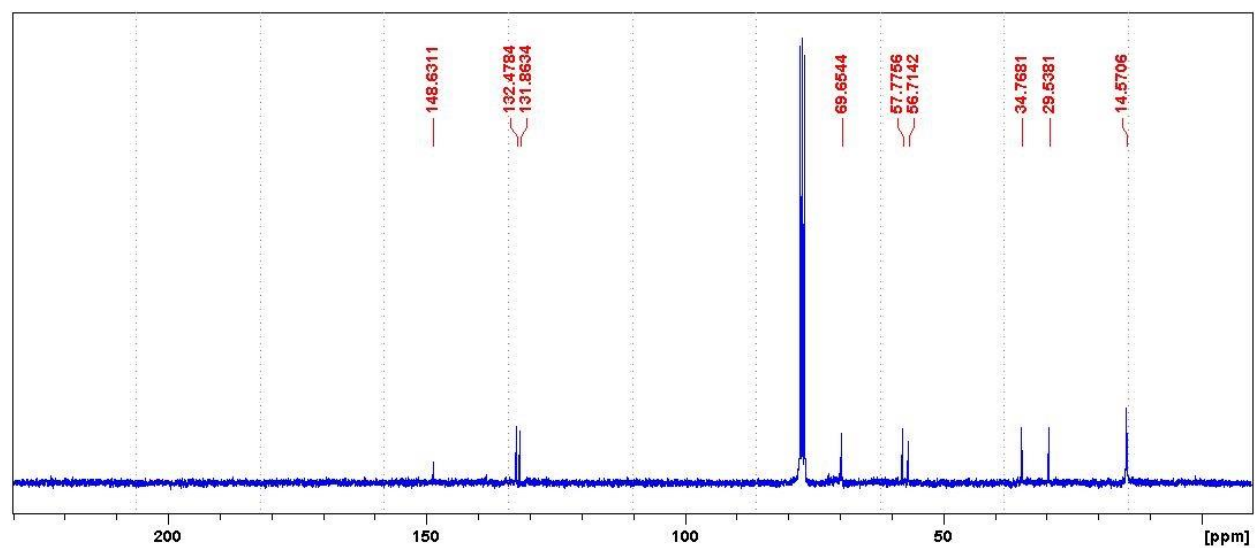


Figure E65. <sup>13</sup>C NMR Spectra of compound **67b** in CDCl<sub>3</sub>.

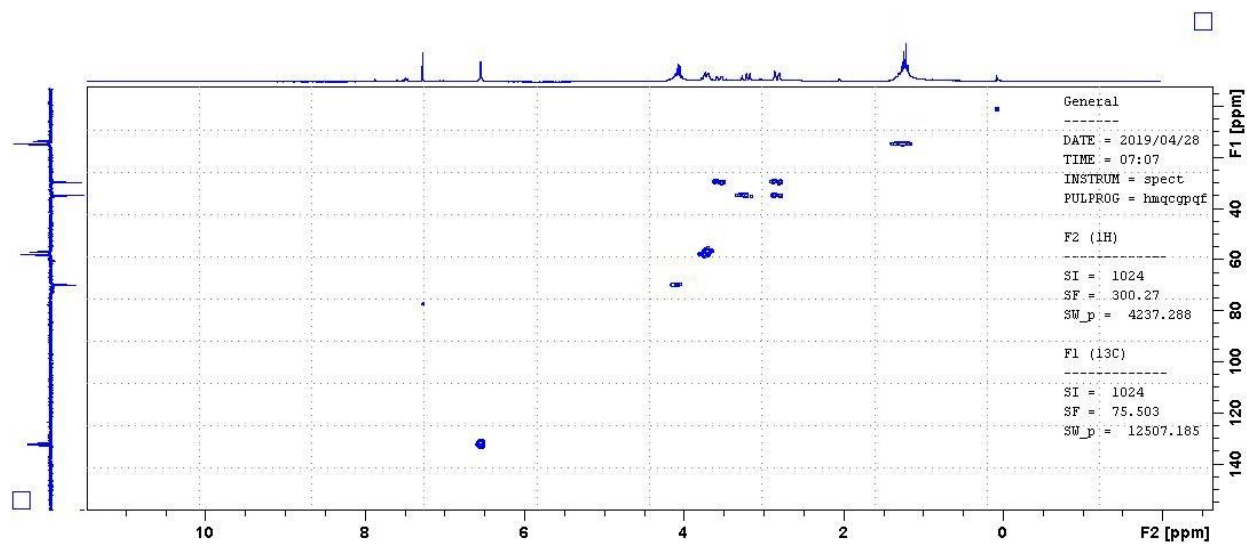


Figure E66. HSQC NMR Spectra of compound **67b** in CDCl<sub>3</sub>.

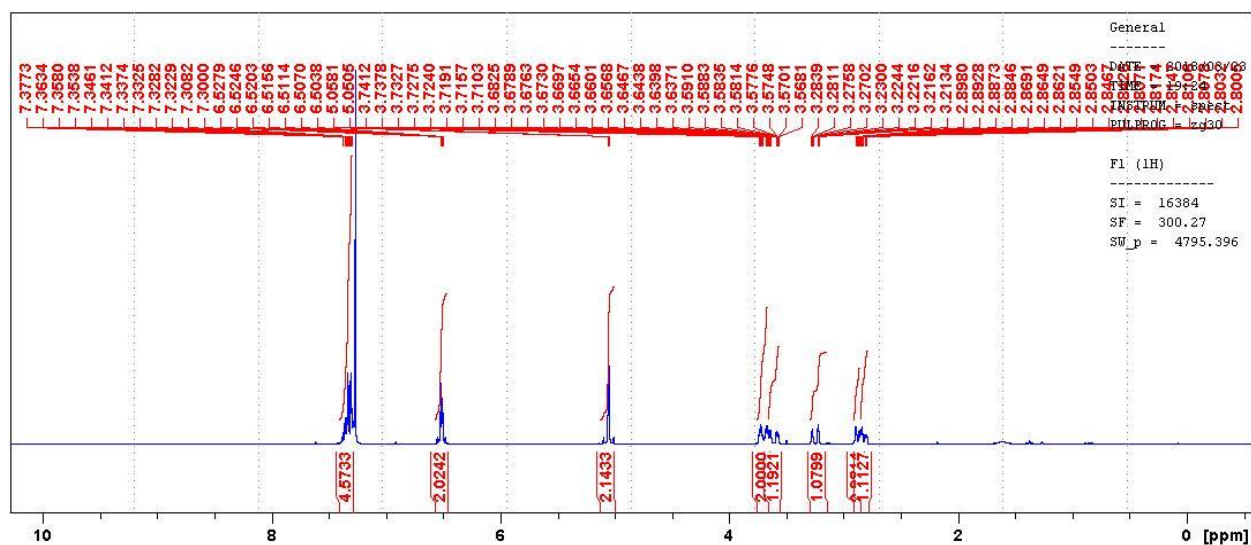


Figure E67.  $^1\text{H}$  NMR Spectra of compound **67c** in  $\text{CDCl}_3$ .

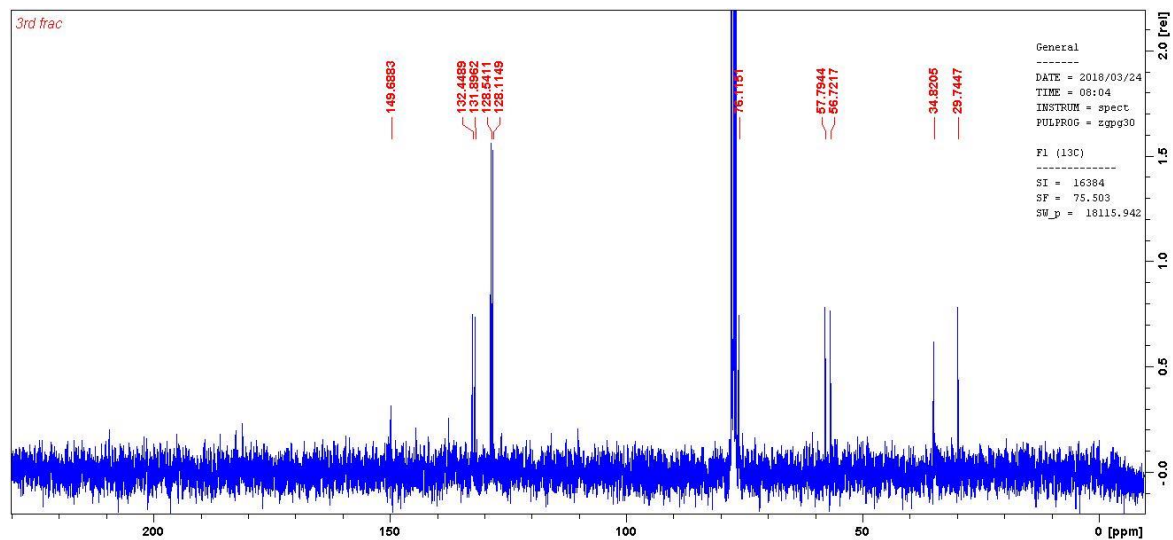


Figure E68.  $^{13}\text{C}$  NMR Spectra of compound **67c** in  $\text{CDCl}_3$ .

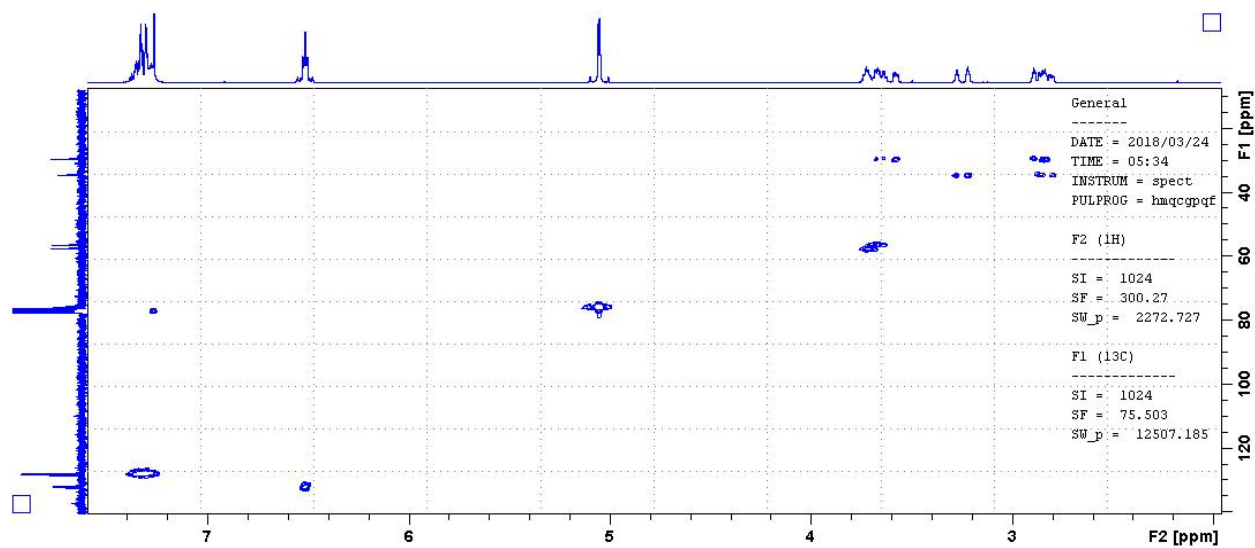


Figure E69. HSQC NMR Spectra of compound **67c** in  $\text{CDCl}_3$ .

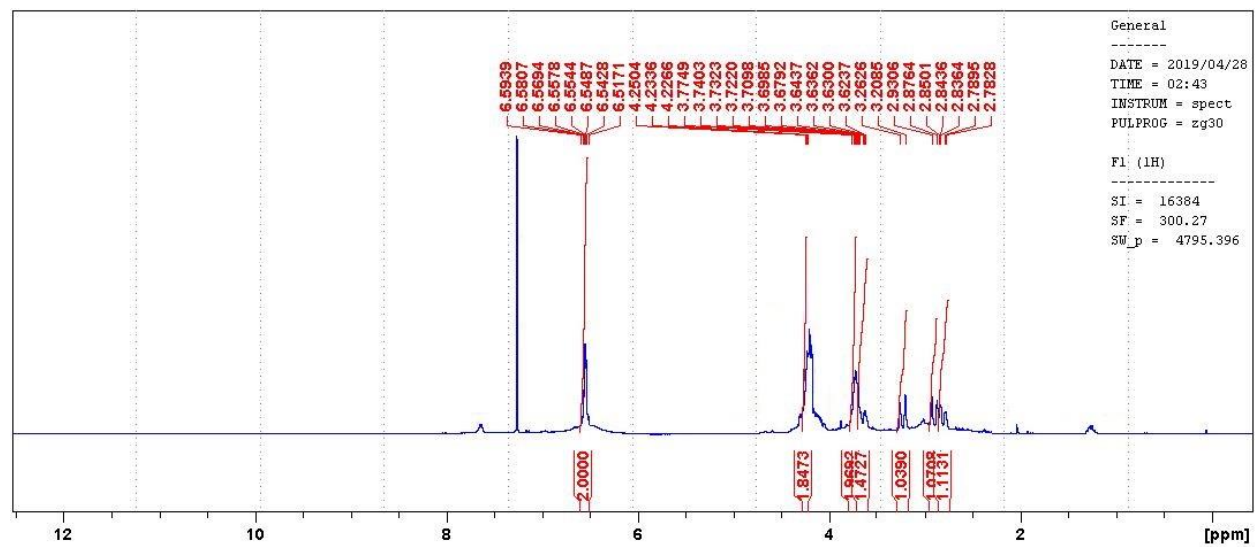


Figure E70.  $^1\text{H}$  NMR Spectra of compound **67d** in  $\text{CDCl}_3$ .

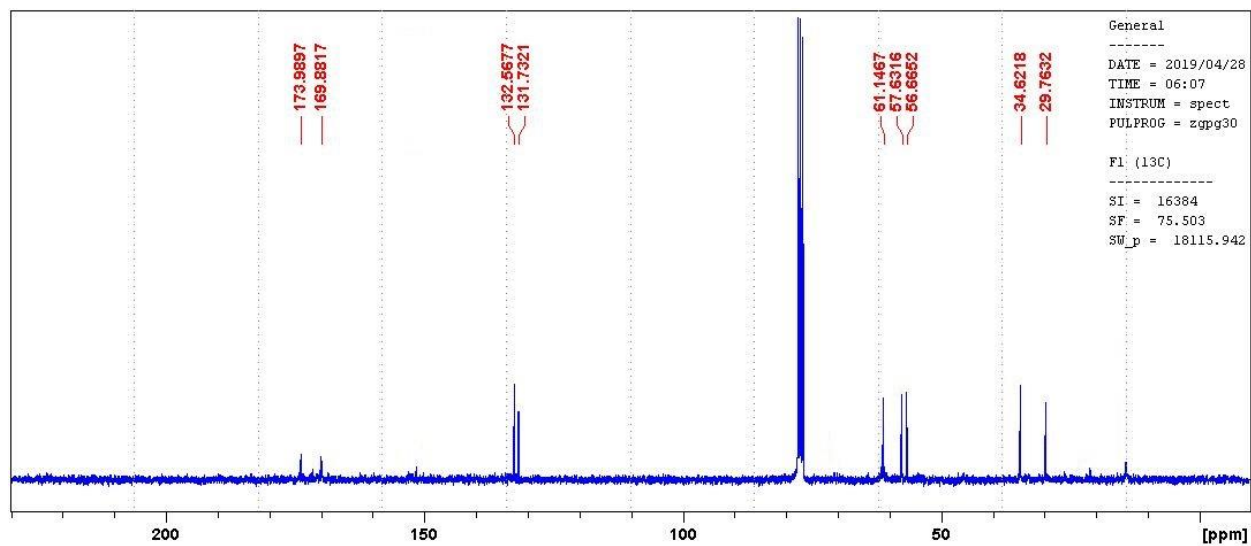


Figure E71.  $^{13}\text{C}$  NMR Spectra of compound **67d** in  $\text{CDCl}_3$ .

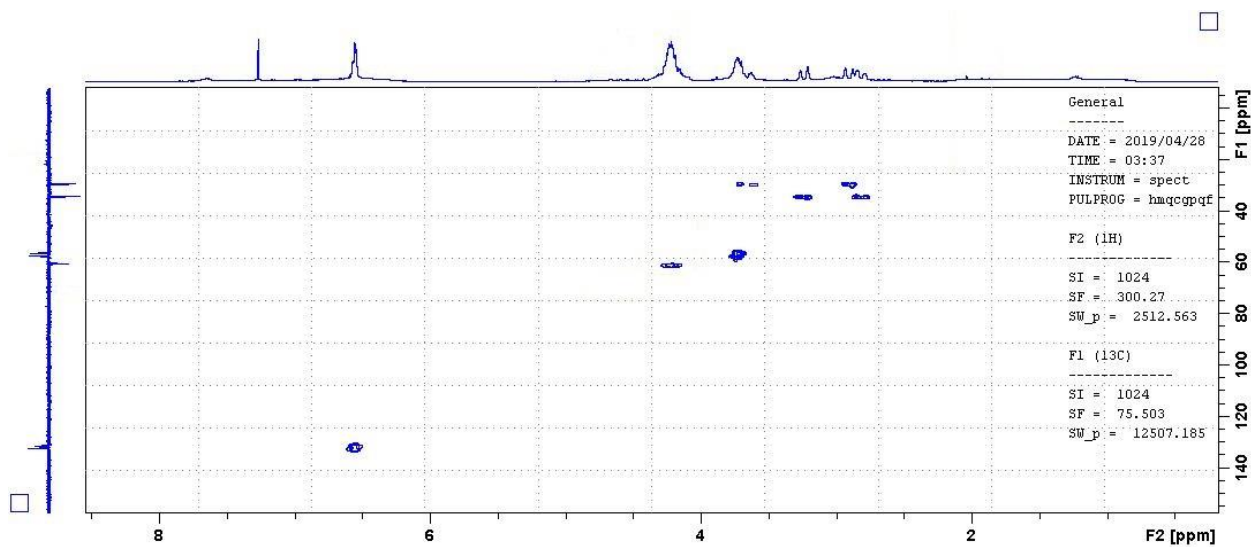


Figure E72. HSQC NMR Spectra of compound **67d** in  $\text{CDCl}_3$ .

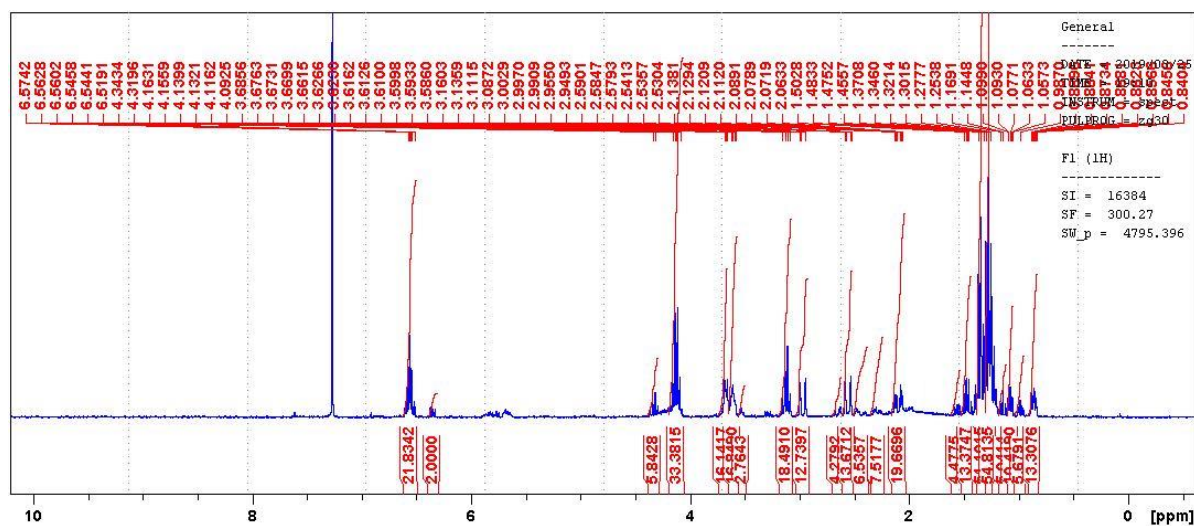


Figure E73.  $^1\text{H}$  NMR Spectra of compounds **68a** and **68b** in  $\text{CDCl}_3$ .

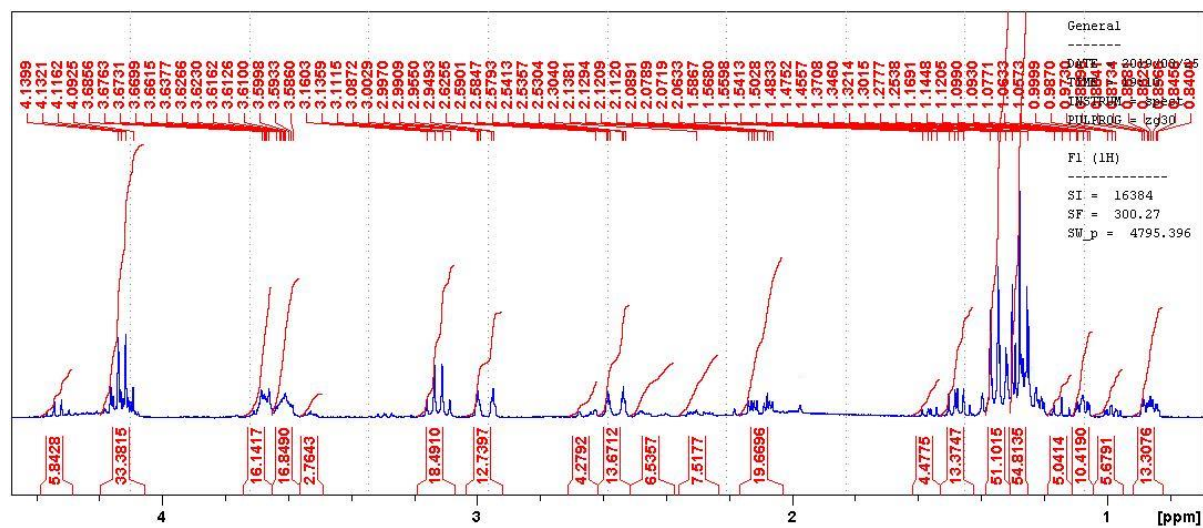


Figure E74. Magnified regions of  $^1\text{H}$  NMR Spectra of compounds **68a** and **68b** in  $\text{CDCl}_3$ .

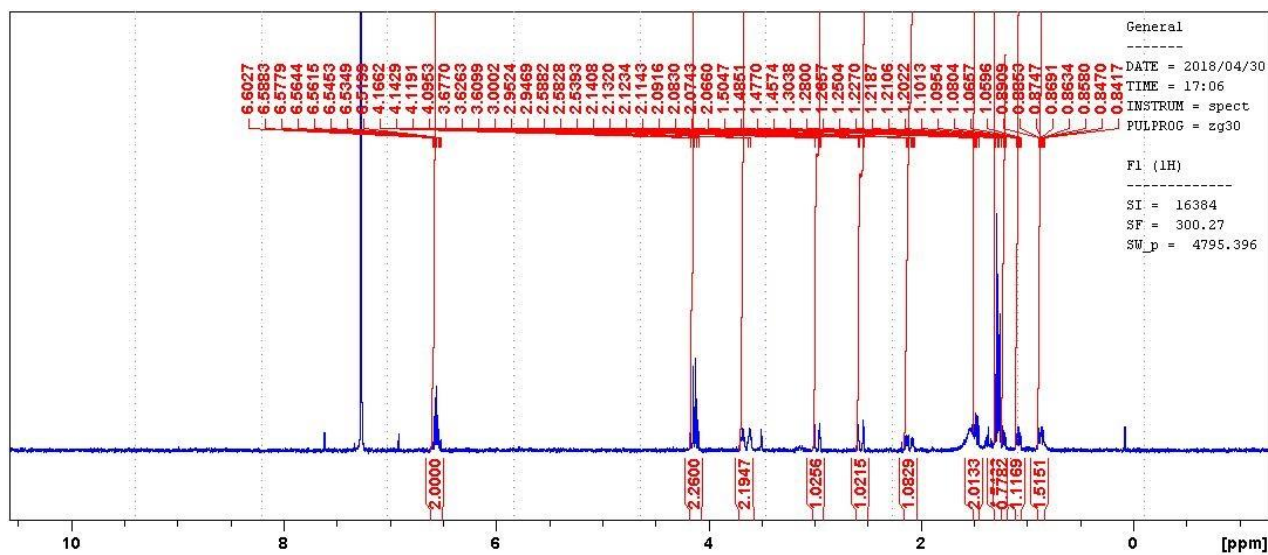


Figure E75.  $^1\text{H}$  NMR Spectra of compound **68a** in  $\text{CDCl}_3$ .

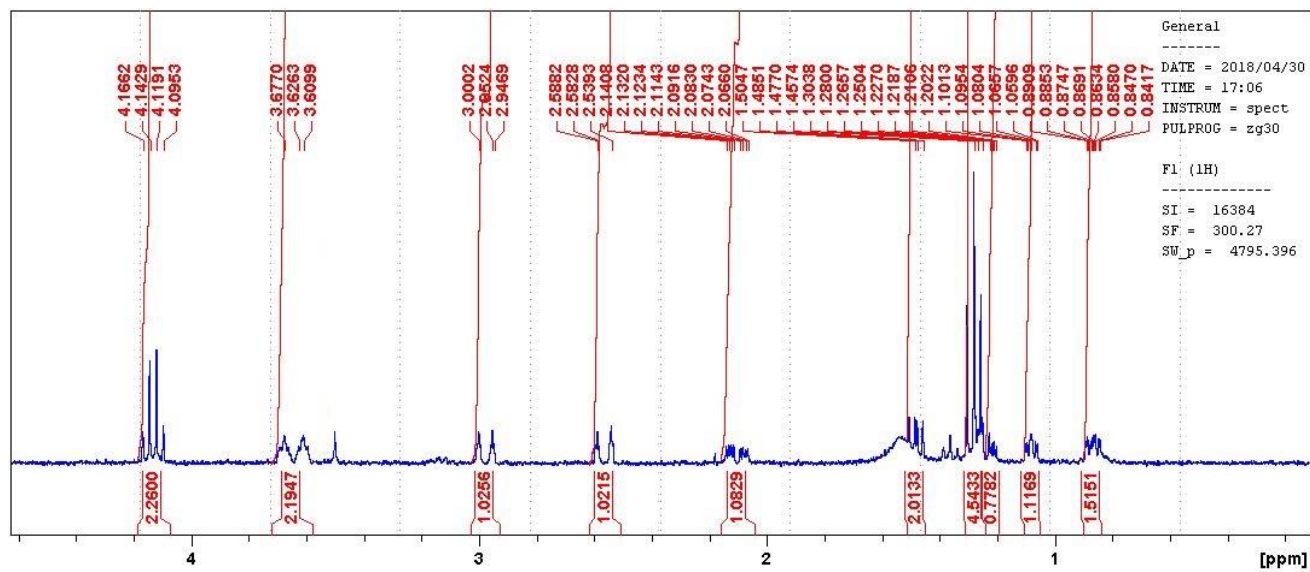


Figure E76. Magnified regions of  $^1\text{H}$  NMR Spectra of compound **68a** in  $\text{CDCl}_3$ .

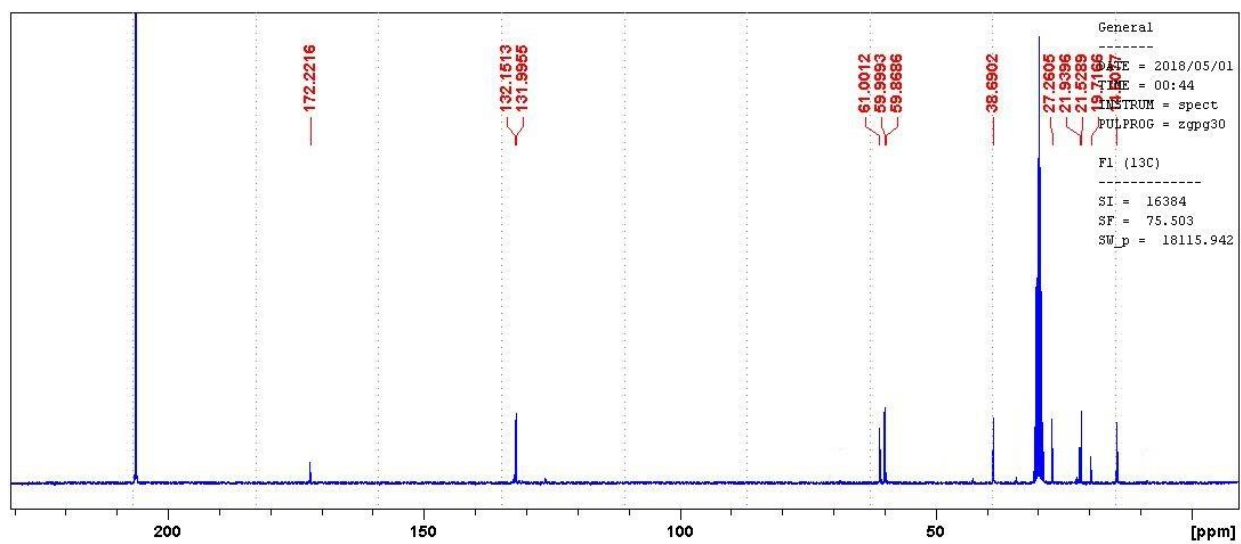


Figure E77.  $^{13}\text{C}$  NMR Spectra of compound **68a** in acetone- $d_6$ .

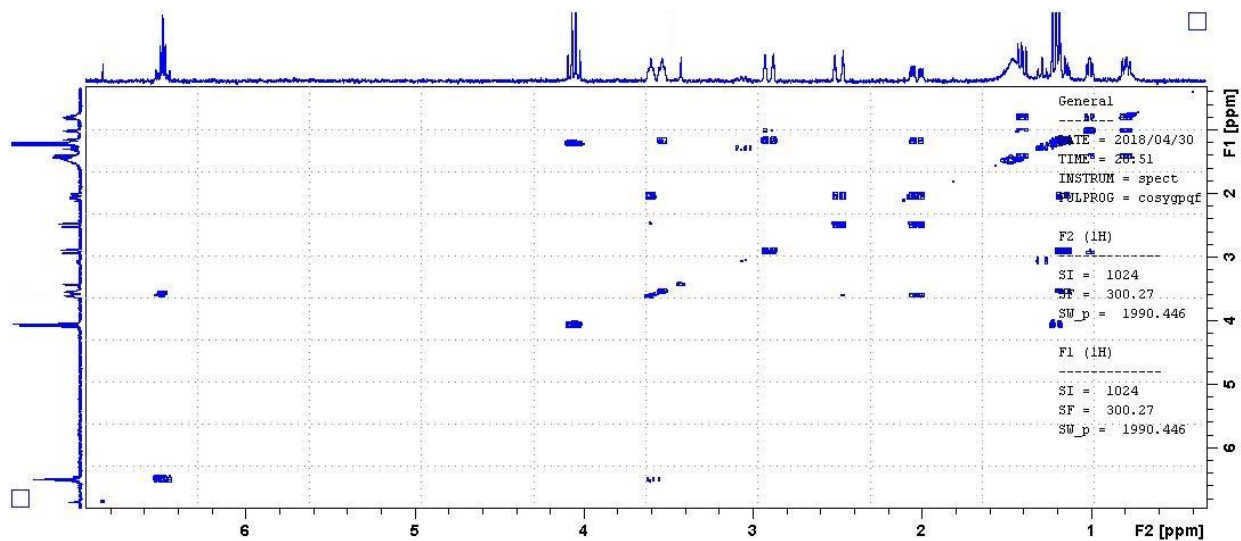


Figure E78. COSY NMR Spectra of compound **68a** in  $\text{CDCl}_3$ .

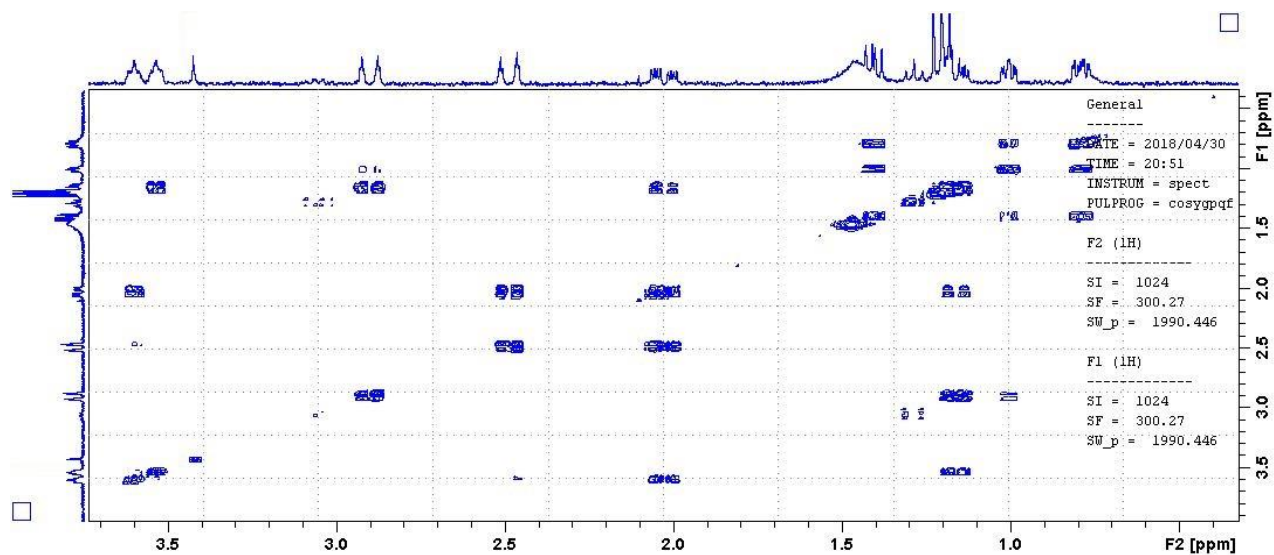


Figure E79. Magnified regions of COSY NMR Spectra of compound **68a** in  $\text{CDCl}_3$ .

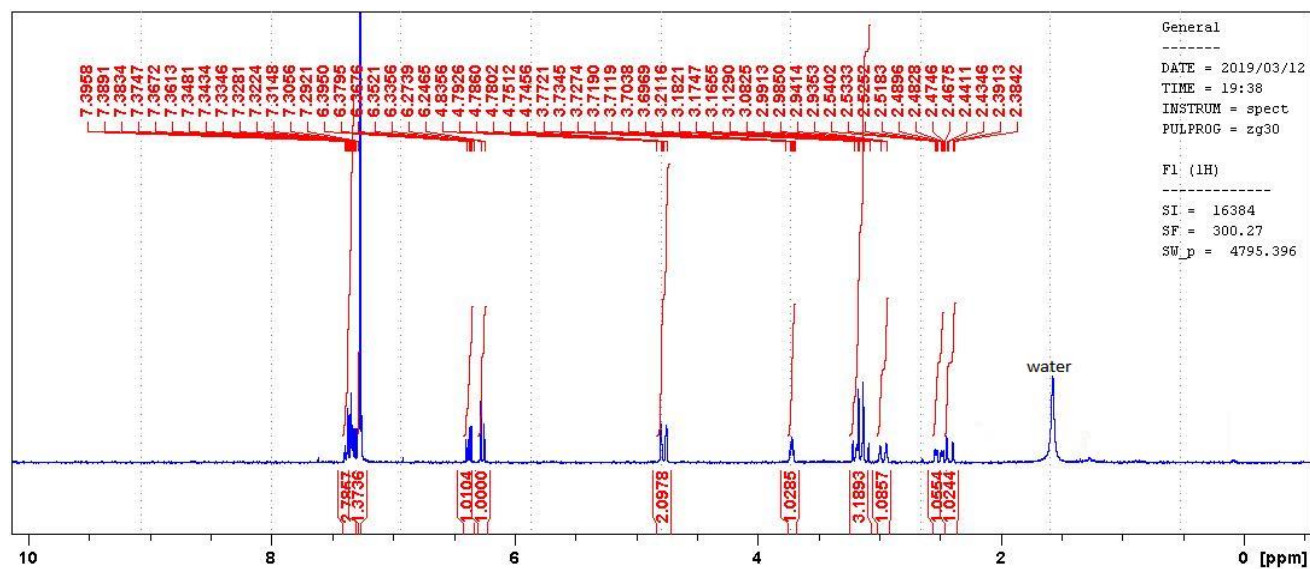


Figure E80.  $^1\text{H}$  NMR Spectra of compounds **76b** in  $\text{CDCl}_3$ .

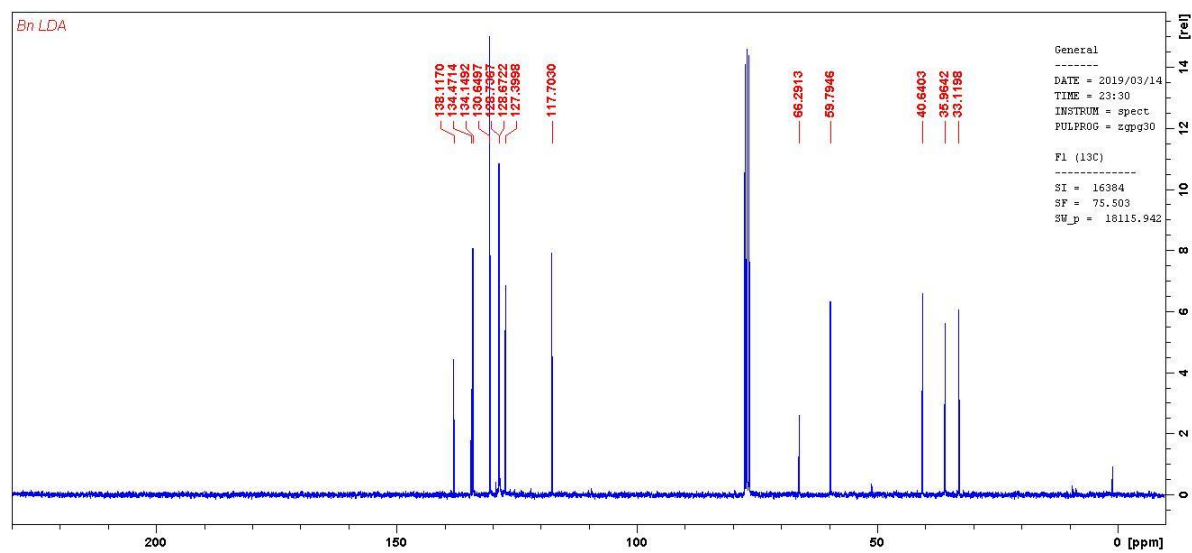


Figure E81.  $^{13}\text{C}$  NMR Spectra of compounds **76b** in  $\text{CDCl}_3$ .

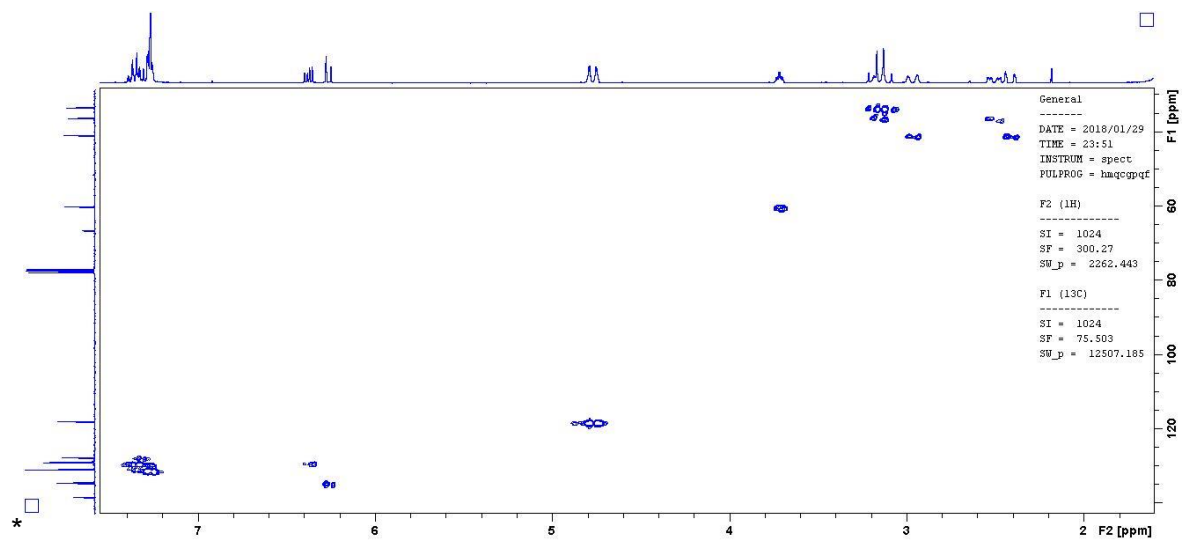


Figure E82. HSQC NMR Spectra of compounds **76b** in  $\text{CDCl}_3$ .

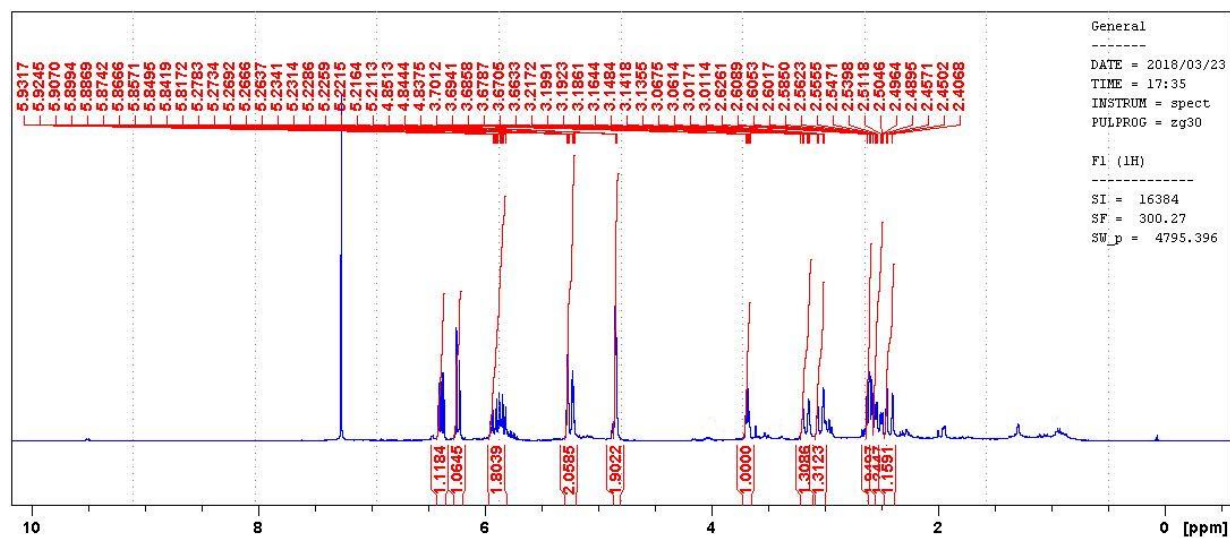


Figure E83.  $^1\text{H}$  NMR Spectra of compounds **76c** in  $\text{CDCl}_3$ .

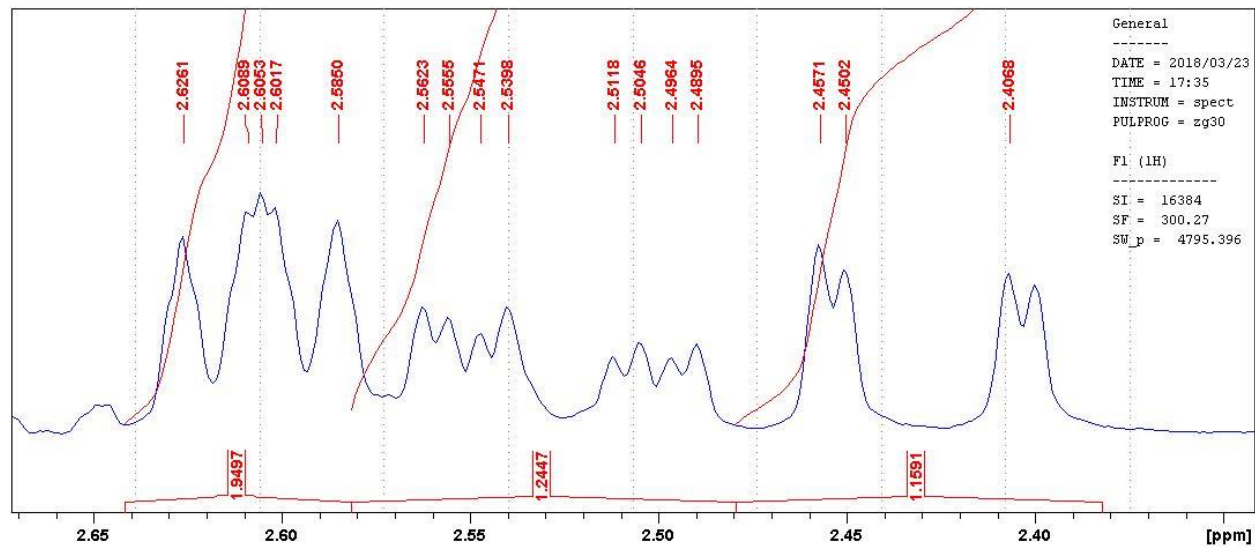


Figure E84. Magnified regions of  $^1\text{H}$  NMR Spectra of compounds **76c** in  $\text{CDCl}_3$ .

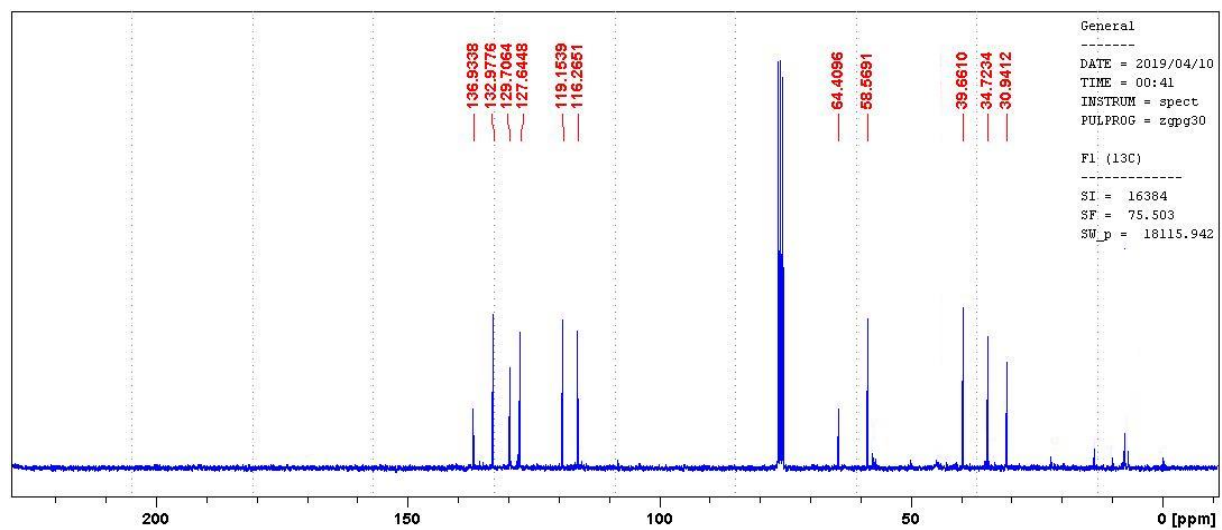


Figure E85.  $^{13}\text{C}$  NMR Spectra of compounds **76c** in  $\text{CDCl}_3$ .

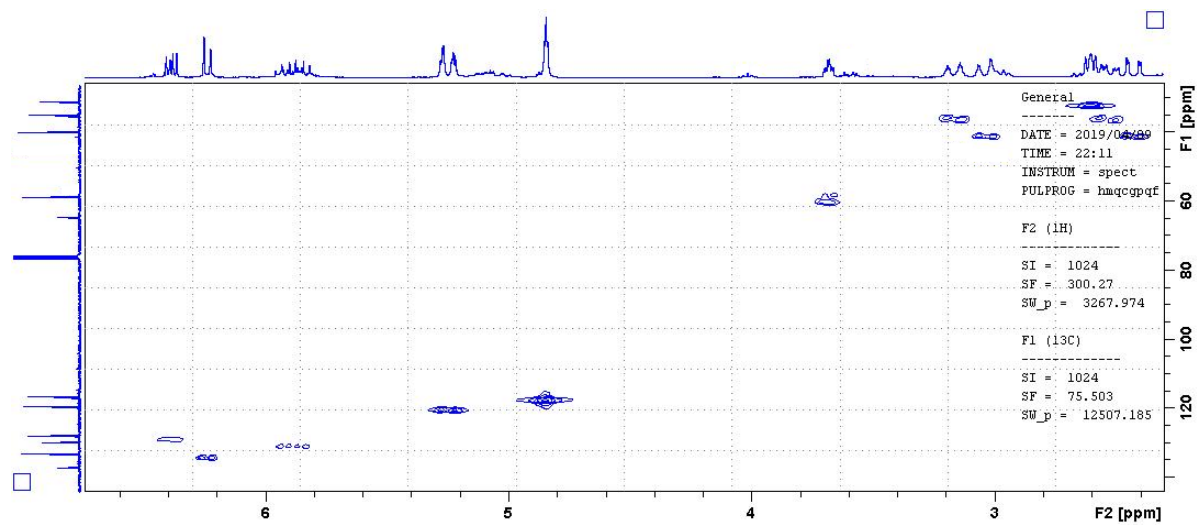


Figure E86. HSQC NMR Spectra of compounds **76c** in  $\text{CDCl}_3$ .

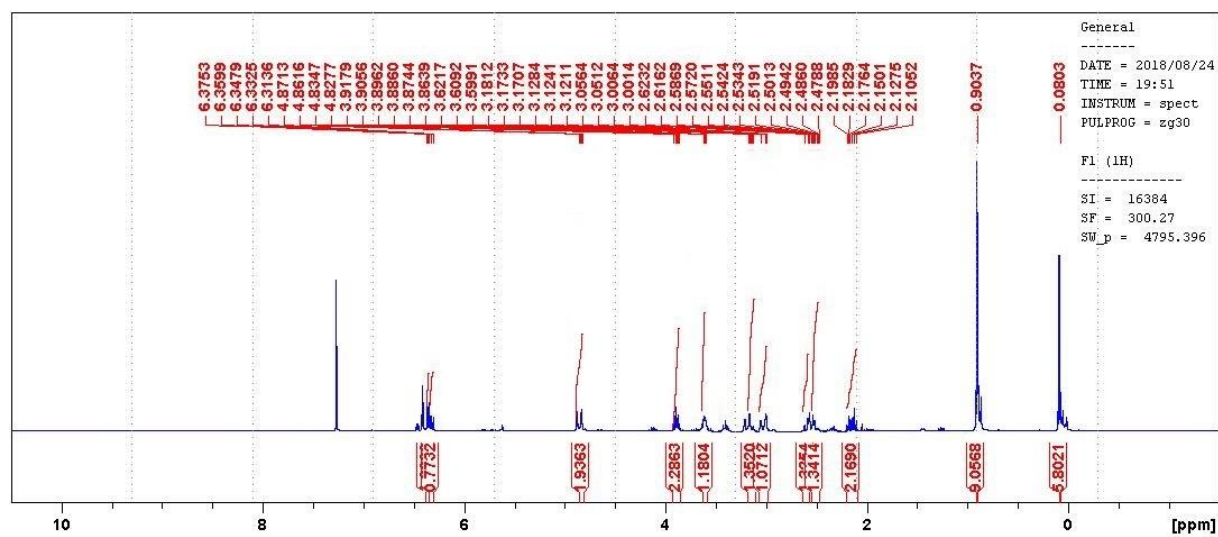


Figure E87.  $^1\text{H}$  NMR Spectra of compounds **76d** in  $\text{CDCl}_3$ .

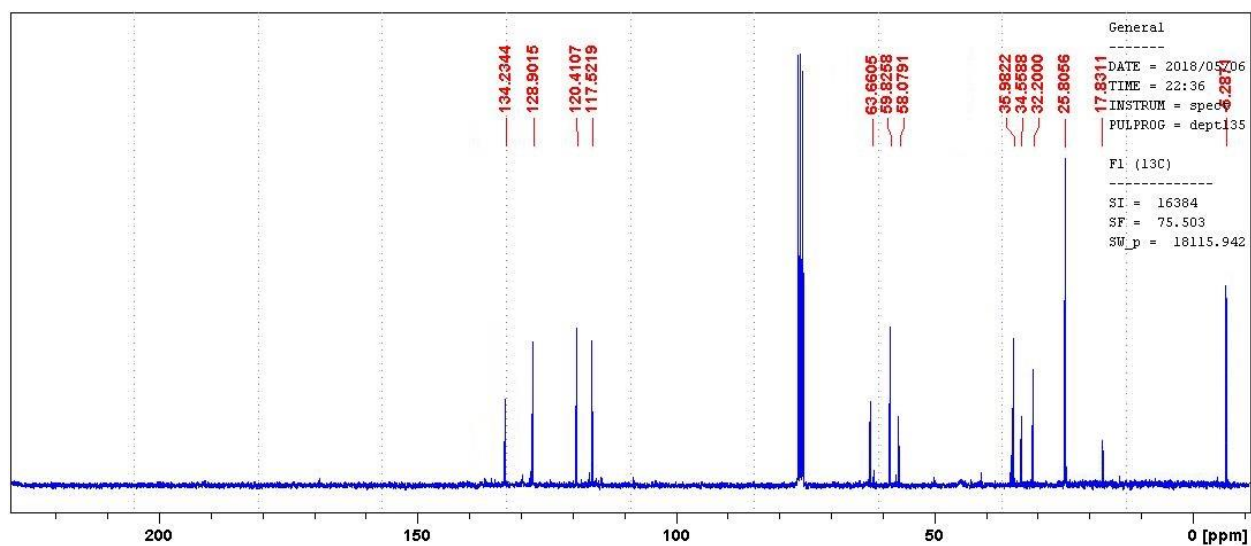


Figure E88.  $^{13}\text{C}$  NMR Spectra of compounds **76d** in  $\text{CDCl}_3$ .

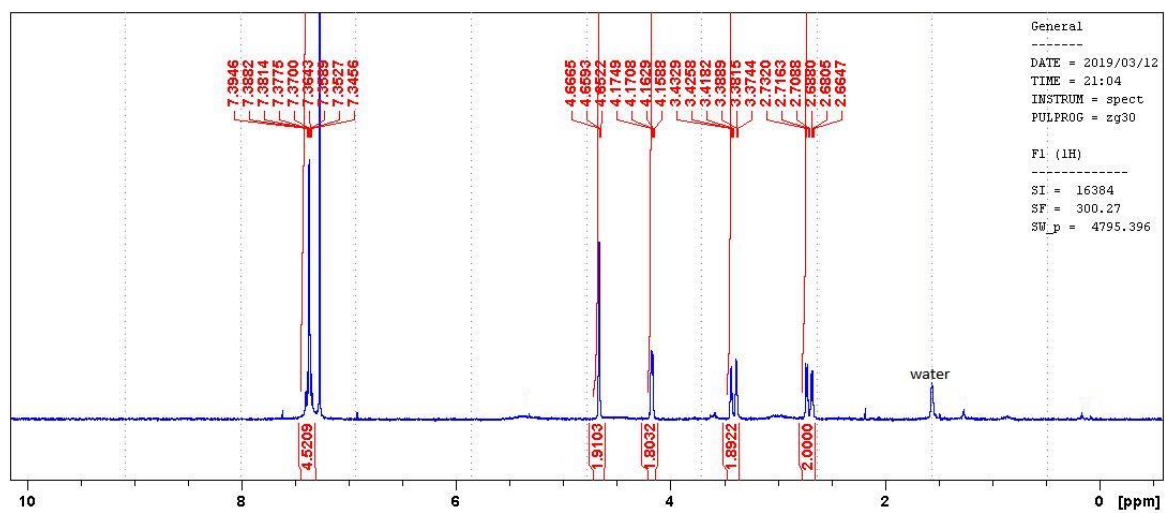


Figure E89.  $^1\text{H}$  NMR Spectra of compounds **82** in  $\text{CDCl}_3$ .

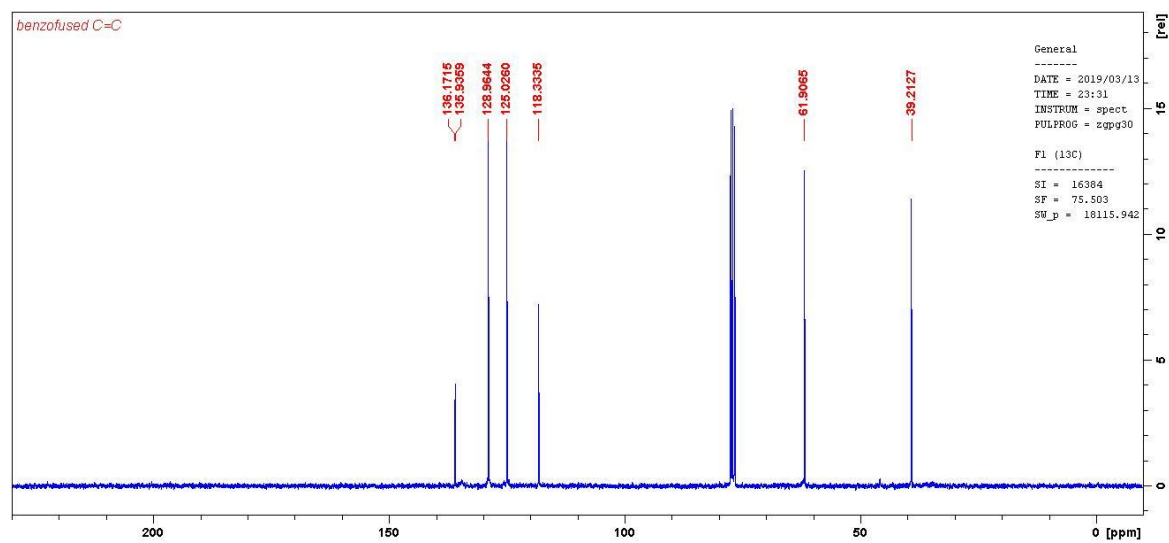


Figure E90.  $^{13}\text{C}$  NMR Spectra of compounds **82** in  $\text{CDCl}_3$ .

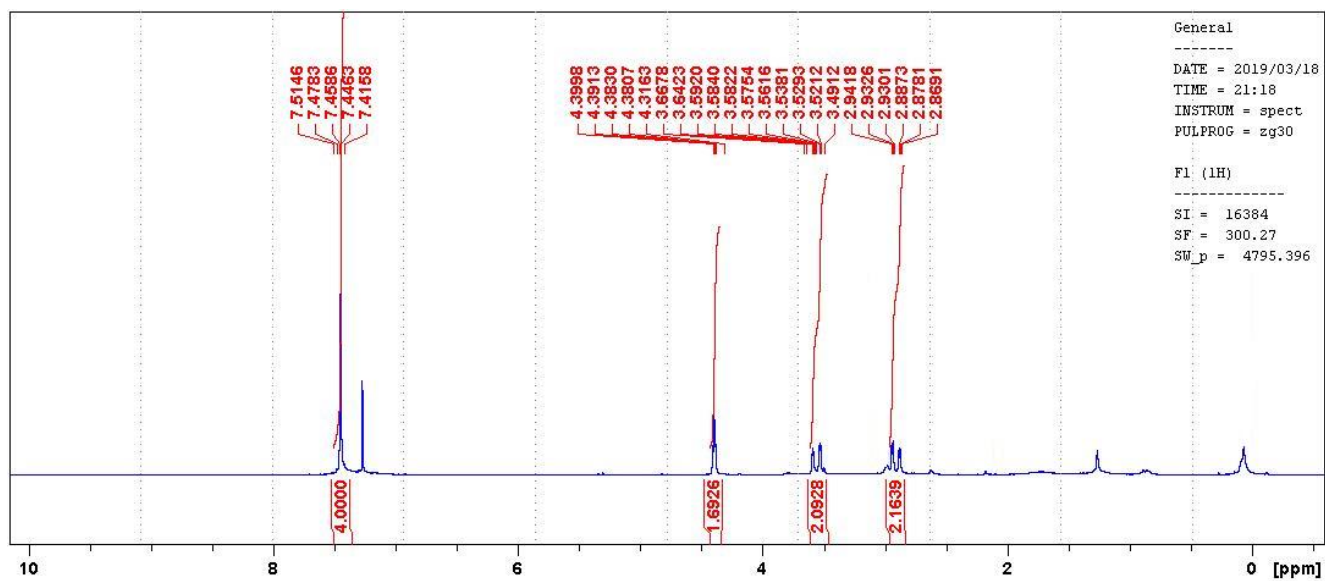


Figure E91.  $^1\text{H}$  NMR Spectra of compound **83** in  $\text{CDCl}_3$ .

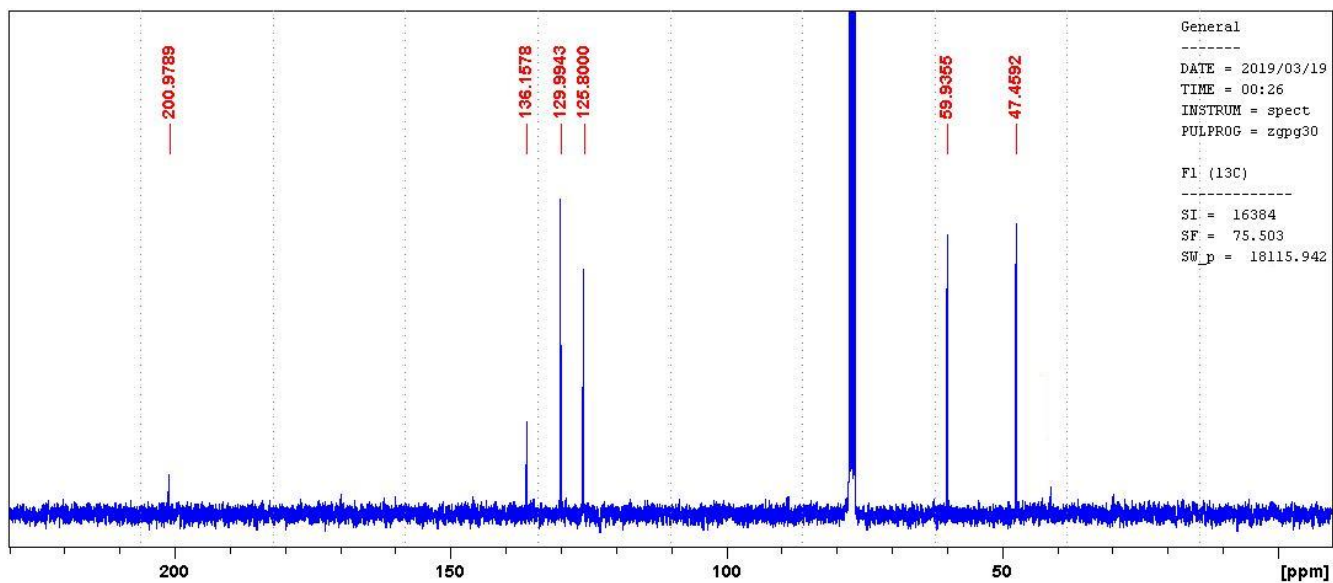


Figure E92.  $^{13}\text{C}$  NMR Spectra of compound **83** in  $\text{CDCl}_3$ .

## Appendix C – Biological Data

### Antibacterial data collection

Inhibition of bacterial growth was determined measuring absorbance at 600 nm ( $OD_{600}$ ), using a Tecan M1000 Pro monochromator plate reader. The percentage of growth inhibition was calculated for each well, using the negative control (media only) and positive control (bacteria without inhibitors) on the same plate as references.

### Antifungal data collection

Growth inhibition of *C. albicans* was determined measuring absorbance at 530 nm ( $OD_{530}$ ), while the growth inhibition of *C. neoformans* was determined measuring the difference in absorbance between 600 and 570 nm ( $OD_{600-570}$ ), after the addition of resazurin (0.001% final concentration) and incubation at 35 °C for additional 2 h. The absorbance was measured using a Biotek Synergy HTX plate reader. The percentage of growth inhibition was calculated for each well, using the negative control (media only) and positive control (bacteria without inhibitors) on the same plate as references.

### Inhibition Values

Percentage growth inhibition of an individual sample is calculated based on negative controls (media only) and positive Controls (bacterial/fungal media without inhibitors). Please note negative inhibition values indicate that the growth rate (or  $OD_{600}$ ) is higher compared to the negative Control (Bacteria/fungi only, set to 0% inhibition). The growth rates for all bacteria and fungi has a variation of  $\pm 10\%$ , which is within the reported normal distribution of bacterial/fungal growth.

Compound	Trial 1 inhibition values (%)	Trial 2 inhibition values (%)	Mean inhibition values	Standard deviation
<b>31a</b>	11.06	5.81	8.44	3.71
<b>31b</b>	5.39	6.02	5.71	0.45
<b>31c</b>	50.96	48.10	49.53	2.02
<b>31d</b>	10.78	5.45	8.12	3.77
<b>32a</b>	0.56	-6.66	-3.05	5.11
<b>32b</b>	11.90	6.24	9.07	4.00
<b>32c</b>	10.36	6.88	8.62	2.46
<b>32d</b>	5.04	9.87	7.46	3.42
<b>40</b>	28.70	0.67	14.69	19.82
<b>41</b>	3.99	4.24	4.12	0.18
<b>42</b>	-0.14	5.81	2.84	4.21
<b>43</b>	8.33	3.95	6.14	3.10
<b>45</b>	18.41	8.02	13.22	7.35
<b>47</b>	1.05	29.49	15.27	20.11
<b>52</b>	2.31	9.02	5.67	4.74
<b>57</b>	5.04	5.17	5.11	0.09
<b>59</b>	-1.33	15.58	7.13	11.96
<b>60</b>	4.55	4.81	4.68	0.18
<b>67a</b>	12.74	10.94	11.84	1.27
<b>67b</b>	5.46	7.31	6.39	1.31
<b>67c</b>	11.48	5.74	8.61	4.06
<b>76b</b>	37.24	43.61	40.43	4.50
<b>76c</b>	11.62	16.36	13.99	3.35

Table E1. Biological data of bicyclo[3.2.1]sulfone-containing molecules against *C. albicans* (strain ATCC 90028).

Compound	Trial 1 inhibition values (%)	Trial 2 inhibition values (%)	Mean inhibition values	Standard deviation
<b>31a</b>	9.13	-31.92	-11.40	29.03
<b>31b</b>	-28.70	-31.35	-30.03	1.87
<b>31c</b>	-23.11	-34.35	-28.73	7.95
<b>31d</b>	-20.53	-26.92	-23.73	4.52
<b>32a</b>	-18.38	-25.78	-22.08	5.23
<b>32b</b>	-20.96	-9.50	-15.23	8.10
<b>32c</b>	-14.94	-12.07	-13.51	2.03
<b>32d</b>	4.40	-5.35	-0.48	6.89
<b>40</b>	-21.82	-21.21	-21.52	0.43
<b>41</b>	-12.58	-19.78	-16.18	5.09
<b>42</b>	9.78	30.35	20.07	14.55
<b>43</b>	11.07	-16.21	-2.57	19.29
<b>45</b>	1.18	-43.35	-21.09	31.49
<b>47</b>	-6.34	-14.21	-10.28	5.56
<b>52</b>	6.55	5.64	6.10	0.64
<b>57</b>	6.12	-13.78	-3.83	14.07
<b>59</b>	-19.24	-12.64	-15.94	4.67
<b>60</b>	-2.04	-4.64	-3.34	1.84
<b>67a</b>	-0.96	-15.64	-8.30	10.38
<b>67b</b>	-18.81	-24.21	-21.51	3.82
<b>67c</b>	-6.98	2.64	-2.17	6.80
<b>76b</b>	-96.66	-37.64	-67.15	41.73
<b>76c</b>	9.35	-8.78	0.29	12.82

Table E2. Biological data of bicyclo[3.2.1]sulfone-containing molecules against *C. neoformans* (strain ATCC 20882).

Compound	Trial 1 inhibition values (%)	Trial 2 inhibition values (%)	Mean inhibition values	Standard deviation
<b>31a</b>	11.81	21.72	16.77	7.01
<b>31b</b>	-6.99	-0.72	-3.86	4.43
<b>31c</b>	-11.21	-6.24	-8.73	3.51
<b>31d</b>	9.18	7.76	8.47	1.00
<b>32a</b>	-32.49	-36.53	-34.51	2.86
<b>32b</b>	-12.34	-11.46	-11.90	0.62
<b>32c</b>	-35.65	-30.96	-33.31	3.32
<b>32d</b>	-20.16	-11.50	-15.83	6.12
<b>40</b>	5.26	7.70	6.48	1.73
<b>41</b>	10.19	15.13	12.66	3.49
<b>42</b>	-20.44	-18.26	-19.35	1.54
<b>43</b>	16.45	22.46	19.46	4.25
<b>45</b>	1.79	12.68	7.24	7.70
<b>47</b>	-12.71	-8.52	-10.62	2.96
<b>52</b>	3.57	3.47	3.52	0.07
<b>57</b>	10.79	17.43	14.11	4.70
<b>59</b>	9.83	11.05	10.44	0.86
<b>60</b>	-0.25	5.77	2.76	4.26
<b>67a</b>	9.46	12.01	10.74	1.80
<b>67b</b>	-1.03	-1.38	-1.21	0.25
<b>67c</b>	-2.09	-3.58	-2.84	1.05
<b>76b</b>	-5.93	-8.82	-7.38	2.04
<b>76c</b>	17.60	18.36	17.98	0.54

Table E3. Biological data of bicyclo[3.2.1]sulfone-containing molecules against *S. aureus* (strain ATCC 43300).

Compound	Trial 1 inhibition values (%)	Trial 2 inhibition values (%)	Mean inhibition values	Standard deviation
<b>31a</b>	12.03	15.66	13.85	2.57
<b>31b</b>	-2.99	0.75	-1.12	2.64
<b>31c</b>	-3.07	1.97	-0.55	3.56
<b>31d</b>	7.13	8.37	7.75	0.88
<b>32a</b>	-10.83	-7.32	-9.08	2.48
<b>32b</b>	9.14	7.54	8.34	1.13
<b>32c</b>	-3.70	1.19	-1.26	3.46
<b>32d</b>	5.26	6.63	5.95	0.97
<b>40</b>	14.59	17.06	15.83	1.75
<b>41</b>	18.23	17.65	17.94	0.41
<b>42</b>	8.99	11.38	10.19	1.69
<b>43</b>	12.08	12.56	12.32	0.34
<b>45</b>	10.54	8.29	9.42	1.59
<b>47</b>	8.07	12.33	10.20	3.01
<b>52</b>	14.97	15.76	15.37	0.56
<b>57</b>	10.77	14.27	12.52	2.47
<b>59</b>	23.40	18.99	21.20	3.12
<b>60</b>	10.67	16.46	13.57	4.09
<b>67a</b>	20.60	22.31	21.46	1.21
<b>67b</b>	10.31	12.89	11.60	1.82
<b>67c</b>	10.77	9.32	10.05	1.03
<b>76b</b>	5.84	9.21	7.53	2.38
<b>76c</b>	12.52	17.91	15.22	3.81

Table E4. Biological data of bicyclo[3.2.1]sulfone-containing molecules against *E. Coli* (strain ATCC 25922).

Compound	Trial 1 inhibition values (%)	Trial 2 inhibition values (%)	Mean inhibition values	Standard deviation
<b>31a</b>	10.58	13.32	11.95	1.94
<b>31b</b>	12.59	1.82	7.21	7.62
<b>31c</b>	-9.01	0.63	-4.19	6.82
<b>31d</b>	8.09	8.68	8.39	0.42
<b>32a</b>	-19.96	-10.98	-15.47	6.35
<b>32b</b>	-11.26	4.96	-3.15	11.47
<b>32c</b>	-22.14	-6.13	-14.14	11.32
<b>32d</b>	-0.95	3.88	1.47	3.42
<b>40</b>	3.58	16.10	9.84	8.85
<b>41</b>	10.29	13.11	11.70	1.99
<b>42</b>	-14.31	-21.04	-17.68	4.76
<b>43</b>	14.39	16.64	15.52	1.59
<b>45</b>	1.58	-2.22	-0.32	2.69
<b>47</b>	3.53	8.90	6.22	3.80
<b>52</b>	13.03	25.35	19.19	8.71
<b>57</b>	8.23	10.67	9.45	1.73
<b>59</b>	15.29	13.77	14.53	1.07
<b>60</b>	3.13	11.76	7.45	6.10
<b>67a</b>	14.62	22.93	18.78	5.88
<b>67b</b>	14.33	11.57	12.95	1.95
<b>67c</b>	-4.04	9.49	2.73	9.57
<b>76b</b>	10.75	6.86	8.81	2.75
<b>76c</b>	16.20	17.44	16.82	0.88

Table E5. Biological data of bicyclo[3.2.1]sulfone-containing molecules against *K. pneumoniae* (strain ATCC 700603).

Compound	Trial 1 inhibition values (%)	Trial 2 inhibition values (%)	Mean inhibition values	Standard deviation
<b>31a</b>	32.32	3.58	17.95	20.32
<b>31b</b>	-11.53	-10.86	-11.20	0.47
<b>31c</b>	-22.83	-49.08	-35.96	18.56
<b>31d</b>	-34.55	-38.34	-36.45	2.68
<b>32a</b>	-73.27	-91.01	-82.14	12.54
<b>32b</b>	-11.81	-42.25	-27.03	21.52
<b>32c</b>	-33.14	-61.56	-47.35	20.10
<b>32d</b>	-2.18	-32.05	-17.12	21.12
<b>40</b>	9.55	17.33	13.44	5.50
<b>41</b>	36.67	3.58	20.13	23.40
<b>42</b>	-105.35	-111.54	-108.45	4.38
<b>43</b>	27.46	21.87	24.67	3.95
<b>45</b>	-11.31	-20.02	-15.67	6.16
<b>47</b>	-20.43	-15.39	-17.91	3.56
<b>52</b>	4.13	-5.07	-0.47	6.51
<b>57</b>	-3.40	6.59	1.60	7.06
<b>59</b>	-16.05	-56.04	-36.05	28.28
<b>60</b>	-7.04	-37.15	-22.10	21.29
<b>67a</b>	7.18	0.14	3.66	4.98
<b>67b</b>	-8.26	-34.01	-21.14	18.21
<b>67c</b>	-44.38	-24.47	-34.43	14.08
<b>76b</b>	-14.61	-8.56	-11.59	4.28
<b>76c</b>	-3.29	-33.90	-18.60	21.64

Table E6. Biological data of bicyclo[3.2.1]sulfone-containing molecules against *A. baumannii* (strain ATCC 19606).

Compound	Trial 1 inhibition values (%)	Trial 2 inhibition values (%)	Mean inhibition values	Standard deviation
<b>31a</b>	-4.37	-7.61	-5.99	2.29
<b>31b</b>	-8.86	-2.68	-5.77	4.37
<b>31c</b>	-3.93	-9.76	-6.85	4.12
<b>31d</b>	0.71	-2.81	-1.05	2.49
<b>32a</b>	-5.67	-10.02	-7.85	3.08
<b>32b</b>	-3.11	-11.21	-7.16	5.73
<b>32c</b>	-3.09	-14.68	-8.89	8.20
<b>32d</b>	-3.58	-10.85	-7.22	5.14
<b>40</b>	2.35	-10.61	-4.13	9.16
<b>41</b>	1.87	-7.71	-2.92	6.77
<b>42</b>	7.93	2.05	4.99	4.16
<b>43</b>	-6.49	-6.10	-6.30	0.28
<b>45</b>	-8.03	-7.80	-7.92	0.16
<b>47</b>	-8.08	-7.15	-7.62	0.66
<b>52</b>	1.29	-1.85	-0.28	2.22
<b>57</b>	-3.08	-7.46	-5.27	3.10
<b>59</b>	-0.30	-8.19	-4.25	5.58
<b>60</b>	-2.10	-6.25	-4.18	2.93
<b>67a</b>	-1.52	0.06	-0.73	1.12
<b>67b</b>	-3.43	-6.91	-5.17	2.46
<b>67c</b>	-1.47	-10.48	-5.98	6.37
<b>76b</b>	-0.06	-1.22	-0.64	0.82
<b>76c</b>	1.38	-2.72	-0.67	2.90

Table E7. Biological data of bicyclo[3.2.1]sulfone-containing molecules against *P. aeruginosa* (strain ATCC 27853).

***M. Tuberculosis* assay procedure (performed by Eli Lilly & Co.)**

Molecule(s) to be tested were prepared as 10mM stock DMSO solution(s) before shipping off. A diluted solution was prepared by 10x dilution using DMSO before assay.

4 $\mu$ L of said diluted solution was added into 50 $\mu$ L of *M. tuberculosis* cell culture in 96-well plates. The plates were incubated at 37°C for about 72 hours before analysis.

Growth inhibition was calculated by absorbance at 590nm (OD<sub>590</sub>), which was measured using a Synergy 4 plate reader (Biotech). Background value was calculated from the contamination control wells (medium-only).

Compound No.	% Inhibition @ 20 $\mu$ M
<b>31a</b>	2.34
<b>31b</b>	4.16
<b>31c</b>	-6.02
<b>31d</b>	12.42
<b>32a</b>	12.42
<b>32b</b>	3.08
<b>32c</b>	1.21
<b>32d</b>	-0.28
<b>40</b>	5.32
<b>41</b>	-1.4
<b>42</b>	2.34
<b>43</b>	5.32
<b>45</b>	1.96
<b>47</b>	0.16
<b>52</b>	5.61
<b>57</b>	1.21
<b>59</b>	3.46
<b>60</b>	1.21
<b>67a</b>	4.58
<b>67b</b>	6.45
<b>67c</b>	-8.87
<b>76b</b>	8.31
<b>76c</b>	0.84

Table E8. Biological data of bicyclo[3.2.1]sulfone-containing molecules against *M. tuberculosis* (strain ATCC H37Rv).

**NNMT assay procedure (performed by Eli Lilly & Co.)**

Molecule(s) to be tested was prepared as a 10 $\mu$ M stock DMSO solution. An aliquot was mixed with a buffered solution of hNNMT (10 nM), SAM (5.8  $\mu$ M), and nicotinamide (2.9  $\mu$ M), and incubated at ambient temperature for 120 minutes.

Internal standards of  $^{13}\text{C}$ -S-Adenosyl-L-homocysteine (0.625  $\mu\text{g}/\mu\text{L}$ ) and  $d_7$  - methylnicotinamide (0.1354  $\mu\text{g}/\mu\text{L}$ ) were added, and then subjected to HPLC analysis. Inhibitory activities are calculated by concentration levels of MNA and SAH respectively.

	hNNMT MNA single point assay	hNNMT SAH single point assay
Compound No.	% Inhibition @ 9.99 $\mu$ M	
<b>31a</b>	8.393	
<b>31b</b>	-1.157	
<b>31c</b>	15.17	
<b>31d</b>	35.15	38.14
<b>32a</b>	8.297	
<b>32b</b>	-15.76	28.52
<b>32c</b>	17.49	
<b>32d</b>	17.31	28.65
<b>40</b>	10.67	
<b>41</b>	5.549	
<b>42</b>	-12.1	
<b>43</b>	5.57	
<b>45</b>	1.471	
<b>47</b>	11.04	
<b>52</b>	11.4	
<b>57</b>	11.04	
<b>59</b>	-2.752	
<b>60</b>	7.681	
<b>67a</b>	19.42	
<b>67b</b>	-5.405	
<b>67c</b>	2.327	
<b>76b</b>	12.13	
<b>76c</b>	1.837	

Table E9. Biological data of bicyclo[3.2.1]sulfone-containing molecules against human recombinant NNMT (hNNMT).

### Human keratinocyte cell assay procedure (performed by LEO Pharma)

Molecule(s) are weighed in provided vials, or prepared as 10mM of stock DMSO solution(s) in provided vials before shipping off. If shipped as is, the molecule(s) are diluted in DMSO until complete dissolution, and concentration of freshly prepared DMSO stock solution of molecule(s) is recorded.

Serial dilution is performed in order to obtain a series of diluted DMSO solution of molecules across a wide range of concentrations (1x dilution to 10<sup>6</sup>x dilution).

For each experiment, 80 nL of solution is transferred into 80  $\mu$ L human keratinocyte cell culture, in which EpiLife™ (spiked with 60  $\mu$ M Ca<sup>2+</sup> for long term storage) as the cell media, and is then incubated at 37°C for about 48 to 72 hours before analysis.

Eczema CCL2 Release Assay			Cell Viability Assay		
Concentration (mmol/mL)	Trial #1 % effect	Trial #2 % effect	Concentration (mmol/mL)	Trial #1 % effect	Trial #2 % effect
9.78E-12	-0.8	2.5	9.78E-12	-10.9	-10.3
9.78E-11	-8.8	-2.8	9.78E-11	-12.9	-5.2
9.78E-10	-7.9	-5.8	9.78E-10	-16.3	-9.6
9.78E-09	-15.3	-12.4	9.78E-09	-20.5	-12.7
9.78E-08	-13.6	-13.1	9.78E-08	-12.9	-12.6
3.11E-07	-14.6	5.3	3.11E-07	-16.8	-12.8
9.90E-07	-13.1	3.9	9.90E-07	-13.3	-7.7
3.15E-06	15.1	17.7	3.15E-06	-6.5	-3.2
1.00E-05	55	61.2	1.00E-05	-0.4	3.2

Table E10. Biological data of compound **41** in eczema CCL2 release assay.

Psoriasis IL-8 Release Assay			Cell Viability Assay		
Concentration (mmol/mL)	Trial #1 % effect	Trial #2 % effect	Concentration (mmol/mL)	Trial #1 % effect	Trial #2 % effect
9.76E-11	1.7	3.8	9.76E-11	-1.6	9.2
9.76E-10	4.6	7.9	9.76E-10	-9.1	-1.6
9.76E-09	0	7.3	9.76E-09	-4.8	2.5
9.76E-08	6.6	12.8	9.76E-08	-13.7	-3
9.76E-07	11.1	24	9.76E-07	-2	6.5
3.10E-06	8.6	11.1	3.10E-06	-13.7	-7.4
9.88E-06	18.7	32.9	9.88E-06	17.2	18.1
3.14E-05	65.7	70.2	3.14E-05	87	92.6
1.00E-04	100.5	100.5	1.00E-04	95.4	104.8

Table E11. Biological data of compound **40** in psoriasis IL-8 release assay.

Psoriasis IL-8 Release Assay			Cell Viability Assay		
Concentration (mmol/mL)	Trial #1 % effect	Trial #2 % effect	Concentration (mmol/mL)	Trial #1 % effect	Trial #2 % effect
9.76E-11	-8.3	-6.3	9.76E-11	-11.1	9.6
9.76E-10	-0.6	11.3	9.76E-10	-4.7	1.8
9.76E-09	1.2	11.1	9.76E-09	-1.7	2.1
9.76E-08	4.4	19.1	9.76E-08	-17	-12.4
9.76E-07	7.1	12.3	9.76E-07	-6	1.6
3.10E-06	3.4	4.5	3.10E-06	4.2	4.4
9.88E-06	57.2	57.7	9.88E-06	66.4	80.7
3.14E-05	99.7	99.7	3.14E-05	110.5	111
1.00E-04	19.9	24.8	1.00E-04	-12.2	5.1

Table E12. Biological data of compound **41** in psoriasis IL-8 release assay.

Psoriasis IL-8 Release Assay			Cell Viability Assay		
Concentration (mmol/mL)	Trial #1 % effect	Trial #2 % effect	Concentration (mmol/mL)	Trial #1 % effect	Trial #2 % effect
9.76E-11	-25.9	-10.2	9.76E-11	-7.1	9.1
9.76E-10	-15.5	-6.3	9.76E-10	-18.9	-6.5
9.76E-09	-16.8	-11.3	9.76E-09	-18	7.8
9.76E-08	-14.4	-10	9.76E-08	5	7.5
9.76E-07	-6.2	17.5	9.76E-07	-10.9	0
3.10E-06	-10.3	-7.4	3.10E-06	10.1	17.4
9.88E-06	9.4	10	9.88E-06	19.4	24.5
3.14E-05	42.9	69.1	3.14E-05	55	58.4
1.00E-04	91.3	92.6	1.00E-04	90.1	90.9

Table E13. Biological data of compound **76b** in psoriasis IL-8 release assay.

Psoriasis IL-8 Release Assay			Cell Viability Assay		
Concentration (mmol/mL)	Trial #1 % effect	Trial #2 % effect	Concentration (mmol/mL)	Trial #1 % effect	Trial #2 % effect
9.76E-11	-0.8	5.9	9.76E-11	-17.8	-6.6
9.76E-10	6.7	8	9.76E-10	-8.6	-8.1
9.76E-09	12.6	15.5	9.76E-09	-1.3	3.4
9.76E-08	8.3	11.7	9.76E-08	-5.8	9.5
9.76E-07	14.8	16.1	9.76E-07	-8.8	-7.5
3.10E-06	-1.1	9.4	3.10E-06	-17.1	4.5
9.88E-06	5.5	14.3	9.88E-06	-13.8	0.7
3.14E-05	27.8	33.7	3.14E-05	4.6	15.7
1.00E-04	38.3	39.5	1.00E-04	9.5	27.2

Table E14. Biological data of compound **82** in psoriasis IL-8 release assay.

Eczema CCL2 Release Assay			Cell Viability Assay		
Concentration (mmol/mL)	Trial #1 % effect	Trial #2 % effect	Concentration (mmol/mL)	Trial #1 % effect	Trial #2 % effect
9.76E-11	-6	6.4	9.76E-11	-9.1	-1.8
9.76E-10	-24.6	-9.4	9.76E-10	-22.8	-3.2
9.76E-09	-12.9	-9.1	9.76E-09	-9.2	-3.2
9.76E-08	-5.5	7.4	9.76E-08	-7.8	-5
9.76E-07	-7.5	-1.6	9.76E-07	-0.7	1.5
3.10E-06	10.2	12.1	3.10E-06	-2.7	1.2
9.88E-06	49.3	55.2	9.88E-06	6.4	13.7
3.14E-05	87.2	93.6	3.14E-05	35.7	43.7
1.00E-04	90.3	100.4	1.00E-04	100.2	101.8

Table E15. Biological data of compound **40** in eczema CCL2 release assay.

Eczema CCL2 Release Assay			Cell Viability Assay		
Concentration (mmol/mL)	Trial #1 % effect	Trial #2 % effect	Concentration (mmol/mL)	Trial #1 % effect	Trial #2 % effect
9.76E-11	-6.6	-3.2	9.76E-11	-23.4	-22.9
9.76E-10	-21	-4.9	9.76E-10	-29.5	-24.7
9.76E-09	-21.6	-5.3	9.76E-09	-22.3	-19.9
9.76E-08	-8.4	-5.3	9.76E-08	-27.1	-25.4
9.76E-07	6.2	16.1	9.76E-07	-26.2	-19.7
3.10E-06	20	20.2	3.10E-06	-20.5	-20.2
9.88E-06	75.6	75.7	9.88E-06	-10.2	-6.4
3.14E-05	96.5	99.1	3.14E-05	97.8	97.8
1.00E-04	94.2	95	1.00E-04	86.2	94.9

Table E16. Re-validated biological data of compound **41** in eczema CCL2 release assay.

Eczema CCL2 Release Assay			Cell Viability Assay		
Concentration (mmol/mL)	Trial #1 % effect	Trial #2 % effect	Concentration (mmol/mL)	Trial #1 % effect	Trial #2 % effect
9.76E-11	-15.8	-7.6	9.76E-11	-40.9	-30
9.76E-10	-13.1	-7.6	9.76E-10	-38.9	-22.7
9.76E-09	-13.7	-1.3	9.76E-09	-30.8	-27.2
9.76E-08	-12.9	-12.2	9.76E-08	-26.9	-26.9
9.76E-07	-12.4	1.4	9.76E-07	-28.8	-26.3
3.10E-06	-6	6.5	3.10E-06	-22.2	-21.2
9.88E-06	15.5	16.7	9.88E-06	-16.4	-14.4
3.14E-05	71.2	72.1	3.14E-05	24.9	25.1
1.00E-04	99.8	102.6	1.00E-04	70	73.3

Table E17. Biological data of compound **76b** in eczema CCL2 release assay.

Eczema CCL2 Release Assay			Cell Viability Assay		
Concentration (mmol/mL)	Trial #1 % effect	Trial #2 % effect	Concentration (mmol/mL)	Trial #1 % effect	Trial #2 % effect
9.76E-11	-7.1	2.6	9.76E-11	-14	-10.5
9.76E-10	-14.1	-0.3	9.76E-10	-14.6	-7.5
9.76E-09	-6.7	-5.3	9.76E-09	-10.2	-0.4
9.76E-08	-19.3	7.3	9.76E-08	-2.2	-0.8
9.76E-07	-4.1	8.6	9.76E-07	-1.5	-0.1
3.10E-06	-11.5	4.4	3.10E-06	-6.4	-0.3
9.88E-06	5.2	8.9	9.88E-06	-0.3	0.3
3.14E-05	8.7	16.8	3.14E-05	4.1	7.3
1.00E-04	19	26.1	1.00E-04	17.7	27.5

Table E18. Biological data of compound **82** in eczema CCL2 release assay.

IL-17 Release Assay			Cell Viability Assay		
Concentration (mmol/mL)	Trial #1 % effect	Trial #2 % effect	Concentration (mmol/mL)	Trial #1 % effect	Trial #2 % effect
9.76E-11	-0.16	1.54	9.76E-11	2.58	9.53
9.76E-10	-2	13.52	9.76E-10	10.07	7.68
9.76E-09	-4.21	-9.16	9.76E-09	7.49	8.81
9.76E-08	1.04	10.95	9.76E-08	0.47	0.72
9.76E-07	-1.57	11.93	9.76E-07	11.91	11.95
3.10E-06	10.55	3.67	3.10E-06	14.83	19.33
9.88E-06	17.66	22.44	9.88E-06	14.9	25.76
3.14E-05	67.75	68.04	3.14E-05	21.73	29.19
1.00E-04	100.03	100.06	1.00E-04	100.02	99.15

Table E19. Biological data of compound **40** in IL-17 release assay.

IL-17 Release Assay			Cell Viability Assay		
Concentration (mmol/mL)	Trial #1 % effect	Trial #2 % effect	Concentration (mmol/mL)	Trial #1 % effect	Trial #2 % effect
9.76E-11	-2.58	-5.42	9.76E-11	-3.39	3.21
9.76E-10	-8.08	5.55	9.76E-10	0.27	6.95
9.76E-09	-2.43	-6.51	9.76E-09	0.4	6.43
9.76E-08	11.47	8.85	9.76E-08	-5.13	0.8
9.76E-07	-0.19	2.38	9.76E-07	2.78	4.15
3.10E-06	-0.11	7.51	3.10E-06	4.21	4.82
9.88E-06	3.81	8.93	9.88E-06	6.64	9.13
3.14E-05	58.25	61.73	3.14E-05	19.6	6.93
1.00E-04	96.96	99.94	1.00E-04	64.27	90.52

Table E20. Re-validated biological data of compound **41** in IL-17 release assay.

IL-17 Release Assay			Cell Viability Assay		
Concentration (mmol/mL)	Trial #1 % effect	Trial #2 % effect	Concentration (mmol/mL)	Trial #1 % effect	Trial #2 % effect
9.76E-11	1.87	9.96	9.76E-11	-1.28	-10.46
9.76E-10	14.84	5.13	9.76E-10	-0.01	-3.28
9.76E-09	-0.95	-3.78	9.76E-09	-0.9	4.05
9.76E-08	-6.79	3.71	9.76E-08	-9.46	-9.85
9.76E-07	-1.5	-5.03	9.76E-07	-1.5	1.42
3.10E-06	-12.18	-7.4	3.10E-06	-3.07	-4.21
9.88E-06	-13.18	0.22	9.88E-06	0.42	6.75
3.14E-05	14.2	8.17	3.14E-05	-0.8	4.87
1.00E-04	31.57	47.82	1.00E-04	-4.69	10.85

*Table E21. Biological data of compound **76b** in IL-17 release assay.*

IL-17 Release Assay			Cell Viability Assay		
Concentration (mmol/mL)	Trial #1 % effect	Trial #2 % effect	Concentration (mmol/mL)	Trial #1 % effect	Trial #2 % effect
9.76E-11	2.96	3.79	9.76E-11	-2.96	0.73
9.76E-10	12.95	8.82	9.76E-10	2.26	8.41
9.76E-09	7.33	8.33	9.76E-09	0.32	8.33
9.76E-08	0.82	4.6	9.76E-08	-6.92	6.25
9.76E-07	6.53	7.9	9.76E-07	4.97	7.66
3.10E-06	-3.33	4.7	3.10E-06	6.57	7.53
9.88E-06	-0.53	-6.1	9.88E-06	14.16	14.57
3.14E-05	-4.92	-9.13	3.14E-05	19.08	19.15
1.00E-04	12.16	13.52	1.00E-04	21.37	26.03

*Table E22. Biological data of compound **82** in IL-17 release assay.*